Université Pierre et Marie Curie

Ecole doctorale 398 : Géosciences, Ressources naturelles et Environnement
ISTeP

3D structural model of the Po Valley basin, Northern Italy

Thèse présentée par
Claudio Turrini

Pour obtenir le grade de : **Docteur de l'Université Pierre et Marie Curie**
Discipline / Spécialité : Sciences de la Terre

J. LAMARCHE (Maître de Conférences, Université Aix-Marseille)	Rapporteur
J.P. CALLOT (Professeur, Université de Pau et des Pays de l'Adour)	Rapporteur
M. SEBRIER (Directeur de Recherches CNRS, UPMC)	Examinateur
E. CARMINATI (Professeur Università La Sapienza, Roma)	Examinateur
G. COURRIOUX (Géologue, BRGM)	Examinateur
O. LACOMBE (Professeur, UPMC)	Directeur de thèse
F. ROURE (Directeur Expert IFP)	Co-Directeur de thèse

Acknowledgments

My unconditioned thanks are for Olivier and Francois. They have accepted to follow and support this study while pushing me to expand my perspective on a wider Po Valley geology.

Because this project is the ultimate result of nearly 25 years of professional activity across/around the Po Valley basin, the list of colleagues and friends that I should acknowledge would be too long to be mentioned in this report. Those colleagues and friends know I am deeply in debt and grateful for collaboration, discussion and help they supplied through the years.

Résumé

Cette thèse présente le modèle 3D du bassin de la Plaine du Pô en Italie du nord. Les six parties de la thèse conduisent le lecteur à partir du cadre géologique de base aux géométries et à la cinématique de la déformation à travers la région, ainsi qu'aux possibles applications en milieu académique ou industriel.

Le modèle a intégré des données éparses et de qualité inégale, tirées exclusivement de la littérature publique. L'ensemble de données utilisées pour la création du modèle se base strictement sur des données en profondeur (i.e. dans leur dimension de profondeur). Les données sismiques disponibles ont été intentionnellement écartées pour les raisons suivantes: a) elles sont mal distribuées à travers le secteur d'étude, b) elles se rapportent à des images de basse qualité, d) leur intégration dans le modèle aurait impliqué un long et difficile travail d'évaluation du meilleur modèle de vitesse de propagation des ondes sismiques dans les sédiments, le mieux à même d'être employé pour une conversion finale temps-profondeur, la variation latérale et verticale des vitesses sismiques à l'échelle régionale étant douteuse ou, au mieux, incertaine. La méthodologie appliquée, la création de modèles et l'analyse des améliorations du modèle 3D fournissent un certain nombre de conclusions sur la géométrie, le style structural et la cinématique de la Plaine du Pô et leur contribution en terme de sismicité du bassin et de son potentiel pétrolier, avec une confirmation mutuelle des, mais aussi par, les résultats locaux et épars obtenus par d'autres auteurs.

Le résultat principal du projet est d'avoir prouvé la capacité du modèle à visualiser et analyser la complexité du bassin de la Plaine du Pô dans les 3 dimensions à différentes échelles d'observation, de l'échelle crustal jusqu'au niveau des prospects.

En termes de géométrie de la déformation, le modèle 3D illustre comment la géométrie du Moho traduit la différenciation de deux domaines crustaux distincts dans la Plaine du Pô (occidentaux et orientaux), et comment la distribution des différentes unités tectoniques est contrôlée par les couches mésozoïques les plus profondes du modèle, même si l'on peut suivre les déformations associées jusqu'en surface à travers les sédiments tertiaires. Cette architecture crustal et les variations latérales et verticales de la stratigraphie mécanique

semblent bien commander la complexité des styles de déformation du bassin qui augmente du domaine oriental vers le domaine occidental de l'avant-pays. Ceci est compatible avec la géodynamique, qui a induit une rotation anti-horaire de l'ensemble constitué par l'Adriatique et la Plaine du Pô (plaque apulienne), avec un axe de rotation situé à la limite entre la Plaine du Pô et les Alpes occidentales, juste au sud de l'arc tectonique du Monferrato). Par la suite, la zonation de la déformation mentionnée ci-dessus correspond à une implication du socle dans le domaine occidental de la Plaine du Pô et à une tectonique de couverture dans le domaine plus oriental.

En termes de cinématique des structures, l'amélioration progressive du modèle avec quelques couches de référence dans la succession sédimentaire tertiaire et la restauration 2D des géométries structurales de coupes régionales à travers le modèle 3D fournissent une nouvelle analyse de l'influence que le grain tectonique-stratigraphique mésozoïque a exercé sur la progression de la déformation à travers et autour de la Plaine du Pô, du Paléogène à l'Actuel. Les résultats montrent que la tectonique extensive mésozoïque et la géométrie et les faciès des carbonates qui y sont associés ont localisé et contraint les structures alpines dans et autour du bassin. Leur contrôle sur la déformation et la sédimentation cénozoïque est évident pendant le Paléogène et le Miocène tandis que leur rôle devient plus modeste pendant le Plio-Pléistocène. En effet, l'inversion du bassin et la réactivation (avec une composante oblique indéfinie) des failles pré-alpines (approximativement orientées N-S) ont eu lieu par intermittence pendant le Paléogène et le Miocène. Pendant cette période, le couplage mécanique entre les chaînes des montagnes et l'avant-pays a favorisé la déformation à l'intérieur de la plaque, loin des orogènes, la tectonique de socle étant alors la plus forte. Durant cette période, la flexure de la plaque Adria répondait au début (Paléogène) à la croissance des Alpes méridionales et seulement plus tard, au Miocène, au développement du nord des Apennins, laissant de l'espace pour le remplissage du bassin d'avant-fosse associé. Au contraire, pendant le Plio-Pléistocène, la présence d'une avant-fosse étroite et profonde à l'avant de l'Apennin du nord se rapporte à une asymétrie claire de la flexure de la plaque Adria. La déformation de l'avant-pays, qui date du Plio-Pléistocène, se manifeste principalement au front de l'Apennin septentrional par des failles inverses, et par l'inversion-réactivation localisée de failles liées à la flexure (orientées approximativement WNW-ESE), ou des failles pré-alpines (orientées approximativement N-S) : a) les deux familles de failles sont actives et forment des arcs tectoniques dans les sédiments mésozoïques, b) la tectonique de couverture domine dans le domaine oriental de l'avant-pays, c) la déformation du socle

dans cette région est possible mais improbable. Le bassin étroit et profond de l'avant-fosse Plio-Pléistocène tout au long du front des Apennines du nord suggère que a) la flexure de l'avant-pays demeure plutôt homogène, b) les faiblesses possibles de la lithosphère orientées N-S et liées à la tectonique extensive triasique-liasique n'exercent pas un contrôle important sur la déformation de la croûte de la plaque Adria qui entre en subduction (ce qui est probablement dû à une quantité faible d'extension pré-orogénique ainsi qu'à un ré-équilibrage thermique postérieur au rifting triasique-liasique).

Pour ce qui concerne la sismicité du bassin, le modèle 3D confirme que les caractéristiques tectoniques principales autour de la Plaine du Pô expliquent les tremblements de terre les plus forts enregistrés par les catalogues de l'INGV. Par conséquent, la sismicité localisée par a) les unités superficielles des Alpes du sud et leur front de déformation depuis le secteur de Milan à l'ouest jusqu'à la région du Frioul à l'est, b) les racines profondes de l'arc de l'Apennin septentrional (70 km) et leur front aveugle (par exemple le domaine de Ferrare), c) le paléo-linéament judicarien réactivé, ressort clairement dans cette analyse 3D. La reconstruction de la sismo-tectonique tridimensionnelle suggère également l'existence d'une stratigraphie sismologique où le Moho, le toit du socle et les sédiments mésozoïques semblent concentrer l'activité sismique. Cette stratigraphie sismologique, en parallèle avec la stratigraphie mécanique de la région, induit des styles structuraux variés. En liaison avec certains domaines structuraux, le modèle 3D semble être plus efficace que les études 2D antérieures pour illustrer les structures complexes qui ont été vraisemblablement responsables des tremblements de terre: a) l'interférence active entre les Alpes et les Dinarides dans la région du Frioul, au pied de la zone faillée de la région de Valsugana, b) les zones de relais entre les failles en-échelon dans la région de Cavone sont des exemples clairs de cette situation. Finalement, le modèle 3D indique que la litho-stratigraphie (pré-alpine) mésozoïque et les failles associées sont les éléments-clés les plus à même de contrôler les associations principales de structures sismogènes dans la région. En particulier, il est intéressant de noter que les changements importants de faciès et d'épaisseur des sédiments mésozoïques pourraient par la suite localiser des tremblements de terre moyens à forts plus efficacement que les failles normales préexistantes.

Pour l'application suivante, un modèle thermique a été bâti à partir du modèle structural 3D. La simulation offre une description claire de l'évolution thermique des roches mères mésozoïques et de la génération/migration des hydrocarbures. En particulier, les résultats du

modèle 1D confirment que la maturité thermique ou les seuils d'expulsion peuvent être surestimés de façon significative si l'on considère seulement l'histoire de la température. Au contraire, quand les effets de la surpression observée dans les puits du secteur occidental de la Plaine du Pô sont pris en compte dans la prévision de la maturité thermique ou des volumes d'hydrocarbures susceptibles d'avoir migré vers les réservoirs, le modèle semble produire une meilleure corrélation avec les données observées. Deux modèles de maturité ont été générés à partir du modèle structural 3D: le premier basé sur un modèle de flux de chaleur géologique et le deuxième basé sur un modèle de flux de chaleur réduit, ce dernier étant destiné à répliquer les effets de retard de la surpression sur la génération ou d'expulsion d'hydrocarbures. L'analyse comparative suggère qu'à l'échelle régionale, les deux modèles sont comparables avec la distribution d'hydrocarbures observée dans les gisements de la Plaine du Pô. Dans le détail cependant, le modèle en surpression a) semble fournir une meilleure corrélation entre les volumes des hydrocarbures calculés en place et la charge disponible dans la région de génération des huiles, b) prédit également la phase d'hydrocarbures (mesurée par son GOR) plus exactement que le modèle sans surpression. Du point de vue de l'exploration des hydrocarbures, deux conclusions majeures peuvent être tirées de l'intégration et de l'analyse finale des modèles cinématiques et thermiques: a) dans la partie occidentale de la Plaine du Pô, le synchronisme entre la maturation des roches, la migration des hydrocarbures et la formation de pièges structuraux est favorable pour l'exploration. La formation des pièges s'est très probablement produite entre l'Oligocène et la fin du Miocène, avec une génération et une expulsion significatives d'hydrocarbures qui ont pu arriver dans les pièges après le Miocène; b) dans le secteur oriental de la Plaine du Pô, les pièges d'âge Plio-Pléistocènes sont plus tardifs que la phase principale de génération des hydrocarbures, ou la génération d'HC y est encore dans sa phase initiale, n'étant donc pas suffisamment avancée pour que la migration se produise et que les pièges soient alimentés.

En dépit de la simplicité relative de l'approche de modélisation adoptée et du niveau variable des incertitudes dû à la dimension modèle et à la qualité et la répartition des données disponibles, le modèle réalisé ici ouvre la voie à de nombreuses applications pour les milieux universitaires et industriels. En particulier, le géo-volume actuel, une fois amélioré avec des données supplémentaires, pourra constituer:

1. un outil important et un exemple extrêmement didactique pour l'activité éducative;

2. le scénario préliminaire pour des investigations futures dans le domaine de l'exploration des hydrocarbures (revue des gisements existants, nouvelles régions de prospections, prévision de la stratigraphie des puits, analyse post-mortem des puits);
3. un volume prêt à l'usage pour l'hydrogéologie dans les formations sédimentaires Plio-Pleistocène (hydro-stratigraphie, modèles hydrologiques 3D);
4. la référence structurale pour les études de faisabilité du stockage de CO_2 et CH_4;
5. le support possible pour des projets de géo-archéologie.

Abstract

This thesis deals with the 3D model building of the Po Valley foreland basin in northern Italy. The six parts of the thesis lead from the basic geological framework to the deformation geometries and kinematics across the region, to some of the possible model applications, for both academia and industry.

The model has integrated sparse and variable quality data, exclusively taken from the public literature. The complete dataset used for the performed model building, strictly relies on depth-data (i.e. in their depth dimension). As such, the few available seismic data have been intentionally left apart because: a) they are poorly distributed across the study-area, b) they definitely refer to low quality images, d) their integration into the model would have implied a long and difficult work about the definition of the most-likely sediment velocities to be used for an ultimate time-depth conversion, uncertain and, at best, questionable.

The applied methodology, the related model building and the progressing analysis of 3D model results suggest and discuss a number of conclusions about the Po Valley structural geometries-style-kinematics. From such results can be derived implications on basin seismicity and hydrocarbon potential, while confirming (thus being supported by) the local and sparse results of previous authors.

The major result from the project is to have proven the model capability in rendering and analyzing the entire Po Valley basin structural complexity in 3D dimensions, from crustal to field scale. Thanks to this, the model is unique in the literature of the region.

In terms of deformation geometries, the performed 3D model illustrates how the Moho controls the presence of the Po Valley crustal domains (western and eastern) and the associated tectonic units' distribution, at any of the shallowest model layers (i.e. inside the basement-Mesozoic section and across the Tertiary sediments). Such crustal architecture, together with the variable mechanical stratigraphy, appears then to drive the basin deformation complexity which increases from the eastern towards the western domain of the foreland. This is consistent with the anticlockwise roto-translation geodynamics of the Po Valley-Adria plate and the possible existence/presence of the related structural pivot at the western Alps-western Po Valley boundary zone (i.e. below-southwards of the Monferrato

tectonic arc). Eventually the final deformation zonation results into clear thick-skinned and mainly thin-skinned structural style in the western and eastern Po Valley respectively.

In terms of structures' kinematics, the continuous refining of the model with some key layers in the Tertiary sediment succession and the 2D restoration of selected cross-section, sliced from the 3D model, provide new insight into the influence that the Mesozoic tectono-stratigraphic grain exerted on the subsequent deformation progression across and around the Po Valley foreland, from the Paleogene to the present. Results show that the Mesozoic, extension-related tectonics and the associated carbonate facies geometry and distribution have localized and constrained the Alpine structures inside/around the basin. Their control on the Cenozoic deformation and sedimentation is evident during the Paleogene and the Miocene whereas it becomes more subtle during the Plio-Pleistocene. Indeed, basin inversion and reactivation (with undefined strike-slip component) of pre-Alpine faults (approximately N-S oriented) intermittently occurred during the Paleogene and Miocene. At that time crustal mechanical coupling between the belts and the foreland enhanced intra-plate deformation, far from the advancing orogens: thick skinned tectonics was then dominant across the belt-foreland system. In addition, flexure of the Po Valley/Adria plate was responding initially (Paleogene) to the Southern Alps growth and lately (Miocene) to the Northern Apennines development also, leaving room for the associated foredeep basin deposition. Conversely, in Plio-Pleistocene times, the presence of a narrow and deep foredeep at the front of the Northern Apennines refers to a clear asymmetry of the Po Valley/Adria flexure. Plio-Pleistocene deformation of the foreland mainly occurs at the external front of the Northern Apennines by thrusting, with local inversion-reactivation of both flexure-related faults (approximately WNW-ESE oriented) and pre-Alpine discontinuities (approximately N-S oriented): a) the two fault families compete to form tectonic arcs in the Mesozoic section, b) thin-skinned tectonics prevails across the eastern Po Valley foreland domain, c) involvement of the basement in that region is possible yet still debatable. The narrow and deep Plio-Pleistocene foredeep basin, all along the front of the Northern Apennines, suggests that: a) the foreland flexure is rather homogeneous below the belt, b) the N-S oriented lithospheric weaknesses, derived from the Triassic-Liassic extensional tectonics, do not exert a major control on the crustal deformation of the subducting Po Valley-Adria plate (possibly due to a weak amount of pre-orogenic extension together with a re-gained thermal equilibrium since the Triassic-Liassic rifting).

Concerning the basin seismicity, the 3D model confirms that the major tectonic features around the Po Valley region account for the strongest earthquake events recorded by the INGV catalogues (5-7 M). Hence, the seismicity is localized by: a) the Southern Alps thrust front (from Milano to the Friuli area), b) the Northern Apennines belt crustal roots (down to 70 km) and their buried front (e.g. the Ferrara domain), c) the reactivated Giudicarie paleo-lineament, which from the Alps outcrops extends southwards into the basin. In addition, the three-dimensional seismo-tectonic reconstruction also suggests that there might be an earthquake-stratigraphy where the Moho, the top basement and the Mesozoic package seem to better concentrate the seismic activity. Such an earthquake stratigraphy works with the well-known Po Valley mechanical stratigraphy to develop the final variable structural style. Within certain domains, the 3D model looks more capable than the previous 2D investigations to illustrate the complex structures that have been likely responsible for strong earthquakes: a) the active interference between Alpine and Dinaric structures in the Friuli area, in the footwall of the regional Valsugana fault zone, b) the relay zones among the en-echelon thrust planes in the Cavone region, are clear examples of such a situation. Ultimately and notwithstanding, the model indicates that the Mesozoic (pre-Alpine) litho-stratigraphy and the related fault pattern are the most likely key elements in controlling the major structure-earthquake associations in the region. In particular, it is interesting to note that important facies and thickness changes in the Mesozoic sediment distribution could eventually trigger medium-to-strong earthquake events more efficiently than pre-existing faults.

As a further application, 1D and 3D thermal modeling was built on the performed 3D structural model. The simulation provided a consistent description of the possible Mesozoic source evolution and the hydrocarbon generation/migration timing. In particular the 1D model results confirm that thermal maturity or the overall volume of hydrocarbons expelled from the source rocks can be significantly over-predicted if we rely only on temperature history. In contrast, when the effects of the substantial overpressure observed in the western Po Valley wells are incorporated into the prediction of thermal maturity, the model seems to produce a better fit to the observed data. Two maturity models were then generated from the Po Valley 3D structural model: one based on the geological heat flow model and another based on a reduced heat flow model, aimed at replicating the retarding effects of overpressure on hydrocarbon generation. The comparative analysis of the different models suggest that, at the regional scale, both non-overpressure and overpressure models are reasonably consistent with the observed hydrocarbon distribution around the Po Valley oil fields. However, in detail, the

overpressure model a) seems to provides a better match between calculated hydrocarbon-in-place volumes and predicted charge available from the kitchen area, since effective trap formation, b) predicts the hydrocarbon phase (as measured by GOR) more accurately than the non-overpressure model. From a hydrocarbon exploration point of view, two main conclusions can be drawn from the final structural-thermal model integration and analysis: a) in the Western Po Valley the timing of hydrocarbon maturation is favorable for exploration. Trap formation is thought to have occurred during the Oligocene to late Miocene, with the timing of significant hydrocarbon generation and expulsion expected to have occurred post-Miocene; b) in the eastern Po Valley, timing is less favorable as traps (Plio-Pleistocene age) tend to either post-date the main hydrocarbon generation phase, or generation is at a very early stage and is not far enough advanced for migration to occur, or for traps to be filled.

Despite the relative simplicity of the modelling approach adopted and the variable level of uncertainty due to the model dimension and the available data quality/distribution, the final structural/seismo-tectonic/thermal model opens to numerous future perspectives for both academia and industry. Particularly, once strengthened with additional data, the current geo-volume can represent:

1. a powerful tool and a highly didactic example for the education activity,
2. the preliminary scenario for further investigations in the domain of the exploration hydrocarbons (reviewing of the existing fields, new prospect areas, pre-well-prognosis and post-well analysis),
3. a ready-to-use volume for the hydrogeology of the Plio-Pleistocene layers (hydro-stratigraphy, 3D groundwater flow models),
4. a structural reference for CO_2-CH_4 storage feasibility studies,
5. a possible support to geo-archeological projects.

Table of contents

Part 1 - Forewords

I. Introduction

From the hieroglyphics of Egypt to Giotto, human kinds needed thousands of years to develop a new way of observing reality and nature: the 3D perspective. Today, thanks to 3D computer graphics, various fields of investigation in science and technology aims at reproducing three-dimensionality as the primary objective for research projects or new developing tools.

In modern Geology, 3D representation and analysis of geometric data have become part of the standard workflow in many fields of application (field-work, hydrocarbons, water, geothermal, mineral, CO_2-CH_4 storage, civil engineering) with immediate benefits in terms of data managing, results reproducibility, cost/time effectiveness.

Concerning structural geology, 3D model building is a powerful procedure for tackling the complexity of deformation geometries and kinematics. Indeed, tectonic-derived structures are rarely cylindrical and their evolution implies inhomogeneity and variability, thus uncertainty, about the related geodynamics (roto-translation?), deformation directions (obliquely-oriented?), fracture distribution (e.g., strata-bounded?), fold-fault termination-connection, mass transfer (in/out-of-plane?), sediment geometry and depositional facies (i.e. horizontal and vertical mechanical stratigraphy).

Without replacing 2D analysis, the 3D modeling technique brings a key support to the structure validation workflow (Egan et al., 1999; Moretti, 2008; Calcagno et al., 2008; Guillem et al., 2008; Caumon et al., 2009; Cherpeau & Caumon, 2015; Ellis & Armstrong, 2015). The methodology eventually provides the user with deterministic or stochastic solutions, these being geometrically consistent even where, thanks to the model extrapolation, data are initially poor or totally lacking.

When specific references in the recent literature are considered, many and various aspects concerning structural-geology issues have been investigated using 3D models, irrespective of the chosen scale of observation:

- the crustal architecture of the earth is possibly among the most common targets for 3D model building (Calcagno et al., 2007; Schreiber et al., 2010; Farrington et al., 2010; Dhont et al., 2012; Vouillamoz et al., 2012; Maystrenko et al., 2013; Autin et al., 2015; Klitzke et al., 2015; Berthoux et al., 2016; Grad et al., 2016);
- 3D analysis of field-to-regional scale structures is applied on worldwide examples (Turrini & Rennison, 2004; Lamarche et al., 2005; Guillaume et al., 2008; Guyonnet-Benaize et al., 2010, 2015; D'Ambrogio et al., 2010; Leslie et al., 2012; Gisquet et al., 2013; Cardoso et al., 2016);
- fold/fault patterns, fault-zones, outcrop studies and fractured structures have been investigated in their 3D characteristics (Bailey et al., 2002; Masaferro et al., 2003; Rivenaes et al., 2005; Lapponi et al., 2011; Schober & Exner, 2011; Ramon et al., 2013; Campani et al., 2014; Fernandez & Kaus, 2014; Katsuaki et al., 2015; Schopfer et al., 2016);
- 3D modeling is widely used to improve understanding about hydrocarbon fields and the related hydrocarbon system elements or exploration strategy (Johannesen et al., 2002; Mitra & Lislie, 2003; Badics et al., 2004; Dischinger & Mitra, 2006; Mitra et al., 2006; Valcarce et al., 2006; Mitra et al., 2007; Yin & Groshong, 2007; Turrini et al., 2009; Cherpeau & Caumon, 2015);
- the 3D technique can be applied for reconstruction and further analysis of sand box experiments (Guglielmo et al., 1997; McClay & Bonora, 2001; Paul & Mitra, 2013; Ferrer et al., 2014; Galuppo et al., 2016);
- CO_2 storage and geothermal evaluations have often benefited from 3D model building (Calcagno et al., 2012; Guglielminetti et al., 2013; Alcade et al., 2014);
- 3D numerical models are used to support different tectonic related issues from fault-zone evolution (Friedman et al., 2008; Katsuaki et al, 2015; Schopfer et al., 2016) to multilayer fold growth and fold deformation simulations/restoration (Durand-Riard et al., 2011; Ramon et a., 2013; Fernandez & Kaus, 2014), to lithospheric stress/dynamics investigations (Farrington et al., 2010; Petricca & Carminati; 2014); stochastic solutions have been proposed as a way to constrain the 3D model uncertainty distribution (Lecour et al., 2001; Cherpeau & Caumon, 2015).

From the meso to the mega scale, from surface to deep sub-surface, all these case studies essentially suggest how tectonic structures can be partially or completely misinterpreted when

observed in 2D, yet, notwithstanding the models' simplification, they result complex but consistent if viewed in 3D.

Undoubtedly, 3D models allow any structure across the entire range of domains that can be found in nature (thrust-belts, foreland, foredeep, rift, wrench zones etc. etc.) to be navigated through, rendered, anatomically observed, analyzed, sectioned, rapidly implemented with new data/interpretations, estimated in all its dimensions (volume, surfaces, lengths), populated with mathematical attributes and punctual values, virtually explored and drilled.

The Po Valley (northern Italy) is a sedimentary basin (see references in Part 2, Section I-III; Part 4, Section III-V; Part 5, Section III-V) which developed from Triassic to present, by the combination of different types of geological environments, all defined by a highly variable mechanical stratigraphy and a complicated tectono-sedimentary evolution.

The following characteristics can be listed to introduce the basin setting and the related complexity:

- it is 40.000 km^2 wide,
- it has undergone a wide spectrum of geological processes (lithosphere stretching and heating, thermal subsidence, tectonic extension, inversion, compression, wrenching, fluid circulation, burial and associated cooling, tectonic-sedimentary compaction, mechanical decoupling inside the sedimentary succession, erosion and unconformity formation, crustal flexuring and bulging),
- past and present geodynamics refer to rotation and translation of the intervening crustal plates,
- it is the foreland-foredeep basin of two opposing mountain chains (the Southern Alps and the Northern Apennines),
- the ultimate compression-related, Alpine structures have developed perpendicularly to the pre-existing, extension-related tectonic fabric,
- most of the sediments (especially the Mesozoic ones) are non-homogeneous in distribution, dimensions (area, thickness) and associated facies,
- it generated hydrocarbons from different source rocks inside the stratigraphic succession while showing the full range of effective trapping mechanisms and geometries,

- public data are sparse and they relate to very different sources and interpretation criteria,
- the majority of the investigations around the region refer to 2D maps and cross-sections.

The coexistence of the aforementioned factors makes the Po Valley basin a rather unique, geological object/province which, since the beginning of this thesis, suggested an interesting case study for application of the 3D modeling methodology.

Once the *Po Valley 3D structural model* goal identified and accepted, a number of general questions seeded the work and progressively arose as the model developed:

- Is the model worth building and why?
- At which level of detail will be possible to reconstruct such a complex tectonic region only using the available data from the public literature?
- What can constrain uncertainty in such hardly-constrainable 3D model case study?
- Can the well-established, standard 3D modeling methodology be implemented somehow?

The results from the performed model (Part 4 and 5 in this thesis) are implicit answers to those first order, philosophical (?), interrogations.

The same results also provide (or struggle to provide) possible answers to the many, second-order (?), regional queries that puzzle any researcher/explorer's mind working on the region (see the Discussion Section in Part 6).

Conclusively, the model has by definition an explicit regional significance: it illustrates the three-dimensional geometries and the associated kinematics which, by tectonic inversion of the north-western sector of the Apula passive margin, formed the current Po Valley foreland-foredeep basin. Nevertheless, by comparison with the sparse and isolated data/interpretations that preceded it, the model clearly demonstrates the impact that switching from 2D to 3D perspective may have on unraveling of any tectonic setting worldwide, especially where a) seismic data are lacking, b) correlation among the structural domains may be open to questions, c) tectono-sedimentary inhomogeneity is dominant both spatially and temporally.

II. Objectives

By loosely following the questions enucleated in the previous chapter while trying to keep a balance between philosophical and scientific answers, the aim of this thesis is many-folded.

The **primary objective** of the project is to perform and illustrate the Po Valley 3D structural model from crustal to field scale with focus on the deformation geometries and kinematics of the Mesozoic carbonates.

The **second objective** is to prove its viability and applicability as a possible support to both industry and academia related research topics.

A **third objective** of the study is to demonstrate that three-dimensional model building is a powerful technique that can really expand the user perspective during the interpretation and analysis of tectono-sedimentary basins. In these terms, the methodology allows new and unpredictable problems to be recognized and tackled by simple twisting of the mouse and changes of the observation direction.

Despite the singleness of the Po Valley tectono-stratigraphic configuration, the **fourth objective** is to provide a possible case-study and workflow for analog situations, worldwide.

III. Plan of the thesis

This thesis is divided into 6 parts.

Part 1 presents the project background, motivations, objectives and structure.

Part 2 provides the framework to the study area. As such the basic information about the geology of Italy and the Po Valley are described by specific sections and the related main references from the available literature. In particular, the Po Valley foreland is briefly presented in terms of its crustal architecture, sediment stratigraphy, shallow and deep structures, seismicity and hydrocarbon content. **Noteworthy, an extended presentation about most of these items is provided in section III and V of Part 4 and 5 where they form the introduction to the papers so far published or currently under-review about the Po Valley 3D model and its applications.**

Part 3 introduces to 3D structural modeling criteria and briefly discusses some of the recent 3D structural models taken from the available literature.

After a short introduction, **Sections II and III of Part 4** present and discuss the deformation geometries that constitute the Po Valley 3D structural model with particular emphasis on the Mesozoic carbonates. **Sections IV and V** focus on the deformation evolution of the basin from Paleogene to present. The influence of the inherited extensional tectonics on the foreland evolution and the associated Tertiary foredeep geometry/migration is hence illustrated.

Part 5 shows and arguments the viability of the performed 3D model as a support to specific applications, namely the earthquake-structures reviewing **(Sections II and III)** and the basin thermal modeling and hydrocarbon generation **(Sections IV and V)**.

Part 6 is devoted to a general discussion of the results against the overall model uncertainty, together with the enouncement of the 3D model conclusions, perspectives and lesson-learned.

Part 2 – The Po Valley

I. Introduction

The Po Valley basin is a major geographical feature of northern Italy (Fig.1). The basin covers an area of approximately 40.000 square kilometres as it is caught in between the Alps, to the west and the north, and the Northern Apennines, to the south. Towards the east, the topographic surface of the plain gradually sinks into the Adriatic Sea where the Po River, after approximately 450 kilometres from the source, forms its delta apparatus.

Figure 1 - Po Valley location and geographical setting

II. Regional Framework

The Italian peninsula results from the long-lasting geodynamic process which led to the current, high-complex structural and stratigraphic puzzle (Fig.2) (Elter & Pertusati, 1973; Dercourt et al., 1986; Laubscher, 1996; Castellarin, 2001; Castellarin & Cantelli, 2010; Cuffaro et al, 2010; Mosca et al., 2010; Frisch et al., 2011; Carminati et al., 2012; Carminati & Doglioni, 2012; Handy et al., 2014 and references therein).

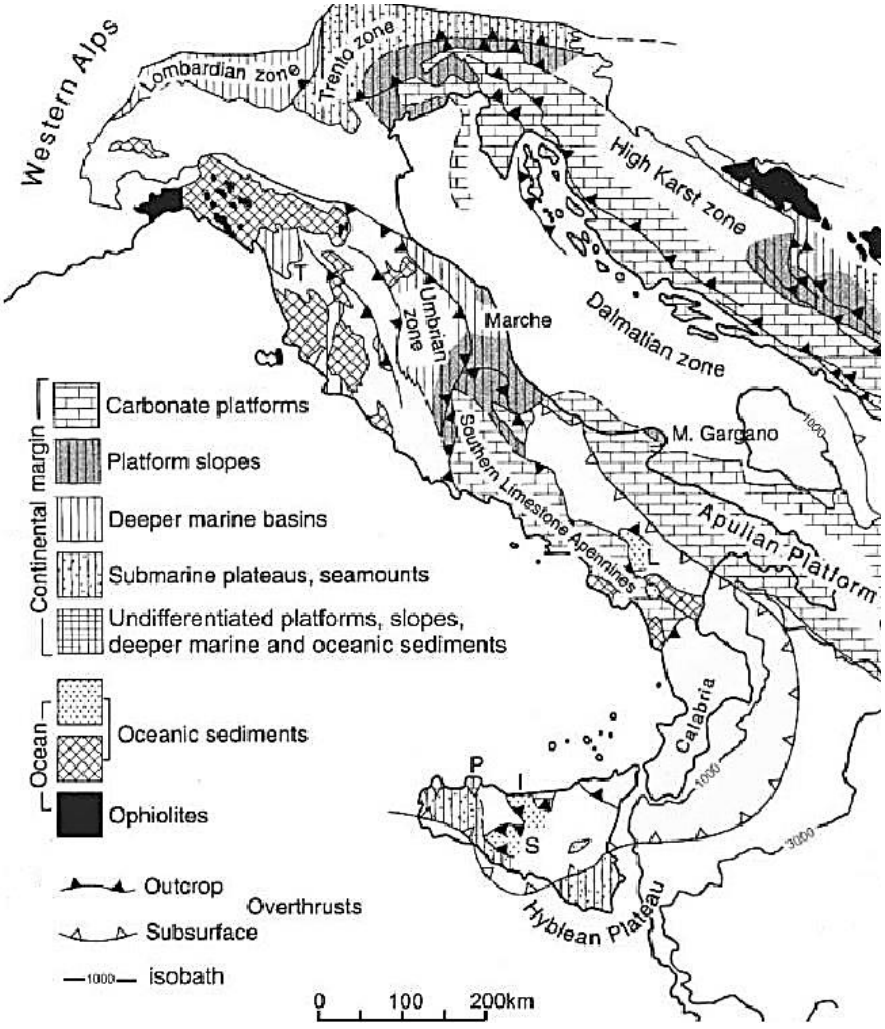

Figure 2 - Tectonic units across the Italian peninsula (Karakitsios, 2013)

During Mesozoic and Cenozoic times (Fig.3), rifting, break-up, passive margin drift and ocean spreading, subduction and collision tectonics modeled the origin and the evolution of the African and Eurasian plate boundaries. The superposition of the related deformation events created the Alps and the Apennines mountain chains while the Po Valley-Adriatic tectonic system progressively developed at the front of both the advancing belts.

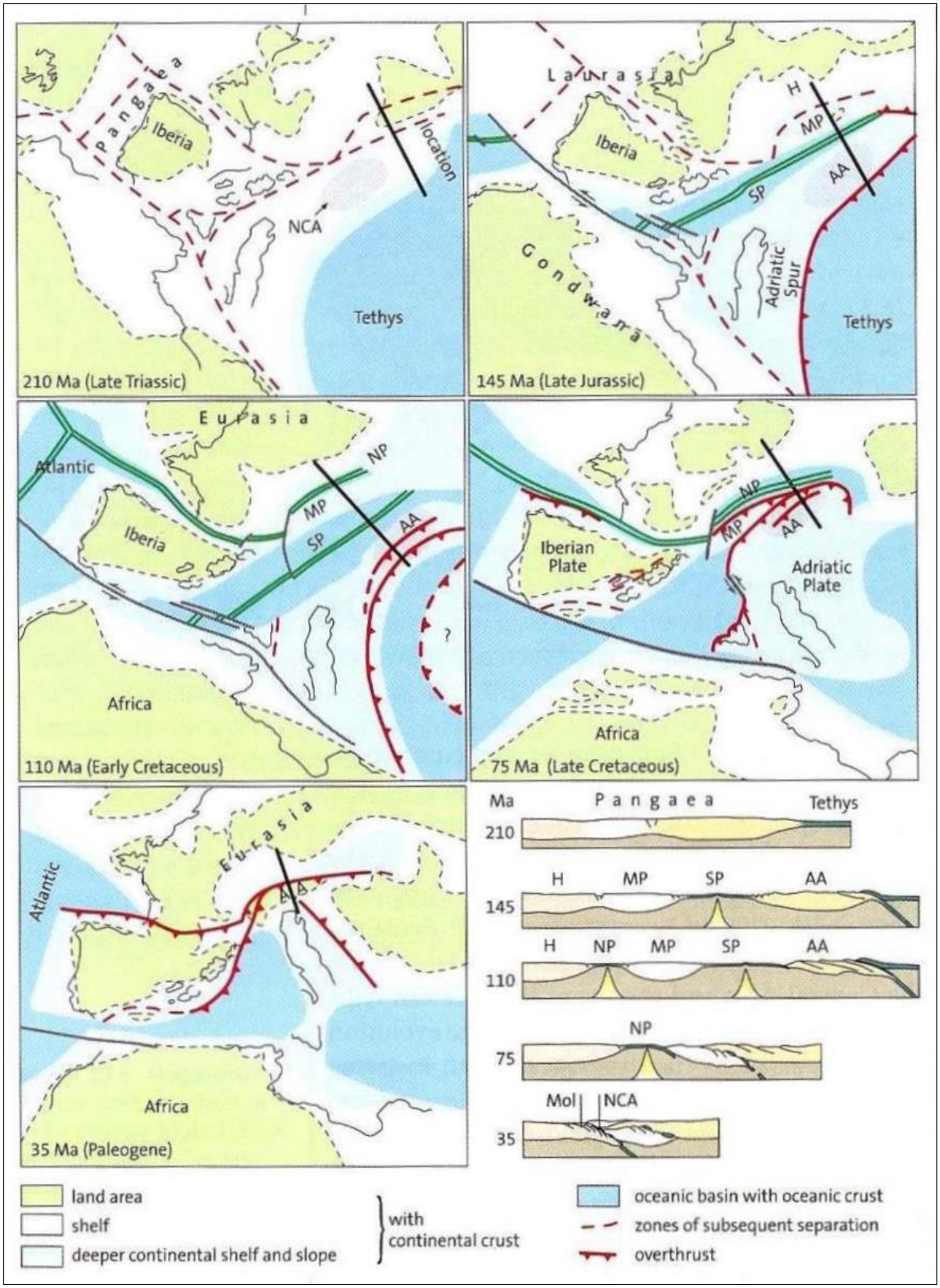

Figure 3 - Plate tectonic evolution of the Alps-Apennines belts and adjacent parts of Europe and North Africa. Time slices from Late Triassic to Eocene show evolution in both map and cross-section views (Frisch et al., 2011)

III. The Po Valley foreland basin

Within the described geological setting, the Po Valley represents the north-westernmost buried sector of the African plate, the foreland-foredeep basin to the Southern Alps and the Northern Apennines and, eventually, one of the major onshore hydrocarbon provinces in Europe.

A. Crustal Architecture

The Po Valley lithosphere is recognized as the Adria-Apulian indenter. As such, while intermittently rotating anti-clockwise, the Adria plate is continuously and currently forced against the Eurasian plate. The western domain of the indenter is supposed to provide the crustal pivot to the system and it accounts for the Northern Apennines-Southern Alps tectonic junction (Fig.4) (Vignaroli et al., 2008; Handy et al., 2010, 2014; Carminati et al., 2012; Mantovani et al., 2015).

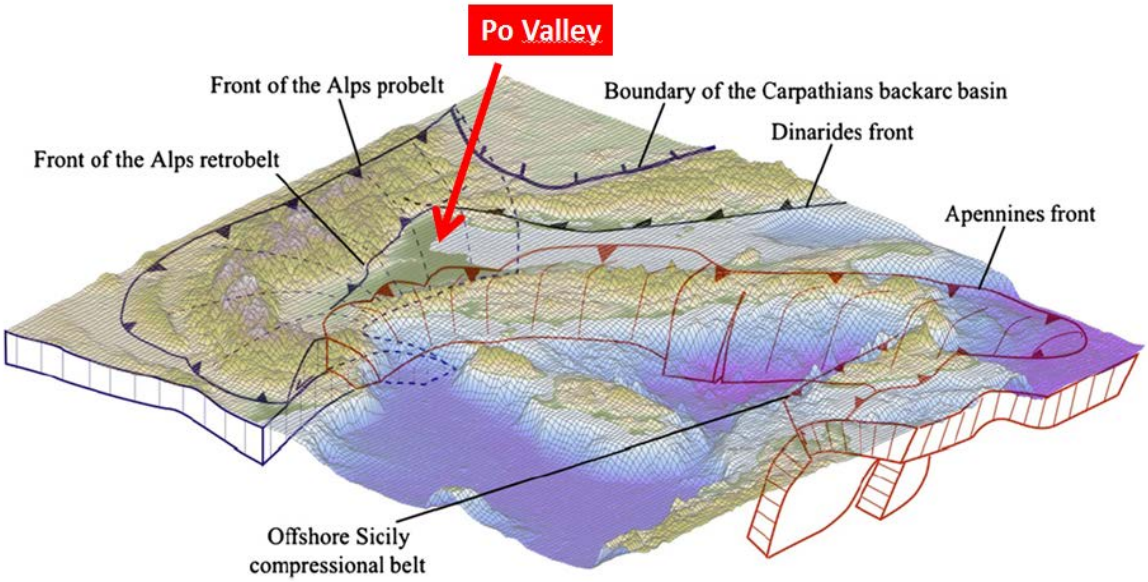

Figure 4 - The Po Valley and surrounding tectonic units (Carminati & Doglioni, 2012)

At present, following the Mesozoic-Cenozoic extension-compression evolution, the Adria plate architecture mainly relates to differential subduction and flexure of the lithosphere: at high angle towards the SW, below the Northern Apennines belt and at low angle towards the NE, below the Southern Alps (Carminati & Doglioni, 2012 and all references therein).

Given such a configuration (and the related geodynamic history), the Po Valley-Adria-Apulian plate shows the following crustal characteristics (Cassano et al., 1986; Della Vedova et al., 2001; Scrocca et al., 2003; Carminati & Doglioni, 2012 and all references therein) (Fig.5):

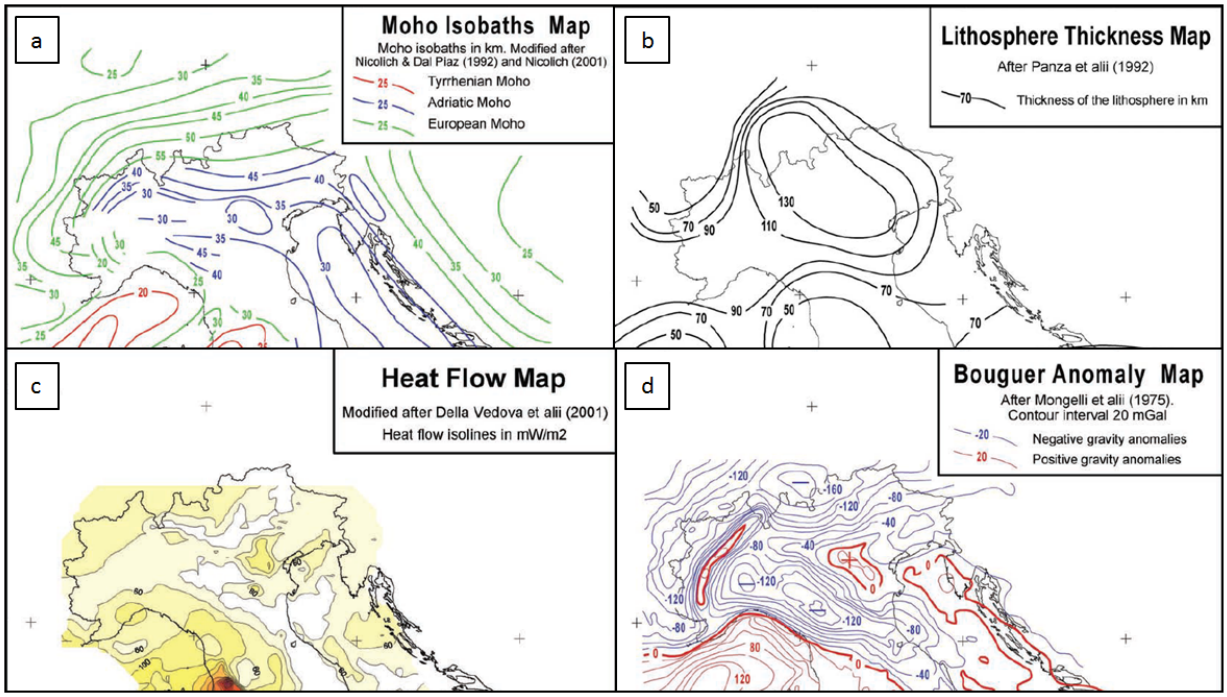

Figure 5 - Crustal characteristics of the Po Valley-Adria-Apulian plate (Scrocca et al., 2003).

- Depth to the Moho increasing from 0 to 30 km, from west (the Ivrea zone, i.e. along the boundary with the western Alps) to east (the Po Valley-Adriatic boundary), with a maximum depth below the Northern Apennines and the Southern Alps (Fig.5a);
- Lithosphere thickness between 70 (i.e. the foreland) and 130 (i.e. the belts) km (Fig.5b);
- Heat flow between 30 and 80 mW/m2 in the western and eastern domain of the foreland region, respectively (Fig.5c);
- Bouguer anomaly values between 0 (the Ivrea zone, along the boundary with the western Alps, and the eastern foreland domain, the Veneto region) and -120mGal (below the belts) (Fig.5d);
- Approximately NNW oriented plate motion with respect to Eurasia (Mantovani et al., 2015, Pfiffner, 2014);
- Active stress and Shmin directions mainly following the geometry of the buried tectonic arcs (with local deviation) (Fig.6).

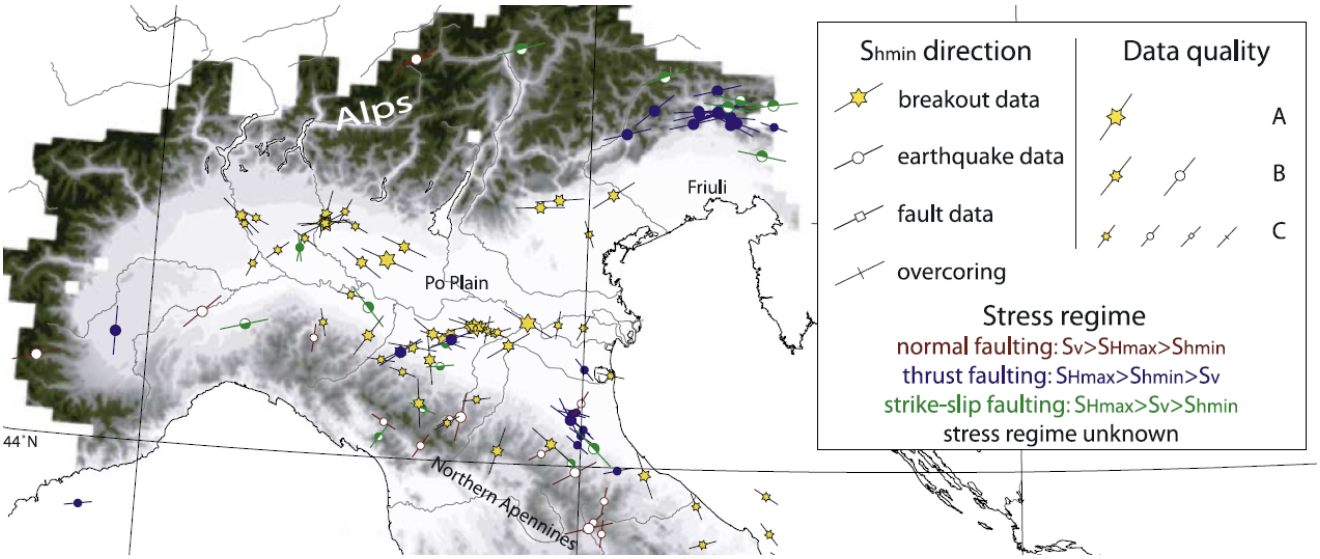

Figure 6 - Active stress map with minimum horizontal stress orientation (Montone et al., 2004).

B. Sediment stratigraphy

The sediment stratigraphy inside the Po Valley consists of Tertiary and Mesozoic deposits. The whole succession overlays Hercynian metamorphic basement rocks (Fig.7).

The *Mesozoic succession* is formed by Triassic platform-type carbonates (with possible basal evaporites: the Burano Formation in the eastern Po Valley – Cassano et al., 1986) and by Jurassic to Cretaceous pelagic carbonates. The Triassic-Jurassic deposits refer to the rifting and drifting events that built the Adria plate margin (Jadoul & Rossi, 1982; Bertotti et al. 1991; Berra et al. 2009) and their facies/distribution can be highly variable both vertically and horizontally (Cassano et al., 1986; Fantoni & Franciosi, 2010; Masetti et al.,2012). Conversely, the Cretaceous deposits mainly relate to thermal subsidence of the Adria margin: in this case, facies and thickness are rather homogeneous across the entire Po Valley basin.

The *Tertiary sediments* consists of Paleogene marls, some Messinian evaporites, sand-shale Pliocene turbidites, Early Pleistocene marine sands and Late Pleistocene alluvial deposits. Such deposits are the infilling of the foredeep basins which developed from late Cretaceous to present at the front of the Northern Apennines and Southern Alps belts (Di Giulio et al., 2010; Ghielmi et al., 2013; Rossi et al., 2015) thus contributing to the flexure of the foreland lithosphere (Fig.8) (Kruse, S.E., Royden, L.H., 1994; Carminati & Doglioni 2003): thickness

of the related sedimentary wedges is between 0 to 8 kilometers (maximum depth being the depocenters at the front of the Southern Alps and Northern Apennines belts).

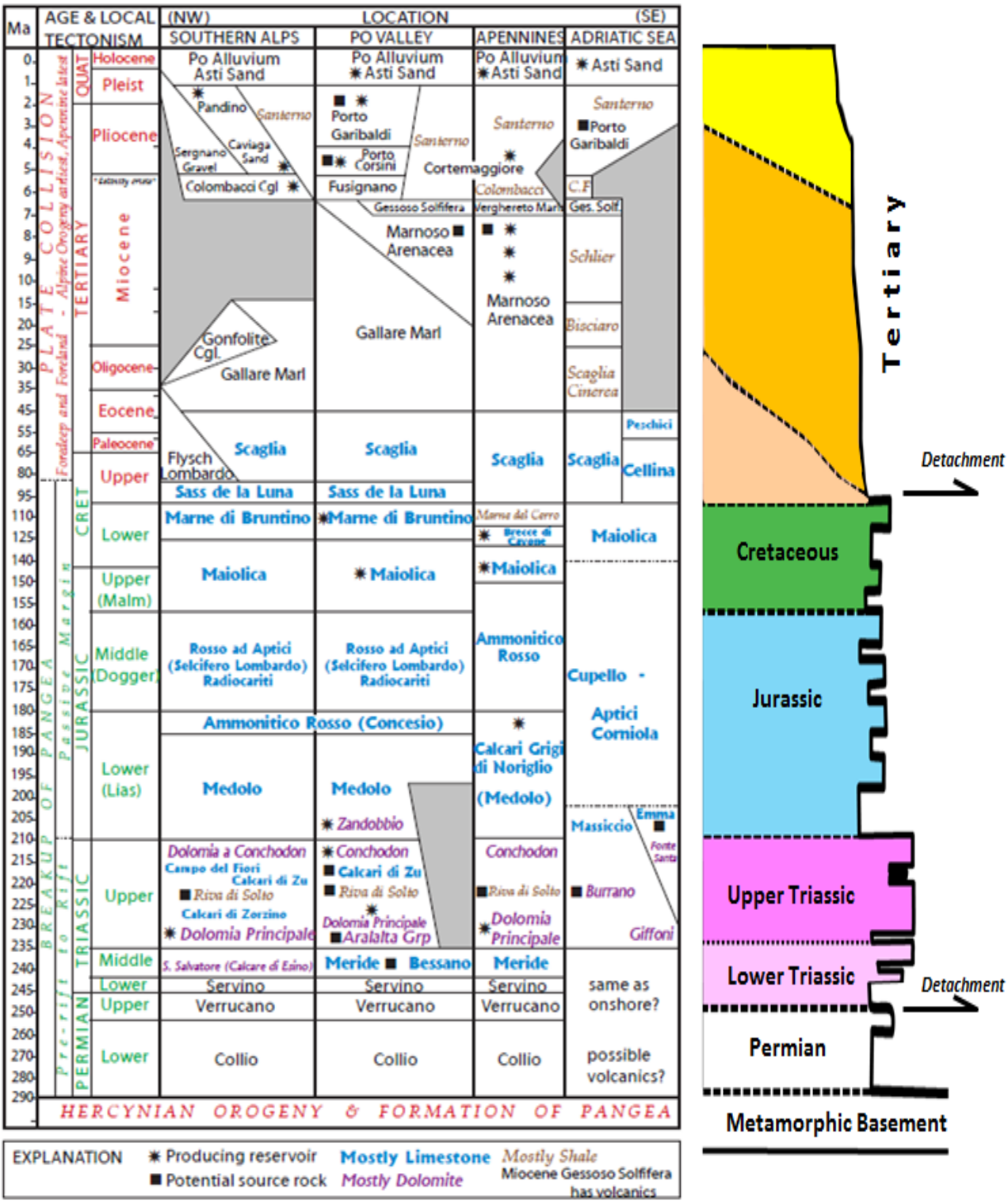

Figure 7 – (left) Po Valley sediment stratigraphy and hydrocarbon system (Lindquist, 1999 - formation lithology by colour code); (right) simplified mechanical stratigraphy.

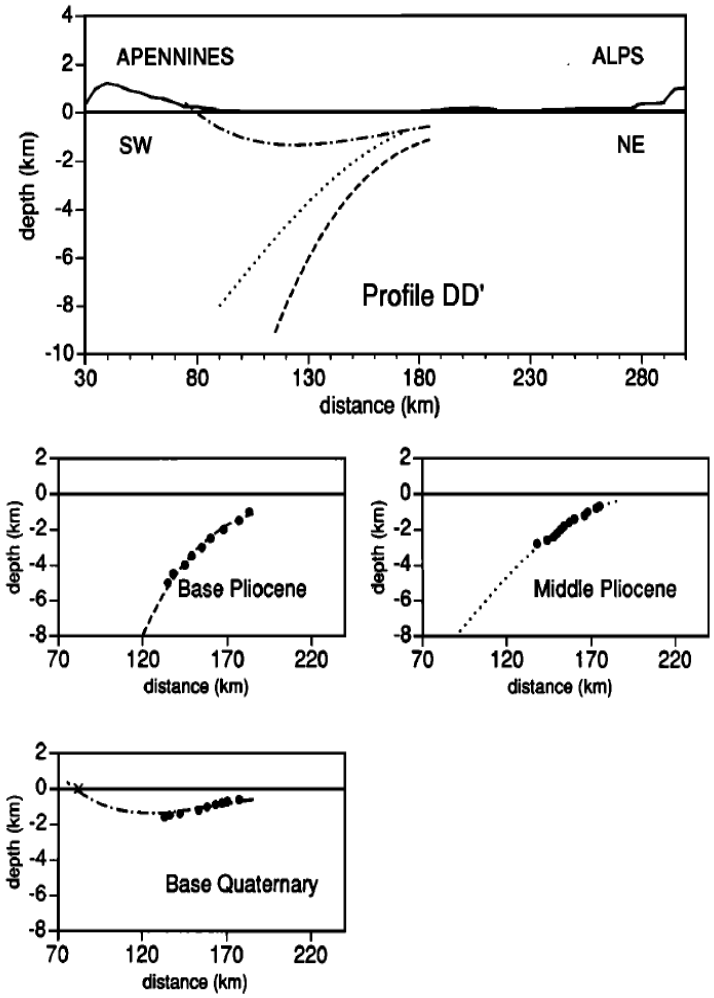

Figure 8 - Flexure evolution across the Northern Apennines-Po Valley-Southern Alps domain (Kruse & Royden, 1994)

The *Hercynian basement* to the Mesozoic deposits has been drilled by a few wells inside the basin (Battuda 1, Monza 1, Assunta 1) and locally outcrops in the hinterland of the Southern Alps (Cassano et al., 1986; Carminati, 2009; Fantoni & Franciosi, 2010; Ponton, 2010; Pfiffner, 2014).

Noteworthy and despite the huge amount of data gathered during the last century of research, the current knowledge about the Po Valley sediment distribution is mainly related to the information coming from the Southern Alps outcrops (Fig.9) (Castellarin & Vai, 1982; Jadoul & Rossi, 1982; Bertotti et al. 1991; Zanchi et al., 1990; Bello & Fantoni, 2002; Fantoni et al, 2003; Doglioni & Carminati, 2008; Berra et al. 2009; Fantoni & Franciosi, 2010) and the exploration industry data (i.e. public well composite logs, Fig.10) (http://unmig.sviluppoeconomico.gov.it) and reporting (Pieri & Groppi, 1976; Cassano et al., 1987; Fantoni et al, 2004; Ghielmi et al., 2010 and 2012).

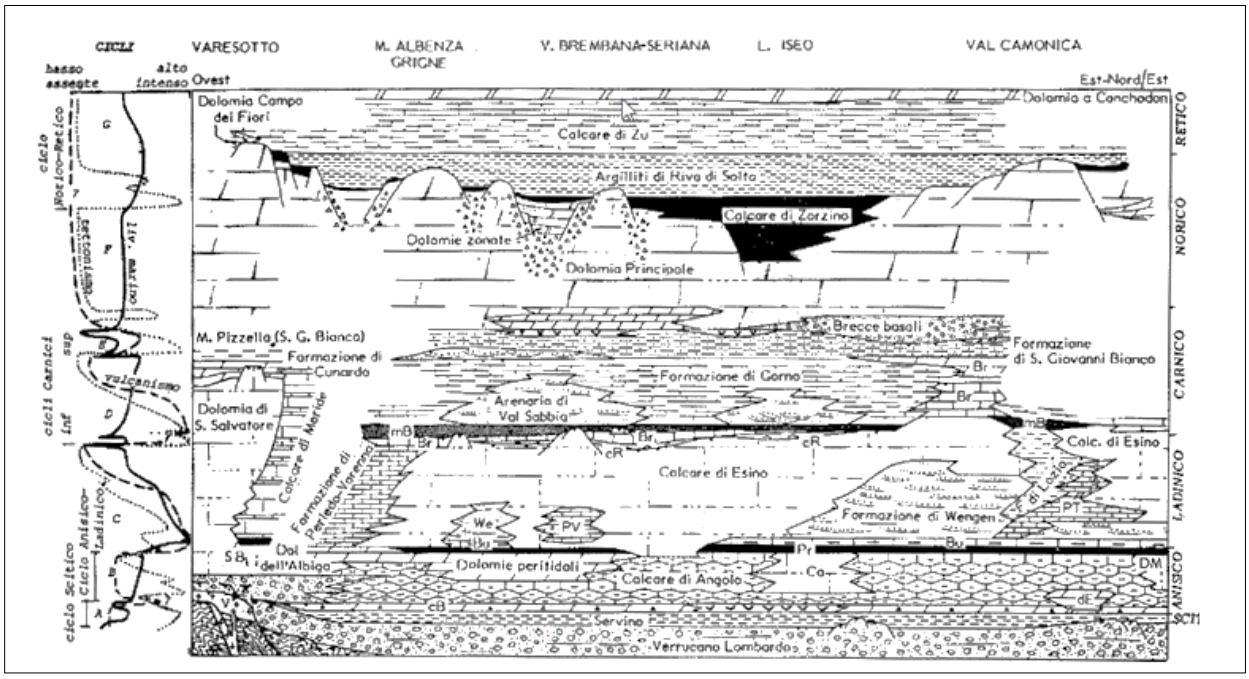

Figure 9 - Triassic facies and formation from the western and central Southern Alps (Jadoul & Rossi, 1982).

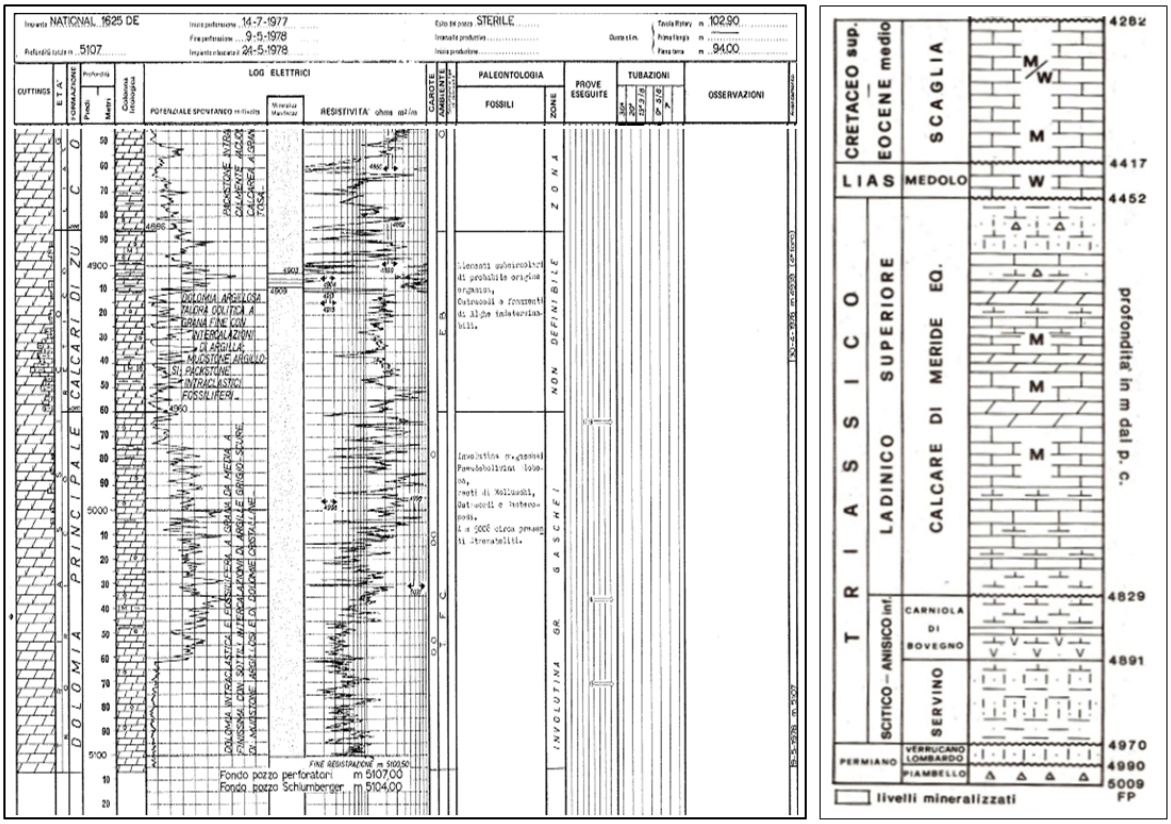

Figure 10 – (left) Detail from the Lacchiarella 1 well composite log (http://unmig.sviluppoeconomico.gov.it); (right) Mesozoic litho-stratigraphy from the Gaggiano 1 well (Buongiorni 1987).

C. Structures

Structures across the Meso-Cenozoic units mainly refer to the external domains of the Southern Alps and the Northern Apennines and intervening foreland, those belts creating outstanding tectonic arcs (Fig.11) and controlling sedimentation occurrence, directions and rate (Pieri & Groppi, 1981; Cassano et al., 1986, Castellarin et al., 1986; Carminati & Doglioni, 2012; Ghielmi et al., 2013; Rossi et al., 2015).

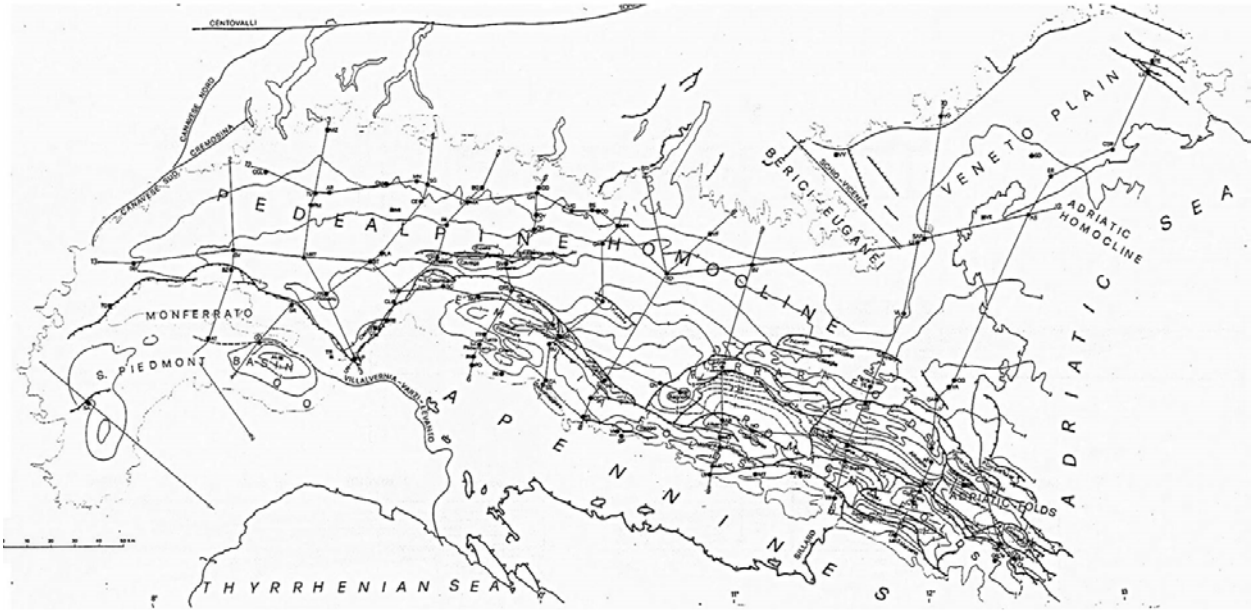

Figure 11 - The Po Valley tectonic arcs and structural geometries at Base Pliocene level from seismic interpretation and well data (Pieri & Groppi, 1976).

Two major décollement levels (see Fig.7) inside the Po Valley succession strongly impact the structural style across the basin (Cassano et al., 1986; Bello & Fantoni, 2002; Fantoni et al., 2004; Ravaglia et al., 2006; Toscani et al, 2014): the deeper detachment appears to correspond to the Burano evaporites of the eastern Po Valley, at the bottom of the Mesozoic carbonate units; the shallower detachment often occurs on top of the carbonate series, in correspondence of Late Eocene-Early Oligocene marls. Decoupling between the Tertiary and the Mesozoic deposits is also due to over-pressured sandstones-shales intervals (Bosica & Shiner, 2013), these acting as stress guides and activated as further detachment horizons.

The final mechanical stratigraphy allows shallow and deep structural geometries to be identified as follows (Fig.12):

1. shallow structures are folds and thrusts in the Tertiary clastic succession;
2. deep structures relate to faulting of the Mesozoic carbonates and their basement, with local inversion of pre-compressional basin and thin-skinned tectonic imbrication.

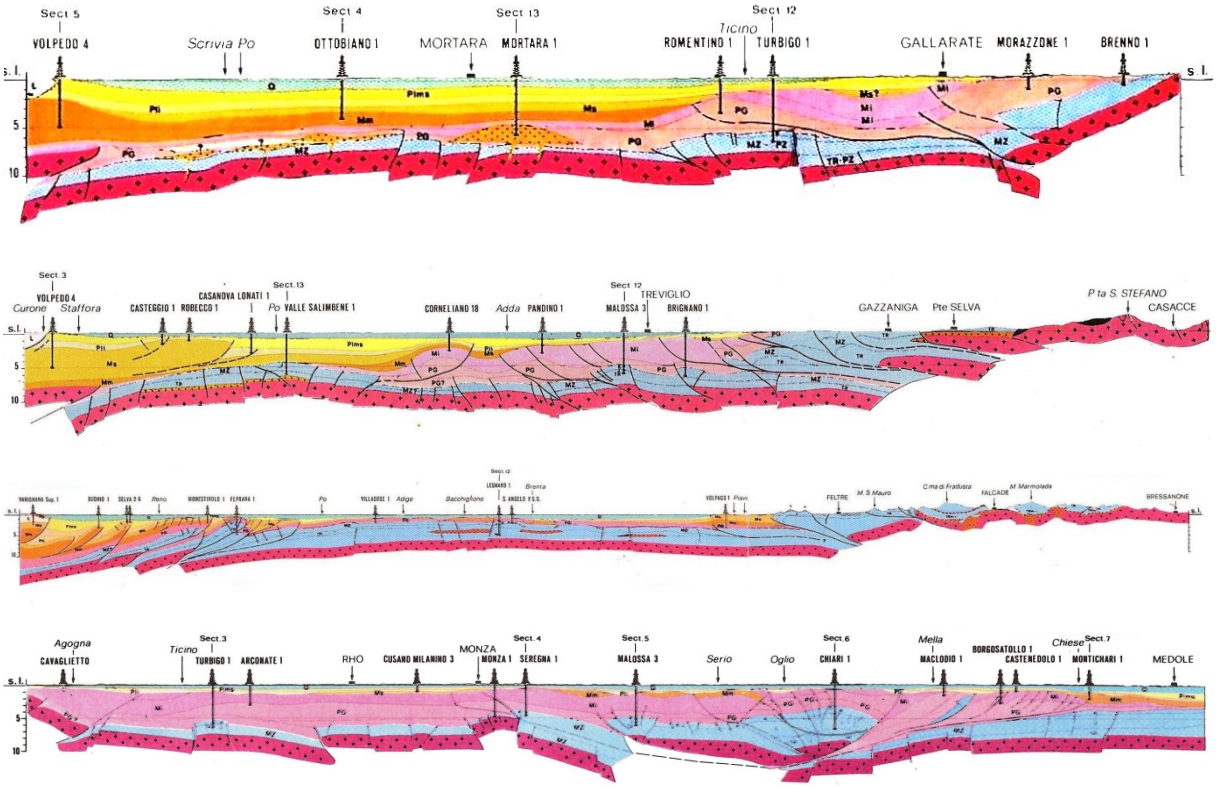

Figure 12 - Structures across the Meso-Cenozoic sedimentary formations (Cassano et al. 1986): red is basement, blue is Mesozoic carbonates; v:h = 1: 1. North is to the right (i.e. towards the Southern Alps) with the exception of the bottom section where WNW is to the left.

D. Deformation kinematics

In Triassic times (Jadoul et al., 1992), extension took place so that the Adria plate, as part of the northern Africa carbonate-platform realm, was deformed into horst and graben units, with faults approximately oriented north-south and east-west (Bertotti et al., 1993; Fantoni & Scotti, 2003; Fantoni et al. 2004; Berra et al. 2009). During the Liassic, a renewed phase of crustal extension led to a structural fabric made up of half-grabens and ridges, mainly elongated along the NE-SW direction (Fig.13).

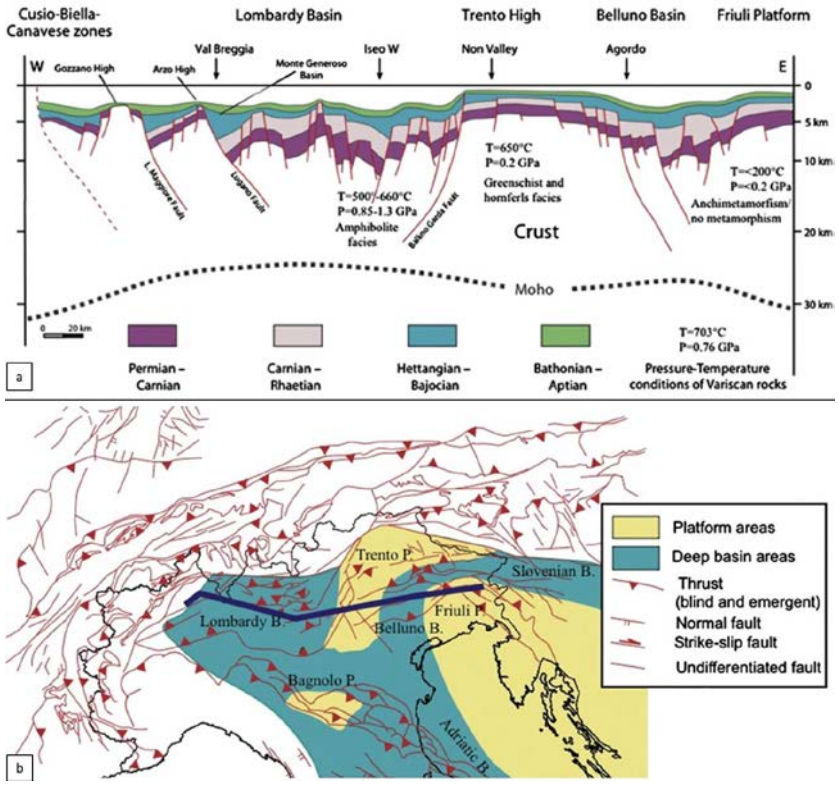

Figure 13 - Late Liassic-Neocomian paleogeographic units (in Carminati & Doglioni, 2012: above - modified from Fantoni & Scotti, 2003; below – modified from Zappaterra, 1994).

Sedimentation of the carbonates kept pace with such tectonics so that shelf, marginal and basin type deposits developed all through the region. Contraction of the Triassic-Jurassic rifted units initiated during the late Cretaceous (Dal Piaz et al., 2004; Schmid et al. 2004) when inversion of selected structures occurred with coeval reactivation of some of the existing normal faults (Cassano et al., 1986; Buongiorni, 1987; Fantoni et al., 2004) (Fig.14).

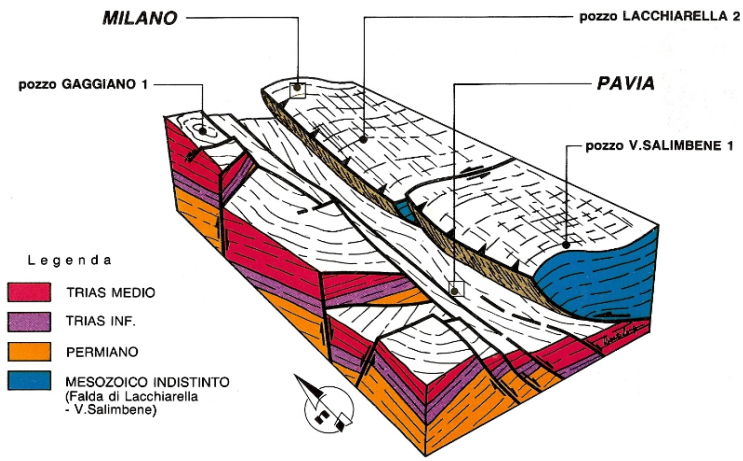

Figure 14 - Triassic-Jurassic extensional structures and Alpine inverted basin in the central Po Valley (Buongiorni, 1987).

Later on, during the Miocene and Pliocene, the basin architecture evolved to become the foreland of the advancing fold-and-thrust belts from the Alps and the Apennines, while the Mesozoic rocks became deeply buried beneath Neogene clastics in the related foredeeps (Trumpy, 1973; Fantoni et al., 2004).

E. Seismicity

Although earthquakes happen continuously all through the Italian peninsula, the northern part of Italy is characterized by patchy hypocenter occurrence with highly concentrated clusters (see Fig.15).

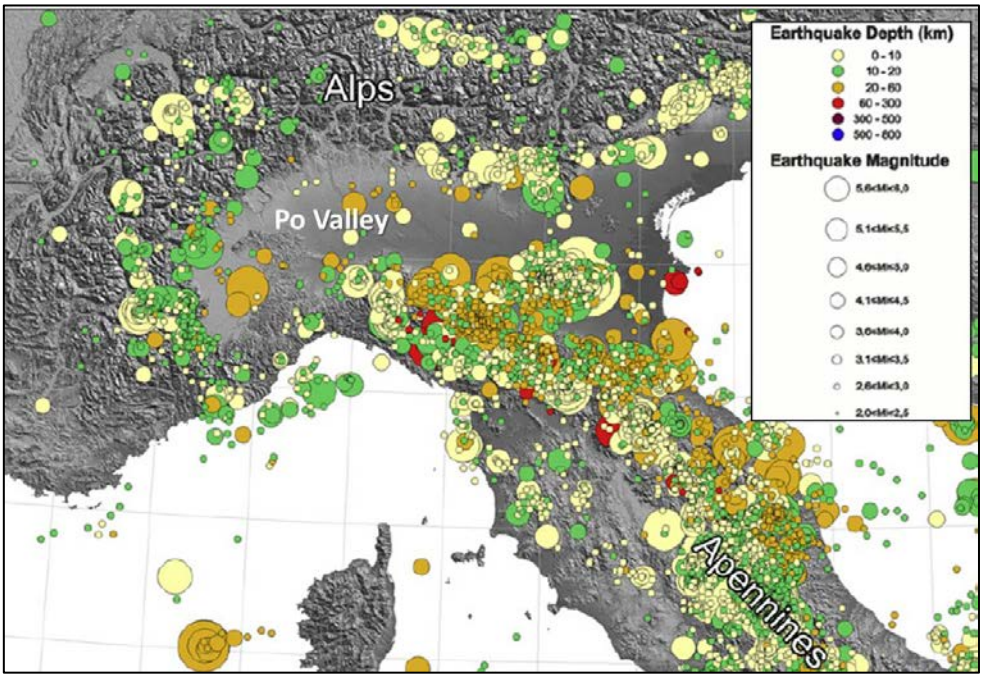

Figure 15 - Instrumental seismicity across the Po Valley basin and surrounding regions from ISIDe database (Di Bucci & Angeloni, 2012).

Magnitude (*local*) of the reported earthquakes across the region is between 0 and 7. Depth of the events is between 0-70 km below the mean sea level. Focal mechanisms from the available literature indicate mainly north-south active shortening with thrust-related and strike-slip structures, these being supported by regional stress, thrust-slip rates, GPS-derived maps and geomorphological criteria (Burrato et al., 2003; Maesano et al., 2010, 2011; Rovida et al., 2011; Burrato et al, 2012; Carminati & Doglioni, 2012; Michetti et al., 2012; Di Bucci & Angeloni, 2013; Maesano et al, 2013, 2014; and all references therein).

Seismicity is preferentially concentrated around the Po Valley basin, along the outcropping structures of the Alps and the Apennines. Nevertheless some areas inside the basin demonstrated to be recently active, with level of seismic hazard comparable to well-known seismic areas of the Apennines internal domains (Michetti et al., 2012). Those areas are the buried front of the Southern Alps between the Lake Garda and the Lake Maggiore and the buried front of the eastern Northern Apennines (i.e. the Ferrara arc).

F. Exploration for hydrocarbons

Since the end of the 19th century (Pieri, 1984) both gas and oil have been progressively produced from a number of fields in the Po Valley (Fig.16) of which the Villafortuna-Trecate field (1984, 30 km west of Milan, 240 MMbbls from Triassic reservoir. Lindquist, 1999) has been, by far, the most successful.

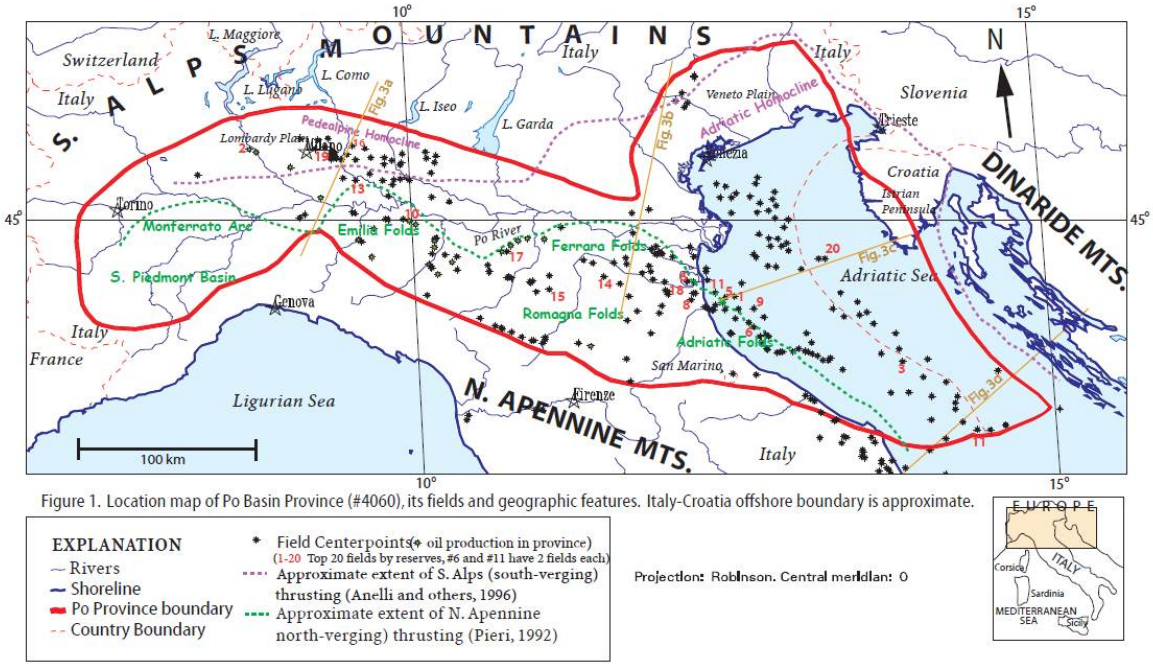

Figure 1. Location map of Po Basin Province (#4060), its fields and geographic features. Italy-Croatia offshore boundary is approximate.

Figure 16 - Hydrocarbon gas-oil fields in the Po Valley basin (Lindquist, 1999)

Hydrocarbons are trapped at different stratigraphic levels, with the deep Mesozoic carbonates (3000-6000 mbsl) representing the preferential target for oil exploration. Instead, the arenaceous intervals, of Miocene, Pliocene and Pleistocene age, are principally drilled for shallow (1000-3000mbsl) gas accumulations, thermogenic and biogenic in origin.

Remarkably, a large part of the geological knowledge in the region is related, directly or indirectly, to the oil business (Pieri & Groppi, 1967; Errico et al, 1980; Pieri, 1984;

Buongiorni, 1987; Cassano et al., 1987; Mattavelli & Novelli, 1987; Mattavelli & Margarucci, 1992; Casero et al. 1990; Nardon et al., 1991; Lindquist, 1999; Bello & Fantoni, 2002; Casero, 2004; Fantoni et al., 2004; Bertello et al., 2010; Fantoni et Franciosi, 2010; Rossi et al., 2015).

In particular, thanks to a) the extensive exploration activity performed in the 60-to-90ties period (Fig.17), b) several exploration wells drilled to a total depth in the range of 4000-7000 m and c) new modern 2d-3d reflection surveys, the buried structures of the Po Valley and the related hydrocarbon systems have been eventually described and revealed to the scientific community (Fig.18-19; see also Fig.11-12).

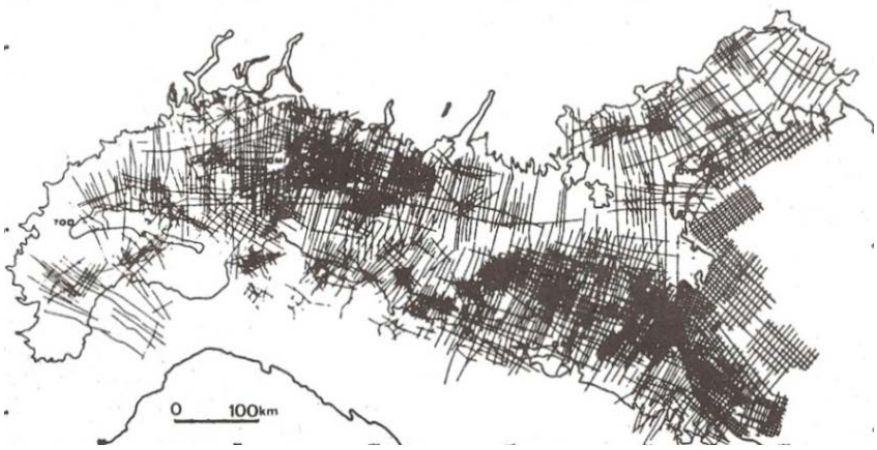

Figure 17 - Seismic data in the Po Valley (Buongiorni, 1987).

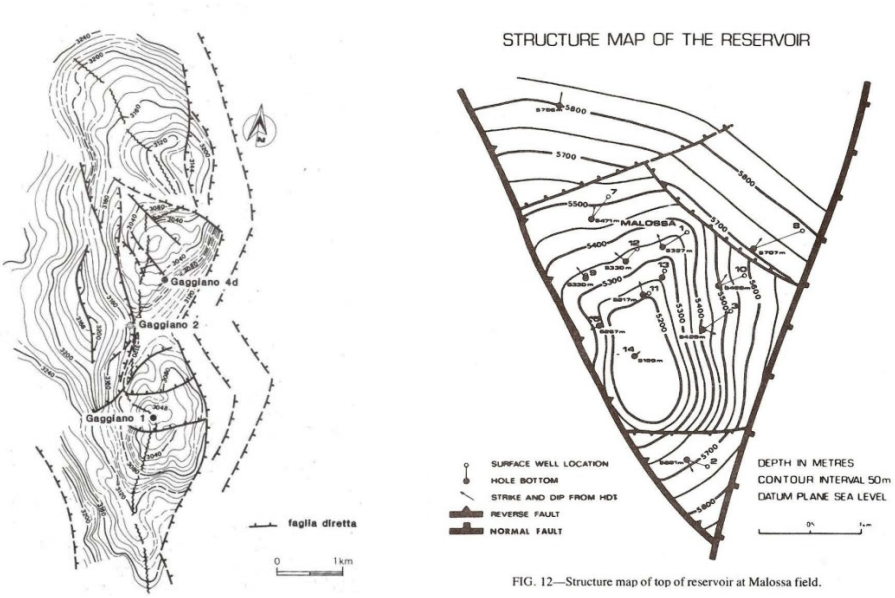

Figure 18 - (left) Time map of the Triassic Meride level in the Gaggiano field; (right) depth map of the Triassic reservoir in the Malossa field (Errico et al., 1980).

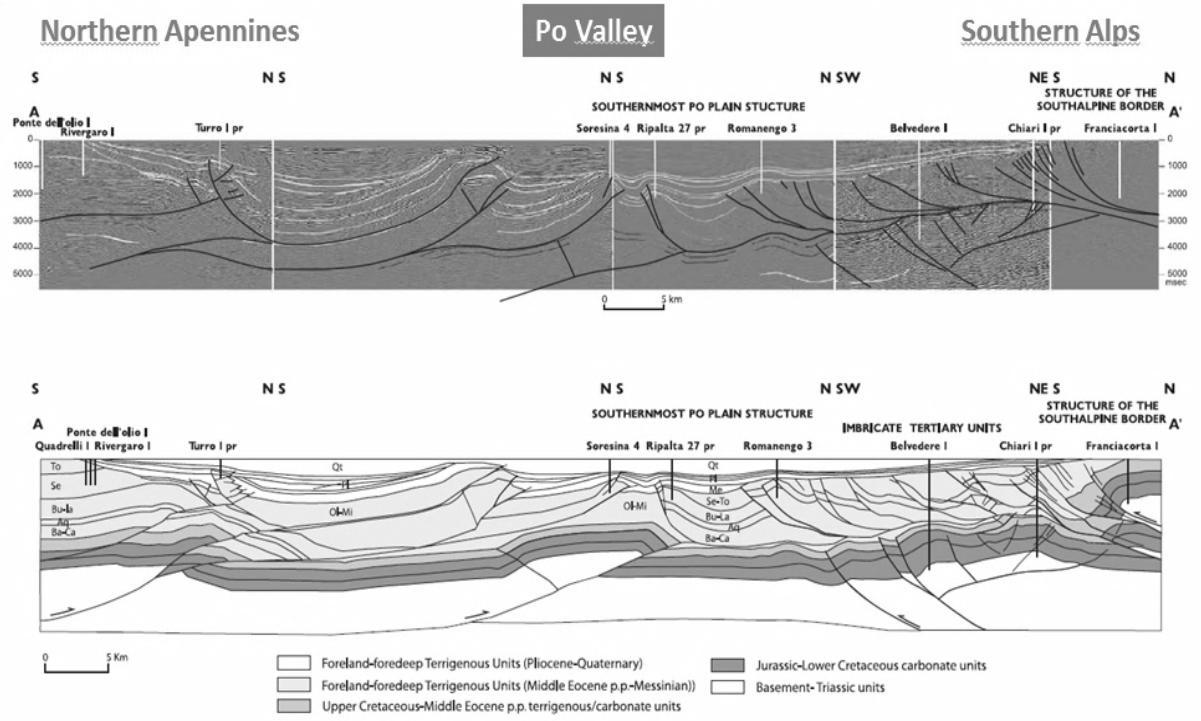

Figure 19 - Seismic profile and relative depth-converted geological section across the Northern Apennines-Po Valley-Southern Alps domains (Fantoni et al., 2004).

Part 3 – 3D Structural Models

I. Introduction

A 3D structural model aims at building (reproducing), rendering, analyzing, checking for geometrical consistency in the three dimensions of space, any structure which has been created in nature by tectonic forces.

The model results relate to the specific scope of investigation, the model dimension, the data availability and the methodologies applied during the modeling workflow (all references in Tab.1). In that light, 3D structural models can result into crustal to field scale reconstruction/simulation. They can be purely geometrical (i.e. built on surfaces), numerical (mathematically based) or kinematics (i.e. implying restoration or forwards modelling). They can be derived from inhomogeneous and sparse datasets (i.e. any geological-geophysical data), 2D-3D seismic data only, outcrops, geophysical data (velocity, gravity, magnetic or magneto-telluric), numerical elaborations, mechanical simulations (e.g. sandbox). They can provide single (deterministic) or multiple-automatic (stochastic) solutions. They can be produced by a mix of data-types and elaboration processes (e.g. geometrical + numerical).

Models' uncertainty directly refers to both the modeled data types and the modeling processes, these factors also being the driver to the model prediction capability:

- integration of inhomogeneous and sparse data will likely result into deterministic 3D structural models where uncertainty is likely moderate to high;
- 2D/3D seismic data are normally used to build stochastic solutions. In this case, uncertainty mainly refers to seismic data quality (e.g. shadow fault zones), time-to-depth conversion of the elaborated grids and interpretation pitfalls (e.g. fault correlation);
- 3D fracture models can be particularly detailed if built on outcrops yet they can suffer from moderate to high uncertainty when they depend on sparse well logs and the related upscaling operations. Stochastic analysis can eventually constrain the solution spectrum.

II. Reference case studies & considerations about 3D structural models

In order to suggest key references about the 3D modeling technique applications in the multiple domains which characterize the structural geology discipline, a number of papers from the recent literature are listed in Tab.1, ordered by publication date and marked by a) geographical area, b) 3D modeling technique/criteria, c) scope of investigation.

Given the selected examples some specific considerations about 3D structural models are hereafter formulated.

- 3D structural models are surprisingly successful for the visualization, rendering and analysis of the deformation geometries (all references in Tab.1; e.g. Leslie et al., 2012); they can eventually be used to a) evaluate the regional geothermal potential (Guglielminetti et al., 2013); b) validate the structures' CO_2 storage capability (Alcade et al., 2014); c) simulate a calculated-gravity or magnetic field to be successively compared with the observed one (Guillen et al., 2008; Guglielminetti et al., 2013);

- on the other hand, 3D structural models are rarely used for deformation kinematics analysis (Calcagno et al., 2007; Yin & Groshong, 2007; Lohr et al., 2007; Durand-Riard et al., 2011);

- regional scale 3D models are commonly used for wide understanding of crustal tectonics (Lamarche & Scheck-Wenderoth, 2005; Schreiber et al., 2010; Dhont et al., 2012; Vouillamoz et al., 2012; Maystrenko et al. ; 2013; Campani et al., 2014; Autin et al., 2015; Klitzke et al., 2015; Berthoux et al., 2016; Grad et al., 2016), thermal evolution and simulation of the hydrocarbon maturation, generation and migration processes (Johannesen et al., 2002; Badics et al., 2004; Maystrenko et al.; 2013), interpretation of the petroleum system elements (Turrini & Rennison, 2004; Turrini et al., 2009);

- such crustal scale models are often a) coupled with the regional velocity/gravity field distribution to support the tectono-stratigraphic architecture (Drakatos et al., 2005;

Maystrenko et al. ; 2013; Sala et al., 2013; Autin et al., 2015; Klitzke et al., 2015; Berthoux et al., 2016; Grad et al., 2016), b) populated with the available earthquake events to provide the seismo-tectonics in the region (Sue et al., 2010; Drakatos et al., 2005);

- detailed 3D structural models are normally performed to illustrate oil fields and manage their exploration/production strategy (Mitra & Lislie, 2003: Rivenaes et al., 2005; Rivenaes et al., 2006; Mitra et al., 2006, 2007; Dishinger & Mitra, 2006);

- outcrop structures provide exceptionally illustrated 3D structural models (Guillaume et al., 2008; Schober & Exner, 2011); they are eventually used to build fracture network model for hydrothermal studies or sub-surface reservoir analog (Bailey et al., 2002; Masaferro et al., 2003; Lapponi et al.,2011; Gisquet et al., 2013; Katsuaki et al, 2015);

- sandbox-derived 3D models are often built to better understand the internal architecture of the modeled structures while gaining insight in the possible deformation processes and seismic analogs (Guglielmo et al., 1997; 2001; Paul & Mitra, 2013; Ferrer et al., 2014; Galuppo et al., 2016);

- numerical models are performed within various contexts: crustal dynamics and plate tectonics (Farrington et al., 2014; Petricca & Carminati, 2014), fracture prediction, fault/fold geometry and kinematic descriptions (Friedman et al., 2008; Ramon et al., 2013; Fernandez & Kaus, 2014; Schopfer et al., 2016);

- the combination of geometrical and mathematical models provides stochastic simulations that can be used for uncertainty definition on reservoir volume estimation (Lecour et al., 2001; Cherpeau & Caumon; 2015).

Tab.1 – Selected 3D structural model from recent literature (see Annexes for related images)

Authors	Year	Geographical area of application	3D modelling technique	Scope
Berthoux et al.	2016	Alps/Corsica	Geometrical *Velocity*	Crustal architecture carachteristics
Cardoso et al.	2016	Northern Colombia	Geometrical	Structural analysis deformation mechanisms
Galuppo et al.	2016	nn	Geometrical *(from sandbox experiments)*	Fracture pattern evolution in fault-related anticlines
Grad et al.	2016	Poland	Geometrical *Velocity*	Crustal architecture carachteristics
Schopfer et al.	2016	nn	*Numerical*	Fault zone evolution in multilayers
Autin et al.	2015	Argentina	Geometrical *Gravity*	Crustal architecture carachteristics
Cherpeau & Caumon	2015	Middle east	Geometrical *Stochastic*	3D Faults and reservoir compartment uncertainty
Guyonnet-Benaize et al.	2015	Southern Farnce	Geometrical	Structural analysis geometries kinematics
Katsuaki et al.	2015	Central Japan	Geometrical *Numerical*	Fracture model
Klitzke et al.	2015	Barents Sea Kara Sea	Geometrical *Velocity*	Crustal architecture carachteristics
Alcade et al.	2014	North-western Spain	Geometrical	CO2 storage
Campani et al.	2014	Central Alps	Geometrical	Folding faulting interplay
Fernandez & Kaus	2014	Zagros	*Numerical*	Mulilayer fold growth simulation
Ferrer et al.	2014	Northern Spain	Geometrical *(from sandbox experiments)*	Role of salt in the HNGW of an extensional fault
Petricca & Carminati	2014	Mediterranean	*Numerical*	Lithospheric stress in convergent margin
Gisquet et al.	2013	Southern France	Geometrical	Reservoir-analog deformation mechanisms
Guglielminetti et al.	2013	Western Alps	Geometrical *Gravity*	Regional Geothermal prospection
Maystrenko et al.	2013	Western Africa margin	Geometrical *Gravity*	Crustal architecture & Thermal modeling
Maystrenko et al.	2013	Central Europe	Geometrical	Crustal architecture carachteristics

Paul & Mitra	2013	nn	Geometrical *(from sandbox experiments)*	Rift-basins Transfer zone evolution
Ramon et al.	2013	Southern Pyrenees	Mechanical *Numerical*	Fold deformation patterns
Sala et al.	2013	Paris basin	Geometrical *Velocity*	Basin reconstruction by well/velocity analysis/correlation
Calcagno et al.	2012	French West Indies	Geometrical	Regional Geothermal resources evaluation
Dhont et al.	2012	Venezuela Andes	Geometrical	Crustal model
Leslie et al.	2012	UK	Geometrical	Structure definition
Vouillamoz et al.	2012	Western Alps	Geometrical	Crustal architecture definition
Durand-Riard et al.	2011	Western Alps	Geometrical *Numerical*	Decompaction Restoration
Lapponi et al.	2011	Zagros	Geometrical *Stochastic*	3D model from outcrops
Schober & Exner	2011	Eastern Alps	Geometrical *Photogrammetry*	Outcrop reconstruction
Trocme et al.	2011	Zagros	Geometrical	Salt-related structure analysis
D'Ambrogio et al.	2010	Italy	Geometrical	Structural analysis visualization
Farrington et al.	2010	Eastern Australia	*Numerical*	Crustal - Upper mantle convection
Guyonnet-Benaize et al.	2010	South-eastern France	Geometrical	Structural analysis evolution
Schreiber et al.	2010	Southwestern Alps	Geometrical *Gravity*	Crustal tectonics
Sue et al.	2010	Western Alps	Geometrical	Seismo-tectonic modelling
Jahn & Riller	2009	South Africa	Geometrical	Impact structure deformation mechanisms
Turrini et al.	2009	Jura Mountains	Geometrical	Tectonics & hydrocarbons
Friedman et al.	2008	nn	*Numerical*	Fault-facies simulation
Guillaume et al.	2008	Pyrenees	Geometrical	Basin geometry reconstruction
Calcagno et al.	2007	Western Alps	Geometrical *Kinematics*	Structure reconstruction & kinematics
Lohr et al.	2007	Germany	Geometrical	Structure restoration strain distribution

Mitra et al.	2007	Mexico	Geometrical	Exploration/production strategy
Yin & Groshong	2007	Various	Geometrical	Salt-related structure Geometries/Kinematics
Dishinger & Mitra	2006	USA	Geometrical	Oil field definition
Mitra et al.	2006	Mexico	Geometrical	Oil field definition/evolution
Valcarce et al.	2006	Argentina	Geometrical	Exploration/well drilling strategy
Drakatos et al.	2005	Greece	Geometrical *velocity*	Regional Seismo-tectonics
Lamarche & Scheck-Wenderoth	2005	Polish basin	Geometrical	Structural and sedimentary kinematics
Rivenaes et al.	2005	Offshore Norway	Geometrical *Stochastic*	Well planning from 3D stochastic models
Badics et al.	2004	Ungary	Geometrical	Petroleum system modelling
Turrini & Rennison	2004	Southern Apennines	Geometrical	Structural reconstruction/analysis
Masaferro et al.	2003	Northwest Argentina	Geometrical	Structures Fracture distribution
Mitra & Lislie	2003	Algeria	Geometrical	Exploration/well drilling strategy
Bailey et al.	2002	UK	Geometrical *Stochastic*	Faults & 3D connectivity
Johannesen et al.	2002	Norwegian North Sea	Geometrical	Oil generation and migration
Lecour et al.	2001	nn	Geometrical *Stochastic*	Stochastic faults & fracture network
McClay & Bonora	2001	nn	Geometrical *(from sandbox experiments)*	Structures inside Strike-slip fault system
Guglielmo et al.	1997	Gulf of Mexico	Geometrical *(from sandbox experiments)*	Structural analysis of salt related geometries

Part 4 – The Po Valley 3D model: deformation geometries, kinematics & structural heritage

I. Introduction

The development of the Po Valley 3D structural model has been completed in two steps by building of the deep and shallow geometries (Section III in this Chapter) and the successively analysis of the associated deformation kinematics (Section V).

Construction of the model was based on data from the literature and the public archives exclusively (see Section III, figure 3 for data distribution).

The 3D model building and the related analysis have been performed by standard workflow (see Sections V for complete description of the adopted methodology) and by different software with respect to the specific objectives:

- The MOVE package (http://www.mve.com/) was used to perform model building (data integration and layer gridding by interpolation of the input points/lines – tessellation algorithms) and vertical/horizontal slicing of the model structures;
- The Kingdom software (https://www.ihs.com/products/kingdom-seismic-geological-interpretation-software.html) was used for the model reviewing/refining, detailed fault modelling and tie to existing wells;
- The Structure Solver software software (http://www.structuresolver.com/) was used for 2D restoration of selected cross-sections.

Results from the model have been the subject for two papers which have been submitted to the Marine and Petroleum Geology (MPG) journal:

- the Po Valley deformation geometries paper has been published as Turrini et al., 2014, MPG vol. 56, pp. 266-289 (Section III);

- the Po Valley deformation kinematics study (Section V) has been performed in collaboration with Dr. Giovanni Toscani of the Pavia Earth Science Dpt. (Italy) and is currently being revised after a first round of reviews.

II. Po Valley Structural geometries

Since the very first studies of Porro (1927), the Po Valley structural geometries have been described by many authors (ref. section III). With the exception of the regional studies from Pieri & Groppi (1981), Cassano et al., (1986) and, more recently yet only dealing with the geophysical aspects of the basin (i.e. velocity distribution), Molinari et al. (2015), all those studies have investigated selected situations which were focusing on specific and detailed geological issues (ref. Section III & V).

The performed Po Valley 3D structural model aimed at integrating, reviewing and updating the various data/interpretations on the region by applying the 3D modeling technology, methodology and key-criteria (phases 1-2 in the workflow of Fig.20).

During the model building process particular attention has been put to cross-checking and validation of the performed geometries. Consequently, the progressive model uncertainty has been constantly monitored and evaluated to ensure the final architecture consistency, in the three dimensions and at both the crustal and field scale of observation.

The model succeeded in correlating the basin structures across laterally inhomogeneous domains, thus revealing the Po Valley foreland by a unique 3D perspective of the basin tectonic complexity.

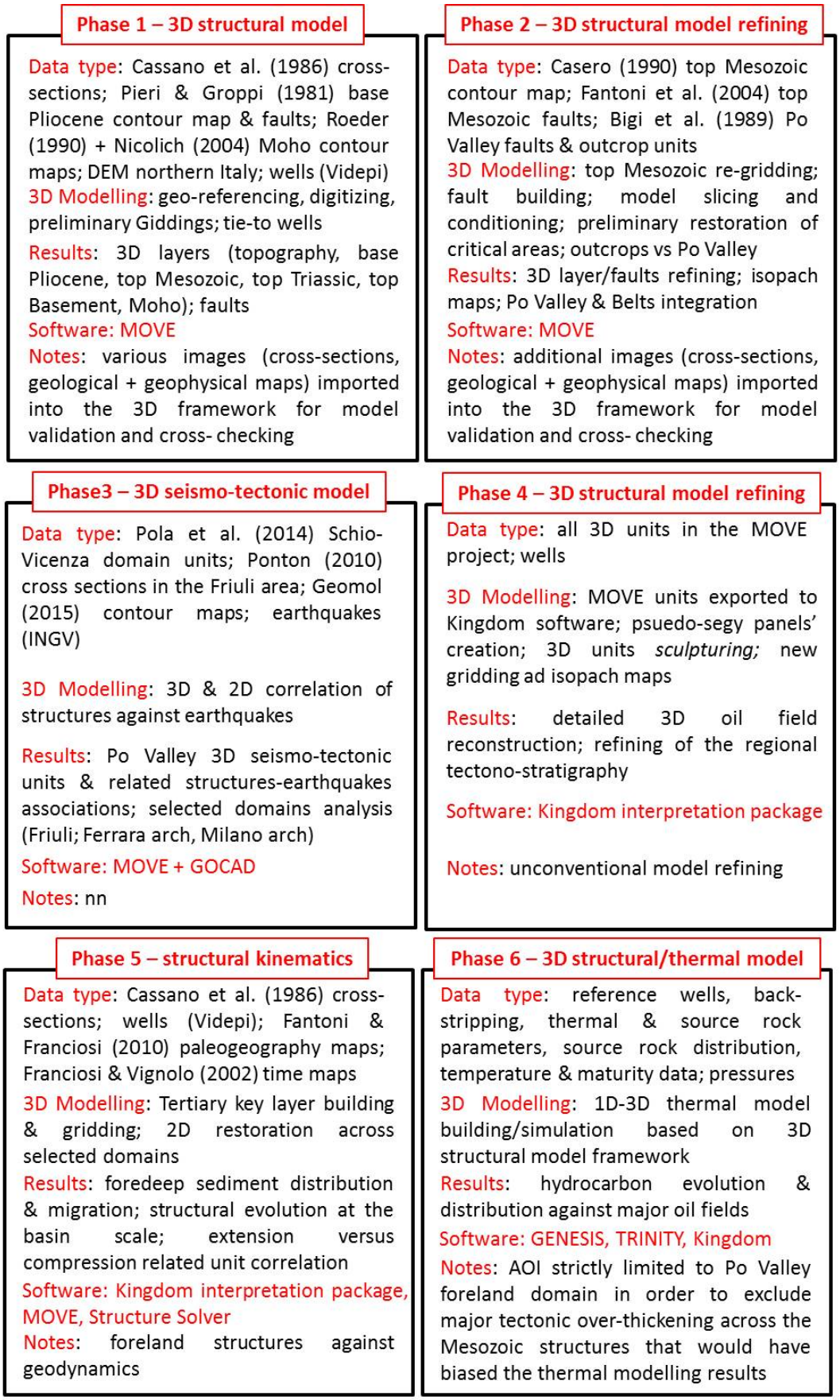

Figure 20 – the Po Valley 3D model building workflow.

Marine and Petroleum Geology 56 (2014) 266–289

Contents lists available at ScienceDirect

Marine and Petroleum Geology

journal homepage: www.elsevier.com/locate/marpetgeo

Present-day 3D structural model of the Po Valley basin, Northern Italy

Claudio Turrini [a,*], Olivier Lacombe [b,c], François Roure [d]

[a] CTGeolConsulting, St. Germain-en-Laye, France
[b] Sorbonne Universités, UPMC Univ Paris 06, UMR 7193, ISTEP, F-75005 Paris, France
[c] CNRS, UMR 7193, ISTEP, F-75005 Paris, France
[d] IFP-EN, Rueil-Malmaison, France and Utrecht University, The Netherlands

ARTICLE INFO

Article history:
Received 11 October 2013
Received in revised form
5 February 2014
Accepted 12 February 2014
Available online 26 February 2014

Keywords:
3D models
Po Valley tectonics
Northern Italy

ABSTRACT

A 3D structural model of the Po Valley basin (Northern Italy) was built by integrating the dataset available from the public domain (DEM, wells, isobath-maps, cross-sections, outcrop-trends).

The model shows the complex foredeep-foreland architecture across the basin, from the Moho level to the topography while illustrating the top Basement, top Triassic, top Mesozoic and base-Pliocene surface-grid structures.

The results, by model slicing and isopach-map reconstruction, suggest that the deep Moho architecture and the original tectonics of the ancient Adria-Po Valley passive continental margin are key factors in controlling the current structures type, orientation and distribution, at any of the shallowest levels across the basin. In particular, the analysis of the final 3D Mesozoic geometries against the pre and post-Alpine trends confirms the structural interference between the mutually perpendicular Triassic–Jurassic extensional structures and the Tertiary compressional ones, this being evident from the regional to the oil-field scale.

Despite the model uncertainty, mainly related to its dimension versus the original non-homogeneous dataset quality and distribution, the final geo-volume offers, for the first time in the region, a continuous three-dimensional visualization of the Po Valley tectonic architecture. It provides, simultaneously, a powerful tool for the reviewing of the basin structures and the potential support to future applications for both industry and academia.

1. Introduction and aims to the study

3D models bring fundamental constraints to the analysis of geological structures. Indeed, a 3D structural model is made of geological interfaces such as horizons and faults honouring available observation data. Anatomical visualisation, model building, model slicing and block-restoration are only a few among the functions that can be performed once a 3D volume is obtained. As software dedicated to 3D structural modelling have spread out on the market (http://www.3d-geology.de/software/geology_and_mining), the technique has become a standard procedure inside the geological community, with main applications to oil and gas fields (Mitra and Leslie, 2003; Turrini and Rennison, 2004; Dischinger and Mitra, 2006; Mitra et al., 2005, 2007; Valcarce et al., 2006; Turrini et al., 2009; Lindsay et al., 2012; Vouillamoz et al., 2012; Shao et al., 2012 and reference therein), groundwater aquifers (Berg et al., 2004 and references therein) and ore deposits (Han et al., 2011 and references therein). Although a complete review of the literature on the subject is beyond the scope of this paper it could be worthy to mention some major references with respect to selected geological domains of research.

a) 3D model building of geological structures: Caumon et al. (2009) present general procedures and guidelines to effectively build a structural model made of faults and horizons from sparse data;
b) Outcrop Geology: the British Geological Survey (Leslie et al., 2012) recently published an astonishing and interactive three-dimensional reconstruction of the Assynt Culmination, in the Moine Thrust Belt of NW Scotland (http://www.bgs.ac.uk/research/ukgeology/assyntCulmination.html);
c) Hydrocarbon Exploration: Mitra and Leslie (2003), Dischinger and Mitra (2006), Mitra et al. (2005, 2007) used 3D structural models to review and validate different oil fields in Algeria, the USA and Mexico;

* Corresponding author. Tel.: +33 672391235.
E-mail address: clturri@wanadoo.fr (C. Turrini).

http://dx.doi.org/10.1016/j.marpetgeo.2014.02.006
0264-8172/

d) Sand-box models reconstruction: Guglielmo et al. (1997), McClay and Bonora (2001), built 3D structural models from sand-box (and silicone) geometries about salt tectonics and strike-slip tectonics, respectively;
e) The Alps: Vouillamoz et al. (2012) built a 3D model of the Western Alps, from the Jura to the Northwest, up to the Bergell granite intrusion and the Lepontine Dome to the East and limited to the South by the Ligurian basin;
f) Italian 3D geology: The Geological Survey of Italy, in collaboration with the Institute of Environmental Geology and Geoengineering and the Department of Earth Sciences of Sapienza University–Rome (D'Ambrogi et al., 2010), promoted the development of a three-dimensional environment where selected crustal and subcrustal-scale structures for the Italian region can be displayed, modelled and retrieved.

Despite the abundance of public data, mainly derived from the hydrocarbon exploration, and certainly because of their great inhomogeneity in terms of quality and distribution, the three-dimensional reconstruction of the Po Valley basin is still a task that has never been tackled so far.

Given such a unique technical challenge, this paper presents for the first time a 3D model of the Po Valley structural and hydrocarbon province from the Moho surface, 30 km deep on average below the mean sea-level, to the topographic level, while especially focussing on the top Mesozoic geometries. Major aims of the study, as part of an in-progress PhD research, are: a) to integrate the available non-homogeneous dataset into a homogeneous and geometrically coherent 3D geo-volume, b) to visualize and validate the three-dimensional crustal architecture of the area, c) to analyse the resulting structures by comparing the deep geometries with the shallow ones, d) to demonstrate how the inherited Triassic–Lower Jurassic tectonics likely controlled the present-day structural architecture (Mariotti and Doglioni, 2000; Ravaglia et al., 2006; Cuffaro et al., 2010; Fantoni et al., 2004) e) to provide a solid and geometrically consistent framework for future industry and academia applications.

2. Geological setting

The Italian peninsula is defined as the result of complex geodynamics where both pre-alpine (Mesozoic and pre-Mesozoic) and alpine (mainly Cenozoic) tectonics have interacted through time to create the current, high-complex structural and stratigraphic puzzle (Elter and Pertusati, 1973; Laubscher, 1996; Castellarin, 2001; Castellarin and Cantelli, 2010; Cuffaro et al., 2010; Mosca et al., 2010; Carminati and Doglioni, 2012 and reference therein). Within the derived geological setting (Fig. 1), the Po Valley represents the north-westernmost buried sector of the Apulian indenter (or Adria plate: Channell et al., 1979; Dewey et al., 1973; Dercourt

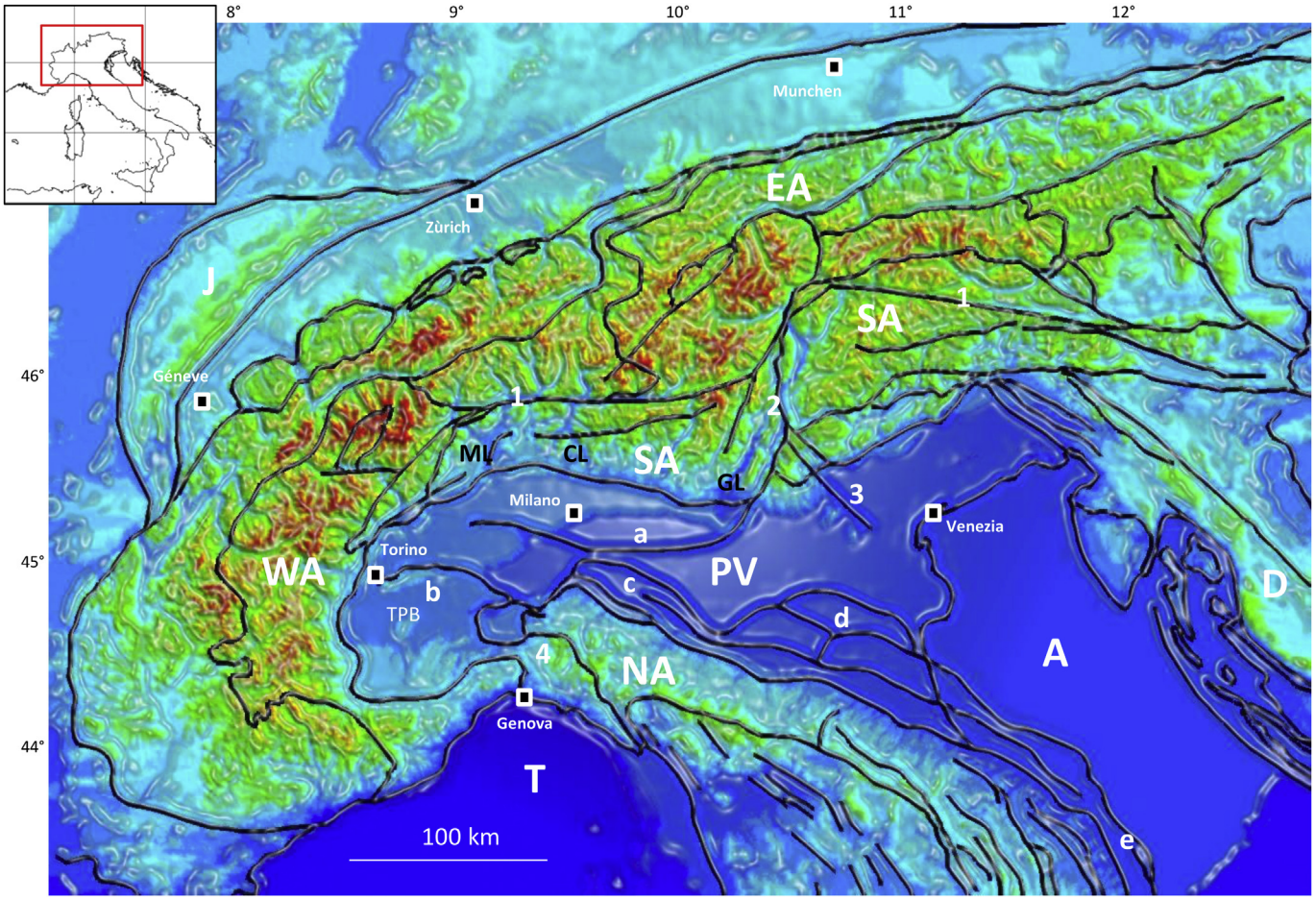

Figure 1. Digital topography and tectonic framework (from Nicolich, 2010) around the Po Valley region. (PV) Po Valley; (SA) Southern Alps; (NA) Northern Apennines; (WA) Western Alps; (EA) Eastern Alps; (D) Dinarides; (J) Jura Mountains; (A) Adriatic; (T) Tyrrenhian; (1) Insubric Line; (2) Giudicarie Line; (3) Schio-Vicenza Line; (4) Villavernia Line; (a–e) buried thrust fronts: a = Milano Thrust Front; b = Monferrato Thrust Front; c = Emilian Thrust Front; d = Ferrara-Romagna Thrust Front; e = Ancona Thrust Front. Tpb = Tertiary Piedmont Basin. ML = Maggiore Lake; CL=Como Lake; GL = Garda Lake. Latitude and Longitude values are North and East of Greenwich. Grid in the insert map is 500 km.

et al., 1986), the foreland-foredeep domain to the Alpine and Northern Apenninic belts and one of the major hydrocarbon provinces of continental Europe. The basin covers an area of approximately 50,000 km^2, it is geologically caught between the Alps, to the west and the north, and the Northern Apennines, to the south. Towards the east, the Po Valley sedimentary formations and structures gradually sink into the Adriatic domain as the topographic surface passes below the sea level.

Across the region, the structural geometries mainly refer to the external domains of the Southern Alps and the Northern Apennines (see Fig. 1) and intervening foreland, those belts creating outstanding tectonic arches while controlling the sediment infilling of the respective foredeep-basins (Pieri and Groppi, 1981; Cassano et al., 1986; Castellarin et al., 1985; Carminati and Doglioni, 2012; Argnani and Ricci Lucchi, 2001; Bartolini et al., 1996; Bertotti et al., 1997; Castellarin and Vai, 1986; Perotti, 1991; Perotti and Vercesi, 1991; Ricci Lucchi, 1986). Sedimentary successions (Fig. 2) encompass broadly Mesozoic carbonates through and dominantly clastic Cenozoic deposits, the whole sedimentary pile sitting on a crystalline basement essentially made of metamorphic rocks of Hercynian age. Most of the tectonic features were initially related to Upper Triassic–Lower Jurassic extension, with local evidence for Cretaceous to Paleogene structural inversion, followed by later Miocene–Pliocene compression affecting the foreland and the surrounding orogenic belts. Indeed, the tectonic history of the region likely started at the end of the Paleozoic and is still going on as accounted by recent studies and the latest earthquake-activity in the central and eastern parts of the basin (Burrato et al., 2003; Carminati et al., 2003, 2010; Toscani et al., 2006, 2009; Picotti and Pazzaglia, 2008; Livio et al., 2009; Di Bucci and Angeloni, 2012; Michetti et al., 2012; Maesano et al., 2013). In Triassic times (Jadoul et al., 1992), extension took place so that the Adria microplate, as part of the northern Africa carbonate-platform realm (Channell et al., 1979), was deformed by a rifting phase characterized by broad NS and EW trending faults generating horsts and grabens. During the Lower Jurassic (Bertotti et al., 1993; Fantoni et al., 2004), a renewed phase of crustal extension led to a structural fabric made up of half-grabens and ridges, mainly elongated along the NE–SW direction. Sedimentation of the carbonates kept pace with such tectonics so that shelf, marginal and basin type

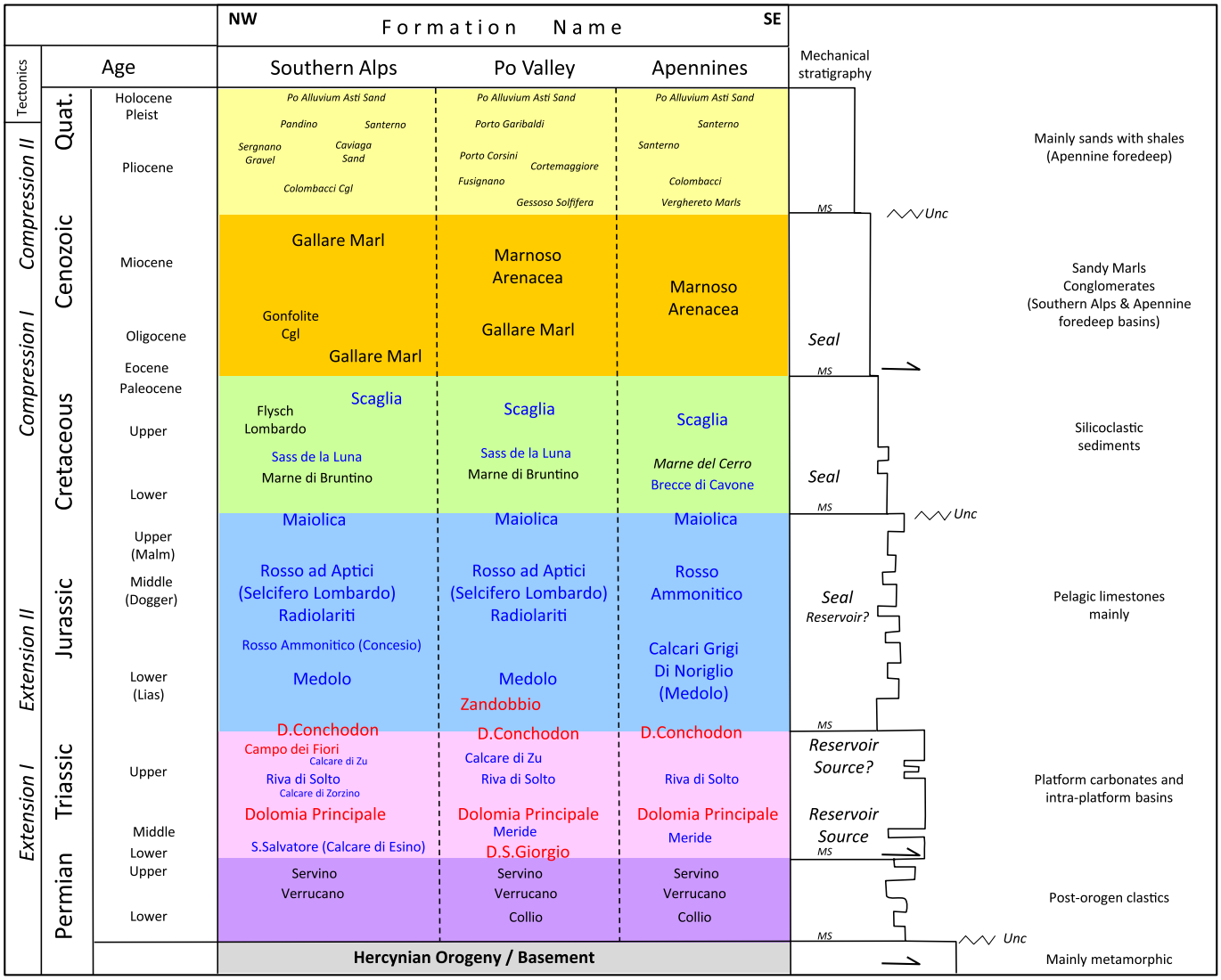

Figure 2. Schematic stratigraphic column of the Po Valley basin (modified from Lindquist, 1999; Casero, 2004). MS = major seismic event; unc = major unconformity. Only the hydrocarbon system related to the Mesozoic oils is described. Major detachment levels are suggested across the mechanical stratigraphy. Formations in blue are mostly limestones. Formations in red are mostly dolostones. (For interpretation of the references to colour in this figure legend, the reader is referred to the web version of this article.)

deposits developed all through the region. Contraction of the Triassic–Lower Jurassic rift related structures was produced by late Cretaceous inversion tectonics with reactivation of some of the existing normal faults (Dal Piaz et al., 2004; Schmid et al., 2004). Later on, during the Miocene and Pliocene, the basin architecture evolved to become the foreland of the advancing fold-and-thrust belts from the Alps and the Apennines, while the Mesozoic rocks became deeply buried beneath Neogene clastics in the related foredeeps (Trumpy, 1973; Fantoni et al., 2004).

Since the end of the 19th century (Pieri, 1984) both gas and oil have been locally produced from a number of fields in the Po Valley, of which the Villafortuna-Trecate field (discovered in 1984 by ENI, 30 km west of Milan) has been, by far, the most successful (with 240 MMbbls from a Triassic carbonate reservoir). Hydrocarbons are trapped at different stratigraphic levels, with the deep Mesozoic carbonates (3000–6000 mbsl) representing the preferential target for oil exploration. Instead, the arenaceous intervals, of Miocene, Pliocene and Pleistocene age, are principally drilled for shallow (1000–3000 mbsl) gas accumulations, thermogenic and biogenic in origin. Remarkably, a large part of the geological knowledge in the region is related, directly or indirectly, to the oil business (Errico et al., 1980; Pieri and Groppi, 1981; Pieri, 1984; Bongiorni, 1987; Cassano et al., 1986; Mattavelli and Novelli, 1987; Mattavelli and Margarucci, 1992; Casero et al., 1990; Nardon et al., 1991; Lindquist, 1999; Bello and Fantoni, 2002; Fantoni et al., 2004). In particular, thanks to the extensive exploration activity performed in the period between 1960 and 2000, namely several exploration wells drilled to a total depth in the range of 3000–7000 m (e.g. Villafortuna-Trecate, Gaggiano, Malossa, Cavone, Assunta; see Fig. 3a for deep wells' name and distribution) and new modern 2d–3d reflection surveys, the buried structures of the Po Valley and the related hydrocarbon systems have been eventually described and

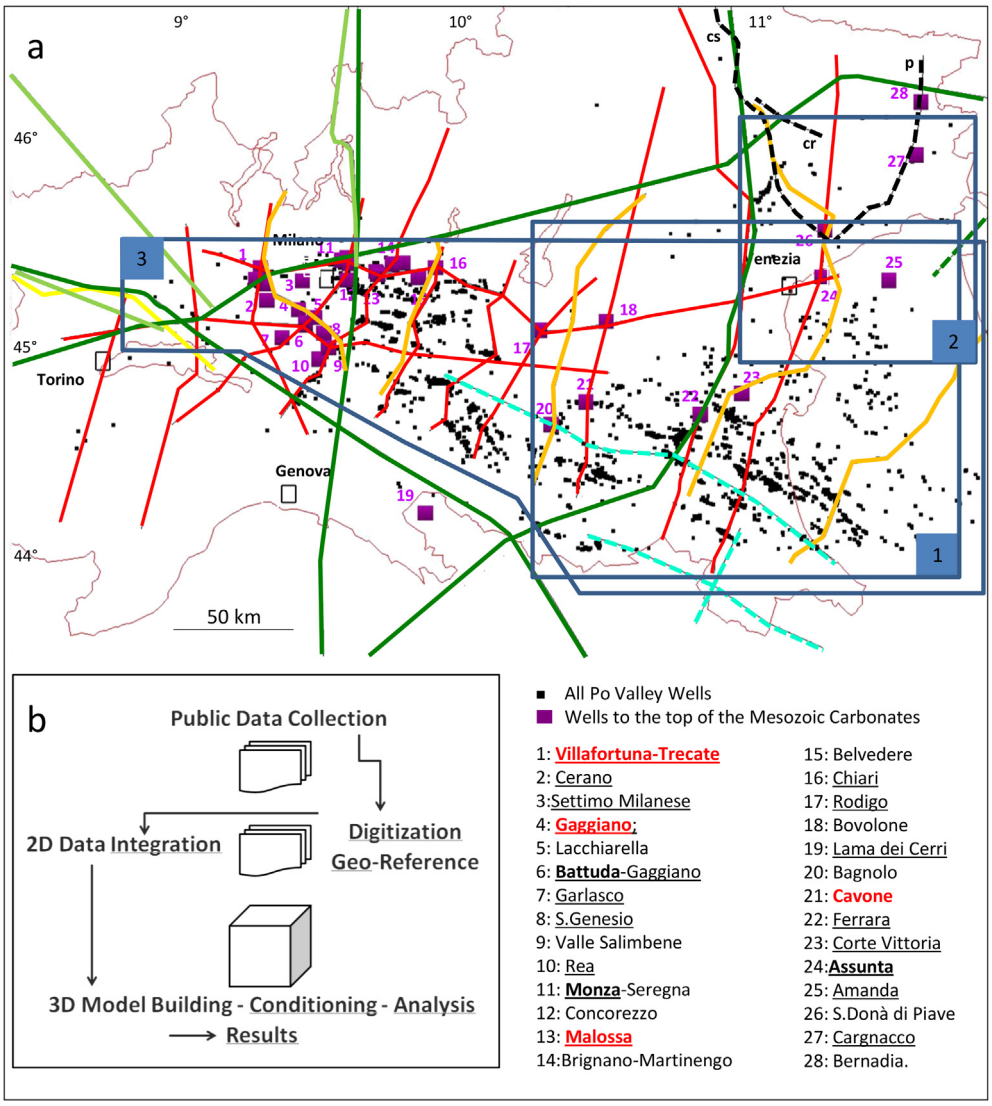

Figure 3. (a) Data distribution: cross-sections available from the public literature and wells (http://unmig.sviluppoeconomico.gov.it/unmig/pozzi/completo.asp; http://unmig.sviluppoeconomico.gov.it/videpi/kml/webgis.asp). In the well list: red = fields; bold black = wells drilling down to the Po Valley basement; underlined = wells drilling down to the Triassic succession. Cross-sections: red set from Cassano et al., 1986; orange set from Fantoni et al., 2004 and Fantoni and Franciosi, 2010; dark-green set from Roeder, 1991; light-green set from Schmid and Kissling, 2000; yellow is CROP-ECORS from Roure et al., 1991; light-blue set from Boccaletti et al., 2010; black set from (cs) Castellarin et al., 2005, (cr) Casero et al., 1990 and (p) Ponton, 2010. Box 1 = top Mesozoic Carbonates depth contour map area, from Casero et al., 1990; box 2 = top Mesozoic Carbonates depth contour map area, from Cimolino et al., 2010; box 3 = top Mesozoic depth map area, from Nicolai and Gambini, 2007. Latitude and Longitude values are North and East of Greenwich. (b) Workflow for the 3D model building process and analysis. (For interpretation of the references to colour in this figure legend, the reader is referred to the web version of this article.)

revealed to the scientific community. Through recent times, academia has provided a conspicuous literature on various subjects about the geology of the region. Livio et al. (2009) analysed the active structures of the Central Po Valley (east of Milan) by integration of seismic and seismicity. Boccaletti et al. (2010) published their results about the Quaternary morpho-tectonics of the central-eastern Po Valley, all along the external zone of the Northern Apennines. Mosca et al. (2010) discussed the structures and the kinematics of Western Po Valley with particular reference to the Tertiary Piedmont Basin region (SE of Torino). Cimolino et al. (2010) produced a top Mesozoic Carbonate depth map of the eastern Po Valley (south of Grado) while describing the interaction between the Dinaric deformation front and the offshore extension of the Po Valley foreland domain. Among the different papers and provided the dimension of the performed 3D modelling, the latest reviewing of the Adria Moho architecture presented by Nicolich (2010) is an important reference to this study. In fact, the related images and interpretative models reveal the crustal characteristics of the different units by their geophysical prospecting signatures (gravity, receiver functions, wide-angle seismic and vertical reflections). Such a review follows and updates a number of works dealing with the crustal anatomy of the Po Valley as part of the Alps–Apennines system: Roeder (1991) is likely the only author who attempted, so far, to build some contour maps of the tectonic units which model the Po Valley Moho and the neighbouring regions. Those maps are supported by key crustal-scale cross-sections which show the complexity and variability of the present crustal architecture. Roure et al. (1990) reported and used the results from the ECORS-CROP deep seismic profile to provide constraints on the post-collisional Alpine evolution and the associated early Miocene deformation beneath the western Po Valley. Schumacher and Laubscher (1996) discussed the possible 3D crustal architecture of the Alps–Apennines junction by reviewing selected seismic images and cross-sections presented by Pieri and Groppi (1981) and (Cassano et al. 1986). Compilations about the Moho crustal anatomy are also presented by Dézes and Ziegler (2004), Dézes et al. (2004) and Tesauro et al. (2008). Noteworthy, Schreiber et al. (2008) discussed a 3D geometrical model of the Moho topography in the south-western Alps by combining gravity, seismic and seismological constraints. At a larger scale, Vignaroli et al. (2008) and Larroque (2009) discussed the role of the Adria micro-plate as part of the Alps–Apennines tectonic system while presenting some former 3D block-diagram about the derived tectonic junction and the related subduction puzzle. More recently Maino et al. (2013) addressed the Alps–Apennines tectonic junction issue, by field-based structural and stratigraphic investigations at the transition between the Tertiary Piedmont Basin (Tpb in Fig. 1) and the Ligurian Alps, approximately 40 year after the review of Vanossi et al. (1986).

Although the buried structural setting of the Po Valley is rather well described by the available literature, the studies about the structural kinematics remains vaguely regional (Castellarin and Cantelli, 2010) or they refer to selected areas (Castellarin et al., 1985; Zoetemeijer et al., 1992; Fantoni et al., 2004). At the same time, although a possible stratigraphic template of the basin has been proposed by Lindquist (1999) and recently reviewed by Casero (2004), the current knowledge about the distribution of sedimentary formations is mainly related to the information coming from the outcrops (Castellarin and Vai, 1982; Jadoul and Rossi, 1982; Bertotti et al., 1993; Fantoni et al., 2003; Doglioni and Carminati, 2008; Berra et al., 2009) and the exploration industry data and reporting (Pieri and Groppi, 1981; Cassano et al., 1986; Fantoni et al., 2004; Ghielmi et al., 2010, 2012). Finally, in terms of geochemical and thermal modelling across the basin, the works from Mattavelli and Novelli (1987, 1990), Mattavelli and Margarucci (1992), Fantoni and Scotti (2003) and Viganò et al. (2011) are so far the key references that can be quoted on the subject.

3. Data and methodology

The data used to build the performed 3D model (Fig. 3a) are strictly derived from the public literature and the archives of the Italian Ministry of Energy (http://unmig.sviluppoeconomico.gov.it, namely the ViDEPI project) (Table 1). As such they mainly refer to geophysical and geological maps, cross-sections, well composite logs and stratigraphic columns. No seismic or confidential data have been used so far. In order to achieve the integration of such heterogeneous type of data-sets, these have been geo-referenced to a common geographical system (Transverse Mercator) and systematically digitized to transform any selected image into its numerical CAD-type format. During the process, images had often to be graphically and spatially re-arranged to correct for a) the image data quality, b) some local distortion, c) errors in the original scale definition. Lines from cross-sections and contours from maps were made ready for gridding into meshes whereas the well-stratigraphic cuts were locally input as control-points. In case the integration of various sources was necessary, the preliminary surfaces, obtained by gridding of the original xyz source points, were cut by serial, vertical slices and the resulting intersection lines were reviewed and averaged into one single line solution before re-gridding of the definitive surface. Continuous iteration between the progressive 2D and 3D models allowed the final structures to be built, validated in terms of geometrical consistency and analysed.

The overall workflow (Fig. 3b), from data collection and integration, to model-building and the final model validation/analysis, has been performed using the MOVE commercial package (2d/3d MOVE by Midland Valley).

4. Model uncertainty

Provided the current model results and the available data source distribution (see Figure 3a) and quality, the following vertical and horizontal uncertainty has been defined for the various 3D model layers.

a) Moho: the surface-grid is essentially averaging the results from Roeder (1991) and CROP (2004). Vertical uncertainty is in the range of 5–10 km, increasing towards the western Po Valley domain and close to the front of the Southern Alps and the Apennines. The final model layer seems reliable at the crustal scale and it has been validated by comparison with a number of crustal sections from the literature (Roure et al., 1990; Roeder, 1991; Schmid and Kissling, 2000; Castellarin et al., 2005) (location in Fig. 3a);
b) Top Basement: the surface grid exclusively refers to the result from Cassano et al. (1986) which used seismic, wells (Monza, Battuda and Assunta; see location in Figure 3a) and grav-mag maps to tie their data interpretation. Our model layer mainly derives from contouring of their basement map which, however and for some unknown reasons, locally deviates from the cross-sections basement geometry. It follows that depth uncertainty in the final 3D model layer ranges between 500 and >2000 m (extreme western sector of the west Po Valley domain, below the Monferrato belt, and at the front of the Appennines to the SW of the Ferrara-Romagna arch) so that it appears strongly reliable at the crustal scale and moderate to low reliable at the structure-scale, away from the reference wells;
c) Top Triassic: the surface grid mainly relates to the cross-sections from Cassano et al. (1986; location in Figure 3a)

Table 1
Data used to perform the 3D model building and validation of the Po Valley basin.

3D model	Data source	Data type	Modelling phase
MOHO	Roeder, 1991	Contour maps	Model building
	Roeder, 1991	Cross-sections	Model validation
	CROP, 2004	Contour map	Model building
	Roure et al., 1990	Cross-section	Model validation
	Schmid and Kissling, 2000	Cross-sections	Model validation
	Castellarin et al., 2005	Cross-section	Model validation
	Nicolich, 2010	Contour map	Model validation
Top Basement	Cassano et al., 1986	Contour map	Model building
	Cassano et al., 1986	Cross-sections	Model building
	Cassano et al., 1986	Well Tops	Model building
	Fantoni et al., 2004	Cross-sections	Model validation
	Fantoni and Franciosi, 2010	Cross-sections	Model validation
Top Trias	Cassano et al., 1986	Cross-sections	Model building
	Cassano et al., 1986	Well Tops	Model building
	Fantoni et al., 2004	Cross-sections	Model validation
	Fantoni and Franciosi, 2010	Cross-sections	Model validation
	ViDEPI Project	Wells locations & Tops	Model validation
Top Mesozoic Carbonates	Cassano et al., 1986	Cross-sections	Model building
	Cassano et al., 1986	Well Tops	Model building
	Bigi et al., 1989	Fault Map	Model validation
	Casero et al., 1990	Contour Map & Fault Map	Model building
	Bello and Fantoni, 2002	Cross-section	Model validation
	Fantoni et al., 2004	Cross-section & Fault Map	Model validation
	Nicolai and Gambini, 2007	Depth Map	Model validation
	Boccaletti et al., 2010	Cross-sections	Model validation
	Cimolino et al., 2010	Contour Map	Model building
	Fantoni and Franciosi, 2010	Cross-sections	Model validation
	Ponton, 2010	Cross-sections	Model validation
	ViDEPI Project	Wells locations & Tops	Model validation
Base Pliocene	Pieri and Groppi, 1981	Contour Map & Fault Map	Model building
	Pieri and Groppi, 1981	Well tops	Model building
	Cassano et al., 1986	Cross-sections	Model validation
	Cassano et al., 1986	Well tops	Model validation
Outcrops	Bigi et al., 1989	Outcrops & Fault trends	Model building
Digital Topography	http://srtm.csi.cgiar.org/SELECTION/inputCoord.asp	Grid	Model building

which have been originally tied to nearly all of the wells that have drilled the possible top Triassic in the Po Valley basin (see these well location in Fig. 3). Major uncertainty relates to lack of interpretation of the top Triassic in part of the original cross-sections. Within such blank areas (i.e. western sector of the western Po Valley, southern sector of the Emilia arch) the most-likely top Triassic has been drawn by 3D model building and consistency check with the top Mesozoic and Basement geometries, above and below it. The related structures have been further validated by comparison with cross sections from Fantoni et al. (2004), Fantoni and Franciosi (2010) and 2 recent wells available from the ViDEPI web-site (Rea 1 and S. Genesio 1; location in Figure 3a). The final model grid is fairly reliable at the crustal scale and moderate to low reliable at the structure-scale, away from the reference wells;

d) Top Mesozoic: data source to the 3D model layer have been (Fig. 3a), a) the cross-sections from Cassano et al. (1986), those being tie to wells, seismic and grav-mag maps, b) the depth contour map from Casero et al. (1990 – from the Adriatic to the Ferrara-Romagna arch included), c) the depth contour map from Cimolino et al. (2010) (in the Friuli onshore-offshore – NE of Venezia), d) cross-sections from Boccaletti et al. (2010). The resulting 3D model layer and the structure distribution have been locally validated by comparison with a) the maps of Fantoni et al. (2004 – fault trends) and Nicolai and Gambini (2007 – regional depth map of the possible Mesozoic Carbonates) and b) cross sections from Casero et al. (1990), Bello and Fantoni (2002), Fantoni et al. (2004), Boccaletti et al. (2010), Fantoni and Franciosi (2010), Ponton (2010). The final surface-grid seems reliable at both crustal and structure scale. Provided the source data robustness (the authors of the reference papers are often coming from the industry thus driving their interpretation by seismic and well information) and their distribution, the 3D model vertical uncertainty is generally in the order 100–500 m with increasing ambiguity towards the Southern Alps and Northern Apennines fronts;

e) Base Pliocene: the 3D layer is exclusively drawn from the base Pliocene depth map, published by Pieri and Groppi (1981) and tied to massive seismic and well data. The related 3D model surface has been then validated by comparison with a) the Cassano et al. (1986) cross-sections and well tops and b) contours and fault trends from the structural model of Italy by Bigi et al. (1989). Wells from the ViDEPI web-site have not been reviewed during the base Pliocene Layer 3D model building thanks to the very weak uncertainty in the data published by the above mentioned authors. The final 3D surface can be considered reliable at both the basin and structure scale. The possible ambiguity in the model geometries and depth could eventually relate to the grid-surface smoothing which had to be run for graphical needs;

f) Isopach-maps: uncertainty about such maps is a natural consequence of the uncertainty described for each of the model layers. Therefore the final sediment thickness distribution and variation illustrated by the model are generically to be considered as crustal scale information rather than detail description of the Mesozoic, pre-compression, basin paleogeography.

Conclusively, uncertainty in the performed 3D model is certainly scale dependent: being essentially a crustal-scale model, the more

we go into the details, the larger the uncertainty. To such extent, a) cross-sections obtained from vertical slicing of the model volume have been conditioned by integrating results from the literature (see references in the related figures), b) smaller and more refined models of some selected structures have been built at the occurrence (e.g. see structures versus hydrocarbons case study at the end of chapter 7.7).

5. The Po Valley 3D structural model

The performed 3D model covers an area of 700 by 400 km (with a core area of approximately 10,000 km^2). It extends at depth to integrate the Moho discontinuity separating the crust from the lithospheric mantle (30–50 km bsl). From top to bottom, the model "layers" are the digital topography, the base of the Pliocene sediments, the top of the Mesozoic Carbonate succession, the "near" top of the Triassic succession, the top of the so called "magnetic basement" (Cassano et al., 1986) and the top of the mantle, (Moho). Given the dimension of the final model, faults and syn-tectonic sediments discontinuously occurring within the Oligo-Miocene units at the front of the Northern Apennines and Southern Alps have only been reviewed locally during the model vertical slicing and the related cross-sections building.

6. Model analysis

The geometrical analysis of the model has been mainly performed by a) visualization and rendering of the model structural layers, b) vertical-horizontal slicing to create key-geological sections and depth-slices and c) isopach-map building between some of the model layers. Those three operations enhanced the general understanding and analysis of the geological 3D framework and they allowed the final grids and structures to be checked for errors and inconsistencies, therefore validated.

The different structural maps have been coloured by depth, and, at the occurrence, put against the outcrops, the shallow buried faults and the well location. As such the comparison and the possible link between all of the geometries (deep and shallow) can be, hopefully, straightforward. At the same time the rationale of the past exploration strategy in the region can also be quickly inferred.

6.1. Model visualization

6.1.1. Structural geometries at the Moho grid-surface

The Moho grid-surface (Fig. 4) is the deepest level in the model. Regionally, the Po Valley Moho, or Adria Moho, appears to be domed in the axial-central domain. It is flexured towards the north, below the Alps, and the south, below the Apennines, and nearly exposed at the surface in the west, north of Torino. Across the derived crustal unit, clearly over-thrusting the European Moho towards the north, deformation increases from east to west so that two separate domains can be defined: the gently deformed Eastern domain and the highly deformed Western domain. Indeed, in contrast with the uniform Moho geometry of the Eastern Po Valley-Adriatic domain, the Western Po Valley Moho architecture shows a complex structural setting at the Alps–Apennines junction (circle area AAJ in Fig. 4). Here we observe the interference between a) the southern termination of some NE–SW oriented, NW verging, thrust-related-imbricates (see also cross-sections in Figs. 11b, 15b, 16b) and b) the north-western segment of a WNW–ESE oriented sub-Apennines anticline feature, verging towards the NE (see also cross-sections in Figs. 12b, 13b, 14b). Within such a framework, a possible NNE–SSW oriented, sinistral transfer zone should accommodate the relative displacement between those two derived structural sectors.

It is relevant to note that the Moho flexure at the front of the Apennines leaves room for the shallow structures (white fault

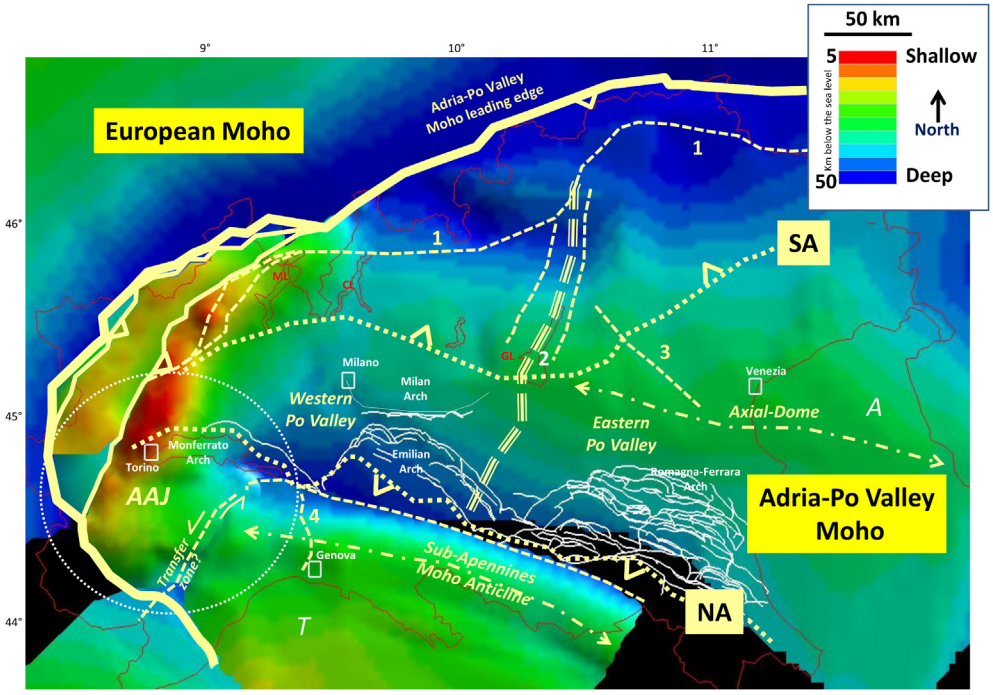

Figure 4. Structural geometries at the Moho grid-surface. Coast-line & northern Italy state boundaries in red. Large dashed segment is possible separation between western and eastern Po Valley domains. White lines are faults at base Pliocene level (Bigi et al., 1989). (SA) Southern Alps outcropping thrust front; (NA) Northern Apennines outcropping thrust front; AAJ = Alps–Apennines Tectonic Junction (circle area). (A) Adriatic; (T) Tyrrhenian. Main regional tectonic lineaments: (1) Insubric Line; (2) Giudicarie Line; (3) Schio-Vicenza Line; (4) Villavernia Line. ML = Maggiore Lake; CL = Como Lake; GL = Garda Lake. Latitude and Longitude values are North and East of Greenwich. (For interpretation of the references to colour in this figure legend, the reader is referred to the web version of this article.)

pattern in Fig. 4). Conversely, no flexure of the Moho is shown at the South Alpine front.

Accordingly to the described structures, the depth of the final grid varies from 50 km to nearly 0 km below the mean sea level.

6.1.2. Structural geometries at the basement grid-surface

The top of the magnetic basement shows a generic structural conformity with the Moho geometry, as illustrated by Figure 5. As such, two major structural domains can be again defined: a) the western domain, deformed into a patchy, low-amplitude, high-and-low fabric and b) the eastern domain, mainly deformed by a large-amplitude crustal scale dome. Across the Po Valley, the basement depth increases from north to southwest reaching a maximum value of 17 km below the Apennine Chain. From the model, two large basement-related units appear to be part of the Northern Apennines arches (see Fig. 5, AB structural elements). Despite their evidence at the grid scale, no wells have drilled those units to prove their existence and constrain their tectonic significance.

6.1.3. Structural geometries at the "near" top Triassic grid-surface

The top Triassic surface-grid (Fig. 6) confirms the western and eastern Po Valley domains existence. At the local scale, the geometries of the western domain can be only guessed so that small highs and lows features appear, which could partly correspond to artifacts due to the data distribution (see Fig. 3a). In the eastern Po Valley, a regional anticlinal feature occurs on top of the basement dome (see Fig. 5) and it largely coincides with the Veneto Platform building. Such a structural element nearly comes to surface at the front of the Southern Alps, to the SE of the Garda Lake and it is recognized at depth by the Rodigo 1 well (well 17 in Fig. 3).

According to the depth model grid, the final Top Triassic unit (i.e. the main reservoir of the Po Valley deep play) is found at 3–15 km bsl, with regional dip towards the South, below the Apennines.

6.1.4. Structural geometries at the top of the Mesozoic carbonate grid-surface

The top of the Mesozoic carbonates (Fig. 7) is an extremely important surface. Infact, it is the top of the deep play for the hydrocarbon exploration in the region and the major seismic marker for the related structure interpretation (see Fig. 2). Depth values for the grid range from 0 to 11 km below the sea level according to the recognized structural architecture.

Once again, the western and eastern Po Valley domains can be immediately recognized also at this level. This confirms the tectonic pattern already observed at the Moho, at the basement and at Triassic level, as well as the geometrical conformity among the four model layers. In the detail, the Mesozoic carbonates of the western Po Valley (Fig. 8b) show dome-and-basin-types features, oriented parallel, oblique and perpendicular to both the Southern Alps and the Apennines mountain fronts. In the eastern Po Valley (see Fig. 7), the Mesozoic top surface is essentially modelled into a large dome, gently elongated in the NW–SE direction. To the south of such a regional feature, some thusted folds, oriented parallel to the Apennines, are shown. Those geometries can be enveloped into an arch where lateral-ramp, frontal-ramp and transfer structural elements can be recognized (Fig. 8c). In the NE corner of the Po Valley (i.e. the Veneto and Friuli domains) the interference between the Alpine and Dinaric tectonics is confirmed by the intersection of the related structural trends, WSW–ENE and NNW–SSE oriented, respectively.

6.1.5. Structural geometries at the base Pliocene grid-surface

This is the shallowest level of the 3D model below the topography and by far the most refined and structurally complex (Fig. 9). In reality, however, the final surface-grid defines a major unconformity across the entire Po Valley basin (bottom of the Pliocene–Quaternary sequence in Pieri and Groppi (1981); that is likely the Messinian unconformity). Therefore a) it properly illustrates the

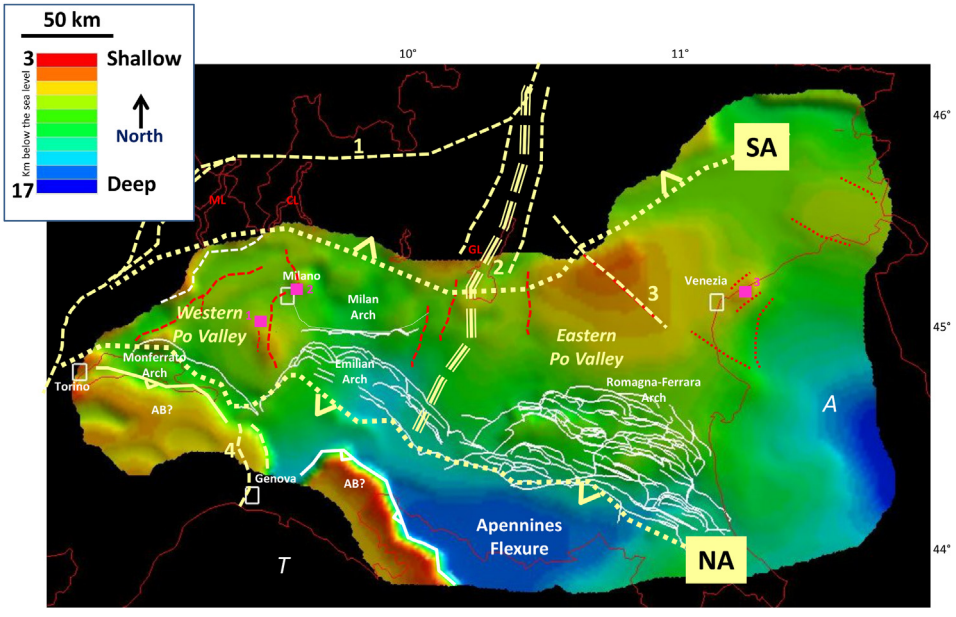

Figure 5. Structural geometries at the Basement grid-surface. Coast-line & northern Italy state boundaries in red. Large dashed segment is possible separation between western and eastern Po Valley domains. White lines are faults at base Pliocene level (Bigi et al., 1989). Purple squares = « basement » wells (1 = Battuda1; 2 = Monza1; 3 = Assunta1). Red stippled lines are possible major basement faults. AB = possible Allochthonous "Basement" units. (SA) Southern Alps outcropping thrust front; (NA) Northern Apennines outcropping thrust front; (A) Adriatic; (T) Tyrrhenian. Main regional tectonic lineaments: (1) Insubric Line; (2) Giudicarie Line; (3) Schio-Vicenza Line; (4) Villavernia Line. ML = Maggiore Lake; CL = Como Lake; GL = Garda Lake. Latitude and Longitude values are North and East of Greenwich. (For interpretation of the references to colour in this figure legend, the reader is referred to the web version of this article.)

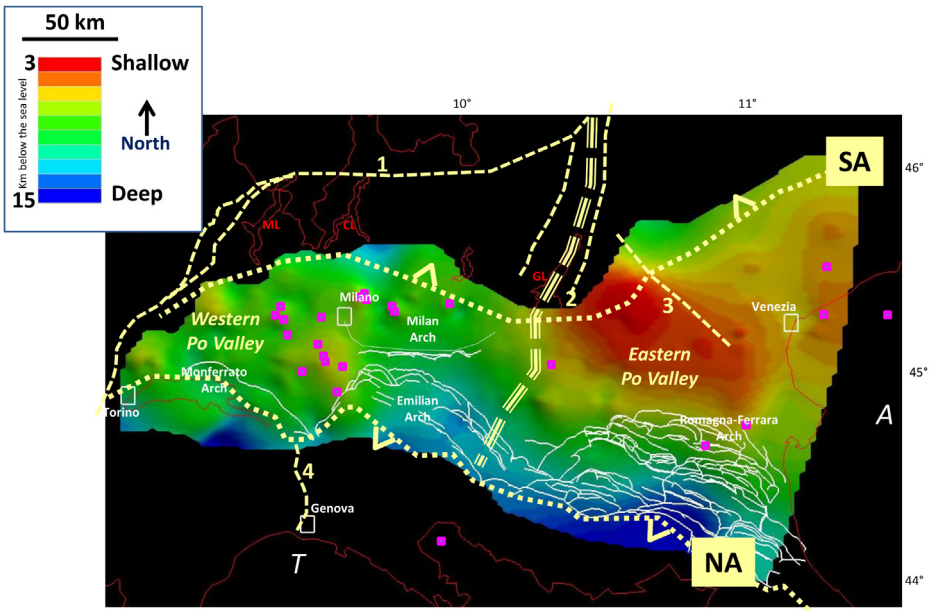

Figure 6. Structural geometries at the top Triassic grid-surface. Coast-line & northern Italy state boundaries in red. Large dashed segment is possible separation between western and eastern Po Valley domains. White lines are faults at base Pliocene level (Bigi et al., 1989). Purple squares = tie-wells to the top of the Mesozoic Carbonates (see Fig. 3 for well name). (SA) Southern Alps outcropping thrust front; (NA) Northern Apennines outcropping thrust front; (A) Adriatic; (T) Tyrrhenian. Main regional tectonic lineaments: (1) Insubric Line; (2) Giudicarie Line; (3) Schio-Vicenza Line; (4) Villavernia Line. ML = Maggiore Lake; CL = Como Lake; GL = Garda Lake. Latitude and Longitude values are North and East of Greenwich. (For interpretation of the references to colour in this figure legend, the reader is referred to the web version of this article.)

Plio-Pleistocene structures, but b) it masks the details of the buried Oligocene and Miocene ones.

At the basin scale, a regional monocline can be observed at the base of the Pliocene, as it goes from 0 km at the front of the Southern Alps, to a maximum of 7 km in the eastern part of the Po Valley, close to the outcropping front of the Apenninic belt (see Fig. 9). Such a monocline is then modelled by 3 major tectonic arches (Monferrato Arch, Emilian Arch, Ferrara-Romagna Arch), their presence implying fold-and-thrusts tectonics and displacement of the related units towards the NE mainly. In details (Fig. 10), the folds seem to show segmented anticline axes and narrow synclines, locally anastomosed and sometimes arranged into an en-echelon pattern. Folds and thrusts within each of the arches are systematically NW–SE oriented and they deviate into the NE–SW direction when they pass to the western sides (i.e. the lateral-ramp domains) of the major arches.

At the front of the Southern Alps only the Milano arch (see Fig. 9) gently deforms the base Pliocene surface, most compressional

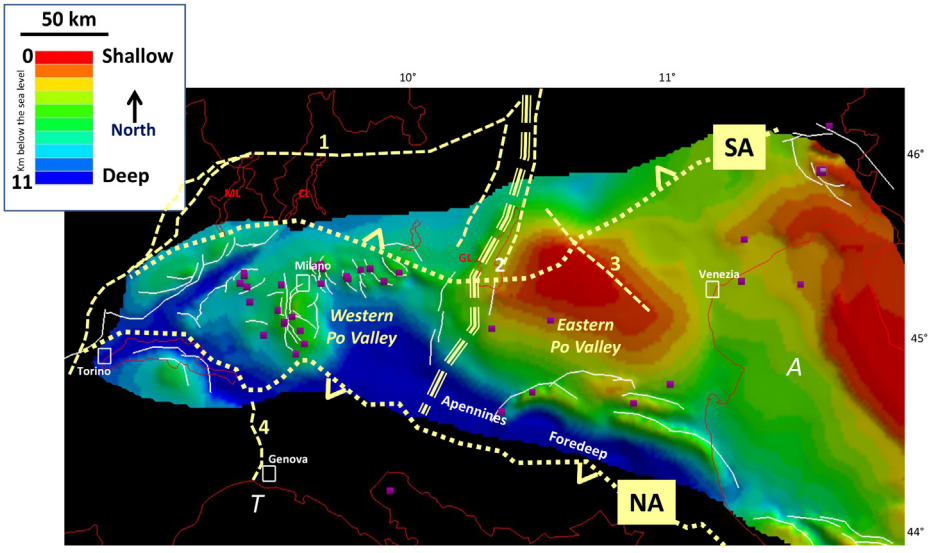

Figure 7. Structural geometries at the top of the Mesozoic Carbonate grid-surface. Coast-line & northern Italy state boundaries in red. Large dashed segment is possible separation between western and eastern Po Valley domains. White lines are faults at Top Mesozoic level. Purple squares = tie-wells to the top of the Mesozoic Carbonates (see Fig. 3 for well name). (SA) Southern Alps outcropping thrust front; (NA) Northern Apennines outcropping thrust front; (A) Adriatic; (T) Tyrrenhian. Main regional tectonic lineaments: (1) Insubric Line; (2) Giudicarie Line; (3) Schio-Vicenza Line; (4) Villavernia Line. ML = Maggiore Lake; CL = Como Lake; GL = Garda Lake. Latitude and Longitude values are North and East of Greenwich. (For interpretation of the references to colour in this figure legend, the reader is referred to the web version of this article.)

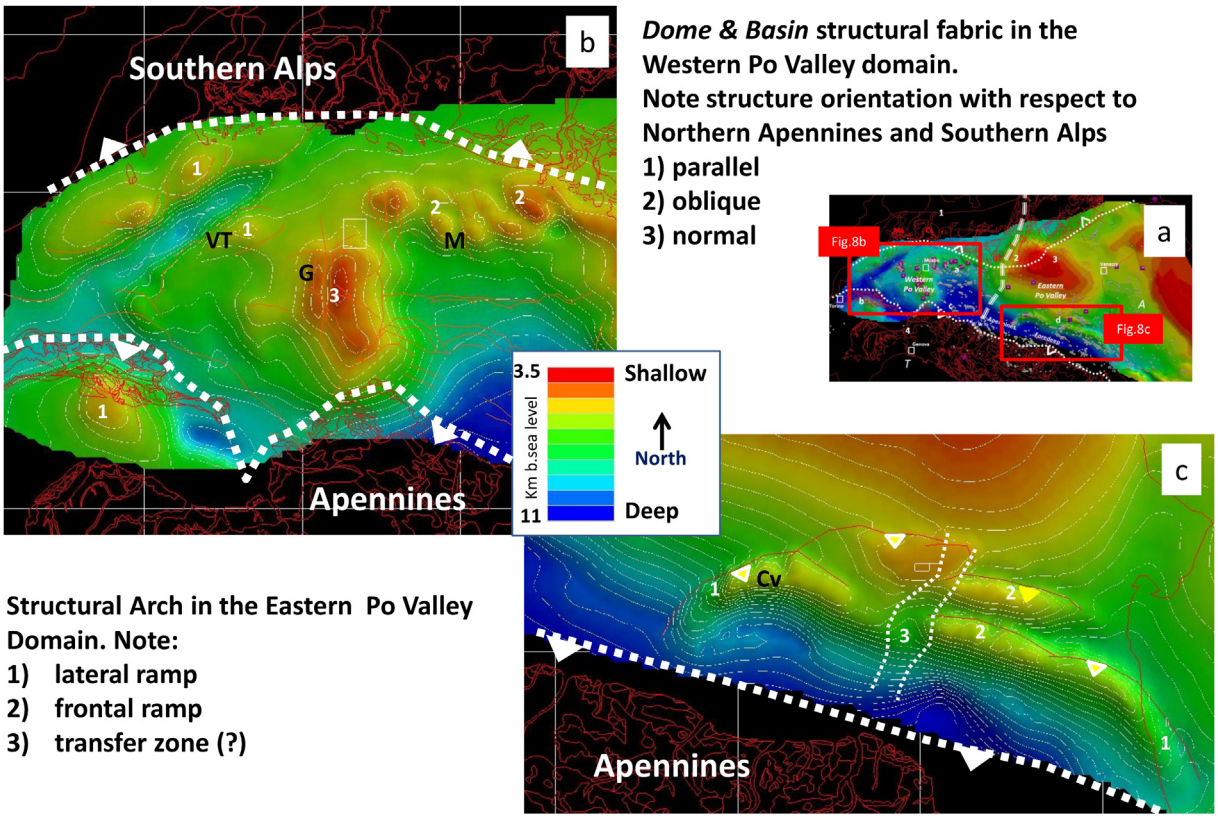

Figure 8. Detail structural geometries from the Top Mesozoic Carbonate grid-surface: (a) Location map for details in figures b and c; (b) Western Po Valley structures. VT = Villafortuna-Trecate field; G = Gaggiano field; M = Malossa field; (c) Eastern Po Valley structures. Cv = Cavone field. Red lines are outcrops. Grid in both figures is 50 km. (For interpretation of the references to colour in this figure legend, the reader is referred to the web version of this article.)

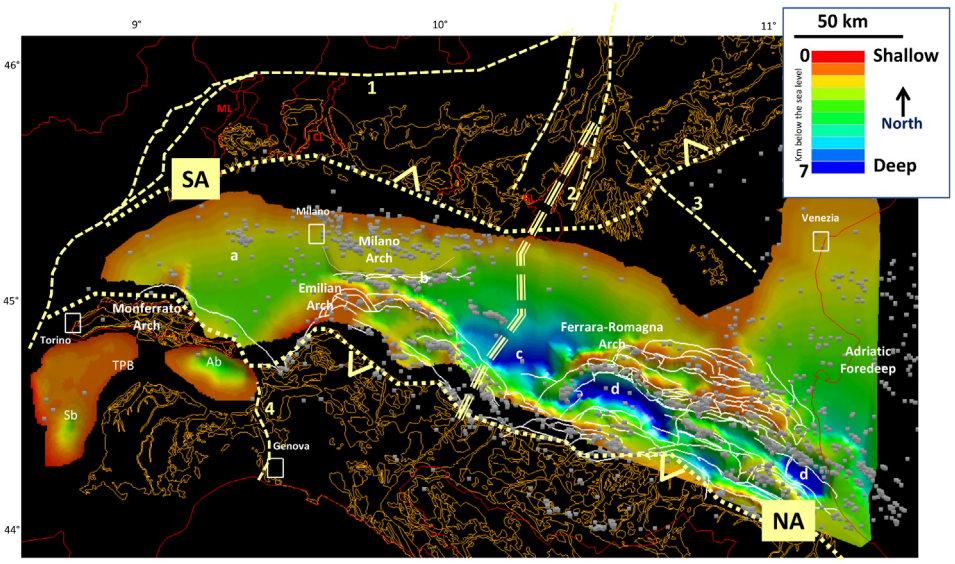

Figure 9. Structural geometries at the Base Pliocene grid-surface. Coast-line & northern Italy state boundaries in red. Southern Alps and Northern Apennines outcrops in orange. (SA) Southern Alps outcropping thrust front; (NA) Northern Apennines outcropping thrust front. Large dashed segment is possible separation between western and eastern Po Valley domains. White lines are faults at base Pliocene level (Bigi et al., 1989). White dots are all the Po Valley wells. a) Regional monocline, b) SA versus NA thrust front clash-zone, c) major Pliocene foredeep depocenter, d) piggy-back basins within the Ferrara-Romagna tectonic arch. TPB = Tertiary Piedmont basin; Sb = Savigliano basin; Ab = Alessandria basin. Main regional tectonic lineaments: (1) Insubric Line; (2) Giudicarie Line; (3) Schio-Vicenza Line; (4) Villavernia Line. ML = Maggiore Lake; CL = Como Lake; GL = Garda Lake. Latitude and Longitude values are North and East of Greenwich. (For interpretation of the references to colour in this figure legend, the reader is referred to the web version of this article.)

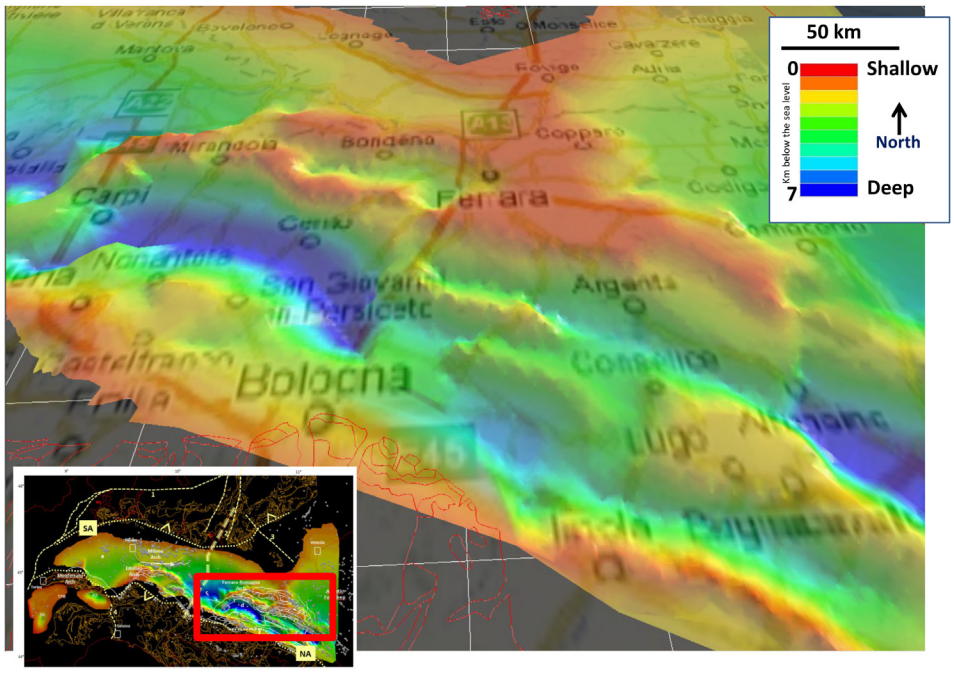

Figure 10. Detail of the Base Pliocene grid-surface structures from the Ferrara-Romagna arch (insert map for location): perspective view looking NNW. Geographic map draped on top of structure map for further references. See text for discussion. Grid is 100 km.

features there being instead sealed by the Pliocene unconformity. The interference between the Milano and the Emilian thrusts and folds define the clash zone between the buried domains of the Alps and the Apennines (b in Fig. 9), as described by Pieri and Groppi (1981).

At the rear of the Monerrato arch, within the Piedmont Tertiary Basin (TPB in Fig. 9), the Savigliano and Alessandria Pliocene basins are clearly illustrated by the 3D model grid-surface. The drastic rotation of the related basin axis, NS (Savigliano) to WNW–ESE (Alessandria), allows the structural interference between Alps and Apennines to be inferred and some change in the deep crustal fabric to be suggested (see paragraph 6.2.8).

In order to confirm and support the 3D model structural pattern, the fault trends from the structural model of Italy (Bigi et al., 1989) have been draped on the final grid surface (white lines in Fig. 9). The positive correlation among grid structures and fault lines is obvious, those latter essentially being the more recent updating by ENI of the original Pieri and Groppi (1981) seismic interpretation.

6.1.6. Dip-map & fault pattern at top Mesozoic

The faults that are shown on top of the 3D model grid-surfaces (see Figs. 6–9) refer to a) crustal scale discontinuities, b) regional trends, c) seismic scale faults and d) outcropping faults) (Pieri and Groppi, 1981; Bigi et al., 1989; Casero et al., 1990; Bertotti et al., 1993; Fantoni et al., 2003, 2004; Cimolino et al., 2010; Ponton, 2010). Hence, they represent the whole spectrum of discontinuities that is expected to cut across the entire 3D geo-volume. Given the main objective of this paper, only the faults that intersect the Mesozoic grid have been systematically reviewed by the model and they will be discussed hereafter with respect to the related top Mesozoic dip-map (Fig. 11).

The top Mesozoic fault sets that occur across the Po Valley basin (white lines in Fig. 11) show NE–SW and NW–SE dominant orientations with local deviations. Indeed, from Figure 11, a NW-trending fault system is present in the eastern part of the Po Valley while in the western part three fault systems can be recognised: NE–SW (the main system?), N–S and NW–SE. Among the various sets it is interesting to note that the NE–SW one appears to replicate the orientation of some major, crustal scale fault zones that can be recognized at the scale of the whole Alpine and Apennines thrust belts (i.e. the western segment of the Insubric line, the Giudicarie fault zone). In general terms of structural definition, the NE–SW and N–S oriented faults mainly refer to both Triassic and lower Jurassic extensional events (Bongiorni, 1987; Bertotti et al., 1993; Fantoni et al., 2004; Franciosi and Vignolo, 2002; Fantoni and Franciosi, 2010) while a large part of the NW–SE ones clearly show a geometrical correlation with the Alps and Apennines thrust front orientations. In details the tectonic origin of each single fault segment can be simple-to-very complex due to the deformation history of the basin structures: in that respect, some of the faults can be normal faults or thrusts exclusively, whereas others can be normal faults lately reactivated by thrusting with a large degree of possible variations in the final anatomy due to fault orientation and stress direction progression (Castellarin and Cantelli, 2010, and references therein). Irrespective of their tectonic origin, those dominant fault families bound and deform, with different degree of density, both the western and eastern domains. Given the available data, the fault spacing within the derived regional compartments can vary from 10 to 100 km.

The dip-map of Figure 11 shows the variation in dip of the top Mesozoic grid-surface across the Po-Valley. The spatial variation of dip on a surface can help locate fault zones that have been gridded during initial surface creation. The derived display that can be automatically generated by a computer is commonly used in structural geology analysis and, by successive mathematical elaborations, during seismic interpretation of faulted and fractured regions (Roberts, 2001; Klein et al., 2008; Resor, 2008). Such rendering tool can a) either confirm the presence of a major discontinuity for steep dip value localization or b) suggest the existence of subtle, minor discontinuities where gentle dip variations show geometrical consistency with the tectonic directions that can be defined in-around the study area. It follows that steep dip

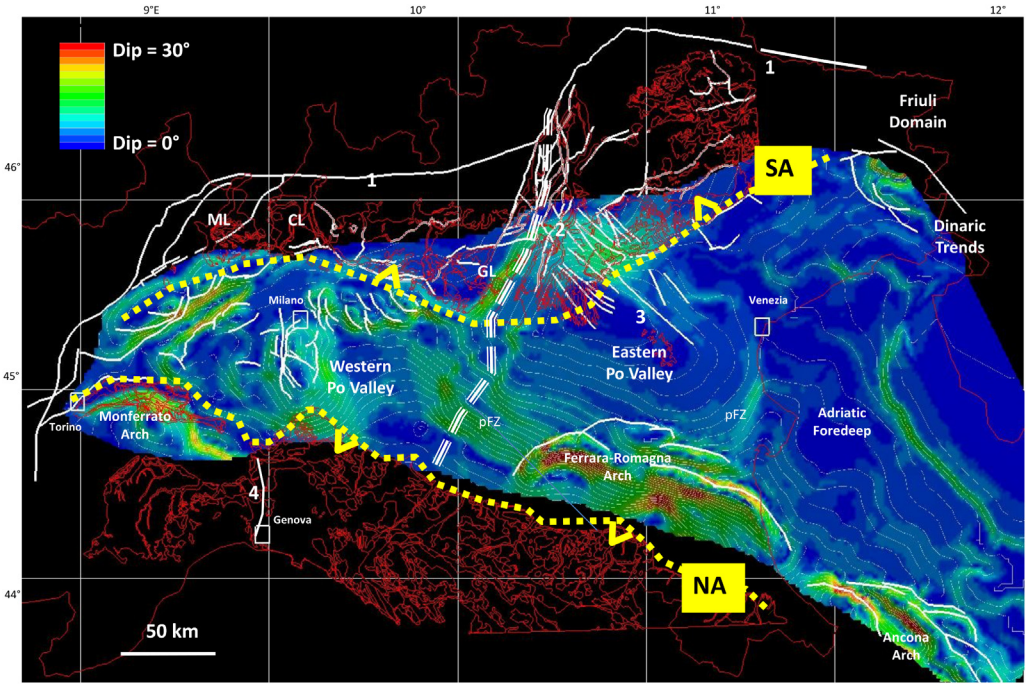

Figure 11. Top Mesozoic major faults from available literature (white lines) against 3D Model top Mesozoic dip-map (contouring is every 500 m). pFZ = possible fault zone (see text for discussion). Outcrops, coast-line & northern Italy state boundaries in red. (SA) Southern Alps outcropping thrust front; (NA) Northern Apennines outcropping thrust front. Main regional tectonic lineaments: (1) Insubric Line; (2) Giudicarie Line; (3) Schio-Vicenza Line; (4) Villavernia Line. Latitude and Longitude values are North and East of Greenwich. Grid is 100 km. (For interpretation of the references to colour in this figure legend, the reader is referred to the web version of this article.)

alignments in the vicinity of already known tectonic features will likely validate the presence of important faults, whereas subtle dip-variation on a gentle monocline can allow some small faults, hidden to interpretation, to be suspected. It should be noted that the methodology cannot suggest by any means the kinematic nature of the discontinuity (i.e. normal, reverse, transcurrent) if the map is not coupled with the surrounding tectonic framework analysis.

The dip-map of Figure 11 seems to supports the regional scale compartments (east and west Po Valley), as well as the local scale structural complexity already shown by the top Mesozoic depth map (Figs. 7 and 8). Particularly outstanding are the Ferrara-Romagna tectonic arch and the dome-and-basin structural pattern in the western Po Valley. The performed rendering a) suggests the Po Valley fault density as it increases from east-to-west, b) confirms the structural interference between NE–SW and WNW–ESE fault sets, c) indicates some possible fault zones which have not been recognized so far around the eastern Po Valley regional scale dome features (i.e. pFZ green trends not overlaid by faults in Fig. 11).

6.2. Slicing the model

Slicing of the geo-volume at any chosen orientation is an important result from the performed 3D model. Observation of the resulting geometries along key directions or selected depths allows the structural uncertainty to be identified while improving the geological understanding across the entire Po Valley basin, from the crustal to the field scale. The final cross-sections are eventually used to refine the original 3D model.

6.2.1. Cross-section 1 (Fig. 12)

The section, SSE–NNW oriented, slices the western domain of the Po Valley foreland-foredeep system, this being tightly caught in between the Southern Alps and the Ligurian Alps (Fig. 12b). Folding and thrusting of the Moho discontinuity at depth seem to control the shallow deformation. As such, the relatively thin Po Valley Mesozoic carbonates (Fig. 12c) are deformed into a crustal scale syncline and thrusted towards both the north (below the Ligurian Alps–Northern Apennines stack) and the south (south of the Insubric line). At the Monferrato front, the Lower Tertiary clastic sediments are tectonically squeezed below the base Pliocene unconformity, this last surface being only mildly folded. Below the Asti1 well the allochthonus Ligurides unit overthrusts the Po Valley crust and carries the Eocene-to-Pleistocene formations of the Tertiary Piedmont basin in a piggy-back fashion.

6.2.2. Cross-section 2 (Fig. 13)

The cross-section is NNE–SSW oriented and it runs through the central part of the Po Valley basin, in the eastern sector of the western domain. The Europe-Adria lithospheric mantle subduction zone is shown below the Alps, whereas folding of the Adria-Po Valley Moho surface dominates the crustal scale picture (Fig. 13b). Across the region (Fig. 13c), N-to-S thinning of the Mesozoic succession occurs so that the thickest section in the Belvedere area is structurally inverted by compression at the front of the Southern Alps. On the other side of the basin, at the front of the Apennines, thrusting in the Mesozoic and in the Tertiary sections cause thickening of the whole sedimentary pile. Across the whole area structures are both south and north verging and their interference in the central part of the basin defines the tectonic clash between the external domains of the Alps and Apennines (AACZ in Fig. 13c).

6.2.3. Cross-section 3 (Fig. 14)

The long section connects the Alps and the Apennines fronts, the two being approximately 150 km apart. Below the Po Valley basin the Moho is strongly folded and, like in the previous section, an intra-Adria-Po Valley major inflection point can be again suggested

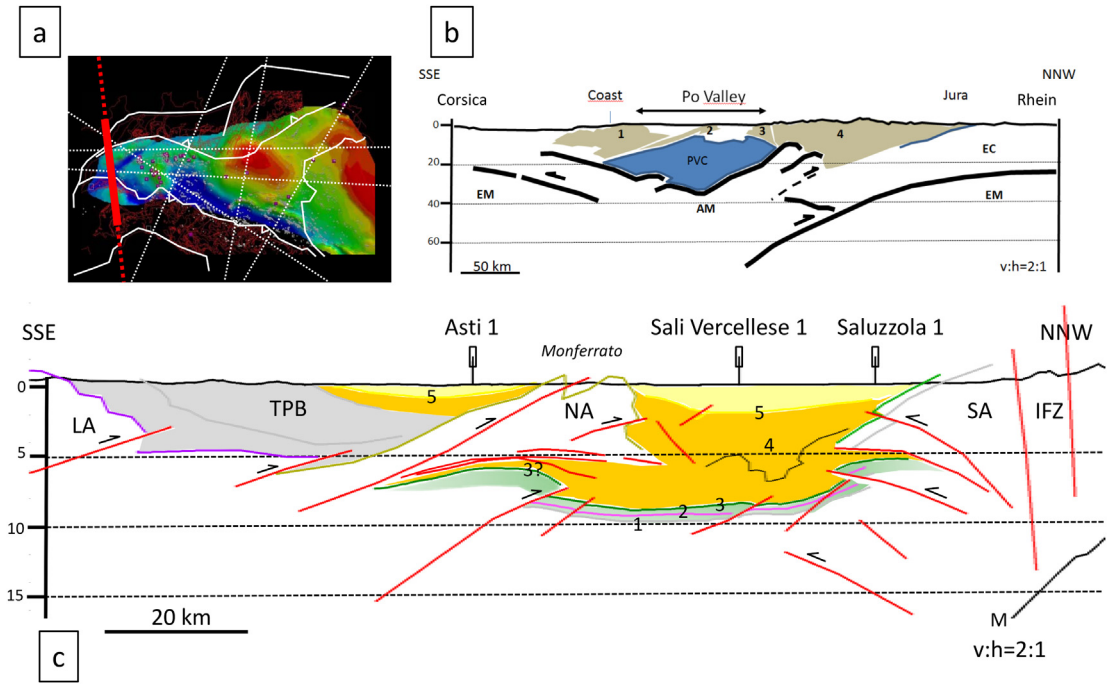

Figure 12. 3D Model Cross-section 1. (a) Location map by Top Mesozoic grid surface from this study. (b) Crustal-scale section (red dotted line in Fig. 12a). Black-thick line = Moho; EM = European Mantle; EC = European Crust; PVC = Po Valley Crust-to-Top Mesozoic; AM = Adria (Po-Valley) Mantle; 1 = Ligurian Alps; 2 = Northern Apennines (Allochthonous Ligurides, Monferrato Belt); 3 = Southern Alps; 4 = Western Alps. (c) Regional-scale section (red segment in Fig. 12a). 1 = Near Top Basement; 2 = Near Top Triassic; 3 = top Mesozoic Carbonates; 4 = Cenozoic succession; 5 = Base-Pliocene unconformity; NA = Northern Apennines, Allochthonous Ligurides); BTLP = Bacino-Terziario-Ligure-Piementese sediments; LA = Ligurian Alps; SA = Southern Alps; IFZ = Insubric Fault Zone; M = Moho. (For interpretation of the references to colour in this figure legend, the reader is referred to the web version of this article.)

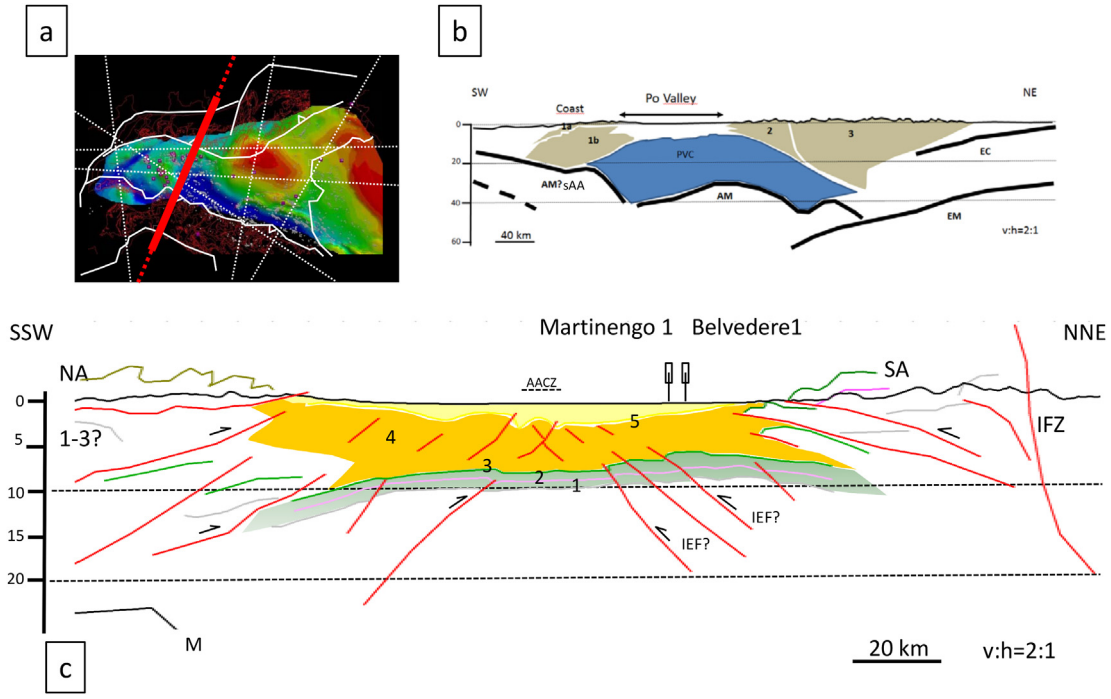

Figure 13. 3D Model Cross-section 2. (a) Location map by Top Mesozoic grid surface from this study. (b) Crustal-scale section (red dotted line in Fig. 13a). Black-thick line = Moho; EM = European Mantle; EC = European Crust; PVC = Po Valley Crust-to-Top Mesozoic; AM = Adria (Po-Valley) Mantle; 1 = Northern Apennines (Allochthonous Ligurides); 2 = Southern Alps; 3 = Western + Northern Alps. (c) Regional-scale section (red segment in Fig. 13a). 1 = Near Top Basement; 2 = Near Top Triassic; 3 = top Mesozoic Carbonates; 4 = Cenozoic succession; 5 = Base-Pliocene unconformity; NA = Northern Apennines; SA = Southern Alps; IFZ = Insubric Fault Zone; AACZ = Alps–Apennines clash zone; M = Moho; IEF = Inverted extensional fault (?). (For interpretation of the references to colour in this figure legend, the reader is referred to the web version of this article.)

(Fig. 14b; see paragraph 7.2 for discussion about such a lithospheric feature). Figure 14c illustrates how the Northern Apennines foothill-structures cut through the Mesozoic foreland and eventually deform the Miocene and Pliocene deposits (Cavone and Modena structures). As such, on the Apenninic margin, structures are disharmonically imbricated and intensively thrusted as they are displaced onto the foreland. Here, the related Mesozoic stratigraphic section, intruded by localized volcanic bodies (Cassano et al., 1986), is thickening towards the Alps (i.e. the Veneto Platform) whereas the overlying Plio-Pleistocene sedimentary wedge is thinned to nearly zero.

6.2.4. Cross-section 4 (Fig. 15)

Even longer than the previous one (i.e. the Alps and the Apennines fronts are 250 km apart) the cross-section links the Northern Apennines to the extreme eastern sector of the Southern Alps (the Friuli Alps). The two domains are separated by a wide and rigid Po Valley foreland unit (Fig. 15c), where the basement culmination of the Assunta1 well represents a kind of geometrical divide. With respect to the previous section, the structural disharmony between Tertiary and Mesozoic sediments is less obvious and, at the large scale, the derived structures appear to be conformably deformed and displaced on top of the basement (evaporites at base Triassic level?).

6.2.5. Cross-section 5 (Fig. 16)

The cross-section is oriented east–west and it cuts through the entire Po Valley foreland so that the western and eastern domains can be shown in terms of both sediment thickness and structural style. The western domain shows a) stratigraphic and tectonic thickening of the Tertiary clastic sediments, b) thin Mesozoic package and c) rather intense deformation of the structural units, with thrusting, possible local reactivation of the pre-Alpine extensional faults and inversion of the related half-graben basins. Conversely the eastern domain shows a thin Tertiary layer and a thick Mesozoic one, mostly Triassic in age. The domain appears gently domed and less deformed. The regional conformity among the deep and shallow model layers is outstanding over the entire section. Indeed, the shallow level deformation gradient, increasing from east to west, can be directly related to gentle folding, progressive tectonic imbrication and vertical expulsion of the Moho, in the same direction (Fig. 16b): from an average depth of 30 km below the mean sea level, that unit nearly reaches the surface at the Po Valley–Alps boundary.

6.2.6. Cross-section 6 (Fig. 17)

The cross-section runs slightly oblique to the Northern Apennines front, from WNW to ESE and it connects the Western Alps–Po Valley structural boundary with the northern-central Apennines zone. At the Moho level (Fig. 17b) the picture is similar to what has been already discussed for the previous cross-section. At the crust level (Fig. 17c), the western domain is again clearly shown with basement involvement by thrusting and inversion tectonics (i.e. the Lacchiarella inverted basin in figure). In the NW of the section, the collision between the Po Valley and the Western Alps is outstanding by extreme uplift of the Moho close to the Insubric Fault Zone (IFZ in figure) and the associated SE verging thrust-related structures. Towards the SE of the section, the Northern Apennines likely appear in the form of a major thrust-related anticline which involves the Mesozoic carbonates while pushing the very southern portion of the eastern Po Valley down to more than 10 km below the sea level.

6.2.7. Cross-section 7 (Fig. 18)

The cross-section intersects the Po Valley foreland and the external front of the Southern Alps along the east-west direction. At the crustal scale (Fig. 18b) the possible tectonic imbrication of the Moho so far observed (see Figs. 12b, 16b and 17b) is confirmed below the Western Alps. Across the rest of the region, the Moho is only gently buckled. At the Mesozoic and basement levels (Fig. 18c)

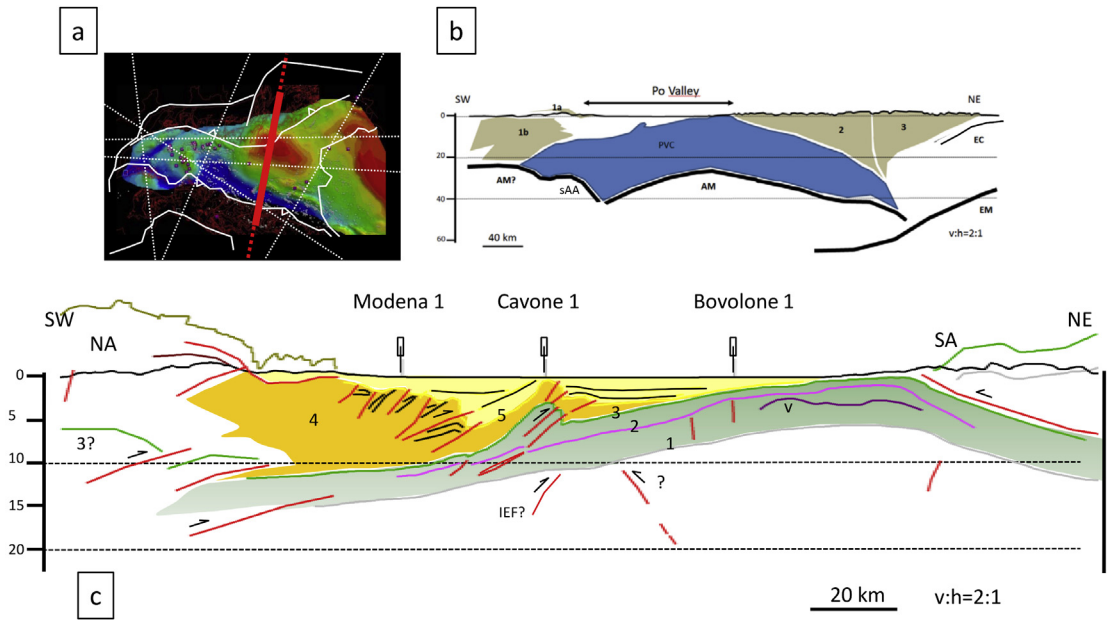

Figure 14. 3D Model Cross-section 3. (a) Location map by Top Mesozoic grid surface from this study. (b) Crustal-scale section (red dotted line in Fig. 14a). Black-thick line = Moho; EM = European Mantle; EC = European Crust; PVC = Po Valley Crust-to-Top Mesozoic; AM = Adria (Po-Valley) Mantle; 1a+1b = Northern Apennines (Allochthonous Ligurides + Autochthonous Mesozoic?); 2 = Southern Alps; 3 = Western + Northern Alps. (c) Regional-scale section (red segment in Fig. 14a). 1 = Near Top Basement; 2 = Near Top Triassic; 3 = top Mesozoic Carbonates; 4 = Cenozoic succession; 5 = Base-Pliocene unconformity; NA = Northern Apennines; SA = Southern Alps; v = volcanics; IEF = Inverted extensional fault (?). Constraints to the Tertiary geometries from Cassano et al., 1986. (For interpretation of the references to colour in this figure legend, the reader is referred to the web version of this article.)

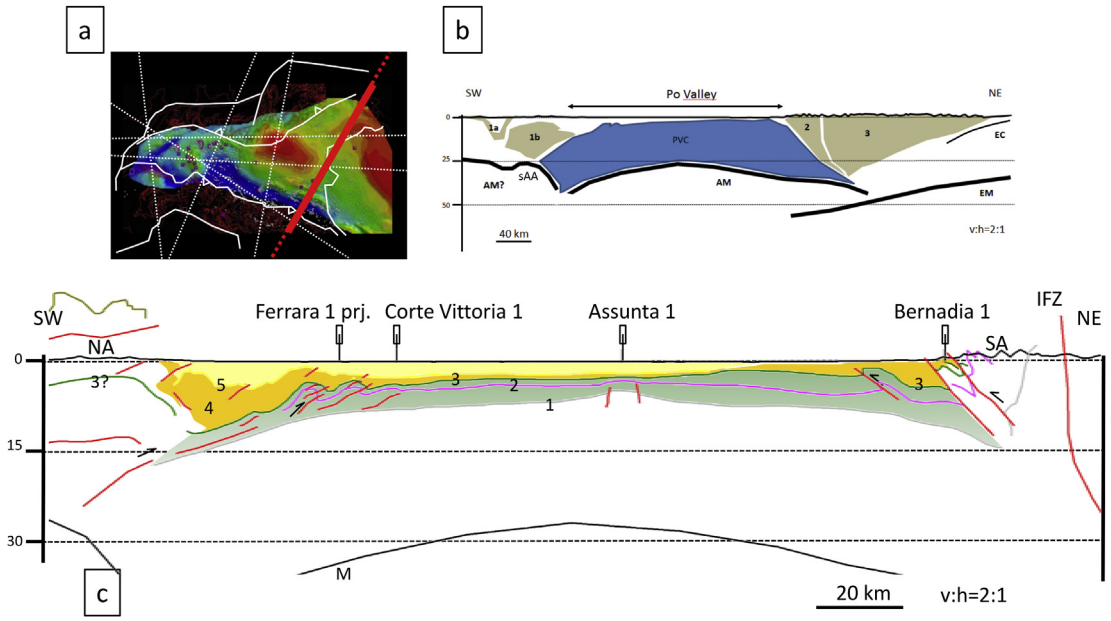

Figure 15. 3D Model Cross-section 4. (a) Location map by Top Mesozoic grid surface from this study. (b) Crustal-scale section (red dotted line in Fig. 15a). Black-thick line = Moho; EM = European Mantle; EC = European Crust; PVC = Po Valley Crust-to-Top Mesozoic; AM = Adria (Po-Valley) Mantle; 1a + 1b = Northern Apennines (Allochthonous Ligurides + Autochthonous Mesozoic?); 2 = Southern Alps; 3 = Eastern Alps. (c) Regional-scale section (red segment in Fig. 15a). 1 = Near Top Basement; 2 = Near Top Triassic; 3 = top Mesozoic Carbonates; 4 = Cenozoic succession; 5 = Base-Pliocene unconformity; NA = Northern Apennines; SA = Southern Alps; IFZ = Insubric Fault Zone; M = Moho. Constraints to the Northern Apennines Tertiary and Mesozoic geometries from Cassano et al., 1987. Constraints to the Southern Alps geometries from Nicolai and Gambini, 2007, Boccaletti et al., 2010, Ponton, 2010. (For interpretation of the references to colour in this figure legend, the reader is referred to the web version of this article.)

the western domain is evidently separated from the eastern one: Triassic–Liassic extensional faults and pre-Pliocene thrusts intensively deform the Western domain causing local inversion of the Mesozoic basins. In the eastern domain the possible top Triassic and its basement mimic the Moho crustal geometry and they are cut by isolated normal faults or wrench-type swarms (Schio-Vicenza fault zone).

6.2.8. Depth slicing

Horizontal depth slicing of the volume has been used to visualize and analyse the deep structures versus the shallow ones.

In Figure 19a the Moho architecture is cut at a depth of 30 km below the sea level whereas the base-Pliocene geometries are derived from the oblique slicing of the related surface, to better account for its regional variable dip, generally increasing west-to-

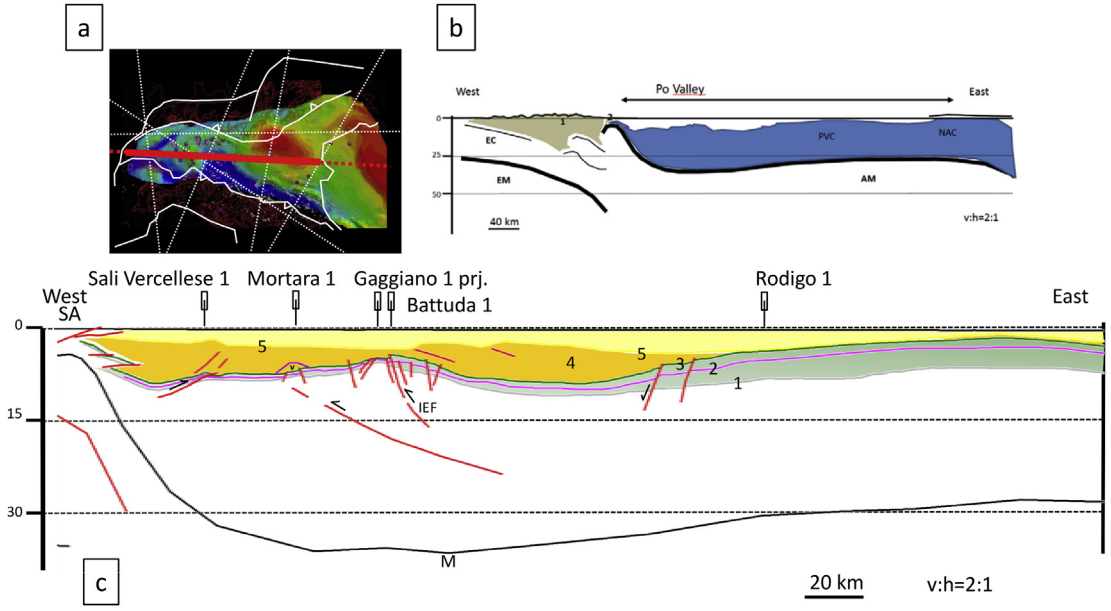

Figure 16. 3D Model Cross-section 5. (a) Location map by Top Mesozoic grid surface from this study. (b) Crustal-scale section (red dotted line in Fig. 16a). Black-thick line = Moho; EM = European Mantle; EC = European Crust; PVC=Po Valley Crust-to-Top Mesozoic; AM = Adria (Po-Valley) Moho; 1 = Western Alps; 2 = Southern Alps; 3 = Dinarides. (c) Regional-scale section (red segment in Fig. 16a). 1 = Near Top Basement; 2 = Near Top Triassic; 3 = top Mesozoic Carbonates; 4 = Cenozoic succession; 5 = Base-Pliocene unconformity; NA = Northern Apennines; SA = Southern Alps; v = Eocene volcanics; IEF = Inverted extensional fault; M = Moho. (For interpretation of the references to colour in this figure legend, the reader is referred to the web version of this article.)

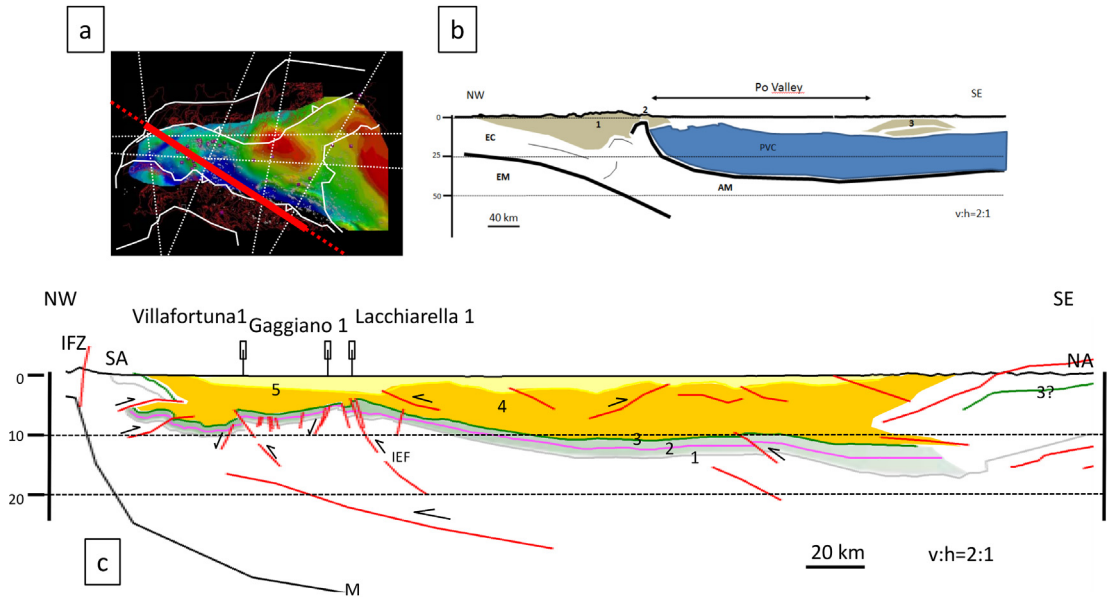

Figure 17. 3D Model Cross-section 6. (a) Location map by Top Mesozoic grid surface from this study. (b) Crustal-scale section (red dotted line in Fig. 17a). Black-thick line = Moho; EM = European Mantle; EC = European Crust; PVC = Po Valley Crust-to-Top Mesozoic; AM = Adria (Po-Valley) Mantle; 1 = Western Alps; 2 = Southern Alps; 3 = Northern Apennines. (c) Regional-scale section (red segment in Fig. 17a). 1 = Near Top Basement; 2 = Near Top Triassic; 3 = top Mesozoic Carbonates; 4 = Cenozoic succession; 5 = Base-Pliocene unconformity; NA = Northern Apennines; SA = Southern Alps; IFZ = Insubric Fault Zone; M = Moho. (For interpretation of the references to colour in this figure legend, the reader is referred to the web version of this article.)

east (2.5–5°). The integration of the deep and shallow slices shows that the base-Pliocene anticline-syncline structures are generally parallel to the Moho crustal directions, all through the eastern domain and the western domain. Here, the Monferrato structures which at the large view appear perpendicular to the Moho axis anticline (the two being W–E and NNE–SSW oriented respectively) become approximately parallel to that one (i.e. NS) once buried below the Plio-quaternary sediments of the Savigliano basin (Sb in Fig. 19a). Figure 19b allows the comparison between the 30 km Moho depth slice and the top Mesozoic contour geometries. The control of the Moho architecture on the top Mesozoic structures is outstanding so that: a) the eastern Po Valley Moho dome provides a SW dipping ramp-surface to the Mesozoic WNW–ESE oriented, NE verging thrusted folds, b) the western Po Valley dome-and-basin

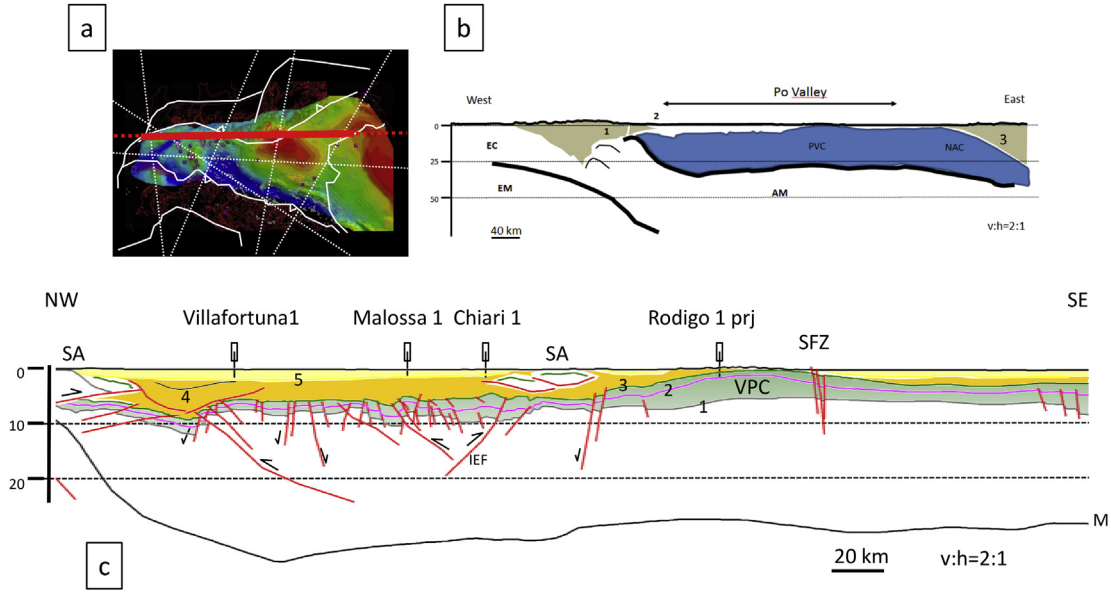

Figure 18. 3D Model Cross-section 7. (a) Location map by Top Mesozoic grid surface from this study. (b) Crustal-scale section (red dotted line in Fig. 18a). Black-thick line = Moho; EM = European Mantle; EC = European Crust; PVC = Po Valley Crust-to-Top Mesozoic; NAD = North Adriatic Crust-to-Top Mesozoic; AM = Adria (Po-Valley) Mantle; 1 = Western Alps; 2 = Southern Alps; 3 = Dinarides. (c) Regional-scale section (red segment in Fig. 18a); 1 = Near Top Basement; 2 = Near Top Triassic; 3 = top Mesozoic Carbonates; 4 = Cenozoic succession; 5 = Base-Pliocene unconformity; SA = Southern Alps; VPC = Venetian Platform Carbonate; SFZ = Schio-Vicenza Fault Zone; M = Moho. (For interpretation of the references to colour in this figure legend, the reader is referred to the web version of this article.)

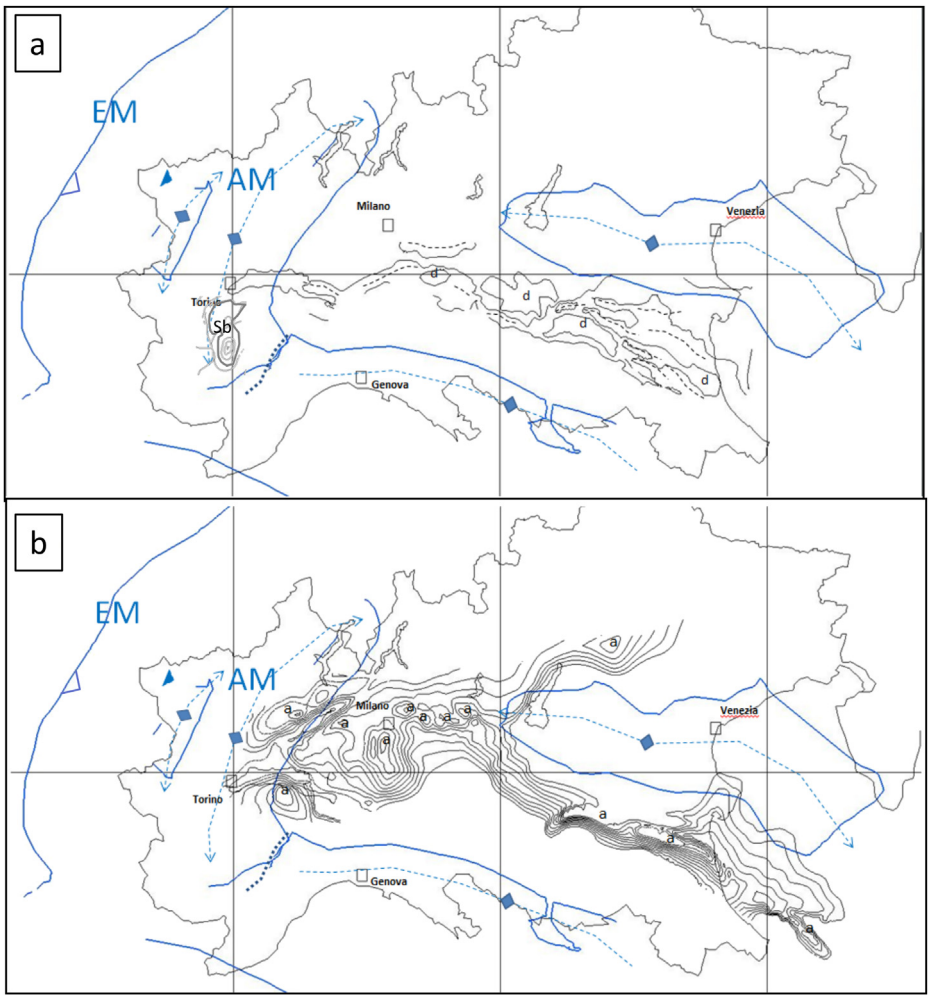

Figure 19. Moho horizontal-depth slice (dark blue) at 30 km below the mean sea level against base Pliocene depth slices (a) and structure contouring of the Mesozoic grid-surface (b). Blue dotted lines are thrusts and anticline axis of the Moho. EM = European Moho; AM = Adria Moho. Grid for scale is 200 km Figure 18a: black dot lines are fold hinges of the Pliocene structures; d = major Pliocene depocenters; AB = Asigliano basin. Figure 18b: a = major anticline culminations. Grid for scale is 200 km. See text for discussion. (For interpretation of the references to colour in this figure legend, the reader is referred to the web version of this article.)

Mesozoic structures develop inside the crustal scale low that results from folding and thrusting of the Moho in the surrounding regions.

6.3. Isopach maps

The isopach maps of the crust, of the Mesozoic, of the Cretaceous–Jurassic and of the Triassic sedimentary formations were produced from the performed 3D model to infer the architecture of the Adria passive margin to which the Po Valley basin did belong in pre-Alpine time (see Discussion section).

The thickness map of the crust (Fig. 20a) shows a dramatic east-to-west thinning of the crust layer, from a thickness of about 30 km in the central Po Valley to less than 10 km close to the Western Alps boundary. Conversely, along the north–south direction, the crust thickness shows two maximum values of about 40 km below the Apennines and the Alps and a relative minimum value of 30 km below the Po Valley basin.

The isopach map of the Mesozoic formations (Fig. 20b) suggests a regional-scale thinning towards the west and the south. In more details, the thickness-related fabric indicates the presence of some basins and highs oriented N–S and NNE–SSW, perpendicular to the Alps and Apennines belt directions.

The thickness distribution of the Cretaceous–Jurassic sediments (Fig. 20c) confirms the thinning direction, to the south and the west, and the paleo-trends NS orientation already shown by the Mesozoic isopach. Possible dimensions of the related units are 5–10 km by 10–30 km, normal and parallel to the basin axis respectively.

The Triassic isopach (Fig. 20d) supports the Mesozoic thinning directions, to the west and south. Nevertheless, the detail depositional trends are, at the map scale, invisible in the western Po Valley and masked by the Veneto carbonate platform across a large part of the eastern Po Valley. Such trends become eventually evident by some Triassic basins recently interpreted on 3D seismic data at the boundary between the eastern Po Valley and the northern Adriatic domain (Franciosi and Vignolo, 2002). Like the Cretaceous-Jurassic ones, they are NNE–SSW oriented and their dimensions are 30–50 km by 80–100 km normal and parallel to the basin axis, respectively.

7. Discussion

The results from the performed 3D model leave a number of points open for discussion. They will be addressed hereafter by answers to selected questions.

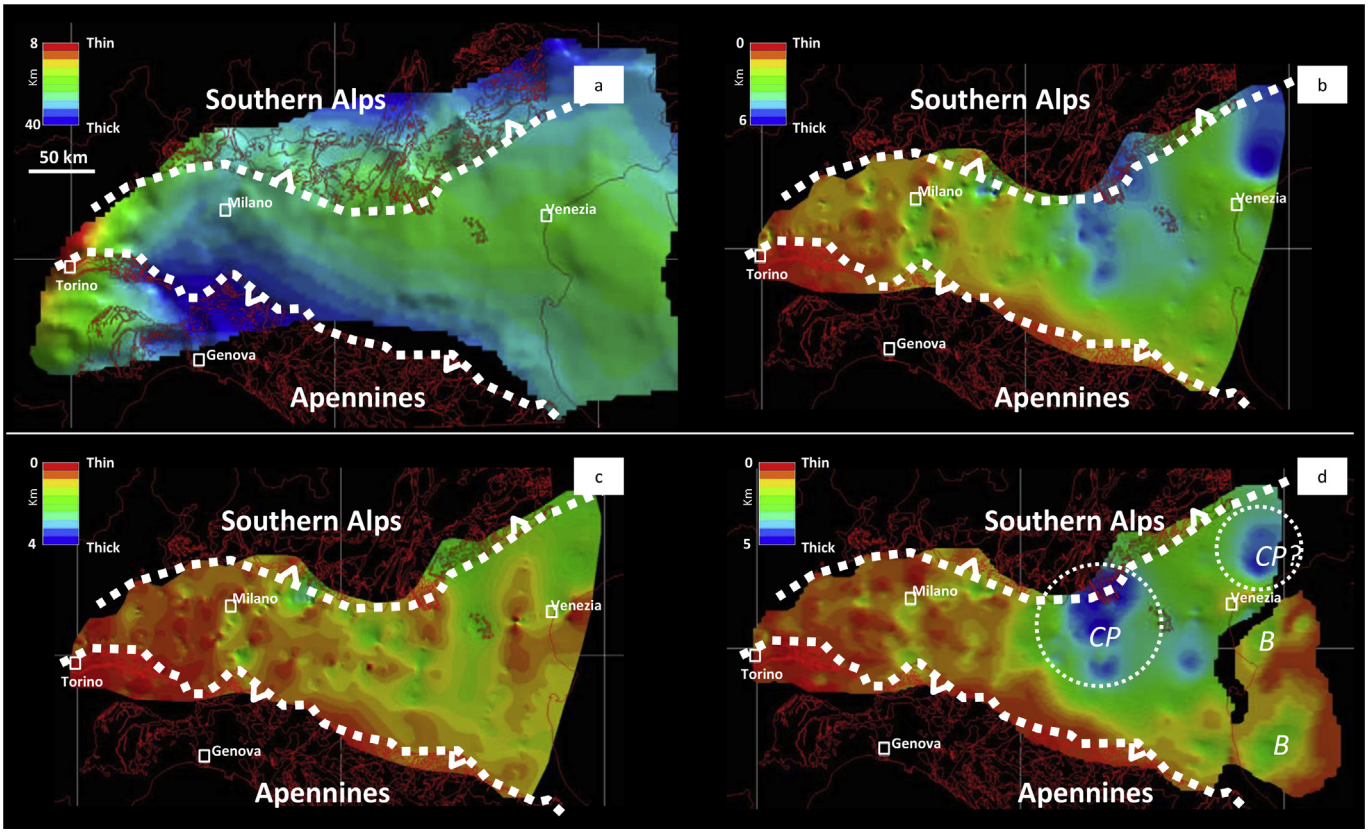

Figure 20. (a) Isopach map of the crust in the Po Valley basin. (b) Isopach map of the Mesozoic sedimentary successions in the Po Valley basin. (c) Isopach map of the Cretaceous–Jurassic sedimentary successions in the Po Valley basin. (d) Isopach map of the Triassic sedimentary successions in the Po Valley basin. (CP) Carbonate Platform facies from outcrops and wells; (B) Triassic basins from 3D seismic data (Franciosi and Vignolo, 2002); Outcrops, coast-line & northern Italy state boundaries in red. Grid in all maps is 200 km. (For interpretation of the references to colour in this figure legend, the reader is referred to the web version of this article.)

7.1. Was the 3D model worth the effort?

It may sound obvious nevertheless the immediate answer is: yes, it was. Indeed, although the data that have been collected and put together are well known in the public domain, the final 3D geo-volume offers a new and interactive view of the structures that form the Po Valley basin, from the very deep Moho to the surface topography. Such integration allows the different interpretations published during the last 50 years to be compared and progressively validated. The model, despite the many uncertainties, is definitely a big step ahead for a modern review of the basin. It can be used as precious analog for the understanding of any other foreland-foredeep domain world-wide.

7.2. What is the major suggestion from the model in terms of present-day crustal architecture?

The model shows (Fig. 21; see all cross-sections in Figs. 12–18) at which level of deformation the present Adria-Po Valley crustal unit is caught in between the Alps and the Apennines belts, apparently detached and floating above the Moho mega-tectonics. Not surprisingly, inspection of the final geo-volume demonstrates that the Moho geometries and the supposed geodynamics definitely control the structure distribution at any of the model layers: in the western Po Valley domain, the horizontal torsion and vertical squeezing of the mantle is accommodated at the basement, Mesozoic and Cenozoic level by intense faulting, folding and tectonic over-thickening of the crust with large dispersion of the structural orientations. In the eastern Po Valley, lithospheric flexuring of the related Adria plate allows contrasting displacement of the Southern Alps and the Apennines onto the regionally bulged Po Valley foreland. Some possible NNE–SSW oriented transfer zones can be argued to be fragmenting the present Moho unit thus separating the western Po Valley domain from the eastern one (see TZ elements in Fig. 21).

The performed 3D model also points to the issue of a possible connection between the sub-Apenninic Moho and the Adria-Po Valley Moho. This hypothesis would imply that the Po Valley Moho is folded but not vertically offset below the Apennines while the underlying Adria mantle would undergo progressive delamination and subduction. Despite any tomography and crustal refraction acquisition (Margheriti et al., 2006, and reference therein), hard data about the Moho-mantle mechanical coupling or decoupling inside the Apennine subduction are still ambiguous. Nevertheless the aforementioned crustal framework, although largely debatable, would support some of the available models about the Apennine kinematics while eventually neglecting others. Indeed, Roure et al. (1991 and 2012) and the RETREAT working group (see Figure 1 in Picotti and Pazzaglia, 2008) propose similar kinematics for the southern and the northern Apennines respectively where delamination, subduction and wedging of the Adria mantle occur below a folded yet continuous Adria Moho surface. Conversely, Doglioni (1991, 1994), Doglioni et al. (1996) and Carminati et al. (2003) suggest steep subduction of the Adria slab and the related Moho below the Apennines. This model seems also the preferred one for Picotti and Pazzaglia (2008) when they try to integrate deep and shallow structures of the south-eastern segment (i.e. the Bologna region) of the Northern Apennines. The

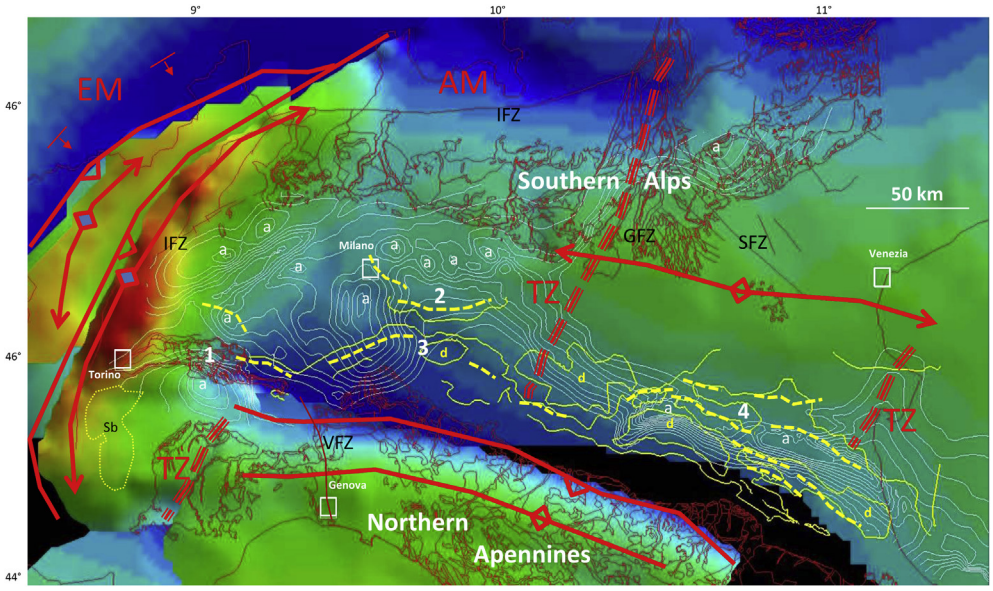

Figure 21. Tectonic summary in the Po Valley basin by Moho Mesh-surfaces (related tectonics in red), top Mesozoic contouring (white) and base Pliocene fold hinge distribution (yellow dot lines). EM = European Moho; AM = Adria Moho; TZ = transfer zone at Moho level. 1 = Monferrato Arch; 2 = Milano Arch; 3 = Emilian Arch; 4 = Ferrara-Romagna Arch; a = anticline culmination at top Mesozoic; d = depocenters at base Pliocene level. Sb = Savigliano basin. IFZ = Insubric Fault zone; VFZ = Villavernia Fault Zone; GFZ = Giudicarie Fault Zone; SFZ = Schio-Vicenza Fault Zone. Outcrops, coast-line & northern Italy state boundaries in red. Latitude and Longitude values are North and East of Greenwich. (For interpretation of the references to colour in this figure legend, the reader is referred to the web version of this article.)

process would guide back-arc progradation and limited frontal compression across the belt while partly controlling the tectonic subsidence of the foreland. The in-progress integration of the 3D model structures with the earthquake data from the Italian catalogue (INGV) will eventually provide further insights on the issue.

7.3. *What about the Po Valley unit within the so-called Alps–Apennines structural junction?*

At the Alps–Apennines junction (see Figs. 4 and 21), the 3D model shows a very complex architecture of the Po Valley Moho, with possible NW verging tectonic imbricates, below the Western Alps (Figs. 12b, 16b, 17b) and a NW–SE oriented fold, with short limb towards the NNE, below the Northern Apennines (Fig. 13b). The Moho deformation in the region is accommodated within the Po Valley crust by intense folding and faulting, these being imaged by the dip-map of the carbonate surface-grid (see Fig. 11). Not by coincidence, the map shows that the structural complexity across the basin increases from NE to SW and it appears to reach its maximum in the extreme western Po Valley, the likely Alps–Apennines junction.

The described framework appears three-dimensionally consistent although neither in the model nor in the literature there are evidences of the possible transfer zone (see Fig. 4) that would allow the opposite motion between the Alpine and the Apennines Moho sectors.

7.4. *What about the Po Valley structural style?*

The 3D model analysis, through slicing of the volume and the isopach-map building, proves that the Po Valley structural style strictly refers to the interaction among the lithosphere dynamics, the related geometry and the paleo-margin architecture (thickness, stratigraphy, fault orientation).

Indeed thick-skinned tectonics can be largely demonstrated in the western Po Valley where a thin Mesozoic sequence is reported and modelled (see also Cassano et al., 1986; Bello and Fantoni, 2002; Fantoni et al., 2004; Picotti and Pazzaglia, 2008; Fantoni and Franciosi, 2010). As such, involvement of the basement prevails with local reactivation of the Triassic–Jurassic faults and inversion of the related extensional basins (see cross-sections in Figs.12 and 13, 16–18). In the region structures at the different stratigraphic levels are vertically coupled with local exception at the front of the thrust belts.

Conversely, in the eastern Po Valley, mainly thin-skinned tectonics occurs by folding and thrusting (see Figs. 14 and 15), these being likely controlled by a relatively thick Mesozoic package detached and displaced from the basement below (see also Cassano et al., 1986; Castellarin et al., 1985; Picotti and Pazzaglia, 2008; Toscani et al., 2006, 2009; Fantoni and Franciosi, 2010). Involvement of that basement becomes evident towards the Apennines and the Southern Alps yet it can also be speculated to enhance the regional doming of the foreland.

In detail, when referring to each of the Po Valley tectonic arches (and the related foreland), the structural style can be defined by some specific elements:

a. Monferrato Arch (see Fig. 12c): basement involvement, thrust-related structures across the Mesozoic carbonates and the Cenozoic succession; weak detachment (base of Gallare? Top of the Scaglia?) of the Cenozoic sediments from the Mesozoic one. A major detachment decouples the possible Mesozoic structures from the Ligurides Allochthonous in the Monferrato belt region.
b. Emilian Arch (see Figs. 13c, 16c, 17c): possible basement involvement and thrust-related structures across the Mesozoic carbonates below the Apennines. Thrust-related structures across the foreland Mesozoic carbonates, with structural inversion of extension-related basin and basement up-thrusts. The buried Emilian arch is essentially made by thrusts and folds in the Cenozoic succession which is almost completely detached (base of Gallare? Top of the Scaglia?) from the related substratum (compare structures at the base Pliocene grid with the top Mesozoic ones in Figs. 9 and 7 respectively).

c. Milano arch: this arch is essentially provided by thrust-related structures across both the Mesozoic carbonates and the Cenozoic succession, with basement involvement and local inversion of Triassic–lower Jurassic basins (Fig. 13c, northern sector, and 18c, the Malossa-Chiari structures in the western sector). A weak structural disharmony can be demonstrated among the different structural levels (basement, Mesozoic carbonates, Cenozoic succession) so that the major detachment would likely be intra-basement.
d. Ferrara-Romagna arch: the Mesozoic and Cenozoic structures are mechanically coupled at the large structural wavelength (Figs.14c and 15c; again, compare structures at the base Pliocene grid with the top Mesozoic ones in Figs. 9 and 7 respectively). In detail, close to the Northern Apennine front and on top of the major anticlines, the Cenozoic succession appears to be strongly decoupled from the Mesozoic one (top of the Scaglia level?), this being diffusely detached in its turn from the underlying basement (base Triassic detaching level?). A minor detachment level is likely located at the transition between the Miocene and the Pliocene successions. Eventually the basement is a) likely involved by thrusting below the Apennines, b) locally reactivated by compression in correspondence of extensional faults within the tectonic arch domain (IEF in Fig. 14c below the Cavone structure), c) buckled by folding into a crustal scale "pop-up" feature in the foreland.

7.5. *What is the 3D model contribution to the understanding of the Adria passive margin anatomy?*

The Po Valley is the remnant of the northern sector of the Adria plate which collided with the European plate during the Alpine orogeny. Therefore, and despite the great uncertainty, the isopach maps that have been derived from the 3D model can be used to speculate about the anatomy of the ancient Adria passive continental margin.

The isopach map of the crust implies thinning of the Po Valley lithosphere from east to west. This is then compatible with a former Adria passive margin thinning towards the present West orientation. Conversely, the same isopach-map shows some tectonic over-thickening of the crust to the north and south of the Po Valley basin, that is likely due to the Alps and Apennines orogenies. Deep over-thickening inside the foreland domain around the Milano area (see cross-sections in Figs. 16–18 and isopach-map of the crust in Fig. 20a) could be eventually due to some possible intra-plate tectonics that inverted the pre-alpine faulted blocks. Such a thickness distribution suggests that the ancient Adria plate was eventually much wider than what it shows at present.

In terms of the possible pre-compressional Mesozoic grain the Cretaceous–Jurassic isopach map and the analysis of the Triassic thickness distribution allow some primary NNE–SSW oriented trends to be speculated, with second order EW-oriented ones. Such extension-related fabric confirms and completes the results of a number of studies performed across the South Alpine outcrops (Bertotti et al., 1993; Fantoni and Scotti, 2003; Berra et al., 2009) and the ones provided by some regional studies from the industry in the Po Valley sub-surface (Bongiorni, 1987; Fantoni et al., 2003, 2004; Franciosi and Vignolo, 2002).

The integration of the extension-related fault trends coming from the literature and the performed 3D model allows the possible pre-alpine margin kinematics to be suggested:

a) during the Triassic, extension caused symmetric stretching of the Adria lithosphere in the western Po Valley and asymmetric stretching in the eastern Po Valley (i.e. towards the current Adriatic and Dinarides geological realms). Symmetric stretching led to a sort of chocolate-table tectonic fabric in the western Po Valley, with fault sets perpendicular to each-others (NNE–SSW and E–W). At the same time asymmetric stretching made N–S oriented faults the predominant ones in the eastern Po Valley.
b) In Liassic times, the margin was definitely stretched in the present-day E–W direction all through the Po Valley-Adria

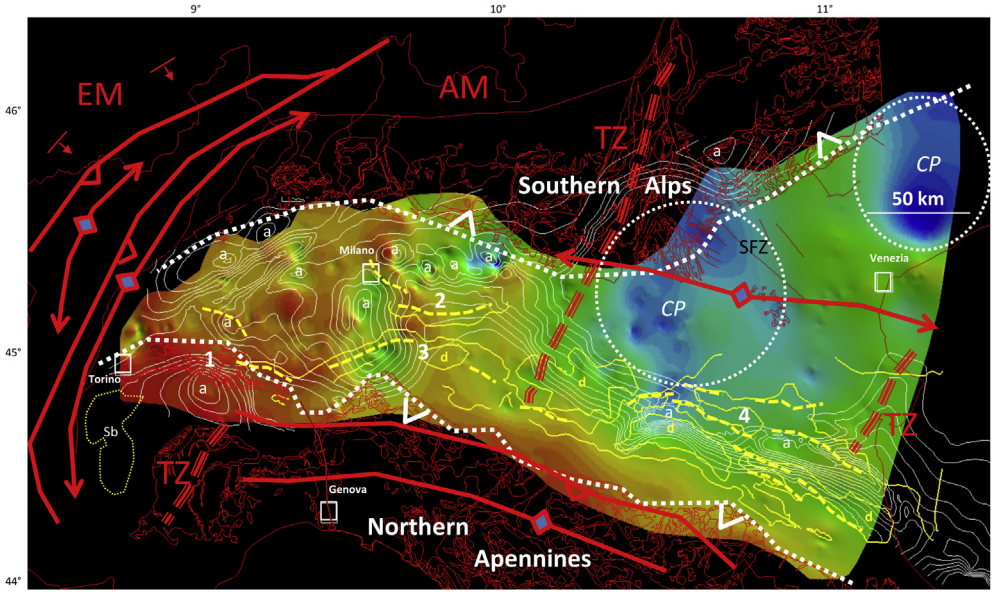

Figure 22. Structural interference and Tectonic heritage in the Po Valley basin by Mesozoic isopach-map, top Mesozoic contouring (white) and base Pliocene fold hinge distribution (yellow dot line). EM = European Moho; AM = Adria Moho; TZ = transfer zone at Moho level; CB = Triassic Carbonate Platform. 1 = Monferrato Arch; 2 = Milano Arch; 3 = Emilian Arch; 4 = Ferrara-Romagna Arch; a = anticline culmination at top Mesozoic; d = depocenters at base Pliocene level. Sb = Savigliano basin. IFZ = Insubric Fault zone; VFZ = Villavernia Fault Zone; GFZ = Giudicarie Fault Zone; SFZ = Schio-Vicenza Fault Zone. Outcrops, coast-line & northern Italy state boundaries in red. Latitude and Longitude values are North and East of Greenwich. (For interpretation of the references to colour in this figure legend, the reader is referred to the web version of this article.)

micro-plate. The derived half-graben and horst features are hence univocally NS oriented.

7.6. What is the 3D model contribution to the understanding of the estension-compression structural interference that modelled the Adria-Po-Valley plate?

As by the above considerations, the entire Adria-Po Valley passive margin was modelled by the Mesozoic extension into highs and basins that were oriented at high angle with respect to the Alpine belts. Indeed, when comparing the 3D model isopach maps with the present structure orientation (Fig. 22), the heritage of the extension-related units on the current compressional ones becomes evident by the west-to-east change in structural style across the basin (see above):

a) thin Mesozoic and chocolate-table extension-related fault trends enhanced thick-skinned alpine tectonics and dome-and-basin structural fabric in the western Po Valley, west of Milan;
b) lateral change in facies of the Mesozoic sediments constrained the localized inversion of few of the Jurassic basins, to the east of Milan (see the Lacchiarella structure in Fig. 17 and the Chiari structure in Fig. 18);
c) in the eastern Po Valley, the presence and areal extension of a huge Triassic platform carbonate units locked the progression of both the South-Alpine and Northern Apennines fronts as they try to advance towards the Po Valley foreland;
d) although extremely speculative at present, the inferred NNE–SSW oriented transfer zones that separated into mega-compartments the Po-Valley pre-alpine crust possibly controlled the indentation of the margin into the European Plate and partly constrained the development of the Northern Apennines tectonic arches.

Once again the performed 3D model integrates and completes at the scale of the entire Po Valley basin what has been locally suggested by various papers in the past (Fantoni and Franciosi, 2010; Ravaglia et al., 2006; Doglioni and Carminati, 2008 and various references therein).

It is interesting to note that a similar structural interference can be observed all along the Adriatic foreland-foredeep domain, this being the prosecution of the Po Valley unit towards the SSE. Across that domain, caught between the central and southern Apennines from the west and the Dinarides–Albanides–Hellenides belts from

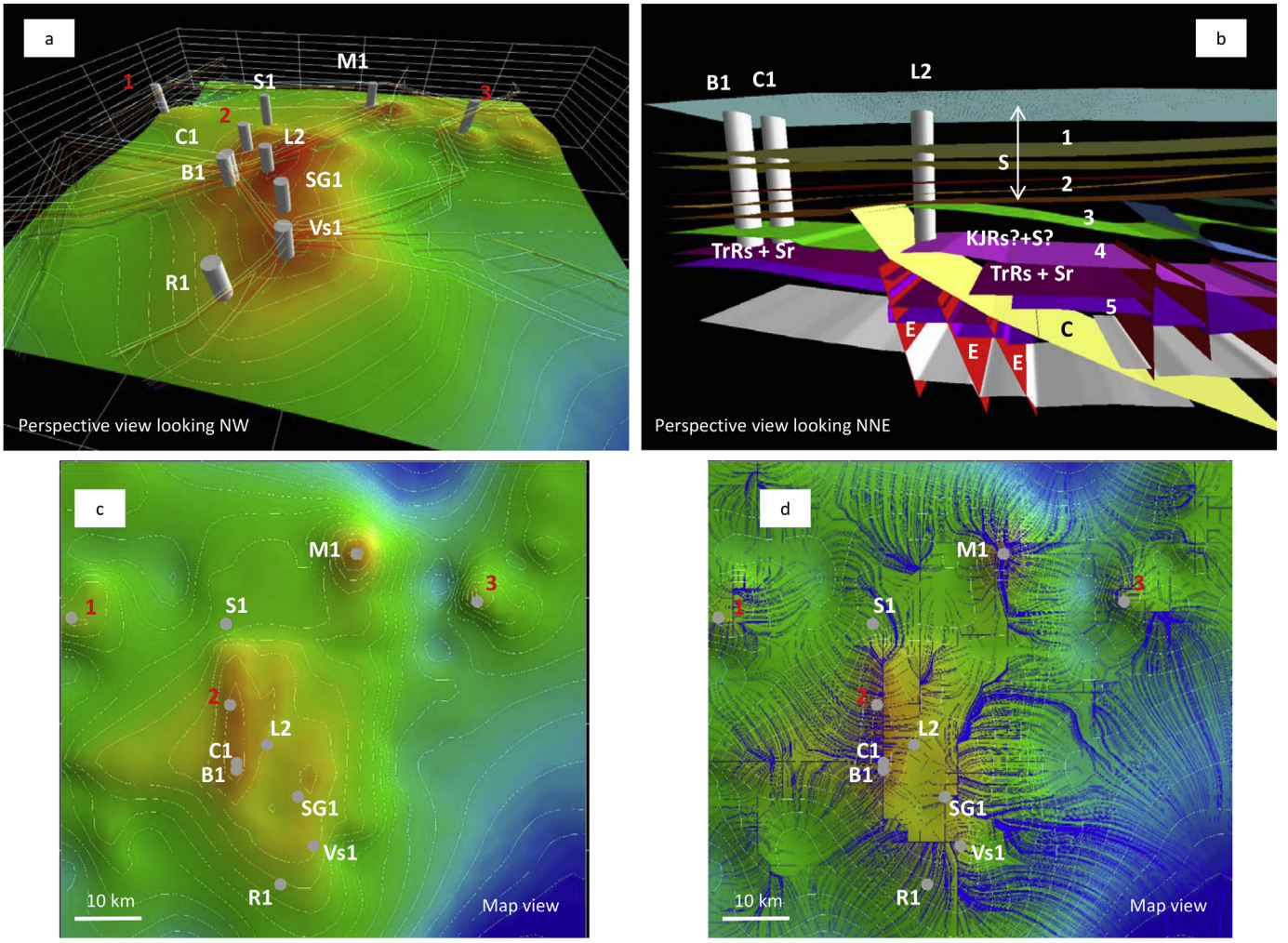

Figure 23. (a) Structures at the Top Mesozoic and source data for 3D model building in the Milano area. 1 = Villafortuna Field; 2 = Gaggiano Field; 3 = Malossa Field. Wells: L2 = Lacchiarella2, Mz1 = Monza1, B1 = Battuda1, C1 = Cerro1, S1 = Settimo Milanese1, Vs1 = Vallesalimbene1, R1 = Rea1. (b) Structural interference among extensional and compressional structures (modified from Cassano et al., 1986): 1 = Base Pliocene, 2 = Top Oligocene, 3 = Top Mesozoic Carbonates, 4 = Top Trias, 5 = Basement. E = Extension-related normal faults; C = contraction-related thrusts. TrRs + Sr = Triassic reservoir & source rock; KJRs?+S? = Cretaceous–Jurassic possible Reservoir + Possible Seal (see text for discussion); S = Seal. (c) Structural geometries at Top Triassic. (d) Migration paths at Top Triassic.

the east, the Jurassic–Cretaceous extensional units, NNE–SSW oriented are overprinted by the compressional ones, generally NW–SE oriented. The result of such an overprinting is outstanding on both the sides of the Adriatic region where the compartmentalization of the Apennines, and Dinarides–Hellenic thrust fronts often relates to pre-compression lateral facies transitions (Roure et al., 2004; Shiner et al., 2013).

7.7. What is the impact of the 3D model on the reviewing of the Mesozoic hydrocarbon system across the Po Valley basin?

The application of the performed 3D structural model to some exploration target validation across the Po Valley (Petroceltic internal reports) indicates that the model can be a precious tool especially during the regional scale play risk-analysis and hydrocarbon-system definition. Once some extra data are added to the base-framework, the model results would also become useful during the progressive and more refined lead–prospect evaluation.

Slicing across the regional 3D model provides a preliminary imaging of the possible trap types that can be found at the Mesozoic structural level.

The isopach maps derived from the 3D model give some guidelines about the Triassic and Jurassic tectonic trends and the related possible source thickness distribution across the basin.

Because the Cretaceus–Jurassic successions are a debated seal to the underlying Triassic reservoir, the ultimate (ubiquitous and laterally continuous) top seal to the Mesozoic traps is generally provided by the Tertiary clastic formations. Therefore the 3D model top Mesozoic depth map can be an immediate estimation of the possible top seal presence and efficiency.

The trap type that the model helps to define across the different Po Valley domains might be used to suggest a lateral-seal risk. As such, presence, geometry, age of the faults associated to the possible trap can be recognized from the model and the related juxtaposition diagram (Allan, 1989) can easily be approximated once the permeable rock formations are defined in the geometries under study.

In terms of reservoir, the Mesozoic isopach map can be used to define the reservoir-thickness domain whereas the trap-type that the 3D model allows to visualize, immediately contributes to a qualitative estimation of the distribution of the possible fracture sets that would be associated to the target structure. Eventually the performed 3D structural model would provide a preliminary support to the generation and migration issue by the integration of the different isopach maps into the necessary thermal-maturity model and by the qualitative visualization of the final hydrocarbon catchment areas and the related migration paths.

As an example of the 3D model application to the exploration workflow at the oil-field scale, Figure 23 illustrates the major steps in the evaluation of the Mesozoic play in the central area of the western Po Valley.

a. Figure 23a: the 3D model is built from the source data (sections, maps and wells) and rendered by depth of the top Mesozoic grid. Current burial of the structure is defined and, eventually, a dip-map can be derived to gain information about the possible fault trends and potential fracture sets with respect to the actual stress-field. By the Allan diagram analysis (Allan, 1989), lithology juxtaposition across the model faults can be defined.
b. Figure 23b: a refined 3D model building of the structure anatomy is performed so that 1) trap-type, 2) reservoir-seal-source presence-distribution from the wells, 3) fault geometries are investigated. At this stage, the structures supply the framework for compaction analysis and the possible thermal modelling across the selected area.
c. Figure 23c: the present depth geometries of the near top Triassic are visualized to constrain the possible top reservoir architecture. Reservoir presence and distribution can be added as attributes on the top grid; isopach maps can be built to understand the reservoir thickness distribution and the paleotrends.
d. Figure 23d: the migration paths are derived from the model to check for drainage area distribution and potential accumulation (note Oil-field location).

7.8. What are the future applications of the performed 3D model?

The possible applications of the performed 3D structural model are multiple for both industry and academia. Despite the many uncertainties, the geo-volume that has been built can work as a geo-referenced 3D geological box where all kind of data and measurements can be input and analysed against the recognized geometries. In addition, the tectonic kinematics that built the basin architecture can also be studied from both 3D block restoration and 2D cross-sections sliced from the volume. As a result it can represent a powerful tool for different actions: in the hydrocarbon domain the comparative analysis between the exploration results and the 3D model structures can supply a way to review the past exploration strategy and support the future one. The modelled geometries can also provide understanding and operational suggestions for methane and CO_2 storage within the basin. Finally, the reconstructed crustal scale architecture of the model can also be referenced as a unique geometrical support in the analysis of the Po Valley earthquake catalogue (INGV) and the review of the derived seismogenic zonation.

For all of the aforementioned applications it is to be said that the model needs strong refining at the structure scale, so that all of the crustal layers, from basement to base Pliocene, will be able to perfectly tie to the well information and the available seismic data. Very likely a number of additional, local scale 3D models will be used to tackle the goal and interact with the crustal scale one.

8. Conclusions

A 3D model of the Po Valley basin from the Adriatic to the Western Alps has been built by integration and consistency check of the available data-set. It is definitely an interactive model and it shows by its geometrical continuity and consistency all of the principle layers from the Moho to the digital topography.

The performed 3D Model represents a unique result in the region as it is able to illustrate the Po Valley architecture like none of the previous work in the area did so far. Also, the model can be seen as a possible analog to other deformed foreland-foredeep basins around the world.

Results from the modelling show how the Moho crustal-scale architecture strongly constrains geometry and distribution of all of the structures that have been built at any of the shallowest model layers. The structure reconstruction illustrates the structural interference between Triassic–Jurassic extension and late Cretaceous–Tertiary compression from the crustal to the oil-field scale.

While a review of the exploration results and strategy in the basin against the 3D model structures is currently in progress, a number of future applications (CO_2–CH_4 storage, earthquake analysis among them) could be eventually supported by the final geo-volume once refined to its maximum detail.

Acknowledgements

The authors would like to thank two anonymous reviewers for the detailed revision of the paper and the related valuable suggestions. C.Turrini thanks also A.Ravaglia (PetroSa) for the review of an early draft of the manuscript.

References

Allan, U.S., 1989. Model for hydrocarbon migration and entrapment within faulted structures. Am. Assoc. Pet. Geol. Bull. 73, 803–881.

Argnani, A., Ricci Lucchi, F., 2001. Terziary silicoclastic turbidite systems of the Northern Apennines. In: Vai, G.B., Martini, I.P. (Eds.), Anatomy of an Orogen: the Apennines and Adjacent Mediterranean Basins. Kluwer Academic Publishers, pp. 327–350.

Bartolini, C., Caputo, R., Pieri, M., 1996. Pliocene-Quaternary sedimentation in the Northern Apennine Foredeep and related denudation. Geol. Mag. 133, 255–273. http://dx.doi.org/10.1017/S0016756800009006.

Bello, M., Fantoni, R., 2002. Deep Oil Plays in the Po Valley: Deformation and Hydrocarbon Generation in a Deformed Foreland. AAPG HEDBERG CONFERENCE, "Deformation History, Fluid Flow Reconstruction and Reservoir Appraisal in Foreland Fold and Thrust Belts" May 14–18, 2002, Palermo – Mondello (Sicily, Italy).

Berg, R.C., Russell, H., Thorleifson, L.H. (Eds.), 2004. Three-dimensional Geological Mapping for Groundwater Applications – Workshop. Extended Abstracts. Illinois State Geological Survey. Open-File Series 2004-8. http://library.isgs.uiuc.edu/Pubs/pdfs/ofs/2009/ofs2009-04.pdf.

Berra, F., Galli, M.T., Reghellin, F., Torricelli, S., Fantoni, R., 2009. Stratigraphic evolution of the Triassic–Jurassic succession in the Western Southern Alps (Italy): the record of the two-stage rifting on the distal passive margin of Adria. Basin Res. 21, 335–353.

Bertotti, G., Picotti, V., Bernoulli, D., Castellarin, A., 1993. From rifting to drifting: tectonic evolution of the South-Alpine upper crust from the Triassic to the Early Cretaceous. Sediment. Geol. 86, 53–76.

Bertotti, G., Capozzi, R., Picotti, V., 1997. Extension controls Quaternary tectonics, geomorphology and sedimentations of the N-Apennines foothills and adjacent Po Plain (Italy). Tectonophysics 282, 291–301.

Bigi, G., Castellarin, A., Catalano, R., Coli, M., Cosentino, D., Dal Piaz, G.V., Lentini, F., Parotto, M., Patacca, E., Praturlon, A., Salvini, F., Sartori, R., Scandone, P., Vai, G.B., 1989. Synthetic Structural-kinematic Map of Italy, Scale 1:2.000.000. CNR, Progetto Finalizzato Geodinamica, Roma.

Boccaletti, M., Corti, G., Martelli, L., 2010. Recent and active tectonics of the external zone of the Northern Apennines (Italy). Int. J. Earth Sci. Geol. Rundsch. http://dx.doi.org/10.1007/s00531-010-0545-y.

Bongiorni, D., 1987. La ricerca di idrocarburo negli alti strutturali mesozoici della Pianura Padana: l'esempio di Gaggiano. In: Atti Tic. Sc. Terra, vol. XXXI, pp. 125–141.

Burrato, P., Ciucci, F., Valensise, G., 2003. An inventory of river anomalies in the Po Plain, Northern Italy: evidence for active blind thrust faulting. Ann. Geophys. 46 (5), 865–882.

Carminati, E., Doglioni, C., 2012. Alps vs. Apennines: the paradigm of a tectonically asymmetric Earth. Earth-Sci. Rev. 112, 67–96.

Carminati, E., Doglioni, C., Scrocca, D., 2003. Apennines subduction-related subsidence of Venice (Italy). Geophys. Res. Lett. 30 (13), 1717. http://dx.doi.org/10.1029/2003GL017001.

Carminati, E., Scrocca, D., Doglioni, C., 2010. Compaction-induced stress variations with depth in an active anticline: northern Apennines, Italy. J. Geophys. Res. 115, B02401. http://dx.doi.org/10.1029/2009JB006395.

Casero, P., 2004. Structural setting of petroleum exploration plays in Italy. In: Crescenti, V., D'Offizi, S., Merlino, S., Sacchi, L. (Eds.), Geology of Italy. Special Volume of the Italian Geological Society for the IGC 32 – Florence.

Casero, P., Rigamonti, A., Iocca, M., 1990. Paleogeographic relationship during Cretaceous between the Northern Adriatic area and the Eastern Southern Alps. Mem.Soc.Geol.It. 45, 807–814.

Cassano, E., Anelli, L., Fichera, R., Cappelli, V., 1986. Pianura Padana, interpretazione integrata di dati Geofisici e Geologici. In: 73° Congresso Soc. Geol. It., Roma.

Castellarin, A., 2001. Alps–Apennines and Po Plain-Frontal Apennines relationships. In: Vai, G.B., Martini, I.P. (Eds.), Anatomy of an Orogen. The Apennines and Adjacent Mediterranean Basins. Kluver, London, pp. 177–196.

Castellarin, A., Cantelli, L., 2010. Geology and evolution of the Northern Adriatic structural triangle between Alps and Apennines. Rend. Fis. Acc. Lincei 21 (Suppl. 1), S3–S14. http://dx.doi.org/10.1007/s12210-010-0086-0.

Castellarin, A., Vai, G.B., 1982. Introduzione alla geologia strutturale del Sudalpino. In: Castellarin, A., Vai, G.B. (Eds.), - Guida alla gelogia del Sudalpino centro orientale, Guide Geol. Reg., Soc. Geol. It., pp. 1–22.

Castellarin, A., Vai, G.B., 1986. Southalpine versus Po Plain apenninic arcs. In: Wezel, F.C. (Ed.), The Origin of Arcs, Development in Geotectonic. Elsevier, Amsterdam, pp. 253–280.

Castellarin, A., Eva, C., Giglia, G., Vai, G.B., 1985. Analisi strutturale del Fronte Appenninico Padano. G. Geol., Sez. 3° 47 (1–2), 47–75.

Castellarin, A., Nicolich, R., Fantoni, R., Cantelli, L., Sella, M., Selli, L., 2005. Structure of the lithosphere beneath the Eastern Alps (southern sector of the TRANSALP transect). Tectonophysics 414, 259–282.

Caumon, G., Collon-Drouaillet, P., Le Carlier, C., Viseur, S., Sausse, J., 2009. Surface-based 3D modeling of geological structures. Math. Geosci. 41, 927–945. http://dx.doi.org/10.1007/s11004-009-9244-2.

Channell, J.E.T., D'Argenio, B., Horvath, F., 1979. Adria, the African promontory, in Mesozoic Mediterranean palaeogeography. Earth Sci. Rev. 15, 213–292.

Cimolino, A., Della Vedova, B., Nicolich, R., Barison, E., Brancatelli, G., 2010. New evidence of the outer Dinaric deformation front in the Grado area (NE-Italy). Rend. Fis. Acc. Lincei 21 (Suppl. 1), S67–S179. http://dx.doi.org/10.1007/s12210-010-0096-y.

CROP Project, 2004. In: Finetti, I. (Ed.), Deep Seismic Exploration of the Central Mediterranean and Italy, first ed. Elsevier, Amsterdam, ISBN 9780080457604.

Cuffaro, M., Riguzzi, F., Scrocca, D., Antonioli, F., Carminati, E., Livani, M., Doglioni, C., 2010. On the geodynamics of the northern Adriatic plate. Rend. Fis. Acc. Lincei 21 (Suppl. 1), S253–S279. http://dx.doi.org/10.1007/s12210-010-0098-9.

D'Ambrogi, C., Scrocca, D., Pantaloni, M., Valeri, V., Doglioni, 2010. Exploring Italian geological data in 3D; J. Virtual Explor., Electronic Edition, ISSN 1441-8142, volume 36, paper 33. In: Marco Beltrando, Angelo Peccerillo, Massimo Mattei, Sandro Conticelli, Carlo Doglioni (Eds.), The Geology of Italy, 2010. ftp://ftp.ingv.it/pub/filippo.muccini/SGI_VIRTUAL%20EXPLORER/exploring-italian-geological-data-in-3d.pdf.

Dal Piaz, G.V., Bistacchi, A., Massironi, M., 2004. Geological Outline of the Alps. Episodes 26, pp. 175–180.

Dercourt, J., Zonenshain, L.P., Ricou, L.-E., Kazmin, V.G., Le Pichon, X., Knipper, A.L., Grandjacquet, C., Sbortshikov, I.M., Geyssant, J., Lepvrier, C., Pechersky, D.H., Boulin, J., Sibuet, J.-C., Savostin, L.A., Sorokhtin, 0, Westphal, M., Bazhenov, M.L., Laurer, J.P., Biju-Duval, B., 1986. Geological evolution of the Tethys belt from Atlantic to Pamirs since the Lias. Tectonophysics 123, 241–315.

Dewey, J.F., Pitman, C., Ryan, B.F., Bonnin, J., 1973. Plate tectonics and the evolution of the Alpine systems. Geol. Soc. Am. Bull. 84 (3), 137–180.

Dèzes, P., Ziegler, P.A., 2004. Moho Depth Map of Western and Central Europe. EUCOR-URGENT Home Page. http://www.unibas.ch/eucor-urgent.

Dèzes, P., Schmid, S.M., Ziegler, P.A., 2004. Evolution of the European Cenozoic Rift System: interaction of the Alpine and Pyrenean orogens with their foreland lithosphere. Tectonophysics 389, 1–33.

Di Bucci, D., Angeloni, P., 2012. Adria seismicity and seismotectonics: review and critical discussion. Mar. Pet. Geol. http://dx.doi.org/10.1016/j.marpetgeo.2012.09.005.

Dischinger, J.D., Mitra, S., August 2006. Three-dimensional structural model of the Painter and East Painter reservoir structures, Wyoming fold and thrust belt. AAPG Bull. 90 (no. 8), 1171–1185.

Doglioni, C., 1991. A proposal of kinematic modelling for W-dipping subductions – possible applications to the Tyrrhenian–Apennines system. Terra Nova 3, 423–434.

Doglioni, C., 1994. The Puglia uplift (SE Italy): an anomaly in the foreland of the Apenninic subduction due to buckling of a thick continental lithosphere. Tectonics 13 (n°5), 1309–1321.

Doglioni, C., Carminati, E., 2008. Structural style and Dolomites field trip. Mem. descr. della carta geol. d'italia LXXXII.

Doglioni, C., Harabaglia, P., Martinelli, G., Mongelli, F., Zito, G., 1996. A geodynamic model of the Southern Apennines accretionary prism. Terra Nova 8, 540–547.

Elter, P., Pertusati, P., 1973. Considerazioni sul limite Alpi–Appennino e sulle sue relazioni con l'arco delle Alpi occidentali. Mem. Soc. Geol. Ital. 12, 359–375.

Errico, G., Groppi, G., Savelli, S., Vaghi, G.C., 1980. Malossa Field: a deep discovery in the Po Valley, Italy. AAPG Mem. 30, 525–538.

Fantoni, R., Franciosi, R., 2010. Tectono-sedimentary setting of the Po Plain and Adriatic foreland. Rend. Fis. Acc. Lincei 21 (Suppl. 1), S197–S209. http://dx.doi.org/10.1007/s12210-010-0102-4.

Fantoni, R., Scotti, P., 2003. Thermal record of the Mesozoic extensional tectonics in the Southern Alps. Atti ticin. Sc. Terra SS9, 96–101.

Fantoni, R., Decarlis, A., Fantoni, E., 2003. L'Estensione Mesozoica al Margine occidentale delle Alpi Meridionali. Atti Ticin. Sci. della Terra 44, 97–110.

Fantoni, R., Bersezio, R., Forcella, F., 2004. Alpine structure and deformation chronology at the Southern Alps–Po Plain border in Lombardy. Boll. Soc. Geol. It. 123, 463–476.

Franciosi, R., Vignolo, A., 2002. Northern Adriatic foreland – a Promising Setting for the Southalpine Mid-Triassic Petroleum System. EAGE, 64th Conference & Exhibition, Florence, Italy, 27–30 May, H-25.

Ghielmi, M., Minervini, M., Nini, C., Rogledi, S., Rossi, M., Vignolo, A., 2010. Sedimentary and tectonic evolution in the eastern Po-Plain and northern Adriatic Sea area from Messinian to Middle Pleistocene (Italy). Rend. Fis. Acc. Lincei 21 (Suppl. 1), S131–S166. http://dx.doi.org/10.1007/s12210-010-0101-5.

Ghielmi, M., Minervini, M., Nini, C., Rogledi, S., Rossi, M., 2012. Late MioceneeMiddle Pleistocene sequences in the Po Plain e Northern Adriatic Sea (Italy): the stratigraphic record of modification phases affecting a complex foreland basin. Mar. Pet. Geol. http://dx.doi.org/10.1016/j.marpetgeo.2012.11.007.

Guglielmo, G., Jackson, M., Vendeville, B., 1997. Three-dimensional visualization of salt walls and associated fault systems. AAPG Bull. 81–1, 46–61.

Han, J., Yeon, Y., Hyun, H., Hwang, D., 2011. 3D Geological Model of Mining Area. In: http://www.asiageospatialforum.org/2011/proceeding/pps/Jonggyu%20Han_AGF.pdf.

Jadoul, F., Rossi, P.M., 1982. Evoluzione paleogeografico-structturale e vulcanismo triassico nella Lombardia centro-occidentale. In: Castellarin, A., Vai, G.B. (Eds.),

Guida alla geologia del Sudalpino centro-occidentale. Guide Geol.Reg. S.G.I, pp. 143–155. Bologna.
Jadoul, F., Berra, F., Frisia, S., 1992. Stratigraphic and palaeogeographic evolution of a carbonate platform in an extensional tectonic regime: the example of the Dolomia Principale in Lombardy (Italy). Riv. Ital. Paleontol. Stratigr. 98, 29–44.
Klein, P., Richard, L., James, H., 2008. 3D curvature attributes: a new approach for seismic interpretation. First break 26, 105–112.
Larroque, C., 2009. Aléa sismique dans une région intraplaque à sismicité modérée: la junction Alpes-Bassin Ligure. In: Memoire d'Habilitation à Diriger des Recherches. UMR 6526 Géosciences Azur, CNRS.
Laubscher, H.P., 1996. Shallow and deep rotations in the. Miocene Alps Tect. 15, 1022–1035.
Leslie, G., Krabbendam, M., Kearsey, T., 2012. Assynt Culmination Geological 3D Model. British Geological Survey. http://www.bgs.ac.uk/research/ukgeology/assyntCulmination.html.
Lindquist, S.J., 1999. Petroleum Systems of the Po Basin Province of Northern Italy and the Northern Adriatic Sea: Porto Garibaldi (Biogenic), Meride/Riva di Solto (Thermal), and Marnoso Arenacea (Thermal). Open-File Report 99-50-M. U.S. Geological Survey, p. 19, 15 figs., 3 tables.
Lindsay, M., Aillères, L., Jessell, M., de Kemp, E., Betts, P., 2012. Locating and quantifying geological uncertainty in three-dimensional models: analysis of the Gippsland Basin, southeastern Australia. Tectonophysics. http://dx.doi.org/10.1016/j.tecto.2012.04.007.
Livio, F., Berlusconi, A., Michetti, A., Sileo, G., Zerboni, A., Trombino, L., Cremaschi, M., Mueller, K., Vittori, E., Carcano, C., Rogledi, S., 2009. Active fault-related folding in the epicentral area of the December 25, 1222 (Io=IX MCS) Brescia earthquake (Northern Italy): seismotectonic implications. Tectonophysics 476, 320–335.
Maesano, F.E., Toscani, G., Burrato, P., Mirabella, F., D'Ambrogi, C., Basili, R., 2013. Deriving thrust fault slip rates from geological modeling: examples from the Marche coastal and offshore contraction belt, Northern Apennines, Italy. Mar. Petr. Geol. 42, 122–134. http://dx.doi.org/10.1016/j.marpetgeo.2012.10.008.
Maino, M., Decarlis, A., Felletti, F., Seno, S., 2013. Tectono-sedimentary evolution of the Tertiary Piedmont Basin (NW Italy) within the Oligo-Miocene central Mediterranean geodynamics. Tectonics 32 (3), 593–619.
Margheriti, L., Pondrelli, S., Piccinini, D., Piana Agostinetti, N., Giovani, L., Salimbeni, S., Lucente, F.P., Amato, A., Baccheschi, P., Park, J., Brandon, M., Levin, V., Plomerová, J., Jedlička, P., Vecsey, L., Babuška, V., Fiaschi, A., Carpani, B., Ulbricht, P., 2006. The subduction structure of the Northern Apennines: results from the RETREAT seismic deployment. Ann. Geophys. 49 (4/5). http://earth.geology.yale.edu/~jjpark/Margheriti_etal_Annali_2006.pdf.
Mariotti, G., Doglioni, C., 2000. The dip of the foreland monocline in the Alps and Apennines. Earth Planet. Sci. Lett. 181, 191–202.
Mattavelli, L., Margarucci, V., 1992. Malossa field – Italy, Po Basin. In: Foster, N.H., Beaumont, E.A. (Eds.), Treatise of Petroleum Geology, Atlas of Oil and Gas Fields, Structural Traps, vol. VII. American Association of Petroleum Geologists, Tulsa, OK, pp. 119–137.
Mattavelli, L., Novelli, L., 1987. Origin of the Po basin hydrocarbons. Memoires la Soc. Geol. Fr. nouv. ser. 151, 97–106.
Mattavelli, L., Novelli, L., 1990. Geochemistry and habitat of the oils in Italy. Am. Assoc. Pet. Geol. Bull. 74 (10), 1623–1639.
McClay, K., Bonora, M., 2001. Analog models of restraining stepovers in strike-slip fault systems. AAPG Bull. 85 (2), 233–260.
Michetti, A.M., Giardina, F., Livio, F., Mueller, K., Serva, L., Sileo, G., Vittori, E., Devoti, R., Riguzzi, F., Carcano, C., Rogledi, S., Bonadeo, L., Brunamonte, F., Fioraso, G., 2012. Active compressional tectonics, Quaternary capable faults and the seismic landscape of the Po Plain (N Italy). Ann. Geophys. 55 (5). http://dx.doi.org/10.4401/ag-5462.
Mitra, S., Leslie, W., 2003. Three-dimensional structural model of the Rhourde el Baguel. AAPG Bull. 87 (2), 231–250.
Mitra, S., Figueroa, G.C., Hernandez Garcia, J., Murillo Alvarado, A., 2005. Three-dimensional structural model of the Cantarell and Sihil structures, Campeche Bay, Mexico. AAPG Bull. 89 (1), 1–26.
Mitra, S., Gonzalez, A., Hernandez Garcia, J., Kajari, G., 2007. Ek-Balam field: a structure related to multiple stages of salt tectonics and extension field, Algeria. AAPG Bull. 91 (11), 1619–1636.
Mosca, P., Polino, R., Rogledi, S., Rossi, M., 2010. New data for the kinematic interpretation of the Alps–Apennines junction (Northwestern Italy). Int. J. Earth Sci. Geol. Rundsch. 99, 833–849. http://dx.doi.org/10.1007/s00531-009-0428-2.
Nardon, S., Marzorati, D., Bernasconi, A., Cornini, S., Gonfalini, M., Mosconi, S., Romano, A., Terdich, P., 1991. Fractured carbonate reservoir characterization and modeling a multidisciplinary case study from the Cavone oil field, Italy. First Break 9 (12), 553–565.
Nicolai, C., Gambini, R., 2007. Structural architecture of the Adria platform-and-basin system. Boll. Soc. Geol. It. (Ital. J. Geosci.), Spec. Issue No. 7, 21–37, 15 figs., 1 pl., CROP-04 (ed. by A. Mazzotti, E. Patacca and P. Scandone).
Nicolich, R., 2010. Geophysical investigation of the crust of the Upper Adriatic and neighbouring chains. Rend. Fis. Acc. Lincei 21 (Suppl. 1), S181–S196. http://dx.doi.org/10.1007/s12210-010-0093-y.
Perotti, C.R., 1991. Osservazioni sull'assetto strutturale del versante padano dell'Appennino Nord-Occidentale. Atti Tic. Sc. Terra 34, 11–22.
Perotti, C.R., Vercesi, P.L., 1991. Assetto tettonico ed evoluzione strutturale recente della porzione nord-occidentale dell'Appennino emiliano. Mem. Descr. Carta Geol. d'Italia XLVI, 313–326.
Picotti, V., Pazzaglia, F.J., 2008. A new active tectonic model for the construction of the Northern Apennines mountain front near Bologna (Italy). J. Geophys. Res. V. 113 (B8), 1–24.
Pieri, M., 1984. Storia delle ricerche nel sottosuolo padano fino alle ricostruzioni attuali – Cento anni di geologia Italiana, pp. 155–177 volume Giubilare, 1° Centenario della Soc. Geol. Ital. 1881–1981, Roma.
Pieri, M., Groppi, G., 1981. Subsurface geological structure of the Po Plain, Italy. Prog. Fin. Geodin. CNR pubbl. 414, 1–113. Roma.
Ponton, M., 2010. Architettura delle Alpi Friulane. Pubblicazione 52. Edizioni del Museo Friulano di storia naturale, Comune di Udine.
Ravaglia, A., Seno, S., Toscani, G., Fantoni, R., 2006. Mesozoic extension controlling the Southern Alps thrust front geometry under the Po Plain, Italy: insights from sandbox models. J. Struct. Geol. 28, 2084e2096.
Resor, P., 2008. Deformation associated with a continental normal fault system, western Grand Canyon, Arizona. GSA Bull. 120 (3/4), 414–430.
Ricci Lucchi, F., 1986. The Oligocene to recent foreland basins of the northern Apennines. In: Allen, P.A., Homewood, P. (Eds.), Foreland Basins, I.A.S. Special Publication 8, pp. 105–139.
Roberts, A., 2001. Curvature attributes and their application to 3D interpreted horizons. First Break 19, 85–100.
Roeder, D., 1991. Structure and tectonic evolution of alpine lithosphere. In: EUG VI Symposium, the European Geotraverse (EGT) Final Results, Strasbourg.
Roure, F., Polino, R., Nicolich, R., 1990. Early Neogene deformation beneath the Po plain: constraints on the post-collisional Alpine evolution. In: Roure, F., Heitzmann, P., Polino, R. (Eds.), Deep Structure of the Alps, Mem.Soc.Geol. France, vol. 156, pp. 309–322.
Roure, F., Casero, P., Vially, R., 1991. Growth processes and mélange formation in the southern Apennine accretionary wedge. Earth Planet. Sci. Lett. 102, 395–412.
Roure, F., Nazaj, S., Mushka, K., Fili, I., Cadet, J.P., Bonneau, M., 2004. Kinematic evolution and petroleum systems—an appraisal of the Outer Albanides. In: McClay, K.R. (Ed.), Thrust Tectonics and Hydrocarbon Systems, vol. 82. AAPG Memoir, pp. 474–493.
Roure, F., Casero, P., Addoum, B., 2012. Alpine inversion of the North African Margin, and delamination of its continental crust. Tectonics 31, TC3006. http://dx.doi.org/10.1029/2011TC002989.
Schmid, S.M., Kissling, E., 2000. The arc of the Western Alps in the light of geophysical data on deep crustal structure. Tectonics 19, 62–85.
Schmid, S., Fugenschuh, B., Kissling, E., Schuster, R., 2004. Tectonic map and overall architecture of the Alpine orogen. Eclogae Geol. Helv. 97, 93–117.
Schumacher, M.E., Laubscher, H.P., 1996. 3D crustal architecture of the Alps–Apennines join: a new view on seismic data. Tectonophysics 260, 349–363.
Schreiber, D., Lardeaux, J.M., Courrioux, G., Martelet, G., Guillen, A., 2008. 3D modelling of alpine Mohos in south-western Alps. In: International Geological Congress Abstracts. Congres Geologique International, Resumes, p. 33.
Shao, Y., Zheng, A., He, Y., Xiao, K., 2012. 3D geological modeling under extremely, complex geological conditions. J. Comput. 3, 699–705.
Shiner, P., Bosica, B., Turrini, C., 2013. The Slope Carbonates of the Apulian Platform – an Under-explored Play in the Central Adriatic. http://www.petroceltic.com/~/media/Files/P/Petroceltic-V2/pdf/AAPG-barcelona-2013-slope-carbonates-of-the-apulian-platform.pdf.
Tesauro, M., Kaban, M.K., Cloetingh, S.A.P.L., 2008. Eu-CRUST-07: a new reference model for the European crust. Geophys. Res. Lett. 35.
Toscani, G., Seno, S., Fantoni, R., Rogledi, S., 2006. Geometry and timing of deformation inside a structural arc: the case of the western Emilian folds (Northern Apennine front, Italy). Boll. Soc. Geol. It. 125, 59–65.
Toscani, G., Burrato, P., Di Bucci, D., Seno, S., Valensise, G., 2009. Plio-Quaternary tectonic evolution of the Northern Apennine thrust front (Bologna-Ferrara section, Italy): seismotectonic implications. It. J. Geosci. 128 (2), 605–613. http://dx.doi.org/10.3301/IJG.2009.128.2.605.
Trumpy, R., 1973. The timing of orogenic events in the Central Alps. In: De Jong, K.A., Scholten, R. (Eds.), Gravity and Tectonics. Wiley and Sons, New York, pp. 229–251.
Turrini, C., Rennison, P., 2004. Structural style from the Southern Apennines' hydrocarbon province—an integrated view. In: McClay, K.R. (Ed.), Thrust Tectonics and Hydrocarbon Systems, vol. 82. AAPG Memoir, pp. 558–578.
Turrini, C., Dups, K., Pullan, C., 2009. 2D and 3D structural modelling in the Swiss-French Jura Mountains. First break 27, 65–71.
Valcarce, G., Zapata, T., Ansa, A., Selva, G., 2006. Three-dimensional structural modeling and its application for development of the El Portón field, Argentina. AAPG Bull. 90 (3), 307–319.
Vanossi, M., Cortesogno, L., Galbiati, B., Messiga, B., Piccardo, G.B., Vannucci, R., 1986. Geologia delle Alpi Liguri: dati, problemi, ipotesi. Mem. Soc. Geol. It. 28, 5–75.
ViDEPI Project, http://unmig.sviluppoeconomico.gov.it/videpi/kml/webgis.asp.
Viganò, A., Della Vedova, B., Ranalli, G., Martin, S., Scafidi, D., 2011. Geothermal and rheological regime in the Po plain sector of Adria (Northern Italy). It. J. Geosci. 131 (2), 228–240.
Vignaroli, G., Faccenna, C., Jolivet, L., Piromallo, C., Rossetti, F., 2008. Subduction polarity reversal at the junction between the Western Alps and the Northern Apennines, Italy. Tectonophysics 450, 34–50.
Vouillamoz, N., Sue, C., Champagnac, J., Calcagno, P., 2012. 3D cartography modeling of the Alpine Arc. Tectonophysics 2012. http://dx.doi.org/10.1016/j.tecto.2012.06.012.
Zoetemeijer, R., Sassi, W., Cloetingh, S., 1992. Stratigraphic and kinematic modeling of thrust evolution, northern Appennines, Italy. Geology 20, 1035–1038.

IV. From structural geometries to kinematics

The first-phase 3D model results (see Section III) essentially a) confirmed the basin structures' type and distribution interpreted so far by the various authors, b) visualized the entire basin anatomy in the 3D space, c) tied the shallow and deep structures to the very deep Moho architecture, d) linked the foreland architecture to the surrounding Southern Alps and Northern Apennines belts.

The model uncertainty distribution raised questions in terms of structural style, geodynamics and tectonic evolution of the Po Valley foreland-foredeep system (see Discussion in section III). Notably, the influence that the inherited structures (mainly Mesozoic and extension-related; subordinately Tertiary and likely related to the foreland flexure) likely had on the Po Valley foreland-foredeep tectonic system represented a major query from the model discussion.

Following the 3D structural model building, and in parallel with the definition of the possible model applications (Part 5), the reconstruction of the Po Valley tectonic evolution (phase 5 in the workflow of Fig.20) aimed at the following specific objectives:

- defining the basin structural kinematics,
- illustrating the role that the various extensional and compressional units had during the basin tectonics (parallel, normal and oblique to the associated stress field),
- understanding of the progressive foreland-foredeep tectono-stratigraphic framework.

The whole exercise was tackled by further refining and implementation of the 3D layering and the associated faults. Hence, regional building of some key Tertiary stratigraphic horizons and local detailing of the oil field configurations, across the Mesozoic-basement units, were performed.

2D restoration of selected cross-sections sliced from the 3D model has been run to suggest the key steps of the Po Valley basin evolution, since Paleogene to present.

With respect to previous works, the main model achievement was once again the three-dimensional integration of the structural-kinematic components. In particular during this

modeling phase, the 4D (space + time) interplay among distribution of the Tertiary-Mesozoic-basement units and lithospheric phenomena (flexure, belt progression) from Paleogene to present could be illustrated and demonstrated with new questions for discussion.

Remarkably, given the available literature (Castellarin et al., 1985; Toscani et al. 2013), the performed 2D restoration exercise represents the first attempt to analyse the basin evolution systematically and across a geometrically consistent regional framework.

Marine and Petroleum Geology 77 (2016) 376–398

Contents lists available at ScienceDirect

Marine and Petroleum Geology

journal homepage: www.elsevier.com/locate/marpetgeo

Research paper

Influence of structural inheritance on foreland-foredeep system evolution: An example from the Po valley region (northern Italy)

Claudio Turrini [a, *], Giovanni Toscani [b], Olivier Lacombe [c], François Roure [d, e]

[a] CTGeological Consulting, St.Germain-en-Laye, France
[b] University of Pavia, Earth and Environmental Science Department, Pavia, Italy
[c] Sorbonne Universités, UPMC Univ Paris 06, CNRS, Institut des Sciences de la Terre de Paris (iSTeP), 4 place Jussieu 75005 Paris, France
[d] IFP-EN, Rueil-Malmaison, France
[e] Tectonic Group, Utrecht University, The Netherlands

ARTICLE INFO

Article history:
Received 2 April 2016
Received in revised form
15 June 2016
Accepted 22 June 2016
Available online 24 June 2016

Keywords:
3D models
Po valley tectonics
Structural inheritance
Foreland basins

ABSTRACT

Understanding the development of foreland-foredeep systems and the influence exerted by pre-existing structures on their evolution is an important step for defining the key factors that control long-term basin and lithosphere dynamics, comprehending the associated seismic hazard and assessing their economic potential in the domain of hydrocarbon exploration.

The Po Valley is a rather unique foreland basin for two major reasons: a) it developed intermittently at the front of two different mountain chains, the Northern Apennines and the Southern Alps, progressively converging one towards the other; b) the inherited structures, mainly derived from the Mesozoic extensional tectonics, are oriented at high angle to the advancing belts. The coexistence of these two factors and their various implications make the Po Valley basin a complex case study that deserves attention.

Taking advantage of the recent building of a 3D structural model across the region, we reconstructed the possible geometry and migration pattern of the Tertiary basins that developed at the front of the Northern Apennines and the Southern Alps, as part of the Po Valley tectonic evolution. In addition, a number of sections sliced from the 3D model across selected domains have then been used to restore the present-day structural units to their pre-compressional setting, while highlighting the key stages of their geological history.

Results from the model analysis show that the Mesozoic extension-related tectonics and the associated carbonate facies geometry and distribution localized and constrained the Alpine structures inside/around the basin. Their control on the Cenozoic deformation and sedimentation is evident during the Paleogene and the Miocene whereas it becomes more subtle during the Plio-Pleistocene when lithospheric-scale mechanisms need to be invoked.

Notwithstanding the model uncertainties and its explicit regional significance, our results may be taken as reference for any foreland-foredeep setting worldwide, especially in complex systems where tectono-sedimentary inhomogeneity is spatially and temporally dominant.

1. Introduction and aim of the study

A foreland basin is a structural basin that forms at the front of a mountain belt basically by bending of the lithosphere as a function of its flexural rigidity and the associated loading from the belt itself (De Celles and Giles, 1996). The consequent foreland width and depth define the accommodation space for the sediments that fill the basin, thus developing the derived foredeep sedimentary successions (Beaumont et al., 1999). According to the polarity of the subduction system that controls the evolution of an orogenic belt, foreland basins are normally separated into two different categories: peripheral or pro-wedge and retro-arc or retro-wedge (De Celles and Giles, 1996; Ziegler et al., 2002; Naylor and Sinclair, 2008). During development of foreland-foredeep domains, the inherited crustal structural fabric as well as the thermal state of the lithosphere may impact the progressive deformation history

* Corresponding author.
E-mail address: clturri@wanadoo.fr (C. Turrini).

http://dx.doi.org/10.1016/j.marpetgeo.2016.06.022
0264-8172/

depending (among the many factors) on the pre-existing mechanical stratigraphy (horizontal and vertical), the distribution/geometry of structures (notably, their orientation with respect to the evolving regional stress field) and at a larger scale on the flexural rigidity of the foreland lithosphere.

The Po Valley (Fig. 1a,b) is a foreland basin (Bello and Fantoni, 2002; Fantoni et al., 2004; Turrini et al., 2014, 2015; Rossi et al., 2015) where the above cited factors have interacted through time and space to give birth to the present-day tectonic system. This system was formed as a result of a rather complex geodynamics, which controlled deformation and sedimentation, respectively of and onto the northern segment of the Adria micro-plate (Carminati and Doglioni, 2012; see also references hereinafter in Section 2). The long-lasting convergence process created opposite verging belts, namely the Northern Apennines and Southern Alps. From Paleogene to present times, the amplification and propagation of those mountain chains controlled the differential flexure of the Po Valley-Adria lithosphere, the associated tilting and bulging of the foreland domain, the rapid sedimentation of thick foredeep-type deposits and their successive involvement within the developing tectonic wedges (e.g., Carminati and Doglioni, 2012 and references therein). Remarkably, part of the described tectonic evolution caused non-homogeneous deformation of the common foreland region, where mainly extension-related Mesozoic structures have been reactivated and/or overprinted by the Cenozoic folds and thrusts.

The influence of the inherited Mesozoic extensional structures on the Alpine tectonics in and around the Po Valley region has been already discussed by various authors in the literature (Castellarin et al., 1985; Doglioni and Bosellini, 1987; Zanchi et al., 1990; Schonborn, 1992; Fantoni et al., 2004; Ravaglia et al., 2006, Castellarin and Cantelli, 2010; Cuffaro et al., 2010; Carminati and Doglioni, 2012; Vannoli et al., 2015; Pfiffner, 2014; Turrini et al., 2014). Key message from those studies is that the extension-related structures which formed the Adria plate margin during the Mesozoic have strongly controlled the progressive Alpine tectonics in the region. The derived interference between late-Triassic to early Jurassic, mainly N-S-oriented, extension-related structures and Cenozoic, generically WNW-ESE-oriented compression-related structures can be tracked at different scales of observation, especially across the Southern Alps outcrops and by the exploration wells drilled inside the Po Valley basin (Cassano et al., 1986; Bertotti et al., 1993; Schonborn, 1992; Fantoni et al., 2004).

As a follow-up to the 3D structural and seismo-tectonic models that have been recently built and analyzed across the Po Valley region (Turrini et al., 2014, 2015), this study aims at providing new evidences of the long-term influence that the distribution and geometry of pre-Alpine Mesozoic structures have had on the evolution of the Po Valley foreland-foredeep system since the Paleogene.

With respect to the previous works (Turrini et al., 2014, 2015) the main achievement of the study was certainly the integration of the structural-kinematic component with the 3D model geometries across the entire basin. In particular during this modeling phase, the 4D (space + time) interplay among distribution of the Tertiary-Mesozoic-basement units and lithospheric phenomena (flexure, belt progression) from Paleogene to present could be illustrated and demonstrated with new questions for discussion. Remarkably, given the available literature, the performed 2D restorations represent the first attempt to analyse the basin evolution systematically and across a geometrically consistent regional framework.

Despite the region uniqueness and beyond the derived regional implications, this study also intends at providing an interesting and solid term of comparison for other complex foreland basin systems worldwide, where large-scale structures and sediment distribution are highly variable both in time and space owing to structural inheritance.

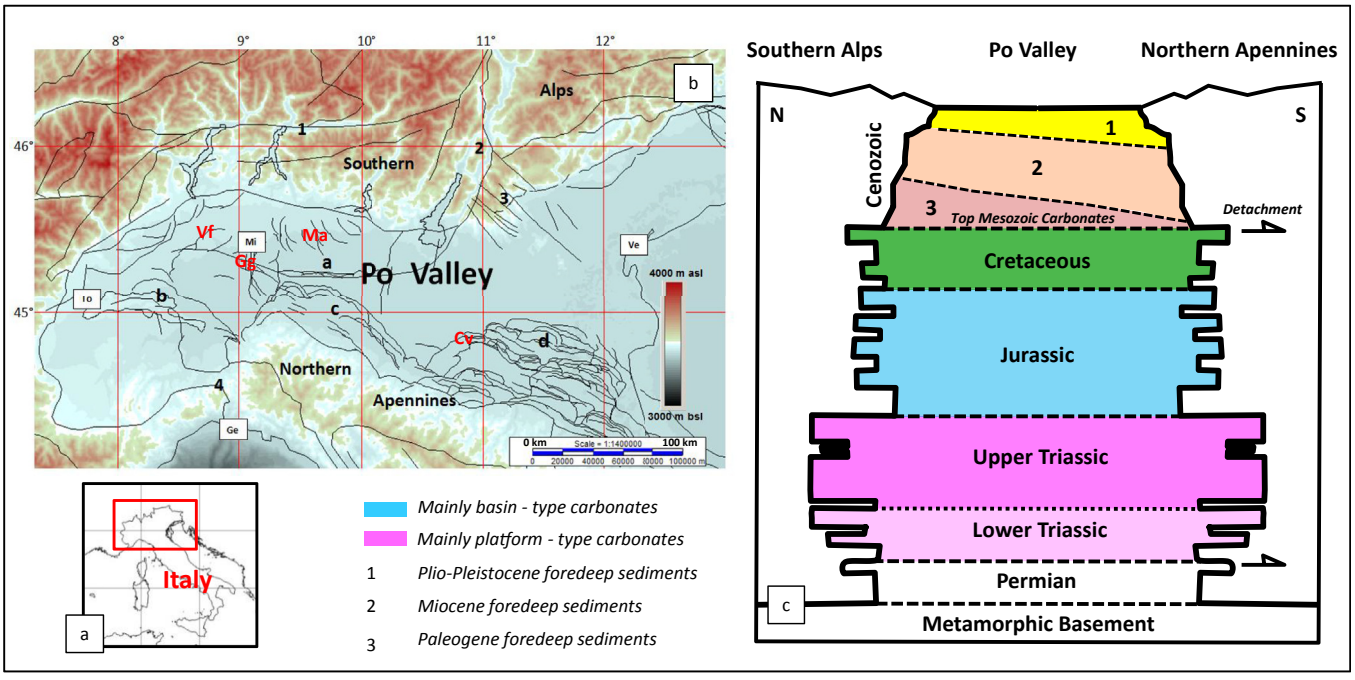

Fig. 1. a) - Location map. b) Digital topography and tectonic framework (modified from Turrini et al., 2014) around the Po Valley region. (1) Insubric Line; (2) Giudicarie Line; (3) Schio-Vicenza Line; (4) Sestri-Voltaggio-Villavernia Lines; (a–e) buried thrust fronts (modified after Bigi et al., 1990): a = Milano Thrust Front; b = Monferrato Thrust Front; c = Emilian Thrust Front; d = Ferrara-Romagna Thrust Front. Main cities are indicated: Mi = Milano, To = Torino, Ge = Genova, Ve = Venezia. c) Simplified stratigraphy of the Po Valley. 1, 2 and 3 in the Cenozoic units indicate respectively the foredeep deposits of Fig. 5c, b and a,.

2. The Po valley

2.1. Regional framework

The interaction between Eurasia and Africa plates drove the geodynamic evolution of the Alps and Apennines belts. The Adria microplate is commonly known as the African promontory involved in the collision with Eurasia (Dercourt et al., 1986). The convergence of the two plates caused indentation between the Northern Alps metamorphic belt and the Insubric domain, active since the Cretaceous up to the present (Coward et al., 1989; Dewey et al., 1989; Dal Piaz et al., 2003; Carminati and Doglioni, 2012). The development of the Southern Alps, and the growth of the Northern Apennines (Boccaletti et al., 1990; Cibin et al., 2004; Di Giulio et al., 2013) led to the formation of the Neogene Po Plain foreland basin, interposed between the two opposite verging chains (Fig. 1b).

The Southern Alps derive from the deformation of a passive continental margin, progressively involved into a collision (e.g., Castellarin et al., 1992; Bertotti et al., 1993; Di Giulio et al., 2001; Barbieri et al., 2004). The outermost buried fronts of that belt are formed by S-verging thrust systems, trending WNW-ESE partly outcropping in the foothill zone and partly buried under Neogene-Quaternary sediments of the Po Plain (Castellarin and Vai, 1986; Castellarin et al., 1992; Fantoni et al., 2004; Ravaglia et al., 2006). The Apennine sector facing the Po Valley consists of buried compressional structures bounded to the south by the Pedeapenninic Thrust Front (PTF) (Pieri and Groppi, 1981; Boccaletti et al., 1985; Castellarin et al., 1985; Cassano et al., 1986; Bigi et al., 1990; Fantoni and Franciosi, 2010; Ghielmi et al., 2010, 2013). These structures mainly refer to N to NE-verging blind thrusts and folds which controlled the rapid deposition of up to 7–8 km thick Neogene-Quaternary syntectonic sediments. Three main buried structural arcs were formed in different times and are associated with different amounts of shortening. From west to east they are (Fig. 1b): 1) the Monferrato arc (an allochthonous tectonic wedge with undefined shortening - Mosca, 2013 - successively re-folded and thrusted between Messinian and Pleistocene); 2) the Emilia arc (20–25% of shortening – Castellarin et al., 1985; Perotti, 1991; Toscani et al., 2014 - mainly active during Pliocene) and 3) the Ferrara-Romagna arc (more than 30–35% of shortening – Castellarin et al., 1985 - tectonically active at present time – Maesano et al., 2015a). The eastward increase in shortening is consistent with the Northern Apennine counter clockwise rotation during its emplacement within an oblique collisional framework (Bally et al., 1986; Vanossi et al., 1994; Cibin et al., 2003; Carminati et al., 2012; Maino et al., 2013).

The Po Valley units separate the Southern Alps and the Northern Apennines and they constitute the common foreland-foredeep system of these two diachronous and opposite verging chains since the Paleogene (see recent synthesis by Turrini et al., 2014, 2015 and references therein). The ancient foreland units, as part of the Mesozoic passive margin, currently form thrust imbricates variably dipping and hidden below thick Cenozoic clastic sediments (Pieri and Groppi, 1981; Cassano et al., 1986; Mariotti and Doglioni, 2000; Fantoni and Franciosi, 2010; Turrini et al., 2014). The ancient foredeep units, derived from the erosion of the Southern Alps (e.g. Carrapa and Di Giulio, 2001; Di Giulio et al., 2001) and of the Northern Apennines (Rizzini and Dondi, 1978; Dondi and D'Andrea, 1986; Ravaglia et al., 2004; Mancin et al., 2009) form a thick sedimentary wedge that, as a whole, can exceed 9 km in total thickness.

The Mesozoic succession is formed by Upper Triassic carbonate platform rocks and by Jurassic to Cretaceous pelagic carbonates resting on top of metamorphic basement rocks (Cassano et al., 1986) (Fig. 1c). The overlying Tertiary sediments (Fig. 1c) consists of Paleogene marls, some Messinian evaporites, sand-shale Pliocene turbidites, Early Pleistocene marine sands and Late Pleistocene alluvial deposits. From the mechanical point of view, the Po Plain stratigraphy includes two major décollement levels (Fig. 1c) which strongly impact the structural style in the basin (Fantoni et al., 2004; Ravaglia et al., 2006, Turrini et al., 2014, 2015): the deeper detachment corresponds to the evaporites at the bottom of the Mesozoic carbonate units; the shallower detachment occurs on top of the carbonate series, in correspondence of Late Eocene-Early Oligocene marls.

The Po Valley tectono-stratigraphic units and sedimentary infill provide a quite complete record of the compressional tectonic phases that affected, from Cretaceous onwards, the Triassic-Jurassic passive margin and giving rise to the formation of a Neogene-Quaternary foredeep basin (Dondi and D'Andrea, 1986; Argnani and Ricci Lucchi, 2001; Ghielmi et al., 2010, 2013). Timing of the related tectonic events is provided by the age of syntectonic deposits and the associated growth strata geometries (Ghielmi et al., 2010, 2013; Rossi et al., 2015).

During the Late Oligocene the Adria plate ended its rotation (Carminati et al., 2012; Malusà et al., 2016) yet continued to move NNW-ward and collided with the Eurasian plate. At the same time, the Apennine fronts rotated counter-clockwise while the Southern Alps fronts were translated southwards, both belts thrusting onto the common Po Valley foreland (Carminati et al., 2012). During the Middle Miocene, due to the progressive advance of the Apennine belt (Carminati et al., 2012), the Southern Alps and the Northern Apennine fronts were closer. The foredeep space was further reduced at early Pliocene times when the Southern Alps fronts (almost no longer tectonically active) and the active Northern Apennine became parallel and faced each other. From early Pliocene onwards only the Northern Apennine fronts remained tectonically active, deforming the buried geometries to their present configuration. GPS measurements and slip rates calculations describe the present (last 20–30 years) and recent (last 1.8My) deformations, respectively. GPS velocities show a general NNE trend with decreasing values going from the outcropping Northern Apennines to the Po Valley region (Bennett et al., 2012; Serpelloni et al., 2005, 2007). Tectonic motion along the Plio-Pleistocene thrust segments is essentially concentrated on the Northern Apennine buried fronts (particularly the Ferrara region). Slip rate values calculated for the last 1.8My are higher (Maesano et al., 2013, 2015a) with respect to the rest of the Po Valley as they occur in regions where major earthquakes have been reported (Basili et al., 2008; DISS Working Group, 2015; Turrini et al., 2015; Bonini et al., 2014). Being a flat alluvial plain, outcrops or field evidences of neotectonic activities are lacking in the Po Valley. Hence, the most recent tectonic events are evidenced by drainage anomalies (Burrato et al., 2003) and, locally, anticline hinges outcrop creating isolated reliefs. Examples of these are the San Colombano hill, belonging to the buried fronts of the Northern Apennines (Toscani et al., 2014), the Capriano del Colle hill, in the Southern Alps (Livio et al., 2009b) and the Montello hill, in the Eastern Southern Alps (Burrato et al., 2008; Caputo et al., 2010).

3. Data & methodology

The 3D model building workflow has been already presented and discussed in terms of the associated data, methodology and uncertainty by previous papers (Turrini et al., 2014, 2015). Nevertheless, because of the continuous refining and updating of the model structural geometries it is worth to briefly review the entire process while describing the new features and operations.

3.1. Model building phase 1

The base framework of the model has been performed by integrating most of the public data available for the region, i.e., cross-sections, contour maps and wells (Turrini et al., 2014, 2015 and reference therein) and they are all measured in depth (Fig. 2). Noteworthy, no seismic data have been used during the entire building workflow, this being due to two particular reasons: a) seismic lines in the Po Valley region are exclusive property of ENI (previously Agip S.p.a., the national oil company) and the few available for public access cannot provide an homogeneous distribution of information for the aimed model building; b) the use of depth data allows any problem derived from time-to-depth conversion and the related velocity distribution to be circumvented. Noticeably, the initial model framework was based on a net of widely used cross-sections published by Agip and built from seismic, wells, geophysical maps (gravity and magnetic) and full knowledge of the region (Pieri and Groppi, 1981; Cassano et al., 1986) (Fig. 3a). The above mentioned set of depth data was georeferenced, digitized and cross-checked for geometrical compatibility in 3D. Once the different interpretations have been transformed into their digital 2D format (xyz lines), they have been gridded to form the surfaces which constitute the model elements. The primary aim was to construct a number of key surfaces that define the model 'stratigraphy', i.e. from top to bottom, topography, base Pliocene, top Mesozoic carbonates, near top Triassic, top basement and Moho. A preliminary, crustal scale 3D geo-volume was then obtained and was used to illustrate (Turrini et al., 2014): a) the regional setting across the basin and b) the possible link among the very deep (Moho), deep (basement and Mesozoic carbonates) and shallow (base Pliocene and outcrops and major tectonic trends from the surrounding Southern Alps and Northern Apennines belts) structures. The entire model building process was performed by the MOVE structural package.

3.2. Model building phase 2

Phase 2 of the model building workflow was particularly devoted to the fault reconstruction, essentially across the Mesozoic layers (Fig. 3b) and subordinately across the Tertiary deposits. The model was then integrated with the earthquake events taken from the INGV web site (Turrini et al., 2015).

As part of phase 2-workflow, still performed using the MOVE software, all key fault maps selected from the literature (Pieri and Groppi, 1981; Casero et al., 1990; Fantoni et al., 2004, Cimolino et al., 2010; Rogledi, 2010) were a) digitized as lines, b) draped onto the specific model layer, c) the composing fault segments projected to depth as planes, accordingly to the most valuable dip angle, d) the reconstructed surfaces sliced for 3D consistency inside the final model. The process was rigorously performed across the main oil field in the region (Fig. 3c). An original technique was used to review and refine both the model stratigraphic layers and the 3D faults: all model surfaces were exported from the MOVE software and imported into the 2D/3D Kingdom package (normally used for seismic interpretation) where, once transformed to gridded layers, they could be re-picked and tied to the well data on a regular and dense net of blank pseudo-SEGY panels (Fig. 3d) created inside the software. With such a technique, all structural features were

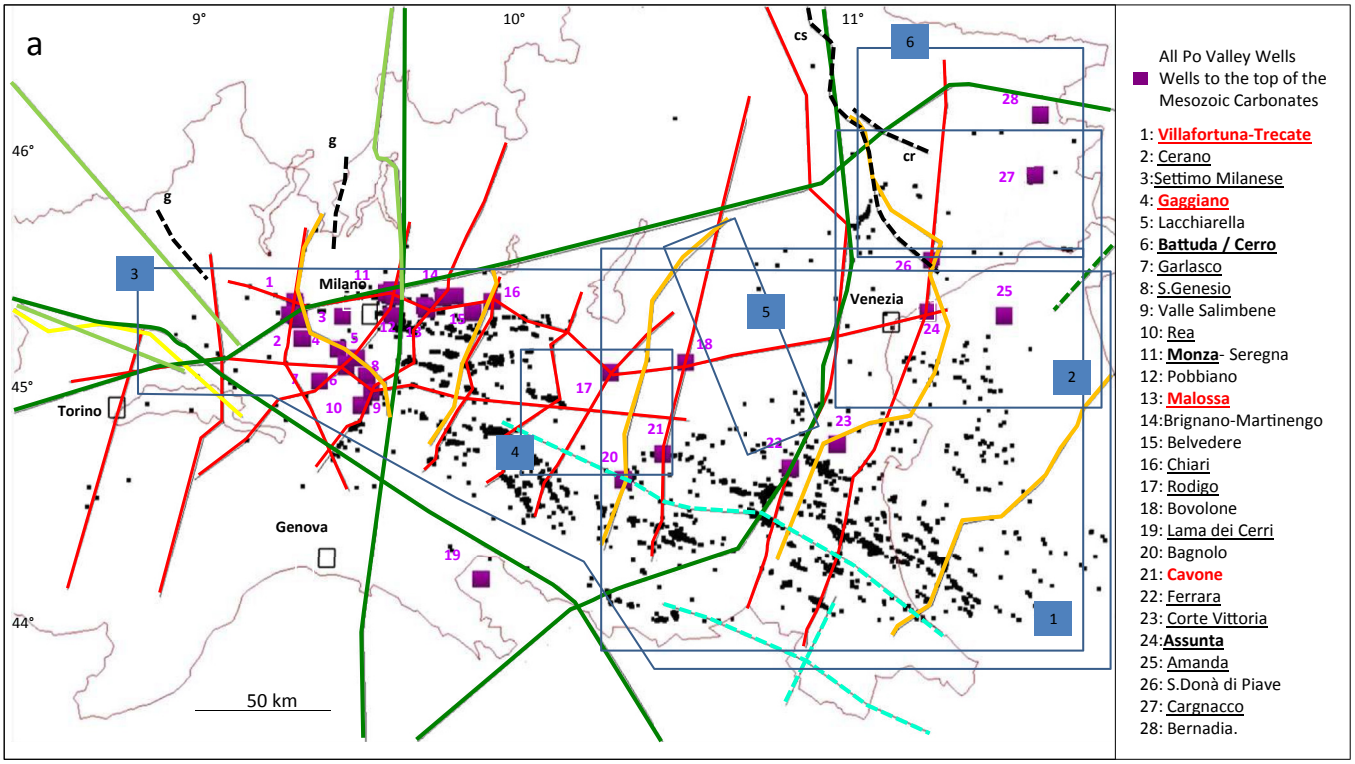

Fig. 2. (a) Data distribution: maps, cross-sections and wells available from the public domain. In the well list: red = fields; bold black = wells drilling down to the Po Valley basement; underlined = wells drilling down to the Triassic succession. Cross-sections: red set from Cassano et al., 1986; orange set from Fantoni et al., 2004 and Fantoni and Franciosi, 2010; dark-green set from Roeder, 1991; light-green set from Schmid and Kissling (2000; yellow is CROP-ECORS from Roure et al. (1990); light-blue set from Boccaletti et al. (2010); black set from (cs) Castellarin et al., 2005, (cr) Casero et al., 1990 and (g) Greber et al., 1997. Box 1 = top Mesozoic Carbonates depth contour map area, from Casero et al., 1990; box 2 = top Mesozoic Carbonates depth contour map area, from Cimolino et al., 2010; box 3 = top Mesozoic depth map area, from Nicolai and Gambini (2007); box 4 = depth maps from GEOMOL project, 2015; box 5 = serial depth sections from Pola et al., 2014; box 6 = serial depth sections from Ponton, 2010. Latitude and Longitude values are North and East of Greenwich. (For interpretation of the references to colour in this figure legend, the reader is referred to the web version of this article.)

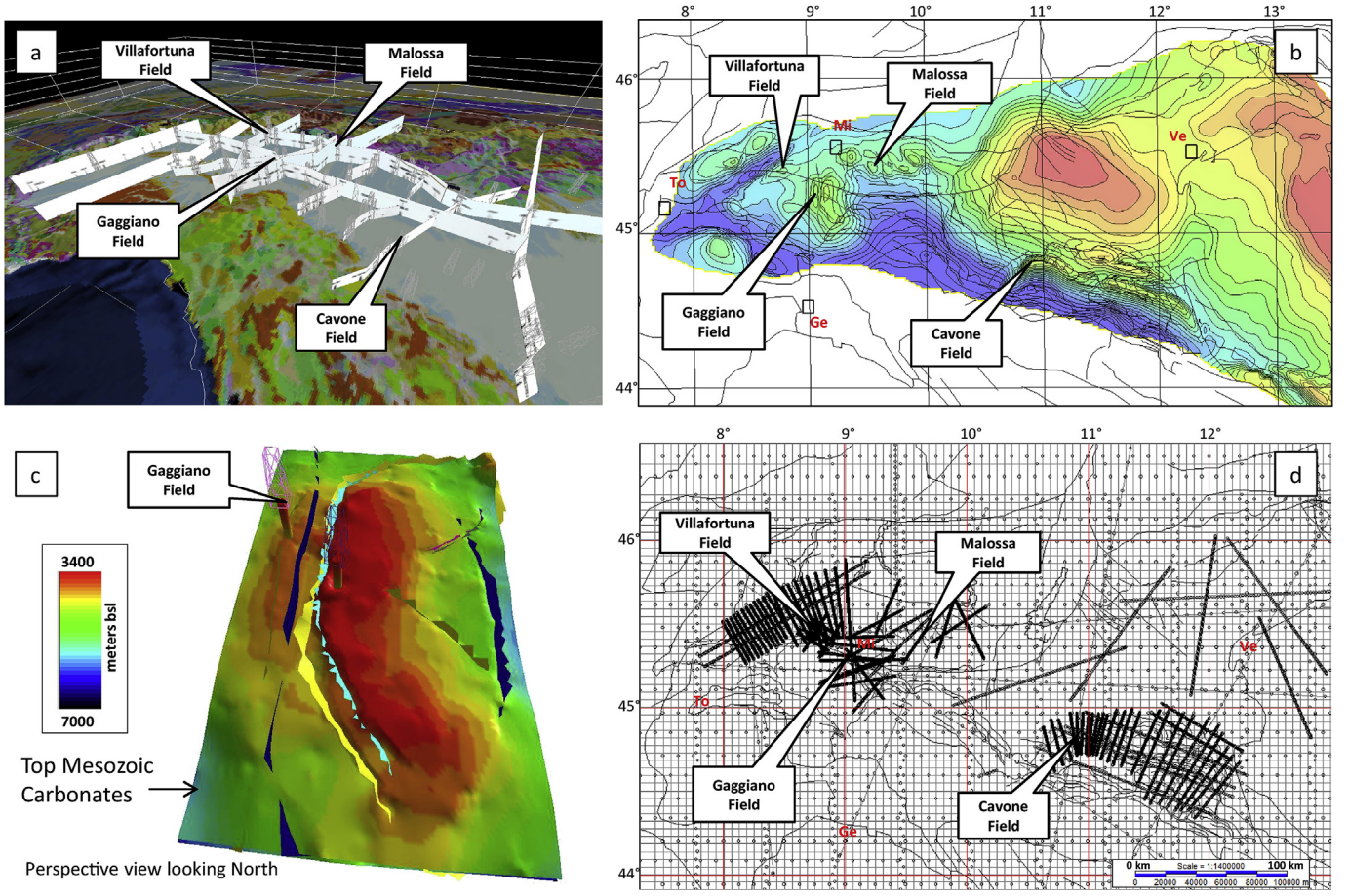

Fig. 3. Different images and views taken from the 3D model. a) DEM of the Po Valley (view from SE) with simplified geological map on the surface and cross sections from Cassano et al. (1986); b) depth structure contour map of the top of Mesozoic carbonates; c) 3d view of the Gaggiano field and the Lacchiarella inversion basin; d) Pseudo-sgy panels imported into the Kingdom project across the Po Valley basin (see text for explanation).

systematically analyzed every 5 km and the model structures were progressively validated along those sections much like in-lines and dip-lines inside a crustal scale pseudo-3D seismic survey. To be mentioned, the fault-surface building tool available in the Kingdom software was particularly useful for revisiting existing faults as well as building new ones when necessary.

3.3. Model building phase 3

The last phase of the 3D structural model reconstruction essentially consisted of infilling the Tertiary stratigraphy between the base Pliocene and the top Mesozoic layers. The exercise was entirely performed with the Kingdom software along the same pseudo-SEGY panels and by the same technique described for the model building phase 2. Noteworthy, some further integration of structural data/interpretation from the public literature was performed (Pola et al., 2014; GEOMOL project). Phase-1 cross-sections from Cassano et al. (1986) were again used as references to the work because they provide a real homogeneous set of data, seismic derived and tied to the key wells in the region. However, given the sparse distribution of those data and the tectono-stratigraphic complexity of the Po Valley Tertiary section, we acknowledge that the modeled top Oligocene, mid-early and mid-late Miocene grids a) represent, at present, a first approximation of the possible geological surfaces, b) would need further refining in order to interpret in detail the associated faults. Despite such an approximation, the new Tertiary layering can be considered a valid representation of the regional framework at the selected geological times. Hence the modeled layers were used to build isopach maps that do eventually describe the paleogeographic context of the different major foredeep basins (Fig. 5). In particular: a) the Paleogene as a whole (Paleocene-Eocene-Oligocene undifferentiated section), Miocene and Plio-Pleistocene foredeep wedges can now be identified in terms of specific geometry and dimension, b) because a clear-cut separation between the early-mid Miocene and the mid-late Miocene wedges remains problematic at the scale of the model, only the total Miocene isopach is presented in this paper whereas specific annotations have been added to that map to suggest the possible prevalence and extension of the different Miocene basins and the associated overlap zones. To be ultimately noted, the current results can be biased by local deviations from the average thickness, being related either to local tectonic overthickening within the different Miocene units and/or to erosional events (Pieri and Groppi, 1981; Ricci Lucchi, 1986; Rossi et al., 2015; Ghielmi et al., 2013; Di Giulio et al., 2013). Nevertheless, at the scale of the entire Po Valley region, the reconstructed Tertiary geometries are geologically sound and are consistent with the available public data and interpretations.

3.4. Restoration

2D restoration of selected cross-sections sliced from the model has been performed by the Structural Solver software (Nunns & Logan LLC). Key principles and assumptions behind the restoration

algorithm (Nunns, 1991) are that length is conserved along the reference horizon and that the deformed units are restored using vertical shear.

The purpose of the 2D restoration exercise is to validate the modeled 3D geometries in the respect of the standard balancing/restoration criteria (Dahlstrom, 1969; Hossack, 1979; Gibbs, 1983; Moretti and Raoult, 1990; Moretti et al., 1990), while attempting to define the key timing of the structure evolution (see Section 4.3). Also, the methodology is specifically used for the recognition of the Mesozoic framework in the central Po Valley foreland after vertical slicing of a number of serial cross-sections that were drawn in order to intersect the major oil fields in the region (see Section 4.3).

Important notes to the performed restorations are:

1. All of the structures cut from the 3D model had to be slightly edited to correct obvious geometrical inconsistencies derived from the model building and the related surface gridding. As such, those structures could be reasonably balanced before proceeding with the 2D restoration;
2. Given the available data, the model crustal-scale and the difficulty in choosing the required dip-direction due to the various structure orientations and the possible oblique movements along the faults (see discussion Section 5.2), the restored configurations should be considered as schematic and over-simplified solutions to the present-day structure complexity;
3. Provided the above consideration, the performed restorations were particularly devoted to unraveling the first-order crustal-scale tectono-sedimentary framework in terms of successive foredeeps, rather than to restoring the single structures in detail;
4. Results from restoration of the selected cross-sections in terms of structure timing, together with the kinematics information from the available literature (Castellarin et al., 1985; Doglioni and Bosellini, 1987; Nardon et al.,1991; Roure et al., 1990; Schonborn, 1992; Greber et al., 1997; Bello and Fantoni, 2002; Benedetti et al., 2003; Fantoni et al., 2003, 2004; Toscani et al., 2006, 2009; Livio et al., 2009a,b; Boccaletti et al., 2010; Mosca et al., 2010; Ponton, 2010; Masetti et al., 2012; Bresciani and Perotti, 2014; Pola et al., 2014), have been used to compile a deformation-time map that helps visualize the deformation progression across the Po Valley basin (see Fig. 15): in this sense, the derived deformation ages have been posted as punctual values across the basin and successively gridded into a continuous map representation of the regional tectonic evolution.

4. Structural geometries and kinematics in the Po Valley foreland basin

While few and isolated cross-sections have been built and restored in the past to gain information about selected areas of the Po Valley (Castellarin et al., 1985; Toscani et al., 2014), we use hereinafter the 3D model elements to provide a regional view of the basin tectonic kinematics from the Paleogene to the present. The derived structural evolution was defined by two different approaches. The first one relies upon the spatial definition of the successive foredeep basin geometries and dimensions: this allowed the recognition of the migration through time of the foredeep while considering the possible sediment contribution from the South Alpine and the Northern Apennines belts. The second approach refers to the restoration of the model structural units, which will expectedly improve recognition of the main stages of development of structures with reference to the associated syntectonic deposits. The restoration also further allows the pre-alpine paleogeography and the influence of the inherited structural pattern on the present-day regional structural fabric to be demonstrated.

4.1. Geometry of the present-day foreland at top Mesozoic level

The 3D structural model performed across the Po Valley basin has fully described the present-day deformation geometries in the region (Turrini et al., 2014, 2015). In particular, the top Mesozoic surface provided an outstanding picture of the deep foreland structures where two major domains can be observed caught in between the Southern Alps and the Northern Apennines belt (Fig. 4a). The western domain is deformed into a basin-and-dome pattern where variably oriented, thick-skinned structures occur. The eastern domain is essentially dominated by a large foreland high onto which the thin-skinned (mainly) Ferrara tectonic arc is thrust and displaced as part of the Apennines external front.

The current tectonic architecture of the carbonates essentially results from interference among a) Cenozoic, compression-related structures, b) pre-existing, Mesozoic (late Triassic-Early Jurassic) extension-related geometries, c) Mesozoic tectono-stratigraphic domains/facies (Fig. 4b) (Castellarin et al., 1985; Doglioni and Bosellini, 1987; Zanchi et al., 1990; Schonborn, 1992; Fantoni et al., 2004; Ravaglia et al., 2006, Castellarin and Cantelli, 2010; Cuffaro et al., 2010; Carminati and Doglioni, 2012; Vannoli et al., 2015; Pfiffner, 2014; Turrini et al., 2014). Within such a framework the foreland units are buried below Tertiary clastic sediments, these being deposited coevally with the progressive tectonic advancement of the Southern Alps and Northern Apennines belts towards the common foreland domain. Structures in the Tertiary deposits refer to folds and thrusts essentially oriented WNW-ESE (Pieri and Groppi, 1981; Bigi et al., 1990; Turrini et al., 2014 and references therein).

For the scope of this work it is important to stress that facies and geometry of the Triassic and Liassic carbonate formations are particularly discontinuous across the Po Valley basin (Fig. 4b) (Fantoni and Franciosi, 2010; Masetti et al., 2012; Turrini et al., 2016). Here, the derived syn-rift pelagic deposits and intra-pelagic ridges and plateaus, highly variable in terms of both thickness and rheology, likely constitute a non-homogeneous mechanical framework to the Alpine tectonic evolution of the basin.

4.2. Geometry and migration of the Tertiary foredeeps

4.2.1. The Paleogene foredeep

The Paleogene foredeep is shown in Fig. 5a by the isopach map which has been computed between the top of the Mesozoic Carbonates and the top Oligocene 3D grids. The map mainly considers the interpreted, undifferentiated, Paleogene section and aims at reproducing the possible paleogeography at top Oligocene time. As such, the derived thickness map of the foredeep deposits delineates the regional geometry of the basin which consists of two different zones at the front of the Southern Alps. The western zone (west of the Giudicarie trend; Giudicarie FZ in Fig. 5a) reaches a maximum thickness of 6–8 km and can be separated into two sub-zones, west and east of Milano, at the front of the western and central sectors of the Southern Alps, respectively. The eastern zone (east of the Giudicarie trend) shows a maximum thickness of 2 km at the front of the eastern sector of the Southern Alps.

The Paleogene foredeep map also shows two important anomalies which, due to their thickness, stand out from the regional basin fabric (Fig. 5a, A and B). The A anomaly is defined by a reduced thickness of the Paleogene deposits (approximately 1.5 km) as also indicated by a number of deep wells in the area: Seregna 1, Malossa 1, Chiari 1, Belvedere 1 (see Fig. 2 for well location) (Videpi database (http://unmig.sviluppoeconomico.gov.it/videpi/en/; Cassano et al., 1986). The structural restoration performed in Section 4.3 suggests the presence of a pre-existing structural high which corresponds to the Malossa oil field area. Conversely, the B anomaly is

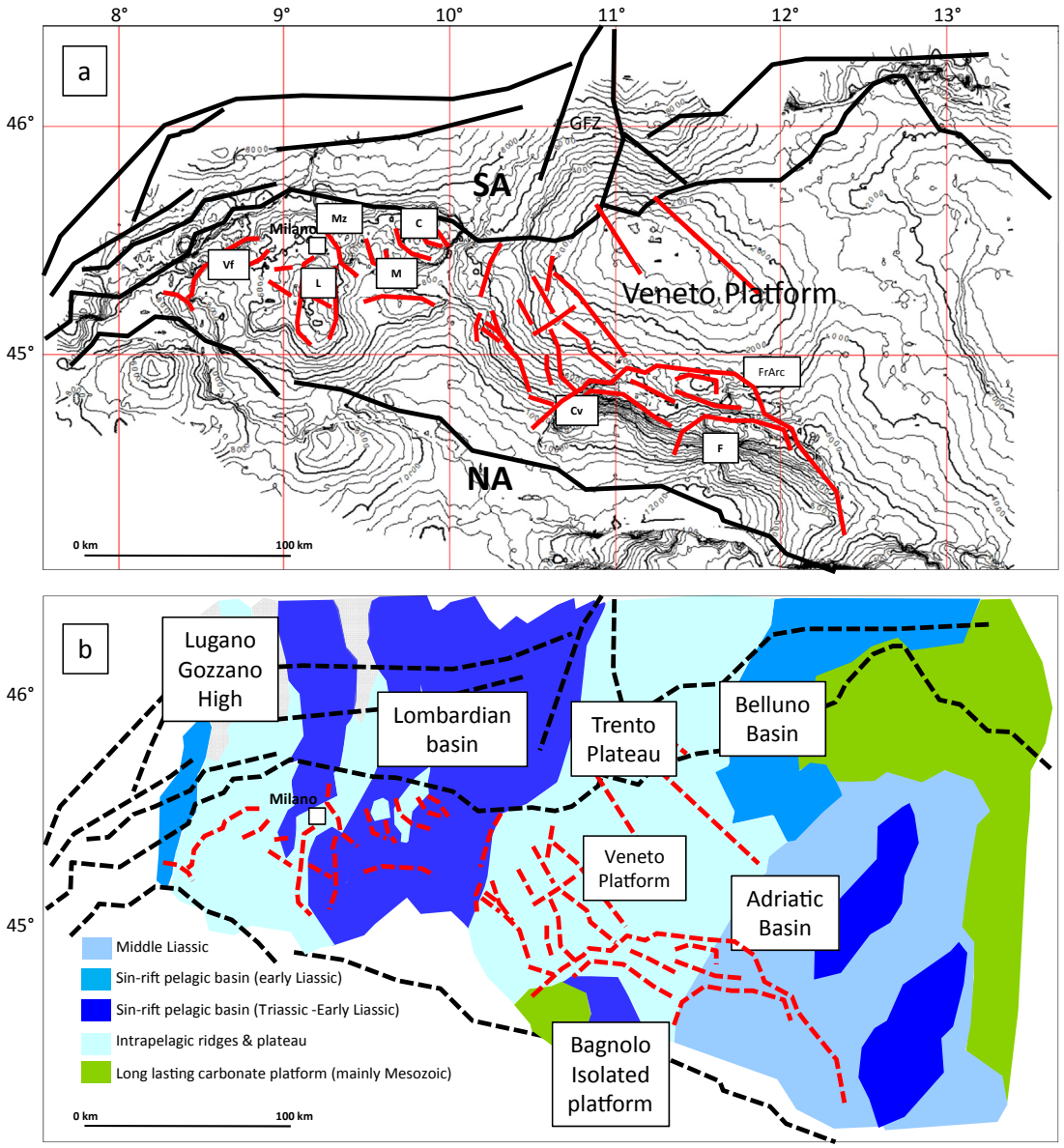

Fig. 4. a) Structure contour map (contour lines every 400 m) of the present day top Mesozoic Carbonates as derived from the Po Valley 3D structural model (Turrini et al., 2014): red and black lines are main buried faults and outcropping tectonic trends, respectively. Labels in the map are referred to hydrocarbon fields and/or geological structures described in the text (Vf = Villafortuna; L = Lacchiarella; M = Malossa; C = Chiari; Mz = Monza; Cv = Cavone; F = Ferrara; FrArc = Ferrara Arc). b) Tectono-stratigraphic unit distribution and facies (modified from Fantoni and Franciosi, 2010). Main structural elements (from Fig.4a) as dotted thick red and black lines. (For interpretation of the references to colour in this figure legend, the reader is referred to the web version of this article.)

defined by an important thickness of the Paleogene sediments (approximately 2–3 km). Although some local tectonic over-thickening is evident from the available data (Cassano et al., 1986) and confirmed by the structural restoration, the B zone might represent the northern termination of a Paleogene basin, which cannot be associated to the Southern Alp belt progression (see Discussion).

4.2.2. The Miocene foredeep

The 3D model Miocene isopach map (Fig. 5b) looks more complex than the one obtained for the Paleogene period. This complexity seemingly results from the interference between the Southern Alps and the Northern Apennines contributions to sedimentary input and tectonics.

At the scale of the Po Valley basin, two major zones can again be defined east and west of the Giudicarie trend (i.e. like for the Paleogene foredeep basin map, Fig. 5a). In the eastern part of the basin, the Miocene units are thin to nearly absent. Nevertheless, the isopach map shows differential thickening inside the Ferrara tectonic arc region with values between 1 km and 4 km. Here, the maximum thickness of Miocene sediments can be correlated with the B anomaly zone already recognized in the Paleogene foredeep map. In the western part of the basin, the thickness of the Miocene sediments varies between 1 km and 5 km on average. Inside this region, a N-S and a WSW-ENE oriented culminations (minimum sediment thickness) separate three different sub-zones:

1. East of Milano, the Miocene sedimentary wedge thickness gently increases towards the Northern Apennines. The 3D model reveals the present-day overlap between the early-mid

Miocene wedge and the late-mid Miocene which can be positioned at the mid-distance between the Southern Alps and the Northern Apennines outcrops. In this context, the early-mid Miocene basin has its depocenter to the north of the overlap zone and is possibly related to the Southern Alps foredeep accumulation (emM in Fig. 5b). Conversely, the mid-late Miocene basin and associated depocenter can be located to the south of the overlap zone and related to the Northern Apennines foredeep (mlM in Fig. 5b);
2. North-west of Milano the 3D shape of the early-mid Miocene deposits indicates the presence of a foredeep basin (emM in Fig. 5b) related to the western Southern Alps segment;
3. South-west of Milano, the modeled mid-late Miocene deposits thickness (mlM in Fig. 5b) defines the foredeep depocenter at the front of the Monferrato tectonic arc.

4.2.3. The Plio-Pleistocene foredeep

The Plio-Pleistocene foredeep geometry and dimension are illustrated in Fig. 5c which also is the representation of the current setting in the Po Valley region. Notwithstanding the intense tectonics, the map shows that the thickness of the present sedimentary wedge increases southwards and eastwards, as it reaches some maximum values (7–9 km) at the front of the Northern Apennines outcrops, inside and NW of the Ferrara tectonic arc. These geometries are in agreement with previous works (Pieri and Groppi, 1981; Cassano et al., 1986, Ghielmi et al., 2013; Turrini et al., 2014).

4.3. 2D restoration across the Po valley foreland basin

A number of selected cross-sections representative of the major Po Valley domains has been sliced from the 3D model and restored into their possible pre-compressional geometry. While checking the three-dimensional consistency of the modeled structures, 2D restoration helps in identifying the timing of their formation with respect to the larger-scale foredeep migration and reconstructing the pre-Alpine, Mesozoic extensional pattern.

Cross-section 1 cuts through the western Southern Alps foothills and the adjacent foreland domain (the Gattinara and the Villafortuna units respectively) (Fig. 6a). The present-day structures show a classic tectonic wedge configuration across the Southern Alps foothills domain. The north-dipping faults (arising from the belt) cut across the metamorphic basement and the Mesozoic units; they are flat at the base of the Tertiary sedimentary section and ramp again onto the Villafortuna foreland structure. The latter is deformed by south-dipping and antithetic north-dipping thrusts, which involve both the basement and the overlying Mesozoic thin cover. Well data in the region (Turbigo 1, Videpi database) indicate that the Paleogene section on top of the Villafortuna structure is faulted and tectonically over-thickened. The early-mid Miocene sediments are folded according to the thrust propagation and eroded at the crest culmination. Ultimately, the base of Pliocene deposits is tilted towards the south (i.e. towards the Northern Apennines). The restoration exercise (Fig. 6b) allows reconstruction of the foredeep and foreland units back into their pre-compressional configuration: a) the Paleogene sedimentary wedge is revealed with a possible maximum thickness of 4 km in between the Southern Alps and the foreland; b) the Jurassic-Cretaceous section is thinning southwards with a minimum thickness to the south of the Villafortuna location; c) here Triassic-Liassic faults should be invoked to justify the well-stratigraphy where a regional Jurassic high is interpreted (Cassano et al., 1986; Fantoni et al., 2004). From the comparison of the present geometries and their restoration, the mid-late Miocene appears to be the key moment in the structural timing of the foreland units due to folding and thrusting across the entire basement-Mesozoic-Tertiary rock package. Interestingly, the reconstructed geometry of the Paleogene wedge suggests the possible existence of early compressional structures (Oligocene?) inside the Southern Alps tectonic stack, in agreement with earlier works (Cassano et al., 1986; Schonborn, 1992).

Cross-section 2 (Fig. 7a) has been sliced across the units which form the foreland-foredeep domain at the front of the central Southern Alps, between Milano and the Giudicarie trend. The section shows: a) Plio-Pleistocene foredeep sedimentary wedge thinning northwards (i.e. towards the Southern Alps outcrops); b) a variable thickness of mainly early-mid Miocene sediments; c) evidence for a Paleogene wedge, involved in the compressional deformation; d) folds and faults that deform the Mesozoic section and the underlying basement. Despite the possible presence of thrusts across the Tertiary sedimentary package (Pieri and Groppi, 1981; Cassano et al., 1986, Fantoni et al., 2004) and the consequent over-estimate of the original sediment thickness, the presence of a Paleogene foredeep wedge, with a depocenter at the front of the Southern Alps belt, is supported by the restored sections at top Paleogene time (Fig. 7b). The resulting configuration highlights the regional dip of the Mesozoic carbonates towards the front of the advancing Southern Alps located north.

Cross-section 3 cuts through the western Po Valley (south of Milano) with a west-east orientation (Fig. 8a). The section essentially focuses on the structural geometries below the top of the Mesozoic carbonates, namely the Lacchiarella inverted Jurassic extensional graben and the adjacent Gaggiano high. The Tertiary deposits on top of those structures consist of thin mid-Miocene to nearly absent Paleogene clastics, below a thick Plio-Pleistocene package. Restoration of the cross-section to top Oligocene (Fig. 8b) allows the early basin inversion of the Lacchiarella Jurassic-Cretaceous graben to be highlighted (Fantoni et al., 2004) (see Fig. 12 for a pseudo-3D representation of the Mesozoic pre-compressional setting). The comparison with the present-day structure (Fig. 8a) suggests weak reactivation of the Lacchiarella fault system during the Miocene. To the west of the Lacchiarella basin, the Tertiary evolution of the Gaggiano units is revealed: a) since Triassic time (Fig. 8a–b) the Gaggiano structures constitute the footwall faulted blocks of the Lacchiarella fault as the Lacchiarella basin formed by extension and was subsequently inverted by compression; b) since the Paleogene and during the whole Neogene (Fig. 8 a–b), the Gaggiano structures were progressively buried and tilted westwards in response to lithospheric flexure of the Po Valley foreland.

The structures which form the zone of interaction between the buried fronts of the Northern Apennines (Emilia arc) and the Southern Alps (Milano arc) are represented in cross-section 4 (Fig. 9a). Along this section, the Tertiary sediments are deformed by folding and thrusting (Pieri and Groppi, 1981; Cassano et al., 1986) detached close to the top of the Mesozoic carbonates. At depth (6 km bsl), the carbonates are modeled to be eventually deformed by compression and tectonically displaced northwards below the Tertiary section, as suggested by Bello and Fantoni (2002). The restoration of the structures at the base Pliocene time (Fig. 9b) reveals that the Miocene sedimentary wedges are thinning northwards, over the south-dipping Mesozoic carbonates. Conversely, the Paleogene foredeep basin is thickening northwards (Fig. 9c), thus suggesting a regional dip of the associated Po Valley foreland towards the Southern Alps, as already shown by cross-sections 1 and 2 (Figs. 6 and 7). Timing of development of the shallow structures is clearly Plio-Pleistocene whereas, given the available constraints (Bello and Fantoni, 2002), the deep thrust-anticline in the Mesozoic carbonates could have developed at any moment from the top Oligocene to the present.

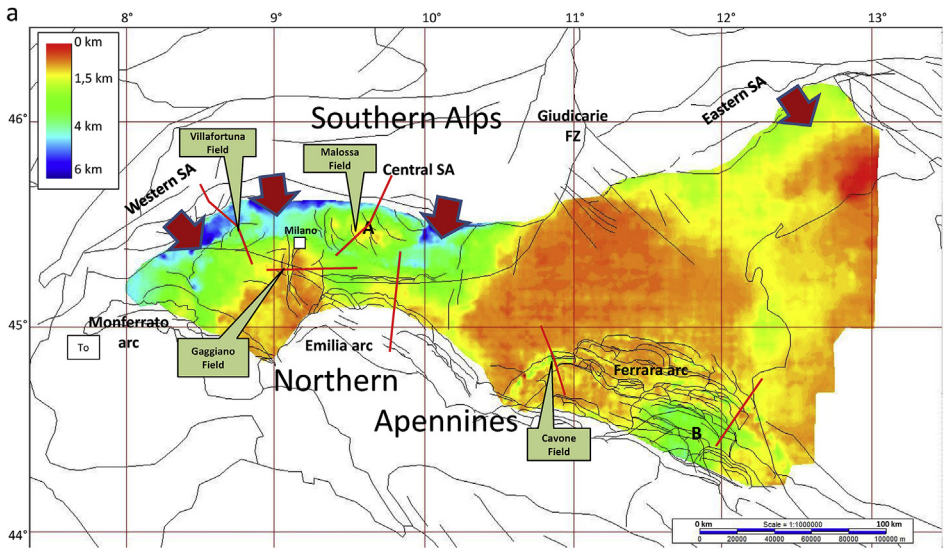
a
0 km
1,5 km
4 km
6 km
Southern Alps
Giudicarie FZ
Eastern SA
Western SA
Central SA
Villafortuna Field
Malossa Field
Milano
A
Monferrato arc
To
Gaggiano Field
Emilia arc
Northern Apennines
Ferrara arc
Cavone Field
B
8°
9°
10°
11°
12°
13°
46°
45°
44°

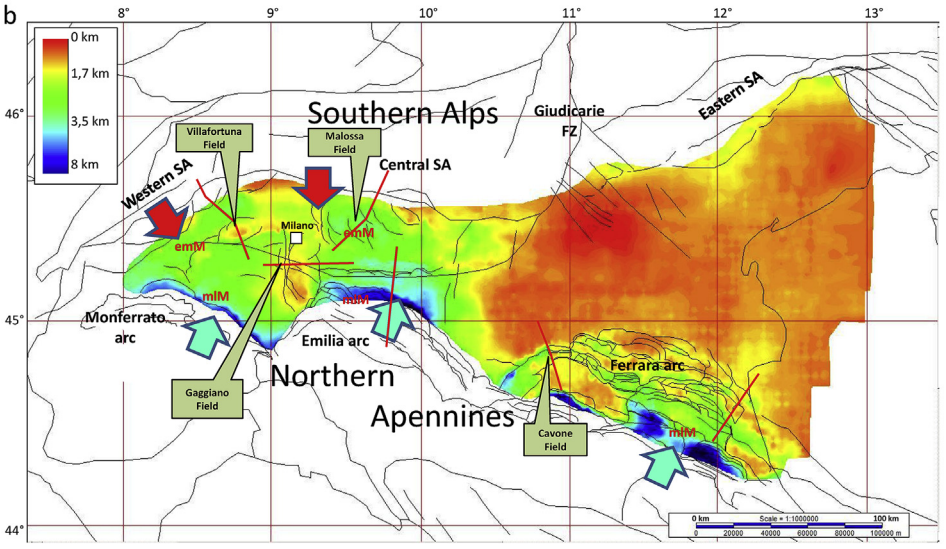
b
0 km
1,7 km
3,5 km
8 km
Southern Alps
Giudicarie FZ
Eastern SA
Western SA
Central SA
Villafortuna Field
Malossa Field
Milano
emM
emM
mlM
mlM
Monferrato arc
Gaggiano Field
Emilia arc
Northern Apennines
Ferrara arc
Cavone Field
mlM
8°
9°
10°
11°
12°
13°
46°
45°
44°

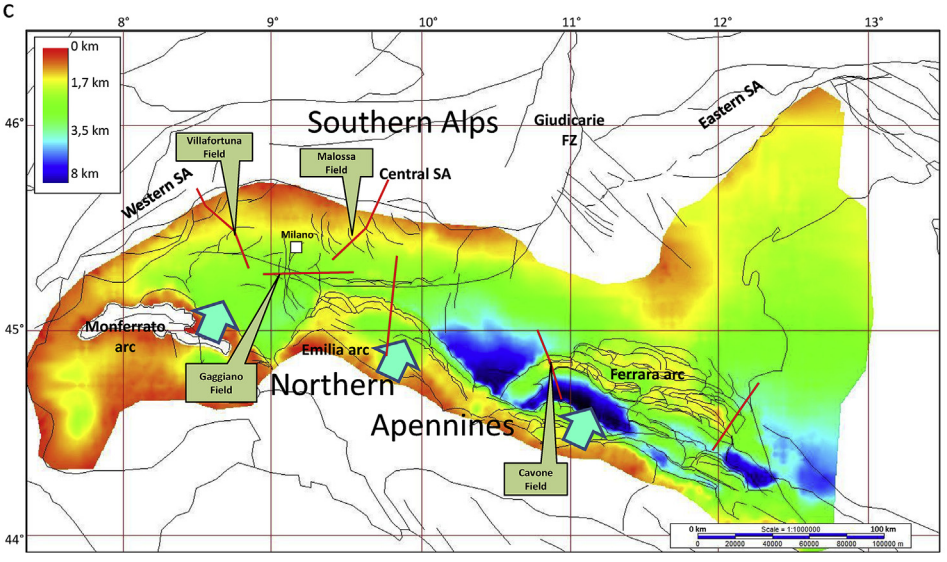
c
0 km
1,7 km
3,5 km
8 km
Southern Alps
Giudicarie FZ
Eastern SA
Western SA
Central SA
Villafortuna Field
Malossa Field
Milano
Monferrato arc
Gaggiano Field
Emilia arc
Northern Apennines
Ferrara arc
Cavone Field
8°
9°
10°
11°
12°
13°
46°
45°
44°

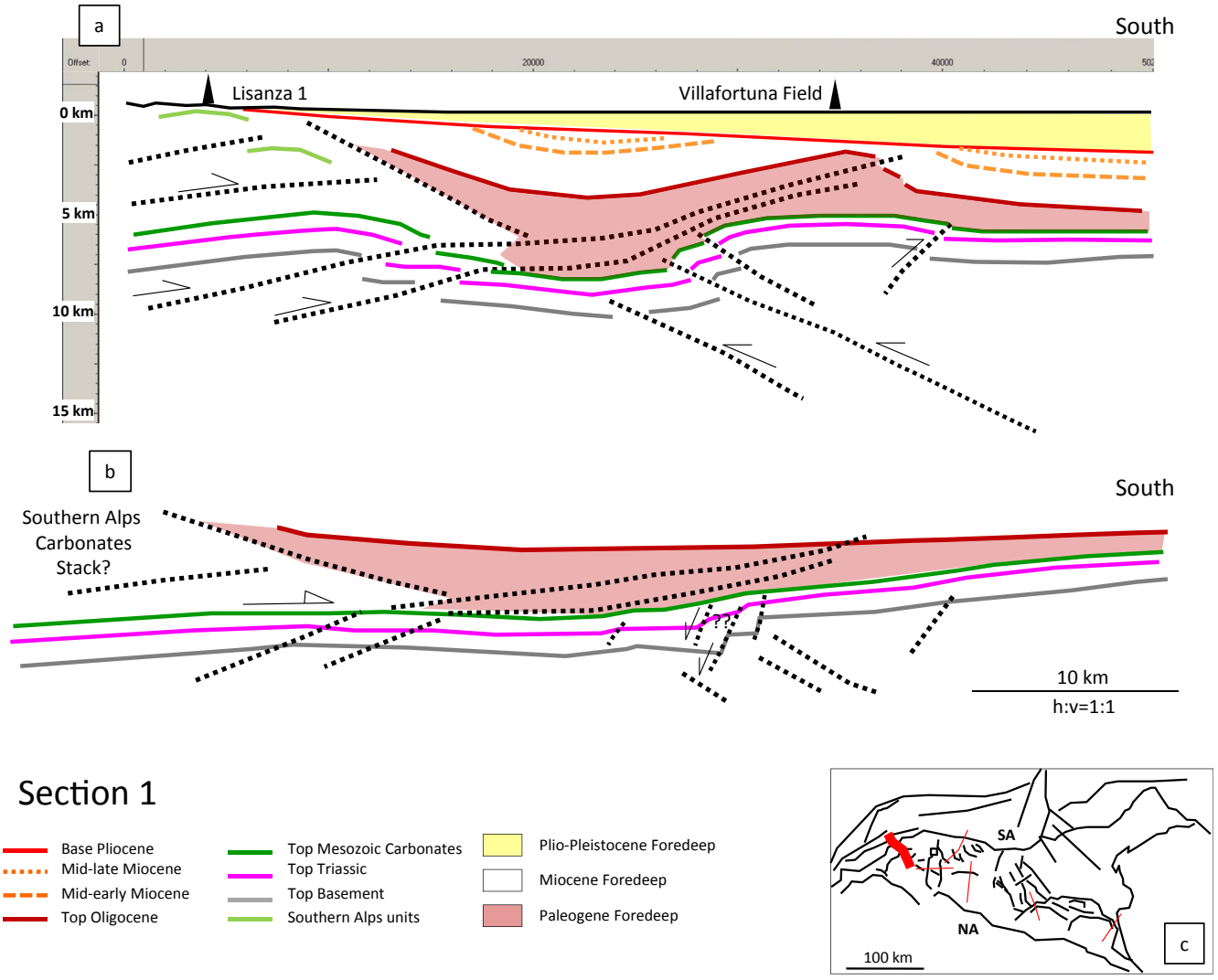

Fig. 6. Section 1: a) present-day structures in the Southern Alps-Villafortuna field region; b) structures restored at top mid-early Miocene time; c) cross-section location and tectonic elements from Fig. 4a.

Cross-section 5 and 6 (Figs. 10 and 11) show the structure-types forming the Ferrara arc, where the external front of the Northern Apennines is thrusting onto the Po Valley foreland (Pieri and Groppi, 1981; Castellarin et al., 1985; Cassano et al., 1986; Turrini et al., 2014 and references therein). Along section 5 (Fig. 10a), i.e., across the western lateral ramp of the Ferrara arc, the Cavone culmination results from strong tectonic imbrication of the Pre-Pliocene rocks detached along the top Triassic and the top of the crystalline basement. All across the thrusted fold, the Paleogene-Miocene sediments are relatively thin (Cassano et al., 1986) and nearly absent on the footwall-foreland side of the faulted anticline. The shape of the Plio-Pleistocene sedimentary wedge clearly indicates a regional southward dip of the foreland domain. The restoration (Fig. 10b) confirms the presence of a variable thickness Tertiary section, which becomes very thin northwards, and is possibly controlled by the presence of Paleogene-Miocene normal faults. The onset of the compressional structure is essentially Plio-Pleistocene in age as indicated by: a) folding and thrusting of the entire Meso-Cenozoic stratigraphic package, b) faults cutting through the base Pliocene surface, c) regional tilting of the foreland (and the faults within it) southwards (i.e. towards the Northern Apennines belt).

Cross-section 6 cuts through the eastern sector of the Ferrara tectonic arc (Fig. 11a) and shows NE verging faulted anticlines detached at multiple levels, with shallow pop-up structures involving post-Mesozoic deposits. At depth, faulting appears to deform also the basement, ahead and below the external, main thrust front. The pre-compressional configuration (Fig. 11b) highlights that Tertiary

Fig. 5. a - Isopach map of the Paleogene deposits, built from the 3D model. Thickness variations highlight foredeep geometry across the Po Valley. Red lines represent the traces of the cross-sections selected for restoration and discussed in the text. Red arrows indicate prevalent foredeep sediment sources (Pfiffner, 2014). b) - Isopach map of the Miocene deposits, built from the 3D model. Thickness variations allow imaging of the foredeep basin geometry across the Po Valley region: emM = area for prevalent early-mid Miocene foredeep deposition; mlM = area for prevalent mid-late Miocene foredeep deposition. Red lines are location of the cross-sections selected for restoration. Red arrows and blue arrows indicates the prevalent foredeep sediment sources from the Southern Alps and Apennines belts, respectively. c) - Isopach map of the Plio-Pleistocene deposits, built from the 3D model. Thickness variations highlight foredeep geometry across the Po Valley. (For interpretation of the references to colour in this figure legend, the reader is referred to the web version of this article.)

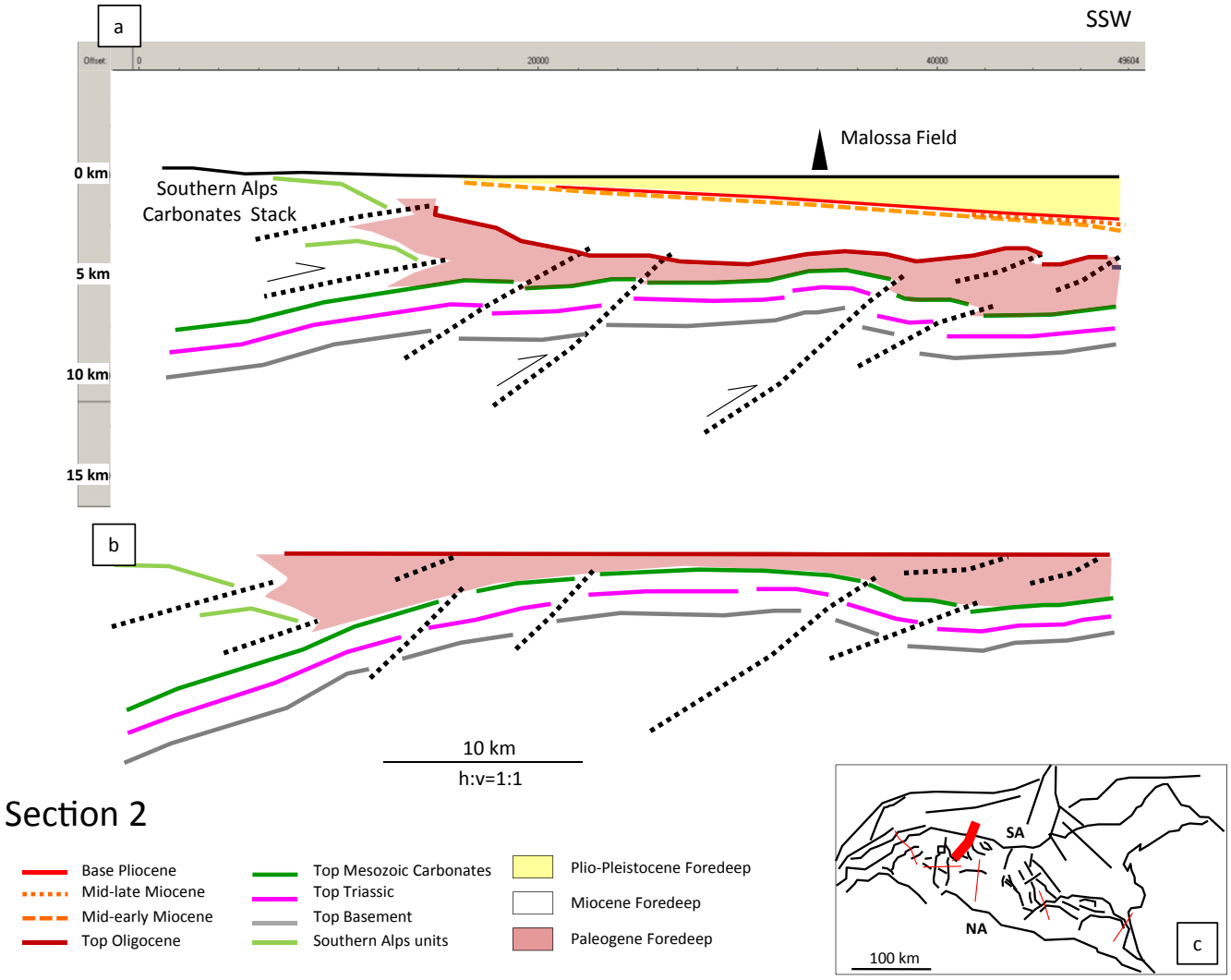

Fig. 7. Section 2: a) present-day structures in the Southern Alps-Malossa field region; b) structures restored at top Oligocene time; c) cross-section location and tectonic elements from Fig. 4a.

sediments, possibly Paleogene and Miocene in age (Cassano et al., 1986), become thinner northwards. The presence of some possible Paleogene-Miocene faults can again be speculated to control the Tertiary sediment variation, like for cross-section 5 (Fig. 10b). Also in this case, timing of main deformation is Plio-Pleistocene.

Cross-sections 7 to 12 (Figs. 12 and 13) have been sliced from the 3D model with the aim to intersect the deep units which form the Mesozoic foreland in the most suitable orientation for restoration. Due to the nearly N-S direction of the Mesozoic paleogeographic elements (Turrini et al., 2014 and reference therein), the sections are oriented approximately east-west and they extend from the central to the westernmost Po Valley. For all of the chosen cross-sections, the overlying Tertiary sediments and tectonics are excluded from the exercise, provided their main sense of displacement along the north-south direction (i.e. perpendicular to the section planes). The present-day structures in the area (Fig. 12) show faulting and folding of the Mesozoic carbonates and their basement (Cassano et al., 1986; Fantoni et al., 2004; Ravaglia et al., 2006; Turrini et al., 2014). The final tectono-stratigraphic setting suggests basin inversion as the dominant deformation process with a) vertical expulsion of the Jurassic-Cretaceous basins, b) limited displacement along the single faults, c) localized thrust-related stacking and possible short-cutting of the pre-Alpine extensional hinge blocks (Fig. 12: below the Monza 1 location and structures to the west of the Malossa field).

Restoration of the structures (Fig. 13) allows the possible Mesozoic, extensional geometries to be reconstructed back to their pre-compressional configuration (this latter essentially referring to the early Liassic episode of extensional deformation, the late Triassic episode being nearly impossible to be distinguished around the basin). Diffuse faulted blocks-forming horsts and deep grabens are revealed together with their possible original dimensions (30 km long and 15 km wide, maximum thickness of the Mesozoic package of 4 km). Basins show lozenge-shape geometry and curved fault traces with relay zones at the transition between the different basins (Fig. 13a). Thickening of the Jurassic-Cretaceous sediments is also revealed (Fig. 13: the Belvedere and the Lacchiarella basins).

In details, all of the mentioned extension-related features are confirmed. In the northernmost region (cross-sections 11 and 12 in Fig. 13) the major boundary fault is west dipping yet east-dipping faults are developed as well. The two fault sets control the thickness increase of both the Jurassic and Triassic sediments from west

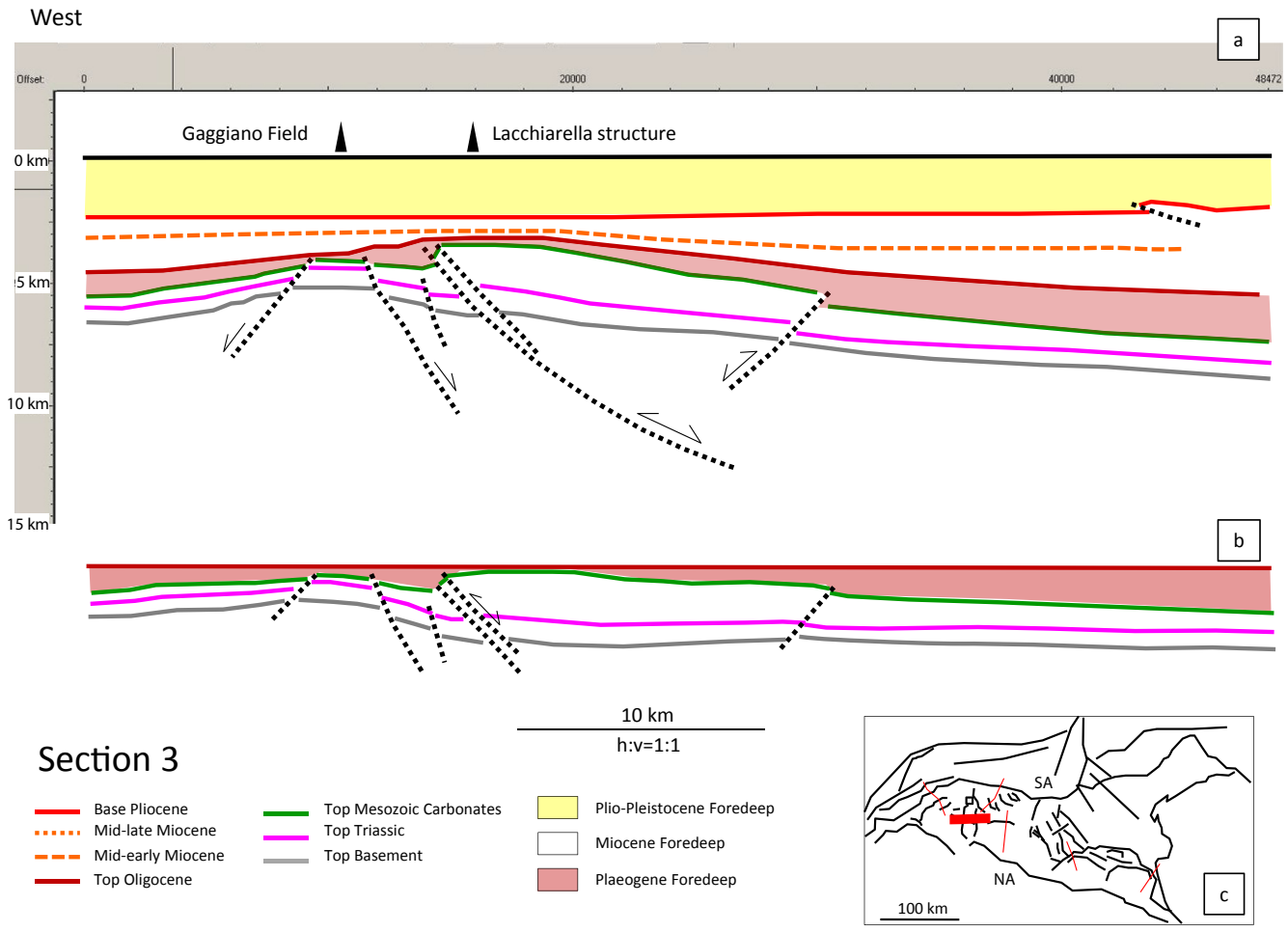

Fig. 8. Section 3: a) present-day structures in the Gaggiano field-Lacchiarella structure region; b) structures restored at top Oligocene time; c) cross-section location and tectonic elements from Fig.4a.

to east. In the southernmost region (cross-sections 13-16 in Fig. 13) the master fault dips towards the east so that the west dipping faults are mainly minor antithetic faults. Nevertheless and once again, thickness of the Mesozoic deposits appears to increase towards the east of the region. The pseudo-3D perspective observation of the serial cross-sections clearly reveals the possible correlation across the modeled faults.

The comparison between Figs. 12 and 13 helps to recognize those faults which could have been re-activated during the Alpine inversion tectonics. At the same time it is also possible to define which of the present faults have been newly created under compression (see fault legend Fig. 13).

The restoration of the various cross-sections indicates an average shortening between 10% and 15% with a minimum value (5%) measured in the Lacchiarella inversion basin (Fig. 8) and a maximum value (28%) across the Cavone structure (Fig. 10). The shortening values correspond to a cumulative displacement along the faults which have been modeled along the various cross-sections in the range of 2–5 km in the western Po Valley and 10–12 km across the Ferrara arc in the eastern Po Valley.

5. Discussion

Worldwide examples available from the literature (e.g. Beydoun et al., 1992; Uliana et al., 1995; Maţenco et al., 1997; Muñoz-Jiménez and Casas-Sainz, 1997; Garfunkel and Greiling, 2002; Ziegler et al., 2002; Lacombe al., 2003; Norman Kent and Dasgupta, 2004; McQuarrie et al., 2005; Mann et al., 2006; Naylor and Sinclair, 2008; Oszczypko, 2006; Fantoni and Franciosi, 2010; Toscani et al., 2014) allows the Po Valley to be considered as a rather unique foreland basin. This is essentially because of the occurrence of two key-characteristics: a) it developed intermittently at the front of two different mountain chains, the Northern Apennines and the Southern Alps, progressively converging one towards the other; b) the inherited structures, mainly derived from the Mesozoic extensional tectonics, are oriented at high angle to the advancing belts.

Starting from such considerations, in the following discussion we use the outcomes of this study to argue about the Oligocene-Neogene Po Valley foreland evolution under a new, basin scale and quantitative perspective. In particular, a) the reconstructed Tertiary basins' geometry/migration (section 4.2) is used to substantiate the foreland development as a function of the Mesozoic tectonics and carbonate facies distribution during the Alpine structural history; b) the performed 2D restorations (section 4.3) are used to suggest the Cenozoic tectonics in terms of structures' timing and structural mechanics across the basin; c) the overall results are used to focus on the Po Valley lithosphere geodynamics while comparing them to some foreland-foredeep configurations taken from the available literature.

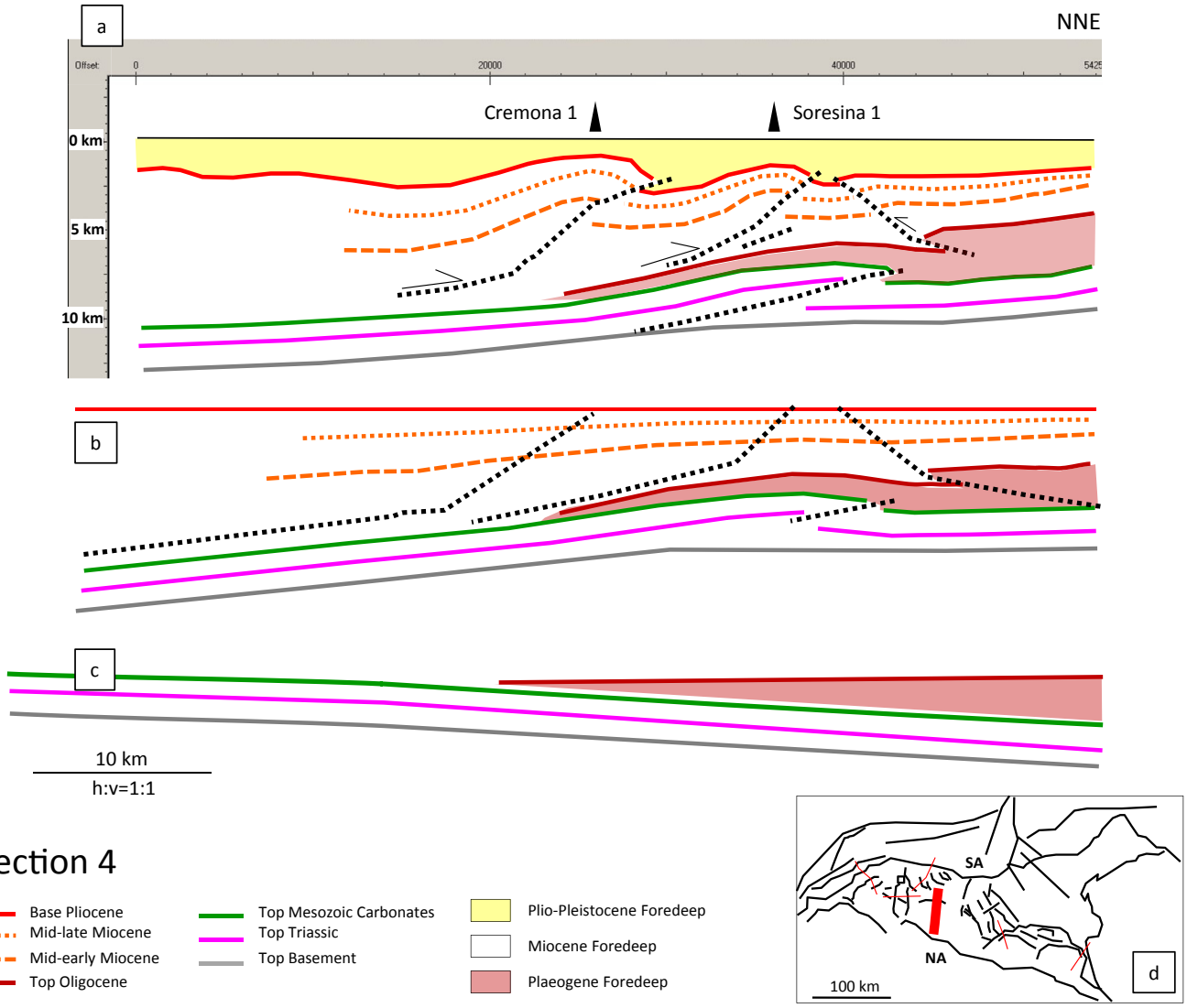

Fig. 9. Section 4: a) present-day structures in the Cremona-Soresina structure region; b) structures restored at near top Miocene time; c) cross-section location and tectonic elements from Fig. 4a.

5.1. Influence of the Mesozoic inherited structures on the foreland tectonics

5.1.1. Foredeep migration-geometry versus Mesozoic tectono-stratigraphic grain

Deposition of the Paleogene foredeep sediments (Fig. 14a) appears to have taken place predominantly in the northern sector of the western Po Valley region. Here the sedimentary wedge of the Gonfolite formation (Bernoulli et al., 1993; Di Capua et al., 2015) was deposited along and deformed by the Southern Alps external front (Figs. 14a, 6–7 km of sediment thickness). Over the eastern Po Valley, the deposition of the Paleogene successions (1–2 km) was largely impeached by the foreland architecture. In that area, the Mesozoic carbonates and their underlying basement provide a crustal-scale structural high and an obstacle to the belt propagation (i.e. the Veneto Platform in Fig. 14a; Masetti et al., 2012; Turrini et al., 2014; Toscani et al., 2016 and references therein). The deformation-time map of the basin (Fig. 15) shows that the western Po Valley was strongly affected by the Alpine compression, which resulted in some early-stage thrusting inside the Southern Alps (Fig. 6) (Schonborn, 1992; Greber et al., 1997) and local inversion of pre-existing extensional basins at the front of the advancing belt (Fig. 8) (Fantoni et al., 2004).

In Miocene times, compression was particularly concentrated all along the front of the Southern Alps (Fig. 15) and, through time, it progressively migrated eastwards (Castellarin et al., 1985; Doglioni and Bosellini, 1987; Ponton, 2010). Both the foredeep geometry and the foreland deformation inside the Po Valley basin appear to have been strongly influenced by the pre-Alpine configuration (Fig. 14b). The modeled geometry of the Miocene basins suggests a setting similar to the Paleogene one: the foreland backbone controlled the distribution of the foredeep sediments whose major depocenters occurred in the western Po Valley (1–4 km), likely responding to both the Southern Alps and the Northern Apennines tectonic pulses and sedimentary input (Fig. 16b). On the other hand and again, the eastern Po Valley foreland domain was an area of reduced sedimentation (1–2 km) and still stood as a barrier to the progression of the buried Southern Alps and Northern Apennines deformation fronts (Figs. 14b and 16b).

Ultimately, during Plio-Pleistocene times, deformation was essentially occurring at the front of the Apenninic belt and along the eastern sector of the Southern Alps (Figs. 14c and 15) (Turrini

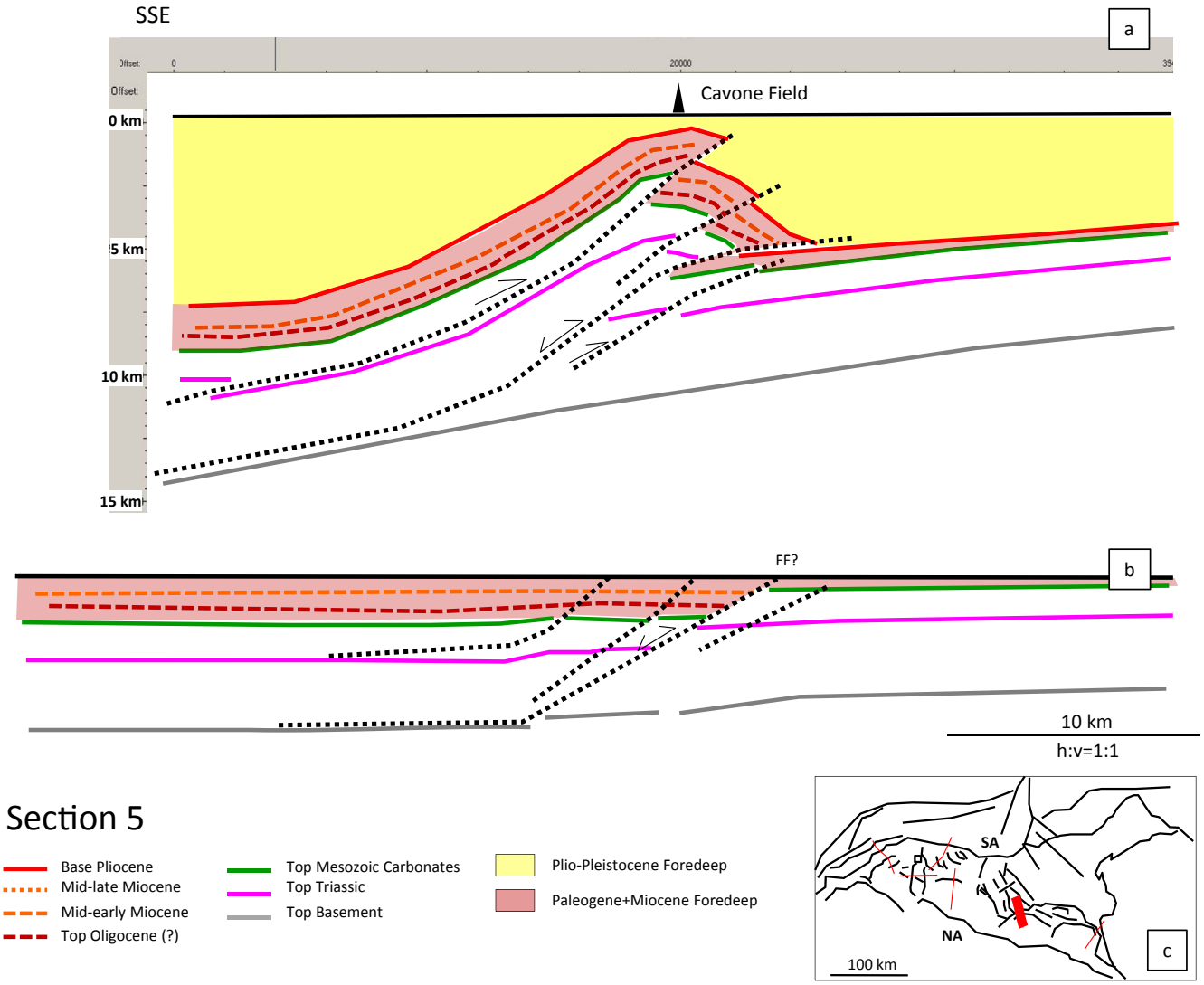

Fig. 10. Section 5: a) present-day structures in the Cavone field region, across the western Ferrara arc (Northern Apennines buried external front); b) structures restored at near top Miocene time; FF = possible flexure related fault c) cross-section location and tectonic elements from Fig. 4a.

et al., 2015 and references therein). The reconstructed Plio-Pleistocene basin geometry confirms that the crustal scale configuration has dramatically changed during that period. Indeed, the related isopach map indicates progressive thinning of the associated sedimentary wedge towards the Southern Alps and the development of some major depocenters (4–8 km) along the Northern Apennines (Fig. 16c). Due to the ongoing processes (subduction, lithosphere flexuring; see below) the influence of the Apenninic orogeny on the Po Valley tectonics became dominant while the inheritance from the Mesozoic fabric appears more subtle: a) the Apennines external front cuts across the foreland domain in the eastern Po Valley foreland while forming the Ferrara arc; b) here, the pre-compressional boundary between the Trento platform and the Adriatic basins (Fantoni and Franciosi, 2010; Masetti et al., 2012) was displaced towards the NE, c) the derived transfer zone (Pieri and Groppi, 1981; Bigi et al., 1990; Turrini et al., 2014, 2015 and references therein) that can be observed to separate the Ferrara arc into two different structural units (see Figs. 4b and 14c) may represent the ultimate indicator of the Mesozoic structural inheritance.

5.1.2. Alpine tectonics versus Mesozoic tectono-stratigraphic grain

It is noticeable that during the entire Cenozoic, the foreland tectono-stratigraphic elements inherited from the Mesozoic extensional phases remained oriented at high angle with respect to the advancing belt fronts (see and compare Figs. 14 and 16). Such faults are the only ones which localize important thickness variations of the Mesozoic deposits (Fig. 13: the Belvedere and Lacchiarella basins). Considering the general NNW motion of the Adria plate (Carminati et al., 2012; Pfiffner, 2014, Fig. 16a) and the nearly N-S orientation of the pre-Alpine faults, an important component of wrenching (i.e. oblique compression) along these faults can be likely speculated during the inversion process. Further, 3D model geometries shows that only part of the extension-related faults were reactivated by compression while others were not (see and compare Figs. 12 and 13). At the same time, newly formed thrusts cut through the Mesozoic stratigraphic succession and the underlying basement.

Following the examples and studies from Letouzey (1990), Lowell (1995) and Ziegler (1989) while considering the structure kinematics and the geodynamic time-steps illustrated in Figs. 15 and 16, it is then possible to suggest that:

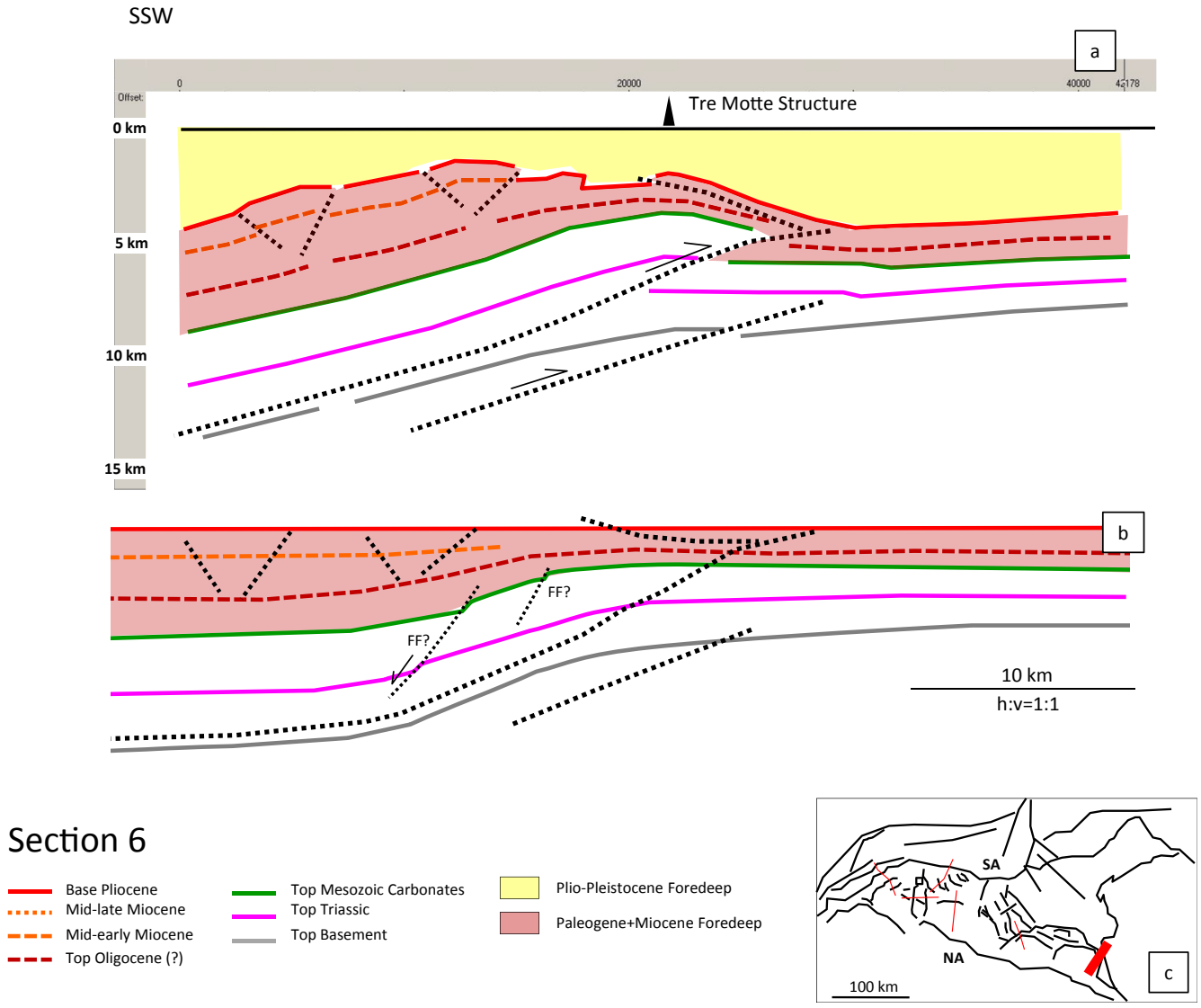

Fig. 11. Section 6: a) present-day structures in the Tre Motte well region, across the eastern Ferrara arc (Northern Apennines buried external front); b) structures restored at near top Miocene time; FF = possible flexure related fault c) cross-section location and tectonic elements from Fig. 4a.

1. Inherited Mesozoic faults that were reactivated across the Po Valley foreland (see and compare Figs. 12 and 13) must have undergone an important strike-slip deformation component due to their obliquity with respect to the direction of tectonic transport of the Alpine fronts. As an extreme case, those faults oriented parallel to the maximum compressional direction possibly did not suffer any strike-slip deformation at all (Lowell, 1995). However, the final, variable oblique component would be difficult to assess by the current crustal-scale 3D model. Further specific analysis based on fault slip tendency (Maesano et al., 2015b), sedimentation rates (Maesano and D'Ambrogi, 2016) and high resolution 3D seismic data would serve that objective. Similar structural configuration are rare yet the Ceara Piaui basin in northeast Brazil and the Salta Province in northern Argentina (Lowell, 1995 and reference therein) might be considered as possible analogs to the deep setting in the Po Valley;
2. the newly formed Alpine faults likely account for generic oblique deformation with a dominant reverse component. These thrusts eventually decapitate pre-existing hinge zones (short-cut structures; e.g. the Monza structure: see and compare Figs. 12 and 13) or they passively displace old normal faults (e.g. the Villafortuna and Malossa field structures: see and compare Figs. 12 and 13) (Errico et al., 1980; Fantoni et al., 2004). In such a case, the strike-slip component is subordinate to the compressional one. Similar configurations are widely known from the North Sea region (see examples from Buchanan and Buchanan, 1995), the Atlas foreland (Letouzey, 1990; Lowell, 1995), the western and central Argentina (Uliana et al., 1995) and the Pyrenees foreland (Bond and McClay, 1995; Guimera et al., 1995);
3. the interaction among pre-orogenic (approximately N-S oriented, extension-related) and orogenic (approximately ESE-WNW oriented, compression-related) faults could eventually play a key role in controlling the localization of arc-shaped fronts in the Mesozoic-basement rock package, namely the Ferrara arc (Fig. 4a). In this case, together with the carbonate facies distribution (Fig. 4a–b), fault interference would control the development of lateral ramps, tear-transfer zones and some possible differential displacement inside the thrust-related

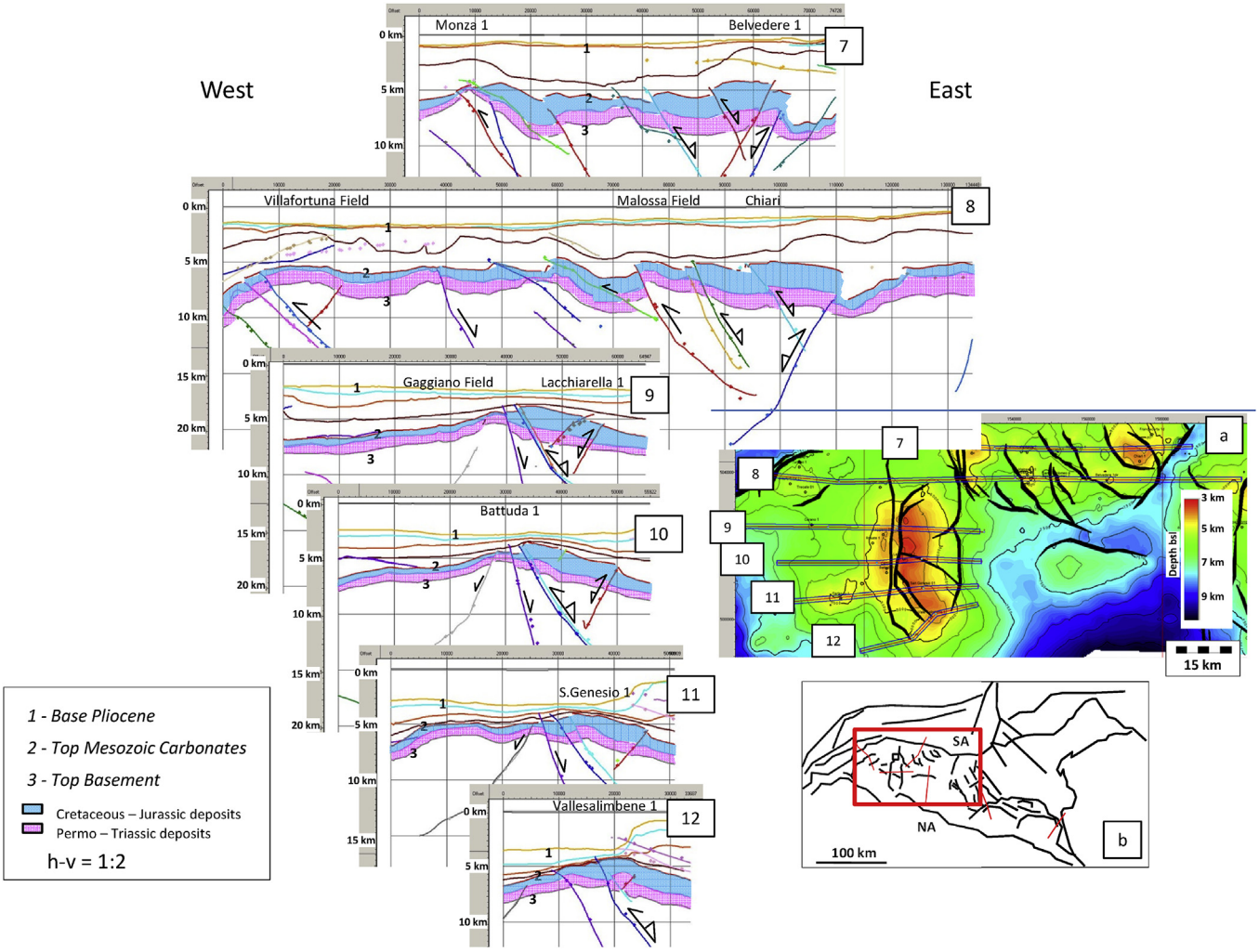

Fig. 12. Serial cross-sections illustrating the present-day structures in the western and central Po Valley: fault colour-code derives from correlation criteria only, during interpretation in the Kingdom software (see arrows for main fault kinematics: normal, reverse, inverted); a) Cross-section location on the top Mesozoic carbonate depth map (black polygons are faults); b) study area location in the Po Valley region. The structure and the cross sections are discussed in Section 4.3.

units of the structural arc (Ravaglia et al., 2006; Doglioni and Carminati, 2008; Bonini et al., 2014; Vannoli et al., 2015 and references therein), similar to what has been reported for instance in the Taiwan foreland (Lacombe et al., 2003);

4. bends in the extensional fault patterns, on map view, might have localized releasing-restraining deformation zones (Figs. 4 and 15) (Letouzey, 1990; Lowell, 1995);
5. during the Paleogene, given the distance of the Po Valley foreland from the Alpine orogeny (Fig. 16a: more than 100 km?), localized fault reactivation and basin inversion (Bernoulli et al., 1990, Bertotti et al., 1998, Fantoni et al., 2004, Cuffaro et al., 2010) were likely responding to some intra-plate deformation in response to far-field stress transmission. Such a situation is similar to a multitude of positive inverted features that can be mapped 100-to-1000 km away from the Alpine suture (Ziegler, 1989 and various examples from Buchanan and Buchanan, 1995);
6. in Miocene times, thrusting and pre-compressional fault reactivation might have equally contributed to the Po Valley regional basin inversion because of a relative proximity of the foreland to the Southern Alps and the Northern Apennines chains (Fig. 16b);
7. since the Pliocene, thrusting is the primary deformation mechanism across the foreland units (Castellarin et al., 1985). This is especially striking along the southern sectors of the basin where the foreland domain becomes the regional footwall of the Northern Apennines front (Fig. 16c), as suggested by the earthquake occurrence across the Ferrara tectonic arc (Bonini et al., 2014; Carannante et al., 2015; Turrini et al., 2015 and references therein). During this period, post-Mesozoic, likely flexure-related faults (Fig. 10) were reactivated (WNW-ESE oriented, parallel to the Apennines mountain front?), short-cut geometries developed (Figs. 10 and 11) and inherited pre-Alpine faults were possibly re-used to form lateral ramps/tear-transfer zones inside the tectonic arcs (see discussion above).

5.1.3. - Po valley tectonics and kinematics versus inherited lithospheric weakness

As already mentioned, basin inversion inside the Po Valley region (and the associated foredeep migration) was locally enhanced or impeached by the facies and geometry distribution of the Mesozoic carbonate deposits across the foreland domains (Fig. 4b).

The whole process was eventually influenced by the strength and thermal state of the Po Valley/Adria lithosphere at the time of orogenic shortening as inherited from lithospheric stretching and heating during the Triassic-Liassic rift evolution. Such a generic

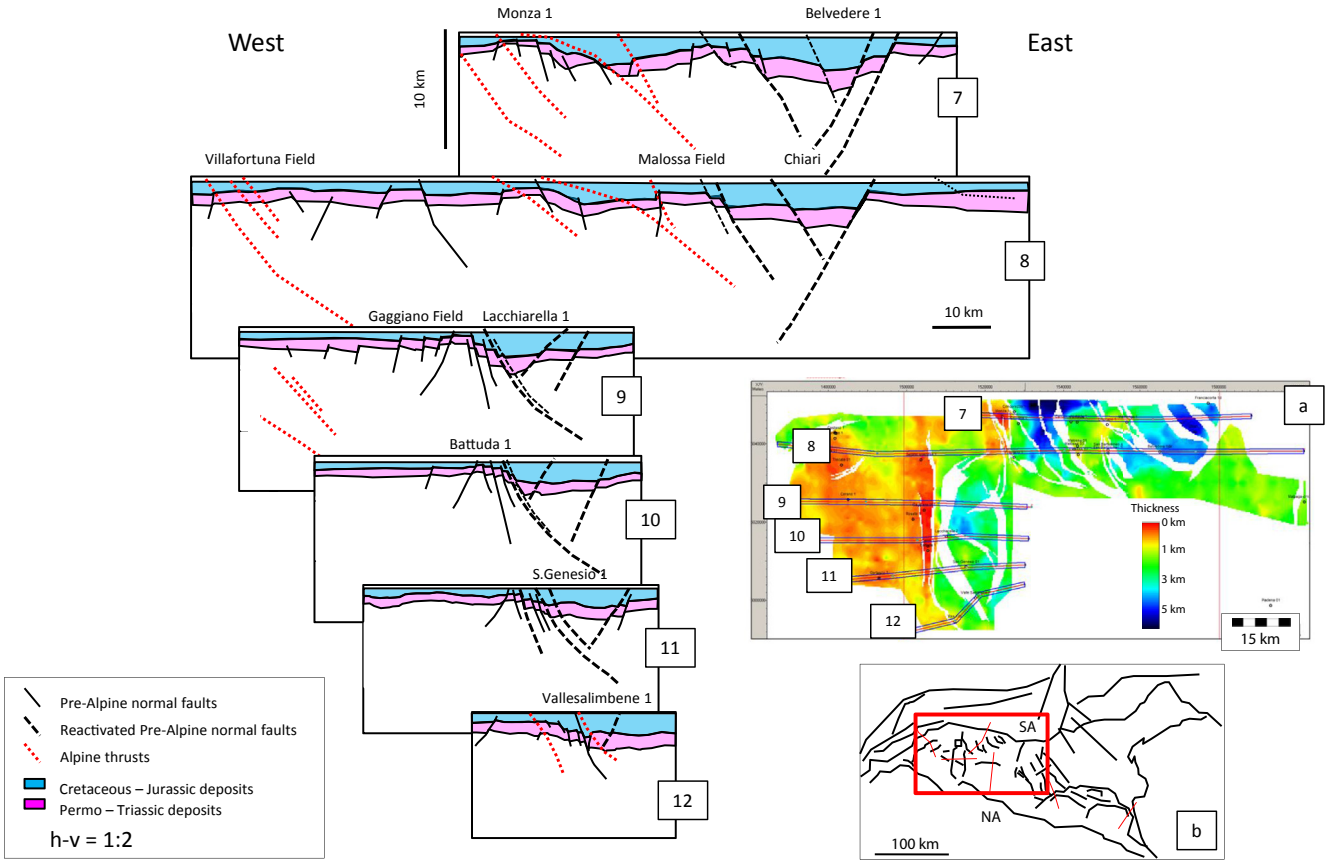

Fig. 13. Serial cross section of Fig. 11 after restoration of the structures at the top of Mesozoic. Pre-alpine normal faults, reactivated normal faults and Alpine thrusts have been distinguished in order to highlight the effect of the Alpine tectonic activity on a pre-existing inherited paleogeography; a) Cross-section location on the Jurassic-Cretaceous isopach map and fault polygons (in white); b) study area location in the Po Valley region. The structure and the cross sections are discussed in Section 4.3.

consideration is supported by theory (Cloetingh et al., 2005) and examples worldwide (e.g. Desegaulx et al., 1990; Mouthereau et al., 2013). Nevertheless, once the weak stretching of the crust during the Mesozoic events is considered (30-25 km of crustal thickness soon after the rifting? Fantoni and Scotti, 2003) together with the progressive thermal re-equilibration from Paleogene to present (e.g. heat flow values went back to a 'normal' 60 mW/m2 by the beginning of Cretaceous: Fantoni and Scotti, 2003 and references therein), we would speculate that both inherited crustal stretching and heating did not act as primary elements in controlling the Alpine structural evolution and the flexural response of the lithosphere within the Po Valley foreland-foredeep system.

5.2. Considerations about the Po valley as a retro/pro wedge foreland basin

Although foreland basins can be found all over the world in association with the development of ancient (pre-Cenozoic) and modern (Cenozoic) mountain ranges, rare are the situations that can be fully compared with the Po Valley foreland-foredeep tectonic system, in terms of interaction between the contributing belts and the derived tectono-stratigraphic complexity.

Indeed, from Cretaceous to present-day the Po Valley region was

1. the retro-wedge foreland basin to the Southern Alps; examples of similar setting include the Andean basins, the Pyrenees-Aquitaine basin, the late Mesozoic to Cenozoic Rocky Mountain basins of North America, the Appalachian basin (e.g., Garfunkel and Greiling, 2002; Ziegler et al., 2002; McQuarrie et al., 2005; Naylor and Sinclair, 2008),
2. possibly the simultaneous retro/pro-wedge foreland basin to the Southern Alps and the Northern Apennines, respectively. This complex setting of a flexural basin trapped in between two convergent orogenic fronts would compare with the Roja through (northern Spain), that is the common foreland of western Pyrenees and Cameros-Demanda Massif, the Adriatic sea (between Apennines et Dinarides-Albanides), the Assam basin (northeastern India) between SE verging Himalaya thrust and NW verging fronts of the Assam-Arakan belt, and the Maracaibo basin between Caribbean belt, Andes de Merida and Sierra de Perija (e.g., Muñoz-Jiménez and Casas-Sainz, 1997; Norman Kent and Dasgupta, 2004; Mann et al., 2006; Fantoni and Franciosi, 2010).
3. the pro-wedge foreland basin to the Northern Apennines, a setting to be compared to the Atlas basin, the Uralian basin, the Ebro basin of the South Pyrenees, the Carpathian basin and the coastal Plain of Taiwan: Maţenco et al., 1997, 2003; Ziegler et al., 2002; Lin and Watts, 2002; Tensi et al., 2006; Oszczypko, 2006; Naylor and Sinclair, 2008).

As the various basin-type systems progressively developed through the Tertiary, the related depozones (De Celles and Giles, 1996) were formed mainly in response to the surrounding geodynamics (Fig. 16).

The Paleogene, Southern Alps-related retro-wedge foreland basin was likely (exclusively?) controlled (Ziegler et al., 2002) by the topographic load of the orogenic wedge and a moderate flexure

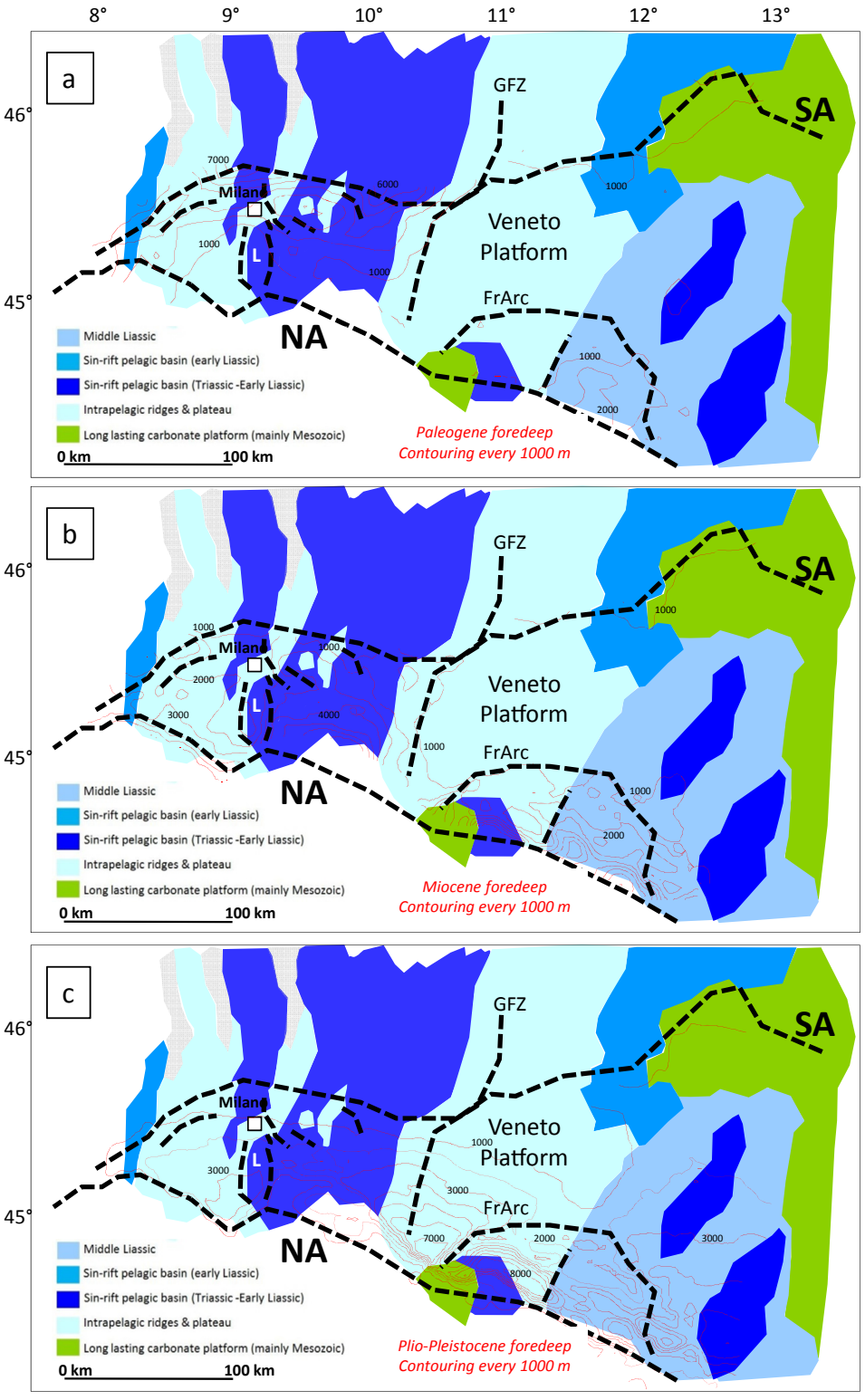

Fig. 14. Foredeep geometry against the simplified present-day, top Mesozoic tectonics (black dashed lines; see Fig. 3a for the complete fault pattern) and the main tectono-stratigraphic unit distribution (from Fig. 4b). Contour lines of the foredeep are represented in red (every 1000 m) respectively for Paleogene (a), Miocene (b) and Plio-Pleistocene (c) times. (For interpretation of the references to colour in this figure legend, the reader is referred to the web version of this article.)

of the Adria lithosphere. From the performed model, the associated foredeep could fill a variable accommodation space 30–50 km wide and 1–6 km thick along the segmented belt (Figs. 5a and 15a). Also clearly illustrated by the modeled top Oligocene foreland-foredeep map, the Mesozoic carbonates units provided a differentiated forebulge depozone (region of potential flexure uplift with possible reduced sedimentation; DeCelles and Giles, 1996), by abrupt, W-to-E lateral changes in the carbonate mechanical stratigraphy and inherited geometry of the pre-Alpine structures (see section 5.1). The anomaly B already described SE of the basin (Figs. 5a and 16a)

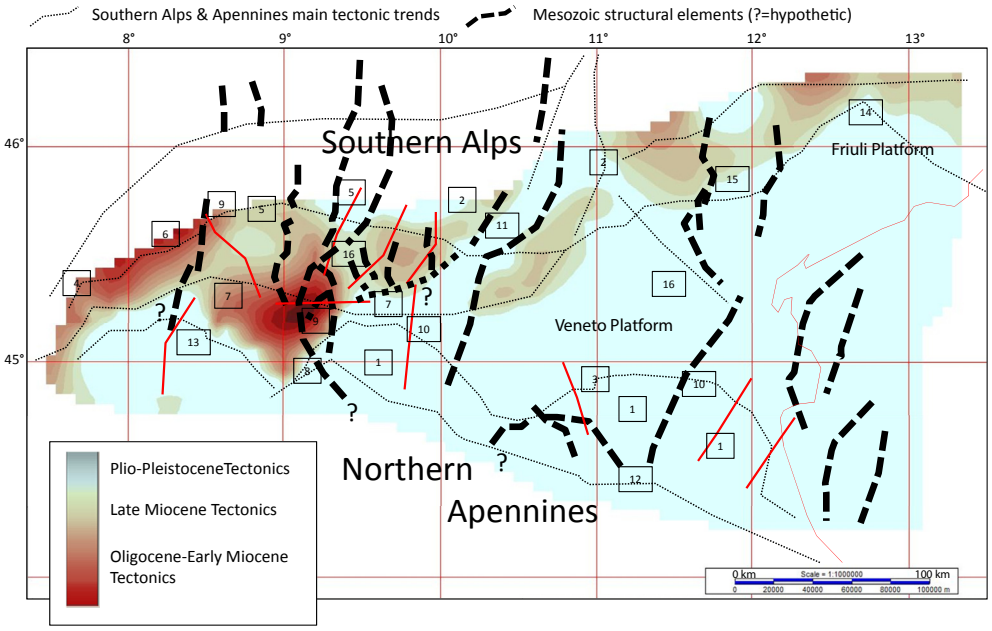

Fig. 15. Deformation-time map illustrating the timing of the main stages of the tectonic evolution of the Po Valley (red Oligocene-Early Miocene to grey Plio-Pleistocene): black thick dashed lines are main pre-Alpine Mesozoic lineaments; black thin dashed lines are main Alpine-Apennine lineaments. Cross-sections traces described in previous pictures and in the text are also indicated by thin red solid lines. Numbers refer to key papers which have been used for adding deformation timing-points for final gridding: 1) Castellarin et al., 1985; 2) Doglioni and Bosellini, 1987; 3) Nardon et al., 1991; 4) Roure et al., 1990; 5) Schonborn, 1992; 6) Greber et al., 1997; 7) Bello and Fantoni, 2002; 8) Benedetti et al., 2003; 9) Fantoni et al., 2003, 2004; 10) Toscani et al., 2006, 2009; 11) Livio et al., 2009a; 12) Boccaletti et al., 2010; 13) Mosca et al., 2010; Ponton, 2010; 14) Masetti et al., 2012; 15) Bresciani and Perotti, 2014; 16) Pola et al., 2014. (For interpretation of the references to colour in this figure legend, the reader is referred to the web version of this article.)

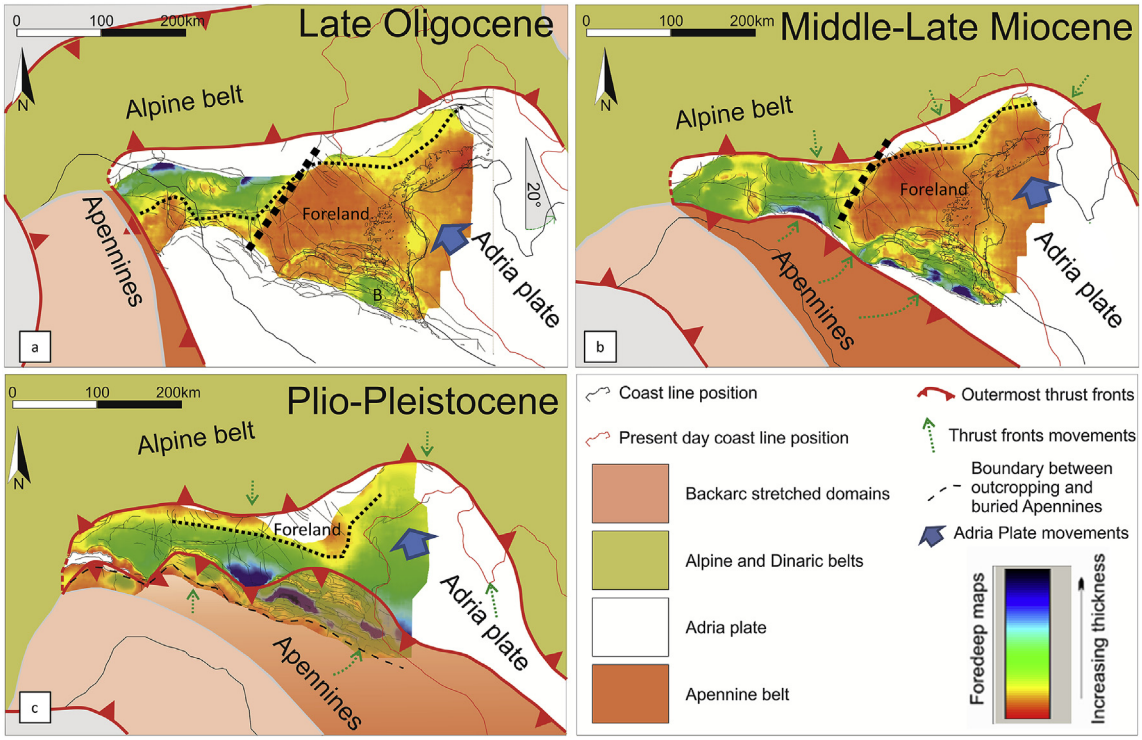

Fig. 16. –Po Valley foredeep geometry and basin migration (see maps in Fig. 5) against the Alps-Apennines geodynamic framework at a) Oligocene, b) upper Miocene and c) base Pliocene time (geodynamic framework modified after Carminati et al., 2012).

could eventually represent part of backbulge domain of the Paleogene foreland basin (could it be, alternatively, the backbulge of the Dinarides foredeep?). Mechanical coupling at crustal level (Ziegler et al., 2002) of the Southern Alps orogenic wedge with its retro-wedge foreland basin can be speculated during the Paleogene when the far-field inversion of the extension-related structures (Fig. 8) are considered.

The Southern Alps retro-wedge and the Northern Apennines

pro-wedge foreland basins interfered with each other during the Miocene period (Fig. 16b). The progressive flexure and bending of the Po Valley-Adria plate below the Northern Apennines have possibly controlled the asymmetry of the overall foredeep sedimentary wedge which became thicker towards the south of the region. The associated wedge-top sediments deposited at the front of both the Southern Alps (on top of the Paleogene foredeep) and the Northern Apennines (Di Giulio et al., 2013; Rossi et al., 2015). The forebulge depozone is difficult to be defined yet it may be represented by the thin sediments which cover the east Po Valley foreland unit (Figs. 5b and 16b). No backbulge depositional areas can be recognized from the Miocene foreland-foredeep map (Figs. 5b and 16b). The thrust-related imbricates by low-angle detachments at the front of the Southern Alps (i.e. below the Lisanza structure on cross-section 1, Fig. 6) suggest mechanical coupling at upper-crustal levels (Ziegler et al., 2002) between the Southern Alps and the northern sectors of the foreland (i.e. the regional footwall to the belt). At the same time involvement of the basement by high angle thrusts (see the Villafortuna structure on cross-section 1, Fig. 6 and the Malossa structures on cross-section 2, Fig. 7) also indicate crustal mechanical coupling between the belts and the far-field foreland domain (Ziegler et al., 2002). The entire thrust-belt-foreland structure associations and the related deformation mechanisms suggest thick skinned tectonics (Lacombe and Bellahsen, 2016).

The Plio-Pleistocene configuration described in Figs. 5c and 16c represents the Northern Apennines pro-wedge foreland basin. The Adria lithosphere flexure controlled the basin geometry (Kruse and Royden, 1994; Doglioni, 1995; Carminati et al., 2003; Carminati and Doglioni, 2012) which is narrow and deep (50 km wide, max 7–9 km deep) (Fig. 16c; see also Fig. 5c). The associated equivalent elastic thickness would be in the order of 20 km (Watts, 1992; Mouthereau et al., 2013). The Pliocene sediments represent the main wedge-top depozone at the front of the Apennine belt. At the same time, the Plio-Pleistocene deposits constitute the foredeep deposits, these being thinning northwards. The forebulge depozone is definitively absent because of the short distance between the Southern Alps and the Northern Apennines mountain belts (Toscani et al., 2014). During this geological period mechanical coupling of the orogenic wedge with the foreland appears mainly restricted to upper crustal levels (Ziegler et al., 2002). In fact, all across the Northern Apennines tectonic arcs, folds and thrusts were mainly controlled by rheologically weak sedimentary layers, such as evaporites (Burano formation in the Ferrara arc; Cassano et al., 1986; Turrini et al., 2014, 2015 and references therein) and overpressured sandstones-shales intervals (Bosica and Shiner, 2013), these acting as stress guides and activated as detachment horizons. Subordinately, crustal mechanical coupling between the belt and the far-field foreland, hence involvement of the basement, may be loosely inferred from the deep earthquakes distribution in the eastern domain of the Po Valley exclusively (Vannoli et al., 2015; Carannante et al., 2015; Turrini et al., 2015).

6. Conclusions

The Po Valley developed as the nearly simultaneous pro/retro-wedge foreland basin to the Southern Alps and the Northern Apennines, respectively.

By implementing the available 3D structural model with some new grid horizons within the Tertiary succession we have provided the possible geometry and migration of the related foreland-foredeep tectonic system from Oligocene to present-day.

The final 3D model reconstruction and the 2D restoration across selected structural domains illustrate the following conclusions:

1. the Mesozoic, extension-related tectonics and the associated carbonate facies geometry and distribution have strongly controlled the Alpine structures inside/around the basin;
2. their control on the Cenozoic deformation and sedimentation is evident during the Paleogene and the Miocene whereas it becomes more subtle during the Plio-Pleistocene;
3. indeed, basin inversion and reactivation (with undefined strike-slip component) of pre-Alpine faults (approximately N-S oriented) intermittently occurred during the Paleogene and Miocene, when crustal mechanical coupling between the belts and the foreland enhanced intra-plate deformation, far from the advancing orogens: thick skinned tectonics was then dominant across the belt-foreland system;
4. in this period, flexure of the Po Valley/Adria plate was responding initially (Paleogene) to the Southern Alps growth and lately (Miocene) to the Northern Apennines development also, leaving room for the associated foredeep basin deposition;
5. in Plio-Pleistocene times the presence of a narrow and deep foredeep at the front of the Northern Apennines refers to a clear asymmetry of the Po Valley/Adria flexure;
6. Plio-Pleistocene deformation of the foreland mainly occurs at the external front of the Northern Apennines by thrusting, with local inversion-reactivation of both flexure-related faults (approximately WNW-ESE oriented) and pre-Alpine discontinuities (approximately N-S oriented): a) the two fault families compete to form tectonic arcs in the Mesozoic section, b) thin-skinned tectonics prevails across the eastern Po Valley foreland domain, c) involvement of the basement in that region is possible yet still debatable;
7. the narrow and deep Plio-Pleistocene foredeep basin all along the front of the Northern Apennines suggests that a) the foreland flexure is rather homogeneous below the belt, b) the N-S oriented lithospheric weaknesses derived from the Triassic-Liassic extensional tectonics do not exert a major control on the crustal deformation of the subducting Po Valley-Adria plate (possibly due to a weak amount of pre-orogenic extension together with a re-gained thermal equilibrium since the Triassic-Liassic rifting).

Once all elements are considered (differential bending of the Po Valley-Adria lithosphere below the two belts, intermittent and variable rate and direction of shortening ahead of the belts, highly differentiated mechanical stratigraphy and non-homogeneous geometry/dimension of the pre-compressional foreland units, variable sedimentation rates along the belts), the geological complexity of the region stands out as a real challenge for integration of all available data and interpretations.

As a follow-up to the 3D structural model (Turrini et al., 2014) and the 3D seismo-tectonic model of the basin (Turrini et al., 2015), this study provides a quantitative, kinematically and geometrically consistent picture of the Po Valley foreland-foredeep evolution at the basin scale: this represents a true novelty, so far missing in the regional literature.

Beyond the explicit regional implications, despite the necessary simplifications of the model and notwithstanding the related uncertainties, this case study can serve as a source of inspiration in terms of both scientific thinking and working methodology for other complex foreland basins worldwide, especially those where tectono-sedimentary inhomogeneity is spatially and temporally dominant and lateral structure correlation is complex and debatable owing to the lack of clear seismic data.

Acknowledgments

The authors would like to thank the Associated Editor Dario

Civile, Giovanni Barreca and another anonymous reviewer for the detailed revision of the paper and the related valuable suggestions.

References

Argnani, A., Ricci Lucchi, F., 2001. Tertiary siliciclastic turbidite systems of the Northern Apennines. In: Vai, G.B., Martini, I.P. (Eds.), Anatomy of an Orogen: the Apennines and Adjacent Mediterranean Basins. Springer, pp. 327–350.

Bally, A.W., Burbi, L., Cooper, C., Ghelardoni, R., 1986. Balanced sections and seismic reflection profiles across the Central Apennines. Mem. Soc. Geol. It. 35, 257–310.

Barbieri, C., Bertotti, G., Di Giulio, A., Fantoni, R., Zoetermeijer, R., 2004. Flexural response of the Venetian foreland to the Southalpine tectonics along the TRANSALP profile. Terra Nova 16 (5), 273–280. http://dx.doi.org/10.1111/j.1365-3121.2004.00561.x.

Basili, R., Valensise, G., Vannoli, P., Burrato, P., Fracassi, U., Mariano, S., Tiberti, M.M., Boschi, E., 2008. The Database of Individual Seismogenic Sources (DISS), version 3: summarizing 20 years of research on Italy's earthquake geology. Tectonophysics 453 (1–4), 20–43. http://dx.doi.org/10.1016/j.tecto.2007.04.014.

Beaumont, C., Ellis, S., Pfiffner, A., 1999. Dynamics of sediment subduction-accretion at convergent margins: short-term modes, long-term deformation, and tectonic implications. J. Geophys. Res. 104, 17573–17601.

Bello, M., Fantoni, R., 2002. Deep oil plays in the po valley: deformation and hydrocarbon generation in a deformed foreland. In: AAPG HEDBERG CONFERENCE, "Deformation History, Fluid Flow Reconstruction and Reservoir Appraisal in Foreland Fold and Thrust Belts" May 14-18, 2002, Palermo e Mondello (Sicily, Italy).

Benedetti, L.C., Tapponnier, P., Gaudemer, Y., Manighetti, I., Van der Woerd, J., 2003. Geomorphic evidence for an emergent active thrust along the edge of the Po Plain: the Broni-Stradella fault. J. Geophys. Res. 108 (B5), 2238. http://dx.doi.org/10.1029/2001JB001546.

Bennett, R.A., Serpelloni, E., Hreinsdóttir, S., Brandon, M.T., Buble, G., Basic, T., Casale, G., Cavaliere, A., Anzidei, M., Marjonovic, M., Minelli, G., Molli, G., Montanari, A., 2012. Syn-convergence extension observed using the RETREAT GPS network, northern Apennines, Italy. J. Geophys. Res. 117, B04408. http://dx.doi.org/10.1029/2011JB008744.

Bernoulli, D., Bertotti, G., Froitzheim, N., 1990. Mesozoic faults and associated sediments in the Austroalpine-South Alpine passive continental margin. Mem. Soc. Geol. Ital. 45, 25–38.

Bernoulli, D., Giger, M., Muller, D.W., Ziegler, U.R.F., 1993. Sr-isotope stratigraphy of the Gonfolite Lombarda Group (South-alpine molasse, northern Italy) and radiometric constraints for its age of deposition. Ecl. Geol. Helv. 86 (3), 751–767.

Bertotti, G., Picotti, V., Bernoulli, D., Castellarin, A., 1993. From rifting to drifting: tectonic evolution of the South-Alpine upper crust from the Triassic to the Early Cretaceous. Sediment. Geol. 86, 53–76. http://dx.doi.org/10.1016/0037-0738(93)90133-P.

Bertotti, G., Picotti, V., Cloetingh, S., 1998. Lithospheric weakening during "retro-foreland" basin formation: tectonic evolution of the central South Alpine foredeep. Tectonics 17 (1), 131–142.

Beydoun, Z.R., Clarke, M.W.H., Stoneley, R., 1992. Petroleum in the Zagros Basin: a late Tertiary foreland basin overprinted onto the outer edge of a vast hydrocarbon-rich Paleozoic–Mesozoic passive-margin shelf. In: Macqueen, R.W., Leckie, D.A. (Eds.), Foreland Basins and Fold Belts. Am. Assoc. Pet. Geol. Memoir, vol. 55, pp. 309–339.

Bigi, G., Cosentino, D., Parotto, M., Sartori, R., Scandone, P., 1990. Structural model of Italy and gravity map, 1:500,000. Quad. Ric. Sci. 114, 3 (S.EL.CA Florence).

Boccaletti, M., Coli, M., Eva, C., Ferrari, G., Giglia, G., Lazzarotto, A., Merlanti, F., Nicolich, R., Papani, G., Postpischl, D., 1985. Considerations on the seismotectonics of the northern Apennines. Tectonophysics 117, 7–38. http://dx.doi.org/10.1016/0040-1951(85)90234-3.

Boccaletti, M., Calamita, F., Deiana, G., Gelati, R., Massari, F., Moratti, G., Ricci Lucchi, F., 1990. Migrating foredeep-thrust belt system in the northern Apennines and southern Alps. Palaeogeogr. Palaeoclim. Palaeoecol. 77, 3–14. http://dx.doi.org/10.1016/0031-0182(90)90095-O.

Boccaletti, M., Corti, G., Martelli, L., 2010. Recent and active tectonics of the external zone of the Northern Apennines (Italy). Int J Earth Sci (Geol Rundsch). http://dx.doi.org/10.1007/s00531-010-0545-y.

Bond, R.M.G., McClay, K.R., 1995. Inversion of Lower Cretaceous extensional basin, south central Pyrenees, Spain. In: Buchanan, J.G. (Ed.). In: Buchanan, P.G. (Ed.), Basin Inversion, Geol. Soc. London Spec. Pub., vol. 8, pp. 415–431.

Bonini, L., Toscani, G., Seno, S., 2014. Three-dimensional segmentation and different rupture behavior during the 2012 Emilia seismic sequence (Northern Italy). Tectonophysics 630, 33–42. http://dx.doi.org/10.1016/j.tecto.2014.05.006.

Bosica, B., Shiner, P., 2013. Petroleum systems and Miocene turbidites leads in the western Po valley". In: 11th Offshore Mediterranean Conference and Exhibition. Ravenna, Italy March 20-22, 2013.

Bresciani, I., Perotti, C.R., 2014. An active deformation structure in the Po Plain (N Italy): the Romanengo anticline. Tectonics 33. http://dx.doi.org/10.1002/2013TC003422.

Buchanan, J.G., Buchanan, P.G., 1995. Basin Inversion. Geological Society Special Publication N°88, pp. 1–589.

Burrato, P., Ciucci, F., Valensise, G., 2003. An inventory of river anomalies in the Po Plain, Northern Italy: evidences for active blind thrust faulting. Ann. Geophys. 46 (5), 865–882. http://dx.doi.org/10.4401/ag-3459.

Burrato, P., Poli, M.E., Vannoli, P., Zanferrari, A., Basili, R., Galadini, F., 2008. Sources of Mw 5+ earthquakes in northeastern Italy and western Slovenia: an updated view based on geological and seismological evidence. Tectonophysics 453 (1–4), 157–176. http://dx.doi.org/10.1016/j.tecto.2007.07.009.

Caputo, R., Poli, M.E., Zanferrari, A., 2010. Neogene-Quaternary tectonic stratigraphy of the eastern Southern Alps, NE Italy. J. Struct. Geol. 32 (7), 1009–1027. http://dx.doi.org/10.1016/j.jsg.2010.06.004.

Carannante, C., Argnani, A., Massa, M., D'Alema, E., Lovati, S., Moretti, M., Cattaneo, M., Augliera, P., 2015. The May 20 (MW 6.1) and 29 (MW 6.0), 2012, Emilia (Po Plain, northern Italy) earthquakes: new seismotectonic implications from subsurface geology and high-quality hypocenter location. Tectonophysics 655, 107–123.

Carminati, E., Doglioni, C., 2012. Alps vs. Apennines: the paradigm of a tectonically asymmetric Earth. Earth Sci. Rev. 112, 67–96. http://dx.doi.org/10.1016/j.earscirev.2012.02.004.

Carminati, E., Doglioni, C., Scrocca, D., 2003. Apennines subduction-related subsidence of Venice (Italy). Geophys. Res. Lett. 30 (13), 1717. http://dx.doi.org/10.1029/2003GL017001.

Carminati, E., Lustrino, M., Doglioni, C., 2012. Geodynamic evolution of the central and western Mediterranean: tectonics vs. igneous petrology constraints. Tectonophysics 579, 173–192. http://dx.doi.org/10.1016/j.tecto.2012.01.026.

Carrapa, B., Di Giulio, A., 2001. The sedimentary record of the exhumation of a granite intrusion into a collisional setting: the lower Gonfolite Group, Southern Alps, Italy. Sedim. Geol. 139 (3–4), 217–228. http://dx.doi.org/10.1016/S0037-0738(00)00167-6.

Casero, P., Rigamonti, A., Iocca, M., 1990. Paleogeographic relationship during Cretaceous between the northern Adriatic area and the eastern southern Alps. Mem. Soc. Geol. Ital. 45, 807–814.

Cassano, E., Anelli, L., Fichera, R., Cappelli, V., 1986. Pianura Padana. Interpretazione integrata di dati geofisici e geologici. In: Proceedings of the 73° Meeting of the Società Geologica Italiana, September 29-October 4, 1986, Rome, Italy, p. 27.

Castellarin, A., Eva, C., Giglia, G., Vai, G.B., 1985. Analisi strutturale del Fronte Appenninico Padano. G. Geol. 47 (1–2), 47–75.

Castellarin, A., Nicolich, R., Fantoni, R., Cantelli, L., Sella, M., Selli, L., 2005. Structure of the lithosphere beneath the Eastern Alps (southern sector of the TRANSALP transect). Tectonophysics 414, 259–282.

Castellarin, A., Vai, G.B., 1986. Southalpine versus Po plain Apenninic arcs. In: Wezel, F.C. (Ed.), The Origin of Arcs, Development in Geotectonic. Elsevier Amsterdam, pp. 253–280.

Castellarin, A., Cantelli, L., Fesce, A.M., Mercier, J.L., Picotti, V., Pini, G.A., Prosser, G., Selli, L., 1992. Alpine compressional tectonics in the southern Alps. Relat. N-Apennines Ann. Tect. 6 (1), 62–94.

Castellarin, A., Cantelli, L., 2010. Geology and evolution of the northern Adriatic structural triangle between Alps and Apennines. Rend. Fis. Acc. Lincei 21 (Suppl. 1), S3–S14. http://dx.doi.org/10.1007/s12210-010-0086-0.

Cibin, U., Di Giulio, A., Martelli, L., 2003. Oligocene-Early Miocene evolution of the Northern Apennines (northwestern Italy) traced through provenance of piggy-back basin fill successions. In: McCann, T., Saintot (Eds.), Tracing Tectonic Deformation Using the Sedimentary Record, Geol. Soc. London Spec. Pub., vol. 208, pp. 269–287. http://dx.doi.org/10.1144/GSL.SP.2003.208.01.13.

Cibin, U., Di Giulio, A., Martelli, L., Catanzariti, R., Poccianti, S., Rosselli, C., Sani, F., 2004. Factors controlling foredeep turbidite deposition: the case of Northern Apennines (Oligocene-Miocene, Italy). In: Lomas, S., Joseph, P. (Eds.), Confined Turbidite Systems, Geol. Soc. London Spec. Pub., vol. 222, pp. 115–134. http://dx.doi.org/10.1144/GSL.SP.2004.222.01.07.

Cimolino, A., Della Vedova, B., Nicolich, R., Barison, E., Brancatelli, G., 2010. New evidence of the outer Dinaric deformation front in the Grado area (NE-Italy). Rend. Fis. Acc. Lincei 21 (Suppl. 1), 167–179. http://dx.doi.org/10.1007/s12210-010-0096-y.

Cloetingh, S., Ziegler, P., Beekman, F., Andriessen, P., Matenco, L., Bada, G., Garcia-Castellanos, D., Hardebol, N., Dezes, P., Sokoutis, D., 2005. Lithospheric memory, state of stress and rheology: neotectonic controls on Europe's intraplate continental topography. Quat. Sci. Rev. 24 (3–4), 241–304.

Coward, M.P., Dietrich, D., Park, R.G., 1989. Alpine tectonics. Geol. Soc. Lond. Spec. Pub. 45, 449 pp.

Cuffaro, M., Riguzzi, F., Scrocca, D., Antonioli, F., Carminati, E., Livani, M., Doglioni, C., 2010. On the geodynamics of the northern Adriatic plate. Rend. Lincei 21 (Suppl. 1), 253–279.

Dal Piaz, G.V., Bistacchi, A., Massironi, M., 2003. Geological outline of the Alps. Episodes 26 (3), 175–180.

Dahlstrom, C.D., 1969. Balanced cross-sections. Can. J. Earth Sci. 6, 743–757.

Dercourt, J., Zonenshain, L.P., Ricou, L.E., Kazmin, V.G., Le Pichon, X., Knipper, A.L., Grandjacquet, C., Sbortshikov, I.M., Geyssant, J., Lepvrirer, C., Pechersky, D.H., Boulin, J., Sibuet, J.C., Savostin, L.A., Sorokhtin, O., Westphal, M., Bazchenov, M.L., Lauer, J.P., Biju-Duval, B., 1986. Geological evolution of the Tethys belt from Atlantic to the Pamirs since the Lias. In: Aubouin, J., Le Pichon, X., Monin, A.S. (Eds.), Evolution of the Tethys. Tectonophysics, vol. 123, pp. 241–315.

Desegaulx, P., Roure, F., Villien, A., 1990. Structural evolution of the Pyrenees tectonic heritage and flexural behavior of the continental crust. In: Letouzey, J. (Ed.), Editions Technip, Petroleum and Tectonics in Mobile Belts, pp. 31–48.

Dewey, J.F., Helman, M.L., Turco, E., Hutton, D.H.W., Knot, S.D., 1989. Kinematics of the western Mediterranenan. Geol. Soc. Lond. Spec. Publ. 45, 265–283.

DeCelles, P.G., Giles, K.A., 1996. Foreland basin systems. Basin Res. 8 (2), 105–123.

Di Capua, A., Vezzoli, G., Cavallo, A., Groppelli, G., 2015. Clastic sedimentation in the

Late Oligocene Southalpine Foredeep: from tectonically controlled melting to tectonically driven erosion. Geol. J. http://dx.doi.org/10.1002/gj.2632.
Di Giulio, A., Carrapa, B., Fantoni, R., Gorla, L., Valdisturlo, A., 2001. Middle Eocene-early Miocene sedimentary evolution of the western Lombardy South Alpine foredeep (Italy). Int. J. Earth Sc. 90 (3), 534–548. http://dx.doi.org/10.1007/s005310000186.
Di Giulio, A., Mancin, N., Martelli, L., Sani, F., 2013. Foredeep palaeobathymetry and subsidence trends during advancing then retreating subduction. The Northern Apennine case (Oligocene-Miocene, Italy). Basin Res. 25 (6), 260–284. http://dx.doi.org/10.1111/bre.12002.
DISS Working Group, 2015. Database of Individual Seismogenic Sources (DISS), Version 3.2.0: a Compilation of Potential Sources for Earthquakes Larger than M 5.5 in Italy and Surrounding Areas. http://dx.doi.org/10.6092/INGV.IT-DISS3.2.0. http://diss.rm.ingv.it/diss/. © INGV 2015-Istituto Nazionale di Geofisica e Vulcanologia – All rights reserved.
Doglioni, C., Bosellini, A., 1987. Eoalpine and mesoalpine tectonics in the southern Alps. Geol. Rundsch. 76 (3), 735–754. http://dx.doi.org/10.1007/BF01821061.
Doglioni, C., 1995. Geological remarks on the relationships between extension and convergent geodynamic settings. Tectonophysics 252 (1–4), 253–267. http://dx.doi.org/10.1016/0040-1951(95)00087-9.
Doglioni, C., Carminati, E., 2008. Structural Style and Dolomites Field Trip – Memorie Descrittive Della Carta Geologica D'italia, LXXXII.
Dondi, L., D'Andrea, G., 1986. La Pianura Padana e Veneta dall'Oligocene superiore al Pleistocene. G. Geol. Ser. 3 48 (1–2), 197–225.
Errico, G., Groppi, G., Savelli, S., Vaghi, G.C., 1980. Malossa field: a deep discovery in the Po valley. Italy AAPG Mem. 30, 525–538.
Fantoni, R., Decarlis, A., Fantoni, E., 2003. L'Estensione Mesozoica al margine occidentale delle Alpi Meridionali. Atti Ticin. Sci. della Terra 44, 97–110.
Fantoni, R., Scotti, P., 2003. Thermal record of the Mesozoic extensional tectonics in the southern Alps. Atti Ticin. Sci. della Terra 9, 96–101.
Fantoni, R., Bersezio, R., Forcella, F., 2004. Alpine structure and deformation chronology at the southern Alps-Po plain border in Lombardy. Boll. Soc. Geol. It. 123, 463–476.
Fantoni, R., Franciosi, R., 2010. Tectono-sedimentary setting of the Po plain and Adriatic foreland. Rend. Lincei 21 (1), S197–S209. http://dx.doi.org/10.1007/s12210-010-0102-4.
Garfunkel, Z., Greiling, R.O., 2002. The implications of foreland basins for the causative tectonic loads. Stephan Mueller Spec. Publ. Ser. 1, 3–16. http://dx.doi.org/10.5194/smsps-1-3-2002.
GEOMOL project: "Assessing subsurface potentials of the Alpine Foreland Basins for sustainable planning and use of natural resources"; project code 10-4-3-DE, co-funded by the Alpine Space Programme – European Territorial Cooperation 2007-2013 http://geomol.eu/home/index_html.
Ghielmi, M., Minervini, M., Nini, C., Rogledi, S., Rossi, M., Vignolo, A., 2010. Sedimentary and tectonic evolution in the eastern Po-Plain and northern Adriatic sea area from Messinian to Middle Pleistocene (Italy). Rend. Lincei 21 (1), S131–S166. http://dx.doi.org/10.1007/s12210-010-0101-5.
Ghielmi, M., Minervini, M., Nini, C., Rogledi, S., Rossi, M., 2013. Late Miocene-Middle Pleistocene sequences in the Po Plain - northern Adriatic Sea (Italy): the stratigraphic record of modification phases affecting a complex foreland basin. Mar. Pet. Geol. 42, 50–81. http://dx.doi.org/10.1016/j.marpetgeo.2012.11.007.
Gibbs, A.D., 1983. Balanced cross-section construction from seismic sections in areas of extensional tectonics. J. Struct. Geol. 5, 153–169.
Greber, E., Leu, W., Bernoulli, D., Schumacher, M.E., Wyss, R., 1997. Hydrocarbon Provinces in the Swiss Southern Alps – a gas geochemistry and basin modelling study. Mar. Pet. Geol. 14 (1), 3–25.
Guimera, J., Alonso, A., Mas, J.R., 1995. Inversion of an extensional-ramp basin by a newly formed thrust: the Cameros basin (N.Spain). In: Buchanan, J.G. (Ed.). In: Buchanan, P.G. (Ed.), Geol. Soc. London Spec. Pub., vol. 88, pp. 433–453.
Hossack, J.R., 1979. The use of balanced cross-sections in the calculation of orogenic contraction: a review. J. Geol. Soc. Lond. 136, 705–711.
Kruse, S.E., Royden, L.H., 1994. Bending and unbending of an elastic lithosphere: the Cenozoic history of the Apennine and Dinaride foredeep basins. Tectonics 13 (2), 278–302. http://dx.doi.org/10.1029/93TC01935.
Lacombe, O., Mouthereau, F., Angelier, J., Chu, H.T., Lee, J.C., 2003. Frontal belt curvature and oblique ramp development at an obliquely collided irregular margin: geometry and kinematics of the NW Taiwan fold–thrust belt. Tectonics 22 (3), 1025. http://dx.doi.org/10.1029/2002TC001436.
Lacombe, O., Bellahsen, N., 2016. Thick-skinned tectonics and basement-involved fold-thrust belts. Insight from selected Cenozoic orogens. In: Lacombe, O., Ruh, J., Brown, D., Nilfouroushan, F. (Eds.), Geological Magazine, Special Issue 'Tectonic Evolution and Mechanics of Basement-involved Fold-thrust Belts', 153 (5-6). http://dx.doi.org/10.1017/S0016756816000078.
Letouzey, J., 1990. fault reactivation, inversion and fold-Thrust belt. In: Letouzey, J. (Ed.), Editions Technip, Petroleum and Tectonics in Mobile Belts, pp. 101–128.
Lin, A.T., Watts, A.B., 2002. Origin of the West Taiwan basin by orogenic loading and flexure of the rifted continental margin. J. Geophys. Res. 107 (B9) http://dx.doi.org/10.1029/2001JB000669.
Livio, F.A., Berlusconi, A., Michetti, A.M., Sileo, G., Zerboni, A., Trombino, L., Cremaschi, M., Mueller, K., Vittori, E., Carcano, C., Rogledi, S., 2009a. Active fault-related folding in the epicentral area of the December 25, 1222 (Io=IX MCS) Brescia earthquake (Northern Italy): seismotectonic implications. Tectonophysics 476 (1–2), 320–335. http://dx.doi.org/10.1016/j.tecto.2009.03.019.
Livio, F., Michetti, A.M., Sileo, G., Carcano, C., Mueller, K., Rogledi, S., Serva, L., Vittori, E., Berlusconi, A., 2009b. Quaternary capable folds and seismic hazard in Lombardia (Northern Italy): the Castenedolo structure near Brescia. Ital. J. Geosci. Boll. Soc. Geol. It.) 128 (1), 191–200.
Lowell, J.D., 1995. Mechanisms of basin inversion from worldwide examples. In: Buchanan, J.G. (Ed.). In: Buchanan, P.G. (Ed.), Geol. Soc. London Spec. Pub., vol. 88, pp. 39–57.
Maesano, F.E., Toscani, G., Burrato, P., Mirabella, F., D'Ambrogi, C., Basili, R., 2013. Deriving thrust fault slip rates from geological modeling: examples from the Marche coastal and offshore contraction belt, Northern Apennines, Italy. Mar. Pet. Geol. 42, 122–134. http://dx.doi.org/10.1016/j.marpetgeo.2012.10.008.
Maesano, F.E., D'Ambrogi, C., 2016. Coupling sedimentation and tectonic control: Pleistocene evolution of the central Po Basin. Ital. J. Geosci 135 (3), 394–407. http://dx.doi.org/10.3301/IJG.2015.17.
Maesano, F.E., D'Ambrogi, C., Burrato, P., Toscani, G., 2015(a). Slip-rates of blind thrusts in slow deforming areas: examples from the Po Plain (Italy). Tectonophysics 643, 8–25. http://dx.doi.org/10.1016/j.tecto.2014.12.007.
Maesano, F.E., D'Ambrogi, C., Toscani, G., Bonini, L., Burrato, P., 2015(b). Influence of inherited normal faults on active thrust-and-fold systems in the Po Plain. Rend. Online Soc. Geol. It vol. 36 (Suppl. 1), 49.
Maino, M., Decarlis, A., Felletti, F., Seno, S., 2013. Tectono-sedimentary evolution of the Tertiary Piedmont basin (NW Italy) within the Oligo-Miocene central Mediterranean geodynamics. Tectonics 32 (3), 593–619. http://dx.doi.org/10.1002/tect.20047.
Malusà, M., Anfinson, O., Dafov, L., Stockli, D., 2016. Tracking Adria indentation beneath the Alps by detrital zircon U-Pb geochronology: implications for the Oligocene-Miocene dynamics of the Adriatic microplate. Geology 44, 155–158. http://dx.doi.org/10.1130/G37407.1.
Mann, P., Escalona, A., Castillo, M.V., 2006. Regional geologic and tectonic setting of the Maracaibo supergiant basin, western Venezuela. AAPG Bull. 90 (4), 445–477.
Mancin, N., Di Giulio, A., Cobianchi, M., 2009. Tectonic vs. climate forcing in the Cenozoic sedimentary evolution of a foreland basin (Eastern Southalpine system, Italy). Basin Res. 21 (6), 799–823. http://dx.doi.org/10.1111/j.1365-2117.2009.00402.x.
Mariotti, G., Doglioni, C., 2000. The dip of the foreland monocline in the Alps and Apennines. Earth Planet. Sci. Lett. 181, 191–202. http://dx.doi.org/10.1016/S0012-821X(00)00192-8.
Masetti, D., Fantoni, R., Romano, R., Sartorio, D., Trevisani, E., 2012. Tectonostratigraphic evolution of the Jurassic extensional basins of the eastern southern Alps and Adriatic foreland based on an integrated study of surface and subsurface data. AAPG Bull. 96 (no. 11), 2065–2089.
Maţenco, L., Bertotti, G., Dinu, C., Cloetingh, S., 1997. Tertiary tectonic evolution of the external South Carpathians and the adjacent Moesian platform (Romania). Tectonics 16 (6), 896–911.
Matenco, L., Bertotti, G., Cloetingh, S., Dinu, C., 2003. Subsidence analysis and tectonic evolution of the external Carpathian - Moesian Platform region during Neogene times. Sediment. Geol. 156 (1–4), 71–94. http://dx.doi.org/10.1016/S0037-0738(02)00283-X.
McQuarrie, N., Horton, B.K., Zandt, G., Beck, S., DeCelles, P.G., 2005. Lithospheric evolution of the Andean fold-thrust belt, Bolivia, and the origin of the central Andean plateau. Tectonophysics 399, 15–37. http://dx.doi.org/10.1016/j.tecto.2004.12.013 (1-4 SPEC. ISS.).
Moretti, I., Triboulet, S., Endignoux, L., 1990. Some remarks on the geometrical modeling of geological deformations. In: Letouzey, J. (Ed.), Editions Technip, Petroleum and Tectonics in Mobile Belts, pp. 155–162.
Moretti, I., Raoult, J.J., 1990. Geological restoration of seismic depth images. First Break 8 (7), 271–275.
Mosca, P., Polino, R., Rogledi, S., Rossi, M., 2010. New data for the kinematic interpretation of the Alps–Apennines junction (Northwestern Italy). Int. J. Earth Sci. Geol. Rundsch. 99, 833–849. http://dx.doi.org/10.1007/s00531-009-0428-2.
Mouthereau, F., Watts, A.B., Burov, E., 2013. Structure of orogenic belts controlled by lithosphere age. Nat. Geosci. 6, 785–789. http://dx.doi.org/10.1038/NGEO1902.
Muñoz-Jiménez, A., Casas-Sainz, A.M., 1997. The Rioja Trough (N Spain): tectono sedimentary evolution of a symmetric foreland basin. Basin Res. 9 (1), 65–85. http://dx.doi.org/10.1046/j.1365-2117.1997.00031.x.
Nardon, S., Marzorati, D., Bernasconi, A., Cornini, S., Gonfalini, M., Mosconi, S., Romano, A., Terdich, P., 1991. Fractured carbonate reservoir characterization and modeling a multidisciplinary case study from the Cavone oil field, Italy: First Break 9 (12), 553–565.
Naylor, M., Sinclair, H.D., 2008. Pro- vs. retro-foreland basins. Basin Res. 20 (3), 285–303. http://dx.doi.org/10.1111/j.1365-2117.2008.00366.x.
Nicolai,C. & Gambini,R., 2007. Structural architecture of the Adria platform-and-basin system. Boll.Soc.Geol.It. (Ital.J.Geosci.), Spec. Issue No. 7, 21-37, 15 figs., 1 pl., CROP-04 (ed. by A. Mazzotti, E. Patacca and P. Scandone).
Norman Kent, W., Dasgupta, U., 2004. Structural evolution in response to fold and thrust belt tectonics in northern Assam. A key to hydrocarbon exploration in the Jaipur anticline area. Mar. Pet. Geol. 21, 785–803. http://dx.doi.org/10.1016/j.marpetgeo.2003.12.006.
Nunns, A., 1991. Structural restoration of seismic and geologic sections in extensional regimes. AAPG Bull. 75, 2.
Oszczypko, N., 2006. Late Jurassic-Miocene evolution of the outer Carpathian fold-and-thrust belt and its foredeep basin (western Carpathians, Poland). Geol. Q. 50 (1), 169–194.
Perotti, C.R., 1991. Osservazioni sull'assetto strutturale del versante padano dell'Appennino Nord-Occidentale. Atti Ticin. Sci. della Terra 34, 11–22.
Pfiffner, A., 2014. Geology of the Alps. Wiley and Sons, New York, 368 pp.

Pieri, M., Groppi, G., 1981. Subsurface geological structure of the Po Plain, Italy. In: Progetto Finalizzato Geodinamica. C.N.R., Publ. n° 414.
Pola, M., Ricciato, A., Fantoni, R., Fabbri, P., Zampieri, D., 2014. 2Architecture of the western margin of the North Adriatic foreland: the Schio-Vicenza fault system. Ital. J. Geosci. 133 (2), 223–234. http://dx.doi.org/10.3301/IJG.2014.04.
Ponton, M., 2010. Architettura delle Alpi Friulane. Museo Friulano di Storia Naturale. Publ. N° 52, Udine. ISBN 9788888192529.
Ravaglia, A., Turrini, C., Seno, S., 2004. Mechanical stratigraphy as a factor controlling the development of a sandbox transfer zone: a three-dimensional analysis. J. Struct. Geol. 26, 2269–2283.
Ravaglia, A., Seno, S., Toscani, G., Fantoni, R., 2006. Mesozoic extension controlling the Southern Alps thrust front geometry under the Po Plain, Italy: insights from sandbox models. J. Struct. Geol. 28, 2084–2096. http://dx.doi.org/10.1016/j.jsg.2006.07.011.
Ricci Lucchi, F., 1986. Oligocene to Recent Foreland Basins Northern Apennines. I.A.S. Special Public. No.8. Blackwell, pp. 105–139.
Rizzini, A., Dondi, L., 1978. Erosional surface of Messinian age in the subsurface of the Lombardian plain (Italy). Mar. Geol. 27 (3–4), 303–325.
Rogledi, S., 2010. Assetto strutturale delle unità alpine nella pianura tra il lago d'Iseo e il Garda. Rischio sismico nella Pianura Padana. http://cesia.ing.unibs.it/index.php/it/eventi/giornate-di-studio/119.
Roeder, D., 1991. Structure and tectonic evolution of alpine lithosphere – EUG VI Symposium, the European geotraverse (EGT) final results, Strasbourg.
Roure, F., Polino, R., Nicolich, R., 1990. Early Neogene deformation beneath the Po plain: constraints on the post-collisional Alpine evolution. In: Roure, F., Heitzmann, P., Polino, R. (Eds.), Deep Structure of the Alps, Mem.Soc.Geol. France, 156, pp. 309–322.
Rossi, M., Minervini, M., Ghielmi, M., Rogledi, S., 2015. Messinian and Pliocene erosional surfaces in the Po Plain-Adriatic Basin: insights from allostratigraphy and sequence stratigraphy in assessing play concepts related to accommodation and gateway turnarounds in tectonically active margins. Mar. Pet. Geol. 66, 192–216.
Schonborn, G., 1992. Alpine tectonics and kinematic models of the central southern Alps. Mem. Sci. Geol. 44, 229–393.
Serpelloni, E., Anzidei, M., Baldi, P., Casula, G., Galvani, A., 2005. Crustal velocity and strain-rate fields in Italy and surrounding regions: new results from the analysis of permanent and non-permanent GPS networks. Geophys. J. Int. 161, 861–880. http://dx.doi.org/10.1111/j.1365-246X.2005.02618.x.
Serpelloni, E., Vannucci, G., Pondrelli, S., Argnani, A., Casula, G., Anzidei, M., Baldi, P., Gasperini, P., 2007. Kinematics of the Western Africa-Eurasia plate boundary from focal mechanisms and GPS data. Geophys. J. Int. 169, 1180–1200. http://dx.doi.org/10.1111/j.1365-246X.2007.03367.x.
Tensi, J., Mouthereau, F., Lacombe, O., 2006. Lithospheric bulge in the west Taiwan basin. Basin Res. 18, 277–299. http://dx.doi.org/10.1111/j.1365-2117.2006.00296x.
Toscani, G., Seno, S., Fantoni, R., Rogledi, S., 2006. Geometry and timing of deformation inside a structural arc; the case of the western Emilian folds (Northern Apennine front, Italy). Boll. Della Soc. Geol. Ital. 125 (1), 59–65.
Toscani, G., Burrato, P., Di Bucci, D., Seno, S., Valensise, G., 2009. Plio-Quaternary tectonic evolution of the Northern Apennines thrust fronts (Bologna-Ferrara section, Italy): seismotectonic implications. Ital. J. Geosci. Boll. della Soc. Geol. Ital. 128 (2), 605–613. http://dx.doi.org/10.3301/IJG.2009.128.2.605.
Toscani, G., Bonini, L., Ahmad, M.I., Bucci, D.D., Giulio, A.D., Seno, S., Galuppo, C., 2014. Opposite verging chains sharing the same foreland: kinematics and interactions through analogue models (Central Po Plain, Italy). Tectonophysics 633 (1), 268–282.
Toscani, G., Marchesini, A., Barbieri, C., Di Giulio, A., Fantoni, R., Mancin, N., Zanferrari, A., 2016. The Friulian-Venetian Basin I: architecture and sediment flux into a shared foreland basin. Ital. J. Geosci. 135 (3), 444–459. http://dx.doi.org/10.3301/IJG.2015.35.
Turrini, C., Lacombe, O., Roure, F., 2014. Present-day 3D structural model of the Po Valley basin, Northern Italy. Mar Petr. Geol. 56, 266–289. http://dx.doi.org/10.1016/j.marpetgeo.2014.02.006.
Turrini, C., Angeloni, P., Lacombe, O., Ponton, M., Roure, F., 2015. Three-dimensional seismo-tectonics in the Po Valley basin. North. Italy Tectonophys. 661, 156–179. http://dx.doi.org/10.1016/j.tecto.2015.08.033.
Turrini, C., Ryan, P., Bosica, B., Shiner, P., Lacombe, O., Roure, F., 2016. 3D structural and thermal modeling in the Po Valley basin, northern Italy. AAPG Bull. (submitted for publication manuscript number BLTN16-072 Version1).
Uliana, M.A., Arteaga, M.E., Legarreta, L., Cerdan, J.J., Peroni, G.O., 1995. Inversion structures and hydrocarbon occurrence in Argentina. In: Buchanan, J.G., Buchanan, P.G. (Eds.), Geol. Soc. London Spec. Pub., vol. 88, pp. 211–233.
Vannoli, P., Burrato, P., Valensise, G., 2015. The seismotectonics of the Po Plain (northern Italy): tectonic diversity in a blind faulting domain. Pure Appl. Geophys. http://dx.doi.org/10.1007/s00024-014-0873-0.
Vanossi, M., Perotti, C.R., Seno, S., 1994. The Maritime Alps arc in the Ligurian and Tyrrhenian systems. Tectonophysics. 230, 75–89.
Watts, A.B., 1992. The effective elastic thickness of the lithosphere and the evolution of foreland basins. Basin Res. 4, 169–178.
Zanchi, A., Chinaglia, N., Conti, M., De Toni, S., Ferliga, C., Tsegaye, A., Valenti, L., Bottin, R., 1990. Analisi strutturale lungo il fronte della dolomia principale in bassa val Seriana (Bergamo). Mem. Soc. Geol. It 45, 83–92.
Ziegler, P.A., 1989. Geodynamic model for alpine intra-plate compressional deformation in western and central Europe. In: Cooper, M.A., Williams, G.D. (Eds.), Geol. Soc. London Spec. Pub., vol. 44(1), pp. 63–85.
Ziegler, P.A., Bertotti, G., Cloetingh, S., 2002. Dynamic processes controlling foreland development – the role of mechanical (de)coupling of orogenic wedges and forelands. EGU Stephan Mueller Spec. Publ. Ser. 1, 17–56.

Part 5 – The Po Valley 3D model: Applications

I. Introduction

At the end of the building process, the performed 3D model seems to consistently illustrate the crustal-to-regional scale tectonics and kinematics of the Po Valley basin. Conversely, further refining and (hopefully) new data will be needed to obtain a more detailed and quantitative field-scale model (see Discussion in Part 6 of this thesis). It derives that applications taking into account the crustal-to-regional scale are, at the moment, definitely the most logic and viable to be tested as direct follow-up to the reconstructed Po Valley 3D architecture.

In that context, the first application of the performed 3D model consisted of the review of the earthquake-structure associations that can be recognized across/around the Po Valley basin (phases 3 in the workflow of Fig.20).

Pamela Angeloni (formerly at the Pavia Earth Science Dpt.) contributed to this project-phase by working on the public earthquake catalogs and transforming the related seismic events into physical points to be analysed inside the MOVE structural model.

Maurizio Ponton (from the Trieste Earth Science Dpt.) supplied his geo-structural knowledge and data/interpretations, while supporting the performed seismo-tectonic model analysis at the boundary between the north-eastern sector of the Po Valley basin and the corresponding Southern Alps domains (i.e. the Friuli domain).

The modeling was run using the MOVE package and the results were published in Tectonophysics (Turrini et al., 2015, vol. 661, pp. 156-179).

The second application concerned the thermal modeling of the Po Valley basin and the simulation of the hydrocarbon evolution and processes (phases 6 in the workflow of Fig.20).

Once again the primary motivation was the crustal-regional scale of investigation implied by such an application. The fact that the Po Valley is one of the major hydrocarbon provinces in continental Europe supported and boosted the initial idea.

The work has been conducted in collaboration with the staff of Petroceltic Italia (Peter Shiner, Technical Manager, and Barbara Bosica, senior Geologist) and Petroceltic International (Paul Ryan, senior Geologist).

The model was mainly performed on the GENESIS and TRINITY software after exporting and conditioning of the MOVE-Kingdom 3D horizon grids.

Results from the combined modeling exercise are under review at the AAPG bulletin (Manuscript Number is: BLTN16-072 Version 1).

II. 3D structures and earthquakes in the Po Valley basin

Since more than a century, earthquakes have been recorded across and around the Po Valley region where destructive seismic energy can occasionally cause damages to both population and infrastructures (e.g. Burrato et al., 2008; Govoni et al., 2014; Vannolli et al. 2014).

In order to review the Po Valley seismicity against the performed 3D model structures, the 3D seismo-tectonic model of the basin (section III) was conceived by the integration and the analysis of the earthquake events taken from the public Italian database with the 3D structural model layers and faults.

Results from such application basically confirm the key conclusions from the available literature. Nevertheless, the complexity of the entire setting is exceptionally shown and illustrated by the integrated and new 3D perspective of the basin.

The three-dimensional view was particularly useful to focus on key issues like:

- presence of faults against earthquakes distribution,
- comparison of the modeled faults against seismogenic surfaces suggested by the official Italian catalogue (DISS),

- interplay between mechanical and possible earthquake stratigraphy.

As a whole, it can be acknowledged that a future and update version of the final seismo-tectonic 3D model should be strongly implemented with/by more refined input earthquake data, more detailed geological constraints and, eventually, new software applications.

Despite any current uncertainties and possible, future implementations, the recognized earthquake-structures associations could be considered an additional support to the 3D model consistency that has been previously suggested by the deformation geometries and kinematics integration and analysis (Part 4, Sections II and IV).

Tectonophysics 661 (2015) 156–179

Contents lists available at ScienceDirect

Tectonophysics

journal homepage: www.elsevier.com/locate/tecto

Three-dimensional seismo-tectonics in the Po Valley basin, Northern Italy

Claudio Turrini [a,1], Pamela Angeloni [b], Olivier Lacombe [c,d], Maurizio Ponton [e], François Roure [f,g]

[a] CTGeolConsulting, 78100 St. Germain-en-Laye, France
[b] Via Antonio Perfetti 25, 00133 Roma, Italy
[c] Sorbonne Universités, UPMC Univ Paris 06, UMR 7193, ISTEP, F-75005 Paris, France
[d] CNRS, UMR 7193, ISTEP, F-75005 Paris, France
[e] Dipartimento di Matematica e Geoscienze, Università degli Studi di Trieste, Trieste, Italy
[f] IFP-EN, Rueil-Malmaison, France
[g] Utrecht University, The Netherlands

ARTICLE INFO

Article history:
Received 1 June 2015
Received in revised form 27 August 2015
Accepted 30 August 2015
Available online 5 September 2015

Keywords:
Seismo-tectonics
3D models
Earthquakes
Po Valley

ABSTRACT

The Po Valley (Northern Italy) is a composite foreland–foredeep basin caught in between the Southern Alps and Northern Apennine mountain belts.
By integrating the 3D structural model of the region with the public earthquake dataset, the seismo-tectonics of the basin is shown at different scales of observation.
The three-dimensional geo-volume is used to review the seismicity around the region and validate the structure–earthquake association for such a complex tectonic framework.
Despite the overall uncertainty due to the original data distribution-quality as well as the crustal scale model dimension, the direct correlation between structures and seismicity a) confirms the Po Valley region as an active tectonic system and b) allows the whole structural architecture to be revised by a unique three-dimensional perspective and approach.
This study also indicates that 3D methodology is a powerful tool for better understanding of highly complex seismo-tectonic situations at both regional and local scales.

1. Introduction

Italy is an active tectonic province within the Mediterranean geodynamic puzzle. In the region, the major structural units and the related crustal scale geological boundaries are clearly revealed by the current stress field and the important seismicity (e.g. Carminati & Doglioni, 2012; Di Bucci & Angeloni, 2013 and reference therein). Through geological time, both pre-Alpine (Mesozoic and pre-Mesozoic) and Alpine (mainly Cenozoic) tectonics have interacted to create the current structural and stratigraphic setting (Elter and Pertusati, 1973; Laubscher, 1996; Castellarin, 2001; Castellarin and Cantelli, 2010; Cuffaro et al., 2010; Mosca et al., 2010; Carminati and Doglioni, 2012 and reference therein). As a result, the Po Valley (Fig. 1) represents the northwesternmost buried sector of the Apulian indenter (or Adria plate: Channell et al., 1979, Dewey et al., 1973, Dercourt et al., 1986), the foreland/foredeep domain to the Alpine and Northern Apenninic belts and, ultimately, one of the major hydrocarbon provinces of continental Europe.

Historical and instrumental earthquakes across the Italian peninsula are recorded, collected and reviewed by the Istituto Nazionale di Geofisica e Vulcanologia (INGV; National Institute for Geophysics and Volcanology). The derived catalogues are constantly updated at each new seismic event and both initial and (re)processed data are available to the public, on the institution's website (http://www.ingv.it/it/).

While earthquakes happen continuously all through the country, the northern part of Italy is characterized by patchy hypocentre occurrence with highly concentrated clusters (Fig. 2a). Magnitude (*local*) of the reported earthquakes across the region is between 0 and 7 while depth of the events is between 0–70 km. Focal mechanisms from the available literature (Fig. 2b) indicate mainly north–south active shortening with thrust-related and strike–slip structures, these being supported by regional stress, thrust–slip rates, GPS-derived maps and geomorphological criteria (Burrato et al., 2003; Montone et al., 2004; Maesano et al., 2010, 2011; Rovida et al., 2011; Burrato et al, 2012; Carminati & Doglioni, 2012; Michetti et al., 2012; Di Bucci & Angeloni, 2013; Maesano et al., 2013, 2014; and all references therein).

Three-dimensional modelling is an important tool to tackle highly complex geological structures. Although such technique has become a standard procedure especially for oil and gas exploration (Mitra and

E-mail address: clturri@wanadoo.fr (C. Turrini).
[1] Tel.: +33 672391235.

http://dx.doi.org/10.1016/j.tecto.2015.08.033
0040-1951/

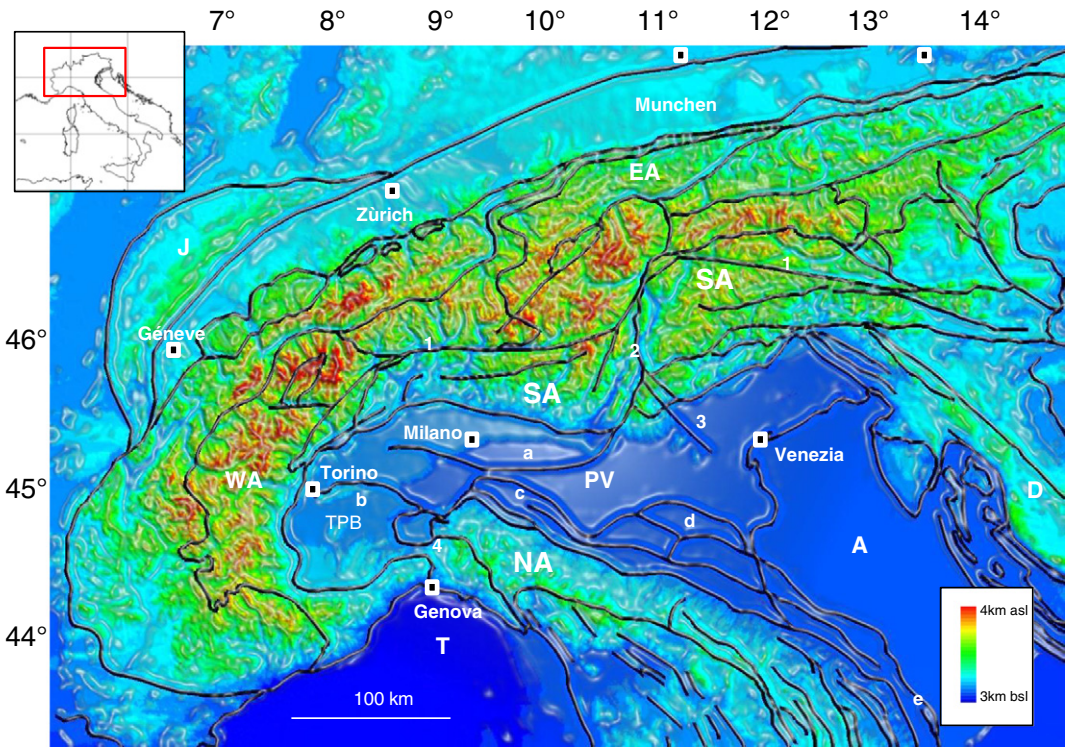

Fig. 1. Digital topography and tectonic framework (modified from Nicolich, 2010) around the Po Valley region. (PV) Po Valley; (SA) Southern Alps; (NA) Northern Apennines; (WA) Western Alps; (EA) Eastern Alps; (D) Dinarides; (J) Jura Mountains; (A) Adriatic; (T) Tyrrenhian; (1) Insubric Line; (2) Giudicarie Line; (3) Schio–Vicenza Line; (4) Sestri–Voltaggio–Villavernia Lines; (a–e) buried thrust fronts: a = Milano Thrust Front; b = Monferrato Thrust Front; c = Emilian Thrust Front; d = Ferrara–Romagna Thrust Front; e = Ancona Thrust Front. TPB = Tertiary Piedmont Basin. Latitude and Longitude values are North and East of Greenwich. Grid in the inset map is 500 km.

Leslie, 2003; Turrini and Rennison, 2004; Dischinger and Mitra, 2006; Mitra et al., 2005, 2007; Valcarce et al., 2006; Turrini et al., 2009; Lindsay et al., 2012; Vouillamoz et al., 2012; Shao et al., 2012 and reference therein), groundwater aquifer studies (Berg et al., 2004 and references therein) and ore deposit analysis (Han et al., 2011, and references therein), the application of 3D models to seismo-tectonic studies is rare (e.g. Bechtold et al., 2009; Burrato et al., 2014; Carena et al., 2002; Maesano et al., 2014). Hence, schematic cross-sections or simple map-view projections constitute the classic tools for the analysis of structures-versus-earthquakes associations.

As follow-up to the recent Po Valley 3D model (Turrini et al., 2014), this study aims to illustrate and discuss the structures and the seismicity of the region from crustal to local scale.

Noteworthy, given the range of uncertainty in both the 3D model and the original earthquake dataset, this study does not aim to offer a quantitative seismological analysis about the selected structural domains. Conversely, the final 3D geo-volume may represent a powerful tool in the unravelling of the basin seismo-tectonic complexity.

2. Regional framework of the Po Valley

2.1. Structures, stratigraphy & exploration

Structures across the Po Valley region mainly refer to the external domains of the Southern Alps and the Northern Apennines and intervening foreland, this latter being a major obstacle to the propagation of large and buried tectonic arcs (Pieri and Groppi, 1981; Castellarin and Vai, 1982; Bartolini et al., 1996; Cassano et al., 1986; Castellarin et al., 1986; Ricci Lucchi, 1986; Perotti, 1991; Perotti and Vercesi, 1991; Bertotti et al., 1997; Argnani and Ricci Lucchi, 2001; Carminati and Doglioni, 2012; Ahmad et al., 2014; Toscani et al., 2014; Turrini et al., 2014, and reference therein). Provided the well results and the outcrops around the region, the Po Valley sedimentary successions are defined by Mesozoic carbonates, clastic Cenozoic deposits and a crystalline basement essentially composed of Hercynian metamorphic rocks. The final tectonic features evolved from late Triassic–early Jurassic extension to late Cretaceous–Cenozoic compression, this providing inversion of the pre-existing extensional structures and shortening across both the foreland and the surrounding orogenic belts (Bertotti et al., 1993; Fantoni et al., 2004; Jadoul et al., 1992). During such a deformation history, sedimentation of the carbonates kept pace with the overall tectonics so that shelf, marginal and basin type deposits developed as part of the northern Africa derived Adria micro-plate. Triassic–early Jurassic rift-related structures were locally inverted by Cretaceous contraction with reactivation of some of the existing N–S and E–W trending normal faults (Dal Piaz et al., 2004; Ravaglia et al., 2006; Schmid et al., 2004). Onset of the foreland flexure at the front of the western Southern Alps is suggested by the deposition of Oligocene turbidites (Gonfolite basin; Gelati and Gnaccolini, 1982; Castellarin and Vai, 1986; Roure et al., 1989, 1990). Finally, in Miocene and Pliocene times, the basin became the foreland of the Alps and the Apennine belts and the Mesozoic rocks were deeply buried beneath the Palaeogene–Neogene clastics and the associated foredeep wedges (Fantoni et al., 2004; Trumpy, 1973).

Since the end of the 20th century a number of hydrocarbon fields have been discovered and developed inside the Po Valley basin (Pieri, 1984). Among others, the Villafortuna–Trecate field, 30 km west of Milano, has been the most successful so far as it produced 240 MMbbls from a Triassic carbonate reservoir, 5000 m below the mean sea level. By the acquisition of modern 2D/3D seismic surveys and the drilling of deep wells (green dots in Fig. 2a), the oil business strongly contributed to the understanding of the basin tectonics, sedimentology and geochemistry (Bello and Fantoni, 2002; Bongiorni, 1987; Casero et al. 1990; Cassano et al., 1986; Errico et al, 1980; Fantoni et al., 2004; Lindquist, 1999; Mattavelli and Margarucci, 1992; Mattavelli and Novelli, 1987; Nardon et al., 1991; Pieri, 1984; Pieri and Groppi, 1981).

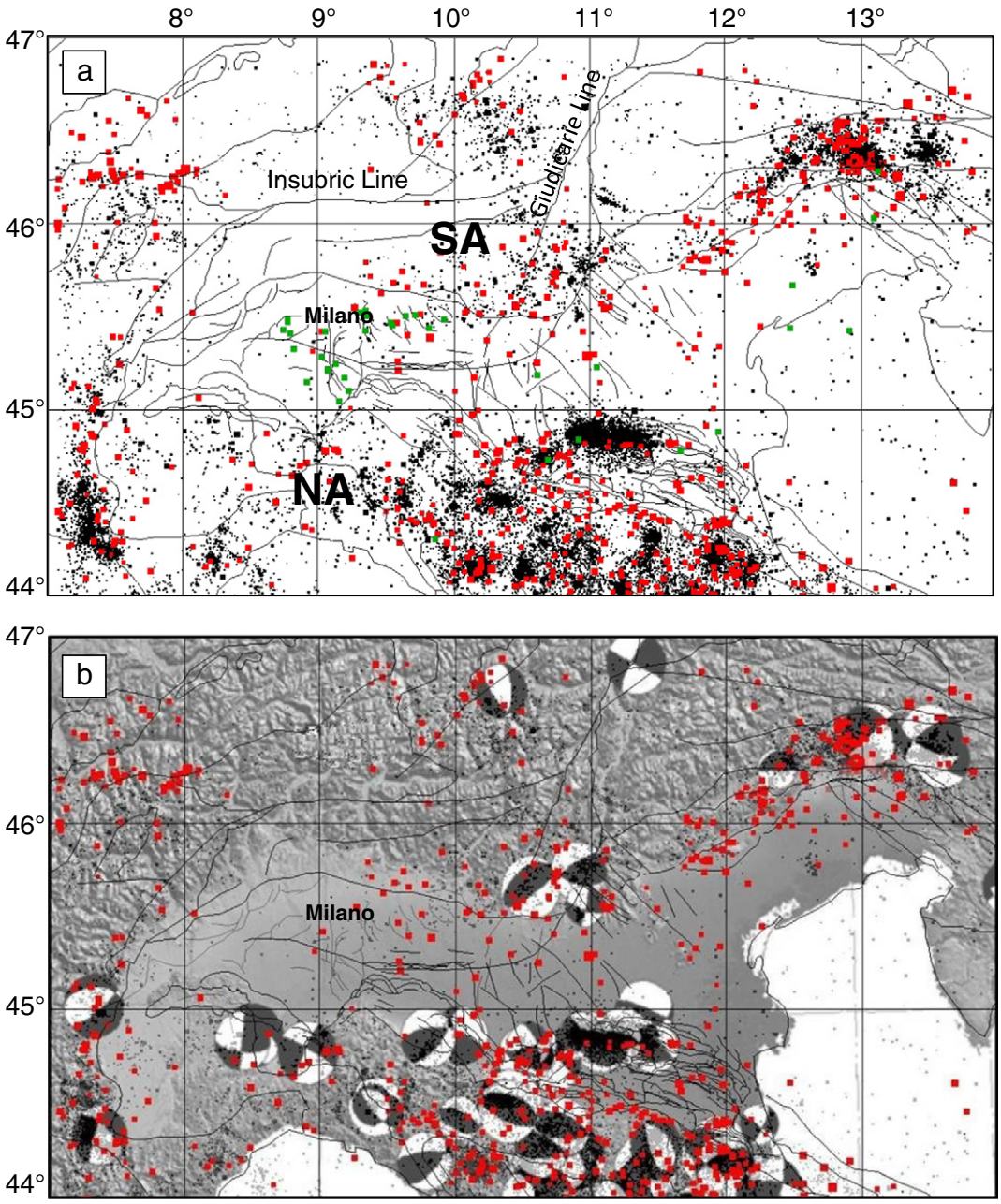

Fig. 2. a–b—Instrumental (black) and historical (red) earthquakes (0 < M < 7) against the Po Valley tectonics (see Fig. 1 for unit distribution and name). Green squares in panel a are deep wells which have penetrated the Mesozoic Carbonates. In panel b the focal mechanisms of the major events (M > 5; from Di Bucci and Angeloni, 2013) are indicated.

2.2. Seismo-tectonic setting

Summarising active tectonic studies and all those works useful for the seismo-tectonic characterization of the Po Valley region is difficult, due to the size of the area and the number of papers. Indeed, numerous research projects have increasingly tackled the Po Valley neotectonic setting, this being especially due to the recent earthquake activity in the region (Michetti et al., 2012; Vannoli et al., 2014).

Previous studies discussed the region as part of the larger Italian seismo-tectonics in terms of seismicity (Chiarabba et al., 2005), seismogenic source characteristics and processes (Basili et al., 2008), present-day stress field and focal mechanisms (Di Bucci and Angeloni, 2013; Montone et al., 2004), and GPS analysis (Serpelloni et al., 2005, 2012, 2013). At the same time, other studies have concentrated on selected areas or specific seismo-tectonic-related topics across the Po Valley and the surrounding regions. Among these many studies, below we put emphasis on those which provided key constraints to the performed 3D modelling, loosely grouped by tectonic domain (foreland, Southern Alps, Northern Apennines).

In the foreland, Castaldini and Panizza (1991) illustrated one of the first inventories of active faults, yet restricted to the eastern sector of the region. Burrato et al. adopted a geomorphological approach, based on the detailed analysis of the drainage network (2003), and pseudo 3D models (2012 and 2014) to contribute to the assessment of the seismic hazard across the basin. Carminati et al. (2007) utilized historical sources to discuss the feasibility of liquefaction-induced subsidence in Venice and the possible associated earthquake phenomena. Livio et al. (2009, 2014) used seismic reflection profiles, field data, exploratory trenching and geomorphic and structural analysis to characterize the Quaternary growth history of selected inferred active buried thrusts.

Bresciani and Perotti (2014) used field surveys, well data and a detailed interpretation of a depth-converted seismic line, to reveal the seismotectonic characteristics of a partially buried structure, still active in recent times (the Romanengo anticline). Toscani et al. (2014) investigated the kinematics of the central sector of the Po Valley foreland–foredeep units, between the Southern Alps and the Apennines, by structure restoration and analogue models. Recently, Maesano et al. (2010, 2011, 2013, 2014) presented the compilation of a slip-rate database about the Plio–Pleistocene blind thrusts of the outer Northern Apennines fronts, these being potential sources of strong earthquakes. North of Milan and at the transition between the Southern Alps and the foreland units, Scardia et al. (2014) documented the tectonics and earthquake activity which deformed that domain since the Pliocene to the present day.

Along the eastern Southern Alps and especially in the Friuli region, seismo-tectonic structures have been investigated using: stress orientation data and focal mechanism inversion (Bressan et al., 1992, 1998, 2003), structures–earthquake association (Carulli and Ponton, 1992), earthquake relocation and hypocentral probability (Poli et al., 2002), seismogenic sources (Barba et al., 2013; Burrato et al., 2008; Galadini et al., 2005), strain accumulation and stress transfer by numerical investigation (Cassola et al., 2007), site velocities from continuous GPS observations and 3D modelling (Bechtold et al., 2009), finite-fault synthetic seismograms and fault models (Moratto et al., 2012), and seismic monitoring experiments (Chiaraluce et al., 2009).

On the southern side of the Po Valley basin, the seismicity of the Northern Apenninic front and the derived buried tectonic arcs has been the subject for different studies (Benedetti et al., 2003; Boccaletti et al., 2011; Di Giovambattista and Tyupkin, 1999; Gunderson et al., 2013; Ponza et al., 2010; Toscani et al., 2006, 2009). In particular, given the recent and important earthquake activity, various techniques have been used to unravel the seismo-tectonic framework of the western sector of the Ferrara tectonic arc, namely the Cavone–Mirandola area (Carminati et al., 2010; Bignami et al., 2012; Di Manna et al., 2012; Marzorati et al., 2012; Scognamiglio et al., 2012; Carannante et al., 2014; Maesano et al., 2013; Bonini et al., 2014; Govoni et al., 2014).

Noteworthy, given the apparent lack of important seismicity, no particular research has tackled the seismo-tectonics of the extreme western Po Valley (i.e. west of Milan). Nevertheless and exceptionally, Delacou et al. (2004) integrated that region as part of the seismotectonics analysis of the western/central Alps using a synthesis of the available and most reliable focal mechanisms.

3. Data & methodology

3.1. Data

The data used to build the performed 3D model are derived from public literature and the archives of the Italian Ministry of Energy (http://unmig.sviluppoeconomico.gov.it, namely the ViDEPI Project, n.d). As such they refer to geophysical and geological maps, cross-sections, well composite logs and stratigraphic columns. No seismic data have been used during the model building process. A complete description of the whole dataset, and its distribution across the basin, is provided in Turrini et al. (2014).

Conversely, the earthquake data comes from the catalogues available to the public on the INGV website (http://bollettinosismico.rm.ingv.it; http://iside.rm.ingv.it). Hypocentres in the database, described by location, magnitude (Mw and Mi for historical and instrumental earthquake respectively) and depth, can be essentially classified as:

1. Historical if their location was derived from the analysis of the damage pattern. They are included in the CPTI11 Catalogue (Rovida et al., 2011; http://emidius.mi.ingv.it/CPTI11/). There are earthquakes from 1000 to 2006, those occurred from 1980 to 2006 are also included in the instrumental catalogues. This is a parametric catalogue with epicentral coordinates, but not depth, and magnitude expressed as moment magnitude (M_w).
2. Instrumental if it occurred after 1980 and registered by the Italian seismic Network (that was established after the 1980 Irpinia earthquake). Usually all these earthquakes were located in semi real time and re-located manually. These earthquakes are included in different catalogues since the ISN was developed during the time and changed also a little bit the procedure to locate them. From 1981 to 2001 they are included in the CSI 1.1 Catalogue (Castello et al., 2006; http://csi.rm.ingv.it/). From 2002 to April 2013 they are included in the Bollettino Sismico Italiano and downloadable from http://bollettinosismico.rm.ingv.it/ and http://iside.rm.ingv.it/. The latter website includes also the real-time seismicity not revised by the analyst seismologists (April 2014 up to now).

3.2. Methodology

The methodology adopted so far refers to four different phases of data collection, editing and analysis.

Phase I: the available data from the literature have been integrated/geo-referenced to a common geographical system and used to build the Po Valley 3D structural model (Turrini et al., 2014). Four layers have been gridded all across the region while key cross-sections, depth-slices and isopach maps have been constructed to analyze the final model. Both the model building and the related analysis have been performed using the MOVE software.

Phase II: in order to a) review the regional 3D model layers, b) improve them across selected structural domains inside the basin, and c) build the final 3D fault pattern, the Kingdom 2D3D package (http://www.ihs.com/products/oil-gas/geoscience-software/kingdom-seismic-interpretation/index.aspx) has been used after creation of a regular grid of SEGY pseudo-seismic lines and import of the MOVE depth grids, these being hence better suitable for re-picking, tie to wells and local modifications. Specifically, the fault building process was performed by:

1. projection of public map fault traces on the model grid layers
2. analysis and slicing of the structural geometries from the 3D model depth-grids and along the available well paths
3. gridding of the final 3D fault plane.

Further, the Kingdom surface-validation tool was used to allow the 3D surface compatibility of the modelled faults to be checked during real-time picking on the pseudo-segy lines.

Phase III: the 3D structural model has been populated with the earthquake data from the INGV catalogues and a 3D seismo-tectonic model could be obtained. For ease, both historical and instrumental events were divided and graphically scaled in different magnitude classes ($0 < M < 7$). The final 3D seismo-tectonic models have been accurately sliced and analyzed versus the hypocentre distribution, the single shock events being eventually coloured by depth and projected onto the model vertical slices from the most suitable distances.

Phase IV: 3 selected 3D seismo-tectonic sub-models and the derived earthquake–structures associations have been analyzed by map view, systematic vertical slicing and hypocentre projection. The MOVE software was used for 3D visualization and rendering of the model structures and earthquake events.

4. Model and data uncertainty

The uncertainties associated with the 3D structural model have been discussed by Turrini et al. (2014) and can be considered to increase as we move downscale from the crustal to the field scale. In order to refine the interpretation and reduce the related uncertainties, the MOVE grids have been reviewed and improved using Kingdom software, where interpretation of horizons and faults can be more easily managed

by cross-picking and wells, such as is done for conventional seismic interpretation. Since no seismic data have been used during the model building, any issue related to the Po Valley litho-tectonic units velocities is directly inherited from the original depth-data (maps, cross-sections, wells; see specific papers referenced in Turrini et al., 2014) so that the related uncertainty is then accepted as part of the 3D structural model one.

Uncertainty concerning the location and magnitude of earthquakes within the extent of the final 3D model can be larger than the structural uncertainty. This is mainly due to the data recording and processing. In particular, depth conversion of the events is critical as the final error will essentially depend on the difference between the selected velocity model and the true, yet unknown, velocity distribution through the Earth. Despite any effort and reviewing by the INGV experts, uncertainty about 3D location (horizontal and vertical) and magnitude of the hypocentres remains a major issue within the Po Valley seismicity database (e.g. Chiarabba et al., 2005), although various filtering of the data may represent a way to reduce it: 1) magnitude cut-off (i.e. >5, Vannoli et al., 2014), 2) selection of the events characterized by a minimum error in the INGV catalogues, and 3) selection of the events recorded by a maximum number of stations. Eventually, although aware of the aforementioned concepts and given the general scarce and patchy seismicity of the Po Valley domain, we have chosen to use the entire INGV earthquake dataset. As a consequence the possible seismo-tectonic scenarios have been analyzed in light of the performed 3D perspective and our experienced/knowledge of the basin. The process suggested that:

1. The validity of the Po Valley structure–earthquake integration seems, at present, *acceptable* at the regional scale, whereas it should be considered *possible* at a smaller scale (e.g. across the selected subdomains);
2. The distance of projection of the earthquakes (HPD = Hypocentre Projection Distance) on the selected cross-sections or maps is based on a) an average 2–5 km horizontal–vertical error (http://www.ingv.it/it/), b) the structural domain specifications (e.g. mainly compression/extension?), c) the 3D structures (geometries, dimensions), and d) the distribution/density of the surrounding earthquakes;
3. This indicates that the earthquakes–structures integration and the derived comparative analysis have the potential to act as a decisive tool for uncertainty reduction and reciprocal validation of the data used to build the final Po Valley 3D seismo-tectonic model.

5. Seismo-tectonics across the 3D Po Valley geo-volume

5.1. 3D model and regional seismicity

Once the outcrop structural trends and the subsurface model layers are put against the entire earthquake dataset, the 3D seismo-tectonic framework across and around the Po Valley is immediately revealed.

In general, the model confirms the positive correlation among the crustal tectonics and the most important earthquake events (Fig. 3a).

In detail, inspection of the 3D model by depth rendering, contouring and perspective visualization of the layer/fault grids and the earthquake events illustrates a number of observations:

1. Most of the events are concentrated at the upper-crust level, between the top basement and the top Mesozoic carbonates (Fig. 3b; red events);
2. Only a minor part of the shocks occur in the lower crust or close to the Moho interface (Fig. 3b; orange and green event);
3. The Adria plate boundary is actively interacting with the Tyrrhenian–Ligurian plate below the Northern Apennines (Fig. 3a; see also Fig. 7c–d) so that the earthquake events can be followed from surface down to 70 km below the Northern Apennines (Fig. 3a and c; see also Fig. 7c–d);
4. Conversely, along the Southern Alps belt, the tectonic interaction between the Adria and the Europe plates appears currently frozen at the deep crust and Moho levels whereas deformation of the upper crust is confirmed by the intense seismicity across the Mesozoic and upper basement units (Fig. 3a and c; see also Fig. 7a–d);
5. At the southern and northern boundaries of the eastern Po Valley domain, overthrusting of the Southern Alps and the Northern Apennines onto the Po Valley Mesozoic foreland controls the earthquake concentration at the buried and segmented front of the two belts (Ferrara arc, Friuli domain) (Fig. 4a);
6. Structures across the Cenozoic clastic successions and above the base-Pliocene surface (Fig. 4b) show poor instrumental seismicity (e.g. in the NW sector the Ferrara tectonic arc).

Seismicity can also be correlated to the Mesozoic Carbonates units which is the main exploration target in the area (see Turrini et al., 2014 for detailed discussion). Indeed, because the earthquakes especially concentrate at the upper-crust level (see Fig. 3b), the final Carbonates-earthquake map-view (Fig. 5a–b) can be taken as representative of the Po Valley foreland seismo-tectonics. The derived picture illustrates the major structures of the eastern and western domain as they stand against a general poor and patchy seismicity: nearly absent west of the Giudicarie lineament and rather intense although extremely localized to the east of that lineament.

5.2. Faults and earthquakes

At present, our seismo-tectonic model is populated with 66 fault surfaces. Most of them are thrust faults (with possible local oblique component of slip) related to Alpine shortening. Nevertheless, a part of those faults can be associated to both extension and compression that occurred through Triassic to present (Turrini et al., 2014 and all references therein). Few faults in the current 3D model are extensional faults only.

In detail, the 3D model faults can be divided into 4 groups (Fig. 6) mainly defined according to their location and depth and each characterized by specific earthquake population:

Group 1 (Fig. 6a): these faults are part of the western Po Valley structural domain and they exclusively cut across the Mesozoic carbonates and their underlying basement (Cassano et al, 1986; Fantoni et al., 2004; Ravaglia et al., 2006). Depth to the fault plane is comprised between 3 and 15 km. Dip is really variable depending on the related structure orientation and tectonic significance (see Turrini et al. 2014, and reference therein). Most of the Group 1 faults appear free from important earthquake activity with the exception of isolated faults to the east of Milan and those below the Monferrato belt (see cross-section AA1 in Fig. 8 and related discussion).

Group 2 (Fig. 6a): faults of this group belong to the eastern Po Valley structural domain, namely the buried front of the Northern Apennines (Ferrara arc). These faults deform the Mesozoic carbonates and propagate into the overlying Cenozoic clastic successions (Pieri and Groppi, 1981; Cassano et al., 1986; Castellarin et al., 1986; Bonini et al, 2014 and all references therein). Basement involvement by some of the more internal faults is a long-standing debate, yet it seems to be eventually demonstrated by recent earthquake activity (Govoni et al., 2014 for the most recent analysis of relocated hypocentres). Depth to the fault plane is comprised between 3 and 15 km. Dip is mainly towards the SW. Inside the group, the faults that deform the NW sector of the Ferrara tectonic arc can be correlated with intense earthquake clusters (see Section 5.4.2 and related references). Only a weak seismicity is recorded along the 3D fault surfaces that have been modelled across the SE sector of the arc.

Group 3 (Fig. 6b): these faults are again part of the western Po Valley domain yet they are shallower than the ones described for group 1 and mechanically detached from them (Bello and Fantoni, 2002; Cassano et al., 1986; Fantoni et al., 2004; Turrini et al., 2014 and references therein). In particular they:

1. displace the South Alpine allochthonous basement (fault 'SAb')
2. displace and imbricate the South Alpine carbonate units (fault 'SAc')

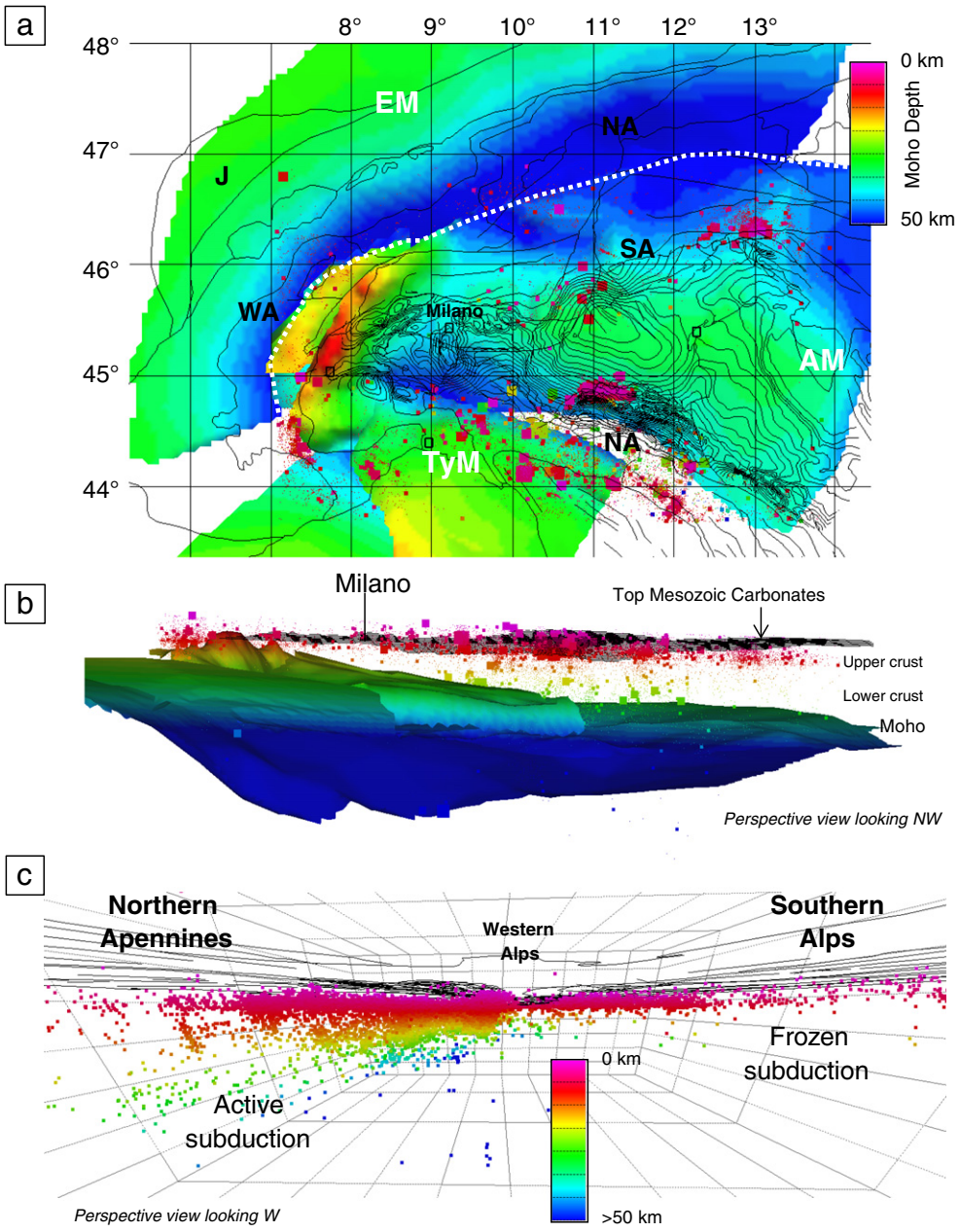

Fig. 3. Images from the 3D seismo-tectonic model. a) Moho and top Mesozoic Carbonates grid-layers with earthquake ($3 < M < 7$) coloured by depth (sea colour scale bar in panel c). Perspective view looking NW; b) map view of the Moho units (EM = European Moho, AM = Adria Moho, TyM = Tyrrenian Moho; white dot line is the northern boundary of the Adria Moho; see Turrini et al, 2014) against contour map of the Po Valley top Mesozoic Carbonates and major tectonics. Earthquakes ($3 < M < 7$) are coloured by depth (sea colour scale bar in panel c). NA = Northern Alps, WA = Western Alps, SA = Southern Alps, Nap = Northern Apennines; c) all instrumental earthquakes ($0 < M < 7$) coloured by depth to show active tectonics across the Northern Apennines and the Southern Alps.

3. induce thrusting of the clastic sediments at the front of the western Southern Alps (fault 'SAw')
4. displace the Northern Apennine Ligurides units in the Monferrato region (fault 'NAm')
5. deform the clastic succession of the Emilia and Milano buried fronts (faults 'NAe' and 'SMf' respectively).

Seismicity around those faults is poor and the related magnitude values vary from low to moderate as we move from west to east, towards the Giudicarie lineament and the NW sector of the Ferrara buried arc.

Group 4 (Fig. 6b): faults in this group define the Veneto and Friuli Southern Alps domains, the latter being deformed by both the Alpine and Dinaric tectonics (see Section 5.4.1, this paper, and references therein). Depth to the fault planes varies between 1 and 15 km as their dip is mostly towards the NNW (Alpine faults) and NE (Dinaric faults). Seismicity around the fault planes can be intense with high magnitude values (see Section 5.4.1).

5.3. 3D model slicing and earthquakes

Vertical slicing of the model provides further insights about the final 3D seismo-tectonic geo-volume and the methodology as well.

The crustal-scale sections in Fig. 7 supply good examples of the Po Valley structure–earthquake associations moving from the western domain (sections 'a' and 'b') to the eastern one (sections 'c' and 'd'). The hypocentres from the INGV database have been projected perpendicularly from a distance of 10 km, on the same cross-sections which

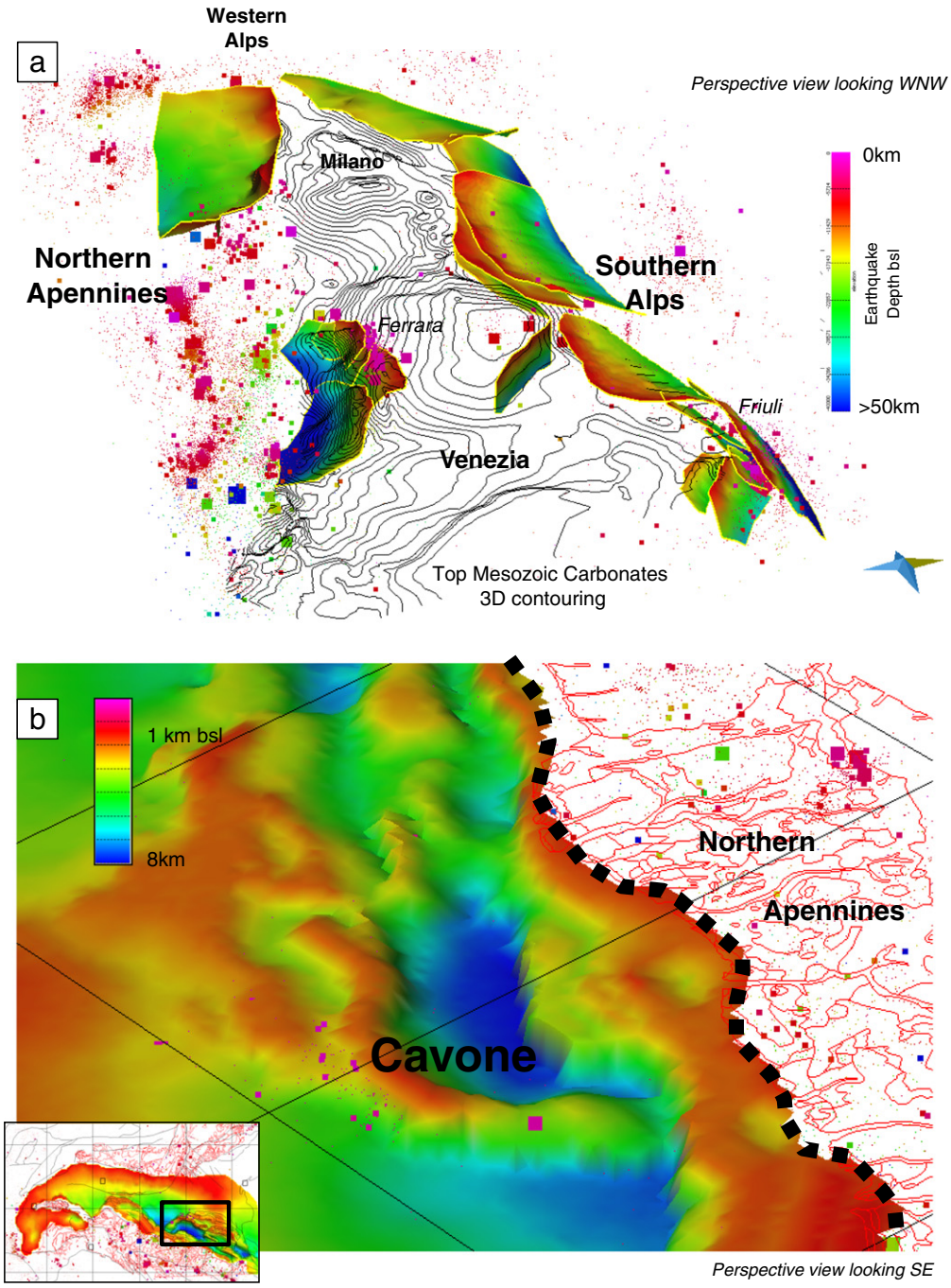

Fig. 4. Images from the 3D seismo-tectonic model. a) Top Mesozoic Carbonates contoured 3D grid and major thrust surfaces at the Northern Apennines (Nap) and Southern Alps (SA) segmented external front; instrumental earthquakes coloured by depth (colour scale bar in Fig. 3c); b) eastern Po Valley Base Pliocene 3D structures (see inset for location) and the associated instrumental earthquakes in the Cavone region. Outcrop geometries (purple) and thrust front of the Northern Apennines (black stipple line) are shown.

have been already discussed in terms of structural geometries by Turrini et al. (2014). The negative and positive correlations between structures and instrumental seismicity are straight-forwards across the region at all of the stratigraphic levels. Once again the major tectonic zones are the *loci* of important earthquake clusters in the eastern Po Valley domain (sections 'c' and 'd'). Conversely the western domain structures (sections 'a' and 'b') appear nearly earthquake-free, even considering the historical event distribution (red dots at depth = 0 on all of the cross-sections).

In order to focus on the seismo-tectonic interpretation of the foreland structure while showing the impact of the earthquake distance of projection on the derived uncertainty, the AA1 cross-section in Fig. 8 has been sliced from the 3D model and the related structure–earthquake associations have been analyzed and compared to one another.

The cross-section runs through the Monferrato arc, the Gaggiano-Lacchiarella domain, the external front of the Southern Alpine belt (and the related foreland units) and the Veneto carbonate platform unit (Fig. 8a). The overall structural setting basically refers to a) Triassic–Jurassic extension which controlled the Mesozoic block-faulting and the related thickness distribution and b) Cretaceous-to-Pliocene contraction which reactivated part of the extensional faults, inverted some of the Jurassic basins and displaced the Apennines and Southern Alps towards the Po Valley foreland (Turrini et al., 2014 and all references therein).

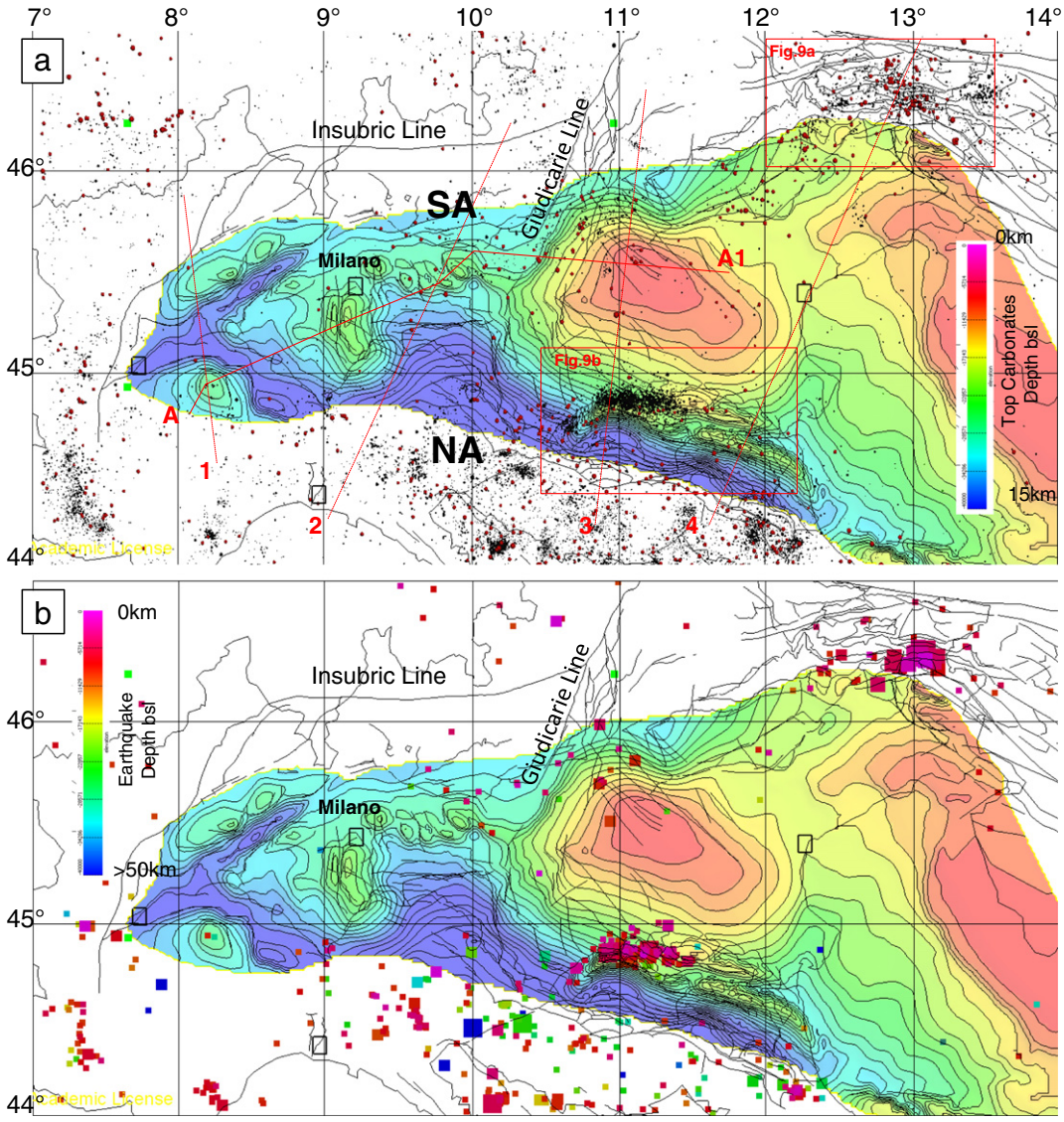

Fig. 5. Po Valley top Mesozoic Carbonates 3D grid by contouring and depth colouring, earthquakes and tectonics: map view; a) structures against all instrumental and historical earthquakes. Location of sections and selected domains in Figs. 7, 8, and 9 is indicated; b) structures against instrumental earthquakes ($4 < M < 7$) coloured by depth. Horizontal net dimension is 80 km. Latitude and longitude values are North and East of Greenwich.

Three different distances of projection of the surrounding earthquakes have been considered with respect to the structure orientation and dimensions (see Fig. 8a and figure caption for explanation). The associated magnitude, variable between 0 and 5 has been rendered using different colours and dimension of the points representing the shocks in the area.

When the projection distance of the events on the cross-section is 5 km (Fig. 8b), no major shock is shown across the structures. Conversely three shocks with $3 < M < 4$ occur in the Veneto Platform domain: near the top of the Mesozoic Carbonates and in the lower crust, at approximately 20 km depth below the mean sea level. One shock with similar magnitude occurs close to the Moho below the Monferrato belt, in correspondence to a strong 'fold' of the Moho. A cloud of shocks with $0 < M < 3$ is loosely distributed to the ENE of the well Chiari 1, between the topography and −10 km depth. Eventually, some isolated shocks can be picked below the Asti 1 well, in the Monferrato region. The picture, despite the absence of major earthquakes, provides a reasonable imaging of the seismo-tectonic of the area with an increasing seismicity from SW to NE.

Using a 10 km (Fig. 8c) distance of projection a couple of $4 < M < 5$ events can now be associated with the basement faults which deform the Veneto Platform. The $3 < M < 4$ earthquakes are spread over a wider area, below and to the east of the Chiari well, both in the foreland and within the Southern Alps units. A few of them also appear close to the Moho: close to the Moho interface between the Lacchiarella inverted structure and the Monferrato belt, and near to the top of the basement, below the Asti 1 well. The seismo-tectonic architecture suggested using a 5 km distance of projection is here confirmed and possibly reinforced: a) seismicity gets stronger from west to east, b) the Southern Alps thrusts do correlate with some shock events, c) some of the extensional faults in the foreland can be correlated to isolated shocks (Chiari basin) and some other are nearly shock-free (Lacchiarella basin), and d) there seems to exist a seismogenic layer above the Moho interface.

Using a 20 km distance (Fig. 8d), the $3 < M < 5$ earthquake clusters previously described are substantially the same while the $0 < M < 3$ events increase in density as a sort of background-seismicity-noise across the crust to the east and west of the Gaggiano–Lacchiarella zone.

From the performed analysis we conclude that:

1. With any of the earthquake projection distance we have chosen, the overall seismo-tectonic picture always indicates moderately active Veneto-Platform and Southern Alps domains and a low active

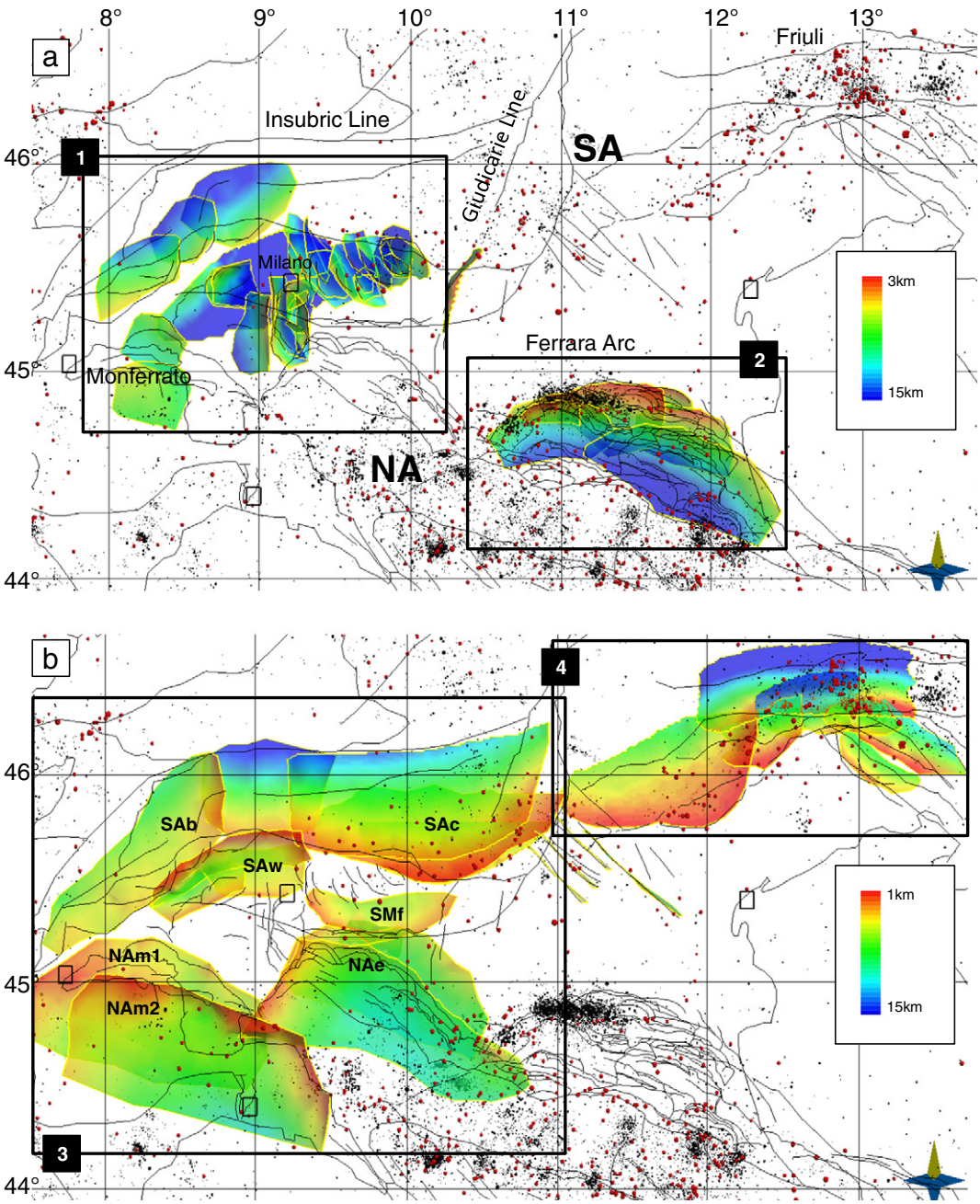

Fig. 6. 3D fault surfaces, coloured by depth, against all earthquake events: see text for description of each fault-group. Horizontal net dimension is 80 km. Latitude and longitude values are North and East of Greenwich.

Monferrato domain, the two being separated by a nearly silent zone which covers the Gaggiano–Lacchiarella structural domain.

2. Along the selected cross-section path, increase in the projection distance from 5 to 20 km results to an increase of the structure seismicity for all of the domains with no visible inconsistency among the different tests.
3. Nevertheless, given the geometry of the structures (dimension and orientation) and the distribution of the available earthquakes, a projection distance of 10 km appears to be the most reasonable for the selected model slice to produce a most likely representation of the possible seismo-tectonic system. Conversely the 5 and 20 km earthquake projection distances seem to account for the extreme situations (minimum or maximum earthquake events), those not allowing the studied case to be completely/correctly represented in its seismo-tectonic elements.

5.4. Seismo-tectonics of selected structural domains around the Po Valley basin

In order to test the final 3D seismo-tectonic model and the related methodology, two domains on the opposite sides of the Po Valley basin, the Friuli domain and the Ferrara arc (Figs. 9–13), have been selected for further and more refined analysis.

5.4.1. The Friuli domain

The Friuli domain is located at the transition between the eastern sector of the Southern Alps-Dinaric fronts and the associated Po Valley foreland (Fig. 9a; see also Fig. 5). The tectonic setting is related to a poly-phase history which created the present tight architecture and the associated arc-shaped configuration, convex towards the north. In this region, N–S faults, transported within the belt and

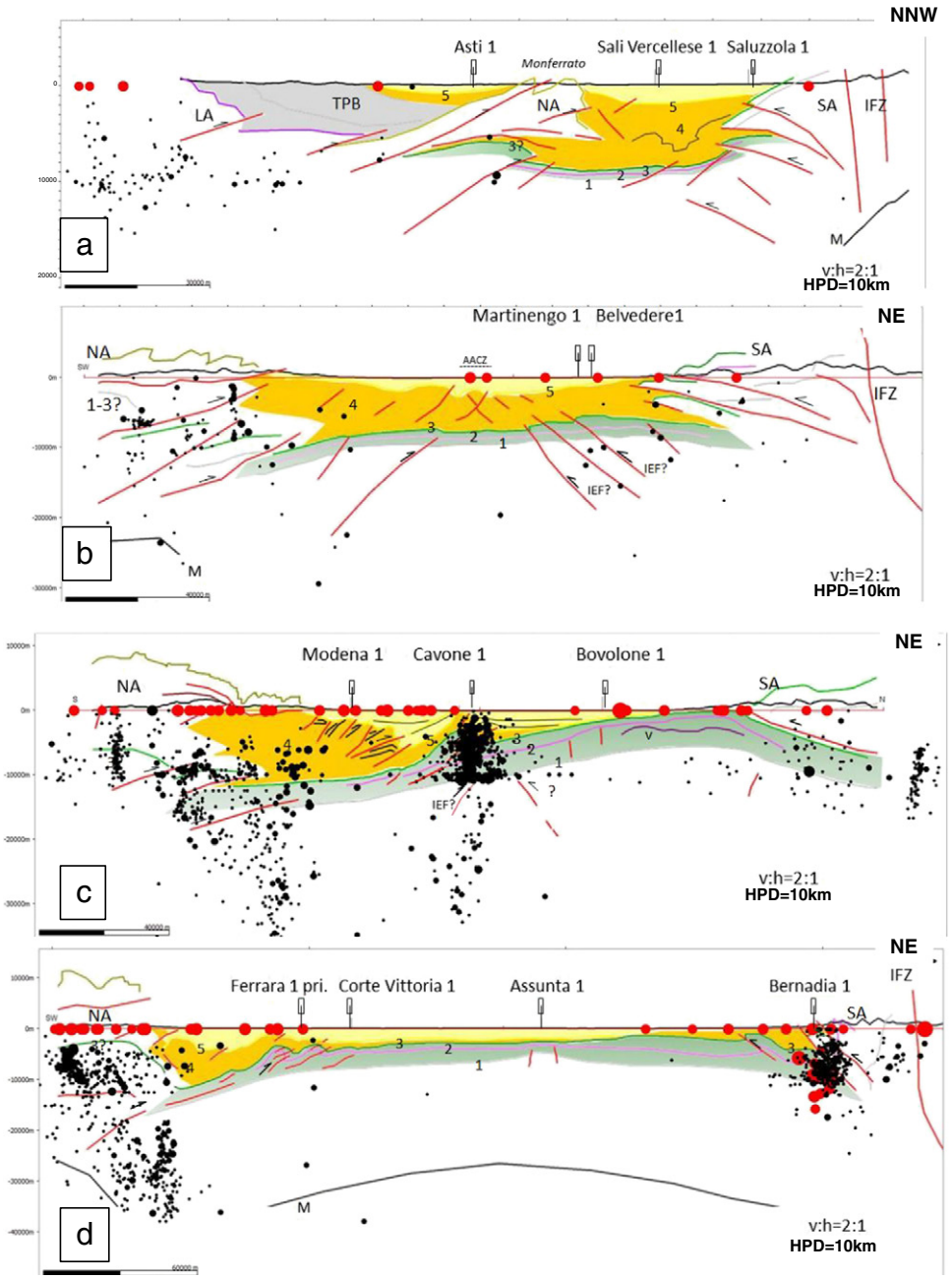

Fig. 7. Crustal-scale cross-sections from Turrini et al. (2014) against the INGV earthquake dataset; black dots: instrumental hypocentres ($0 < M < 7$); red dots: historical hypocentres ($M = 3–7$). HPD = Hypocentre Projection Distance. Deep red dots in section 'd' are historical hypocentres relocated by depth. Section 'a': 1 = Near Top Basement; 2 = Near Top Triassic; 3 = top Mesozoic Carbonates; 4 = Cenozoic succession; 5 = Base-Pliocene unconformity; NA = Northern Apennines (Allochthonous Ligurides); TPB = Tertiary Piedmont Basin sediments; LA = Ligurian Alps; SA = Southern Alps; IFZ = Insubric Fault Zone; M = Moho. Section 'b': 1 = Northern Apennines (Allochthonous Ligurides); 2 = Southern Alps; 3 = Western + Northern Alps. Section 'c': 1 = Near Top Basement; 2 = Near Top Triassic; 3 = top Mesozoic Carbonates; 4 = Cenozoic succession; 5 = Base-Pliocene unconformity; NA = Northern Apennines; SA = Southern Alps; v = volcanics; IEF = Inverted extensional fault. Section 'd': 1 = Near Top Basement; 2 = Near Top Triassic; 3 = top Mesozoic Carbonates; 4 = Cenozoic succession; 5 = Base-Pliocene unconformity; NA = Northern Apennines; SA = Southern Alps; IFZ = Insubric Fault Zone; M = Moho. See Fig. 5a for location of sections.

buried in the foreland, mainly refer to Mesozoic extensional episodes, while two different thrust families result from the progressive interference between the Dinaric (end Cretaceous–Eocene) and Alpine (from end Oligocene onwards) mountain belts (Castellarin et al., 1992, 2006; Doglioni & Bosellini, 1987; Ponton, 2010; Venturini, 1991). The Dinaric structures are particularly evident in the eastern sector (Julian Pre-Alps), with NW–SE oriented folds and thrusts (Placer, 1999; Placer et al., 2010) The Dinaric thrusts appear truncated in the central sector (Gemona) by a dense system of neo-Alpine E–W imbricate thrusts which locally and partially reuse the pre-existing Dinaric ones. In the western sector (Carnian Pre-Alps) NE–SW thrusts, neo-Alpine in age (Upper Miocene onwards), can be observed together with NW–SE coeval dextral strike–slip faults of the eastern zone (Slovenia). Across the area, rocks pertain to both metamorphic and non-metamorphic rocks. The basement is metamorphic to the west, while in Carnia (Central

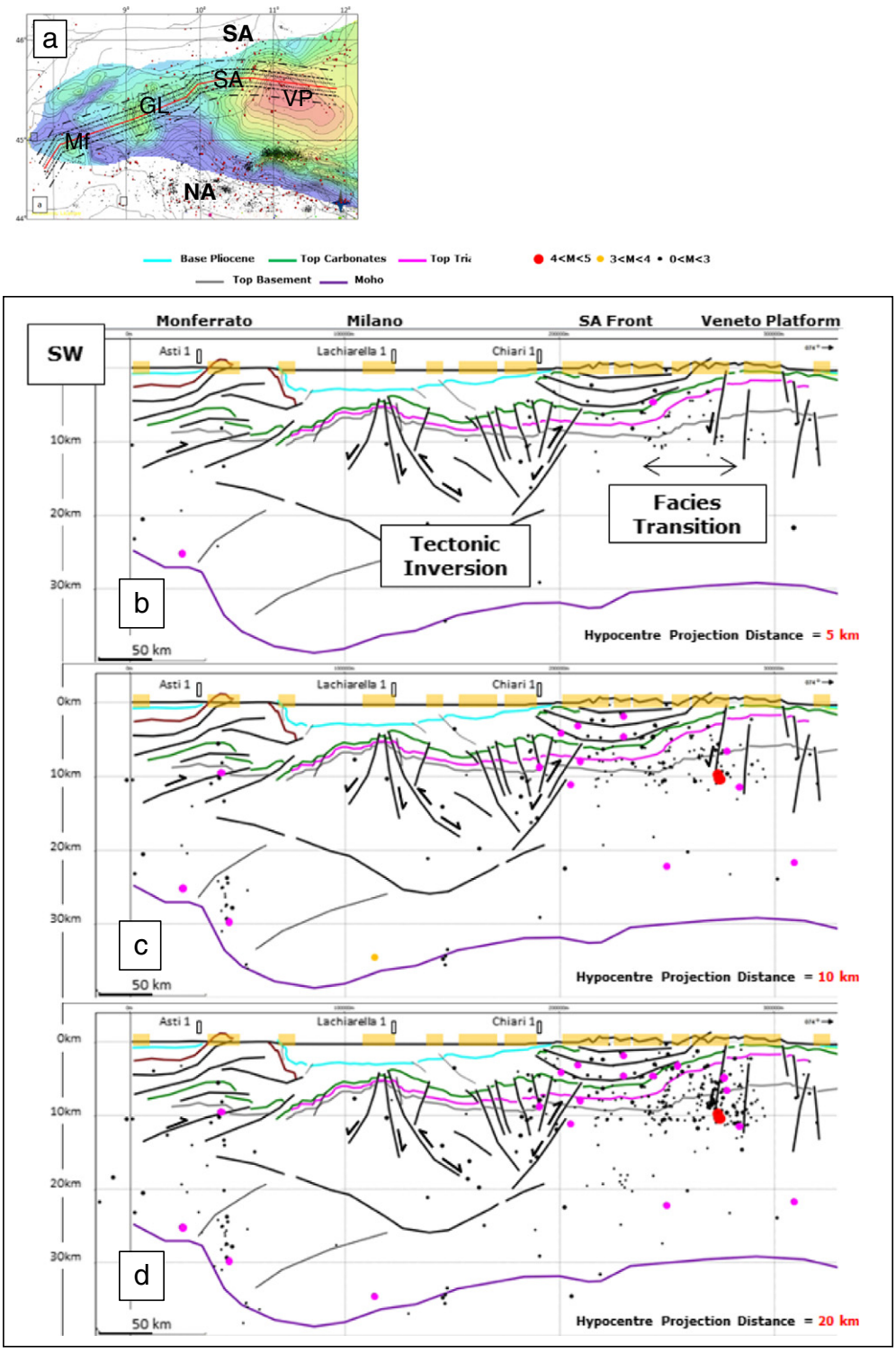

Fig. 8. Vertical slice across the seismo-tectonic 3D model to show the possible structures–earthquakes associations as a function of the hypocentres projection distance: a) section location on the top Mesozoic Carbonates grid layer and all earthquake dataset; red line = vertical slice path, stipple lines = 5, 10 and 20 km Hypocentre Projection Distance for b, c, and d earthquake projection sensitivity; b) 2d structures and earthquakes ($0 < M < 5$) projected from 5 km normal to the section; c) 2d structures and earthquakes ($0 < M < 5$) projected from 10 km normal to the section; c) 2d structures and earthquakes ($0 < M < 5$) projected from 20 km normal to the section.

and Eastern Friuli zone) it corresponds to a non-metamorphosed Palaeozoic succession which has however been deformed by Variscan tectonic phases, and to a late-orogenic Permo-Carboniferous sequence (Ponton, 2010 and reference therein). The sedimentary succession which covers the basement is about 10 km thick. There are two important evaporitic layers: in the Permian (up to 250 m thick) and in the Carnian (up to 250 m thick); Mid-Triassic massive carbonates (up to 1000 m thick) or terrigenous successions; late Triassic to

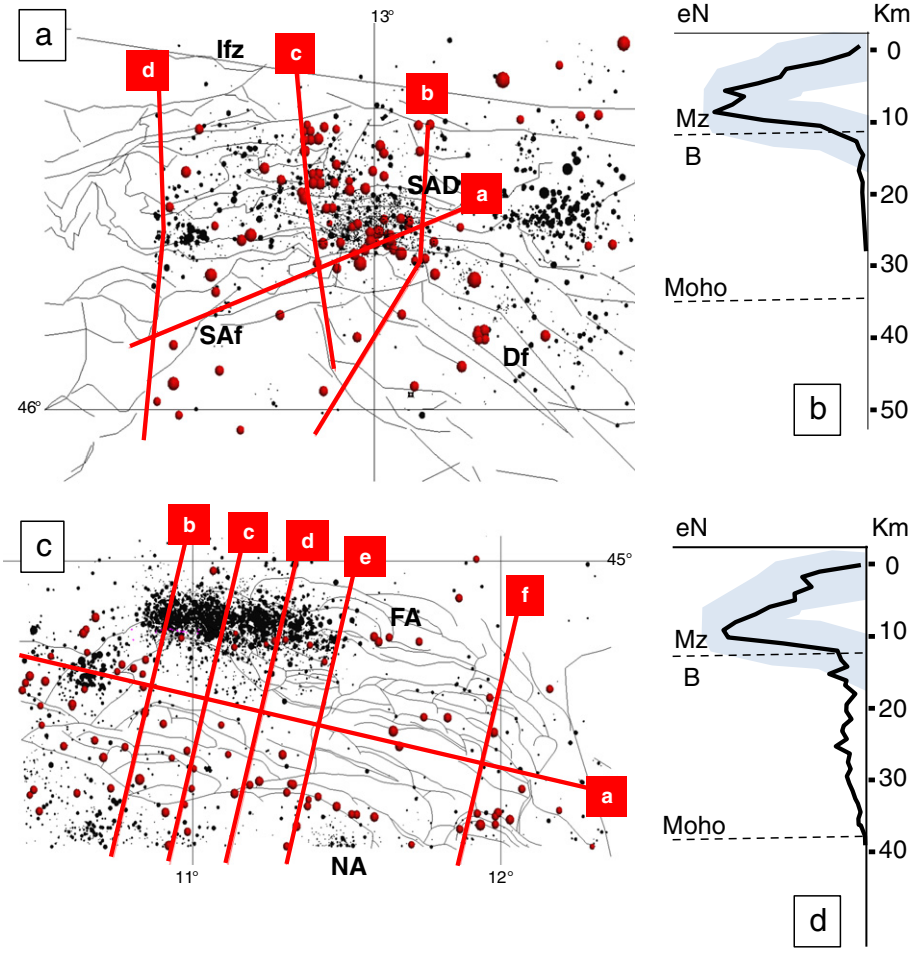

Fig. 9. Selected domains from the Po Valley 3D seismo-tectonic model: a) Friuli domain: section location, tectonics and earthquakes; IFz = Insubric Fault zone, SAf = Southern Alps thrust front, Df = Dinarides thrust front, SAD = Southern Alps–Dinarides Interference zone. Horizontal net dimension is 80 km. Latitude and longitude values are North and East of Greenwich; b) earthquake distribution by number and depth against approximate crustal scale stratigraphy (Mz = Mesozoic carbonates, B = basement; M = Moho); blue shadow area to suggest vertical uncertainty of the earthquake distribution; c) Ferrara arc domain: section location, tectonics and earthquakes; d) earthquake distribution by number and depth against approximate crustal scale stratigraphy (Mz = Mesozoic carbonates, B = basement; M = Moho); blue shadow area to suggest vertical uncertainty of the earthquake distribution.

Cretaceous very thick massive carbonates (up to 3500 m thick); at the top clastic deposits refer to the Dinaric foredeep (Palaeogene turbidites, 2500 m), and to the South Alpine forebulge (Miocene clastics, up to 2500 m).

The domain is seismically active and is classified at the top risk level in the seismic hazard map of northern Italy. Seismicity (Fig. 9a; see also Fig. 5) is distributed in clusters along the mountain fronts and both earthquake concentration and depth decrease towards the foreland. The largest cluster of events is shown in the central pre-Alps, at the interference between the Dinaric structures and the neo-Alpine ones. In this area, most of the hypocentres are reported to be approximately concentrated between 1 and 30 km depth (Fig. 9b) (Carulli & Ponton, 1992; Merlini et al., 2002; Moratto et al., 2012; Ponton, 2010). The associated focal mechanisms (see Fig. 2b) (Burrato et al., 2008; Di Bucci and Angeloni, 2013; Michetti et al., 2012) indicate a) compressional tectonics and N–S oriented principal stress direction in the central sector of the domain, b) compression with NNW–SSE oriented principal stress direction and locally sinistral shear in the western sector (Bechtold et al., 2009; Bressan et al., 1998, 2003; Burrato et al., 2008; Galadini et al., 2005; Peruzza et al., 2002; Poli et al., 2002), and c) dextral strike–slip shear movements in the eastern sector (Slovenia) (Kastelich et al., 2008; Ponton, 2010). Both the stress and GPS-related displacement fields, confirm the afore-mentioned tectonics and the present kinematics (see also Serpelloni et al., 2005, 2012, 2013; Bechtold et al., 2009; Devoti et al., 2011; Michetti et al., 2012).

The 3D analysis of the Friuli domain has been performed using selected cross-sections from recent literature (Fig. 10; Ponton, 2010). These sections have been imported into the Po Valley 3D model so that some of the key thrusts could be digitized, built as three-dimensional surfaces and integrated within the final geo-volume. Hence, the whole setting has been checked for special geometrical compatibility so that the 3D Po Valley model and the 2D cross-sections could be reciprocally validated.

Noteworthy, within this domain, some of the historical hypocentres have been relocated by the INGV specialists and their depth has been assigned (deep red dots in sections 'a–d' of Fig. 10).

Section 'a'

This section is oriented ENE–WSW across the belt (see location in Fig. 9a). It represents a strike line to the Alpine structures and, simultaneously, a dip-line to the Dinaric ones. As such thrusts refer to these two diachronous and distinct structural families thus revealing the derived interference and overprinting kinematics (Ponton, 2010). Given the high-density hypocentre cluster which the section intersects in the NE of the area, an initial earthquake projection distance of 1 km has been

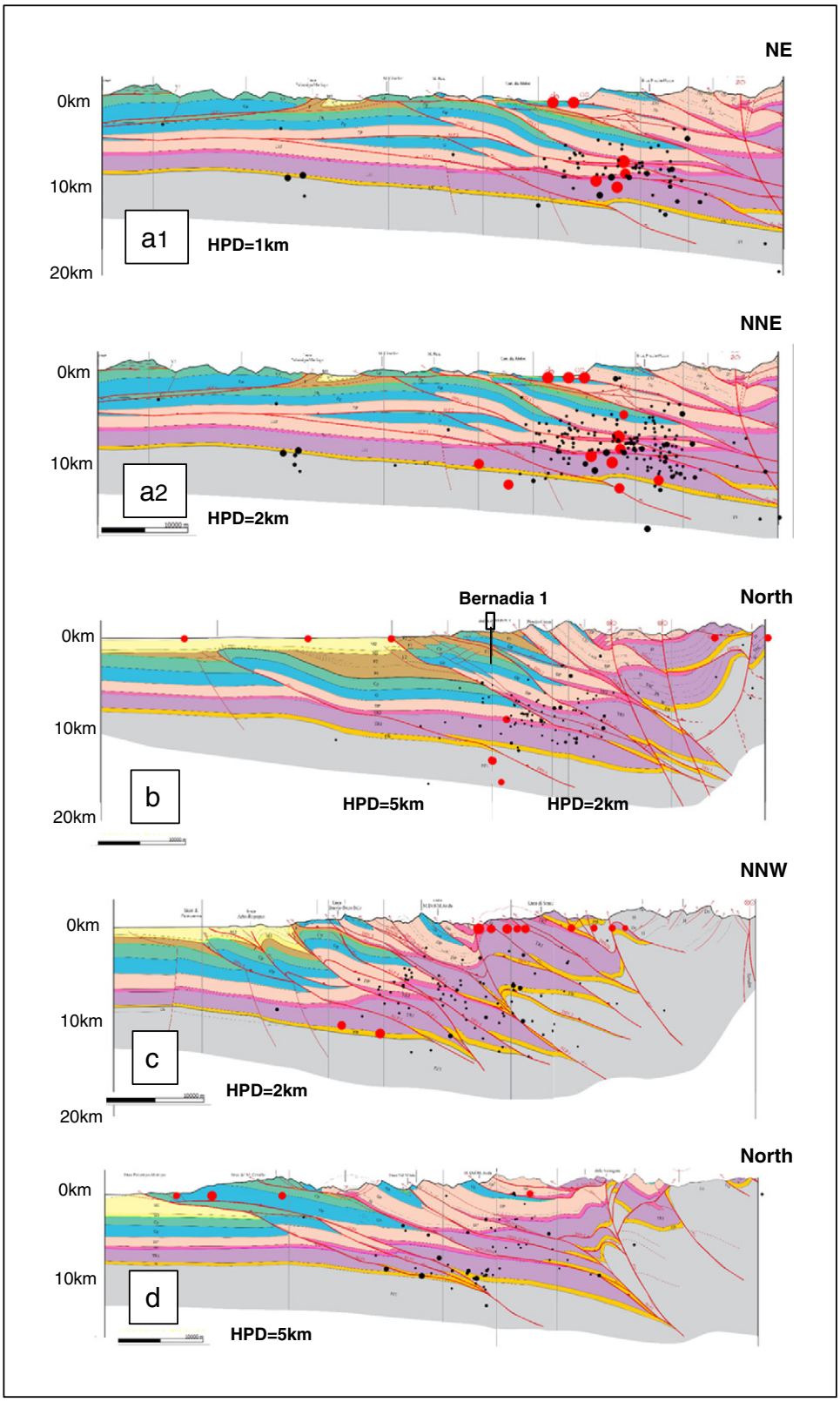

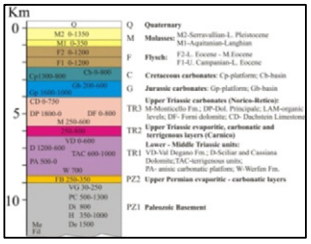

Fig. 10. Seismo-tectonic sections in the Friuli domain of the eastern Southern Alps to show structures–earthquake associations in the region (location in Fig. 9a; modified from Ponton, 2010; HPD = Hypocentre Projection Distance; note different HPD for the same a1 and a2 cross-sections: see text for discussion). Deep red dots are relocated hypocentres.

chosen. The resulting picture (Fig. 10a1) shows low-to-high seismicity in correspondence of the strong thrust-stacking which has been interpreted in the eastern sector of the section, with depth between 5 and 10 km, within the Triassic units and above the basement. Few and isolated minor shocks appear in the central and western sectors, close to the top basement. Interestingly, when the earthquake projection

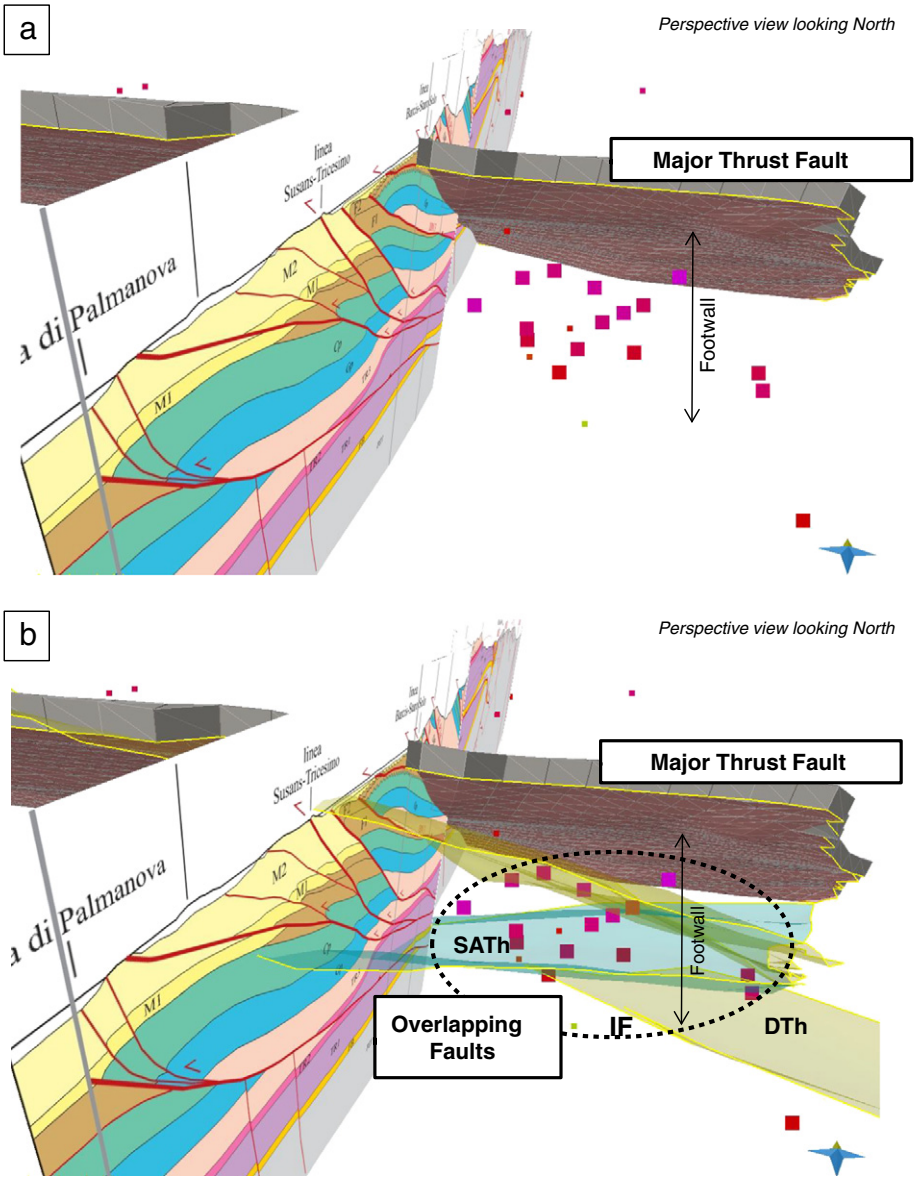

Fig. 11. 3D visualization of the Friuli domain seismo-tectonics: 4 < M < 7 earthquakes against 3D fault surfaces; a) earthquakes in the footwall of major thrust plane, perspective view looking NW; b) same earthquake cluster in panel a at the Southern Alps–Dinarides structural interference (IF = interference zone; SATh = Southern Alps thrust; DTh = Dinaric thrust; see text for discussion). Perspective view looking NW.

distance is 2 km (Fig. 10a2), the results show a slightly different structures–earthquakes association, so that: 1) the cluster in the eastern part of the section is denser, 2) a number of hypocentres occur at higher levels of the eastern tectonic stack (Upper Triassic and Jurassic levels), and 3) some important shocks can be observed in the basement, both below the thrust-related imbricates and in the central part of the section.

Section 'b'

This section can be approximately considered as an oblique line to both the Alpine and Inner Dinaric structures, and a dip line to the Outer Dinaric structures and a dip line to the external Dinaric fronts (see location in Fig. 9a). It also intersects a couple of strike–slip zones in its internal part. The interpreted fault pattern clearly shows the related structural interference (high angle and low angle thrusts cross-cutting each others). Using a variable 2–5 km projection distance (NE and SW of the Bernadia well respectively), the section allows the central Friuli earthquake cluster to be illustrated and compared with the one provided by the previous strike line. The resulting hypocentre distribution confirms the correlation between the deep thrust-stack and the seismicity in the area. The main shocks appear to occur at the top of the Middle Triassic units, at the bottom of Upper Triassic carbonate units and, locally, within the basement. Remarkably, the high-angle (NW–SE) strike–slip faults here seem not to tie with any earthquakes, yet their SE segments are highly seismogenic (Burrato et al., 2008; Ponton, 2010).

Sections 'c' and 'd'

Both the sections are dip-lines with respect to the Alpine structures and cut through the entire Alpine belt (see location in Fig. 9a). The earthquake projection distance is 2 km for section c and 5 for section d.

On section 'c' (see Fig. 10c) the earthquake events are widespread over a large part of the central sector and, once again, they seem to occur 1) especially within the mid-Triassic carbonates and 2) close to the top of the basement. A positive correlation among the projected shocks and the interpreted thrusts is really evident at the footwall of the basement units.

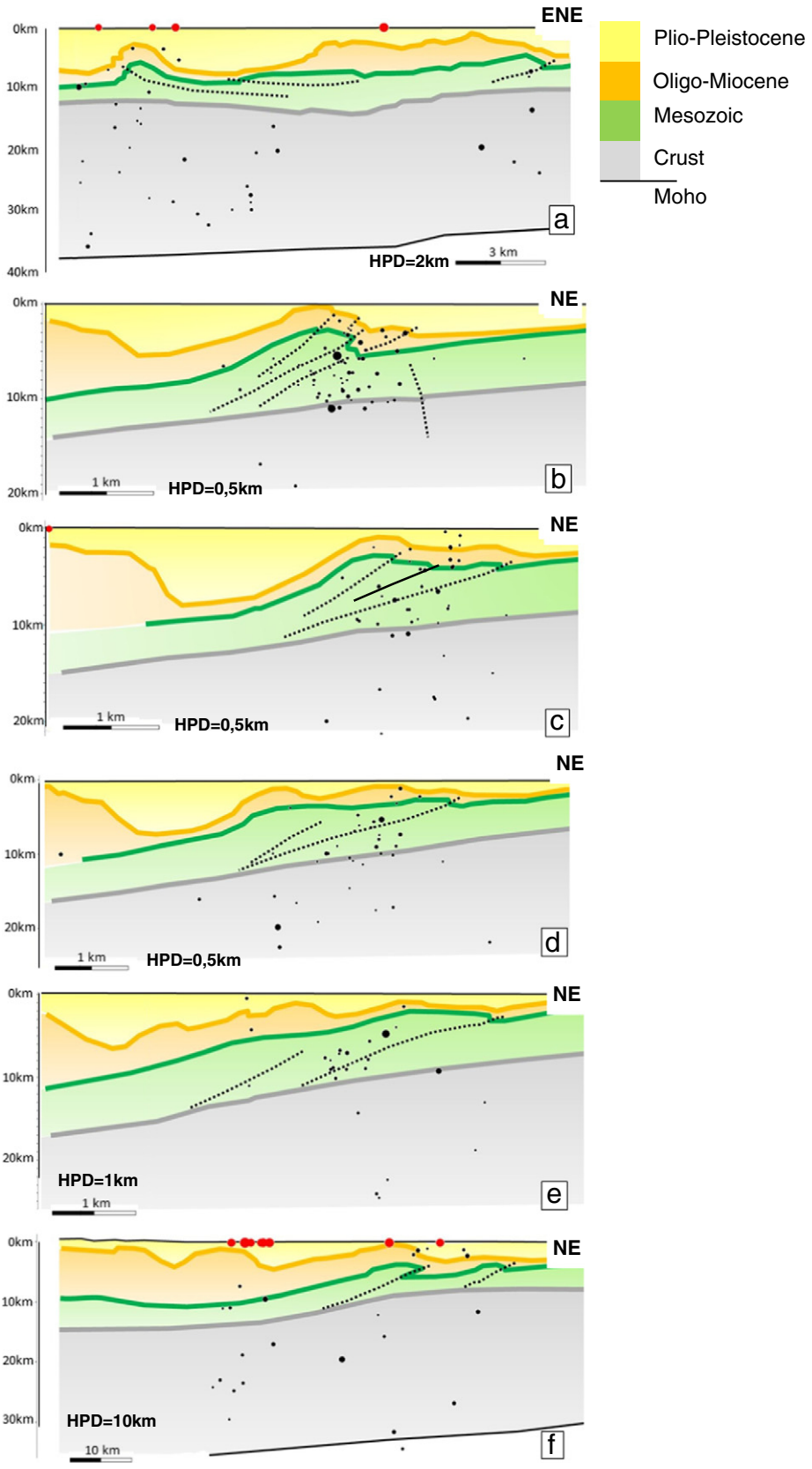

Fig. 12. Seismo-tectonic sections sliced across the 3D volume (location in Fig. 9b) to show structure–earthquake association across the Ferrara tectonic arc; HPD = Hypocentre Projection Distance; see text for discussion.

On section 'd' (see Fig. 10d), seismicity is weak and displays a decreasing trend from north to south of the belt. The positive correlation among instrumental hypocentres and thrusts is impressive at the deep ramp segment of the more external thrust surface. The outer and shallow thrust-anticline can be likely associated with the historical shocks (i.e. 0 m depth).

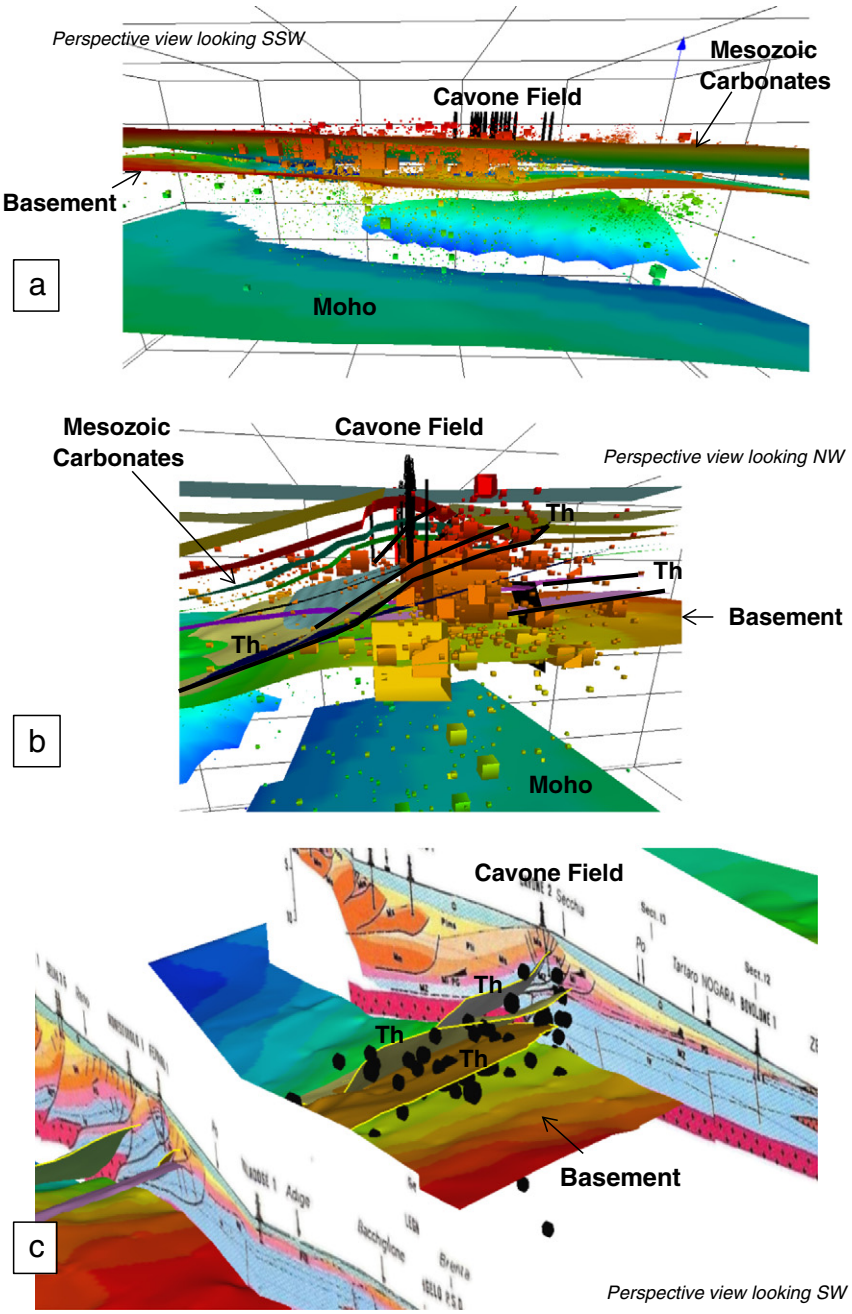

Fig. 13. 3D visualization across the Ferrara domain; a) earthquake stratigraphy, conformable with the model layers; perspective view looking SSW; b) earthquakes (cubes coloured by depth; dimension proportional to magnitude) versus folds and thrusts in the Cavone field area; perspective view looking NW. c) transfer zone, overlapping thrusts and earthquake distribution between the Cavone field and the Ferrara anticline (cross sections from Cassano et al., 1986). Perspective view looking SW; see text for discussion.

3D visualization

The seismo-tectonic pattern of the region is outstanding when observed in the 3D volume (Fig. 11). In particular, the anatomical analysis of the model confirms that the central Friuli high-density earthquake cluster:

1. is localized in the footwall of a major thrust zone whose footwall volume has been imbricated by the recent active tectonic (Fig. 11a)
2. is related to the interference between Alpine and Dinaric structures and the derived overlapping thrust surfaces (Fig. 11b), those being locally active during the 'same' geological interval (i.e. the Alps and the Dinarides are active belts at present).

5.4.2. The Ferrara domain

This domain is located at the front of the eastern sector of the Northern Apennines, in the Ferrara arc (Fig. 9c; see also Fig. 5). Structures refer to thrust folds, displaced towards the NE and deforming both the Mesozoic and Cenozoic deposits (e.g. Turrini et al., 2014 and references therein). The structural style is debated yet major evidence supports mainly thin-skinned tectonics with some partial/local involvement of the basement. Nevertheless, a conclusive thin–thick skinned tectonics can now be admitted, resulting from the interference between possible Mesozoic extensional faults (approximately N–S oriented; Turrini et al., 2014) and Cenozoic thrusts, WNW–ESE oriented. From top to bottom, the rock package refers to Cenozoic terrigenous successions, Mesozoic

carbonates and metamorphic basement (Cassano et al., 1986). An important detachment level made up of evaporite (Burano Formation) enhances the mechanical decoupling between the basement and the Meso–Cenozoic package (e.g. Cassano et al., 1986). Conclusively, the interaction among faults (normal and reverse), mechanical stratigraphy and the flexure-related Pio–Pleistocene subsidence does control the present-day kinematics and mechanics of deformation across the entire domain.

The Ferrara arc is a seismically active domain as testified by the 2012 Emilia seismic sequence (Bonini et al., 2014; Govoni et al., 2014; see all references therein). Earthquakes are mainly concentrated in the west sector of the arc while they are sparse in the eastern sector (Fig. 9c). Focal mechanisms suggest compression and, locally, strike–slip deformation (see Fig. 2b). Magnitude from the available earthquake dataset is comprised between 0 and 6 (historical: 3.5–6; instrumental: 0–6). Depth of the hypocentres varies from 0 to approximately 40 km (Fig. 9d) so that both main shock and aftershock clusters occur 1) within the clastic sediments, 2) inside the Mesozoic carbonates, 3) in the basement and locally 4) below the Moho. In the area the present day tectonic behaviour is supported by the regional stress field, GPS studies, INSAR results and thrust slip analysis (Bonini et al., 2014; Govoni et al., 2014 and reference therein). Following the Mirandola recent earthquake event (29 May 2012; M = 6) the area has been monitored by the temporary seismograph net deployed by INGV (Marzorati et al., 2012). Despite the updated and the re-located hypocentre distribution, a great uncertainty still needs to be accepted about both the location of the seismogenic sources and the related thrust plane geometry.

Vertical slicing of the performed 3D model grids (horizons and faults) allowed the systematic projection of the available earthquakes to be performed on regularly spaced cross-sections and the structure–earthquake associations to be recognised (Fig. 12).

Section 'a'

This section is oriented WNW–ESE, perpendicular to the regional transport direction of structures. Earthquakes, projected from 2 km distance on the chosen vertical plane, are asymmetrically distributed. As such they occur especially in the western sector, this representing one of the lateral ramp of the Ferrara arc. The hypocentres can be observed from the Moho level to the base Pliocene horizons. They tend to disappear in the central sector of the arc. Few events appear in the eastern sector, the eastern lateral ramp domain of the Ferrara arc. On this cross-section no particular correlation can be defined between earthquakes and the faults sliced from the 3D model.

Sections 'b' to 'f'

All sections from 'b' to 'f' are oriented perpendicular to the structural geometries and parallel to the regional shortening and transport direction. Given the earthquake density and the section spacing, the hypocentre projection distance is 500 m for sections 'b', 'c' and 'd'. It is 1 km for section 'e' and 10 km for section 'f'.

On section 'b', cutting across the western Ferrara lateral ramp domain (the Cavone field area), the projected earthquakes seem to fall in the footwall of the thrust-related imbricates and they occur a) close to the basement level, b) mainly within the Mesozoic carbonate layers and c) subordinately inside the Oligo–Miocene layers. The shallower main shock and some of the minor events can be correlated with the 3D model thrusts.

The structural units are more open on section 'c' as we move away from the aforementioned lateral ramp domain. Here (the Mirandola area), the earthquakes occur around the outermost thrust fold where they locally correlate with the model frontal thrust. A few of the projected hypocentres occur across the crust below the Mesozoic. Close to the basement level a number of events rather suggest that the detachment level of the fold-and-thrust structures is seismically active, propagating the deformation towards the NE.

Section 'd' is cut near to the central sector of the Ferrara arc and close to the possible transfer zone which appears at both the 3D model Mesozoic carbonate layer and the base Pliocene one (Turrini et al., 2014). Again, like for section *c*, the earthquake events are projected around the external thrust and its footwall. The more internal structure seems not to be active. Across the basement and down to more than 20 km below sea level the hypocentres are dispersed across a large zone where, so far, no major faults have been modelled inside the 3D seismo-tectonic volume.

Section 'e' runs across the aforementioned Ferrara arc transfer zone. Structures are even more open than in section 'd'. Across the Mesozoic carbonate unit, the projected earthquakes loosely correlate with the external thrust while the internal fault appears nearly inactive. Minor hypocentres below the top basement level confirm that the crust is likely undergoing some seismogenic tectonics (Vannoli et al., 2014).

Seismicity in the eastern sector of the arc is generally sparse. As such we used only one section to represent the seismo-tectonic setting in the region. Indeed, in section 'f' the projected earthquakes are again loosely dispersed from the Moho model level to the Plio–Pleistocene sedimentary unit. While in the Meso–Cenozoic succession they do not show any obvious positive correlation with the model faults their presence and distribution below the top basement would allow active deformation to be inferred at great depth in the crust (Vannoli et al., 2014).

3D visualization

3D visualization of the Ferrara arc units can better show the complex seismo-tectonics across the region. The selected perspective views (Fig. 13)

1. confirm a possible layering of the seismicity a) close to the top basement, b) within the Mesozoic carbonate unit and c) above the base Pliocene layers of the model (Fig. 13a)
2. allow partitioning of the shocks to be observed across the faulted structures, apparently in the footwall of the major faults (Fig. 13b)
3. illustrate the distribution of the hypocentres around and across the thrust surfaces that form the tectonic stack in the western Ferrara arc (Fig. 13c). Here, as the thrusts are progressively anastomosed and tightened towards the lateral ramp domain (the Cavone field area), deformation and the associated earthquakes are transferred across the different, overlapping thrusts and the intervening rely-zones.

6. Discussion

6.1. Methodology

The first point which obviously needs to be discussed is the methodology so far used to build and analyze the performed Po Valley 3D seismo-tectonic model.

As already mentioned (Turrini et al., 2014 and Section 4) the model suffers from different types of uncertainties. Indeed, we acknowledge that it is based on public data only (*yet filtered and organized through the long experience of the authors about the region*), those being sparse and derived from various sources (i.e. *they need systematic cross-check and QC*). Also, the model covers a very large region (*from crustal to field scale*) so that it necessarily represents one solution in the possible spectrum which could be derived from the chosen model building workflow. Conclusively, errors may refer to both structure building/interpretation and earthquake parameters (*magnitude, vertical and horizontal location*).

Once those points are accepted we still need to stress that all of the model layers and the associated fault patterns are reasonably well-constrained by the collected dataset and they do show fair three-dimensional compatibility, at all scales. Hence they do represent a robust framework thanks to which the earthquake family can be analyzed while looking for the most likely interpretation, despite the complex tectonics of the region. Furthermore, starting from the current geo-volume, the 3D model can and will be continuously updated and progressively refined in more and more detail by using different software (MOVE, Kingdom; basin modelling by the Themis-Genesis

software is in progress; the magnitude volume across the whole basin has been recently built using the GOCAD software — Turrini et al., 2015).

In terms of specific earthquakes–structures integration and analysis, let us have a look at the major improvements that the performed model provides with respect to the past results.

Among the many papers that have investigated the seismo-tectonics of the Po Valley basin, none has ever represented the derived framework using a complete 3D approach. So far, the seismo-tectonic setting of the region has been essentially illustrated by maps and cross-sections. Results are that a) on map view the shallow events can drastically hide the deep ones and b) the hypocentres projected on the cross-section may easily be not representative of the cross-section tectonics. Remarkably, most of the papers use one cross-section (often modified/simplified from the literature) and the related hypocentre projection distance (HPD in Figs. 7, 8, 10, 12) is not always indicated. On those sections stratigraphy is approximated from the referenced literature (i.e. not directly tied to the well data) or completely absent. Faults are commonly represented as simple 2D segments so that their three-dimensional consistency is difficult to be checked against the earthquake occurrence.

However, we acknowledge that most of the works are particularly rich with details and measurements that, at the moment, are completely lacking from our model. It is certainly evident that the seismicity dataset that has been imported and used into/within the basin 3D geological volume is still rough and a better selection of the earthquakes can be performed as a base to the final interpretation. With that respect, the precise definition of each event in terms of the related parameters and the associated uncertainties would represent a step forwards while aiming for the *perfect* 3D seismo-tectonic modelling of the region. Furthermore, data/interpretation about the active deformation such as growth strata around the key structures, slip rate along the major thrusts, GPS analysis, focal mechanisms and geomorphological indicators (see references in Section 2 of this paper) could definitely bring to the 3D model immense benefit and improvement.

This might be the road ahead for future development and improvement of the model.

6.2. Po Valley 3D seismo-tectonics

The results from the performed 3D model confirm that the Po Valley is a geological province rather discontinuous and not-homogeneous in terms of tectonic activity. The derived associations between structures and earthquakes clearly suggest that there are regions which at present show an important seismicity (i.e. the Northern Apennines) while others appear relatively quiet, at least silent (i.e. the western Po Valley, from Milano to Torino). Further to that, regions that were silent in the past became suddenly/recently active causing great damage to the country and the population (i.e. the western sector of the Ferrara arc). Ultimately, at the same map location there are shallow portions of the crust which are seismically active whereas the corresponding deep levels appear seismically frozen (i.e. the Friuli area).

Causes of such a patchy seismo-tectonic system can be multiple as they likely refer to a) the complex geodynamics that modelled the region through time and space, b) the present fault-related tectonics, c) the inherited pre-Alpine palaeogeography and d) the region earthquake-mechanical stratigraphy.

All those elements have or should show a corresponding earthquake imprinting. Although being totally aware of the possible bias related to the data uncertainty and the complexity of the overall geodynamics, those causes are addressed here below to raise questions and discussion.

6.2.1. Earthquakes versus Po Valley geodynamics

Extension due to passive margin formation and the successive shortening due to counter-clockwise rotation of the Adria plate towards and against the Europe one are definitely the long-standing events considered as responsible for the overall Po Valley tectonics (see references in Turrini et al., 2014; Weber et al., 2010, and references therein). Such a dynamic started in Triassic time and is believed to be continuing these days. The related long standing deformation process has hypothetically been intermittent in both time and space with sudden pulses of energy relaxation especially within/across specific domains: a) around the well-known rotation pole of the Adria plate, b) above the subduction/indentation regions and c) along the possible associated transverse zones.

The junction between the Western Alps and the Northern Apennines is represented within the 3D structural model by a combination of complex deep and shallow tectonics at the extreme south-western Po Valley basin (Turrini et al., 2014). The earthquake distribution in the western Po Valley illustrates a frozen domain to the north of the Monferrato belt and a moderate active domain to the south of the Monferrato. Seismicity is increasingly more active towards the Ligurian Alps that is in the region where the possible pole of rotation for the Adria/Po Valley plate motion is inferred (Vignaroli et al., 2008).

The subduction/indentation tectonics are evidenced by the performed 3D seismo-tectonics without much of a discussion: a) at the Europe–Adria convergent boundary, the active shallow Southern Alps units float on a deep frozen Moho geometry, those two structural levels being identified by intense and nearly no earthquakes respectively (see also Castellarin et al., 2006); b) simultaneously, the present Northern Apennines seismicity confirms active deformation of the crust from the topography down to approximately 70 km of depth (see Fig. 3c). It is noteworthy to suggest that gridding of the base of the earthquake data below the central and eastern Northern Apennines results in a surface which largely corresponds to the Adria Moho layer of the 3D model. Such an envelope surface is dipping 45° below the Apennine belt yet, although such a geometry would support some subduction dynamics, the subduction type process remaining is still debatable (intra-crustal or sub-crustal; see discussion in Turrini et al., 2014).

Ultimately, the crustal transfer zones (see Vannoli et al., 2014, for previous/alternative interpretation) that would enhance the aforementioned rigid yet non-homogeneous roto-translation process, obliquely oriented to the entire Po Valley–Alps–Apennines tectonic system, can be locally illustrated by some possible structure–earthquake association. These mainly occur across the Northern Apennines belt where horizontal (NNE–SSW) and vertical hypocentre clusters are observed. On the other side of the Po Valley, the Giudicarie transverse lineament and the associated NE–SW aligned earthquake clusters are likely representing the expression of both the Adria geodynamics and the pre-Alpine palaeogeography (Castellarin and Vai, 1982).

6.2.2. Earthquakes versus Po Valley faults

Provided that better knowledge about the faults of a region means better understanding of their seismogenic potential, the faults–earthquakes issue is likely the most important from the performed 3D seismo-tectonic model.

The fault pattern supplied by the Po Valley 3D structural model contains all of the major faults which can be derived from the available subsurface literature, mainly derived from seismic interpretation and tied to the well velocities (see Turrini et al., 2014 for dataset references). As such, they should suggest reliable geometries which actively concur to define the basin tectonic architecture yet they do not necessarily suggest any active seismogenic discontinuity.

In terms of 3D faults versus earthquake distribution, the overall picture appears to support the final seismo-tectonic zonation made of active, silent and frozen domains which have been above suggested as a consequence of the Adria geodynamics:

1. The extreme western Po Valley, south and west of Milano (see Figs. 5 and 6) stands as a frozen or silent domain where faults are generally sealed by the top Messinian unconformity (Cassano et al., 1986; Pieri and Groppi, 1981). In the area, the high number of faults is remarkably in strong contrast with the apparent lack of important recent seismicity (see Figs. 5 and 6);

2. the western Po Valley domain east of Milan is a relatively active domain with low-to-moderate seismicity localized along selected faults (see Fig. 8 and text for discussion);
3. in the southern part of the eastern Po Valley, the Ferrara arc is an active-to-silent domain as we move from the NW to the SE sectors (see Figs. 5, 6, 9, 12). Faults which overlap to form the north-western lateral ramp zone of the arc account for intense seismogenic activity (see Fig. 13c), whereas the eastern sector faults are only expressed by very local/sparse seismicity;
4. in the northern part of the eastern Po Valley, the Friuli domain is definitely an active shallow domain with intensively seismogenic faults across the upper crust of the belt (Figs. 3c, 5, 6, 7d, 9a and 10).

6.3. Earthquakes and palaeogeographical framework

The extensional fault pattern of the Po Valley is made of mainly NS oriented faults and, subordinately, EW oriented ones (Turrini et al., 2014 and reference therein). On section AA1 in Fig. 8 the inversion and reactivation of pre-alpine extensional faults are clearly illustrated by two examples: the Chiari and the Lacchiarella domains. Despite the similar deformation history, the seismicity that has been recorded across the two domains is strikingly different: in the Chiari zone some of the faults appear to show weak seismicity whereas faults in the Lacchiarella area, although clearly reactivated (Fantoni et al., 2004), do not seem to correlate to the available hypocentres within the model. Given a similar orientation of the existing faults with respect to the present regional stress field direction (both approximately NS), the observed different structure–earthquake associations could be related to a) their proximity to active crustal scale lineation, b) important facies changes in the Mesozoic sediments, c) the basement architecture, and d) the interplay among a–b–c factors. In such a perspective a) faults across the Chiari structural domain would result as the most potentially seismogenic faults, those being located at the front of the Southern Alps and close to the Giudicarie crustal lineaments; b) the same Chiari faults occur at the regional platform-to-basin facies transition which separates the western Po Valley domain from the eastern one (see also Fig. 8); and

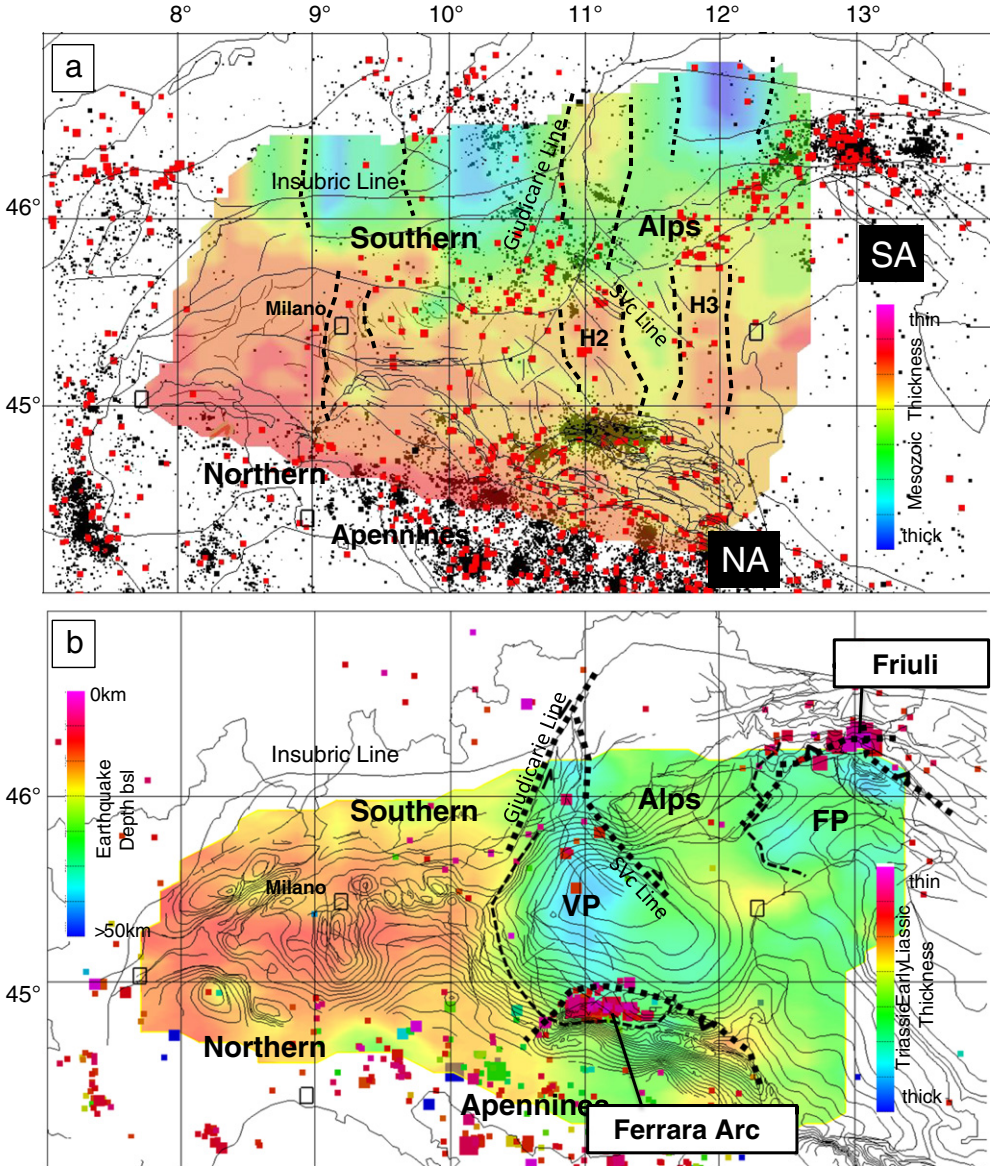

Fig. 14. a) Mesozoic isopach against present-day tectonics (compare with Figs. 1–2 and 5; SA and NA are outcropping Southern Alps and Northern Apennines thrust fronts, respectively) and all earthquakes; H1–3 are High units (see text for discussion); b) Triassic–early Liassic isopach against major earthquakes (4–7 magnitude): VP = Veneto platform carbonate domain, FP = Friuli platform carbonate domain (see text for discussion).

c) the Chiari unit evolves as a Liassic basin so that at the end of Mesozoic it defines the footwall (low-basement feature) to the Veneto basement high (see also Fig. 8).

The control of the pre-alpine structural fabric on the Po Valley seismicity observed in the Lacchiarella–Chiari region (Fig. 8), can eventually be illustrated by the correlation between the earthquake dataset and some of the 3D model isopach maps, these already presented and discussed in Turrini et al. (2014).

If we consider the Mesozoic isopach map (Fig. 14a), some of the N–S basin-and-high features (blue to red areas in the figure), mainly Jurassic in age, can be associated with the final 3D model N–S oriented earthquake trends, transversal to the main NE–SW and NW–SE oriented ones. Among them the most prominent earthquake–palaeo-structure association is definitely the Giudicarie one.

When the Triassic–Early Liassic isopach map is considered (Fig. 14b), the distribution of the platform carbonate facies seems to have a strong control on the current seismicity recorded across the Po Valley region. Indeed while the Ferrara arc seismicity appears to happen at the southern margin of the Veneto Platform, earthquakes in the Friuli region are clearly distributed along the Friuli Platform margin (Ponton, 2010).

6.4. Earthquakes and mechanical stratigraphy

Results from the performed seismo-tectonic model suggest a crustal-scale earthquakes stratigraphy (Fig. 15a) which, together with the regional mechanical stratigraphy (Fig. 15b), would control the final Po Valley structural style.

At the basin scale the derived earthquake stratigraphy shows a maximal hypocentre concentration between 0 and 13 km with a decreasing trend between 15 and 40 km depth below the sea level. When such values are compared with the regional cross-sections sliced from the model (see Figs. 7 and 8) it follows that the 0–15 km earthquake layer can be approximately related to the upper crust structures (mainly within the Mesozoic carbonate layer) with a possible preferential detachment level at about 10 km (near top of the basement?). With increasing depth, the deeper 20–35 km seismogenic layer should possibly refer to some lower crust tectonics in the foreland (see seismicity close to the Moho interface in Fig. 8) and below the Northern Apennines belt (see Fig. 3b and c).

A similar situation is revealed for both the selected Po Valley domains which have been discussed in Section 6 (Friuli and Ferrara arc). By looking at the different earthquake stratigraphy diagrams (Fig. 9b and d), seismicity is mainly localized 1) across the competent Mesozoic carbonates, 2) close to the top of the basement and subordinately 3) within the upper crust.

Following the previous considerations, we can conclude that the combination of earthquake and mechanical stratigraphy supports the structural distribution and the associated structural style that can be observed across the whole Po Valley basin (see discussion in Turrini et al., 2014). Indeed a thick–thin skinned tectonics likely fits the described earthquake-layering, so that a Po Valley seismogenic thrust surface (Fig. 15c) would progressively develop as follows:

1. nucleate along a mid-crust detachment level
2. ramp across the upper crust

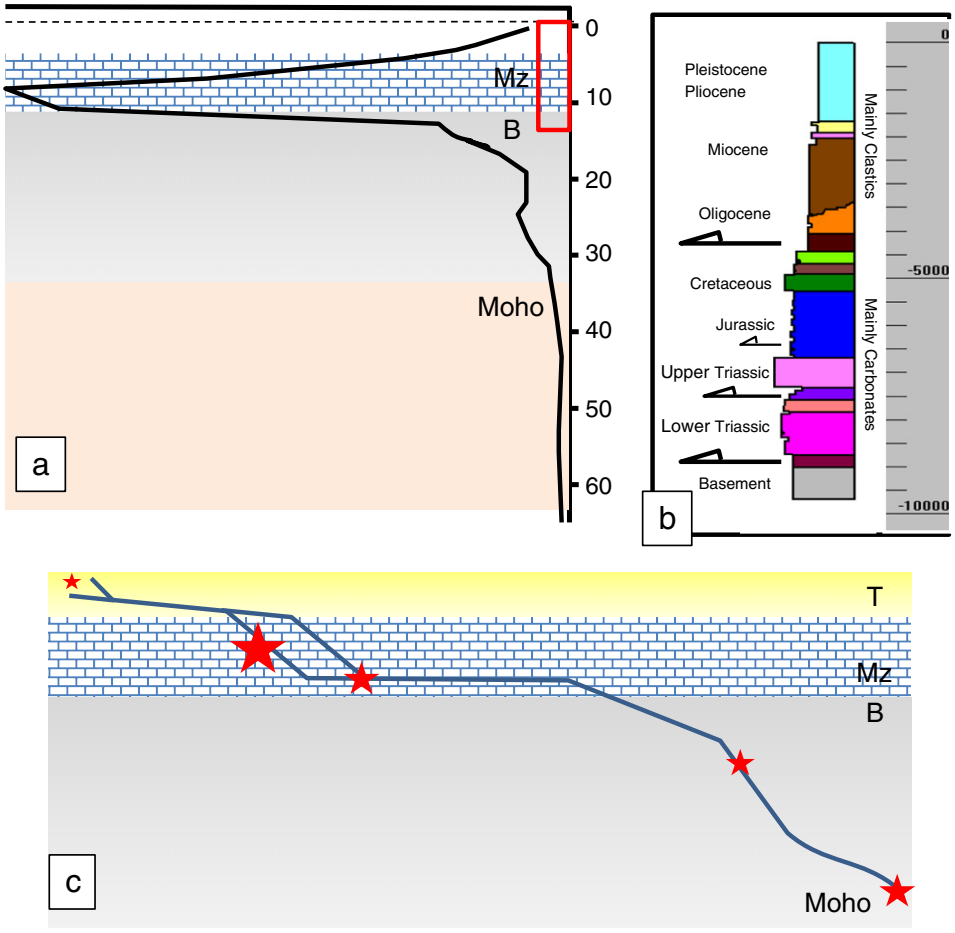

Fig. 15. Earthquake stratigraphy and mechanical stratigraphy from the Po Valley basin; a) crustal scale earthquake distribution; b) simplified mechanical stratigraphy (note detachment levels and lithology profile by qualitative strength of the different units); c) generic Po Valley thrust geometry and most likely earthquake shocks derived from this study (dimension of red star by earthquake magnitude).

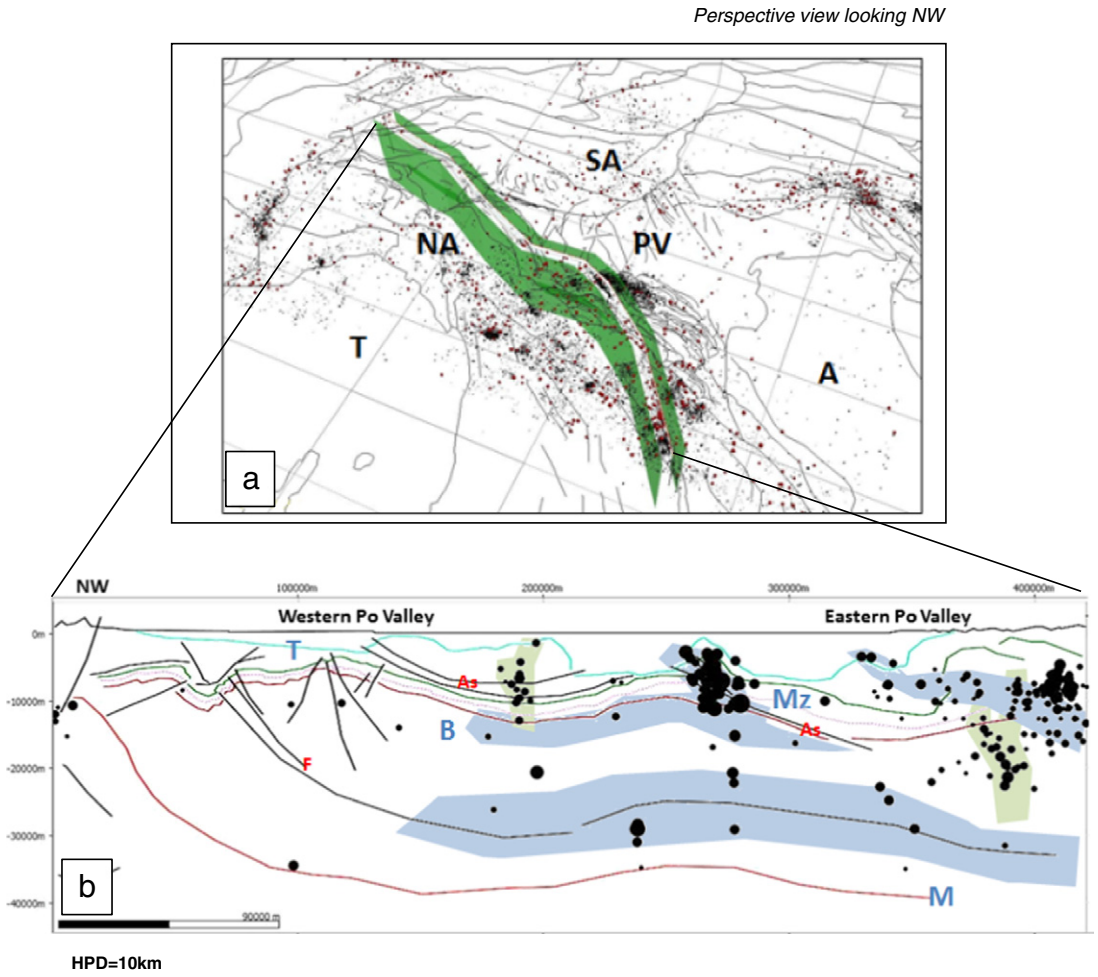

Fig. 16. Crustal section across the Po Valley and main seismogenic zones (light blue shadows). T: Tertiary sediments; Mz: Mesozoic sediments; B: basement; M: Moho. HPD = Hypocentre Projection Distance; v:h = 2.5:1.

3. flatten near the top basement interface
4. ramp again across the carbonates
5. flatten at the base of the Tertiary succession
6. ramp across the Mio–Pliocene sediments.

Depending on the available lithologies and sediment thickness (i.e. the mechanical stratigraphy) the propagating fault zones would generate major earthquake events at the various ramp-segments and minor events at the transition between the basement and the Mesozoic layer (Figs. 15c and 16). Seismicity may also occur along the flat-segments yet eventually be reduced

1. at the Upper-Triassic level (i.e. the Burano evaporites, a major detachment in the Apennines)
2. at the base of the Tertiary clastic successions where fluid overpressures are reported (Bosica and Shiner, 2013) and likely to be expected nearly all through the Po Valley basin.

Eventually, given the described palaeo-tectonics (see Fig. 14) the fault zone geometry may deviate in both the horizontal and vertical directions.

7. Conclusions

The integration of the Po Valley 3D structural model (Turrini et al., 2014) with the earthquake data available from the INGV catalogues resulted in a comprehensive and unique 3D seismo-tectonic geo-volume of the region.

Nevertheless, given the final uncertainty, extreme caution needs to be considered in the definition of the possible structure–earthquake associations, being that uncertainty greater as investigation is performed across restricted structural domains.

Despite any uncertainty, the 3D model has been proven to be a valuable and reliable tool particularly in the rendering and evaluation of the Po Valley crustal scale seismo-tectonic template. Indeed, it confirmed that the major tectonic features around the region do account for the strongest earthquake events recorded by the INGV catalogues. In that respect, the seismicity localized by a) the Southern Alps shallow units and their thrust front from Milano to the Friuli area, b) the Northern Apennines belt in their crustal roots (down to 70 km) and at their burial front (e.g. the Ferrara domain), and c) the reactivated Giudicarie palaeo-lineament, is revealed with great evidence by the performed perspective analysis.

Furthermore the reconstructed crustal framework also suggests that there might exist an earthquake-stratigraphy where the Moho, the top basement and the Mesozoic package seem to better concentrate the seismic activity. Such an earthquake stratigraphy works with the well-known Po Valley mechanical stratigraphy to develop the final variable structural style.

At the scale of some selected domains, the 3D model looks more capable than the previous 2D investigations to illustrate the complex structures that have been likely responsible for strong earthquakes: a) the active interference between Alpine and Dinaric structures in the Friuli area, in the footwall of the regional Valsugana fault zone, and b)

the relay zones among the en-echelon thrust planes in the Cavone region, are clear examples of such a situation.

Ultimately and notwithstanding, the model seems to suggest that the Mesozoic (pre-Alpine) litho-stratigraphy and the related fault pattern are the most likely key elements in controlling the major structure–earthquake associations in the region. In particular it seems interesting to note that important facies and thickness changes in the Mesozoic sediment distribution could eventually trigger medium-to-strong earthquake events more efficiently than pre-existing faults.

Future updating and improving of the model may rely on more refined selection of the earthquake data, integration of geomorphological interpretation, detailed analysis about the syn-tectonic growth of the identifiable seismogenic structures, and new software applications for an alternative elaboration of the earthquake dataset.

Acknowledgements

Giovanni Toscani, Peter Shiner, two anonymous reviewers and, in particular, Pierfrancesco Burrato are kindly acknowledged for reviewing and actively concurring to the improvement of this paper.

References

Ahmad, M.I., Dubey, A.K., Toscani, G., Bonini, L., Seno, S., 2014. Kinematic evolution of thrusts wedge and erratic line length balancing: insights from deformed sandbox models. Int. J. Earth Sci. (Geol. Rundsch.) 133, 329–347. http://dx.doi.org/10.1007/s00531-013-0947-8.

Argnani, A., Ricci Lucchi, F., 2001. Tertiary silicoclastic turbidite systems of the Northern Apennines. In: Vai, G.B., Martini, I.P. (Eds.), Anatomy of an Orogen: The Apennines and Adjacent Mediterranean Basins. Kluwer Academic Publishers, pp. 327–350.

Barba, S., Finocchio, D., Sikdar, E., Burrato, P., 2013. Modelling the interseismic deformation of a thrust system: seismogenic potential of the Southern Alps. Terra Nova http://dx.doi.org/10.1111/ter.12026.

Bartolini, C., Caputo, R., Pieri, M., 1996. Pliocene–Quaternary sedimentation in the Northern Apennine Foredeep and related denudation. Geol. Mag. 133, 255–273. http://dx.doi.org/10.1017/S0016756800009006.

Basili, R., Valensise, G., Vannoli, P., Burrato, P., Fracassi, U., Mariano, S., Tiberti, M., Boschi, E., 2008. The Database of Individual Seismogenic Sources (DISS), version 3: summarizing 20 years of research on Italy's earthquake geology. Tectonophysics 453, 20–24.

Bechtold, M., Battaglia, M., Tanner, D.C., Zuliani, D., 2009. Constraints on the active tectonics of the Friuli/NW Slovenia area from CGPS measurements and three-dimensional kinematic modeling. J. Geophys. Res. 114, B03408. http://dx.doi.org/10.1029/2008JB005638.

Bello, M., Fantoni, R., 2002. Deep oil plays in the Po Valley: deformation and hydrocarbon generation in a deformed foreland. AAPG Hedberg Conference, "Deformation History, Fluid Flow Reconstruction and Reservoir Appraisal in Foreland Fold and Thrust Belts" May 14–18, Abstract Book, 1–4 (http://www.searchanddiscovery.com/documents/2003/bello/images/bello.pdf).

Benedetti, L.C., Tapponnier, P., Gaudemer, Y., Manighetti, I., Van der Woerd, J., 2003. Geomorphic evidence for an emergent active thrust along the edge of the Po Plain: the Broni–Stradella fault. J. Geophys. Res. 108 (B5), 2238. http://dx.doi.org/10.1029/2001JB001546.

Berg, R.C., Russell, H., Thorleifson, L.H. (Eds.), 2004. Three-dimensional Geological Mapping for Groundwater Applications — Workshop. Extended Abstracts, Illinois State Geological Survey. Open-File Series 2004–8 (http://library.isgs.uiuc.edu/Pubs/pdfs/ofs/2009/ofs2009-04.pdf).

Bertotti, G., Picotti, V., Bernoulli, D., Castellarin, A., 1993. From rifting to drifting: tectonic evolution of the South-Alpine upper crust from the Triassic to the Early Cretaceous. Sediment. Geol. 86, 53–76.

Bertotti, G., Capozzi, R., Picotti, V., 1997. Extension controls Quaternary tectonics, geomorphology and sedimentations of the N-Apennines foothills and adjacent Po Plain (Italy). Tectonophysics 282, 291–301.

Bignami, C., Burrato, P., Cannelli, V., Chini, M., Falcucci, E., Ferretti, A., Gori, S., Kyriakopoulos, C., Melini, D., Moro, M., Novali, F., Saroli, M., Stramondo, S., Valensise, G., Vannoli, P., 2012. Coseismic deformation pattern of the Emilia 2012 seismic sequence imaged by Radarsat-1 interferometry. Ann. Geophys. 55 (4), 789–795. http://dx.doi.org/10.4401/ag6157.

Boccaletti, M., Corti, G., Martelli, L., 2011. Recent and active tectonics of the external zone of the Northern Apennines (Italy). Int. J. Earth Sci. 100, 1331–1348. http://dx.doi.org/10.1007/s00531-010-0545-y.

Bongiorni, D., 1987. La ricerca di idrocarburo negli alti strutturali mesozoici della Pianura Padana: l'esempio di Gaggiano. Atti Tic Sci. Terra XXXI, 125–141.

Bonini, L., Toscani, G., Seno, S., 2014. Three-dimensional segmentation and different rupture behavior during the 2012 Emilia seismic sequence (Northern Italy). Tectonophysics 630, 33–42.

Bosica, B., Shiner, P., 2013. Petroleum systems and Miocene turbidites leads in the Western Po Valley". 11th Offshore Mediterranean Conference and Exhibition. Ravenna, Italy March 20-22, 2013.

Bresciani, I., Perotti, C.R., 2014. An active deformation structure in the Po Plain (N. Italy): the Romanengo anticline. American Geophysical Union http://dx.doi.org/10.1002/2013TC003422.

Bressan, G., De Franco, R., Gentile, F., 1992. Seismotectonic study of the Friuli (Italy) area based on tomographic inversion and geophysical data. Tectonophysics 207, 383–400.

Bressan, G., Snidarcig, A., Venturini, C., 1998. Present state of tectonic stress of the Friuli area (eastern Southern Alps). Tectonophysics 292, 211–227.

Bressan, G., Bragato, L.P., Venturini, C., 2003. Stress and strain tensors based on focal mechanisms in the seismotectonic framework of the Friuli-Venezia Giulia region (Northeastern Italy). Bull. Seismol. Soc. Am. 93 (3), 1280–1297.

Burrato, P., Ciucci, F., Valensise, G., 2003. An inventory of river anomalies in the Po Plain, Northern Italy: evidence for active blind thrust faulting. Ann. Geophys. 46 (5), 865–882.

Burrato, P., Poli, M.E., Vannoli, P., Zanferrari, A., Basili, R., Galadini, F., 2008. Sources of Mw 5+ earthquakes in northeastern Italy and western Slovenia: an updated view based on geological and seismological evidence. Tectonophysics 453, 157–176.

Burrato, P., Maesano, F.E., D'Ambrogi, C., Toscani, G., Valensise, G., 2012. From drawing anticline axes to 3D modelling of seismogenic sources: evolution of seismotectonic mapping in the Po Plain. 7° EUropean Congress on REgional GEOscientific Cartography and Information Systems (EUREGEO), 12–15 June 2012, Bologna (Available from: http://ambiente.regione.emilia-romagna.it/geologia-en/temi/euregeo2012/presentations/09_Burrato_etal_Euregeo.pdf).

Burrato, P., D'Ambrogi, C., Maesano, F.E., Toscani, G., 2014. Regional earthquake source model of the Po Plain based on full 3D definition of active faults. GeolMol Mid-term Conference, Montanuniversität Leoben, 5–6 June, 2014.

Carannante, S., Argnani, A., Augliera, P., Cattaneo, M., D'Alema, E., Franceschina, G., Lovati, S., Massa, M., Monachesi, G., Moretti, M., 2014. Risultati da Progetto Sismologico S1 (INGV-DPC 2013) Base-knowledge improvement for assessing the seismogenic potential of Italy Section n: D18/b2 Relocated seismicity in the Po Plain. Workshop Terremoto Emilia 2012, Roma 26 Maggio 201.

Carena, S., Suppe, J., Kao, H., 2002. Active detachment of Taiwan illuminated by small earthquakes and its control of first-order topography. Geology 30 (10), 935–938.

Carminati, E., Doglioni, C., 2012. Alps vs. Apennines: the paradigm of a tectonically asymmetric Earth. Earth Sci. Rev. 112, 67–96.

Carminati, E., Enzi, S., Camuffo, D., 2007. A study on the effects of seismicity on subsidence in foreland basins: an application to the Venice area. Glob. Planet. Chang. 55, 237–250.

Carminati, E., Scrocca, D., Doglioni, C., 2010. Compaction-induced stress variations with depth in an active anticline: Northern Apennines, Italy. J. Geophys. Res. 115, B02401. http://dx.doi.org/10.1029/2009JB006395.

Carulli, G.B., Ponton, M., 1992. Interpretazione strutturale profonda del settore centrale Carnico-Friulano. Studi Geol. Camerti 275–284 (Special Volume, CROP 1-1A).

Casero, P., Rigamonti, A., Iocca, M., 1990. Paleogeographic relationship during Cretaceous between the Northern Adriatic area and the Eastern Southern Alps. Mem. Soc. Geol. Ital. 45, 807–814.

Cassano, E., Anelli, L., Fichera, R., Cappelli, V., 1986. Pianura Padana, interpretazione integrata di dati Geofisici e Geologici. 73° congresso Soc. Geol. It., Roma.

Cassola, T., Battaglia, M., Doglioni, C., Zuliani, D., 2007. A two dimensional elastic deformation model of the strain accumulation in Friuli — Venezia Giulia (Julian Alps). Excerpt from the Proceedings of the COMSOL Users Conference 2007 Grenoble.

Castaldini, D., Panizza, M., 1991. Inventario delle faglie attive tra I fiumi Po e Piave e il lago di Como (Italia Settentrionale). Quaternario 4 (2), 333–410.

Castellarin, A., 2001. Alps–Apennines and Po Plain–Frontal Apennines relationships. In: Vai, G.B., Martini, I.P. (Eds.), Anatomy of an OrogenThe Apennines and Adjacent Mediterranean Basins. Kluver, London, pp. 177–196.

Castellarin, A., Cantelli, L., 2010. Geology and evolution of the Northern Adriatic structural triangle between Alps and Apennines — Rend.Fis.Acc.Lincei, 21, (Suppl 1):S3–S14, DOI 10.1007/s12210-010-0086-0.

Castellarin, A., Vai, G.B., 1982. Introduzione alla geologia strutturale del Sudalpino. In: Castellarin, A., Vai, G.B. (Eds.), Guida alla gelogia del Sudalpino centro orientale. Guide Geol. Reg., Soc. Geol. It., pp. 1–22.

Castellarin, A., Vai, G.B., 1986. In: Wezel, F.C. (Ed.), The Origin of Arcs. Elsevier Sc. Pul., pp. 253–280.

Castellarin, A., Eva, C., Giglia, G., Vai, G.B., 1986. Analisi strutturale del Fronte Appenninico Padano. Giorn. Geol. Sez. 3° (47/1-2), 47–75.

Castellarin, A., Cantelli, L., Fesce, A.M., Mercier, J.L., Picotti, V., Pini, G.A., Prosser, G., Selli, L., 1992. Alpine compressional tectonics in the Southern Alps. Relationships with the N-Apennines. Ann. Tectonicae 6, 62–94.

Castellarin, A., Nicolich, R., Fantoni, R., Cantelli, L., Sella, M., Selli, L., 2006. Structure of the lithosphere beneath the Eastern Alps (southern sector of the TRANSALP transect). Tectonophysics 414, 259–282.

Castello, B., Selvaggi, G., Chiarabba, C., Amato, A., 2006. CSI Catalogo della sismicità italiana 1981–2002, versione 1.1. INGV-CNT, Roma. http://csi.rm.ingv.it/.

Channell, J.E.T., D'Argenio, B., Horvath, F., 1979. Adria, the African promontory, in Mesozoic Mediterranean palaeogeography. Earth Sci. Rev. 15, 213–292.

Chiarabba, C., Jovane, L., DiStefano, R., 2005. A new view of Italian seismicity using 20 years of instrumental recordings. Tectonophysics 395, 251–268.

Chiaraluce, L., Valoroso, L., Anselmi, M., Bagh, S., Chiarabba, C., 2009. A decade of passive seismic monitoring experiments with local networks in four Italian regions. Tectonophysics 476, 85–98.

Cuffaro, M., Riguzzi, F., Scrocca, D., Antonioli, F., Carminati, E., Livani, M., Doglioni, C., 2010. On the geodynamics of the northern Adriatic plate — Rend. Fis. Acc. Lincei, 21 (Suppl 1): S253–S279 DOI 10.1007/s12210-010-0098-9.

Dal Piaz, G.V., Bistacchi, A., Massironi, M., 2004. Geological outline of the Alps. Episodes 26, 175–180.

Delacou, B., Sue, C., Champagnac, J.D., Burkhard, M., 2004. Present-day geodynamics in the bend of the western and central Alps as constrained by earthquake analysis. Geophys. J. Int. 158, 753–774. http://dx.doi.org/10.1111/j.1365-246X.2004.02320.x.

Dercourt, J., Zonenshain, L.P., Ricou, L.-E., Kazmin, V.G., Le Pichon, X., Knipper, A.L., Grandjacquet, C., Sbortshikov, I.M., Geyssant, J., Lepvrier, C., Pechersky, D.H., Boulin, J., Sibuet, J.-C., Savostin, L.A., Sorokhtin, O., Westphal, M., Bazhenov, M.L., Laurer, J.P., Biju-Duval, B., 1986. Geological evolution of the Tethys belt from Atlantic to Pamirs since the Lias. Tectonophysics 123, 241–315.

Devoti, R., Esposito, A., Pietrantonio, G., Pisanil, A.R., Riguzzi, F., 2011. Evidence of large scale deformation patterns from GPS data in the Italian subduction boundary. Earth Planet. Sci. Lett. 311 (3–4), 230–241. http://dx.doi.org/10.1016/j.epsl.2011.09.034.

Dewey, J.F., Pitman, C., Ryan, B.F., Bonnin, J., 1973. Plate tectonics and the evolution of the Alpine systems. Geol. Soc. Am. Bull. 84 (3), 137–180.

Di Bucci, D., Angeloni, P., 2013. Adria seismicity and seismotectonics: review and critical discussion. Mar. Pet. Geol. 42, 182–190. http://dx.doi.org/10.1016/j.marpetgeo.2012.09.005.

Di Giovambattista, R., Tyupkin, Y., 1999. The fine structure of the dynamics of seismicity before M > 4.5 earthquakes in the area of Reggio Emilia (Northern Italy). Ann. Geofis. 42 (5).

Di Manna, P., Guerrieri, L., Piccardi, L., Vittori, E., Castaldini, D., Berlusconi, A., Bonadeo, L., Comerci, V., Ferrario, F., Gambillara, R., Livio, F., Lucarini, M., Michetti, A., 2012. Ground effects induced by the 2012 seismic sequence in Emilia: implications for seismic hazard assessment in the Po Plain. Ann. Geophys. 55, 4. http://dx.doi.org/10.4401/ag-6143.

Dischinger, J.D., Mitra, S., 2006. Three-dimensional structural model of the Painter and East Painter reservoir structures, Wyoming fold and thrust belt. AAPG Bull. 90 (8), 1171–1185.

Doglioni, C., Bosellini, A., 1987. Eoalpine and mesoalpine tectonics in the Southern Alps. Geol. Rundsch. 76 (3), 735–754.

Elter, P., Pertusati, P., 1973. Considerazioni sul limite Alpi–Appennino e sulle sue relazioni con l'arco delle Alpi occidentali. Mem. Soc. Geol. Ital. 12, 359–375.

Errico, G., Groppi, G., Savelli, S., Vaghi, G.C., 1980. Malossa Field: a deep discovery in the Po Valley, Italy. AAPG Mem. 30, 525–538.

Fantoni, R., Bersezio, R., Forcella, F., 2004. Alpine structure and deformation chronology at the Southern Alps–Po Plain border in Lombardy. Boll. Soc. Geol. Ital. 123, 463–476.

Galadini, F., Poli, M.E., Zanferrari, A., 2005. Seismogenic sources potentially responsible for earthquakes with M > 6 in the eastern Southern Alps (Thiene–Udine sector, NE Italy). Geophys. J. Int. 161, 739–762.

Gelati, R., Gnaccolini, 1982. Evoluzione tettonico-sedimentaria della zona al limite tra Alpi a Appennino tra l'inizio dell'Ologocene e il Miocene medio. Mem. Soc. Geol. Ital. 24, 183–191.

Govoni, A., Marchetti, A., De Gori, P., Di Bona, M., Lucente, F.P., Improta, L., Chiarabba, C., Nardi, A., Margheriti, L., Agostinetti, N.P., Di Giovanbattista, R., Latorre, D., Anselmi, M., Ciaccio, M.G., Moretti, M., Castellano, C., Piccinini, D., 2014. The 2012 Emilia seismic sequence (Northern Italy): imaging the thrust fault system by accurate aftershock location. Tectonophysics 622, 44–55. http://dx.doi.org/10.1016/j.tecto.2014.02.013.

Gunderson, K.L., Pazzaglia, F.J., Picotti, V., Anastasio, D.A., Kodama, K.P., Rittenour, T., Frankael, K.F., Ponza, A., Berti, C., Negri, A., Sabbatini, A., 2013. Unraveling tectonic and climatic controls on synorogenic growth strata (Northern Apennines, Italy). Geol. Soc. Am. Bull. 126 (3–4), 532–552. http://dx.doi.org/10.1130/B30902.1.

Han, J., Yeon, Y., Hyun, H., Hwang, D., 2011. 3D Geological Model of Mining Area. http://www.asiageospatialforum.org/2011/proceeding/pps/Jonggyu%20Han_AGF.pdf.

Jadoul, F., Berra, F., Frisia, S., 1992. Stratigraphic and palaeogeographic evolution of a carbonate platform in an extensional tectonic regime: the example of the Dolomia Principale in Lombardy (Italy). Riv. Ital. Paleontol. Stratigr. 98, 29–44.

Kastelich, V., Vrabek, M., Cunningnam, D., Gosar, A., 2008. Neo-alpine structural evolution and present-day tectonic activity of the Eastern Southern Alps: the case of the Ravne Fault, NW Slovenia. J. Struct. Geol. 30, 963–975.

Laubscher, H.P., 1996. Shallow and Deep Rotations in the Miocene Alps Tectonics, 15, 1022–1035.

Lindquist, S.J., 1999. Petroleum systems of the Po Basin province of northern Italy and the northern Adriatic Sea: Porto Garibaldi (biogenic), Meride/Riva di Solto (thermal), and Marnoso Arenacea (thermal). U.S. Geological Survey Open-File Report 99-50-M (19 pp., 15 figs., 3 tables).

Lindsay, M., Aillères, L., Jessell, M., de Kemp, E., Betts, P., 2012. Locating and quantifying geological uncertainty in three-dimensional models: analysis of the Gippsland Basin, southeastern Australia. Tectonophysics 546–547, 10–27. http://dx.doi.org/10.1016/j.tecto.2012.04.007.

Livio, F., Berlusconi, A., Michetti, A., Sileo, G., Zerboni, A., Trombino, L., Cremaschi, M., Mueller, K., Vittori, E., Carcano, C., Rogledi, S., 2009. Active fault-related folding in the epicentral area of the December 25, 1222 (Io = IX MCS) Brescia earthquake (Northern Italy): seismotectonic implications. Tectonophysics 476, 320–335.

Livio, F., Berlusconi, A., Zerboni, A., Trombino, L., Sileo, G., Michetti, A.M., Rodnight, E., Spötl, C., 2014. Progressive offset and surface deformation along a seismogenic blind thrust in the Po Plain foredeep (Southern Alps, Northern Italy). American Geophysical Union http://dx.doi.org/10.1002/2014JB011112.

Maesano, F., D'Ambrogi, C., Burrato, P., Toscani, G., 2010. Long-term geological slip rates of the Emilia thrust front (Northern Apennines) from 3D modelling of key buried horizons. 85° Congresso Nazionale della Società Geologica Italiana, "L'Appennino nella geologia del Mediterraneo Centrale", 6–8 September 2010, Pisa.

Maesano, F.E., D'Ambrogi, C., Burrato, P., Toscani, G., 2011. Slip-rates of the buried Northern Apennines thrust fronts from 3D modeling of key geological horizons (Po Plain, Northern Italy). VIII Forum della Federazione Italiana di Scienze della Terra, Geoitalia, 19–23 September 2011, Torino (Plio–Pleistocene only & few pseudo 3D blocks from sections).

Maesano, F.E., Toscani, G., Burrato, P., Mirabella, F., D'Ambrogi, C., Basili, R., 2013. Deriving thrust fault slip rates from geological modeling: examples from the Marche coastal and offshore contraction belt, Northern Apennines, Italy. Mar. Pet. Geol. 42, 122–134. http://dx.doi.org/10.1016/j.marpetgeo.2012.10.008.

Maesano, F.E., D'Ambrogi, C., Burrato, P., Toscani, G., 2014. Slip-rates of blind thrusts in the Po sedimentary basin (Italy). Tectonophysics 643, 8–25.

Marzorati, S., Carannante, S., Cattaneo, M., D'Alema, E., Frapiccini, M., Ladina, C., Monachesi, G., Spallarossa, D., 2012. Automated control procedures and first results from the temporary seismic monitoring of the 2012 Emilia sequence. Ann. Geophys. 55, 4. http://dx.doi.org/10.4401/ag-6116.

Mattavelli, L., Margarucci, V., 1992. Malossa Field — Italy, Po Basin. In: Foster, N.H., Beaumont, E.A. (Eds.), Treatise of Petroleum Geology, Atlas of Oil and Gas Fields, Structural Traps VII. American Association of Petroleum Geologists, Tulsa, OK, pp. 119–137.

Mattavelli, L., Novelli, L., 1987. Origin of the Po basin hydrocarbons. Mém. Soc. Géol. Fr. 151, 97–106.

Merlini, S., Doglioni, C., Fantoni, R., Ponton, M., 2002. Analisi strutturale lungo un profilo geologico tra la linea Fella Sava e l'avampaese adriatico (Friuli Venezia Giulia — Italia). Mem. Soc. Geol. Ital. 57, 293–300 (Roma).

Michetti, A.M., Giardina, F., Livio, F., Mueller, K., Serva, L., Sileo, G., Vittori, E., Devoti, R., Riguzzi, F., Carcano, C., Rogledi, S., Bonadeo, L., Brunamonte, F., Fioraso, G., 2012. Active compressional tectonics, Quaternary capable faults and the seismic landscape of the Po Plain (N Italy). Ann. Geophys. 55 (5), 969–1001. http://dx.doi.org/10.4401/ag-5462.

Mitra, S., Leslie, W., 2003. Three-dimensional structural model of the Rhourde el Baguel. AAPG Bull. 87 (2), 231–250.

Mitra, S., Figueroa, G.C., Hernandez Garcia, J., Murillo Alvarado, A., 2005. Three-dimensional structural model of the Cantarell and Sihil structures, Campeche Bay, Mexico. AAPG Bull. 89 (1), 1–26.

Mitra, S., Gonzalez, A., Hernandez Garcia, J., Kajari, G., 2007. Ek-Balam field: a structure related to multiple stages of salt tectonics and extension field, Algeria. AAPG Bull. 91 (11), 1619–1636.

Montone, P., Mariucci, M.T., Pondrelli, S., Amato, A., 2004. An improved stress map for Italy and surrounding regions (central Mediterranean). J. Geophys. Res. 109, B10410. http://dx.doi.org/10.1029/2003JB002703.

Moratto, L., Suhadolc, P., Costa, G., 2012. Finite-fault parameters of the September 1976 M > 5 aftershocks in Friuli (NE Italy). Tectonophysics 536–537, 44–60.

Mosca, P., Polino, R., Rogledi, S., Rossi, M., 2010. New data for the kinematic interpretation of the Alps–Apennines junction (Northwestern Italy). Int. J. Earth Sci. (Geol. Rundsch.) 99, 833–849. http://dx.doi.org/10.1007/s00531-009-0428-2.

Nardon, S., Marzorati, D., Bernasconi, A., Cornini, S., Gonfalini, M., Mosconi, S., Romano, A., Terdich, P., 1991. Fractured carbonate reservoir characterization and modeling a multidisciplinary case study from the Cavone oil field, Italy. First Break 9 (12), 553–565.

Nicolich, R., 2010. Geophysical investigation of the crust of the Upper Adriatic and neighbouring chains — Rend.Fis.Acc.Lincei, 21, (Suppl 1):S181–S196, DOI 10.1007/s12210-010-0093-y.

Perotti, C.R., 1991. Osservazioni sull'assetto strutturale del versante padano dell'Appennino Nord-Occidentale. Atti Tic Sci. Terra 34, 11–22.

Perotti, C.R., Vercesi, P.L., 1991. Assetto tettonico ed evoluzione strutturale recente della porzione nord-occidentale dell'Appennino Emiliano. Memorie Descrittive Carta Geologica d'Italia XLVI pp. 313–326.

Peruzza, L., Poli, M.E., Rebez, A., Renner, G., Rogledi, S., Slejko, D., Zanferrari, A., 2002. The 1976–1977 seismic sequence in Friuli: new seismotectonic aspects. Mem. Soc. Geol. Ital. 57, 391–400.

Pieri, M., 1984. Storia delle ricerche nel sottosuolo padano fino alle ricostruzioni attuali. Cento anni di geologia Italiana, Volume Giubilare, 1° Centenario della Soc. Geol. Ital. 1881–1981, Roma, pp. 155–177.

Pieri, M., Groppi, G., 1981. Subsurface geological structure of the Po Plain, Italy. Prog. Fin. Geodinamica CNR, pubbl.414 pp. 1–113.

Placer, L., 1999. Contribution to the macrotectonic subdivision of the border region between Southern Alps and External Dinarides. Geologija 41, 223–255 (Ljubljana).

Placer, L., Vrabec, M., Celarc, B., 2010. The bases for understanding of the NW Dinarides and Istria Peninsula tectonics. Geologija 53/1 55–86 Ljubljana. Contribution to the macrotectonic subdivision of the border region between Southern Alps and External Dinarides. Geologija 41, 223–255 (Ljubljana).

Poli, M.E., Peruzza, L., Rebez, A., Renner, G., Slejko, D., Zanferrari, A., 2002. New seismotectonic evidence from the analysis of the 1976–1977 and 1977–1999 seismicity in Friuli (NE Italy). Boll. Geofis. Teor. Appl. 43, 53–78 (Trieste).

Ponton, M., 2010. Architettura delle Alpi Friulane. Museo Friulano di Storia Naturale, Publ. No 52, Udine 9788888192529.

Ponza, A., Pazzaglia, F.J., Picotti, V., 2010. Thrust-fold activity at the mountain front of the Northern Apennines (Italy) from quantitative landscape analysis. Geomorphology 123, 211–231.

Ravaglia, A., Seno, S., Toscani, G., Fantoni, R., 2006. Mesozoic extension controlling the Southern Alps thrust front geometry under the Po Plain, Italy: insights from sandbox models. J. Struct. Geol. 28, 2084e2096.

Ricci Lucchi, F., 1986. The Oligocene to recent foreland basins of the northern Apennines. In: Allen, P.A., Homewood, P. (Eds.), Foreland Basins. I.A.S. Special Publication 8, pp. 105–139.

Roure, F., Polino, R., Nicolich, R., 1989. Poinçonnements, rétrocharriages et chevauchements post-basculement dans les Alpes occidentales: evolution intracontinentale d'une chaîne de collision. CR Acad. Sci. Paris 309 (II), 283–290.

Roure, F., Polino, R., Nicolich, R., 1990. Early Neogene deformation beneath the Po plain: constraints on the post-collisional Alpine evolution. In: Roure, F., Heitzmann, P., Polino, R. (Eds.), Deep structure of the Alps. Mem. Soc. Geol. France 156, pp. 309–322.

Rovida, R., Camassi, R., Gasperini, P., Stucchi, M., 2011. CPTI11, the 2011 version of the Parametric Catalogue of Italian Earthquakes, Milano, Bologna (http://emidius.mi.ingv.it/CPTI/).

Scardia, G., Festa, A., Monegato, G., Pini, R., Rogledi, S., Tremolada, F., Galadini, F., 2014. Evidences for the late Alpine tectonics in the Lake Garda area (northern Italy) and seismogenic implications. Geol. Soc. Am. Bull. 127 (1/2), 113–130. http://dx.doi.org/10.1130/B30990.1.

Schmid, S., Fugenschuh, B., Kissling, E., Schuster, R., 2004. Tectonic map and overall architecture of the Alpine orogen. Eclogae Geol. Helv. 97, 93–117.

Serpelloni, E., Anzidei, M., Baldi, P., Casula, G., Galvani, A., 2005. Crustal velocity and strain-rate fields in Italy and surrounding regions: new results from the analysis of permanent and non-permanent GPS networks. Geophys. J. Int. 161 (3), 861–880.

Serpelloni, E., Anderlini, L., Avallone, A., Cannelli, V., Cavaliere, A., Cheloni, D., D'Ambrosio, C., D'Anastasio, E., Esposito, A., Pietrantonio, G., Pisani, A.R., Anzidei, M., Cecere, G., D'Agostino, N., Del Mese, S., Devoti, R., Galvani, A., Massucci, A., Melini, D., Riguzzi, F., Selvaggi, G., Sepe, V., 2012. GPS observations of coseismic deformation following the May 20 and 29, 2012, Emilia seismic events (northern Italy): data, analysis and preliminary models. Ann. Geophys. 55, 4. http://dx.doi.org/10.4401/ag-6168.

Serpelloni, E., Faccenna, C., Spada, G., Dong, D., D. P. Williams, S., 2013. Vertical GPS ground motion rates in the Euro-Mediterranean region: new evidence of velocity gradients at different spatial scales along the Nubia–Eurasia plate boundary. J. Geophys. Res. 118, 6003–6024. http://dx.doi.org/10.1002/2013JB010102.

Shao, Y., Zheng, A., He, Y., Xiao, K., 2012. 3D geological modeling under extremely, complex geological conditions. J. Comput. 3, 699–705.

Toscani, G., Seno, S., Fantoni, R., Rogledi, S., 2006. Geometry and timing of deformation inside a structural arc: the case of the western Emilian folds (Northern Apennine front, Italy). Boll. Soc. Geol. Ital. 125, 59–65.

Toscani, G., Burrato, P., Di Bucci, D., Seno, S., Valensise, G., 2009. Plio-Quaternary tectonic evolution of the Northern Apennine thrust front (Bologna-Ferrara section, Italy): seismotectonic implications. Ital. J. Geosci. 128 (2), 605–613. http://dx.doi.org/10.3301/IJG.2009.128.2.605.

Toscani, G., Bonini, L., Ahmad, M., Di Bucci, D., Di Giulio, A., Seno, S., Galuppo, C., 2014. Opposite verging chains sharing the same foreland: kinematics and interactions through analogue models (Central Po Plain, Italy). Tectonophysics 633, 268–282. http://dx.doi.org/10.1016/j.tecto.2014.07.019.

Trumpy, R., 1973. The timing of orogenic events in the Central Alps. In: De Jong, K.A., Scholten, R. (Eds.), Gravity and Tectonics. Wiley and Sons, New York, pp. 229–251.

Turrini, C., Rennison, P., 2004. Structural style from the Southern Apennines' hydrocarbon province—an integrated view. In: McClay, K.R. (Ed.), Thrust tectonics and hydrocarbon systems. AAPG Memoir 82, pp. 558–578.

Turrini, C., Dups, K., Pullan, C., 2009. 2D and 3D structural modelling in the Swiss–French Jura Mountains. First Break 27, 65–71.

Turrini, C., Lacombe, O., Roure, F., 2014. Present-day 3D structural model of the Po Valley basin, Northern Italy. Mar. Pet. Geol. 56, 266–289.

Turrini, C., Angeloni, P., Lacombe, O., Ponton, M., Roure, F., 2015. Three-dimensional seismo-tectonics in the Po Valley basin, northern Italy. Geophysical Research Abstract, EGU, Vienna.

Valcarce, G., Zapata, T., Ansa, A., Selva, G., 2006. Three-dimensional structural modeling and its application for development of the El Porto'n field, Argentina. AAPG Bull. 90 (3), 307–319.

Vannoli, P., Burrato, P., Valensise, G., 2014. The seismotectonics of the Po Plain (Northern Italy): tectonic diversity in a blind faulting domain. Pure Appl. Geophys. 172, 1105–1142. http://dx.doi.org/10.1007/s00024-014-0873-0.

Venturini, C., 1991. Cinematica neogenico-quaternaria del sudalpino orientale (settore friulano). Studi Geol. Camerti 109–113 (vol. spec. (1990), Camerino).

ViDEPI Project http://unmig.sviluppoeconomico.gov.it/videpi/kml/webgis.asp.

Vignaroli, G., Faccenna, C., Jolivet, L., Piromallo, C., Rossetti, F., 2008. Subduction polarity reversal at the junction between the Western Alps and the Northern Apennines, Italy. Tectonophysics 450, 34–50.

Vouillamoz, N., Sue, C., Champagnac, J., Calcagno, P., 2012. 3D cartography modeling of the Alpine Arc. Tectonophysics 579, 131–143. http://dx.doi.org/10.1016/j.tecto.2012.06.012.

Weber, J., Vrabec, M., Pavlovcic-Preseren, P., Dixon, T., Jiang, Y., Stopar, R.B., 2010. GPS derived motion of the Adriatic microplate from Istria Peninsula and Po Plain sites, and geodynamic implications. Tectonophysics 483, 213–222. http://dx.doi.org/10.1016/j.tecto.2009.09.001.

IV. 3D structures & thermal history of the basin

Reviewing of the Po Valley seismicity in the light of the 3D structural model (Section III) led to a number of conclusions which, provided the cumulative uncertainty about the model geometry and the earthquake distribution, can be reasonable at the crustal scale yet debatable at the local scale.

Once the 3D seismo-tectonic model viability tested, thermal modeling of the Po Valley basin became the next exercise during the Thesis development (phase 6 in Fig.20) (Section V). The model used data taken from published literature and publically available well information as well as a limited amount of proprietary data (Petroceltic Italia).

Regardless the overall simplification, the reconstruction-simulations have provided, for the first time, the integration of the 3D structure-thermal history and the related hydrocarbon maturation-generation process across the entire Po Valley.

It is to be underlined that, while confirming some of the results from previous authors, the performed integration progressively drifted at discussing the possible role that overpressures inside the deep Mesozoic systems of the basin may have in delaying organic matter maturation.

The results from the different modeled scenarios, discussed against the observed oil field distribution, dimension and characteristics, appear to loosely support the overpressure issue yet they still leave room for future debate.

AAPG Bulletin, 2016 (under review)

V. 3D structural, petroleum and thermal modeling of Mesozoic petroleum systems in the Po Valley basin, northern Italy

Claudio Turrini (1), , Barbara Bosica (2), Paul Ryan (3), Peter Shiner (2) Olivier Lacombe (4), and François Roure (5, 6)

1. CTGeological Consulting, 78100, St.Germain-en-Laye, France
2. Petroceltic Italia, Via E.Q: Visconti 20, Roma 00193, Italy
3. Petroceltic International plc, 3 Grand Canal Plaza, Grand Canal Street Upper, Dublin 4, Ireland
4. Sorbonne Universités, UPMC Univ Paris 06, CNRS, Institut des Sciences de la Terre de Paris (iSTeP), 4 place Jussieu 75005 Paris, France
5. IFP-EN, Rueil-Malmaison, France
6. Tectonic Group, Utrecht University, the Netherlands

Abstract

1D and 3D basin modelling techniques were used to investigate the Mesozoic carbonate petroleum systems of the Po Valley basin (northern Italy), through integration of a recent 3D structural model of the study area with the distribution of potential Triassic source rocks, and rock property and heat flow models derived from the literature.

Results from standard 1D maturity models show significant over-prediction of the thermal maturity of deep Triassic carbonates in the western Po Valley, unless the effect of the substantial overpressure observed in these sequences is incorporated into the model. In order to test this observation further, two thermal scenarios were applied to the Po Valley 3D geo-volume: one based on the geological heat flow and a second model based on a reduced heat flow as a proxy for the retarding effect of overpressure on hydrocarbon maturation. The results of these 2 models were then compared with the observed hydrocarbon distribution in the western Po Valley and they suggest that:

1. both the aforementioned scenarios are broadly consistent with the observed hydrocarbon distribution,
2. the overpressure model seems to provide a better match between: a) the predicted charge available from the kitchen areas post critical moment and observed

volumes of hydrocarbons initially in place within the traps; b) observed and predicted hydrocarbon phase, as measured by GOR,

3. overpressure appears to have significantly retarded hydrocarbon maturation in the western domain of the basin, thus confirming results from previous authors.

Despite the relative simplicity and inherent uncertainties of the adopted approach, the models provide for the first time a unique integration in 3D of the thermo-structural history and the related hydrocarbon maturation-generation process across the entire Po Valley.

Key-words: 3D models, thermal maturity, Po Valley tectonics and hydrocarbons, overpressures, Northern Italy.

1. Introduction and objectives

The Po Valley (Northern Italy) (Fig.1a) is the foreland-foredeep basin of the Southern Alps and the Northern Apennines thrust-belts and forms one of the best known hydrocarbon provinces in continental Europe (Errico et al., 1980; Pieri & Groppi, 1981; Pieri, 1984; Cassano et al., 1986; Riva et al., 1986; Bongiorni, 1987; Mattavelli & Novelli, 1987; Nardon et al., 1991; Mattavelli & Margarucci, 1992; Mattavelli et al., 1993; Lindquist, 1999; Casero, 2004; Bertello et al., 2010). The basin stratigraphy consists of a thick carbonate-clastic sedimentary section, with both oil and gas having been produced from different levels across the basin: the deep Mesozoic carbonates represent the preferential target for oil exploration whereas the clastic intervals of Miocene, Pliocene and Pleistocene age are principally drilled for shallow gas accumulations.

Despite the long history of exploration-production activity and the progressive data and knowledge acquired from both academia and industry, the thermal history of the Po Valley region has, until present, been little documented in the public literature (Wygrala, 1988; Chiaramonte & Novelli, 1986), which has focused primarily on the temperature evolution of similar units cropping out in the adjacent Southern Alps fold-and-thrust units instead (Bersezio & Bellantani, 1997; Greber et al., 1997; Calabro' et al., 2003; Fantoni & Scotti, 2003; Scotti, 2005; Carminati et al., 2010).

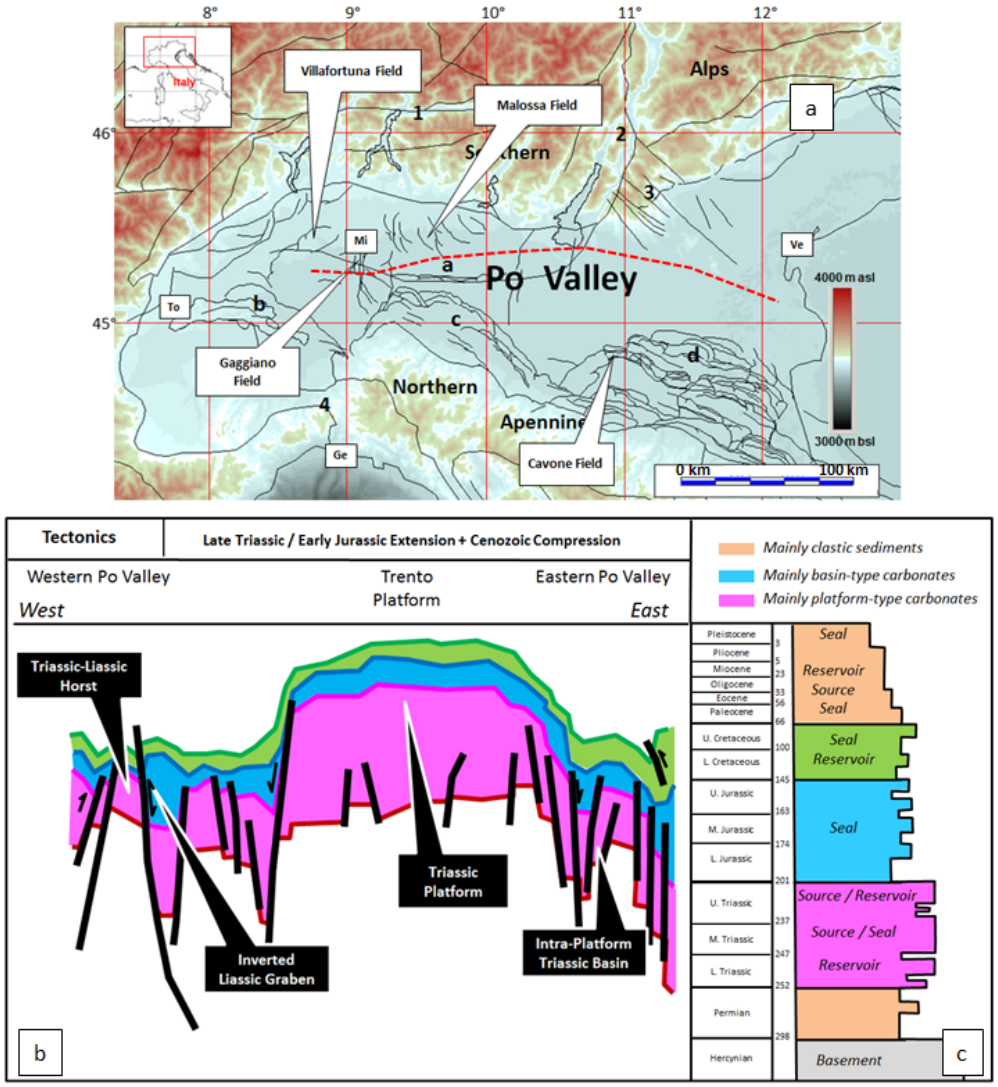

Fig.1 – Regional setting, tectono-stratigraphic framework and petroleum system in/around the Po Valley basin: a) location map of the study area (purple stippled line) and major oil fields at Mesozoic level; a=Milan tectonic arc, b=Monferrato arc, c= Emilia arc, d=Ferrara arc; 1 = Insubric lines, 2=Giudicarie line, 3=Schio-Vicenza line, 4=Sestri-Voltaggio line; b) Structural cross section (red dashed line) through study area showing present day geometries of main structural elements; c) major stratigraphic units and the related hydrocarbon distribution.

As a development of and further application of the 3D structural model of Turrini et al. (2014; 2015), this work considers the 1D and 3D thermal modelling of the entire Po Valley basin, with particular focus on the proven, deep Mesozoic petroleum system. In particular, the aim of this paper is to model and review: a) the trap formation across the Po Valley foreland-foredeep domain, b) the progressive maturation and generation history of the known Triassic

petroleum source rocks, c) the present-day pressure regime and investigate the possible impact of overpressure on hydrocarbon maturation.

2. The Po Valley basin

2.1 Regional framework

The framework to the Po Valley basin has been recently discussed by many papers which cover the different geological aspects of the region (see Turrini et al., 2014, 2015 and references therein). Given this extensive recent literature, only a short summary will be provided hereafter.

The region was affected by repeated extensional and compressional events throughout the Mesozoic and Cenozoic (Fig.1b). These events essentially relate to the long-lasting geodynamic context that produced rifting, drifting, subduction and collision of the Adria and Eurasian plates (Dewey et al., 1973; Castellarin, 2001; Carminati & Doglioni, 2010; Pfiffner, 2014 and references therein). The present-day structural pattern is primarily the result of weak to moderate Cenozoic thrusting of both the Tertiary and the Mesozoic sediments (Pieri & Groppi, 1981; Bongiorni, 1986; Cassano et al., 1986; Castellarin et al., 1985; Fantoni et al., 2004, Ravaglia et al., 2006; Fantoni & Franciosi, 2010; Turrini et al., 2014 and reference therein). While the calculated displacement along faults ranges between 0.5 and 5 km, a large part of the basin substratum shows evidence of the pre-compressional tectonic grain, with autochthonous highs and lows of clearly extension-related origin, partially reactivated by compression. Overprinting of the extension-related structures (approximately North-trending) by the compression-related ones (generically West-trending) resulted in the current crustal-scale interference pattern in which both active and non-active structures can be observed, the former being identified by the present-day earthquake-structure association (Michetti et al., 2013; Vannoli et al., 2014; Turrini et al., 2015 and references therein). The involvement of the basement in the compressional structures of the western domain is proven by both well and seismic data, whilst it is still the subject of debate in the eastern domain (see discussion in Turrini et al., 2014).

The main stratigraphic units across the basin are Triassic platform carbonates, Jurassic to Cretaceous platform and basinal carbonates, overlain by Tertiary clastics (Fig.1c) (Jadoul et

al., 1986; Cati et al., 1987; Jadoul et al., 1992; De Zanche et al., 2000; Ghielmi et al., 2012; Masetti et al., 2012; Pfiffner, 2014). This sedimentary package overlies some possible Permian and the Hercynian metamorphic basement (Fig.1c) which has been drilled by a few wells inside the basin and locally crops out in the hinterland of the Southern Alps (Cassano et al., 1986; Ponton, 2010; Pfiffner, 2014).

2.2 Exploration

Exploration for hydrocarbons in the Po Valley started in the first half of the 20th century (Pieri, 1984). Following the concepts illustrated by Porro (1927) who argued that the Po Valley was underlain by gentle fold structures made up of Oligo-Miocene sediments at the front of the Northern Apennines belt, Agip (now ENI) performed the first gravimetric acquisition across the southern sector of the basin. This resulted in the initial definition of the anticline-syncline geometries that would become recognized, with further data acquisition, as the buried front of the Northern Apennines, namely the Emilia and the Ferrara tectonic arcs (Pieri & Groppi, 1981). Subsequent exploration wells drilled through a thin Pliocene sequence, underlain by Oligo-Miocene sediments and locally reached the Cretaceous without encountering any evidence of hydrocarbons. Soon after the 2nd world war, exploration progressively covered the north-east of the basin and the use of electric logs and cores, the development of micro-palaeontological techniques and, especially, the acquisition of analogue seismic data enabled the recognition and understanding of deeper targets. This resulted in the drilling, to the east of Milano, of the Caviaga 1 well, (1944; 1404 m bsl), the first gas field discovered within the Po Valley and the largest in Western Europe at that time. Between 1945 and 1982, Agip acquired 50.000 km of 2D seismic data across the basin. In particular the new digital recordings allowed the very deep horizons to be imaged while also favouring the development of new hypotheses concerning deep lithologies and their associated rock properties. In the 1980s, new methodologies led to the detailed analysis of the seismo-stratigraphy and the associated tectonic pattern of the basin. The integration of well correlations with seismic interpretation resulted in the reconstruction of the regional base-Pliocene structural map by Pieri & Groppi (1981) which, even today, remains an essential reference for any geological project inside the basin. From 1973 to 1984, hydrocarbon exploration of the Mesozoic carbonates developed through two different phases (Bongiorni, 1987; Bertello et al., 2010). The first phase targeted overthrust structures developed during Alpine orogenesis, whilst the second one led to the investigation and drilling of Mesozoic

structural highs formed by Liassic rifting. Both phases proved to be successful and led to the discovery of four major hydrocarbon fields, namely the Malossa (gas condensate), Cavone, Gaggiano and Villafortuna (all oil) fields. The latter is one of the largest oil fields in continental Europe and has produced, so far, 226 MMbbl of light oil from a record depth of 6000 m below the mean sea level. These discoveries allowed the definition of the different petroleum systems and enhanced understanding of the key elements of each of the play systems (Mattavelli et al., 1987; Bertello et al., 2010). The opening of the basin to foreign exploration companies in the early 1990s led to increased interest in the remaining potential of the area (Rigo, 1991). Today the Po Valley stands as an underexplored region ready for the next exploration phase, based on exploitation of new technologies and the increased knowledge of the basin geology.

2.3 Hydrocarbon systems and hydrocarbon distribution

The hydrocarbon distribution in the Po Valley is complex: oil and gas condensate occurs in the deep Mesozoic carbonates, whereas thermogenic gas is found in former, currently allochthonous terrigenous Oligo-Miocene flexural sequences, and biogenic gas occurs in still autochthonous terrigenous Plio-Pleistocene flexural sequences (Mattavelli et al., 1987; Lindquist, 1999; Casero, 2004; Bertello et al., 2010). This hydrocarbon distribution suggests the presence of numerous, distinct petroleum systems which drilling, outcrop geology and systematic analysis of the associated oil and gas types have progressively identified and defined (Riva et al., 1986; Bongiorni, 1987; Mattavelli et al., 1987, 1993; Wygrala, 1988; Lindquist, 1999; Bello & Fantoni, 2002; Franciosi & Vignolo, 2002; Casero, 2004; Bertello et al., 2010).

The Triassic-Liassic petroleum systems have produced gas, condensate and light oil from Mesozoic carbonates. The reservoir consists of dolomitized carbonate platform units of Mid Triassic–Early Jurassic age charged by Middle to Late Triassic carbonate source rocks deposited in intra-platform lagoons and basins. Traps are mostly provided by Mesozoic structures locally inverted by the Cenozoic compression. The Cretaceous-Jurassic pelagic carbonates provide the seal for the accumulations. The Villafortuna-Trecate Field (discovered 1984; light oil; 226 MMbbl of 43° API oil and 93 bcf gas produced to date), represents the largest oil accumulation pertaining to this play (Bello & Fantoni 2002; Bertello et al., 2010). Second-order oil fields in terms of both dimension and production are the Malossa field

(discovered 1973; gas and condensate; approximately 27 MMbbl and 150 bcf gas produced) (Errico et al., 1980; Pieri & Groppi, 1981; Mattavelli & Margarucci, 1992), the Cavone field (discovered 1974; 23°API oil; 94,5 MMbbl hydrocarbons initially in place (HCIIP)) (Nardon et al., 1991) and the Gaggiano field (discovered 1982; 36°API oil; 20-30 MMbbl estimated reserves) (Bongiorni, 1987; Rigo 1991; Fantoni et al., 2004).

The Oligo-Miocene petroleum system produces thermogenic gas with secondary quantities of oil from the foredeep successions belonging to the Northern Apennine foredeep (Mattavelli et al., 1987, 1993; Bertello et al., 2010). The system is made of thick turbidite sequences that supply the reservoir, source and seal elements and the traps are usually structural, with the Cortemaggiore and Casteggio fields providing typical examples of producing fields belonging to this petroleum system.

The Plio-Pleistocene petroleum system contains large quantities of biogenic gas, notably at the buried external fronts of the Apennine thrust belt (Bertello et al., 2010 and references therein). The system consists of sand-rich turbidites within which thick-bedded sand lobes and thin-bedded, fine-grained basin plain/lobe fringe deposits are the main reservoir facies associations (Ghielmi et al. 2012). Interbedded clays are both the source-rock and the effective topseal. Traps are most commonly structural, yet stratigraphic traps also occur, mainly related to the onlap of turbidite reservoirs onto the flanks of thrust propagation folds or against the foreland ramp. The Settala field (1977) is a remarkable example of a mixed structural–stratigraphic trap in the Plio-Pleistocene play (Bertello et al., 2010).

The 3D basin model discussed in this paper addresses the burial and temperature history of the thermogenic Mesozoic petroleum system. Investigation of the Plio-Pleistocene and Oligo-Miocene systems is beyond the scope of this paper.

3. Data & workflow

Data used for the 3D structural model come from public literature and the archives of the Italian Ministry of Energy (http://unmig.sviluppoeconomico.gov.it, namely the ViDEPI project). These data include geological cross-sections, well composite logs, geophysical and geological maps. No seismic data have been used during the model building process. A full description of the whole dataset, and its distribution across the basin, is provided in Turrini et al. (2014 and 2015).

The structural model was built using Midland Valley's MOVE software (http://www.mve.com/) while progressive refinement of the 3D grids and faults was carried out using IHS's Kingdom interpretation package (https://www.ihs.com/products/kingdom-seismic-geological-interpretation-software.html).

It should be stressed that the area of interest for the present study is strictly limited to the Northern Apennines and Southern Alps foreland domain in order to exclude major tectonic over-thickening across the Mesozoic structures that would have biased the thermal modelling results (see white stippled line in Fig.2).

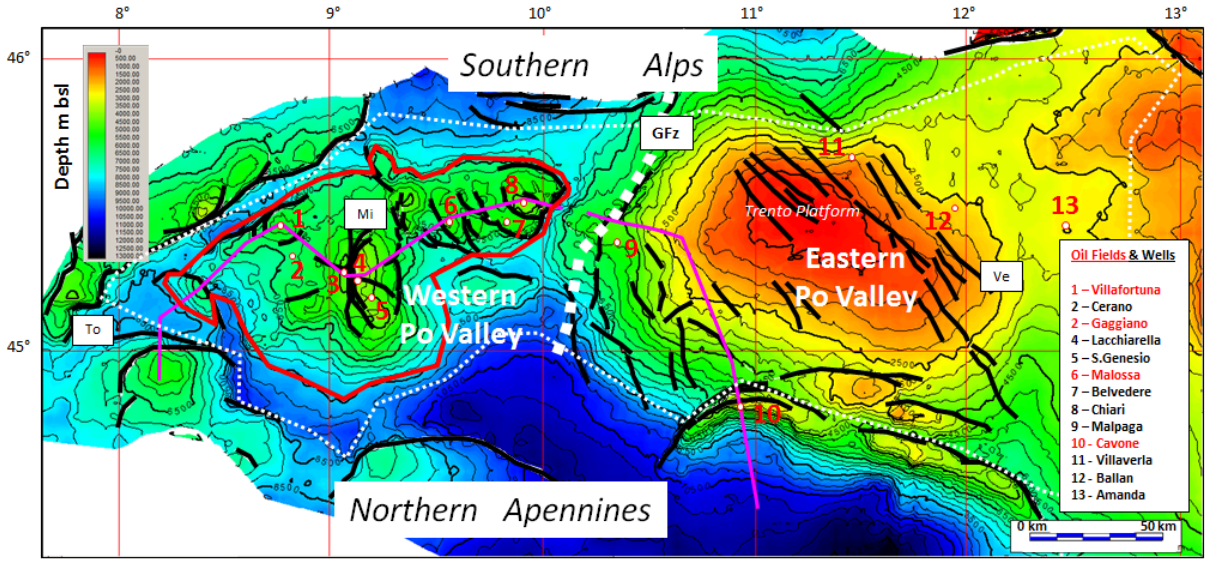

Fig.2 – Grid showing depth to Top Mesozoic Carbonates (referenced to mean sea level, contouring every 500 m; fault polygons in white); 1-4 = major oil fields. Purple lines show the location of the cross-sections in figure 3. GFz = Giudicarie Fault zone trend line (thick stippled line) separating the Eastern domain from the Western one; thin stippled white line shows the area covered by the basin modelling study described in this paper; bold red line is overpressure cell from Chiaramonte & Novelli (1986); Major cities: Mi = Milano, To = Torino, Ge = Genova, Ve = Venezia.

Data used for the basin modelling aspects of this study (back-stripping and thermal parameters, temperature and heat flow data, palaeo-water depths, TOC, HI values, etc.) are taken from published literature and publically available well data (Riva et al., 1986; Mattavelli & Novelli, 1987; Wygrala, 1988; Fantoni & Scotti, 2003, ViDEPI Project) as well as a limited amount of proprietary data. Modelling was carried out using Zetaware Inc.'s Genesis & Trinity 3D software packages (http://www.zetaware.com/) and proprietary

spreadsheets. The basin modelling workflow for this study consisted of three phases, described more fully in subsequent sections of this paper:

Phase1 – 1D model building

- Reference well and pseudo-well chrono-litho-stratigraphy, back-stripping parameters, thermal parameters, source rock parameters, temperature and maturity data loaded into Genesis (http://www.zetaware.com/);
- Definition of geological heat flow and overpressure models, primarily based on the available literature;
- Collation of information about palaeo-water depth and palaeo-sediment/water interface temperature.

Phase 2 – 1D model calibration and outputs

- Calibration of rock property and present-day heat flow model against temperature data;
- Calibration of back-stripping and heat flow models by forward modelling of thermal maturity and comparison against available maturity data;
- 1D modelling of hydrocarbon generation from key source intervals.

Phase 3 – 3D model building & simulation

- 3D stratigraphic grids exported from the Kingdom package into the Trinity software, with additional grids generated by interpolating between imported grids as necessary, particularly to define source rock intervals;
- Further definition of source intervals within the model, including lateral distribution from gross depositional environment (GDE) maps, thickness and kerogen type as described in literature;
- Definition of 3D palaeo-temperature model by calibration against 1D models for key well and pseudo-wells;
- 3D hydrocarbon maturation/generation/migration history modelling across the Po Valley and analysis of kitchen areas associated with key traps;
- Comparison of predicted hydrocarbon distribution with observed distribution.

4. Structural & thermal model of the Po Valley basin

4.1 Structural geometries at the Mesozoic carbonate level

The Po Valley 3D structural model (Turrini et al., 2014, 2015) consists of 66 faults and 5 layer grids, namely: the Moho discontinuity, the basement, the near top Triassic, the top Mesozoic Carbonates, and the base Pliocene. At all levels within the model, the regional-scale architecture indicates the presence of two crustal domains, a western and an eastern domains separated by the Giudicarie Lineament, a NE-SW oriented trend line dissecting the basin (Fig.2). Shallow structures are folds and thrusts in the Tertiary clastic succession. Deep structures relate to faulting of the Mesozoic carbonates and their basement, with local inversion of pre-compressional basin and thin-skinned tectonic imbrication (Fig.3).

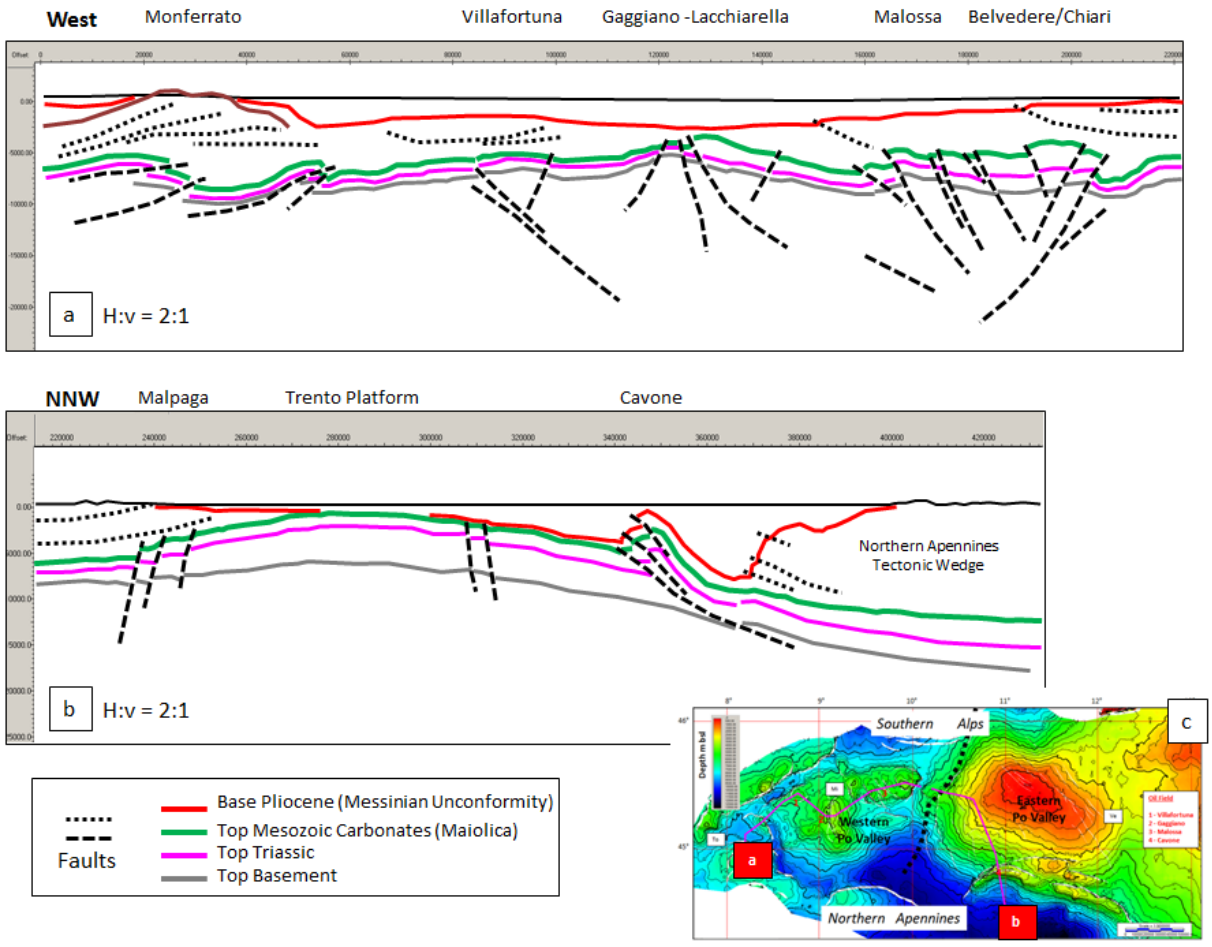

Fig.3 – a, b = regional cross-sections sliced from the 3D Po Valley structural model and main tectonic units; c = cross-section location map at top Mesozoic Carbonate level (see Fig.2 for larger view and the associated legend).

In the following section some of the most significant structures of the Po Valley basin are briefly discussed. Such structures 1) illustrate the common deformation features affecting the

Mesozoic carbonates in the Po Valley foreland, 2) are related to the major tectonic events experienced in the region (Mesozoic extension and Cenozoic compression) and 3) illustrate the main trap types for the deep Mesozoic oil play inside the basin. Despite being located outside the area covered by the thermal model, the Cavone structure is hereafter described for completeness of this chapter devoted to the Mesozoic structural geometries.

4.1.1 The Villafortuna oil-field structure

The Villafortuna field (Fig.3a, 4) (discovered in 1984; light oil; 226 MMbbl pf 43° API oil and 93 bcf of gas produced to date) lies 20 km to the south of the Southern Alpine front (see Fig.2) and corresponds to a major compressional unit that involves the Mesozoic section and the underlying basement (Pieri & Groppi, 1981; Cassano et al., 1986; Bello and Fantoni, 2002; Turrini et al., 2014).

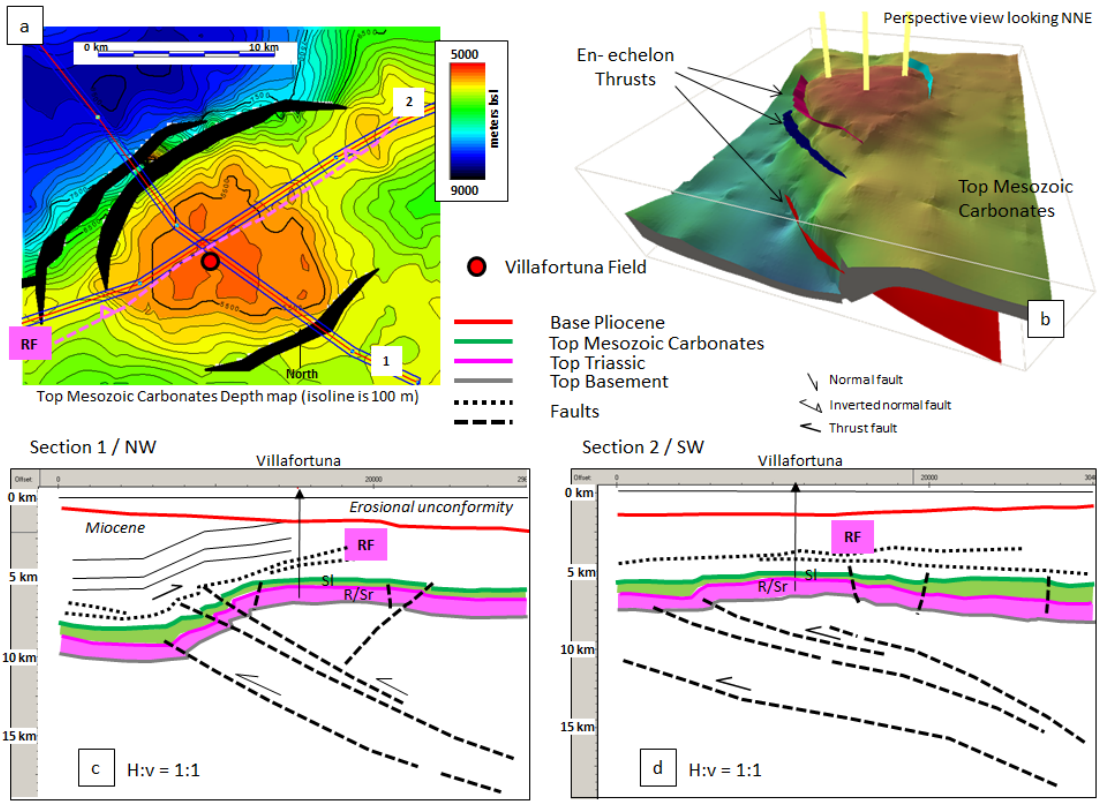

Fig.4 – The Villafortuna oil-field structure (see location in Fig.1 and 2): a) top Mesozoic depth grid, b) 3D structural model of the field structure, c) and d) cross-sections sliced from the 3D model. R/Sr = Reservoir and Source; Sl = Seal; RF = Romentino thrust front. Note: the Romentino unit geometry within the Oligo-Miocene section in Fig.6c is sketched from Pieri & Groppi, 1981, Cassano et al., 1986, Bello-Fantoni, 2002.

The structure is weakly displaced towards the NW and wedges into the overlying Tertiary sediments which, in turn, are thrust to the SE along the Romentino front (RF in Fig.4a, c, d). The base Pliocene unconformity separates the deformed Oligo-Miocene succession from the undeformed Plio-Pleistocene deposits. The field structure consists of a dome-type anticline, regionally plunging towards the SW and the NE (Fig.2 and 4a). Faults are SE and NW-dipping thrusts that cut the basement and enhance the gentle form of the final pop-up geometry below the Tertiary package (Fig.3 and 4c-d). Displacement is essentially towards the NW with an average throw of some 3 km at top carbonate level. In perspective and map view, the faults show an en-echelon pattern (Fig.4b). The presence of a complete Late and Mid Triassic reservoir-source section is reported inside the field while a few hundred meters of Jurassic-early Cretaceous, basinal carbonates seem to provide the topseal (Casero, 2004 and references therein; Bertello et al., 2010). According to the final 3D model, the trap area of the field is approximately 100 km^2 and likely compartmentalized by Triassic-Jurassic normal faults (Casero et al., 2004 and references therein). These, given the available information, are not represented inside the field model. The geometrical relationship between Tertiary sediments and the Mesozoic-basement assemblage within the Villafortuna tectonic wedge seems to indicate that the age of the final trap is mainly late Miocene (with displacement of a pre-compressional Triassic high) (Fig. 4c).

4.1.2 The Gaggiano oil-field and the Lacchiarella structure

The Gaggiano-Lacchiarella structural association (Fig.5) is a crustal-scale tectonic element which cuts across the entire Po Valley basin and extends towards the Southern Alps to the north and the Northern Apennines to the south (see Gaggiano location in Fig.2). The feature has a complex history, having initiated as a north-south striking, east-dipping extensional fault system in the Liassic before undergoing initial inversion in the Oligocene followed by weak reactivation during the Miocene (Fantoni et al., 2004). Liassic extension resulted in significant footwall erosion over the crest of the Gaggiano footwall high and in the deposition of an expanded thickness of deep-water Jurassic and Cretaceous carbonates in the subsiding Lacchiarella hangingwall basin. Oligocene inversion has resulted in approximately no net extension at Top Triassic level across the feature. Inversion and vertical expulsion of the expanded Jurassic-Cretaceous deep-water carbonate sediments, originally deposited in the Lachiarella hangingwall basin, has resulted in the development of a regional north-south

striking anticline immediately to the east of, and above, the trace of the extensional Liassic fault system (Fig.5).

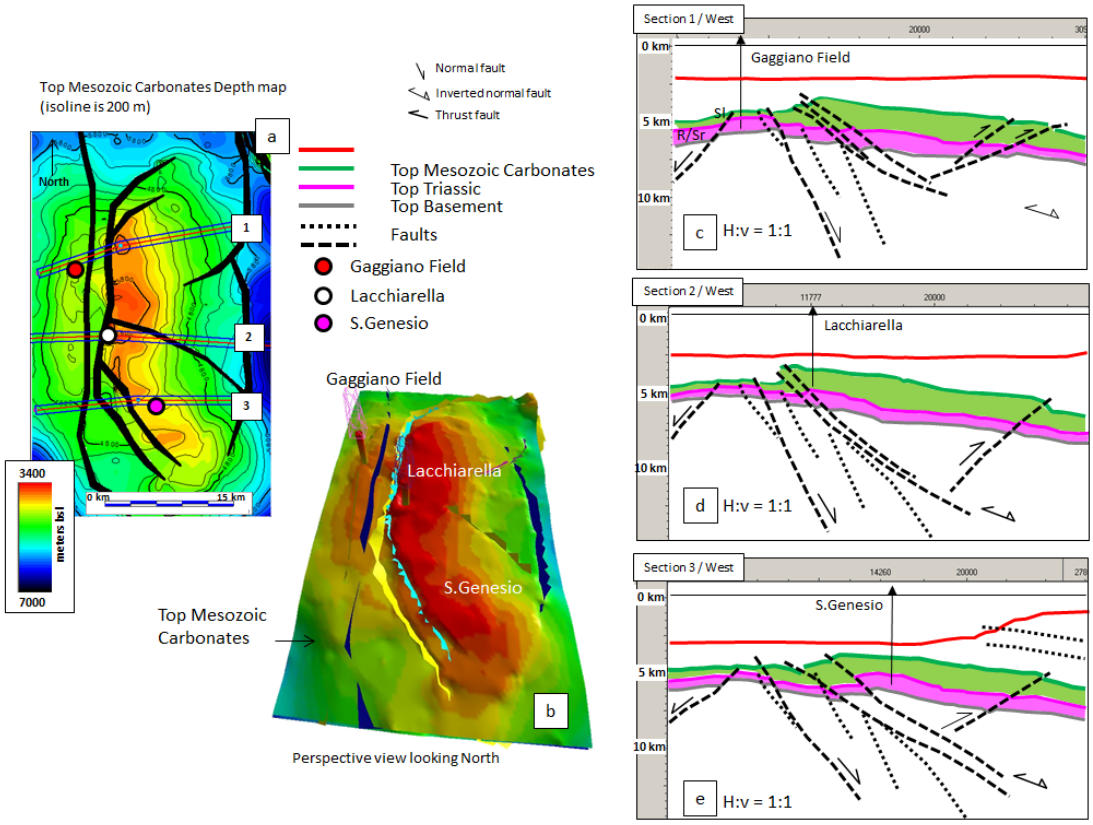

Fig.5 – The Gaggiano oil-field and the Lacchiarella structures (see location in Fig.1 and 2): a) top Mesozoic depth grid, b) 3D structural model of the field and the surrounding structures, c), d) and e) cross-sections sliced from the 3D model. R/Sr = Reservoir and Source; Sl = Seal. Note: the extensional terraces in the footwall of the Lacchiarella inverted fault (dotted-lines) are sketched on the basis of Cassano et al., 1986, Bongiorni, 1987, Fantoni et al.2004.

The structural framework derives from the overprinting of Mesozoic extensional and Tertiary compressional tectonics, as is clearly revealed by slicing of the model-volume (see Fig.5c-e). Major faults in the region are east-dipping whereas the associated secondary faults are west-dipping, with the two fault sets bounding the Gaggiano high and the Lacchiarella basin. A number of exploration wells have been drilled along this regional feature. The Gaggiano field (Fig.3a and 5) was discovered in 1982 (36°API oil; 20-30 MMbbl estimated reserves) (Bongiorni, 1987; Rigo 1991; Fantoni et al., 2004) and is located on the west-dipping footwall crest to the N-S Triassic-Liassic extensional fault system (Cassano et al., 1986; Bongiorni, 1987; Fantoni et al., 2004; Turrini et al., 2014). Within the field, the Mesozoic stratigraphic

section is extremely reduced by erosion associated with syn-extension footwall uplift and the basement is encountered by wells at the exceptionally shallow depths of approximately 5 km bsl (Fig. 5c-e). Based on the 3D model reconstruction, the top reservoir at Gaggiano lies just below the top Mesozoic surface, at an average depth of 4.5 km below mean sea level, giving a closure of approximately 30 km^2 and defining a relatively limited 4 way dip-closed trap at the crest of the regional footwall (Bongiorni et al., 1987). This trap was formed by Liassic extension and underwent minor rotation during the Cenozoic, associated with the deposition of Oligo-Miocene foredeep sediments. The top-seal is provided by the same intra-platform basinal carbonates (Meride formation) which also form the source rock for the field (Bongiorni et al., 1987; Bertello et al., 2010). Wells drilled on the Lacchiarella inversion structure (Lacchiarella-2 - 1978- and San Genesio -1994 -,) have encountered significantly increased thickness of Jurassic and Cretaceous basinal limestones, confirming the overall tectono-stratigraphic model, but have failed to find significant hydrocarbons at the Triassic objective levels.

4.1.3 The Malossa field structural domain

The Malossa field (Fig.3a - 6) (discovered in 1973; gas and condensate; approximately 27 MMbbl and 150 bcf gas produced prior to field abandonment in 1992) is located in the western sector of the Milano tectonic arc (see Fig.2). The field is one of a number of structures which deform the Po Valley Mesozoic foreland and have been buried beneath the Tertiary foredeep wedges to the south of the Southern Alps belt (Errico et al., 1980; Pieri & Groppi, 1981; Mattavelli et al., 1986; Cassano et al., 1986; Fantoni & Franciosi, 2010; Turrini et al., 2014). The reservoir of the field is provided by fractured late Triassic platform carbonates while the overlying Jurassic-Cretaceous basinal carbonates supply the seal and some further reservoir section. The source rock has not been proven inside the field area. However, analysis of the oil (Mattavelli and Novelli, 1987; Mattavelli & Margarucci, 1992; Bertello et al., 2010) suggests a late Triassic source rock (Argilliti di Riva di Solto), a lithology which crops out extensively in the Southern Alps, to the north of the Malossa region (Fantoni and Scotti, 2003). The field stratigraphy indicates that the structure developed by Miocene thrusting of a Triassic-Liassic high during the Alpine compression. The trap of the field is provided by a NW-SE oriented, faulted anticline, plunging towards both the NW and the SE. The associated major thrust is NE dipping and it displaces the structure towards the SW. Minor faults are reported to intersect the fold crest, creating structural compartments within the field (Mattavelli & Margarucci, 1992). From the model, the average depth to the

top Mesozoic structure crest is 5 km bsl, while the field area is approximately 15 km^2 (Fig.6a). The final age of the trap formation is mainly late Miocene with some minor reactivation during the Plio-Pleistocene.

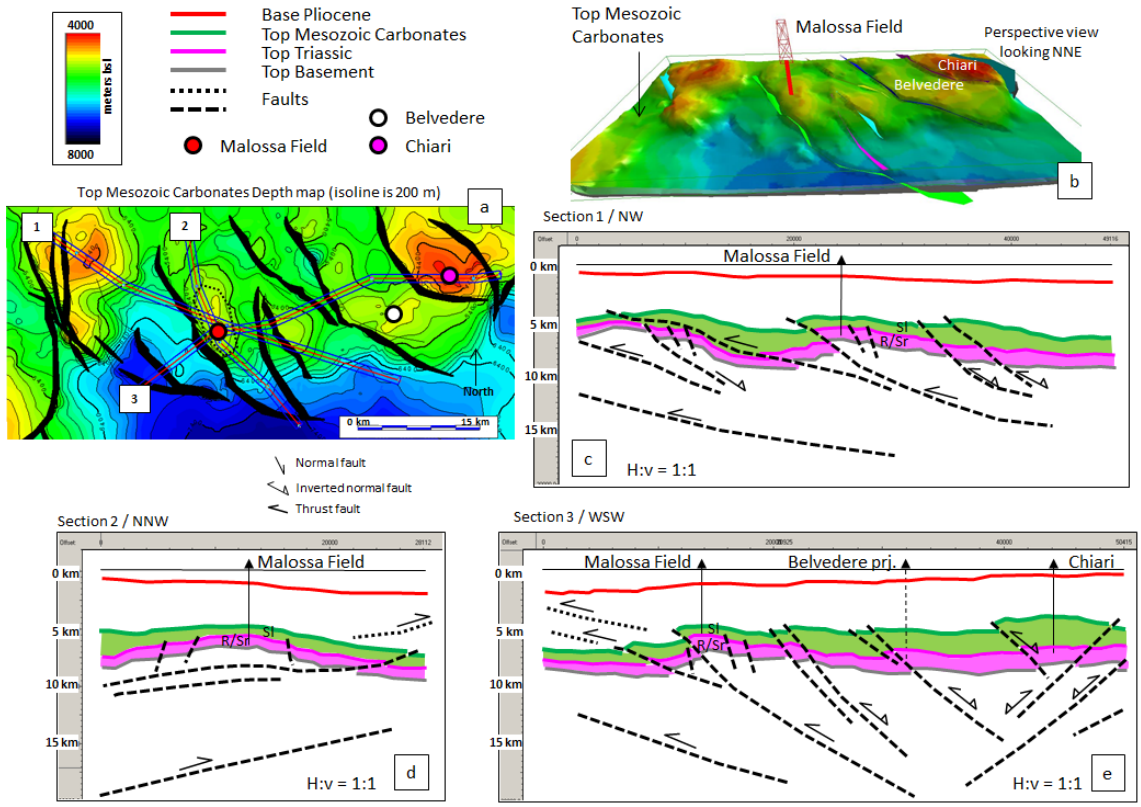

Fig.6 – The Malossa oil-field region (see location in Fig.1 and 2): a) top Mesozoic depth grid, b) 3D structural model of the field and the surrounding structures, c), d) and e) cross-sections sliced from the 3D model. R/Sr = Reservoir and Source; Sl = Seal.

Inspection of the 3D model (Fig.6) shows the Malossa unit as one of a number of structures of similar size, orientation and style, all of which are deformed by folding and thrusting of the Mesozoic carbonates and the related basement. Slicing of the model geo-volume (Fig.6c-e) confirms that inversion of the Triassic-Liassic extensional basins does control the overall structural style in the region (Cassano et al., 1986; Ravaglia et al., 2006; Fantoni & Franciosi, 2010; Masetti et al., 2012) with reactivation of the Mesozoic extensional faults and creation of new footwall shortcuts which locally cut through the pre-existing highs. Particularly important to the aims and results of this study are the Chiari and Belvedere structures, to the NE of the Malossa field. Those structures, together with the Lacchiarella one (see section 4.1.2, Fig. 5), are the main expression of the basin inversion process which took

place in the western Po Valley domain. Key-characteristics of the two structures compared with Malossa are the following:

1. The structures are inverted Liassic half-grabens and the thick (5 km) Mesozoic carbonates are vertically expelled by Miocene inversion (the Malossa structure is essentially a short-cut of a pre-existing Triassic-Liassic high);
2. the Mesozoic faults are reactivated (once the map shown by Mattavelli & Margarucci – 1992 – is considered, it is possible to argue that pre-compressional faults – not represented in the 3D model - are passively displaced by new thrusts in the Malossa structure);
3. some tectonic over-thickening of the Jurassic sediments can be interpreted from the public composite log (the Malossa well data does not seem to show any tectonic repetition);
4. the basement is involved in the structuration (same as Malossa);
5. the age of the present structural geometries is essentially late Miocene with some minor Pliocene tectonics (same as Malossa).

4.1.4 The Cavone oil-field structure

The Cavone field (Fig.3b-7) (discovered in 1974; 23°API oil; 94.5 MMbbl hydrocarbons initially in place (HCIIP)) (Nardon et al., 1991) occurs on the lateral ramp of a major tectonic arc (i.e. the Ferrara arc) at the buried front of the eastern sector of the Northern Apennines (see Fig.2) (Pieri & Groppi, 1981; Cassano et al., 1986; Nardon et al., 1991; Turrini et al., 2014). The structure is a thrust-related fold where Mesozoic and Tertiary sediments are intensively faulted and fractured (Cassano et al., 1986; Nardon et al., 1991; Carannante et al., 2015). The age of the trap is essentially Plio-Pleistocene although Miocene tectonics has been suggested to have contributed to the early stage development of the field (Castellarin et al., 1985; Nardon et al., 1991; Ghielmi et al., 2012). The 3D structural model shows the imbrication of the Mesozoic units and the clear asymmetry of the associated thrust-related fold (see Fig.7): as such, faults inside the tectonic stack are mainly SSE dipping and the derived faulted anticline is NNW verging (Fig.7c). The observed vertical throw that separates the Cavone hanging-wall and foot-wall unit (i.e. the Po Valley foreland) is around 1.5 km on average. The described structural geometry suggests a major detachment surface at the base of the Triassic sediments (i.e., the Burano Evaporite) (light blue thrust in Fig.7c-d) and makes any involvement of the basement particularly unlikely (Cassano et al., 1986; Nardon et al., 1991) unless short-cutting and slicing of the footwall of the foreland unit has

occurred (Carannante et al., 2015). The depth to the Cavone culmination from the available public data is approximately 3 and 4 km below mean sea level, at near top Mesozoic and top Triassic respectively. According to the reconstructed geometry, the field area would be in the order of 30 km^2 (Fig.7a, c, d).

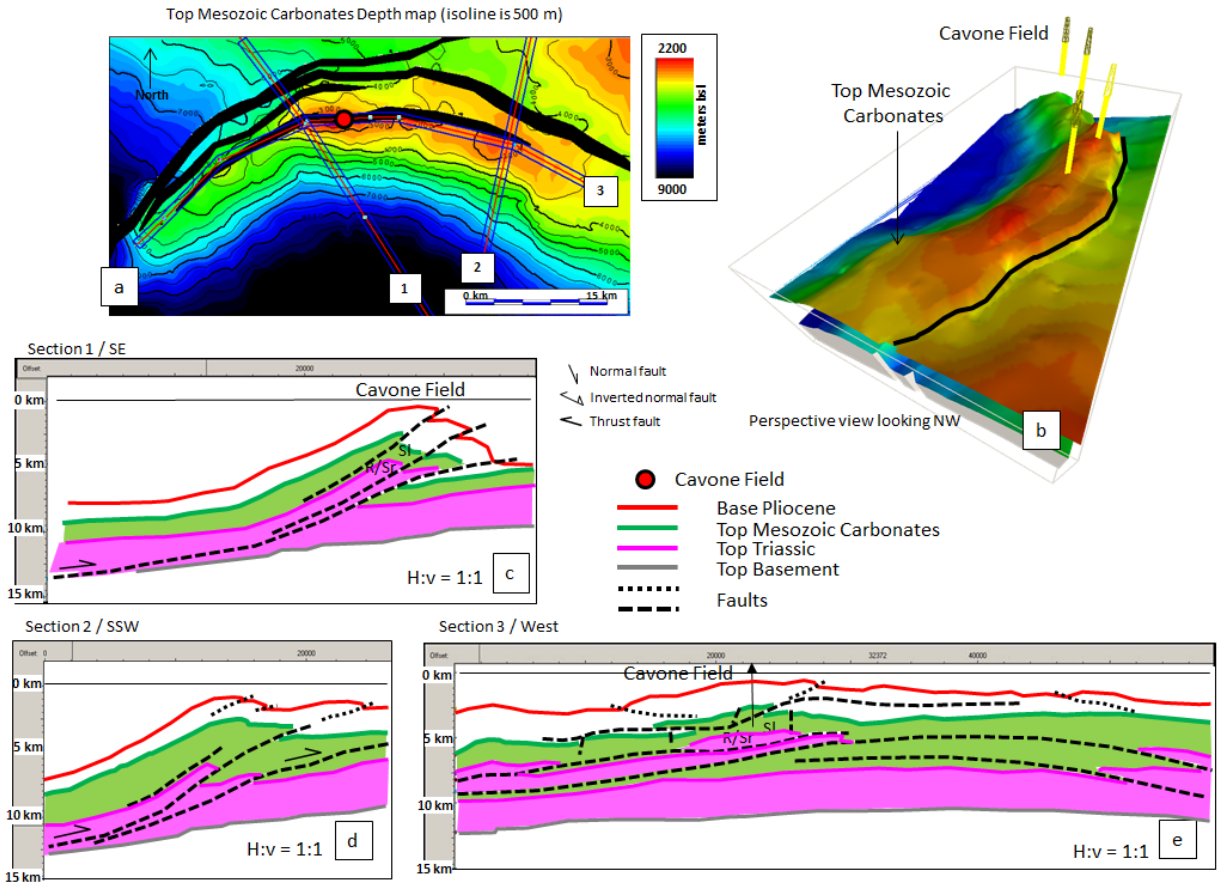

Fig.7 - The Cavone oil-field structure (see location in Fig.1 and 2): a) top Mesozoic depth grid, b) 3D structural model of the field and the surrounding structures, c), d) and e) cross-sections sliced from the 3D model. R/Sr = Reservoir and Source; Sl = Seal. Note: the vertical stippled segments inside the Cavone thrust-related stack are cross-faults sketched from Nardon et al., 1990.

4.2 Source rock distribution & Gross Depositional Environment (GDE) maps in the Mesozoic carbonates

Mid and Late Triassic intervals (Fig. 8a) have been proven as the major source rocks for the deep Mesozoic petroleum system of the Po Valley through the application of geochemical fingerprinting techniques to correlate discovered hydrocarbons with outcropping

source rocks (Mattavelli & Novelli, 1987; Mattavelli et al., 1993; Zappaterra, 1994; Lindquist, 1999; Katz et al., 2000; Casero, 2004; Bertello et al., 2010).

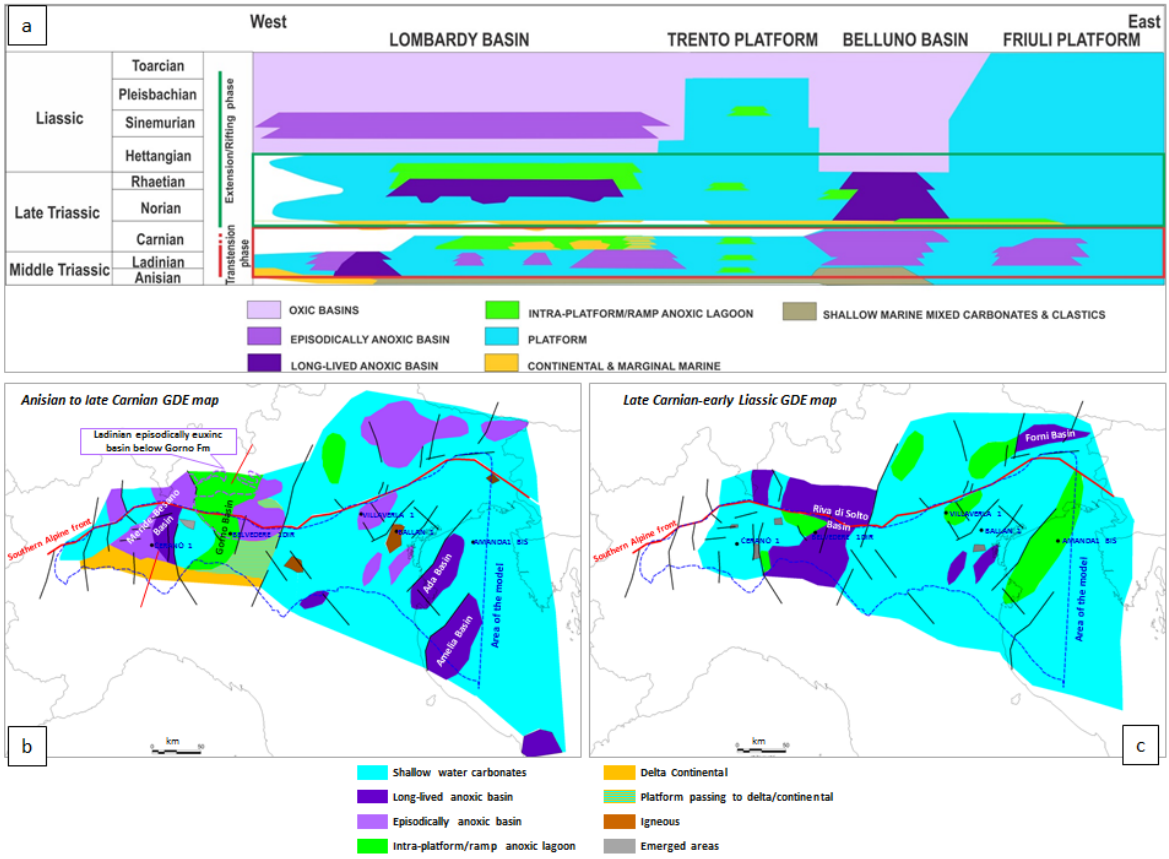

Fig.8 – a) Triassic-Liassic chrono-stratigraphy of the Po Valley region highlighting the main source rock intervals; b) Gross depositional environment map of the Anisian to late Carnian sediments; c) Gross depositional environment map of the late Carnian-early Liassic sediments.

Key inputs for the basin modelling study that is the subject of the present work are a description of the spatial distribution of these source intervals (Fig. 8b-c) and the assignation of the main parameters describing hydrocarbon generation potential (net source thickness, TOC, hydrogen index etc.) to the source intervals (Table 1). The present section describes how the source model was constrained within the 3D basin model. The complex tectonic history of the study area coupled with limited public data coverage and quality, makes delineating source depositional basins difficult: a) only a few deep wells have drilled through the Triassic source intervals; b) mapping the lateral extent of the source rocks is difficult given the lack of a clear seismic expression of the basins where the source rocks were deposited. Given this, source rock distribution in the model is described based on the

construction of Gross Depositional Environment maps (GDE maps) produced for key intervals.

Source Age Interval	Domain	Formation(s)	Net Thickness (m)	TOC (%)	Kerogen Type		Weight (%)	Hydrogen Index	Petroleum Potential		
					Tissot & Welte, 1984	Pepper & Corvi, 1995a			mg HC/ g Rock	mmbbl/ Km^2	bcf/Km^2
Upper Triassic	Long-lived anoxic basin	Argille di Riva di Solto, Formi	50	4	IIS	A	90	550	19.8	17.9	
					III	F	10	160	0.64		3.9
	Intra-platform/ramp lagoon	Dolomia Principale, Monticello, Calcare di Zu, Scisti Bituminosi	12.5	4	IIS	A	90	550	19.8	4.5	
					III	F	10	160	0.64		1
Middle Triassic	Long-lived anoxic basin	Meride, Besano	50	4	IIS	A	90	550	19.8	17.9	
					III	F	10	160	0.64		3.9
	Episodically anoxic basin	Meride, Livinallongo, Moena, Rio del Lago	25	4	IIS	A	90	550	19.8	9	
					III	F	10	160	0.64		2
	Intra-platform/ramp lagoon	Gorno	12.5	4	IIS	A	10	550	2.2	4	
					III	F	90	160	5.76		70.9

Table 1 - Table of source rock parameters used in thermal modelling of the Po Valley. Parameters are consistent with published data on the Po Valley Triassic source intervals as reported for the Villafortuna-Trecate and Malossa fields, as well as outcrop analogues. Colours correspond to Gross depositional environments in Fig 8. IFP – Institut Français du Pétrole, P & C – Pepper & Corvi, 1995a.

These were derived through integration of publicly available well data with the extensive literature describing the time-equivalent outcrops in the Southern Alps (Gortani & Desio, 1925; Mattirolo et al., 1927; Castiglioni et al., 1940 and 1941; Dal Piaz et al., 1946; Desio et al., 1954; Andreatta et al., 1957; Passeri et al., 1967; Braga et al., 1968; Gatto et al., 1968 and 1969; Lipparini et al., 1969; Casati et al., 1970; Nardin et al., 1970; Sassi et al., 1970 ; Cantelli et al., 1971; Castellarin & Vai, 1986; Jadoul, 1986; Cati et al., 1986, 1987; Ciarapica et al., 1986; Doglioni & Bosellini, 1987; Jadoul et al., 1992; Shonborn, 1992, 1999; Bertotti et al., 1993; Zappaterra, 1994; Greber et al., 1997; De Zanche et al., 2000; Franciosi & Vignolo, 2002; Fantoni & Scotti, 2003; Fantoni et al., 2003, 2004; Berra et al., 2009; Bertello et al., 2010; Fantoni & Franciosi, 2010; Masetti et al. 2010; Ponton, 2010; Gianolla et al.,2012, Masetti et al., 2012; Handy et al., 2014; Pfiffner, 2014).

The Triassic depositional systems of the Po valley were strongly influenced by the structural evolution of the basin. Two loosely defined tectonically-controlled megasequences can be identified: a) a mainly Middle Triassic (Anisian to late Carnian) megasequence, associated with extensional-transtensional tectonics and local volcanism driven by plate scale wrench movements or aborted rifting; and b) a mainly Late Triassic (late Carnian to early Liassic) megasequence, associated with extensional rifting related to the initial phase of the opening of Alpine Tethys (Berra & Carminati 2010).

The Middle Triassic megasequence (Fig. 8a) commences with the tectonic dissection of the widespread epeiric carbonate-evaporitic platform system that dominated early Triassic deposition. From the late Anisian onwards intra-platform basins developed within this former platform and euxinic conditions periodically developed within those basins resulting in the deposition of organic-rich basinal carbonates, such as the Meride limestone & Besano and Gorno formations in the Western Po Valley, and the Livinallongo Formation, and bituminous events in Predil Limestone and Rio del Lago Formation in the Eastern Po Valley. From the early Carnian onwards, subsidence slowed and platform carbonates prograded over the basins bringing to an end this first phase of deposition of organic-rich facies. The gross depositional environment map in figure 8b shows the interpreted spatial distribution of potential source rock basins for this megasequence: in the western Po Valley these are interpreted to have an approximately north-south orientation whilst in the eastern Po Valley, the basins are interpreted as oriented north-east to south-west (Franciosi & Vignolo, 2002). In the western Po valley, two potential source basins are identified: the Anisian to Ladinian Meride-Besano basin and the Carnian Gorno basin, to the west and east of Milan, respectively. The source potential of the former is confirmed by geochemical correlation with the oils from the Villafortuna-Trecate and Gaggiano fields (Bello & Fantoni, 2002). The source rocks potential of the Gorno basin is more speculative: enrichment of organic matter is reported from the outcrops (Stefani & Burchill, 1993, Assereto et al, 1977, Wygrala, 1989) within sediments deposited in shallow anoxic lagoons developed within a mixed clastic-carbonate depositional system (Gnaccolini & Jadoul, 1990), but there is little direct evidence for hydrocarbons having been generated in the subsurface from this formation. The interpretation that this facies extends southwards into the subsurface of the Po Valley is based on a similar facies having been encountered in one of the wells within the Malossa field. In the Central Po Valley, along the buried Ferrara arc (i.e. the buried, external front of the Northern Apennines), the presence of a Mid Triassic source basin is inferred from Cavone field oil-source correlation, which indicates a Mid Triassic oil-prone carbonate source rock similar to Meride Formation of the western Po Valley (Mattavelli & Novelli, 1990; Nardon et al., 1990). In the eastern Po Valley and Adriatic foreland, the distribution of potential source basins follows Franciosi & Vignolo (2002) with two offshore Mid Triassic basins identified, the Ada and Amelia basins: the presence and areal extent of these is well constrained by 3D seismic. However the presence of source rock facies within them remains speculative. Onshore, organic-enriched mid Triassic (Anisian-Carnian) basinal marls and wackestones of up to several tens of metres thickness are known within the thick basinal successions of the

Livinallongo, Predil, Rio del Lago and Durrenstein Formations of the south eastern Alps (Brack et al 2000, Fantoni & Scotti 2003, Keim et al 2006). Similar facies are encountered in the subsurface of the Po Valley at the Villaverla-1 well: the latter are interpreted here to lie within one of several north-east to south-west oriented basins, of similar dimensions to those mapped offshore on 3D seismic data, forming a rather speculative proto-Belluno trough (Masetti et al. 2012).

Extensional tectonics recommenced in Middle-Late Norian in the Central Southern Alps and in the Carnian Pre-Alps, resulting in the progressive dismembering of the widespread Dolomia Principale carbonate platform established during late Carnian and early Norian tectonic quiescence. Extension formed approximately north-south oriented intra-platform basins up to several tens of kilometres wide (Jadoul et al., 1992) which expanded as rifting progressed into the Liassic. Eventually drowning of large sectors of the platform occurred ultimately leading to fully open marine deep-water conditions associated with the Tethyan-Ligurian Ocean. Prior to the establishment of open marine circulation, anoxic conditions developed periodically during the Late Triassic within these basins. This resulted in the preservation of high levels of organic material within the basinal limestone facies, for example in the Argilliti di Riva di Solto, Zu, and Aralalta formations in the Central Po Valley, and the Dolomia di Forni of the Eastern Po Valley. The gross depositional environment map in figure 8c shows the interpreted spatial distribution of these potential source basins: the main basin in the western Po valley is the Riva di Solto basin of mid to late Norian age. This basin developed in the subsiding hanging wall to the major late Triassic-Liassic Gaggiano-Lacchiarella extensional fault system (Fantoni & Franciosi, 2010) described previously. Thinner sequences of organic-rich sediments were also deposited in a mid to outer ramp setting, in the successor Rhaetian carbonate ramp represented by the Zu Formation (Stefani & Burchill 1993, Galli et al 2007). The source potential of these successions is well documented both from outcrop descriptions (Jadoul et al., 1992) and through geochemical typing of the oils from the Malossa field to these source rocks (Mattavelli & Novelli, 1990). In the eastern Po valley, the upper megasequence commences with a widespread late Carnian transgression resulting in deposition of the organic rich dolomites of the Monticello Formation in an inner ramp setting. An organic-rich facies, some 60m thick, ascribed to this interval is reported from the offshore Adriatic foreland at the Amanda-1bis well (Carulli et al 1997). As transgression continued into the Norian, differentiation occurred into areas dominated by the widespread Dolomia Principale Platform passing laterally into narrow (kilometres to a few

tens of kilometres) anoxic basins, for example in the area of the future Belluno Trough where the organic rich Dolomia di Forni were deposited (Carulli et al 1997), locally attaining thicknesses of 850m. Within the Dolomia Principale, anoxic intra-platform lagoons developed locally, for example the Rio Resartico organic laminates where over a 100m of laminated dolomites and "scisti bituminosi" are reported (Carulli et al 1997). The same authors have described similar facies within the Dolomia Principale in the offshore of the Adriatic foreland, reaching their maximum development in the Amanda-1bis well. Beyond the reported well penetrations, constraints on the distribution of organic rich sediments in the subsurface are absent: here it has been assumed that these deposits accumulated in successor basins to the mid Triassic basins described previously in the proto-Belluno trough and in the Adriatic foreland, either in long-lived anoxic basins similar to that in which the Dolomia di Forni accumulated, or in anoxic intra-platform lagoons similar to that described at Rio Resartico.

The gross depositional environment maps presented here (Fig.8b-8c) were used to define the lateral source rock distribution within the 3D basin model. Source parameters were then assigned to each polygon. The net thickness of source intervals is poorly constrained, although the gross thickness of the source-bearing interval locally may reach 1 km inside the major depocentres (Pieri, 2001), whilst Fantoni et al.(2002) define 400m of gross thickness for the Meride-Besano source interval in the Villafortuna-Trecate field. On this basis, net source thickness has been assigned with reference to the interpreted gross depositional environment, with long-lived anoxic basins assigned a net source thickness of 50m, episodically anoxic basins assigned 25m and intra-platform/ ramp anoxic lagoons assigned 12.5m.

In general, potential source rocks are carbonate-argillaceous sediments of variable but rather high TOC, varying from a maximum of 40% in the Besano Shales to a minimum of 0.10% within the Meride Limestone with an average of approximately 4% (Novelli et al., 1987, Fantoni et al., 2002, Katz et al, 2000). Kerogen types are dominantly of marine origin, with a secondary component of terrestrial material. These have been parameterized for all sources within the model as 90% Type A kerogen and 10% Type F kerogen using default kinetic parameters as defined by Pepper & Corvi (1995a-b) and as shown in Table 1. The only exceptions are the potential source rocks of the Gorno Formation which are described as dominantly consisting of reworked terrestrial material (Stefani & Burchill, 1993) and have consequently been parameterized as 10% Type A kerogen and 90% Type F kerogen.

The petroleum potentials derived from these source parameters and reported in Table 1 appear to be consistent with those reported in the literature: Fantoni et al (2002) define/suggest a formation average petroleum potential for the Meride-Besano interval at Villafortuna-Trecate of 21 kg HC/ ton rock, whilst Bello & Fantoni (2002) indicate a source potential index of 4t HC/m^2 (or 30 MMbbl/km^2) for the Mid Triassic petroleum system of the western Po Valley and of 3t HC/m^2 (or 22 MMbbl/km^2) for the Late Triassic petroleum system.

4.3 Rock property model

The rock properties needed for the present study include the following: chrono-litho-stratigraphy; surface porosities; compaction coefficients; bulk densities; radiogenic heat generation parameters for each lithology; thermal conductivities and their temperature dependencies. As far as possible, the rock property model used in this study uses locally-derived parameters, taken from the literature on exploration wells drilled in the Po Valley or adjacent outcrop analogues (Berra & Carminati, 2010, Pasquale et al 2011, Pasquale et al, 2012). Where such local parameters are not available, values are derived from global datasets.

The chrono-litho-stratigraphies used in the 1D modelling are taken from the publicly available well composite logs, and the lithological descriptions contained therein were used to assign the percentages of end member lithologies present for each stratigraphic unit described (Fig 9a). Where additional pseudo-well locations are defined within the model, a generalised litho-stratigraphy was ascribed after considering the gross depositional environment of the pseudo-well location, as well as the litho-stratigraphy present in any nearby wells.

Once the lithological model for each unit has been assigned, back-stripping and thermal properties are defined based on lithology. For mixed lithologies, properties are derived from the properties of the end member lithologies combined with the relative percentage of each end member using the appropriate mixing model: simple volumetric weighting is used to calculate surface porosity, compaction coefficient, density, volumetric heat capacity and radioactive heat generation, whilst thermal conductivities are calculated using a geometric mixing law (Pasquale et al. 2011). Temperature dependency of thermal conductivity is incorporated into the model using an approximation to the Sekiguchi Correction (Sekiguchi, 1984). A summary of the properties assigned for each end member lithology is given in Table 2.

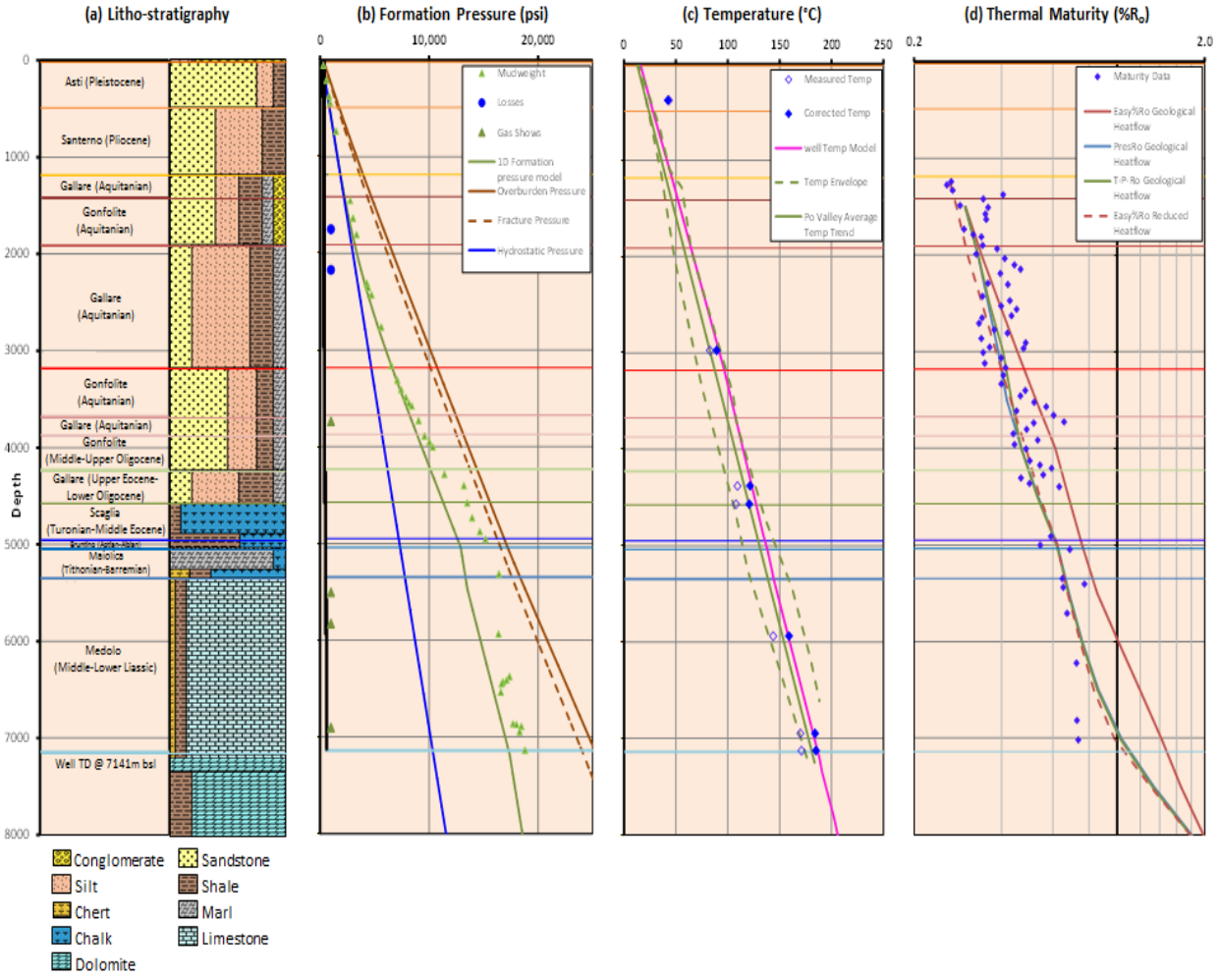

Fig.9 – Belvedere 1 well (a) Chrono- & Litho-stratigraphy; (b) Formation pressure model showing the significant increase in overpressure below 2,000m through the Tertiary foredeep clastics and basinal carbonates into the highly overpressured deep carbonate aquifer consisting of Liassic and Triassic platform limestones and dolomites; (c) temperature model showing good correspondence between corrected well temperature measurements and the prediction from the basin model. The average temperature-depth trend for the Western Po Valley from Pasquale et al (2012) together with the observed range is also shown; and (d) thermal maturity model showing match of various models to the dataset from Chiaramonte & Novelli (1986). Temperature-only models using the geological heat flow (Easy%Ro, shown in the continuous red line) provide a poor match to the data, whilst models based on geological heat flow and pressure history (PresRo & T-P-Ro shown in the blue and green lines) fit much better. These latter models can be approximated using a temperature-only model with a reduced heat flow corresponding to the period of overpressure (Easy%Ro with reduced heat flow shown in the dashed red line).

Rock Properties										
Rock Type	Shale	Sandstone	Chalk	Chert/ Radiolarites	Limestone	Dolomite	Anhydrite	Silt	Marl	Conglomerate
Surface porosity	0.29	0.28	0.70	0.70	0.51	0.30	0.63	0.29	0.50	0.40
Compaction Coefficient	0.38	0.22	0.71	0.71	0.52	0.22	0.52	0.38	0.54	0.23
Porosity at 3000m (using Athy eq. $\varphi(z)=\varphi_s e^{-kz}$)	0.09	0.15	0.08	0.08	0.11	0.16	0.13	0.09	0.10	0.20
Bulk density (kg/m^3)	2720	2650	2710	2650	2710	2710	2270	2650	2715	2650
Thermal conductivity (w/m/K)	1.62	3.85	3.14	7.11	3.14	4.98	4.76	3.35	2.25	4.18
Temperature Dependency of thermal conductivity (1/C)	-0.0004	0.0019	0.0015	0.0030	0.0015	0.0025	0.0024	0.0016	0.0010	0.0021
Specific heat (J/kg/°K)	832	735	815	740	815	870	585	784	824	812
Specific heat (cal/g/°C)	0.20	0.18	0.19	0.18	0.19	0.21	0.14	0.19	0.20	0.19
Radiogenic heat (µW/m^3)	1.33	1.05	0.63	0.43	0.45	0.46	0.09	1.13	0.92	0.90

Gretner, 1981	Waples & Waples, 2004	Pasquale et al, 2011
Middleton, 1993	Berra & Carminati, 2010	Pasquale et al 2012
	Sekiguchi, 1984	

Table 2 - Table of rock properties used in basin modelling of the Po Valley. Where available, local rock properties are used (Berra & Carminati, 2001; Pasquale et al, 2011; Pasquale et al, 2012). Other values are from global averages (Gretner, 1981; Waples & Waples, 2004; Middleton, 2005).

4.4 Pressure model in the Mesozoic Carbonates

The Mesozoic carbonates of the western Po valley are characterized by high overpressures and these overpressures represent a significant challenge to deep exploration (Pietro et al., 1979; Vaghi et al., 1979). Early workers in the Po valley argued that formation pressure exerted a significant control on hydrocarbon maturation in the area, by illustrating a relationship between formation pressure and the difference between observed and theoretically calculated measures of maturity (Chiaramonte and Novelli, 1986). Subsequent workers investigated the relationship between vitrinite reflectance and formation overpressure, using a global dataset that included data points from the western Po Valley (Carr, 1999). This work resulted in a quantitative model based on modifying the Easy%Ro algorithm of Sweeney and Burnham (1990), which is based on the temperature history of a sample, to include an overpressure term. Given this emphasis on overpressure as a retarding factor on thermal maturity in previous works on the area, one of the objectives of the present study was to investigate this effect and, should its importance be confirmed, incorporate it into the 3D basin modelling work.

Novelli et al (1987) briefly reviewed the overpressure distribution in the western portion of the study area, which is characterized by a normally pressured shallow clastic aquifer of Pliocene age and a deep, overpressured carbonate aquifer of Triassic age, corresponding to the units that host the Triassic petroleum systems that are the subject of this paper. These two aquifers are separated by an aquitard consisting of fine-grained clastic rocks of Miocene to Paleogene age and fine-grained basinal carbonates of Paleogene to Jurassic

age. This aquitard is characterized by a strong pressure ramp which connects the normally pressured shallow aquifer to the overpressured deep carbonate aquifer. These authors further go onto interpret the overpressures in the western Po valley as arising from high sedimentation rates .associated with foredeep sedimentation from the Oligocene onwards. Hydraulic isolation of the deep carbonate aquifer occurred during mid to late Miocene times due to alpine thrusting, resulting in creation of the deep carbonate pressure cell, in the western Po Valley. Rapid burial during the Plio-Pleistocene then produced the present distribution of overpressure within both the deep carbonate aquifer and the mixed clastic-carbonate aquitard.

In the present study, the data and models presented by Novelli et al (1987) were developed in 2 ways: a) by the creation of 1D pore pressure models for both the aquitard and the deep carbonate aquifer for key wells, as an input to modelling the thermal maturity of organic matter; b) the distribution of overpressures within the deep carbonate aquifer was reviewed against the structure maps from the 3D model to develop an understanding of the spatial and temporal distribution of these overpressures.

The 1D pore pressure models for individual wells were built in 2 steps: firstly a constant overpressure was estimated for the deep carbonate aquifer, based either on pressure data from the well in question or from data presented by Novelli et al (1987) (their Fig. 7); secondly available pressure data (primarily mud-weight data, but with occasional well test or MDT data) in the aquitard were modelled using the Mann and Mackenzie approach, with the Plio-Pleistocene sedimentation rate as one key input and lithology within the aquitard and top overpressure as the other key inputs (Mann & Mackenzie, 1990). An example of such a model is shown in Fig. 9b for the Belvedere well.

Review of the distribution of overpressures within the deep carbonate aquifer in the context of the 3D structural model clearly indicates that the overpressures are confined to a regional scale anticline developed at the Top Triassic level in the western Po valley (thick red line in Fig. 2), and that this anticline was in existence by the end of the Miocene, although it probably initiated sometimes in the Paleogene. This anticline is isolated from the normally pressured carbonates of the eastern Po valley, observed for example in the Malpaga-1 well (Fig 2, Novelli et al (1987), across the Chiari syncline. However, the 3D structural model (Fig.2) shows that the overpressure cell is not hydraulically isolated from the normally pressured carbonates to the east by a continuous system of sealing faults, as indicated by

Novelli et al (1987). Rather it is suggested here that it is defined by a combination of faults and a depth related reduction in porosity-permeability within the Triassic carbonates to levels that do not permit lateral transmission of overpressure. The 3D model indicates that this depth is in the range 8-8.5 km below the mean sea level. Low permeability within the Triassic carbonates at similar depths is supported by observations from the Adamello contact aureole in the S Alps where a tonalite batholith with associated gabbroic stocks was emplaced into a thick sequence of Triassic dolomites, essentially similar to those in the subsurface of the western Po Valley, at depths of 9-11 km (Pennacchioni et al., 2006). Gerdes et al. (1999) use oxygen stable isotope data to infer that metamorphism within the aureole occurred in a closed system due to the low permeability of the dolomitic country rock into which the batholith was intruded, which prevented regional scale fluid flow.

4.5 Thermal and maturity models

To enable the basin modelling of potential Triassic source intervals, two further inputs are necessary: palaeo-water depths and a heat flow model.

Palaeo-water depths are inferred from the depositional facies present at the well locations used and the gross depositional environment maps for key intervals (Fig.8b-c). The depths used broadly correlate with those considered by Winterer & Bosellini (1981) for the Mesozoic carbonates and by Di Giulio et al. (2013) and Ghielmi et al. (2012) for the Tertiary. Sediment-surface interface palaeo-temperatures are then derived by combining palaeo-water surface temperatures based on the relative latitude of the Po Valley through time with a discrete water depth-temperature relationship such as proposed by Defant, (1961).

The heat flow model (Fig. 10) has been defined following a comparative review of published data, primarily from the Southern Alps (Mattavelli & Novelli, 1987; Greber et al., 1997; Fantoni & Scotti, 2003; Zattin et al., 2006; Scotti & Fantoni, 2008; Carminati et al., 2010; Grobe et al., 2015). There is general consensus amongst authors for two episodes of increased heat flow during the Mesozoic: the first in the mid Triassic, caused by a first pulse of extensional tectonic activity, which resulted in the development of the basins within which the mid Triassic source rocks were deposited, as discussed previously; the second during the early Jurassic, associated with the full development of Tethyan rifting. A late Cenozoic reduction in the heat flow trend is observed due to high sedimentation rates and rapid burial in the Po

Valley in the foredeep to the advancing Southern Alps and Northern Apennine fronts. This is consistent with the basin geodynamics and associated tectono-stratigraphic evolution inside the Po Valley region (see section 2.1 and references therein). The present day heat flow is based on the regional heat flow map of Italy of Della Vedova et al. (1991), with some modifications where corrected well temperature data are available and can be used to constrain the heat flow locally.

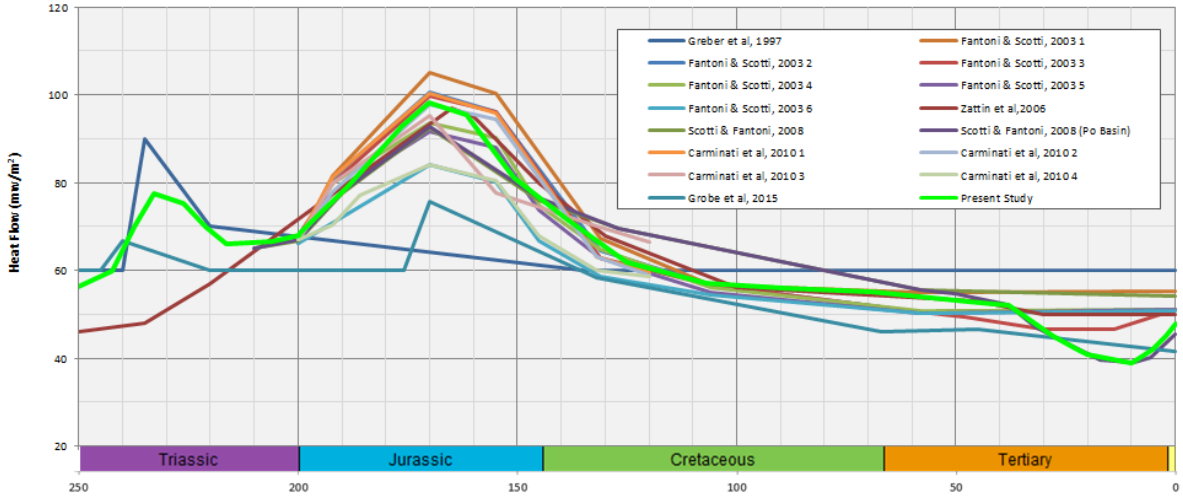

Fig.10 - Heat flow histories of the Po Valley and surrounding regions, from the literature. The high initial heat flow during Triassic and also later during the Jurassic are associated with rifting and extensional tectonics. The lower heat flow during the Tertiary results from high sedimentation rates during the Alpine orogeny.

4.5.1 1D thermal modelling and hydrocarbon generation

A number of well locations, for which temperature and/or maturity data were available, were selected for 1D modelling, with their locations chosen to provide a reasonable geographic spread across the Po Valley region. Maturity data is mainly collated from the literature (particularly Wygrala, 1988; Chiaramonte and Novelli, 1986; Fantoni & Scotti, 2003) with the addition of some proprietary data. Additionally, some pseudo-wells were constructed to fill in the areas where well data were sparse. The chrono- and litho-stratigraphy for each well were derived from the relevant composite log, with physical properties (porosity, density, thermal conductivity) being assigned based on lithology as described in section 4.3. Measured temperature data reported on the composite log were corrected to in-situ temperature using the approach described by Pasquale et al. (2012). In general the available maturity data for the Mesozoic carbonates were limited and of poor quality,

frequently showing substantial scatter. Much of the data consists of RockEval pyrolysis Tmax data and these were converted to vitrinite reflectance (%Ro) equivalent values using the relationship of Jarvie et al. (2001). The satisfactory nature of this relationship in the study area was confirmed at wells with both Tmax and vitrinite reflectance data available.

In the first instance, as a calibration step, the present-day temperature-depth relationship calculated from the model was compared with the corrected temperature values derived from the composite log. An example is shown for the Belvedere-1 well in figure 9c. In general, the match between model and observation was acceptable particularly over the carbonate section that is the subject of the present study. Once a good match was obtained between temperature observations and that predicted from the model, maturity profiles were calculated for each well and pseudo-well and, for wells with maturity data, the calculated profile was compared with observed data. Figure 9d shows the maturity profile for the Belvedere-1 well and clearly indicates that the maturity profile calculated using the Easy %Ro algorithm (Burnham & Sweeney, 1989), which uses only the temperature history of each data point, substantially over-predicts the observed thermal maturity, particularly in the Mesozoic carbonates. In contrast, algorithms that incorporate the overpressure history, in addition to the temperature history, appear to produce a better fit to the observed data, with the PresRo algorithm of Carr (1999) producing very similar results to the alternative T-P-Ro algorithm of Zou & Peng (2001) (Carr,1999, incorporates overpressure effects into the Easy%Ro model by introducing a pressure based modification to the frequency factor, whilst Zou & Peng, 2001, introduce a overpressure based modification to the activation energies). For the purposes of this modelling, it was assumed that pressures were hydrostatic up to the end Miocene isolation of the deep carbonate aquifer in the western Po valley. From the end of the Miocene onwards it was assumed that overpressures increased linearly with time up to the present day overpressure modelled for a particular interval, as described in section 4.4. Other wells included in the dataset showed similar results, with an improved fit to observed maturity data from models incorporating overpressure and over-prediction of maturity using Easy%Ro. Of particular note at Belvedere-1, is the way in which the results of the overpressure algorithms converge with the Easy %Ro model below 7,500m tvdss (Fig.9d). This is due to peak maturity deep within the carbonate section having been achieved in association with the Liassic rift event, long before significant overpressure entered the system. This early maturity was a consequence of the thick syn-rift section deposited at this location, combined with the elevated syn-rift heat flows. Notwithstanding the relatively poor quality and scattered nature

of the maturity data, this analysis would appear to support the contention that overpressure has retarded the thermal maturity of the Triassic source rocks in parts of the Po Valley as maintained by Chiaramonte & Novelli (1986) and Carr (1999).

The Genesis and Trinity 3D modelling software from Zetaware, Inc. used in this study does not incorporate algorithms that include the overpressure effect. It was therefore decided that the most appropriate modelling strategy was to approximate the overpressure effect in the software by applying a reduced heat flow, given that overpressure appears to act to retard maturation (Carr, 1999). Figure 9d shows that the maturity profiles calculated for the Belvedere-1 well using the overpressure algorithms are approximated by a temperature-only maturity model using a heat flow that is 15mW/m^2 lower than the currently observed heat flow at this location. To replicate the overpressure history in the basin, the reduced heat flow model is equal to the geological heat flow up to the end of the Miocene, at which point the heat flow varies linearly to reach a present day value that is 15mW/m^2 lower than the observed present day heat flow. Similar results were obtained for other wells in the dataset. This analysis was also replicated for a number of pseudo-well data points covering the depth range of the Triassic source rocks within the area characterized by overpressure to confirm that the reduced heat flow model satisfactorily replicated the maturity trends generated by the overpressure model.

Figure 11 summarises the 1D modelling results for well and pseudo-well locations in the western, central, east-central and eastern Po Valley. For the western and central Po Valley, two sets of results are provided, one based on the geological heat flow and one which considers the effect of overpressure through application of the reduced heat flow model from end Miocene times. In the western Po Valley, to the west of Milan (Fig. 11a), the Triassic source intervals are shown to have reached maturity during the Miocene as a result of burial beneath the thick sediments deposited in the Alpine foredeep. These source rocks are presently in the late oil window. In contrast, in the central Po Valley to the east of Milan (Fig. 11b), due to the increased thickness of syn-rift Liassic carbonates deposited in the hanging wall to the Gaggiano-Lacchiarella fault system combined with high syn-rift heat flows, Triassic source rocks started generating hydrocarbons during the Jurassic, with renewed generation in the Miocene, and are presently in the late oil to gas windows. For both the western and central Po Valley well locations, the reduced heat flow model shows lower maturity which is attained through the Pliocene to present day. In the western Po Valley, this

equates to the difference between middle oil maturity (%Ro ≈ 0.8) and wet gas maturity (%Ro ≈ 1.3) (discussed further in section 4.5.3).

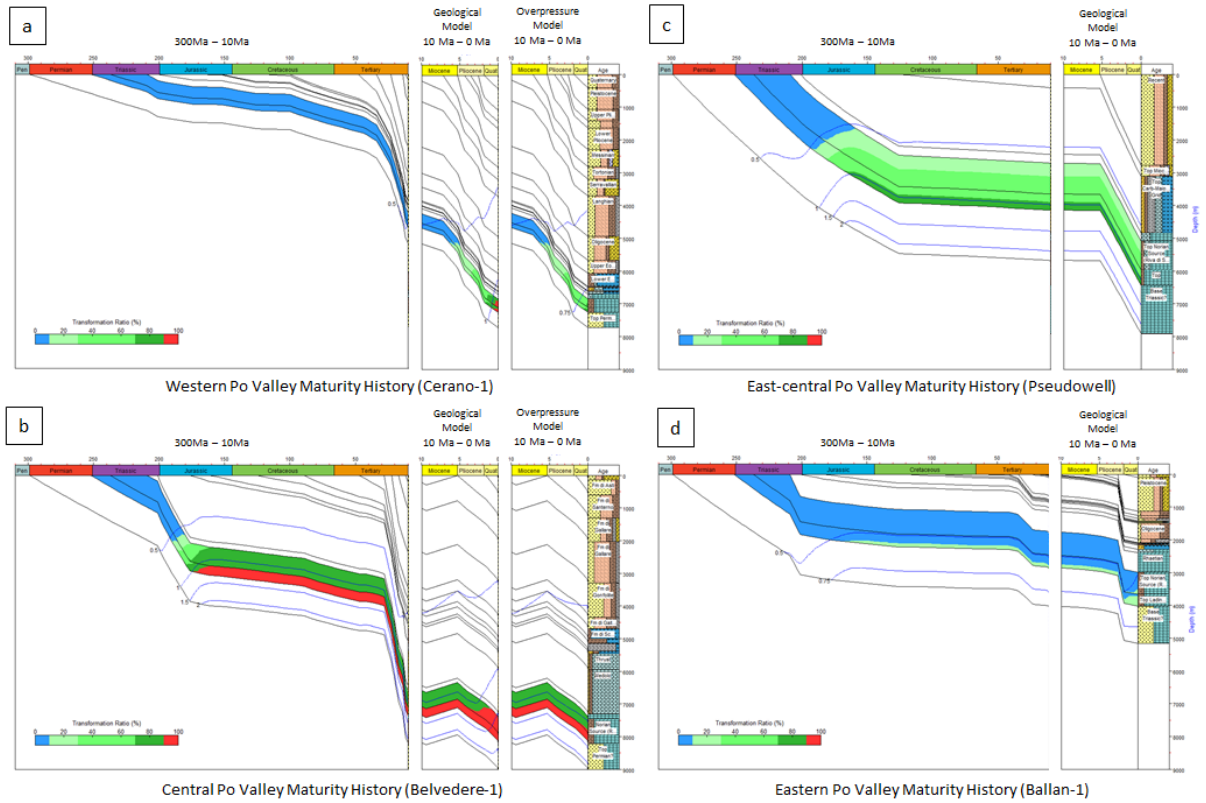

Fig.11 - 1D Transformation Ratio (TR) maturity histories for four wells from the Po Valley based on initial source rock parameters outlined in Table 1: (a) Cerano-1 from the western Po Valley; (b) Belvedere-1 from the central Po Valley; (c) a pseudo-well from the east-central Po Valley; and (d) Ballan-1 from the eastern Po Valley (see Fig. 2 for well locations). Vitrinite reflectance maturities are shown as blue lines. For (a) and (b), two histories are shown for the last 10Ma, one based on the geological heat flow and one based on reduced heat flow from end Miocene times to replicate the effect of overpressure, as described in the text.. (c) and (d) lie outside of the overpressure cell.

Over most of the eastern Po Valley, Middle Triassic source rocks attained early maturity during the Jurassic due to thick carbonate deposition and high heat flows, with only minor increases in maturity to present day as a result of lower heat flow and/or a low sedimentary depositional rate. During the same time interval, Late Triassic source rocks remained immature to very early mature (Fig. 11c). Figure 11d shows a 1D model for part of the Trento Platform in the eastern Po Valley where sedimentation rates remained particularly low. In this

location only limited generation potential is seen, with the early oil window being reached by the mid Triassic source rocks in the late Miocene to Recent, whilst late Triassic source rocks are essentially immature at the present day.

4.5.2 3D thermal modelling and hydrocarbon generation

The results of the 1D modelling and gross depositional environment mapping described above have been integrated with the 3D structural model of Turrini et al (2014, 2015) to create a 3D thermal model of the entire Po Valley foreland basin. Using the 1D well models described in section 4.5.1 as anchor points, two thermal histories for the Po Valley were created and calibrated to best represent the thermal histories of the Middle and Late Triassic source intervals: one based on the geological heat flow model as described in section 4.5 and shown in fig. 10 (i.e. the geological heat flow model) ; the other using reduced heat flow from end Miocene times to replicate the effect of overpressure, as described in the section 4.5.1 (i.e. the overpressure model). The reduced heat flows associated with the overpressure model are confined to the area of the regional scale anticline at Top Triassic level that contains the overpressure cell, as discussed in section 4.4 and as shown in Fig. 2. Outside this area, the two heat flow models are equal.

Figure 12 shows the progressive change in transformation ratio through time across the Po Valley for the Middle and Late Triassic source intervals from the Mesozoic to the end Miocene. For Middle Triassic source rocks early oil maturity is attained during the Jurassic to the east of the Gaggiano Lacchiarella fault system and in most of the eastern Po Valley, while the footwall to the west of the Gaggiano Lacchiarella fault system remains immature (Fig 12a) confirming the results of the 1D modelling discussed above and the results presented by Novelli et al., 1987. This maturity pattern is attributed to high syn-rift heat flows associated with Liassic rifting combined with the deposition of thick sequences of basinal limestones in the hangingwall of the Gaggiano Lacchiarella fault system and of thick shallow marine carbonate deposition in the area of the Trento Platform (Fig. 2) compared with the deposition of thinner basinal sequences west of the Gaggiano-Lacchiarella fault system. Through the Cretaceous only small increases in maturity are observed due to low sedimentation rates in a deep-water, basinal setting, while heat flows during this period return to normal levels for a passive margin setting (Fig. 12b) (Fantoni & Scotti, 2003). Throughout the Jurassic and Cretaceous, the Late Triassic source rocks remain immature, except in the vicinity of locally

thick carbonate deposits, particularly in the central and north-western Po Valley (Fig.12d). Through the early Tertiary and up to the end of the Miocene, increased burial resulting from the increased clastic influx from the Southern Alpine and Northern Apennines thrust belts results in increased burial of both Triassic source intervals and further increases in maturity.

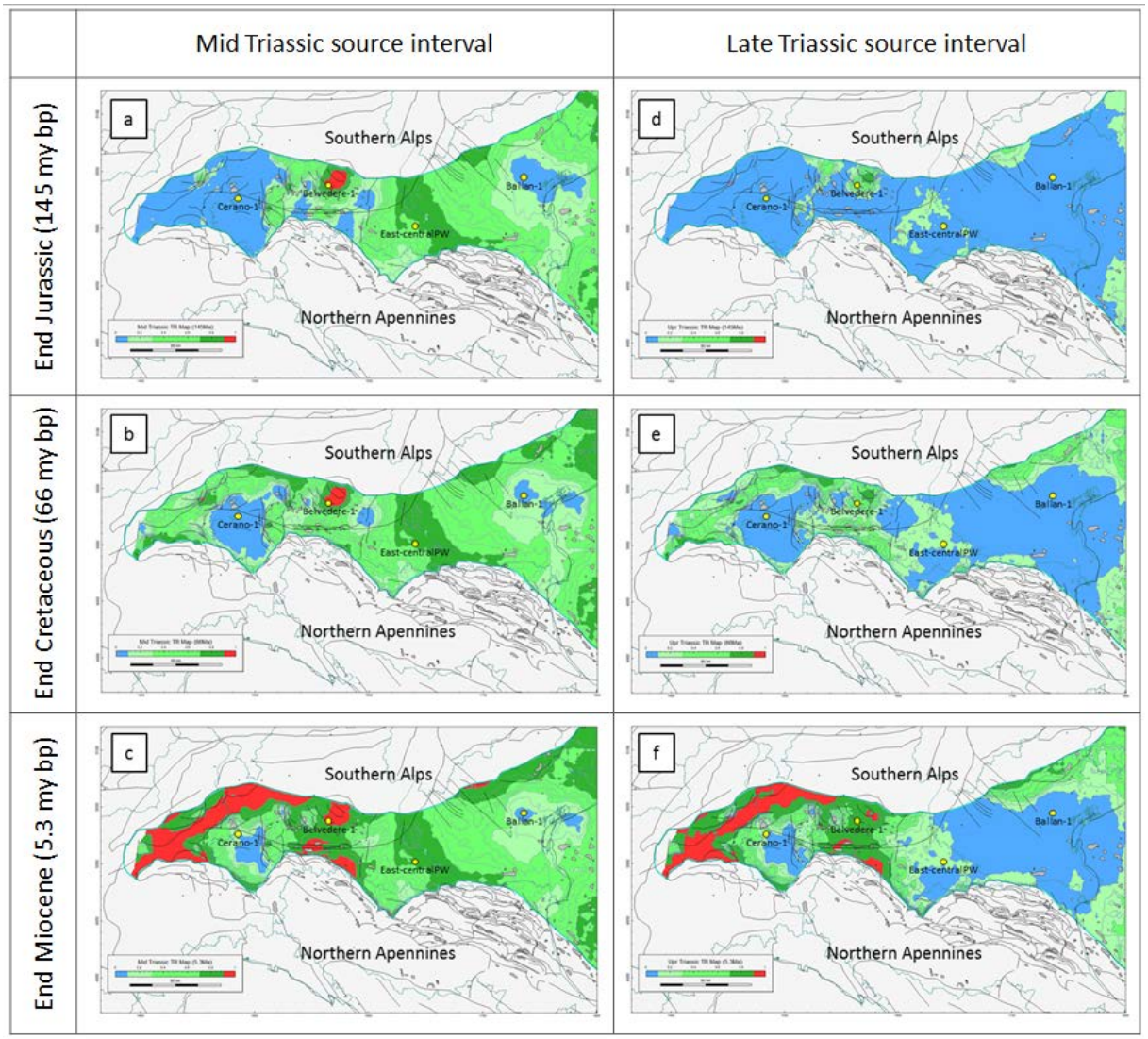

Fig.12 - Transformation ratio (TR) maturity maps for the Middle Triassic (a-c) and the Late Triassic (d-f) source intervals, for end Jurassic (a, d), end-Cretaceous (b, e) and end Miocene (c, f) times. As the onset of overpressure within the carbonate sequences is interpreted to occur at end Miocene, there is no difference between the maturity levels associated with the geological heat flow and the overpressure models for these time intervals.

Locally, where sedimentation rates are highest, such as in portions of the Southern Alpine foredeep, this results in the completion of the kerogen transformation process (Fig 12c). Notwithstanding this, the Liassic structural grain continues to exert an influence on maturity

patterns with much of the Gaggiano footwall and Trento Platform continuing to exhibit low maturities.

During mid to late Miocene times, the deep carbonate aquifer in the western Po Valley becomes isolated and the Triassic source intervals start to experience overpressure, as described in section 4.4. Figure 13 compares the present-day transformation ratio distribution for the geological heat flow and overpressure models.

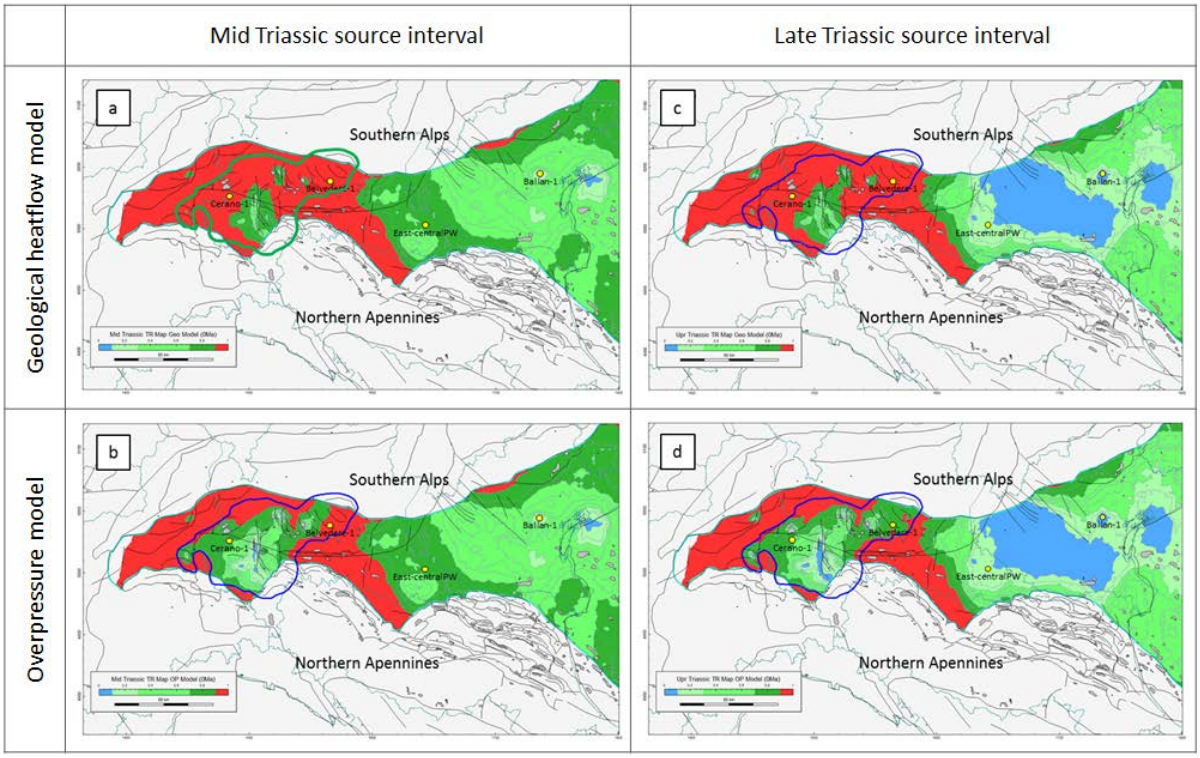

Fig.13 – Present day transformation ratio (TR) maturity maps for the Middle Triassic (a and b) and the Late Triassic (c and d) source intervals. (a) and (c) show the results of geological heat flow model with (b) and (d) showing the results for the overpressure model, based on the application of reduced Plio-Pleistocene heat flow as described in the text. Significantly lower maturity is predicted within the overpressure cell (blue outline) or both source intervals in the overpressure Model.

The high Plio-Pleistocene sedimentation rate results in increased maturity throughout the Po valley, however, as expected, inside the western Po Valley overpressure cell, the increase in maturity is substantially less for the overpressure model than for the geological heat flow model (compare Figs. 13a-c to Figs. 13b-d). This effect is particularly evident over the crest of the Gaggiano footwall: the area shown in blue at end Miocene for both Mid and Late

Triassic intervals (fig. 12c & f), corresponding to a transformation ratio of less than 10%, has completely disappeared at present day for the geological heat flow model (fig 13a & c), whilst for the overpressure model narrow belts with low transformation ratio remain over the crest of the footwall (fig 13b & d).

4.5.3 3D Charge modelling in the western Po Valley

To further compare the geological heat flow and overpressure models, charge modelling for a number of structures within the western Po valley overpressure cell was carried out, and results were then compared against the observed hydrocarbon distribution and properties. This was carried out using the simple kinetic methodology described in Pepper & Corvi (1995a, 1995b) and Pepper and Todd (1995) as implemented in the Trinity Basin Modelling software. Source rock kerogen types and initial HIs and TOCs are defined in section 4.2 and as shown in Table 1. Kitchen areas were defined for each structure based on the area on the present-day top Triassic depth map over which buoyancy forces would drain migrated hydrocarbons towards the relevant structural culmination. The kitchen areas were then further refined by superimposing the source rock polygons from the gross depositional environment maps (GDE maps in Fig.8) on the kitchen areas and using only the areas where the calculated kitchen and source rock polygons coincided. The charge volumes for each trap were then limited to those available after the critical moment for each structure, defined as the later of the moment after the trap formed or the seal became capable of retaining a hydrocarbon column (Fig. 14). The model incorporates the effect of migration losses along the path to the trap, with a loss of 0.75 mmbbl/km^2 considered, derived using the methodology proposed by Mackenzie & Quigley (1988) with a carrier bed thickness of 500m and average porosity of 1.5%. Finally reservoir and topseal parameters are defined to enable the basin model to calculate volumes trapped in each structure with a single Late Triassic reservoir modelled as a 250m thick, 100% net-to-gross slab with an average porosity of 3% (see Bello & Fantoni, 2002 for comparison). Topseal capacity is modelled as 300 psi using simple capillary seal models for pelagic carbonate topseals. Once the basin model had been rerun with these inputs a number of outputs were extracted from the model for traps defined on the 3D structural model that lie within the western Po Valley overpressure cell: namely volume of charge available from the relevant kitchen area since the critical moment, trapped hydrocarbon volume and the GOR of the trapped fluids. Figure 15 shows how these model predictions compare with our estimate of the initially in place hydrocarbon volume (HCIIP) at

each trap and for the GOR of the fluids present in the three main discoveries in the western Po valley.

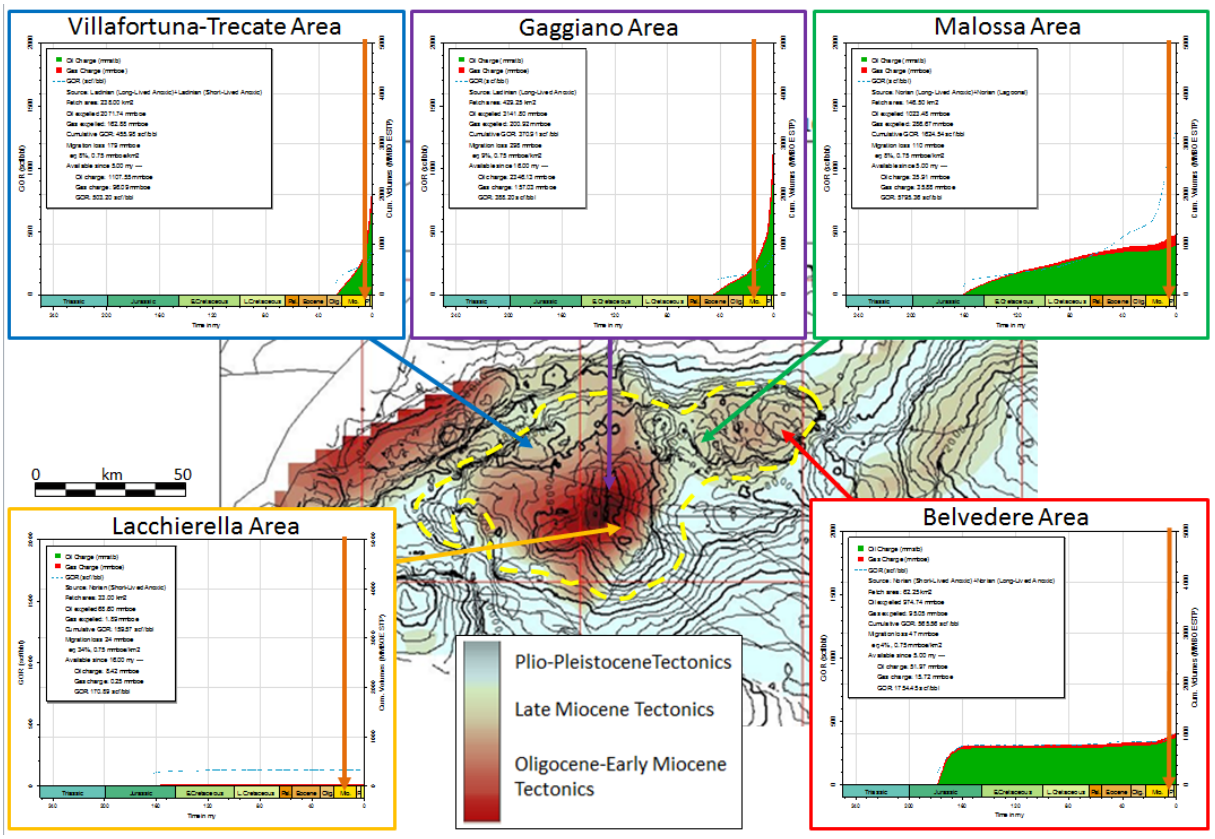

Fig.14 – Charge timing versus trap formation in the Western Po Valley based on preferred Overpressure Model (see text for discussion).

As figure 15 shows, the 3D basin model based on both the geological heat flow model and the overpressure model predict the overall distribution and phase of hydrocarbons in the western Po valley reasonably well. Both models predict significant discoveries at Villafortuna-Trecate and Malossa and a smaller discovery at Gaggiano. Both models predict a rich petroleum system with significant volumes of hydrocarbons being spilled from traps that are full to spill point. This is most evident at Gaggiano where both models predict small trapped volumes to be present due to the small size of the trap in the 3D structural model. However, as this trap is located at the crest of a regional high it accesses a large kitchen area that has generated charge volumes since the Mid-Miocene critical moment some 25 to 50 times larger than the trapped volumes.

Both models also predict liquid hydrocarbons with moderate to low GOR at Villafortuna-Trecate and Gaggiano whilst high GOR fluids are predicted at Malossa.

In detail, however, it is clear that the overpressure model provides a better match to the observed data than the geological heat flow model.

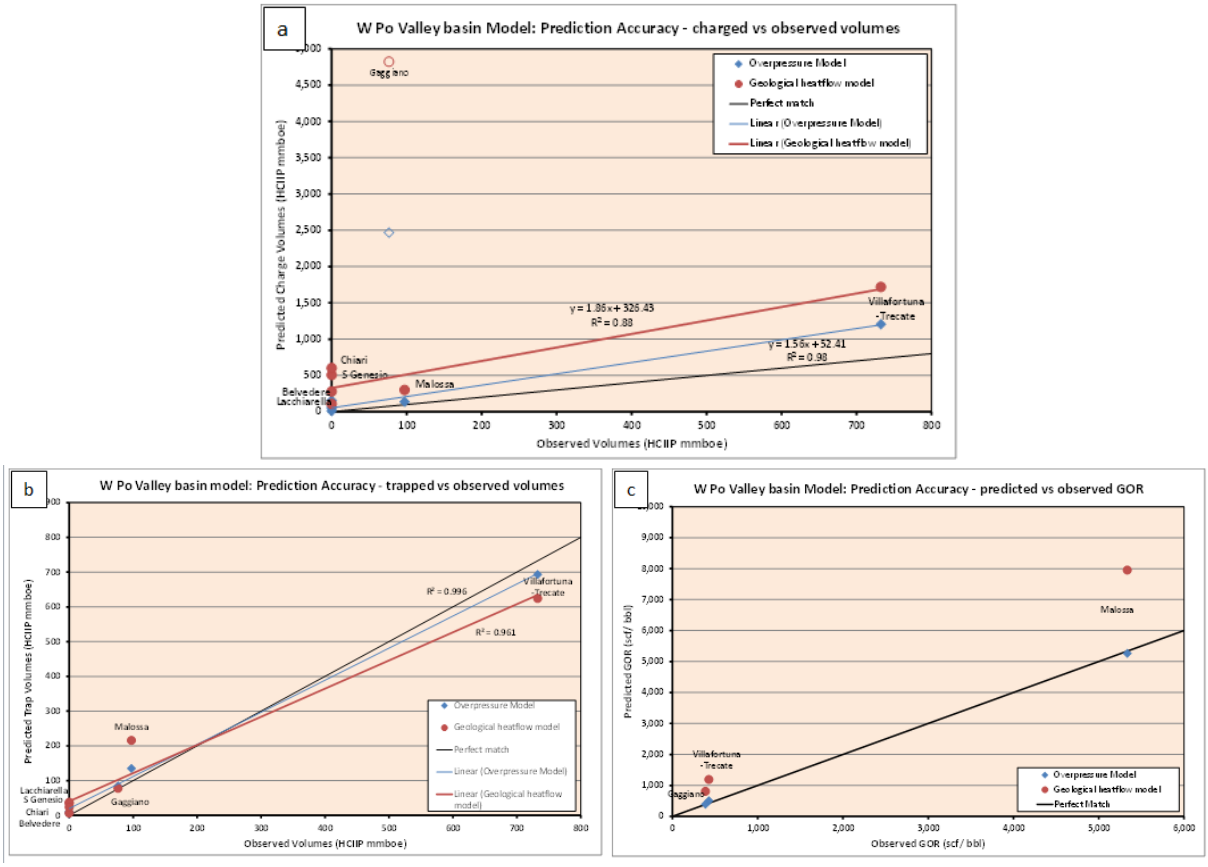

Fig.15 – Model evaluation: (a) cross plot of observed in place volumes for main traps versus available charge from kitchen area since the critical moment predicted by the models, and (b) cross plot of observed in place volumes for main traps versus predicted trapped volumes from the models and (c) cross plot of observed GOR versus GOR predicted from the models. Red data points and regression lines are for the geological heat flow model, blue data points and regression lines are for the overpressure model. For plot (b) regression lines have been fitted to the dataset excluding the Gaggiano outlier. In all plots the black line corresponds to a perfect match between observation and model.

Figure 15a compares calculated trap HCIIP volumes with the predicted charge available from the kitchen area since the critical moment and shows that predictions from the overpressure model (excluding Gaggiano) correlate better with trap HCIIP values than those from the geological heat flow model, largely because the overpressure model can successfully explain the failures in the inversion traps in the Lacchiarella hangingwall (Lacchiarella and San

Genesio) and the deep traps east of Malossa (Chiari, Belvedere), whilst the geological heat flow model predicts significant volumes in several of these traps. Furthermore, charge volumes available to the trap are closer to HCIIP volumes for the overpressure model than for the geological heat flow model, implying smaller volumes being spilled to shallower traps and/ or stratigraphic levels. Given little evidence for large spilled volumes in the Po Valley, the prediction of smaller excess volumes favours the overpressure model. Figure 15b shows how predicted trap volumes from the basin models compare with the calculated trap HCIIP volumes. Given that traps are generally oversupplied with charge in both models there is relatively little difference in the performance of the 2 models. However, Malossa volumes are matched better by the overpressure model as there is a charge limitation on predicted volumes in the trap whilst the geological heat flow model predicts larger volumes with the trap being oversupplied and excess volumes spilled. Finally, figure 15c shows that the overpressure model more successfully predicts fluid phase than the geological heat flow model, which predicts higher maturity fluids with higher GORs than observed for all 3 of the main discoveries.

5. Discussion

The 3D basin model of the Po Valley presented in this paper provides important insights into the geometry and structural evolution of hydrocarbon-bearing traps, and into the generation and migration of hydrocarbons into these traps. However, there is significant uncertainty associated with various aspects of this model and discussion of these and their impact on the results of the model is the subject of this section.

5.1. Structural model uncertainties

The 3D structural model defines the present-day configuration of the Po Valley basin and no kinematic restoration aimed at returning units to their pre-Alpine and/or Mesozoic position has been attempted to date. Hence the modelling approach applied to the evolution of the Mesozoic petroleum system is a conventional one, consisting of vertical back-stripping to describe the tectono-stratigraphic evolution of the basin (see Gusterhuber et al., 2013 and Neumaier et al., 2014 for a 2D kinematic approach of complex petroleum system modelling). Notwithstanding this, we believe the results of the model presented above are valid because:

1. the model has been restricted to the foreland domain, characterized by low deformation and in which vertical displacements are more significant than horizontal ones (Cassano et al., 1986; Turrini et al., 2014). Locally, thrust faults can create a late tectonic over-thickening of the thrust section, particularly where a hangingwall ramp is juxtaposed with a footwall ramp. This is erroneously incorporated into the model as a syn-depositional stratigraphic thickening. An example occurs in the Medolo Formation in the Belvedere well, where an estimated 500m of tectonic thickening occurs on a Miocene thrust fault. This is incorporated into the model as stratigraphic thickening of the Medolo Formation and contributes to the high transformation ratio in the vicinity of the Belvedere well shown at end Jurassic times (Figs 12a and d). However, sensitivity modelling indicates that the effect is minor and local, given the relatively small scale of the thrusting involved, and does not impact the validity of the regional results presented previously;
2. the model confirms earlier studies (Novelli et al., 1987; Mattavelli and Novelli, 1987; Mattavelli et al., 1993; Lindquist, 1999; Bertello et al., 2010) and shows hydrocarbon generation occurring in 2 phases: a Jurassic phase and an Alpine Tertiary phase, which commences in the Oligocene but is mainly concentrated into the last 5-10 million years (Figs 11, 12, 13 & 14). The vertical back-stripping approach utilized here approximately describes the recent evolution of the system, covering the bulk of hydrocarbons generated during the Alpine phase. The model will not adequately describe generation and expulsion of hydrocarbons during the earlier Jurassic phase as trap distribution and geometry were substantially different during this phase. However, the effective charge in the models discussed previously has been limited to post the critical moment, which generally occurs at some point in the Miocene. Consequently hydrocarbons generated earlier are lost to the system and deemed to have leaked to the surface. Given the above, it is not considered that the lack of structural restoration in the model renders the results presented here invalid, although any possible re-migration from reactivated Mesozoic traps has not been considered.

A further simplification in the model is that all surfaces other than the base Pliocene surface have been modelled as conformities. In particular a number of erosional unconformities earlier in the Tertiary have been neglected, due to insufficient data to model them at the regional scale of the model. The literature on the region (Pieri & Groppi, 1981;

Cassano et al., 1986; Ghielmi et al., 2013; Rossi et al., 2015) suggests that: a) erosion of Mesozoic sediments did not occur on a regional-scale, but was restricted to locally uplifted areas, such as the syn-rift footwall erosion experienced over the crest of the Gaggiano footwall, b) erosion of Tertiary deposits associated with intra-Tertiary unconformities is in the order of few hundred meters. Consequently, given limited pre-Pliocene erosion and high Pliocene-Pleistocene sedimentation rates, it is likely that Mesozoic source rocks are at maximum depth of burial and peak thermal maturity at the present day across the vast majority of the basin (Ghielmi et al., 2013; Rossi et al., 2015). Given the limited and local nature of the pre-Pliocene unconformities, it is considered unlikely that their absence from the model significantly affects results, although it may result in some local errors in the maturation history.

5.2. Petroleum systems uncertainties

The main uncertainty pertaining to the petroleum systems analysed here is the source rock distribution as described in the basin model, consisting of both the position and areal extent of the source polygons (Fig. 8b and c) which have been defined based on the gross depositional environment maps, and the net source thicknesses assigned. Given the paucity of data on which these inputs are based there is considerable uncertainty in these aspects of the model. The models applied here are strongly based on outcrop information from the Southern Alps and it should be noted that the South Alpine Front, which separates the outcrops from the subsurface of the Po Valley, is a Tertiary feature with an estimated 50-70 km of shortening (Handy et al., 2014 and references therein). Given this, considerable uncertainty exists in correlating from the outcrop to the subsurface. It is also worth noting that, given the exploration focus of this study, the source rock distribution defined here includes a number of postulated source basins, particularly in the eastern Po Valley and the Adriatic offshore.

A further potential issue arises in the interpretation of the failure wells in the western Po Valley. In section 4.5, the ability of the overpressure model to explain these failures as arising due to lack of access to recent charge was used as a reason for preferring the overpressure model to the geological heat flow model, which predicts the availability of significant recent charge volumes to these traps. Clearly there is a range of other potential failure mechanisms, unrelated to source rock that could explain these well results.

Notwithstanding these uncertainties, however, the models are capable of explaining most first order features relating to hydrocarbon distribution in the Po Valley. Given this, they can be considered as viable realizations, whilst recognising that alternative models may also

be able to explain the observed features. The overpressure model is preferred to the geological heat flow model because a) it is more consistent with the available maturity data (Fig. 9d) and b) it provides a better explanation of the observed distribution and nature of hydrocarbons in the subsurface of the Po Valley (Fig. 15). This conclusion is considered robust in the face of the uncertainties discussed in that whilst it would undoubtedly be possible to amend the model to obtain an equally good fit with the geological heat flow model, the necessary changes would be non-systematic, ad hoc and unsupported by available data.

6. Conclusions

This study develops the recent Po Valley 3D structural model (Turrini et al., 2014 and 2015) by using it as an input for a basin modelling exercise. Despite the relative simplicity of the modelling approach adopted (lack of palinspastic restoration and lack of local structural detail in the regional model) and high levels of uncertainty, particularly as regards source rock distribution, the model provides for the first time a unique integration of the 3D structures with their thermal history and the related hydrocarbon maturation/generation process across the entire Po Valley basin.

The 1D model confirms that, for wells where data in the Mesozoic carbonates are available, thermal maturity can be significantly over-predicted using models based on temperature history only. In contrast, when the effects of the substantial overpressure observed in the western Po Valley wells are incorporated into the prediction of thermal maturity, the model seems to produce much better fits to the observed data. Two maturity models were then generated from the Po Valley 3D structural model: one based on the geological heat flow model and another based on a reduced heat flow model, aimed at replicating the retarding effects of overpressure on hydrocarbon generation.

When compared with the observed distribution of hydrocarbons, the results from the modelling suggest that, at the regional scale, both maturity models appear consistent with the observed hydrocarbon distribution. However, in detail, the overpressure model provides a better match between calculated trap HCIIP volumes and predicted charge available from the kitchen area since the critical moment and also predicts hydrocarbon phase (as measured by GOR) more accurately than the geological heat flow model.

It is concluded that overpressure has significantly retarded hydrocarbon maturation in the western Po valley, as proposed by earlier authors (Chiaramonte and Novelli, 1986, Carr, 1999), on the basis that the overpressure model provides an improved match to both observed maturity data and the observed distribution and nature of hydrocarbons in the subsurface.

The study confirms the importance to the development of a successful petroleum system in the Po valley of both the main tectonic phases experienced in the basin: Mesozoic extension, associated with opening of Tethys, and Tertiary Alpine compression, associated with the closure of Tethys. The earlier phase controlled reservoir and source distribution, trap formation (e.g. Gaggiano) and the early phases of hydrocarbon maturation in subsiding half grabens associated with high heat flows and substantial syn to early post-rift sediment accumulation. The latter phase controlled trap formation, either by generating new traps (Cavone) or by reactivating older ones inherited from the Mesozoic extensional phase (Villafortuna-Trecate, Malossa), and regional hydrocarbon maturation and expulsion related to rapid foredeep burial ahead of the evolving southern Alpine and northern Apenninic thrust belts. From a hydrocarbon exploration point of view, two main conclusions can be drawn:

1. In the Western Po Valley the timing of hydrocarbon maturation is favourable for exploration. Trap formation is thought to have occurred during the Oligocene to late Miocene, with the timing of significant hydrocarbon generation and expulsion expected to have occurred post-Miocene.
2. In the Eastern Po Valley, timing is less favourable as traps - Plio-Pleistocene in age - tend to either post-date the main hydrocarbon generation phase, or generation is at a very early stage and is not far enough advanced for migration to occur, or for traps to be filled.

References

Andreatta, C., Dal Piaz, G., Vardabasso, S., Fabiani, R., Dal Piaz, G., 1957. Carta geologica delle Tre Venezie, scale 1:100,000, Map "10-Bolzano".

Assereto, R., Jadoul, F., Omenetto, P., 1977. Stratigrafia e metallogenesi del settore occidentale del distretto a Pb, Zn, fluorite e barite di Gorno (Alpi bergamasche) - Riv. Ital. Paleont., 83, 3, 395-532.

Bello. M., Fantoni, R., 2002. Deep oil plays in the Po Valley: Deformation and hydrocarbon generation in a deformed foreland – AAPG HEDBERG CONFERENCE, "Deformation History, Fluid Flow Reconstruction and Reservoir Appraisal in Foreland Fold and Thrust Belts" May 14-18, 2002, Palermo – Mondello (Sicily, Italy).

Berra, F., Carminati, E., 2010. Subsidence history from a backstripping analysis of the Permo-Mesozoic succession of the Central Southern Alps (Northern Italy). Basin Research, 22, 952-975.

Berra F., Galli M.T., Reghellin F., Torricelli S., Fantoni R., 2009. Stratigraphic evolution of the Triassic-Jurassic succession in the Western Southern Alps (Italy) : the record of the two-stage rifting on the distal passive margin of Adria– Basin Research, 21, 335-353.

Bersezio, R. & Bellantani, G., 1997. The thermal maturity of the Southalpine mesozoic succession north of Bergamo by vitrinite reflectance data. Atti Tic.Sc.Terra, 5, 101-114.

Bertello. F., Fantoni, R., Franciosi, R., Gatti, V, Ghielmi, M., Pugliese, A., 2010. From thrust-and-fold belt to foreland: hydrocarbon occurrences in Italy. VINING, B.A. & PICKERING, S. C. (eds) Petroleum Geology: From Mature Basins to New Frontiers – Proceedings of the 7th Petroleum Geology Conference, 113–126. DOI: 10.1144/0070113 # Petroleum Geology Conferences Ltd. Published by the Geological Society, London.

Bertotti G., Picotti V., Bernoulli D., Castellarin A.,1993. From rifting to drifting: tectonic evolution of the South-Alpine upper crust from the Triassic to the Early Cretaceous – Sedimentary Geology, 86, 53-76.

Bongiorni, D., 1987. La ricerca di idrocarburi negli alti strutturali mesozoici della Pianura Padana: l'esempio di Gaggiano – Atti Tic. Sc. Terra Vol. XXXI, pp. 125-141.

Brack, P., Rieber, H., 1993. Towards a better definition of the Anisian/Ladinian boundary : New biostratigraphic data and correlations of boundary sections from the Southern Alps. Eclogae geol. Helv. 86/2: 415-527.

Braga, Gp., Castellarin, A., Corsi, M., De Vecchi, Gp., Gatto, Gino., Gatti, Giuseppe, Largaiolli, T., Monese, A., Mozzi, G., Rui, A., Sassi, F.P., Zirpoli, G., 1968. Carta Geologica D'Italia, scale 1:100,000, Map "36-Schio".

Burnham, A.K., and Sweeney, J.J., 1989, A chemical kinetic model of vitrinite maturation and reflectance: Geochimica et Cosmochimica Acta, v. 53, p. 2649–2657.

Calabrò R., Ceriani A., Di Giulio A., Fantoni R., F. Lino, Scotti P, 2003. Thermal history of syn-rift successions between the Iseo Basin and the Trento Plateau: results from the integrated study of organic matter maturity and fluid inclusions. Atti Tic. Sc. Terra, serie sp. v. 9, pp. 88-91.

Cantelli, C., Carloni, G.C., Castellarin, A., Ceretti, E., Colantoni, P., Cremonini, G., Elmi, C., Frascari, F., Monesi, F., Pisa, G., Rabbi, E., Tomadin, L., Vai, G.B., Braga, Gp., Corsi, M., Gatto, G., Locatelli, D., Rui, A., Sassi, P., Zirpoli, G., Dal Cin, R., Largaiolli, T., Gatto, G.O., 1971. Carta Geologica D'Italia, scale 1:100 000, Map "4C-13- Monte Cavallino-Ampezzo".

Carannante, S., Argnani, A., Augliera, P., Cattaneo, M., D'Alema, E., Franceschina, G., Lovati, S., Massa, M., Monachesi, G., Moretti, M., 2014. Risultati da Progetto Sismologico S1 (INGV-DPC 2013) Base-knowledge improvement for assessing the seismogenic potential of Italy Section n: D18/b2 Relocated seismicity in the Po Plain. Workshop Terremoto Emilia 2012, Roma 26 Maggio 201.

Carminati, E., Doglioni,C., 2012. Alps vs. Apennines: the paradigm of a tectonically asymmetric Earth. Earth-Science Reviews, 112, 67-96.

Carminati, E., Cavazza, D., Scrocca, D., Fantoni, R., Scotti, P., Doglioni, C., 2010. Thermal and tectonic evolution of the southern Alps (northern Italy) rifting: Coupled organic matter maturity analysis and thermokinematic modelling. AAPG Bulletin, v. 94, no. 3 (March 2010), pp. 369–397.

Carr, A.D., 1999. A vitrinite reflectance kinetic model incorporating overpressure retardation. Marine and Petroleum Geology, 16, 355-377.

Carulli, G.B, Salvador, G.L., Ponton, M., Podda, F., 1997. La dolomia di forni: evoluzione di un bacino euxinico tardo triassico nelle prealpi carniche. Boll. Soc. Geol. It., 116, 95-107.

Casati, P., Assereto, R., Comizzoli, G., Passeri, L.D., Boni, A., Cassinis, G., Cerro, A., Rosetti, R., Accordi, B., Dieni, I., Malaroda, R., Bianchi, A., Cevales, G., Dal Piaz, Gb., Morgante, S., 1970. Carta Geologica D'Italia scale 1:100,000, Map "34- Breno".

Casero, P., 2004. Structural setting of petroleum exploration plays in Italy. In Crescenti, V., D'Offizi, S., Merlino, S., Sacchi, L. (Eds), Geology of Italy. Special Volume of the Italian Geological Society for the IGC 32nd, Florence, 189-199.

Cassano, E., Anelli, L., Fichera, R., Cappelli, V., 1986. Pianura Padana, interpretazione integrata di dati Geofisici e Geologici. - 73° congresso Soc. Geol. It., Roma.

Castellarin, A., Vai, G.B., 1982. Introduzione alla geologia strutturale del Sudalpino. In: Castellarin, A., Vai,G.B., - Guida alla gelogia del Sudalpino centro orientale. Guide Geol. Reg., Soc.Geol.It., 1-22.

Castellarin A., Eva C., Giglia G., Vai G.B., Rabbi E., Pini G.A. & Crestana G., 1985. Analisi strutturale del Fronte Appenninico Padano. Giornale di Geologia, 47, pp.47-75.

Castellarin, A., 2001. Alps-Apennines and Po Plain-Frontal Apennines relationships. In: VAI G. B. & MARTINI I. P. (Eds.), Anatomy of an Orogen. The Apennines and adjacent Mediterranean Basins, Kluver, London, 177- 196.

Castiglioni,B., Leonardi, P., Merla, G., Trevisan., Zenari, S., 1940. Carta geologica delle Tre Venezie, scale 1:100,000, Map "12- Pieve di Cadore".

Castiglioni, B., Boyer, G., Leonardi, P., Venzio, S., Dal Piaz, G., Vialli, V., Zenari, S., 1941. Carta geologica delle Tre Venezie, scale 1:100,000, Map "23- Belluno".

Cati, A., Sartorio, D., Venturini, S., 1987. Carbonate platforms in the subsurface of the northern Adriatic area. Mem.Soc. Geol.It., v.40. pp. 295-308.

Ciarapica, G., Cirilli, S., D'Argenio, B., Marsella, E., Passeri, L., Zaninetti, L., 1986. Late Triassic open and euxinic basins in Italy. Rend.Soc.Geol.It., 9, pp.157-166.

Chiaramonte, M.,A., Novelli, L., 1986. Organic matter maturation in Northern Italy: some determining agents. Org. Geochem., 10, 281-290.

Dal Piaz, G., Venzo,S., Fabiani, R., Trevisan, L., Pia, J., 1946. Carta geologica delle Tre Venezie, scale 1:100,000, Map "37-Bassano del Grappa".

Defant, A., 1961. Physical Oceanography, Vol. 1, Pergamon Press, 728 pp.

Della Vedova, B., Bellani, S., Pellis, G., Squarci, P., 2001. Deep temperatures and surface heat flow distribution. In: VAI G.B. & MARTINI I.P. (Eds.): "Anatomy of an orogen: the Apenninesand adjacent Mediterranean basins". Kluwer Academic Publishers: 65-76, Dordrecht, The Netherlands.

Desio, A., Venzo, S., 1954. Carta Geologica D'Italia, scale 1:100,000, Map "33- Bergamo".

Dewey, J.F.; Pitman, C., Ryan, B. F., Bonnin, J. 1973. Plate tectonics and the evolution of the Alpine systems. Geological Society of America Bulletin, 84, 3,137-80.

De Zanche, V., Gianolla, P., Roghi, G., 2000. Carnian stratigraphy in the Raibl/Cave del Predil area (Julian Alps, Italy). Eclogae. Geol. Helv., 93, 331–347.

Doglioni, C., Bosellini, A., 1987. Eo-Alpine and meso-Alpine tectonics in the Southern Alps. Geol. Rundsch. 76 (3), 735–754.

Di Giulio, A., Mancin, N., Martelli, L., Sani, F., 2013. Foredeep palaeobathymetryand subsidence trends during advancing then retreating subduction: the Northern Apennine case (Oligocene-Miocene, Italy). Basin Research (2013) 25, 260–284, doi: 10.1111/bre.12002.

Errico, G., Groppi, G., Savelli, S., Vaghi G.C., 1980. Malossa Field: a deep discovery in the Po Valley, Italy – AAPG Memoir 30, 525-538.

Fantoni, R., Bello, M., Ronchi, P., Scotti, P., 2002. Po Valley oil play – From the Villafortuna-Trecate field to South Alpine and Northern Apennine exploration. EAGE 64th Conference & Exhibition — Florence, Italy, 27 - 30 May 2002.

Fantoni, R., Scotti, P., 2003. Thermal record of the Mesozoic extensional tectonics in the Southern Alps – Atti Ticinensi di Scienze della Terra 9, 96-101.

Fantoni, R., Decarus, A., Fantoni E., 2003. Mesozoic extension at the Western margin of the Southern Alps (Northern Piedmont, Italy) – Atti Ticinensi di Scienze della Terra 44, 97-110.

Fantoni, R., Bersezio, R., Forcella, F., 2004. Alpine structure and deformation chronology at the Southern Alps-Po Plain border in Lombardy. Boll.Soc.Geol.It., 123 (2004), 463-476.

Fantoni R., Franciosi R., 2010. Tectono-sedimentary setting of the Po Plain and Adriatic foreland - Rend.Fis.Acc.Lincei, 21, (Suppl 1):S197-S209, DOI 10.1007/s12210-010-0102-4.

Franciosi R. & Vignolo A., 2002. Northern Adriatic foreland- a promising setting for the south Alpine Mid-Triassic Petroleum system. EAGE 64th Conference & Exhibitions, Florence, Italy, 27-30May 2002.

Galli, M.T., Jadoul, F., Bernasconi, S.M., Cirilli, S., Weissert, H., 2007. Stratigraphy and palaeoenvironmental analysis of the Triassic-Jurassic transition in the western Southern Alps (Northern Italy). Palaeogeography, Palaeoclimatology, Palaeoecology, 44, 52-70

Gatto, G.O., Gatto, P., Baggio, P., De Vecchi, Gp., Mezzacasa, G., Piccirillo, E., Zirpoli, G., Friz., Gatto, G., Corsi, M., Sassi, F.P., Monese,A., Gregnanin, A., Zilian, T., Largaiolli, T., 1969. Carta Geologica D'Italia, scale 1:100,000, Map "1 & 4A- Passo del Brennero and Bressanone".

Gatto, P., Rui, A., Dal Pra,A., De Zanche,V., Gatto, G., Gatto, G.O., Corsi, M., Nardin, M., Sacerdoti, M., Largaiolli, T., Ghezzo, C., D'Amico, C., 1968. Carta Geologica D'Italia, scale 1:100,000, Map "21-Trento".

Gerdes, M.L., Baumgartner, L.P., Valley, J.W., 1999. Stable isotopic evidence for limited fluid flow through dolomitic marble in the Adamello contact aureole, Cima Uzza, Italy. Journal of Petrology;40:853-872.

Ghielmi, M., Minervini, M., Nini, C., Rogledi, S., Rossi, M., 2012. Late Miocene-Middle Pleistocene sequences in the Po Plain and the Northern Adriatic Sea (Italy): The stratigraphic record of modification phases affecting a complex foreland basin. Marine and Petroleum Geology, http://dx.doi.org/ 10.1016/j.marpetgeo.2012.11.007.

Gianolla, P., De Zanche, V., Mietto, P., 2012. Triassic sequence stratigraphy in the Southern Alps (Northern Italy): definition of sequences and basin evolution. SEPM Special Publication No. 60, ISBN 1-56576-043-3.

Gnaccolini, M., Jadoul, F., 1990. Carbonate platform, lagoon and delta "high-frequency" cycles from the Carnian of Lombardy (Southern Alps, Italy). Sedimentary Geology, 67, 143-159.

Gortani, M., Desio, A., 1925. Carta geologica delle Tre Venezie, scale 1:100,000, Map "14- Pontebba".

Greber, E., W. Leu, D. Bernoulli, M. Schumacher, and R. Wyss, 1997. Hydrocarbon provinces in the Swiss southern Alps—A gas geochemistry and basin modelling study. Marine and Petroleum Geology, v. 14, p. 3–25, doi:10.1016/S0264-8172(96)00037-2.

Gretener, P.E., 1981. Geothermics: using temperature in hydrocarbon exploration. AAPG, Short Course Notes, 17.

Grobe, A., Littke, R., Sachse, V., Leythaeuser, D., 2015. Burial history and thermal maturity of Mesozoic rocks of the Dolomites, Northern Italy. Swiss Geological Society, doi 10.1007/s00015-015-0191-2.

Gusterhuber, J., Hinsch, R., Sachsenhofer, R.F., 2014. Evaluation of hydrocarbon generation and migration in the Molasse fold and thrust belt (Central Eastern Alps, Austria) using structural and thermal basin models. AAPG Bulletin, v. 98, no. 2, pp. 253–277.

Handy, R., Ustaszewski, K., Kissling, E., 2014. Reconstructing the Alps-Carpathians-Dinarides as a key to understanding switches in subduction polarity, slab gaps and surface motion. International Journal of Earth Science (Geol Rundsch) - DOI 10.1007/s00531-014-1060-3.

Jadoul, F. 1986, Stratigrafia e Paleogeografia del Norico nelle Prealpi bergamasche occidentali. Riv.It.Paleoont.Strat, v.91,n.4 pp.479-512.

Jadoul, F., Berra F. 7 Frisia, S., 1992. Stratigrafic and palaeogeographic evolution of a carbonate platform in an extensional tectonic regime:the example of the Dolomia Principale in Lombardy (Italy). Riv.It.Paleont.Strat., v.98,n.1,pp.29-44.

Jadoul, F., Nicora A., Ortenzi A., Pohar C., 2002. Ladinian stratigraphy and palaeogeography of the Southern Val Canale (Pontebbano-Tarvisiano, Julian Alps, Italy). Mem Soc.geol It., v57, pp29-43.

Jarvie, D.M.., Claxton, B.L., Henk, F., Breyer, J.T., 2001. Oil and Shale Gas from the Barnett Shale, Ft. Worth Basin, Texas, AAPG National Convention, June 3-6, 2001, Denver, CO, AAPG Bull. Vol. 85, No. 13 (Supplement), p.A100.

Katz, B.J., Dittmar, E.I., Ehret, G.E., 2000. A geochemical review of carbonate source rocks in Italy. Journal of Petroleum Geology, v.23 (4), pp.399-424.

Keim, L., Spötl, C., and Brandner, R., 2006. The aftermath of the Carnian carbonate platform demise: a basinal perspective (Dolomites, Southern Alps): Sedimentology, v. 53 p. 361-386, doi: 10.1111/j.1365-3091.2006.00768.x.

Lindquist, S.J., 1999. Petroleum systems of the Po Basin province of northern Italy and the northern Adriatic Sea; U.S. Geological Survey Open-File Report 99-50-M, 19 p., 15 figs., 3 tables.

Lipparini, T., Perrella, G., Medioli, F., Venzo,S., Barbier, F., Malaroda, R., Sturani, C., Carraro, F., Zanella, E., Corsi, M., Gatto, G., Piccoli, G., 1969. Carta Geologica D'Italia, scale 1:100,000, Map "48-Peschiera del Garda".

Mackenzie, A. S., & Quigley, T. M. (1988). Principles of geochemical prospect appraisal. AAPG Bulletin, 72(4), 399-415.

Mann, D. M., Mackenzie, A. S., 1990. Prediction of pore fluid pressures in sedimentary basins: Marine and Petroleum Geology, 7, no. 1, 55–65, http://dx.doi.org/10.1016/0264-8172(90)90056-M.

Masetti, D., Fantoni, R., Romano, R., Sartorio, D., Trevisani, E., 2012. Tectonostratigraphic evolution of the Jurassic extensional basins of the eastern southern Alps and Adriatic foreland based on an integrated study of surface and subsurface data. AAPG Bulletin, v. 96, no. 11, pp. 2065–2089.

Mattavelli, L., Novelli, L., 1987. Origin of the Po basin hydrocarbons – Mémoires de la Société Géologique de France, nouvelle série. 151; 97-106.

Mattavelli, L., Margarucci, V., 1992. Malossa Field – Italy, Po Basin, in Foster, N.H., and Beaumont, E.A., Treatise of Petroleum Geology, Atlas of Oil and Gas Fields, Structural Traps VII: Tulsa, OK, American Association of Petroleum Geologists, p. 119-137.

Mattavelli, L., Pieri, M., Groppi, G., 1993. Petroleum exploration in Italy: a review. Marine and Petroleum Geology, 10, 410-425.

Mattirolo, E. Novarese, V., Franchi, S., Stella, A., 1927. Carta Geologica D'Italia, scale 1:100 000, Map "30-Varallo".

Michetti, A.M., Giardina, F., Livio, F., Mueller, K., Serva, L., Sileo, G., Vittori, E., Devoti, R., Riguzzi, F., Carcano, C., Rogledi, S., Bonadeo, L., Brunamonte, F., Fioraso, G., 2013. Active compressional tectonics, Quaternary capable faults, and the seismic landscape of the Po Plain (northern Italy). Ann. Geophys. 55 (5), 969–1001, doi:10.4401/ag-5462.

Middleton M. (1993) A transient method of measuring the thermal properties of rocks. Geophysics, 58, 357-365.

Nardin, M., Rossi, D., Sommavilla, E., Largaiolli, T., Mozzi, G., Gregnanin, A., Zulian, T., Zirpoli, G., Corsi, M., Gatto, G.O., Gatto, P., Graga, Gp., Rui, a., 1970. Carta Geologica D'Italia, scale 1:100,000, Map "22- Feltre".

Nardon, S., Marzorati, D., Bernasconi, A., Cornini, S., Gonfalini, M., Mosconi, S., Romano, A., Terdich, P., 1991. Fractured carbonate reservoir characterization and modelling a multidisciplinary case study from the Cavone oil field, Italy: First Break, 9, 12, 553-565.

Neumaier, M., Littke, R., Hantschel, T., Maerten, L., Joonnekindt, T., Kukla, P., 2014. Integrated charge and seal assessment in the Monagas fold and thrust belt of Venezuela. AAPG Bulletin, v. 98, no. 7, pp. 1325–1350.

Novelli, L., Chiaramonte, M. A., Mattavelli, L., Pizzi, G., Sartori, L., Scotti, P., 1987. Oil habitat in the northwestern Po Basin, in B. Doligez, ed., Migration of hydrocarbons in sedimentary basins: Paris, Editions Technip, p. 27–57.

Pasquale,V., Gola, G., Chiozzi,P., Verdoya, M., 2011. Thermophysical properties of the Po Basin rocks. Geophys. J. Int., 186, 69–81. doi: 10.1111/j.1365-246X.2011.05040.x

Pasquale,V., Chiozzi, P., Verdoya, M., Gola, G., 2012. Heat flow in theWestern Po Basin and the surrounding orogenic belts. Geophys. J. Int., 190, 8–22. doi: 10.1111/j.1365-246X.2012.05486.x.

Passeri, L.D., Comizzoli, G., Assereto, R., 1967. Carta Geologica D'Italia, scale 1:100,000, Map "14 A-Tarvisio".

Pennacchioni, G., Di Toro, G., Brack, P., Menegon, L., Villa, I.M., 2006. Brittle–ductile–brittle deformation during cooling of tonalite (Adamello, Southern Italian Alps). Tectonophysics 427, 171–197.

Pepper, A. S., Corvi, P.J., 1995a. Simple kinetic models of petroleum formation. Part I: Oil and Gas generation from kerogen. Marine and Petroleum Geology, v. 12, no. 3, p. 291-319.

Pepper, A. S., Corvi, P.J., 1995b. Simple kinetic models of petroleum formation. Part III: Modelling an open system. Marine and Petroleum Geology, v. 12, no. 4, p. 417-452.

Pepper, A.S., Dodd, T.A., 1995. Simple kinetic models of petroleum formation. Part II : oil-gas cracking. Marine and Petroleum Geology, v. 12, no. 3, p. 321-340.

Pieri, M., Groppi,G., 1981. Subsurface geological structure of the Po Plain, Italy. Prog.Fin. Geodinamica CNR, pubbl.414, Roma, 1-113.

Pieri M., 1984. Storia delle ricerche nel sottosuolo padano fino alle ricostruzioni attuali – Cento anni di geologia Italiana, Volume Giubilare, 1° Centenario della Soc.Geol.Ital. 1881-1981, Roma, 155-177.

Pieri, M., 2001, Italian petroleum geology- In: G.B.Vai and I.P. Martini (eds), Anatomy of an Orogen: the Apennines and Adjacent Mediterranean Basins, pp.533-550.

Pietro, B., Raffaele, D., & Diego, G. (1979, January 1). Deep Drilling In Po Valley : Planning Criteria And Field Results. Society of Petroleum Engineers. doi:10.2118/7847-MS

Pfiffner, A., 2014. Geology of the Alps. Wiley Blackwell, pp. 368.

Ponton, M., 2010. Architettura delle Alpi Friulane. Museo Friulano di Storia Naturale, Publ. N° 52, Udine, ISBN 9788888192529.

Porro, C., 1921. In tema di ricerche di petrolio in Italia; La miniera italiana, 5, 137-156, 10 ff, Roma.

Ravaglia, A., Seno, S., Toscani, G., Fantoni, R., 2006. Mesozoic extension controlling the Southern Alps thrust front geometry under the Po Plain, Italy: Insights from sandbox models. Journal of Structural Geology 28, 2084-2096.

Rigo, F., 1991, Italy to open 'exclusive' Po basin area in 1992. Oil and Gas Journal, v. 89, no. 21 102-106.

Riva, A., Salvatori, T., Cavaliere, R., Ricchiuto, T., Novelli, L., 1986. Origin of oils in Po Valley, Northern Italy – Organic Geochemistry, 10, 391-400.

Rossi, M., Minervini, M., Ghielmi, M. & Rogledi, S., 2015. Messinian and Pliocene erosional surfaces in the Po Plain-Adriatic Basin: Insights from allostratigraphy and sequence stratigraphy in assessing play concepts related to accommodation and gateway turnarounds in tectonically active margins. Marine and Petroleum Geology, 66, 192-216.

Sassi, F.P., Zirpoli, G., Nardin, M., Sacerdoti, M., Bosellini, A., Largaiolli, T., Leonardi, P., Sommavilla, E., MOzzi, G., Rossi, D., Proto Decima, F., Dal Monte, M., Paganelli, L., Simboli, G., Gatto, P., 1970. Carta Geologica D'Italia, scale 1:100,000, Map "11- M. Marmolada".

Scotti, P., 2005. Thermal constraints suggested by the study of the organic matter and thermal modelling strategies: A case history from the southern Alps: Atti Ticinensi di Scienze della Terra, Serie Speciale, v. 10, p. 21–35.

Scotti, P., Fantoni, R., 2008. Thermal modelling of the extensional Mesozoic succession of the Southern Alps and implications for oil exploration in the Po Plain foredeep. 70th EAGE Congerence & Exhibition – Rome, Italy, 0-12 June, 2008.

Sekiguchi, K., 1984. A method for determining terrestrial heat flow in oil

basinal areas. Tectonophysics, 103, 67etho

Shonborn,G., 1992. Alpine tectonics and kinematics of the central Southern Alps. Memorie di Scienze Geologiche; vol XLIV, pp. 229-393.

Shonborn,G., 1999. Balancing cross sections with kinematic constraints: the Dolomites (northern Italy). Tectonics, 18, 3, pp. 527-545.

Stefani, M., and Burchell, M., 1990. Upper Triassic (Rhaetic) argillaceous sequences in northern Italy: depositional dynamics and source potential, *in* Hue, A.Y., (Eds.), Deposition of Organic Facies, AAPG Studies in Geology #30: Tulsa, OK, American Association of Petroleum Geologists, p. 93-106.

Sweeney, J.J., and Burnham, A.K., 1990. Evaluation of a simple model of vitrinite reflectance based on chemical kinetics: American Association of Petroleum Geologists Bulletin, v. 74, p. 1559–1570.

Tissot, B. P., and D. H. Welte, 1984, Petroleum formation and occurrence, 2nd ed: New-York, Springer Verlag, 699 p.

Turrini, C., Lacombe, O., Roure, F., 2014. Present-day 3D structural model of the Po Valley basin, Northern Italy. Mar. Pet. Geol. 56, 266–289.

Turrini, C., Angeloni, P., Lacombe, O., Ponton, M., Roure, F., 2015. Three-dimensional seismo-tectonics in the Po Valley basin, northern Italy. Tectonophysics, 661, 156-179. http://dx.doi.org/10.1016/j.tecto.2015.08.033.

Vaghi, G.C., Torricelli, L., Pulga, M., Giacca, D., Chierici, G.L., and Bilgeri, D., 1980, Production in the very deep Malossa field, Italy: Proceedings 10th World Petroleum Congress, Bucharest, v. 3, p. 371-388

Vannoli, P., Burrato, P., Valensise, G., 2014. The seismotectonics of the Po Plain (northern Italy): tectonic diversity in a blind faulting domain. Pure Appl. Geophys., doi:10.1007/s00024-014-0873-0.

Waples, D.W., Waples, J.S., 2004 A review and evaluation of specific heat capacities of rocks, minerals, and subsurface fluids. Part 2, fluids and porous rocks. Nat Resour Res 13:123–130.

Winterer, E. L., Bosellini, A., 1981. Subsidence and sedimentation on Jurassic passive continental margin, southern Alps, Italy: AAPG Bulletin, v. 65, p. 394-421.

Wygrala, B.P., 1988. Integrated computer-aided basin modelling applied to analysis of hydrocarbon generation history in a Northern Italian oil field. Advances in Organic Geochemistry, 13, 1-3, pp. 187-197.

Zou Yan-Rong, Peng Ping'an, 2001. Overpressure retardation of organic-matter maturation : a kinetic model and its application. Marine and Petroleum Geology, 18, 707-713.

Zappaterra, E., 1994. Source-Rock distribution Model of the Periadriatic Region. AAPG Bullettin, v.78, n.3, pp.333-35.

Zattin, M., Cuman, A., Fantoni, R., Martin, S., Scotti, P., Stefani, C., 2006. From middle Jurassic heating to Neogene cooling: the thermochronological evolution of the Southern Alps. Tectonophysics, 414, 191-202.

Part 6 – Discussion, conclusions & perspectives

I. Introduction

By this thesis and the resulting 3D structural/seismo-tectonic/thermal model I tried to integrate and critically examine the dataset/interpretations publicly available across the Po Valley basin. All along the building/analysis workflow, those data/interpretations were filtered by my personal, 25-years-long experience on the region, as a seismic interpreter and structural geologist for different oil companies.

While conducting the PhD work, I soon realized that the three-dimensional model of such a huge, tectonically multi-phased, geological province was an ambitious and rather problematic task.

On the other hand, the study has revealed to be truly exciting, with new challenges arising at any new step of the model building process. Ultimately, it has given me the chance to review most of the results from the authors which have been working on the region during the last century, while putting them into a single, consistent 3D geological volume. That task was demanding yet the derived, endless thinking-loop definitely enhanced my scientific curiosity and strengthened the willingness to reach the final goal.

Today, the model, with its faults and defaults (!), is done and ready for further development.
Let's then discuss the *good and the bad* that I can see at this point of the process, while critically answering and considering the following issues:

- initial questions that triggered the thesis (Section II.A-D)
- model uncertainty and unreached expectations (Section II.E)
- key conclusions (Sections III)
- the 3D model possible future perspectives (Section IV).

II. Discussion

A. My Model

Before coming to any technical debate it is important to state that this model is *my model*: the data integration and the use I made out of them definitely propose *one single, deterministic solution*, although not an *a-priori* one (i.e. based on pre-conceived ideas and concepts). As such, there might exist different and alternative solutions to the one I am presenting and hopefully they will follow in the future from other authors. Nevertheless, at the moment, the performed model can stand as a viable representation of the Po Valley foreland basin architecture and bear the inevitable criticisms.

B. Was the 3D Model worth the effort? Why?

As already written (see discussion in Part 4, Section III), it may sound obvious nevertheless the immediate answer is: *yes, it was*. Indeed, regardless the many uncertainties, the Po Valley 3D model is definitely a big step ahead for a modern review of the basin.

First, although the data that have been collected and put together are well known in the public domain, the model allows the different interpretations published during the last 50 years to be compared and progressively validated (or not).

Second, with respect to previous, sparse and discontinuos interpretations, the performed geo-volume stands as virtual structural scenario suitable for any further, future modifications.

Eventually, it offers a number of important achievements:

- a new and interactive view of the structures that form the Po Valley region, from the very deep Moho to the surface topography;
- the interpretation of the foreland-foredeep deformation kinematics in the light of a homogeneous tectono-stratigraphic standpoint;
- the review of the basin earthquake-structure associations from the new three-dimensional perspective;
- a unique 3D simulation of the hydrocarbon potential in the deep Mesozoic petroleum system as a function of the basin thermal history and pressure compartmentalization;
- an interesting analog to foreland-foredeep systems, world-wide.

C. Data availability vs 3D Model feasibility

Today, the Po Valley 3D structural model is a fact and this is a clear demonstration that *it was feasible*. Nevertheless and once again it is important to stress that:

- data and interpretations made available by the literature on the Po Valley region are very inhomogeneous (i.e. produced by different authors since the first regional interpretation by Pieri and Groppi, 1981) and scattered, with clusters within particular structural levels and regions;
- after 30 years, the reference structural elements across the basin and, as already stated over and over (ref. Part 4, section II and III), the ones on which the 3D model building mainly refer to, are still the cross-sections from Cassano et al., 1986 (as demonstrated by other recent works; e.g. Molinari et al., 2015);
- given the spacing among those cross-sections (10-60 km), the derived horizons and faults resulted into preliminary surfaces which needed to be a) carefully checked for 3D consistency and b) literally sculptured by 3D model building inside the MOVE and Kingdom software (ref. methodology description Part 4, Section III and V, Part 5, Section III);
- the fault maps published so far in the literature (ref. Part 4, section III) provided a key support to the performed 3D model exercise by standard structural model building;
- the entire work a) took advantage from the 3D perspective and analysis which the developing model could allow, b) benefited from my long-lasting experience on the region as a geologist for different major companies (ENI, FINA, TOTAL) and, lately as a consultant for minor ones (Northern Petroleum, Petroceltic).

In the end, until new and fresh data will be offered to the scientific community and despite the overall uncertainty, the model reconstructed across the Po Valley basin is consistent with all the available data and past or recent interpretations.

D. An unconventional 3D modeling procedure?

The Po Valley 3D structural model was performed conformably with a standard model building workflow: (see Fig.20) 2D data (sections, maps) correlation and analysis, surface gridding, 3D visualization and geometry validation, well tie, 2D and block restoration,

integration of the outcrop trends with sub-surface tectonics, all these operations were run to make the model a consistent scenario about the basin tectonic architecture.

Further to that, an original (unconventional?) technique was used to review and refine both the 3D model stratigraphic layers and the associated faults.

Indeed, all model surfaces were exported from the MOVE software and imported into the 2D/3D Kingdom package (normally used for seismic interpretation) where, once transformed to gridded layers, they could be re-picked and tied to the well data on a regular and dense net of blank pseudo-SEGY panels (ref. Part 4, Section V, Fig.2d) created inside the software. With such a technique, all structural features were systematically analyzed every 5 km (1 km around the major oil fields) and the model structures were progressively validated along those sections much like in-lines and dip-lines inside a crustal scale pseudo-3D seismic survey.

As part of the adopted procedure, the fault-surface building tool available in the Kingdom software was used to carefully revisiting existing faults as well as building new ones when necessary.

The whole workflow and the applied technique define a user-friendly and powerful methodology which can be useful whenever available data are sparse and model building mainly relies on *our understanding/knowledge/experience about the geological structures under investigation*.

E. 3D Model uncertainty & possible (future) constraints to it

The model uncertainty can be locally high, as often stressed in the previous chapters (see Sections III and V in Part 4 and 5). *Such uncertainty basically depends on the model dimension, the data distribution and quality, the local lack of deep tie-wells, the extreme non-homogeneity of the geological setting from any point of view: geodynamic, tectonic, sedimentologic and stratigraphic*.

Here are some questions suggesting dimension and distribution of the model uncertainty and some possible way to reduce it:

1 – Given the interaction among the Southern Alps, the Apennines and the Adria domains, where is the triple-junction which should exist in the western domain of the Po Valley basin? How does it work?

Despite any effort, the reconstructed 3D geometries appear currently unable to further illustrate what is known in the literature. Indeed, the model shows the increasing structural complexity of the Mesozoic carbonates-basement structures as we go from the eastern to the western Po Valley domains (i.e. close to the Alps) (Part 4, Section III). Nevertheless the interplay among the various crustal units needs additional thinking, work and data. Possibly, new geophysical images and forwards gravity modeling of the 3D structures would help in that direction.

2 - Where is the possible footwall cut-off of the Mesozoic carbonates below the Southern Alps and Northern Apennines fronts?

The question is relevant in terms of paleogeographic reconstructions, thermal modeling impact and bearing on the hydrocarbon exploration strategy. Nevertheless, a definitive answer is still *blowing in the wind*. Hopefully, a better integration between the outcrops and subcrops (i.e. inside the Po Valley basin), the acquisition of some future crustal seismic lines and the restoration of the complete Alps-Apennines-Po Valley structural puzzle will provide new insights to the issue.

3 - What is the true, pre-Alpine fault orientation and which among the pre-compressional faults have been reactivated, maybe controlling trap formation and fluid migration around the deep Mesozoic carbonate reservoir?

I have provided my possible conjectures about this question in chapter 4 (Part IV, Section V). Irrespective of anyone night-thoughts or theory, faults across the Po Valley are largely unknown in their detailed 3D geometry and only access to the existing 2D-3D seismic data would significantly contribute to unraveling the problem.

4 - Why do the faults that the model shows to intersect the Mesozoic carbonates and underlying basement in the western Po Valley domain appear as quite, non-seismogenic surfaces?

This is a big dilemma: the western Po Valley is supposed to represent a part of the Alps-Apennines-Apula crustal triple-junction (see point 1 above), the modeled deep faults are definitely seismic-scale faults (Fantoni et al. 2004) yet the region is practically not recording

any major earthquake (Part 5, Section III). Some kind of industry-academia *think-tank* might help in solving the problem while considering a) the presence/effect of deep fluid overpressures, b) the re-location of the available hypocenters, c) reviewing of the fault patterns.

5 - What is happening to the Mesozoic pre-Alpine structures and stratigraphy to the west of the Villafortuna-Trecate field?

That region, by its analogy with the Southern Alps outcrops, is supposed to have represented the possible transition between the Adria plate passive margin and the ancient ocean realm.

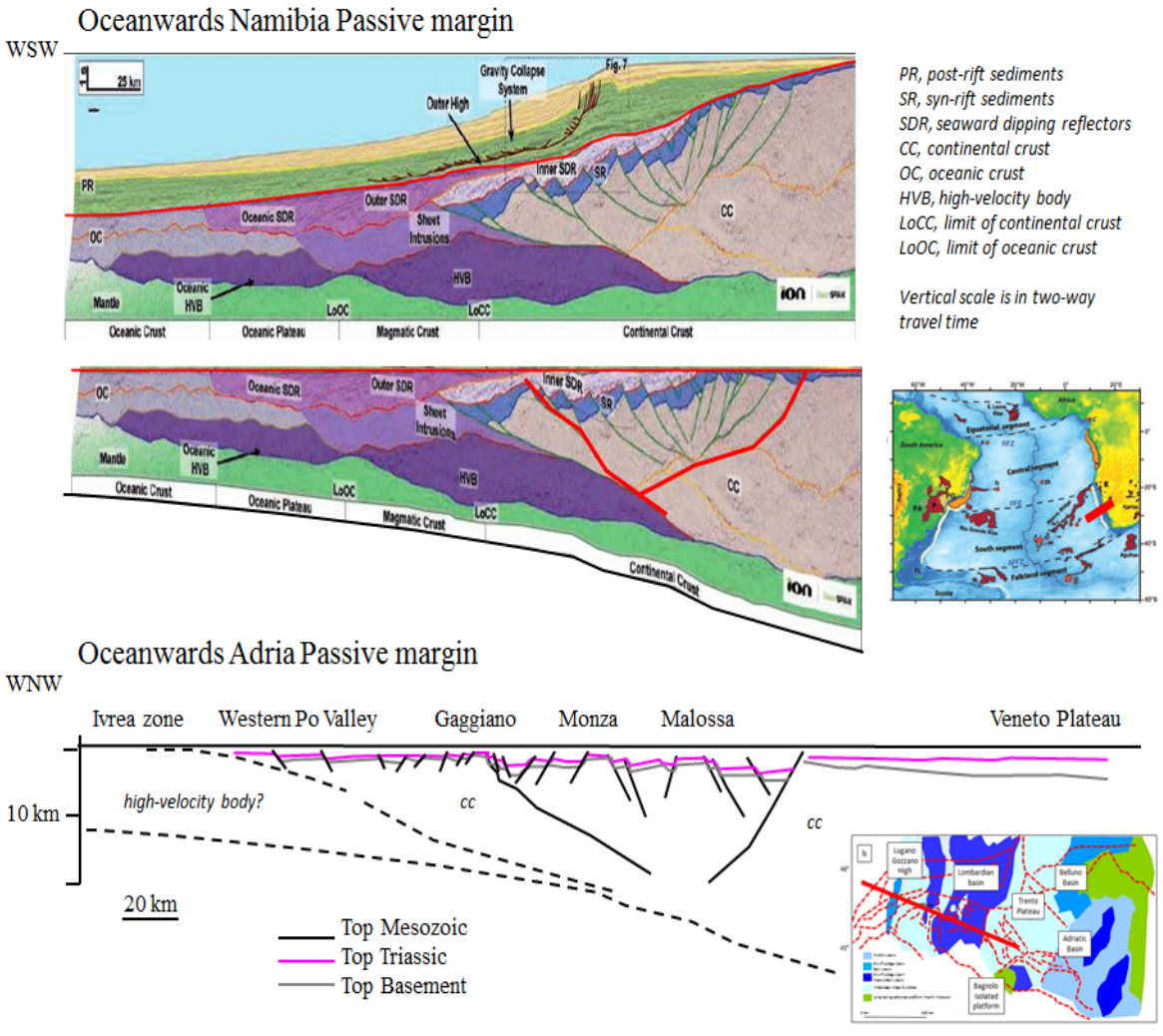

Figure 21 – (top) Geoseismic sections across the Namibia passive margin (McDermott et al., 2015); (center) the Namibia margin restored to pre-thermal subsidence; (bottom) Adria passive margin from the Po Valley 3D structural model restored to pre-Alpine time.

Today it stands as a true *no-man land* inside the basin: no deep well has been drilled so far and the existing seismic data are secretly kept by oil companies which still hold few important targets within the Mesozoic carbonates. The comparison of the pre-compressional structures derived from the 3D model with some of the actual passive margin reconstructions (i.e. SW African margin vs Adria passive margin - Fig.21) would raise new questions to the discussion of the viable scenarios that could be pictured across the under-explored, western domain of the Po Valley region, the related thermal history and the relict exploration potential.

6 - Why, despite the initial intentions, was the 3D restoration of the model not run so far?

This is a major regret. Infact, the original workflow was planning to perform the 3D restoration of the Po Valley structures which form the Mesozoic-basement units. Due to the persisting uncertainties about a) field-scale tectono-stratigraphy, b) faults' throw and lateral terminations, c) definition of the most-likely displacement direction, only a simplified 2D reconstruction along a number of selected cross-sections was ultimately done (see Part 4, Section V).

As an example of possible further works, figure 22 illustrates a preliminary block restoration of the Ferrara tectonic arch at the buried front of the Northern Apennines.

Here, the fold-and-thrust units that constitute the western and eastern sectors across the Mesozoic and basement 3D layers have been defined (Fig.22b), unfolded and restored accordingly to a best-fit movement direction of the different blocks. The workflow allowed the following considerations:

- mainly NW-SE displacement vectors allowed the minimum number of gaps and overlapping zones among the restored blocks (Fig.22c);
- the 3D units unfolding and successive block restoration point to the presence of a pre-existing, NW-SE (?) oriented basin with important thickening of the Mesozoic sediments (Fig.22d);
- inversion of such basin might have controlled the localization of the transfer zone which separates the northwestern and southeastern domains of the tectonic arch (Fig.22a).

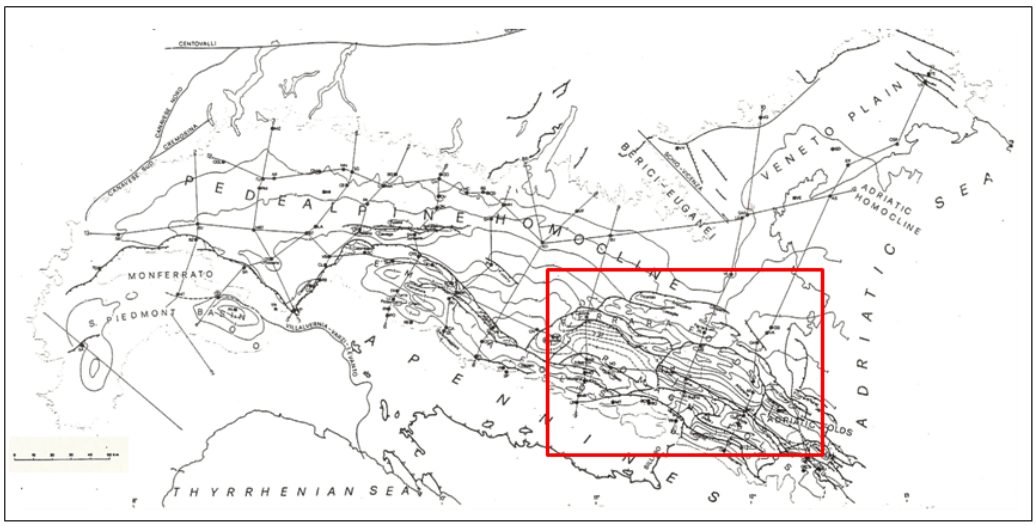

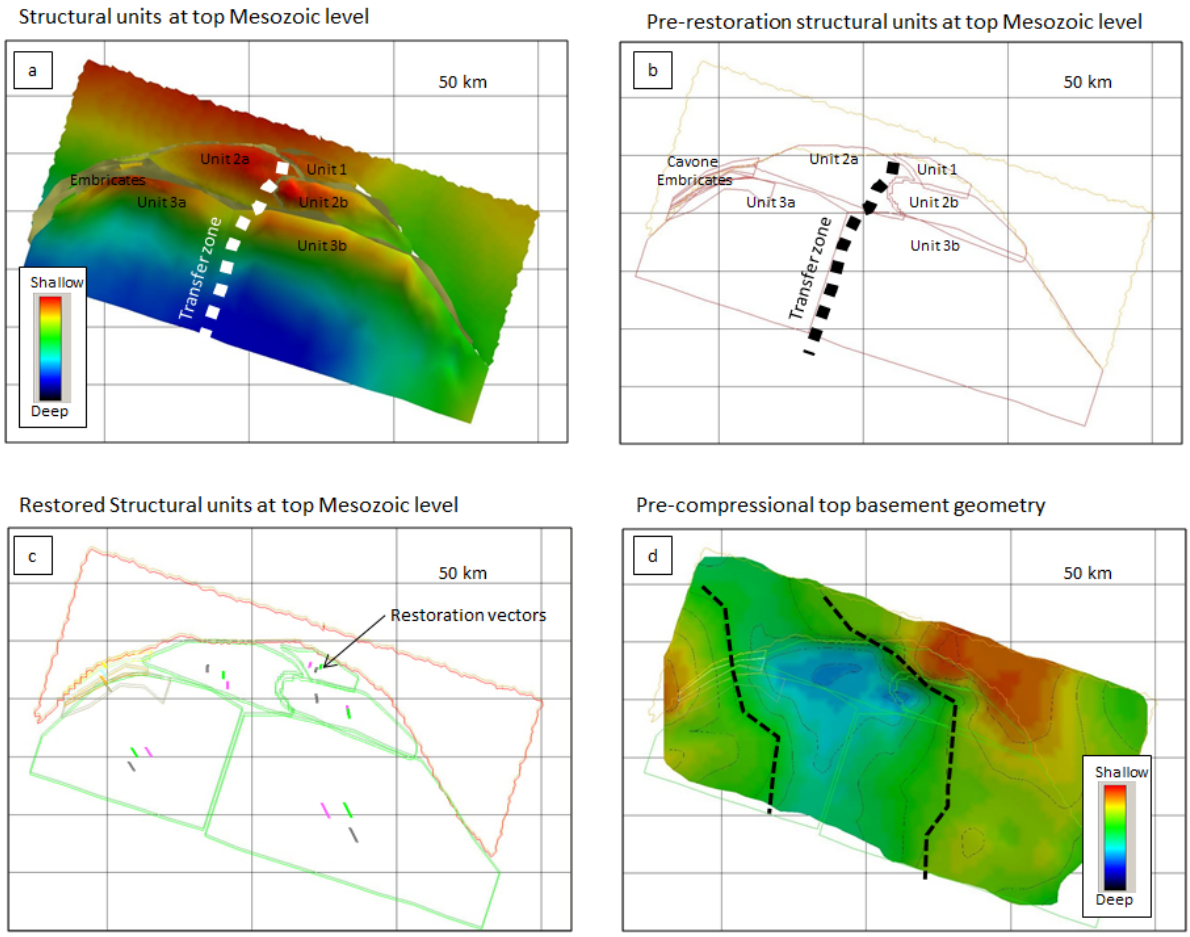

Figure 22 – Location map and block restoration of structures at the Mesozoic level in the Ferrara tectonic arch (see text for explanations).

Although preliminary, the results sound interesting yet they definitely need further investigations. Eventually, the same block-restoration exercise should be repeated for each of the foreland units defined by the 3D model across the entire Po Valley region.

7 - Why the thermal maturity and the hydrocarbon generation history computed around the Po Valley basin can be considered reasonable at the basin scale yet debatable at the field scale?

The maturity data available from public sources used to calibrate the basin thermal evolution are very sparsely distributed. For better modeling, having more maturity data is key. Furthermore, greater details are required in terms of stratigraphy, structures and burial history around the field structures. Once again, availability of seismic data is the fundamental issue. Second, the use of a kinematic approach to the thermal modeling might also represent a possible future objective: local tectonic over-thickening would be compensated by restoration of the structures during the progressive analysis of the tectono-stratigraphic evolution (Gusterhuber et al., 2013 and Neumaier et al., 2014).

8 - Is the Tertiary sediment succession detailed enough inside the 3D model? Actually, only a limited number of key horizons have been built across the Po Valley basin (see cross sections in Part 4, Section V). Noteworthy, public data are available to complete the work (i.e. the Videpi dataset): the issue, in this case, is the huge effort that would be required to analyze the thousands of wells that drilled the post-Mesozoic, clastic successions.

9 - What about the reliability of the structure-earthquake associations illustrated by the performed seismo-tectonic 3D model?

The current model (Part 5, Section III) confirms and shows that the process of populating the 3D structural model with the public earthquake data is possible and it can be a powerful tool in illustrating the Po Valley seismicity. The future interplay with additional software could eventually provide new achievements about the seismo-tectonics of the region.

In figure 23 the GOCAD software has been utilized to build and analyze the Magnitude volume that can be defined around the Ferrara tectonic arch. The software allowed the earthquake-related Magnitude distribution (i.e. point values) to be interpolated across some pre-defined volume units (voxels). These arrays of cells, normally used for the purpose of property or fluid modeling, could then be a) rendered as Magnitude volumes, b) anatomically observed, c) sliced in any direction of the 3D space for specific analysis against the associated

3D structures (see vertical and horizontal slices of Magnitude vs structures around the Ferrara arch in Fig. 23).

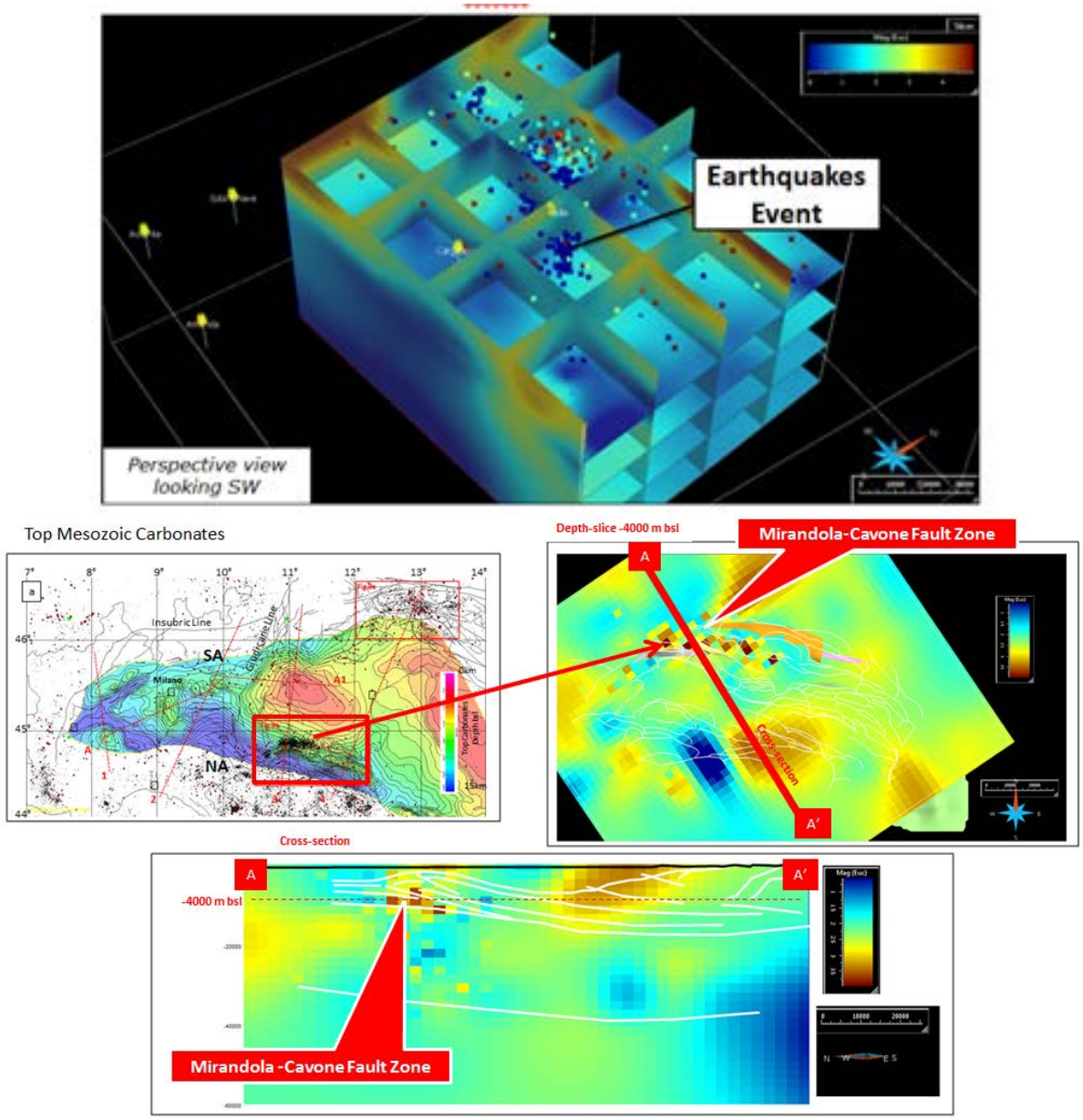

Figure 23 – (above) Magnitude volume; (below) horizontal and vertical slices in the Ferrara tectonic arc (GOCAD software; 1<M<6).

Such methodology, which will need further testing and the correct relocation of the available earthquake events all over the basin, can be exploited to derive Magnitude information a) around fault zones when the fault geometry is questionable (nearly always!?) or b) across structural domains where shocks are absent.

10 - Are the structures' kinematics suggested by the 3D model fully describing the Po Valley tectonic evolution?

Today the answer is simple: *NO, they aren't*. The 3D model confirms the structural complexity of the basin yet, due to the current uncertainties (see point 6 above), it only allowed so far: a) a number of selected 2D restoration (Part 4, Section V), b) some guessing about the Mesozoic-Cenozoic, extension-compression structural interferences (Part 4, Section II and V), c) preliminary and local 3D block restoration (i.e. the Ferrara arch case study).

Further understanding and more constraints about the deformation kinematics of the basin structures could be possibly obtained by comparison of the 3D model geometries with the ones derived from sand-box experiments. This is part of an on-going collaboration with the Earth Science Dpt. of the Pavia University.

The experiments have been run by building a dedicated sand-box apparatus where roto-translational dynamics could possibly replicate the ones which occurred from Paleogene to present in the Alpine-Apenninic region (Boccaletti et al., 1990; Carminati et al., 2012, among the many authors). Successively, the sand-box structures have been reconstructed inside the MOVE software for a detailed analysis of the deformation evolution.

Preliminary results from the simulations and the related 3D model building (Fig.24) suggest the possible progression of the Southern Alps and Northern Apennines units towards the same Po Valley foreland domain.

In particular, once the role of the inherited pre-compressional structures distribution is accepted as a key factor for the initiation and development of the Po Valley buried arches (see Part 4, Section V), the performed sandbox models indicate that:

- arc-shaped thrust fronts can be produced simply as a function of the centripetal belt rotation around the pivot-zone;
- the displacement gradient that is acquired by the different tectonic arches decreases towards the pivot;
- both frontal and lateral ramps are the common geometries as shortening increases during the deformation progression.

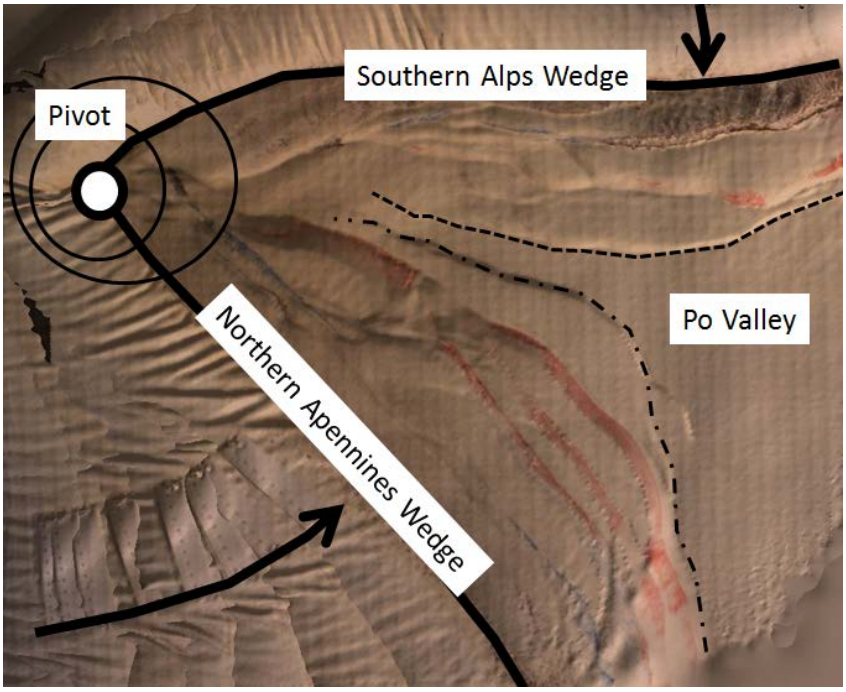

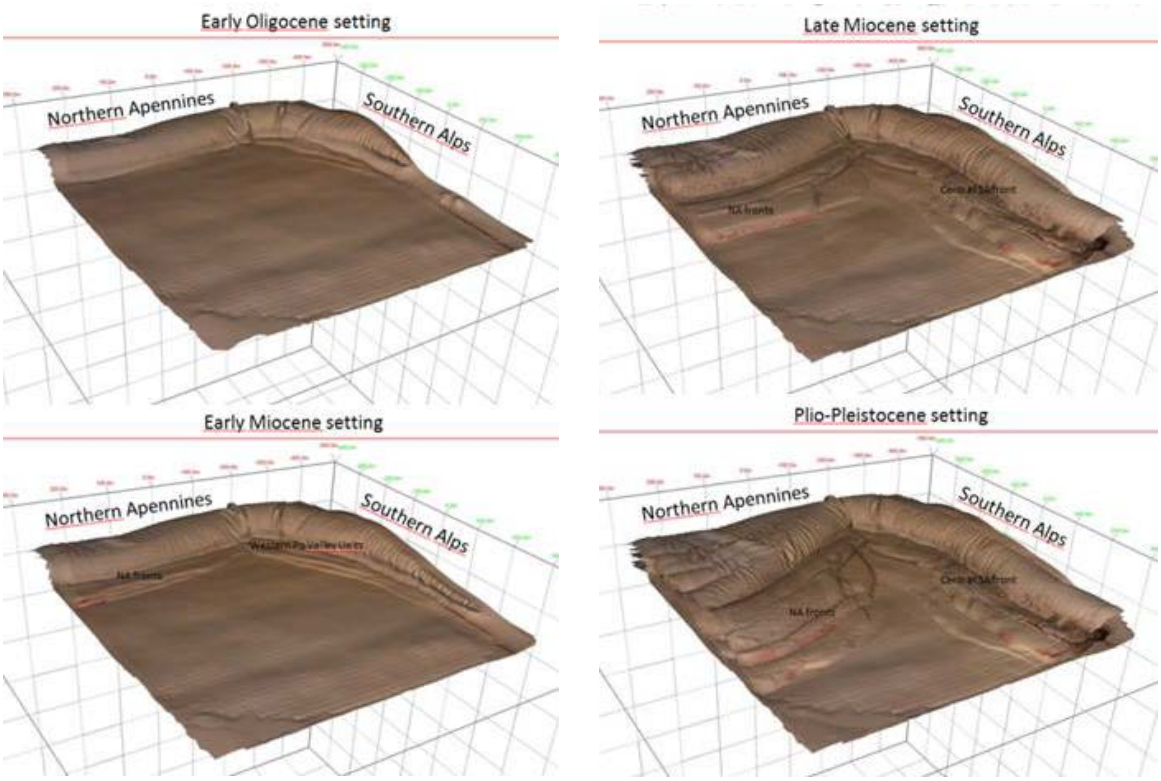

Figure 24 – (above) map view and (below) perspective view of the Northern Apennines-Po Valley-Southern Alps type structures and kinematics by sandbox experiments (see text for explanations).

III. Conclusions

This thesis presents and discusses the 3D structural model of the Po Valley foreland, in northern Italy.

The model has been created by the integration of public depth-data and the progressive sculpting of the performed 3D units, tied to the available cross-sections, maps, outcrops and wells (Fig.25).

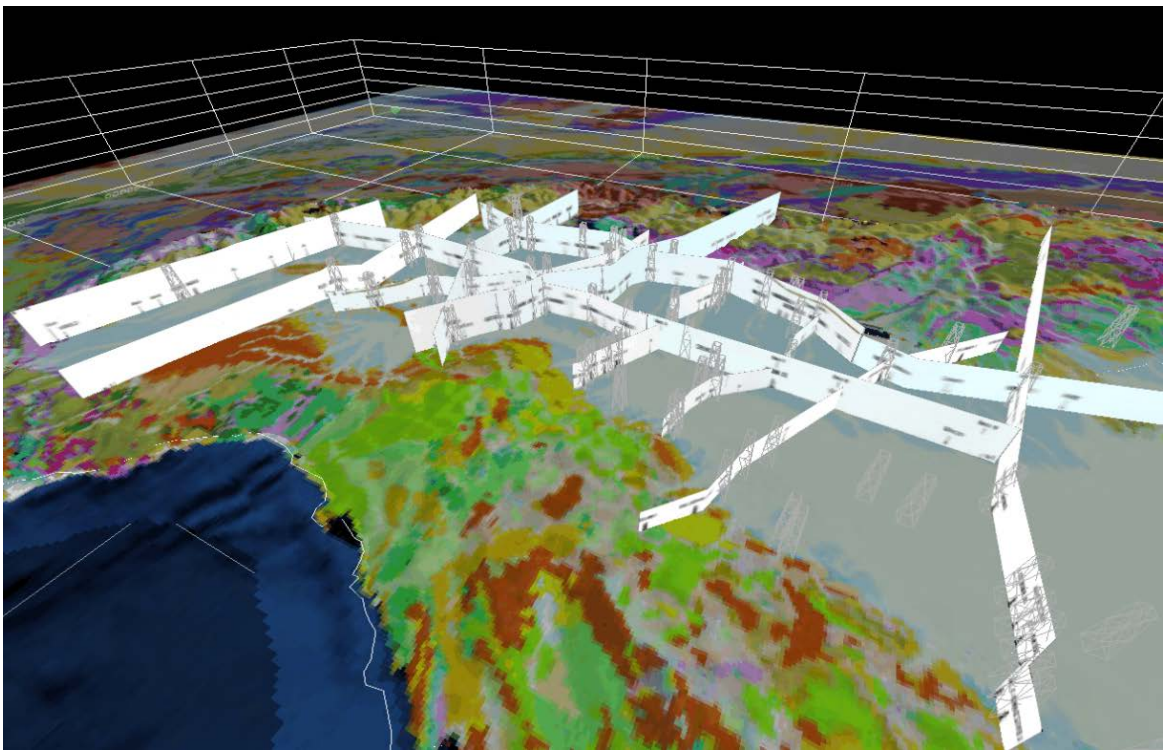

Figure 25- the Po Valley 3D model (perspective view looking NW)

Despite the possible simplification and the associated uncertainty, mainly due to quality and distribution of the initial dataset, the Po Valley model is consistent with the structural setting and the kinematics of the basin from crustal to field scale, with proved applications to reviewing of the basin structure-earthquake associations and thermal modeling of the potential hydrocarbons from the Mesozoic systems.

Key results from the model are the following:

1. The whole Po Valley crustal architecture is controlled by the Moho geometry (Part 4, Section II);

2. The foreland basin is defined by two major structural domains (eastern and western of the NNE-SSW oriented Giudicarie trend), where sediment distribution/thickness and structural style are substantially different (Part 4, Section II);
3. The modeled Tertiary foredeep basin geometry and migration are strongly controlled by the foreland pre-Alpine tectonics (Part 4, Section V);
4. The influence of the inherited extensional structures on the compressional structure evolution is clear until Miocene time, when the foreland show double-flexure towards the north and the south, below the Southern Alps and Northern Apennines advancing chains, respectively (Part 4, Section V);
5. During Pliocene, flexure of the Adria/Po Valley foreland is essentially south-verging below the Apennines: at this stage, the influence of the Mesozoic fabric is subtle and deformation across the foreland is mainly controlled by subduction of the Po Valley lithosphere below the Apenninic belt (Part 4, Section V);
6. Seismicity across the region is mainly related to a) the Northern Apennines buried fronts, b) the eastern sector of the Southern Alps-Po Valley boundary zone, c) some platform-to-basin facies transition in the Mesozoic carbonates around the Veneto and Friuli platform domains (Part 5, Section III);
7. Despite the intensive faulting across the Mesozoic-basement units, the western Po Valley domain shows an apparent low seismicity (Part 5, Section III);
8. The model illustrates a clear earthquake stratigraphy so that major hypocenters seem to be concentrated a) at the Moho-crust transition, b) close to the top of the basement, c) at the top of the Mesozoic carbonates (Part 5, Section III);
9. The final thermal modeling built on the 3D structural model is capable to (Part 5, Section V)
   - confirm the hydrocarbon generation history suggested by previous authors,
   - compare the model results with hydrocarbon production from the major oil fields in the region,
   - correlate hydrocarbon generation, migration and accumulation with trap formation across the basin,
   - suggest the presence of fluid overpressures as a potential key factor in delaying the hydrocarbon maturation inside the deep Mesozoic carbonates of the western Po valley.

The current model is to be intended as the base-case 3D scenario for future applications in the various domains of the earth science, namely education, hydrocarbon exploration, hydrogeology, CO_2-CH_4 storage and geo-archeology.

The model, built and analyzed by a combination of different software (MOVE, Kingdom, Structural Solver, GOCAD) is a ready-to-use product which, in order to reduce uncertainty while increasing the predictive potential, is expected to be locally refined and implemented through addition of further data.

Whether correct or not, the performed 3D structural model of the Po valley region resulted in a number of lessons learned that possibly represent the real achievements of the thesis thanks to their applicability elsewhere and worldwide.

IV. Perspectives

A. Implementation of the Po Valley model

From the considerations listed and discussed above, it is evident that implementation of the performed 3D model layering and geometries are needed for constraining of the current uncertainty and strengthening of the model prediction potential.

In terms of further and future actions it is also suggested that both the uncertainty-reduction and model-implementation targets could be achieved by:

1. access to the 2D/3D seismic data that ENI (mainly) is *concealing* in the company archives (that could be a major benefit for the scientific community with back-impact on the industry as well);
2. integration of more well data for both the Mesozoic and Tertiary sequences (most of them from the public Ministry website; some key deep wells from the ENI archives);
3. the use of alternative software specifically dedicated to particular functions (geostatistics, upscaling of pseudo-reservoir properties, thermo-mechanical simulations);
4. employ more resources (students?) to refine/update the model at both the regional and local scale.

B. Education

Society has a growing need for a wider comprehension of the natural phenomena and processes that impact the everyday life. In this sense, the Po Valley structural-seismo-tectonic 3D model could have a true value in the domain of education.

At a higher level, the model is:

- an exceptional laboratory for viewing and discussing the geology of the Po Valley,
- a reference for tackling the analysis of other foreland-foredeep basin worldwide,
- a complete case-history for understanding of the 3D modeling technique, the related benefits and associated uncertainties.

In its simpler terms, the 3D model perspective could be an effective tool for instruction of a larger audience by:

- displaying the basin structural architecture at any scale of observation,
- presenting/debating the earthquake mechanisms-occurrence-risk (a critical subject for particular areas in the region),
- illustrating/discussing the hydrocarbon exploration activity with its history, energetic advantages and objective ecological impact.

Remarkably, the model could represent the support to a multitude of future geological topics (regional and local): this could be used to draw funds and data from the industry and grants from the EC scientific programs.

C. Future model applications in the Po Valley region

The current 3D model can be considered a preliminary, geo-referenced, virtual volume of the Po Valley foreland basin geology. If handled with caution and, particularly, once implemented (see above), the model would be capable of supporting further applications with respect to the ones already tested (Part 5, Sections III & V).

C1. Hydrocarbon exploration

Definitely, some of the 3D model perspectives fall in the domain of the hydrocarbon exploration.

As already discussed (point 7 in Section II, this chapter), more precise investigations about the hydrocarbon maturation/generation can be obtained with new data and refining of the 3D model geometries and tectono-stratigraphy. Such implementations would also result into a more detailed 3D framework that might be used to support the exploration strategies across under-explored sectors of the basin (e.g. the western Po Valley).

In this sense, the time-conversion of the current 3D depth-structures can be an important exercise for a) checking any interpretation hypothesis based on poor quality seismic data, b) validating the processing operations of complex 2D-3D seismic surveys, c) creating new plays especially where seismic data are absent (i.e. below the Northern Apennines belt).

C2. CO_2 – CH_4 storage

Emission of industrial CO_2 is one of the major problems linked to modern society and the Po Valley is among the regions where such problem is particularly evident (Fig.26), due to overpopulation and presence of factories and electric centrals.

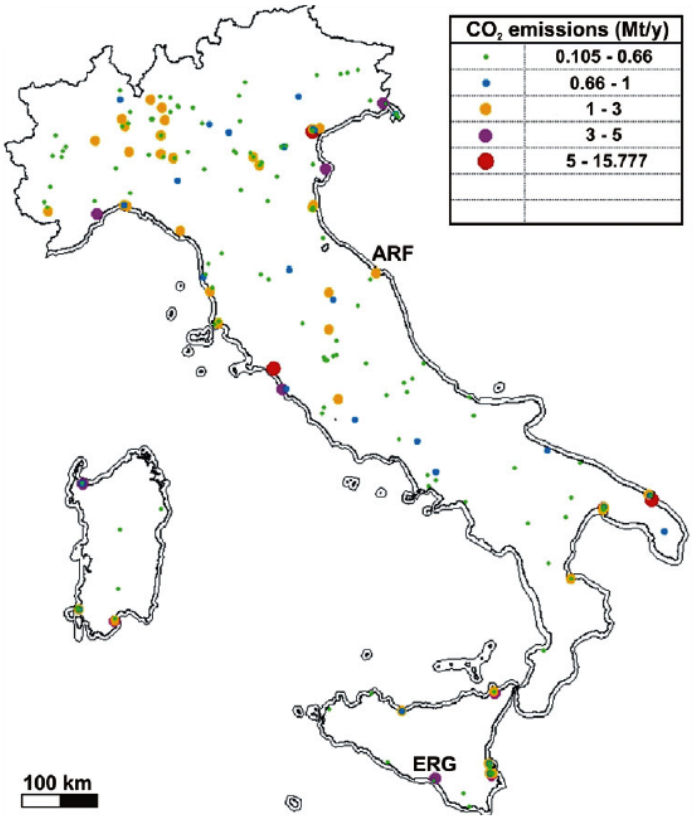

Figure 26 - Location of the major CO2 point sources in Italy (emissions >0.1 Mt/year) (Civile et al., 2013).

In the objectives to find the optimal site for CO_2 storage, the performed 3D model could help in the definition of the possible trapping locations. Any possible traps below the Triassic evaporites of the eastern domain (Burano Fm) or inside the Cenozoic porous successions could provide viable conditions for that storage. In particular depleted gas fields across the basin would possibly benefit from CO_2 injection to enhance production of the remaining hydrocarbons.

Although such application would require important refining of both geometries and tectono-stratigraphy, the *ready-to-use* 3D model would assure a consistent framework around the investigated storage-sites where structures and seismicity have been previously integrated. By the recognized structure orientation and structural style, the model would predict the possible local stress direction and fracture existence/distribution at the reservoir level. At the same time, reservoir type and seal effectiveness of the storage location could be derived from the various model domains.

Ultimately, the model would also provide a preliminary image of the geological conditions around the injection well path while suggesting the presence of faults and their structural behavior (seal, barrier, active, silent, connected to surface). This will have an impact on long-term retention of the injected CO_2, prediction of the movement of the CO_2 during the period in which it is injected and beyond, and monitoring of the emplacement and migration of the CO_2 at appropriate intervals. Slicing of the 3D model will supply the possible scenario on which alternative and more refined solutions could be created. This will reduce the initial uncertainty and risk for storage failure.

Noteworthy, as by the CO_2 rationale, storage of methane (CH_4) in the Po Valley subsurface porous formations can eventually represent an additional perspective for the performed 3D model.

C3. Hydrogeology

In the field of hydrogeology the 3D model of the Po Valley basin can be used to support a hydro-stratigraphy of the Plio-Pleistocene layers (e.g. Fig.27). Of course, the current model would need to be integrated with new data on the aquifer anatomy and distribution across the basin. Focus should be put on the unconsolidated sediment geometry that host and control

water accumulation and migration, in particular along the regions that make the structural and lithologica transition between the outcrop and the Po Valley plain.

Water-wells, piezometric maps and information about river catchment areas could be easily imported and georeferenced into the 3D geo-volume. Results can be expected to help in the definition of a basin-scale 3D groundwater flow models which should then be developed by dedicated software. Full integration of the geological/hydrogeological data and the regional dimension of the final virtual volume would represent the added value to such a project in the objective to manage both surface and ground waters by a homogeneous strategy.

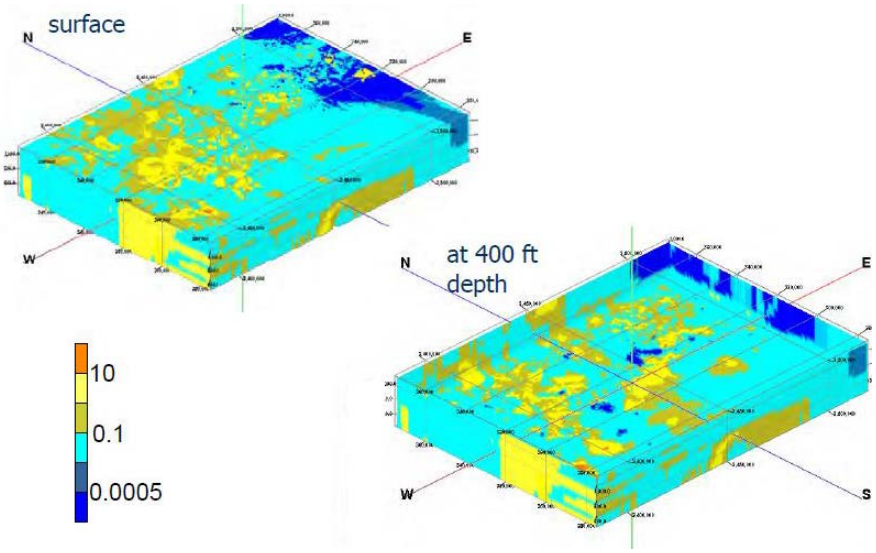

Figure 27– 3D hydro-stratigraphy model sliced at the surface (left) and at 400 ft depth (right) (Kallina et al., 2009); southeastern Wisconsin, USA.

C4. Geo-archeology (?)

It is definitely true that pitfalls to look out for include the use of models outside their validated scope.

However, it seems also true that when the Po Valley surface elements are considered against the top of the Mesozoic carbonate 3D layer, two astonishing informations are immediately revealed (Fig.28):

- most of the culmination at the carbonate level corresponds with cities and towns across the region;
- the hydrography of the basin can surprisingly be correlated with the deep Mesozoic geometry.

Such results seem to indicate that the human history and the modern landscape have been and are somehow controlled by the deep architecture of the region. In this light, geo-archaeology, geo-landscape and human history related studies could represent an extreme yet interesting application of the Po Valley 3D model.

Once the specific data integrated (e.g. aerial photographs, archeological site distribution), back-stripping and restoring of the geological landscape might eventually offer a unique chance to track the evolution of human society in the region.

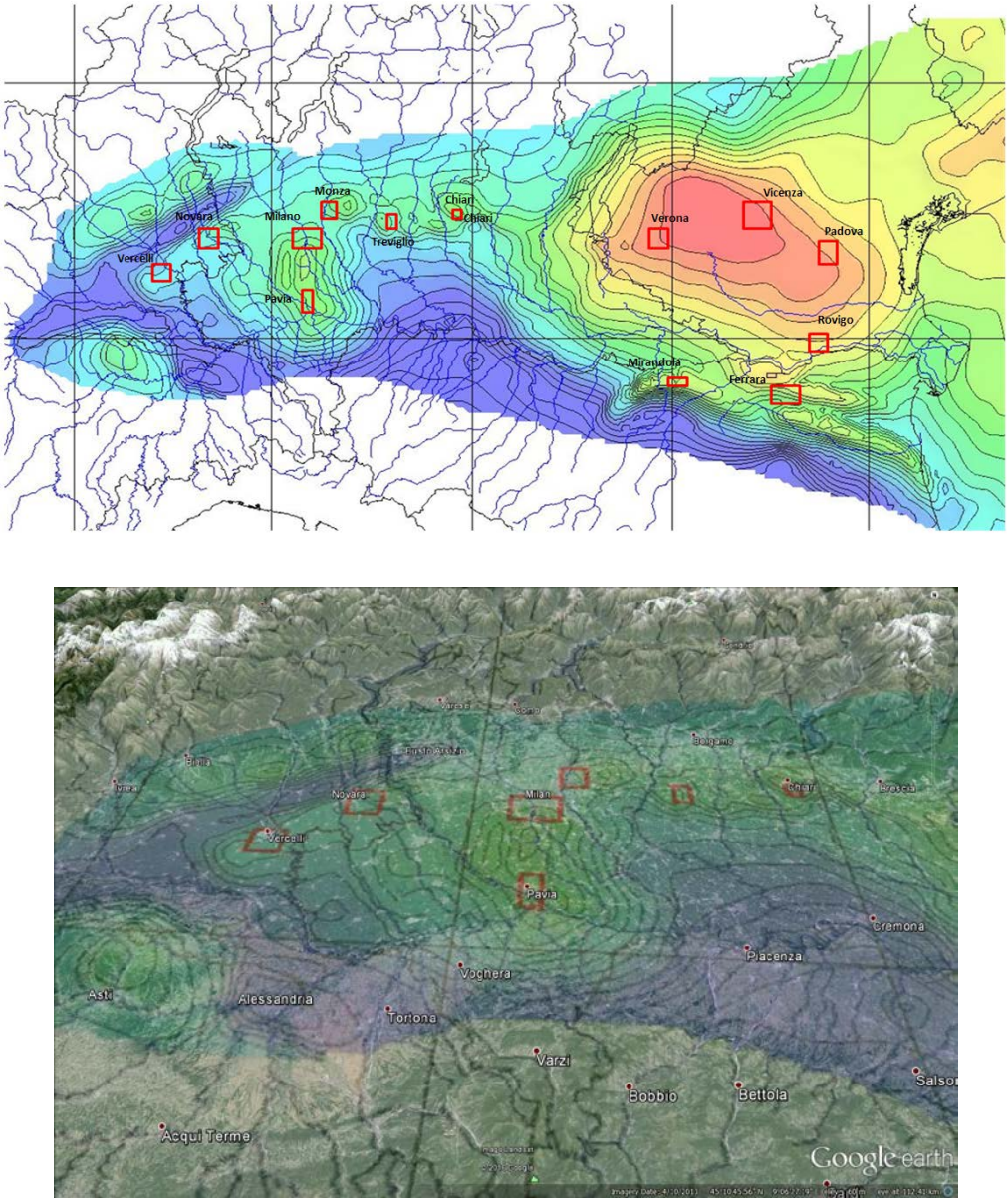

Figure 28- (above) top Mesozoic carbonates from the Po Valley 3D model with hydrography and major towns/cities; (below) perspective view looking north of the western Po Valley topography and hydrography (Google earth) vs top Mesozoic structures (3D Model).

D. Not only the Po Valley

The performed 3D structural model of the Po valley region has been a source of inspiration in terms of both scientific thinking and working methodology. These resulted in a number of lessons-learned that possibly represent the real achievement of the thesis thanks to their possible applicability elsewhere and worldwide.

Methodology Lesson 1: *switching from the 2D to the 3D view always raises new ideas and questions which did not exist before*. They both can be as many as the possible angles of observation. Most of the time, the first interpretation product is questionable yet the methodology allow our perspective to be changed over and over.

Methodology Lesson 2: *integration of all the available data/interpretations is definitely the way to the most likely scenario into which 3D structures will hopefully fit*. Only when 2D data/interpretations are consistently tied together in the 3D space, any domain of the region can be sliced and analysed for further discussion.

Methodology Lesson 3: *building of a 3D model from sparse data requires geological knowledge and creativity as well*. In particular the chance of slicing the model in any direction of the 3D space allows observations that were not immediate (few data) or even possible (no data) before. The review of post-well results or testing of new play-concepts, depth-to-time conversion of lead targets may become feasible operations thanks to the three-dimensional modeling and the related uncertainty evaluation.

Methodology Lesson 4: *any modelling software is different in terms of tools and structural analysis capability*. The best strategy seems to be the combination of different packages and, when needed, their unconventional utilization (ref. Section II.E. here above).

Scientific Lesson 1: *the Moho architecture of a given region can suggest most of the structural trends that are observed at shallower levels*. Indeed such a statement might sound pretentious yet it can be clearly applied to the Po Valley region (Fig.29) and likely all over the earth surface.

As an example, the Moho depth map of central Europe taken from the web public source (https://commons.wikimedia.org/wiki/File:Mohomap.png#filelinks) is here analyzed and interpreted using the major tectonic features that can be derived from the available literature

(Fig.30) (Lamarche et al., 2004; Carminati & Doglioni, 2012; Handy et al., 2014; Grad et al., 2016).

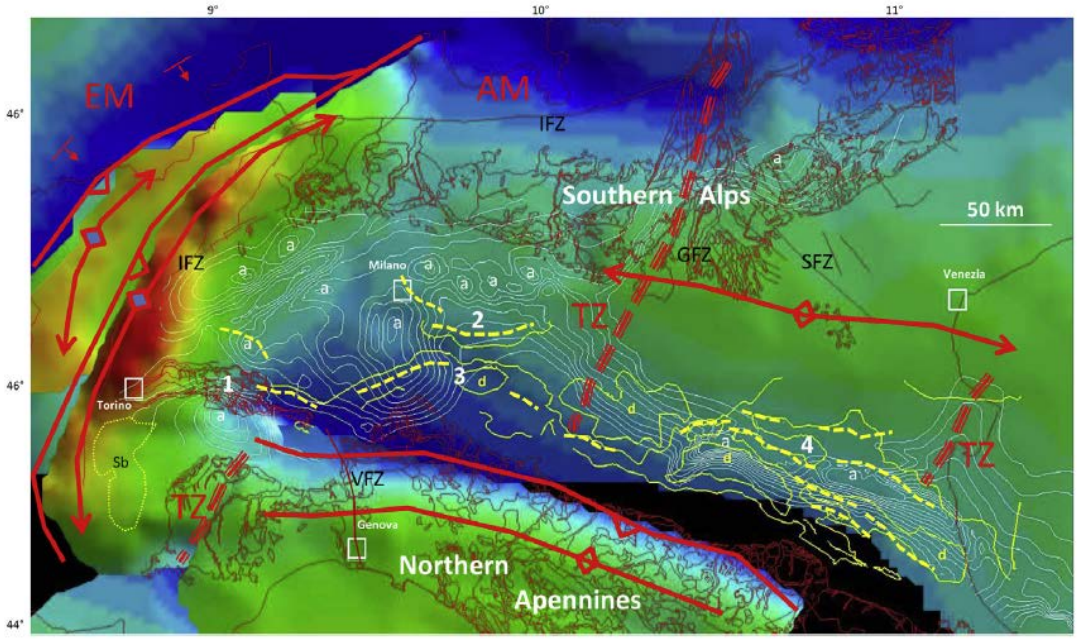

Figure 29 - Po Valley Moho depth map against shallow structural trends (ref. Part 4, section III for explanation).

The result shows a good correlation between depth to the Moho discontinuity and tectonic trends. Following the lesson from the Po Valley 3D model a more detailed Moho depth map would very likely allow a number of minor structural features to be detected.

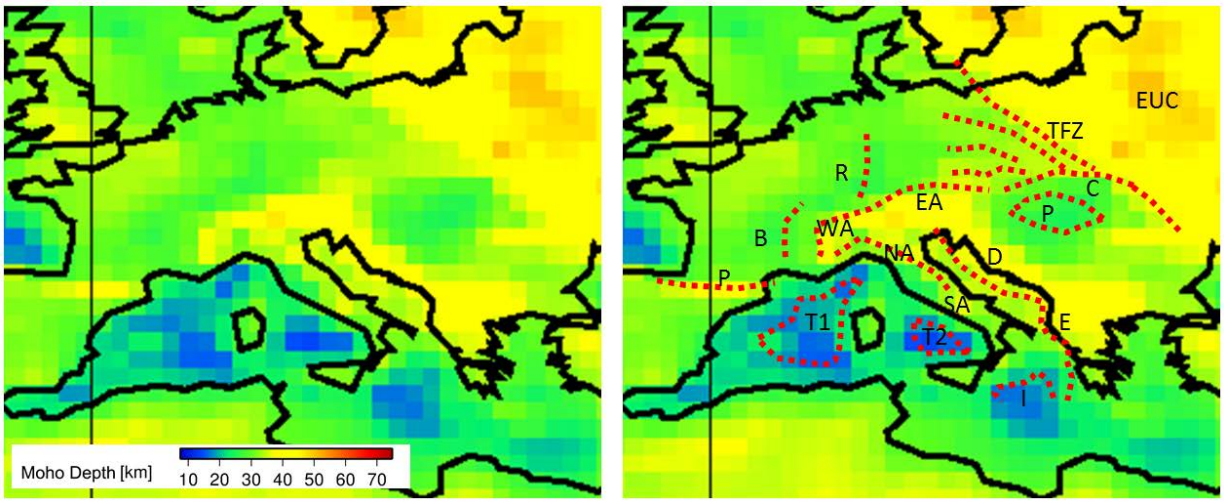

Figure 30 - Moho depth map of the Europe region and major tectonics: P=Pyrenees, T1 & T2=Tyrrenian basins, I=Ionian basin, B & R=Bresse & Rheins grabens, WA & EA=Western & Eastern Alps, NA & SA=Northern & Southern Apennines, D=Dinarides, E=Ellenides, P=Pannonian basin, C=Carpathians, TFZ=Tornquist Fault Zone, EUC=East European Craton.

Scientific Lesson 2: *foreland structures can show a wide spectrum of structural style (thin and thick skinned), families (extension, compression, wrenching related) and the associated structural interference*. Thanks to the basin tectonic history, the Po Valley 3D model definitely supports the aforementioned sentence (ref. Part 4 Section III and V). When other foreland regions are considered, the interference among different structure types can be observed as well, with various degree of final tectonic complexity (e.g., the Pyrenees, the Rocky Mountain, the Appalachian - Garfunkel & Greiling, 2001; Ziegler et al. 2002; McQuarrie et al., 2005; Naylor & Sinclair, 2008 - between Apennines et Dinarides-Albanides, between the Himalaya thrust and the Assam-Arakan belt, between the Caribbean belt, Andes de Merida and Sierra de Perija - Muñoz-Jiménez and Casas-Sainz, 1997; Norman Kent and Dasgupta, 2004; Mann et al., 2006; Fantoni & Franciosi, 2010 – at the front of the the Atlas mountains, the Urales, the Carpathian, the Taiwan belt - Matenco et al., 1997; 2003; Ziegler et al. 2002; Lin & Watts, 2002; Tensi et al., 2006; Oszczypko et al., 2006; Naylor & Sinclair, 2008).

Scientific Lesson 3: *inherited foreland tectonics can strongly constrain the successive structure evolution and the adjacent thrust belt progression*. In Part 4, section V of this thesis the interaction between the Mesozoic fabric and the Alpine tectonics teach such a lesson. From the available literature, clear examples of interference from pre-existing structures on the foreland structural evolution are abundant.

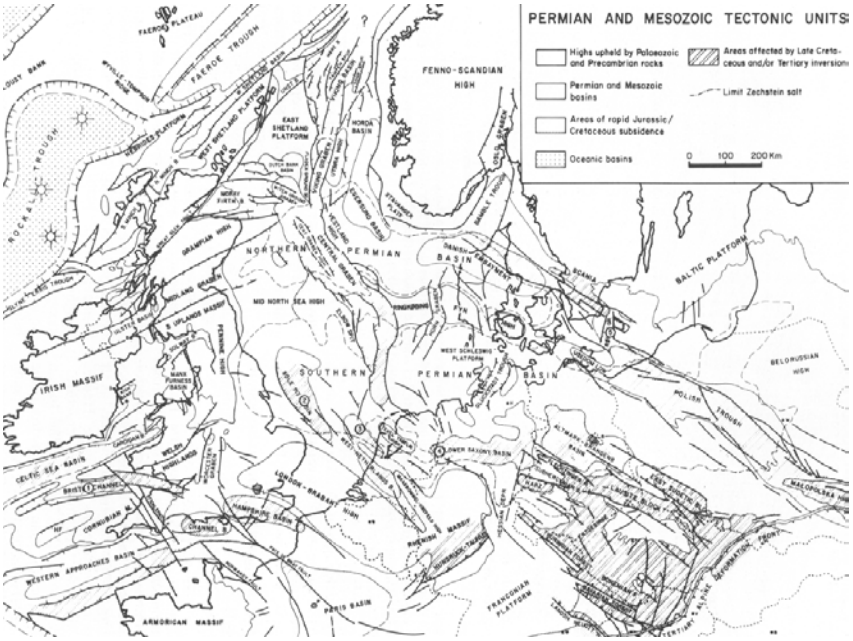

Figure 31- map showing the extent of inversion in Alpine foreland with late Tertiary Alpine deformation front in southeast corner (Ziegler, 1989).

Among the many papers, the works from Ziegler (1989), Letouzey (1990) and Lowell (1995) show by cross-sections, seismic lines and maps (Fig.31), clear examples of positive basin inversion and fault reactivation, taken from the Atlas, Indonesia, the Rockies, Europe and the North sea.

Like in the Po Valley, those situations also suggest that the orientation of the pre-existing discontinuities with respect to the new regional stress field may control the degree of wrenching of the last stage structures (Fig.32): key criteria, especially in foreland domains.

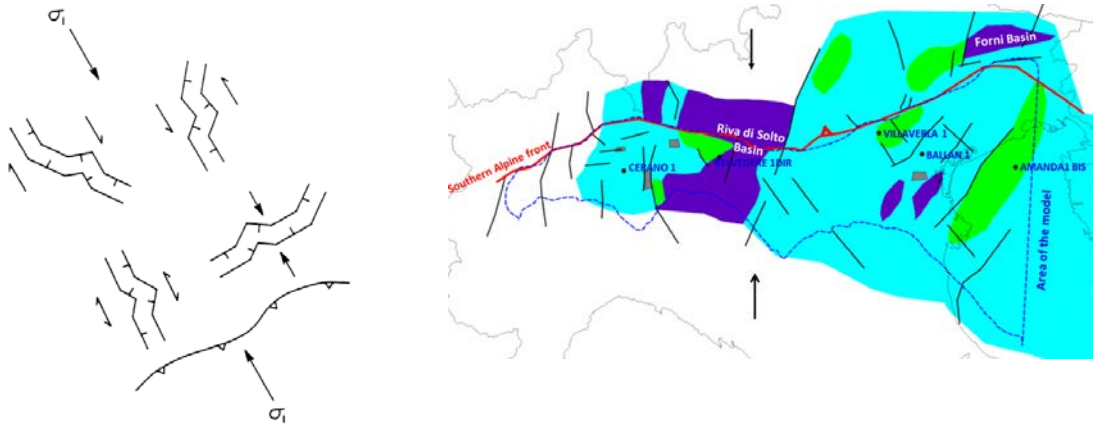

Figure 32- (left) map demonstrating range of possible angles of incidence of compression (during later inversion stage) to original rift-bounding faults (Lowell, 1995); (right) Alpine regional stress (arrows) vs Mesozoic basin and major fault zones in the Po Valley (ref. Part 5, Section V).

Scientific Lesson 4: *intensively faulted foreland domains can be seismically inactive irrespective of the fault orientation*. The Po Valley seismo-tectonic model shows such a situation as a clear fact in the western domain of the basin, between the Western Alps and Milan (ref. Part 5, Section III; Fig.6). In that region nearly none of the shallow and deep faults correlate with important earthquakes and that is true for any fault orientation.
The investigation of similar setting worldwide is out of the remit of this thesis so that we could only speculate about the possible reasons that would cause such phenomena in a wider geological-geographical perspective:

- is it due to lack of data?
- is that due to presence of fluid overpressures (typical in foredeep basins)?
- is that related to compartmentalization of the foreland at the front of an advancing belt with abandon of selected compartments?

The lesson is open for discussion.

Scientific Lesson 5: *sedimentary facies transition can eventually be more seismogenic than faulted domains*. Indeed, the Po Valley 3D seismo-tectonic model indicates that platform-to-basin transitions inside the Mesozoic carbonates appear to localize some earthquake activity more evidently than the associated faults (ref. Part 5, section III; Fig.14). Is it a matter of resolution of the modeled fault system? Is it a matter of fluid concentration along the transition between different porosity facies? Once again, the message from the performed 3D model is difficult to be confirmed by other examples worldwide. As a generic rule, faults are normally reputed for concentrating the energy that will result into an earthquake event. In order to substantiate the model conclusion, some local scale, detailed seismo-tectonic analysis is needed, instead of the common crustal/regional scale ones (Fig.33 & 34).

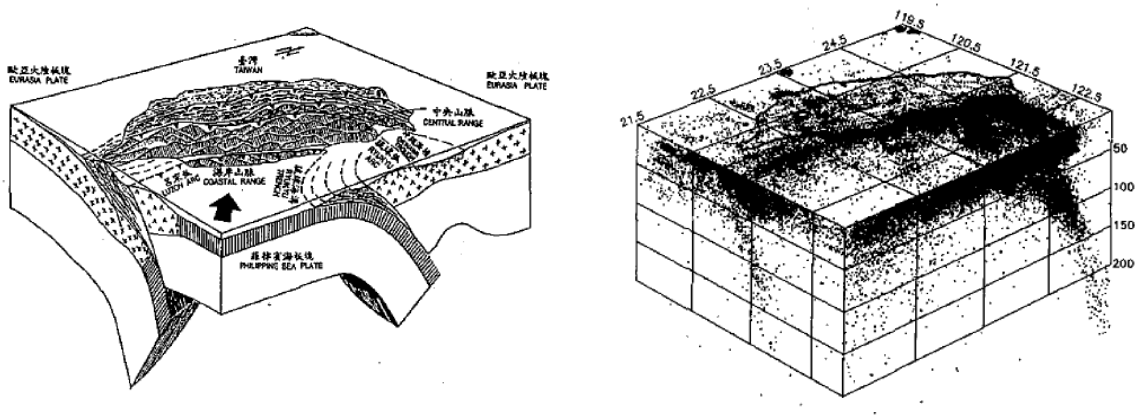

Figure 33- Taiwan seismicity against crustal tectonics (Wang & Shin, 1998)

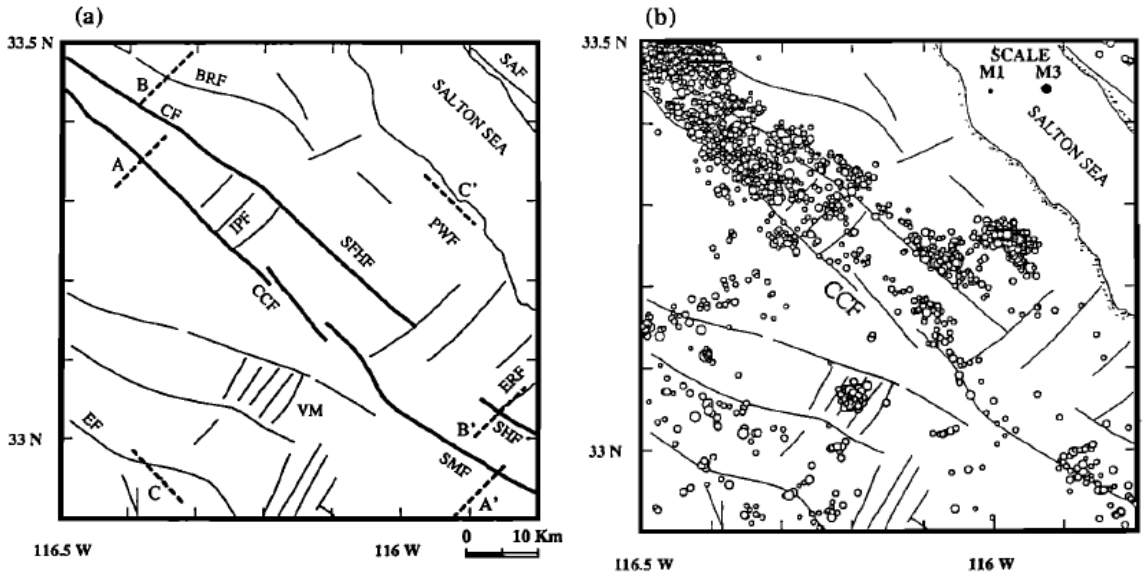

Figure 34 – Faults vs seismicity of the S.Jacinto fault zone (California) (Petersen et al. 1991)

Scientific Lesson 6: *overpressures in deep-seated carbonate lithologies might retard hydrocarbon maturation*. The thermal modeling that has been run using the Po Valley 3D model points to such a conclusion (ref. Part 5, Section V). It is true that retardation of maturation is one of the aspects pertaining to reservoir quality, migration, maturation, prospect identification and hydrocarbon retention that are demonstrably influenced by pore pressure (Fig.35) (Green et al. 2016). Although a few analogs can be spotted in the public literature (Carr, 1998; Zhou & Peng, 2001) various uncertainties in the hydrocarbon modeling process (source rock distribution and volume, TOC content, % of expulsed hydrocarbons vs % of retained hydrocarbons, reservoir heterogeneity, % of hydrocarbon losses along the path from source to reservoir), still bias the possible overpressure effects.

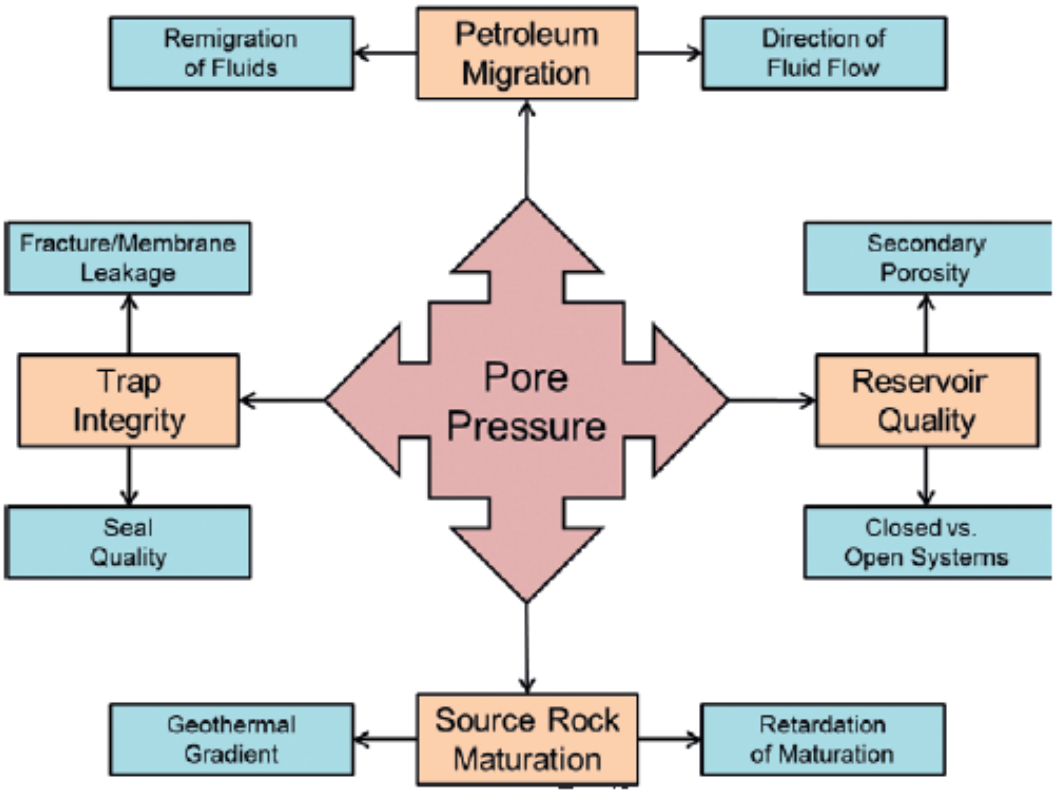

Figure 35 – Flow chart summarising the key influences of pore pressure on the major elements of the petroleum system (Green et al. 2016).

Scientific Lesson 7: *lateral ramps are preferential structures for accumulation of hydrocarbons.* Refing of the Po Valley 3D structures revealed a common characteristic to the major oil fields in the region (Part 5, Section 5): with the exception of the Gaggiano field, they appear to be located in correspondence of lateral-ramp domains (Fig.36).

Such an observation may just be a coincidence yet like Agata Christie (possibly) wrote "*One coincidence is just a coincidence, two coincidences are a clue, three coincidences are a proof*".

Whether A.C. intuition is right or wrong, the possible correlation between hydrocarbon accumulations and lateral ramp structures can be repeatedly observed in different part of the world (Fig.37).

The Cusiana field is sitting on a clear lateral ramp thrust-related feature in the Llanos foothills (personal communication from confidential report). The Tempa Rossa and M.te Alpi fields drilled some lateral ramp units which deform the Southern Apennines apulian carbonates (Turrini et al., 2004). The Shpiragu discovery penetrated the lateral ramp structures which model the southern Albanides thrust belt, at the front of Kruja front (Roure et al., 2004; Graham, 2006.). Further to these proofs (!) and from a theoretical standpoint, no doubts that fluids can circulate more easily, at least intermittently, across highly faulted and fractured domain (especially in carbonate lithologies – see Shpiragu cross-section and cores from the well in Fig.37) like transfer zones, strike-slip units, lateral ramp structures (Verges).

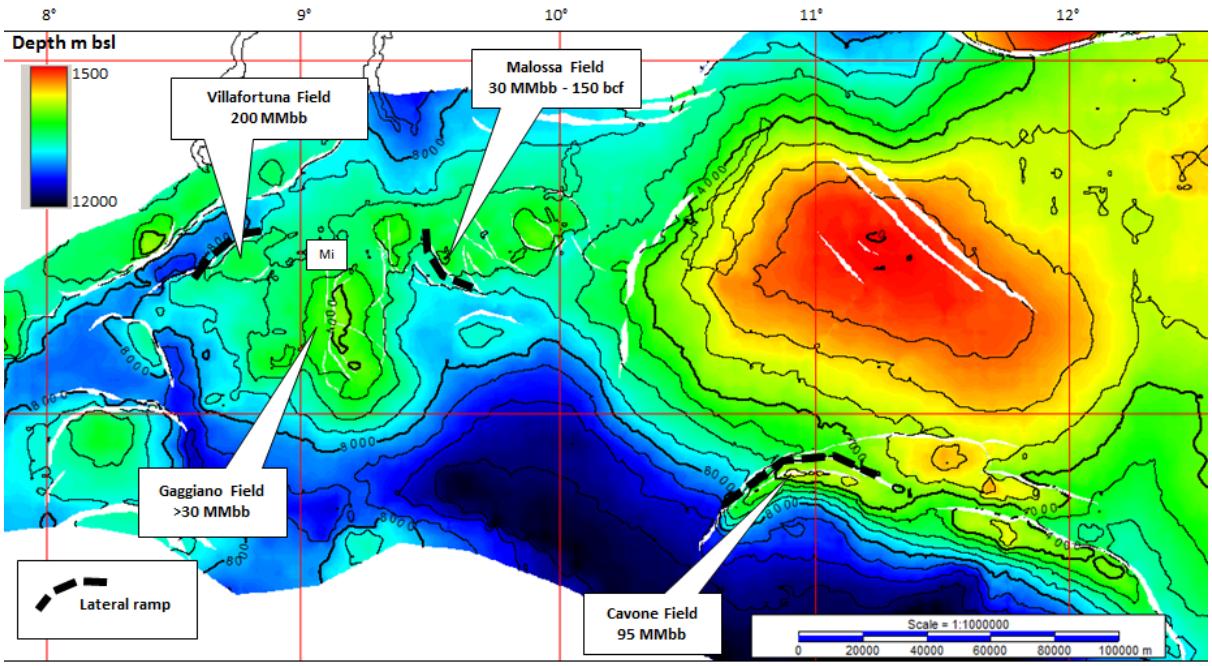

Figure 36 - Top Mesozoic Carbonate depth grid and lateral-ramp domain related oil-field structures in the Po Valley.

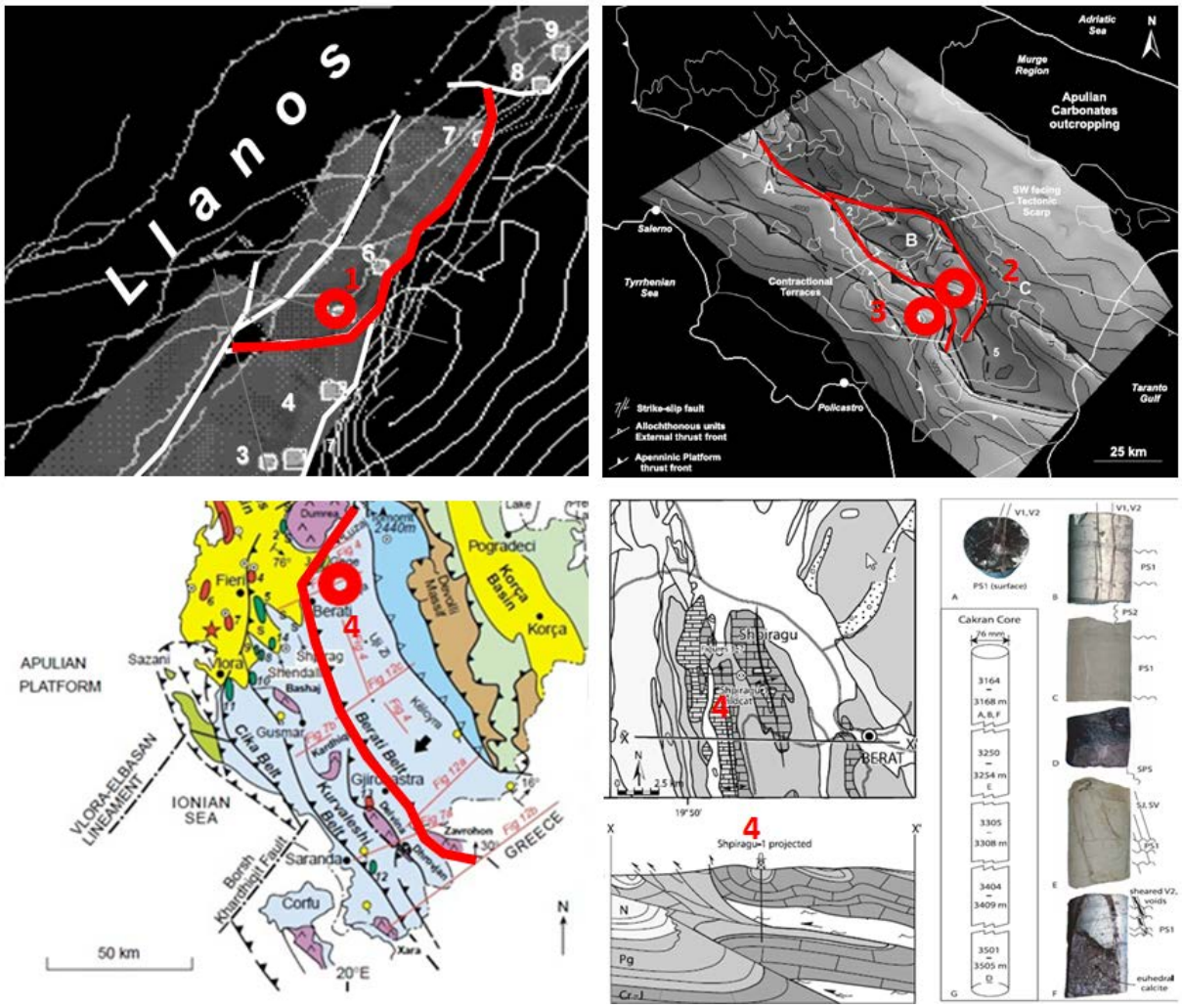

Figure 37- Oil fields in lateral-ramp structures; 1=Cusiana-Cupiaga (map view), 2=T.Rossa, 3=M.te Alpi (map view), 4=Sphiragu (map view & cross-section). Red are major thrusts. (See text for references and discussion).

List of Figures *(outside Papers)*

Annexes

In order to provide key references about some of the recent applications of 3D modeling to structural analysis, a number of case studies from the recent literature (ref. Part 3, Section II – Tab.1) are hereafter briefly described and illustrated by selected images.

Berthoux et al. (2016) elaborated from geological and geophysical constraints a 3D structural-seismo-tectonic model of the region between the inner zones of the Alps and Corsica to implement the seismic hazard evaluation in the area.

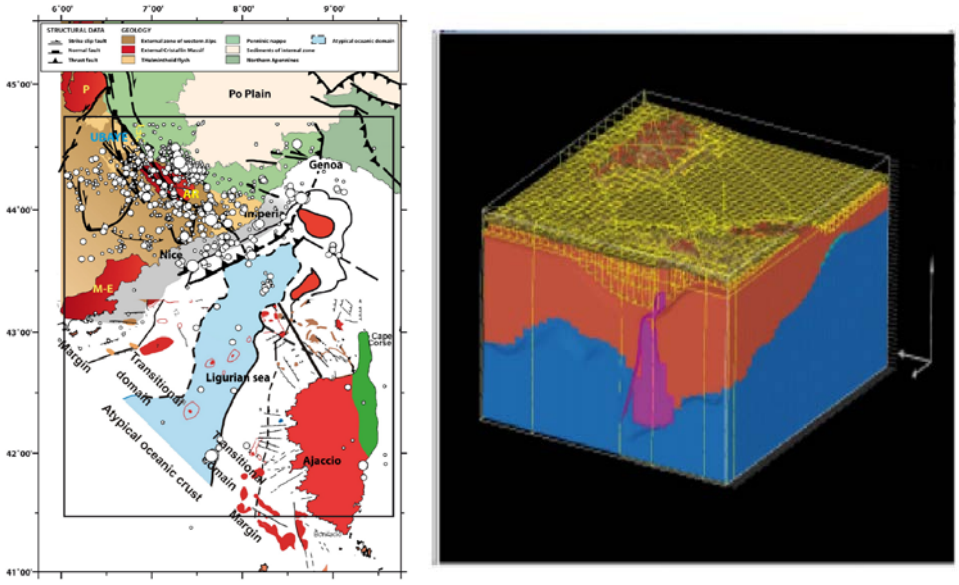

Fig.A1 – (left) location map; (right) 3D model (see papers for extended discussion).

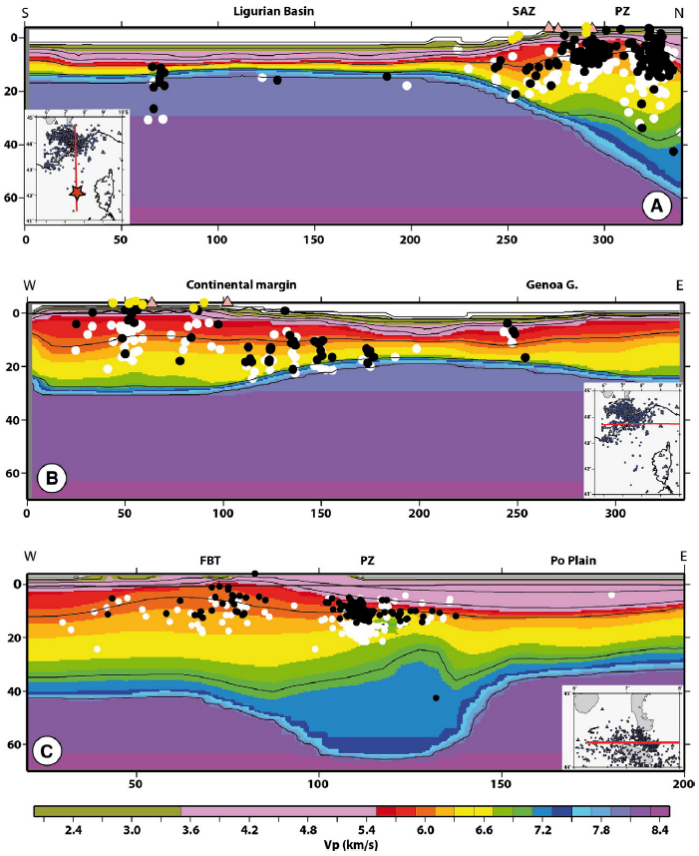

Fig.A2 – Sections across the 3DP-velocitymodel, showing earthquakes projected onto the section if their distance from the section is smaller than 10 km (see paper for extended discussion).

By systematic mapping of coal seams and faults, **Cardozo et al. (2016)** built the 3D structural model of the Tabaco anticline (northern Colombia) resulting into the understanding of the transpressive structural evolution of the area.

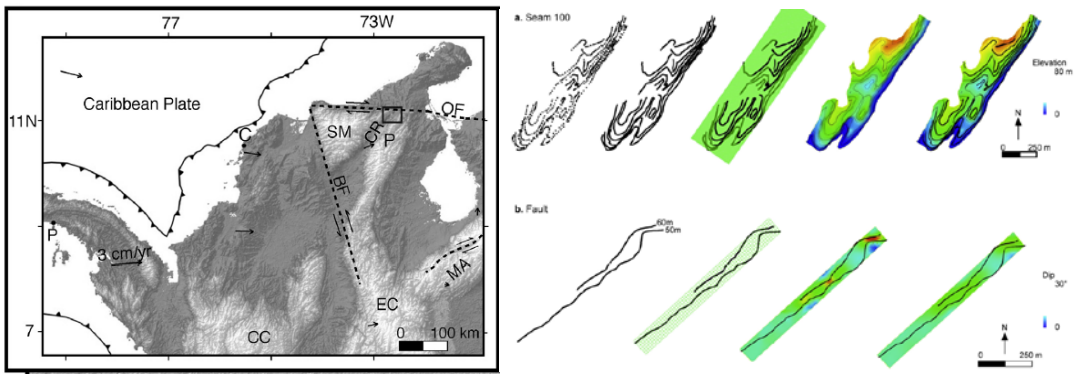

Fig.A3 – (left) location map; (right) steps taken in the 3D model building (see paper for extended discussion).

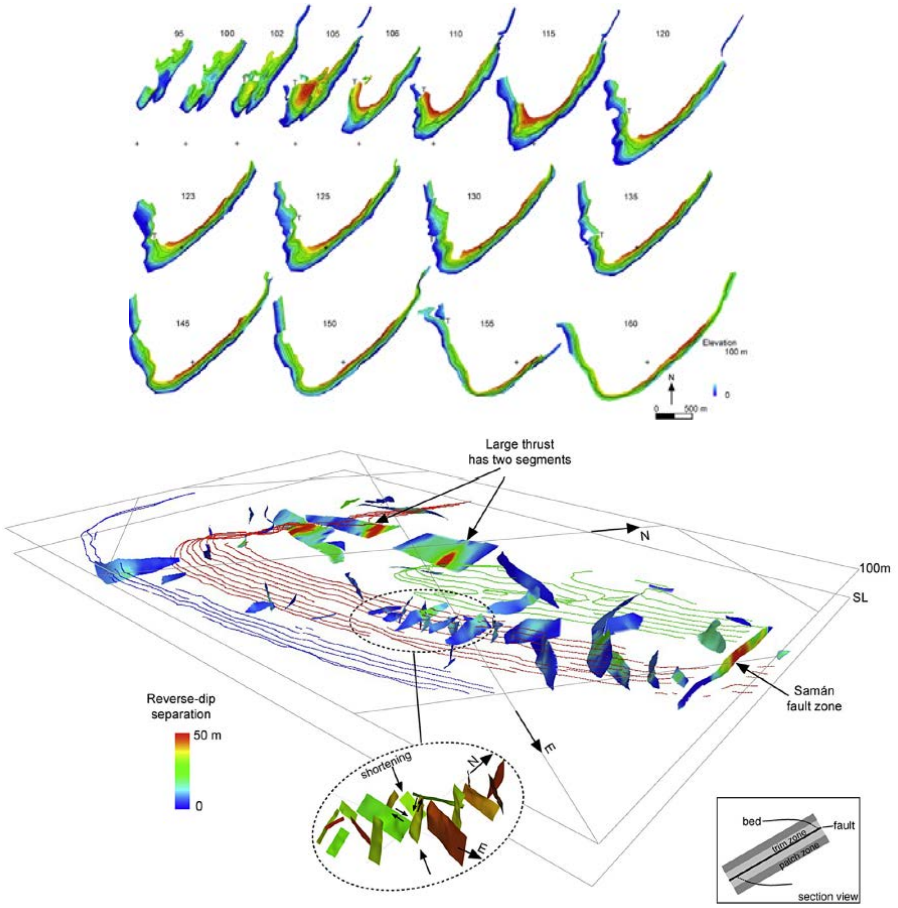

Fig.A4 – 3D model analysis (see paper for extended discussion).

Galuppo et al. (2016) performed 3D models from sandbox experiments to investigate the fracture patterns evolution in fault-related anticlines, e.g. fault-propagation and fault-bend fold.

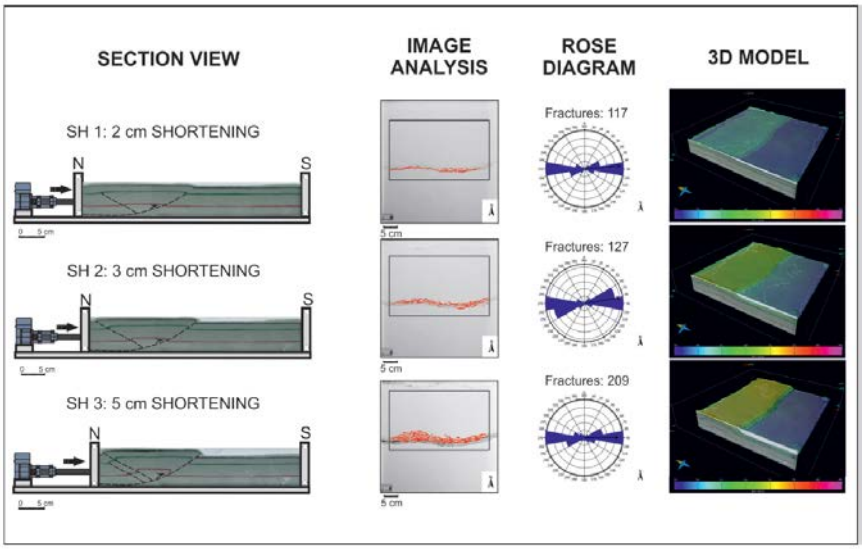

Fig.A5 - Progressive evolution of fault-propagation fold model; first column = section view, second column = fracture patterns in map view, third column = rose diagrams of fractures relative to the represented passages, fourth column = 3D models of the three different deformation steps (see paper for extended discussion).

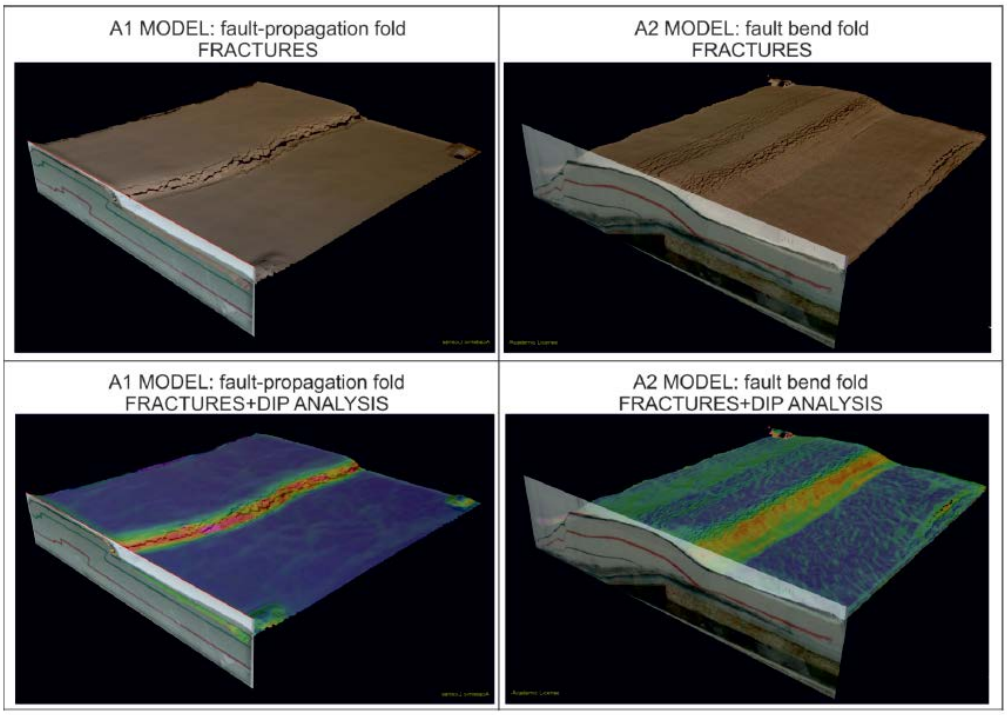

Fig.A6 - Three-Dimensional reconstructions of the A1 Model (fault-propagation fold, top left) and A2 Model (fault-bend fold, top right) at final step of deformation (5 cm of shortening); (see paper for extended discussion).

Schöpfer et al. (2016) use a discontinue numerical approach, the 3D distinct element method (DEM), to model the evolution of normal fault zones in mechanically layered sequences.

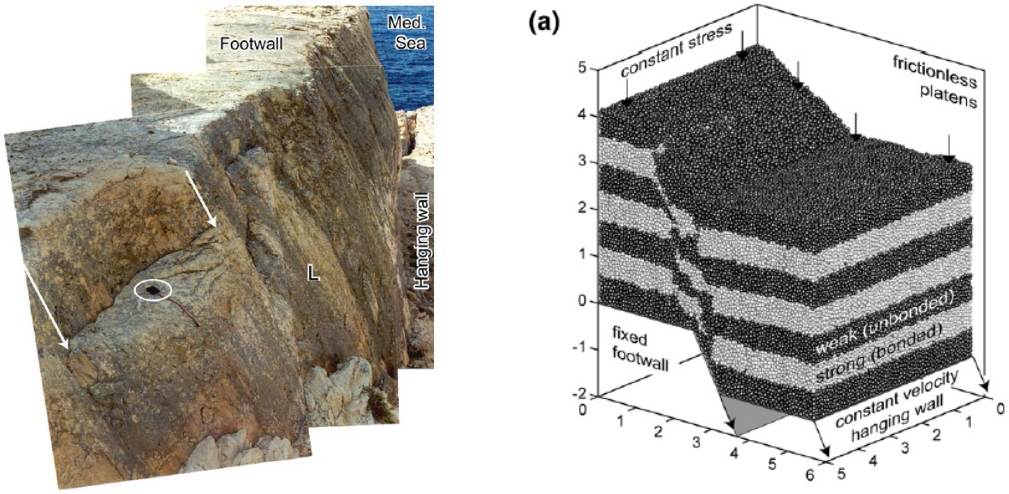

Fig.A7 – (left) fault outcrop example (Malta); (right) DEM modeling of fault growth on a multilayered sequence and stress-strain (see paper for extended discussion).

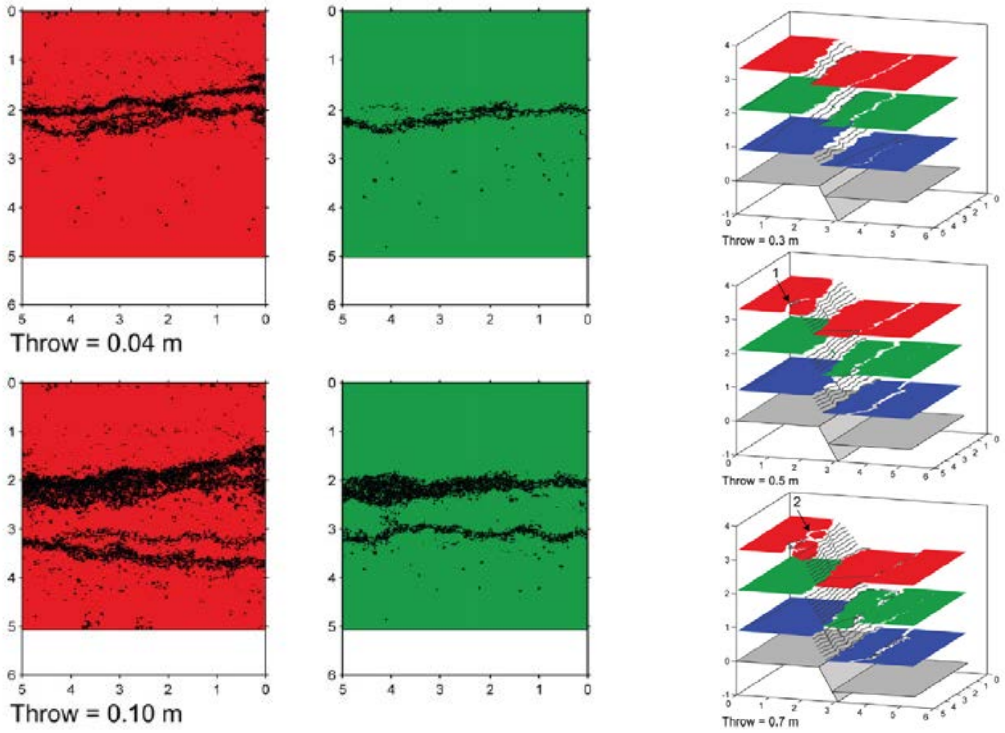

Fig.A8 – map and 3D perspectives of fault zone evolution for progressive throw increments (see paper for extended discussion).

Cherpeau & Caumon, (2015) introduces a stochastic structural modelling method that honors interpretations of both faults and stratigraphic horizons on maps and cross-sections in conjunction with prior information, such as fault orientation and statistical size–displacement relationships. The authors focus on fault uncertainties in settings where the number and overall topology of faults is poorly constrained. The goal of the method is to help interpretation tasks by automatically generating alternative models of field geometry and compartmentalization compatible with observations.

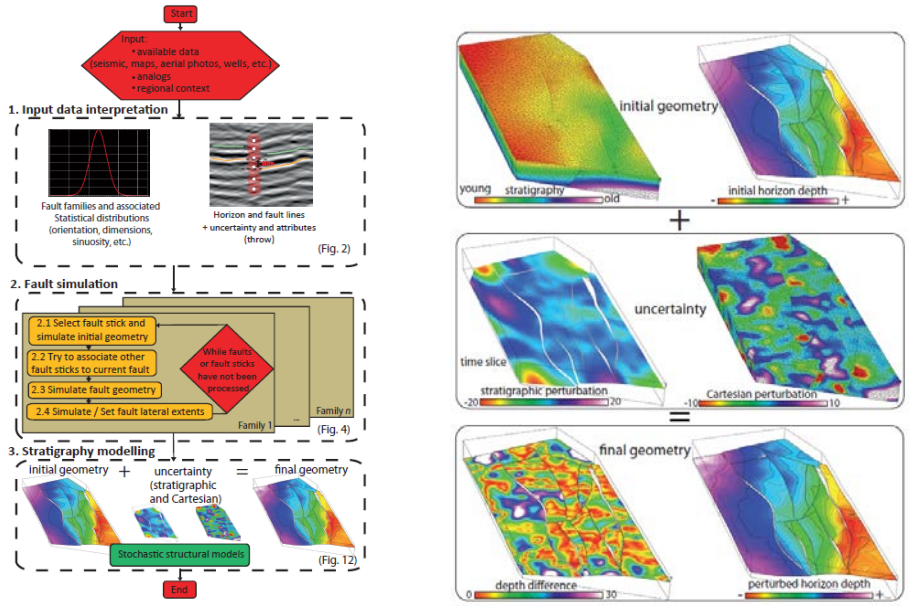

Fig.A9 – (left) flow chart showing the general simulation process; (right) method for modelling stratigraphic uncertainty (see paper for extended discussion).

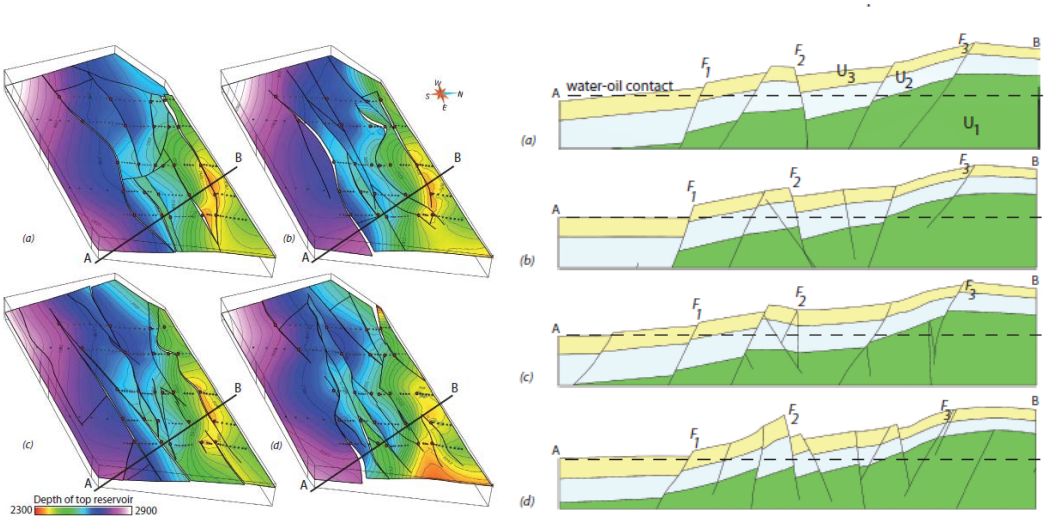

Fig.A10 – (left) Example of stochastic model in map view (top reservoir surfaces) and (right) the related cross-sectional structures (see paper for extended discussion).

Guyonnet-Benaize et al. (2015) performed a 3D model of the deep basin structure of the Middle Durance region by integration of geological and geophysical data, to evaluate the segmented fault geometry and the associated tectonic history.

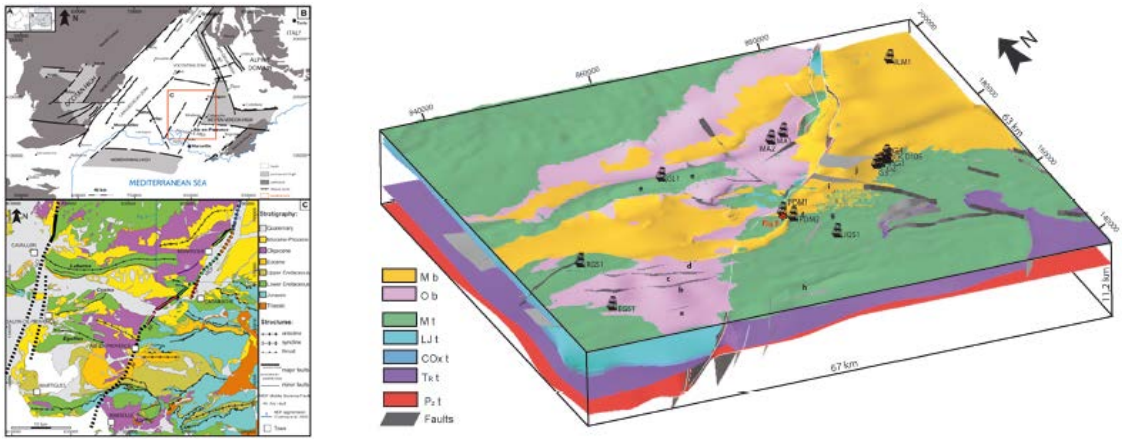

Fig.A11 – (left) location map; (right) 3D model of the studied region (see paper for extended discussion).

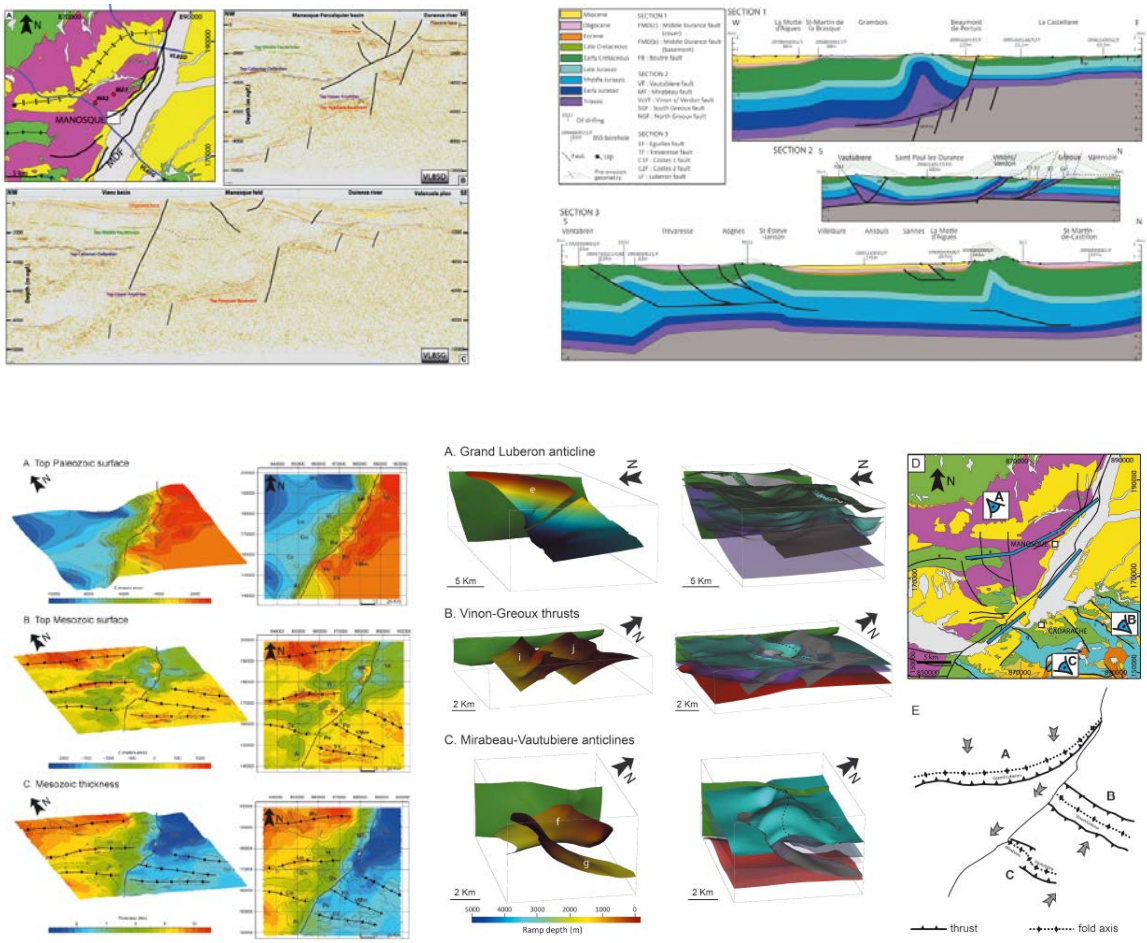

Fig.A12 – (top) seismic and structural sections; (bottom) 3D model horizons and structures (see paper for extended discussion).

The study of **Katsuaki et al. (2015)** integrates 3D models of rock fractures from different sources (particularly boreholes) and hydraulic properties aimed at identifying relationships between fractures and permeability in the Tono area, central Japan.

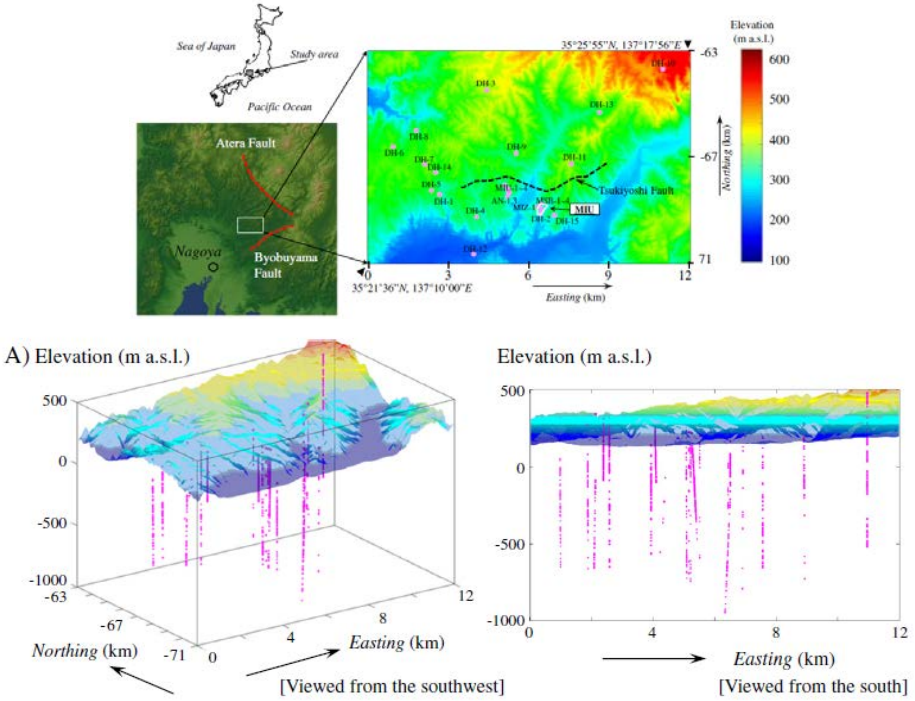

Fig.A13 – (above) location map and DEM of the study area; (below) perspective view of topography and boreholes (see paper for extended discussion).

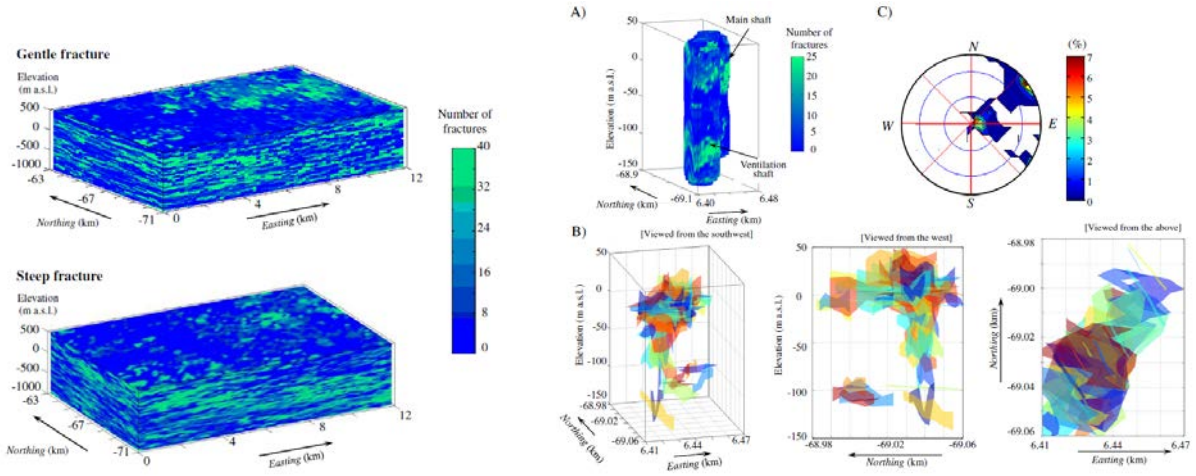

Fig.A14 – (left) 3D simulated fracture density; (right) (A) Density map of fractures through boreholes, (B) perspective views of the relatively continuous fracture planes by GEOFRAC, and (C) orientations of the simulated fractures by the Schmidt's net lower projection (see paper for extended discussion).

By the integration of all available geological and geophysical data (interpreted seismic refraction and reflection data, seismological data, geological maps and previously published 3-D models) **Klitzke et al. (2015)** present a regional 3-D structural model of the Barents Sea and Kara Sea region which combine information on the sediments and the crystalline crust as well as the configuration of the lithospheric mantle.

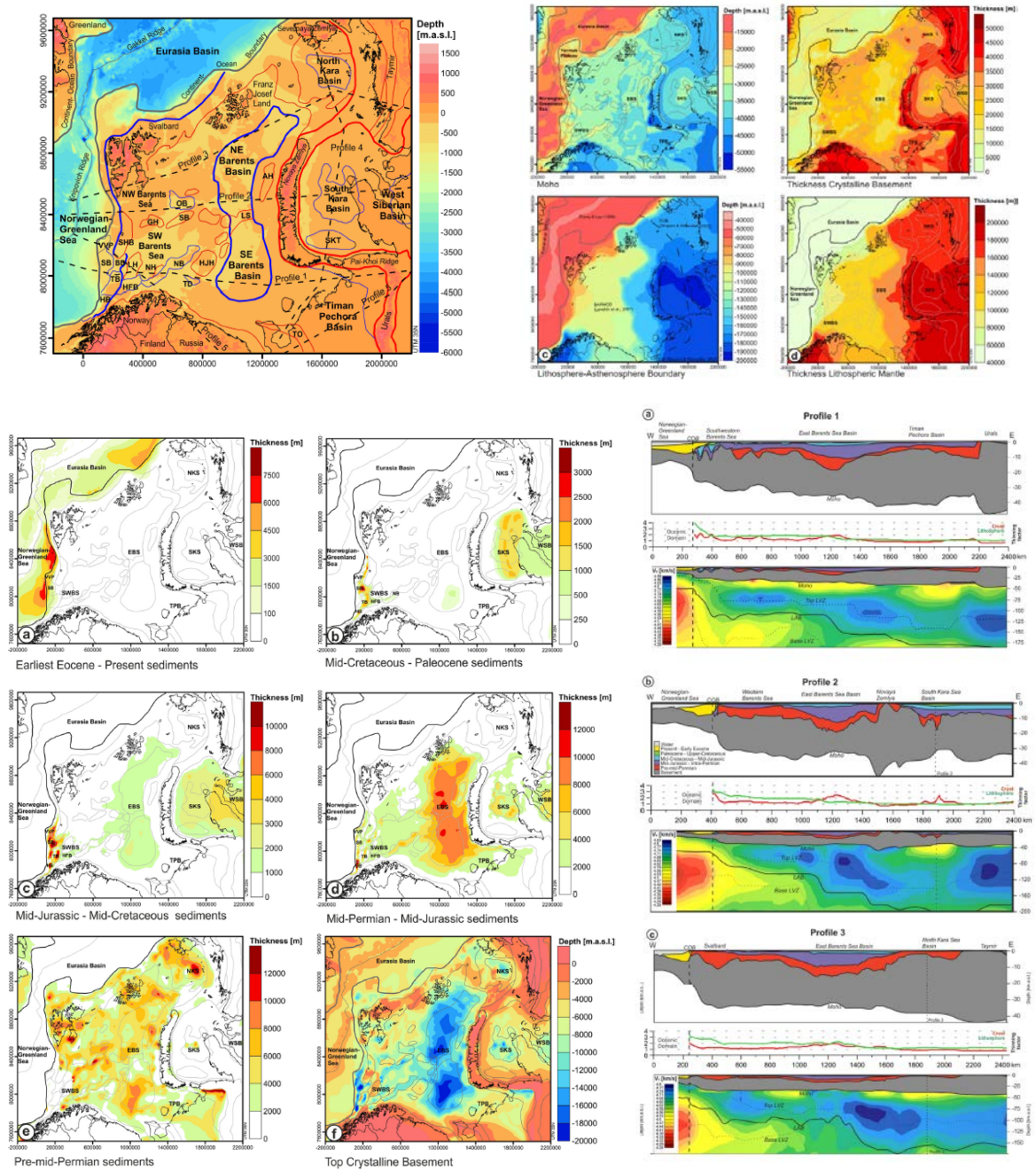

Fig.A15 – (top left) location map; (top right) structure of the deeper crust and upper mantle; (bottom left) thickness of mega-sequence and depth to top crystalline crust; (bottom right) crustal section illustrating main geological units and velocity distribution (see paper for extended discussion).

Using well-log and 3D seismic reflection data **Alcade et al. (2014)** built a subsurface 3D geological model of the Hontomín site (north-western Spain) to estimate CO2 storage capacity of the investigated structure and the associated fractured carbonate reservoir.

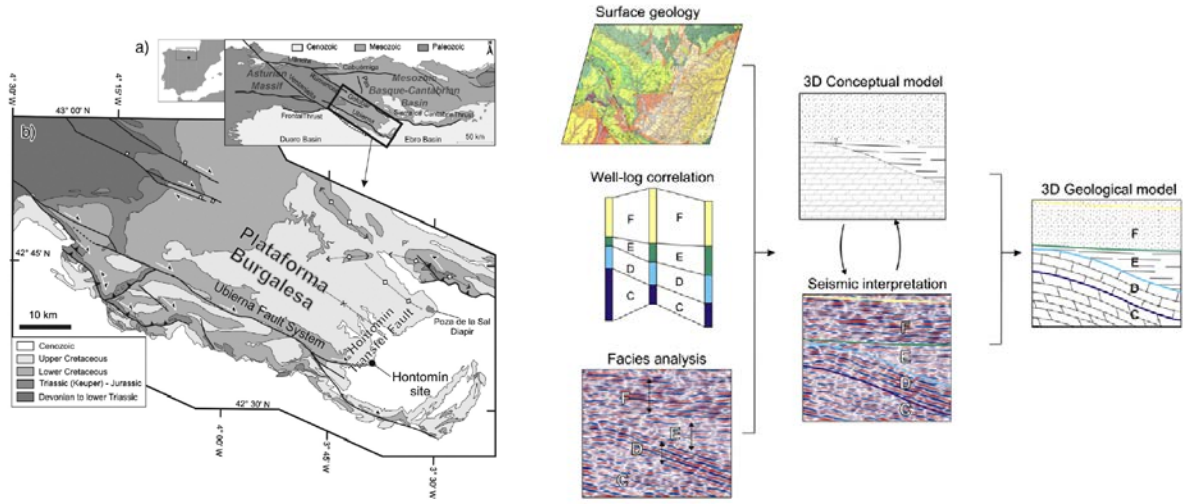

Fig.A16 – (left) Location map; (right) 3D model workflow (see paper for extended discussion).

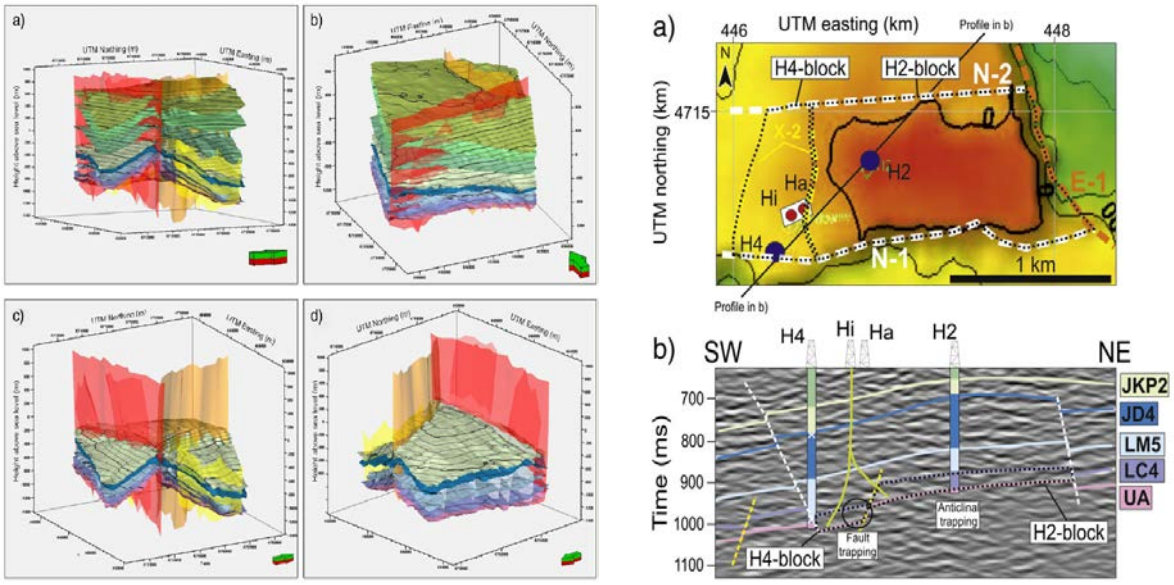

Fig.A17 – (left) 3D model of the Hontomin site; (right) map from the 3D model of the potential CO2 reservoir and section through the interpreted structures (see paper for extended discussion).

Campani et al. (2014) present a regional study that investigates the interplay between folding and faulting and its implications for the resulting exhumation pattern of the gneiss dome using 3D geometric modelling**.**

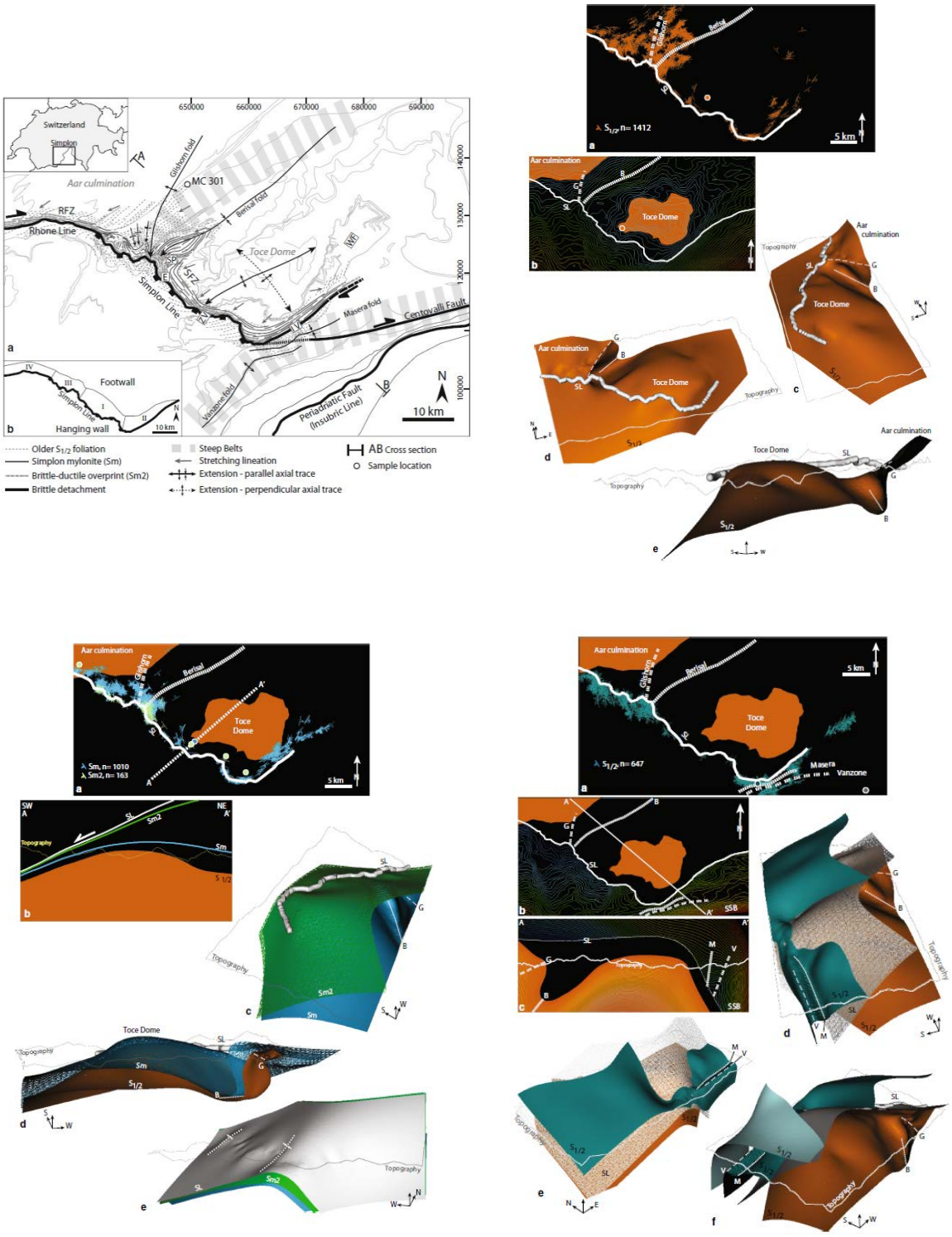

Fig.A18 – Location map and 3D model development as by recognized deformation history of the study region (see paper for extended discussion)

Fernandez and Kaus (2014) perform 2D and 3D numerical simulations about multilayerd fold growth as a function of fold segment interactions and evolution of fold width–length aspect ratio. The numerical simulations show a number of similarities with the Fars region of the Zagros fold-and-thrust belt.

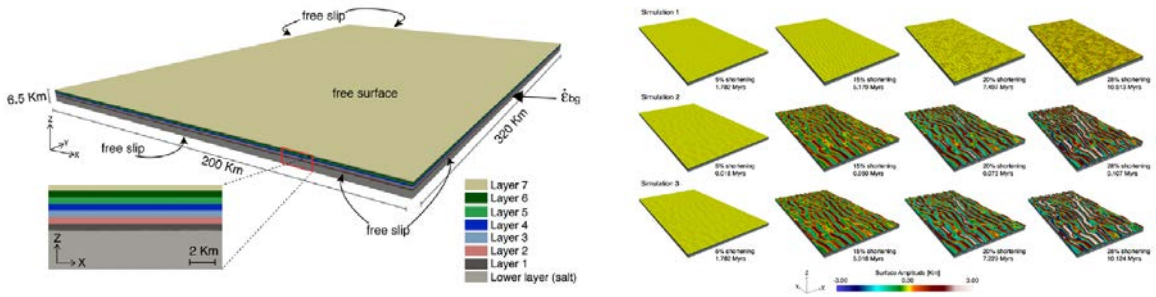

Fig.A19 – (left) Setup of the 3D multilayer detachment folding; (right) time and strain evolution of Simulations 1 to 3. Amplitude is coloured with the same scale for all the simulations for direct comparison (see paper for extended discussion).

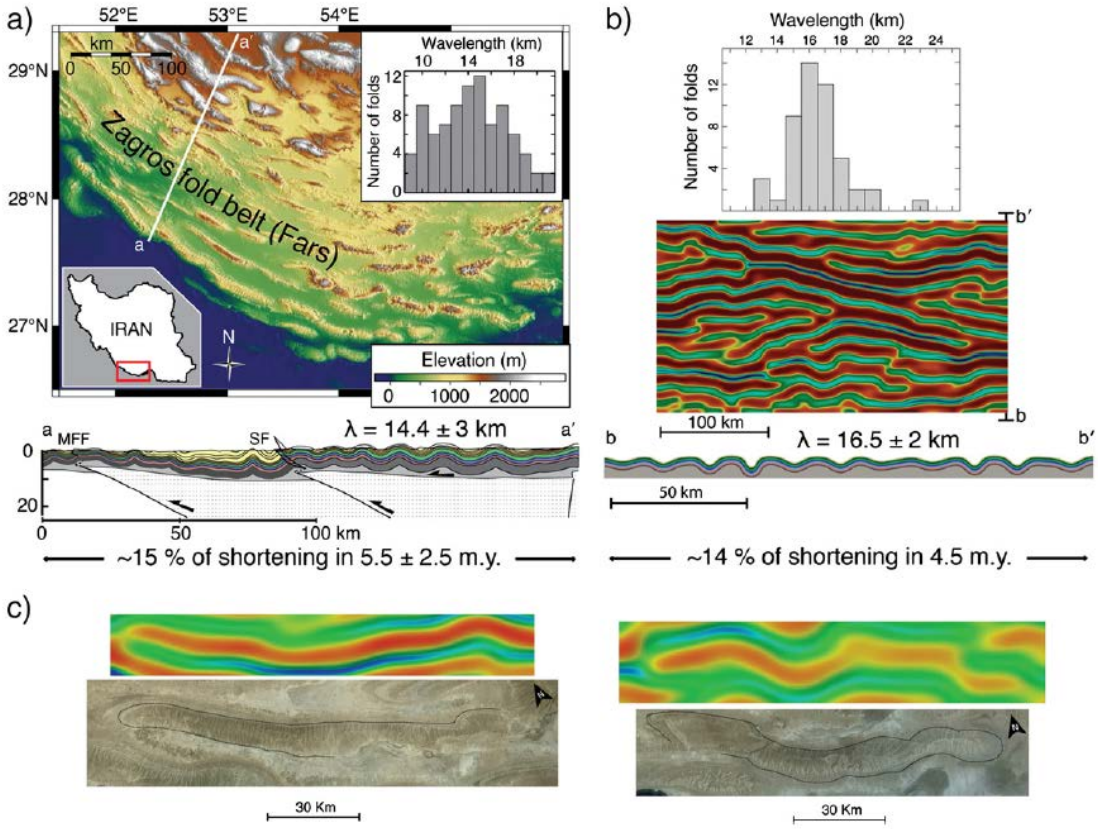

Fig.A20 - Comparison of some features observed in Simulation 6 with the Fars province in the Zagros Folded Belt (see paper for extended discussion).

Petricca & Carminati (2014) use 3D viscoelastic models to investigate the impact of geometry and kinematics on the lithospheric stress in convergent margins.

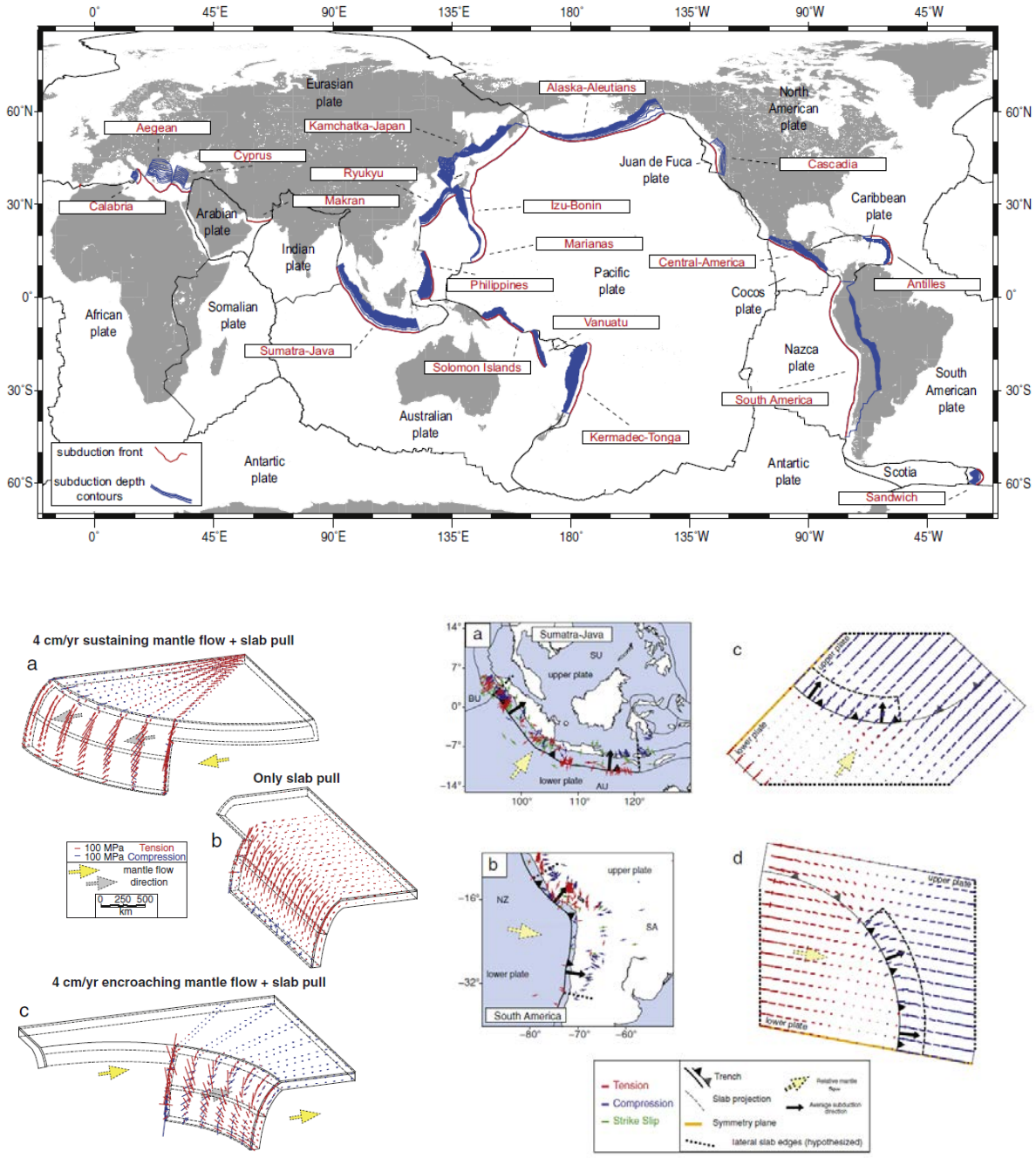

Fig.A21 – (top) active subduction zones; (bottom left) 3D modeling results; (bottom right) intraplate stress orientation for the sustaining mantle flow subduction zone cases (see paper for extended discussion).

Gisquet et al. (2013) applied a subsurface modeling method to perform an outcrop-based 3-D structural, stratigraphic, and diagenetic model. Our goal was to unravel composite dolomite bodies in a folded area and to realize a true 3-D geometric model using the case of the Etoile massif complex ramp anticline.

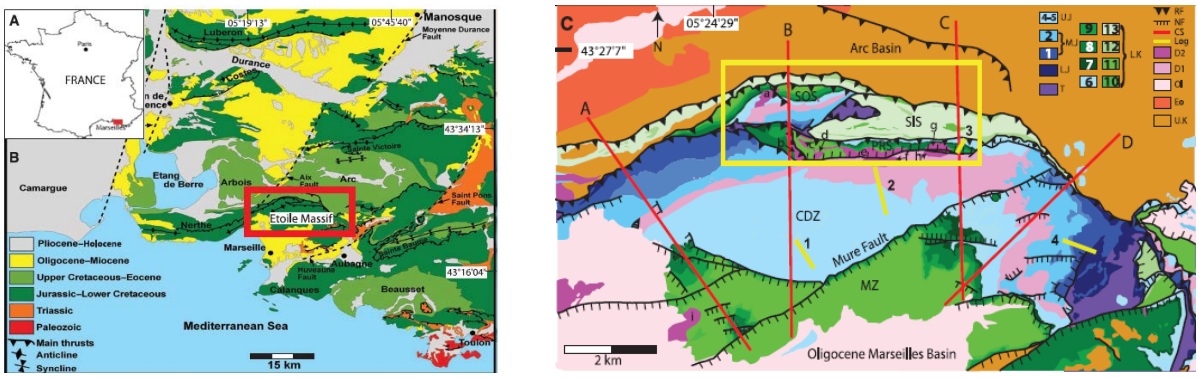

Fig.22 – (left) location map; (right) tectonics and 3D model boundary (see paper for extended discussion).

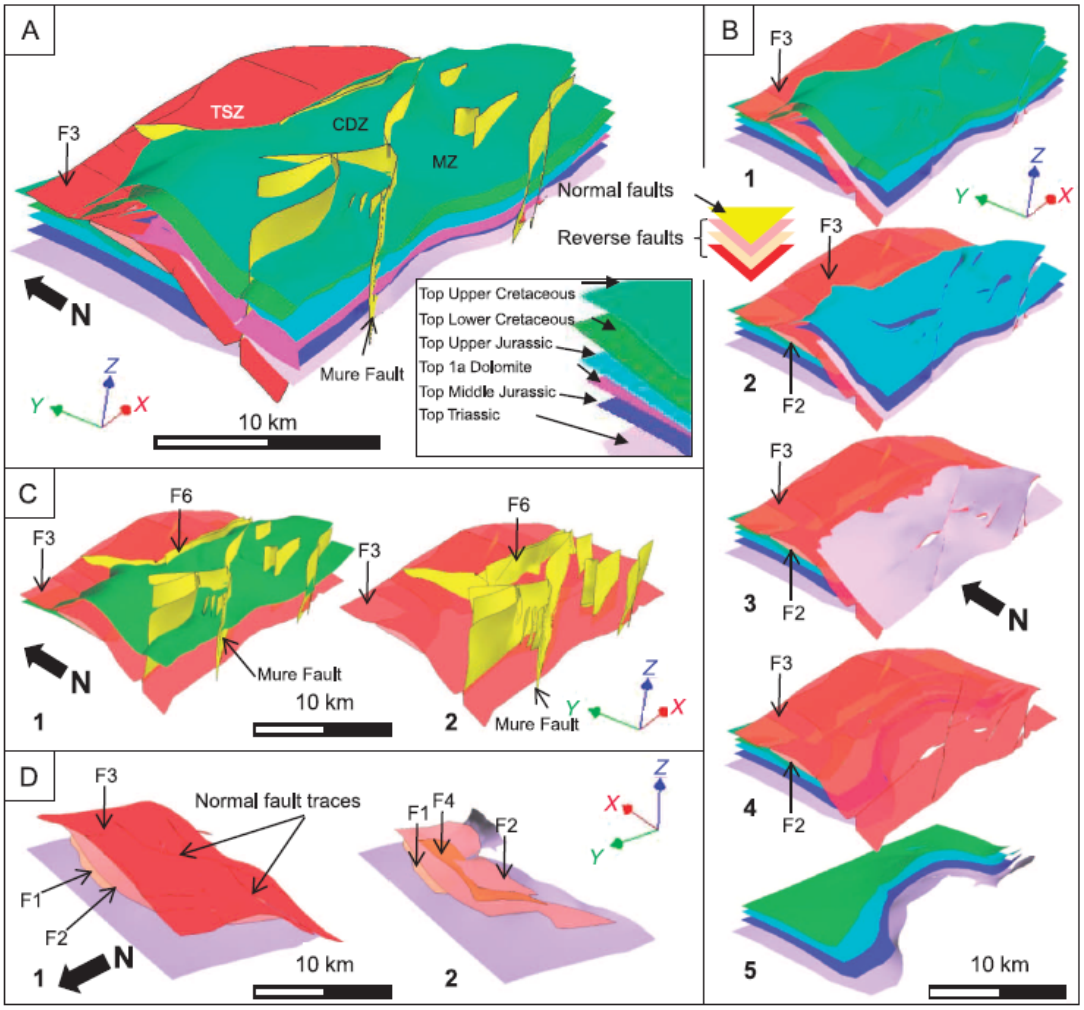

Fig.23 – different views of the Etoile massif 3D model (see paper for extended discussion).

Guglielminetti et al. (2013) combined use of 3D geological modeling and gravity surveys for geothermal prospection of a hydrothermal area in the western Alps where a very complex geological and structural setting is expected.

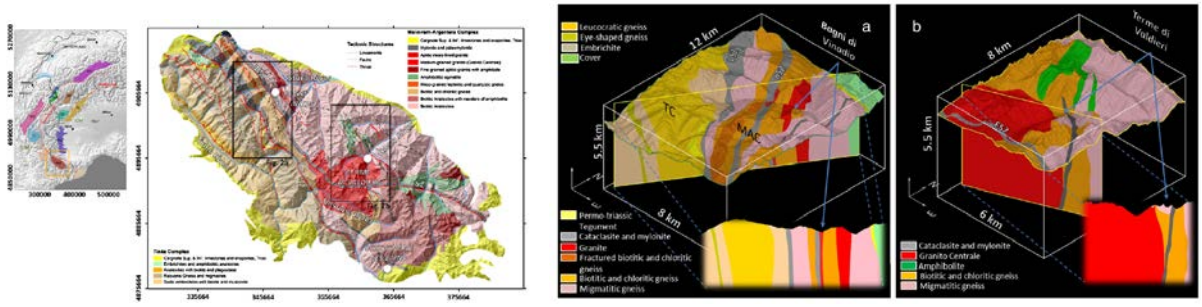

Fig.A24 – (left) geological map of the Argentera Massif, in the western Alps; (right) 3D modeling across the study region (see paper for extended discussion).

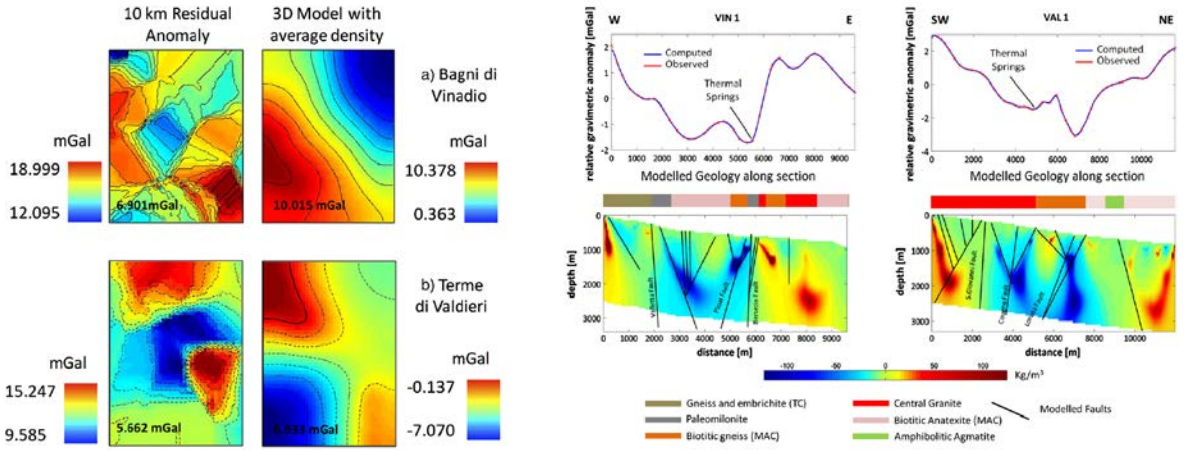

Fig.A25 – comparison between measured and calculated (using the 3D geological model) gravity fields (see paper for extended discussion).

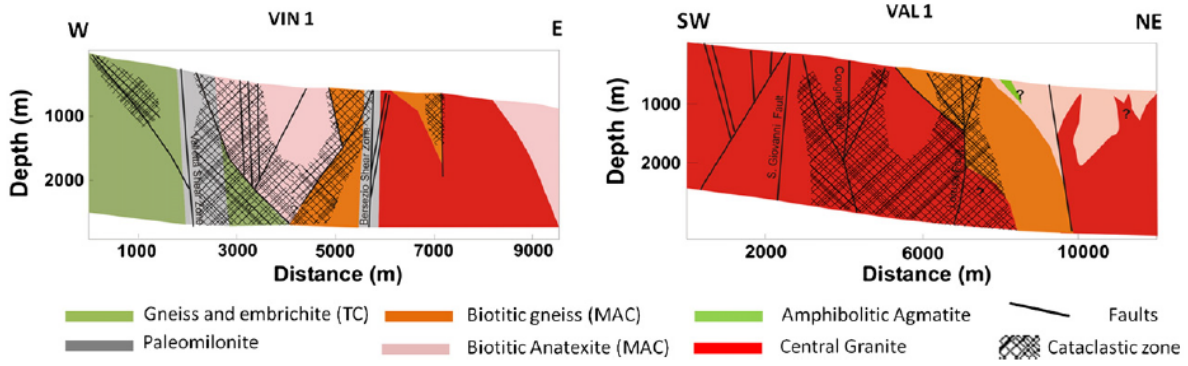

Fig.A26 – final interpretation along selected profiles across the 3D geological-gravity model (see paper for extended discussion).

Based on well constrained data/interpretations of the Central European Basin System, **Maystrenko et al. (2013)** carried out and analyzed the 3D crustal-scale model of the region to understand the influence of the major post-Permian tectonic events on the geometries and kinematics of the Upper Permian (Zechstein) salt.

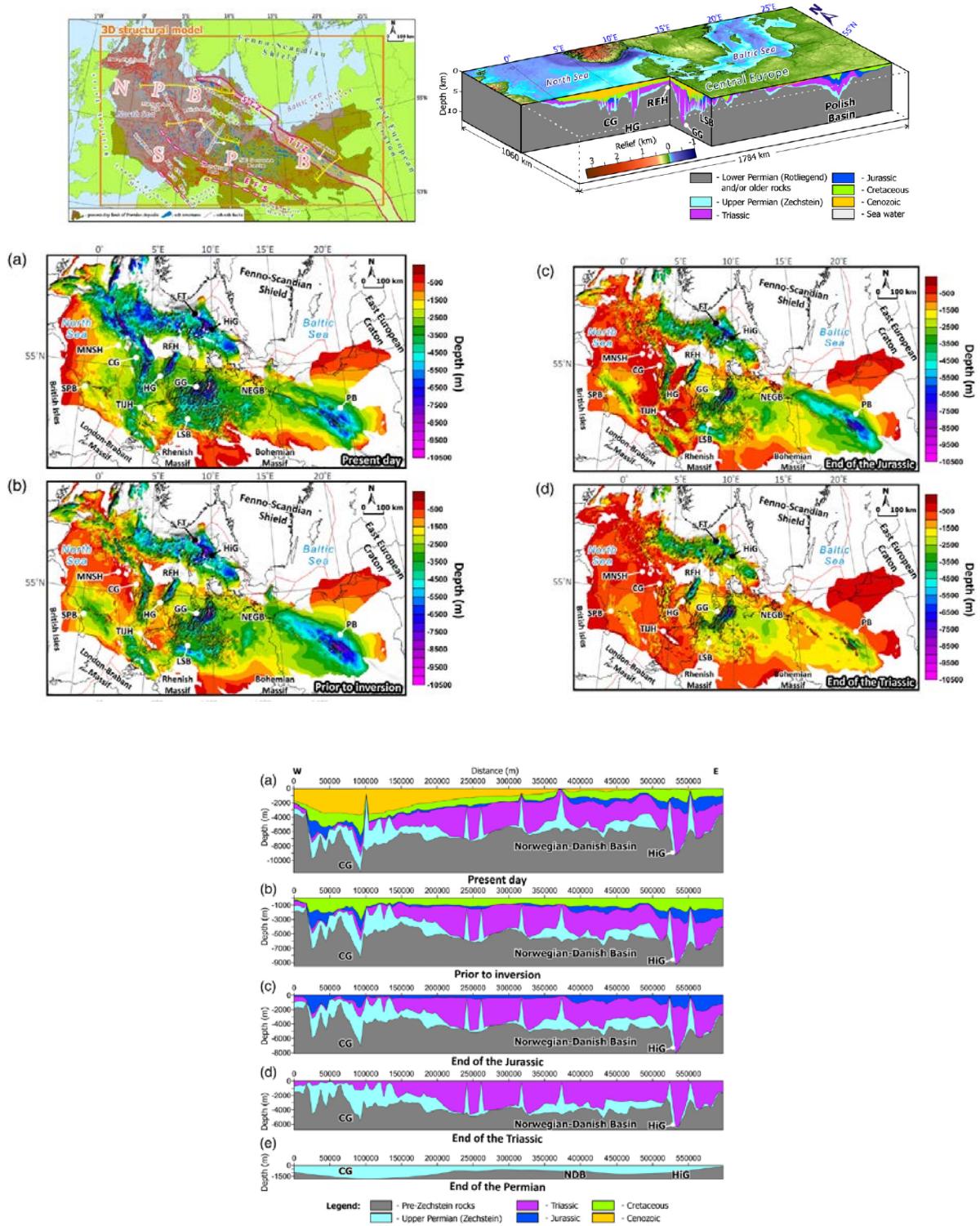

Fig.A27 – (top) location map and 3D model; (center) paleo-top of upper Permian salt through time; (bottom) 2D Permian-to-present tectonics (see paper for extended discussion).

Paul and Mitra (2013) present and analyze 3D models based on clay experiments to determine the geometry, evolution, and fault patterns associated with transfer zones in rift basins.

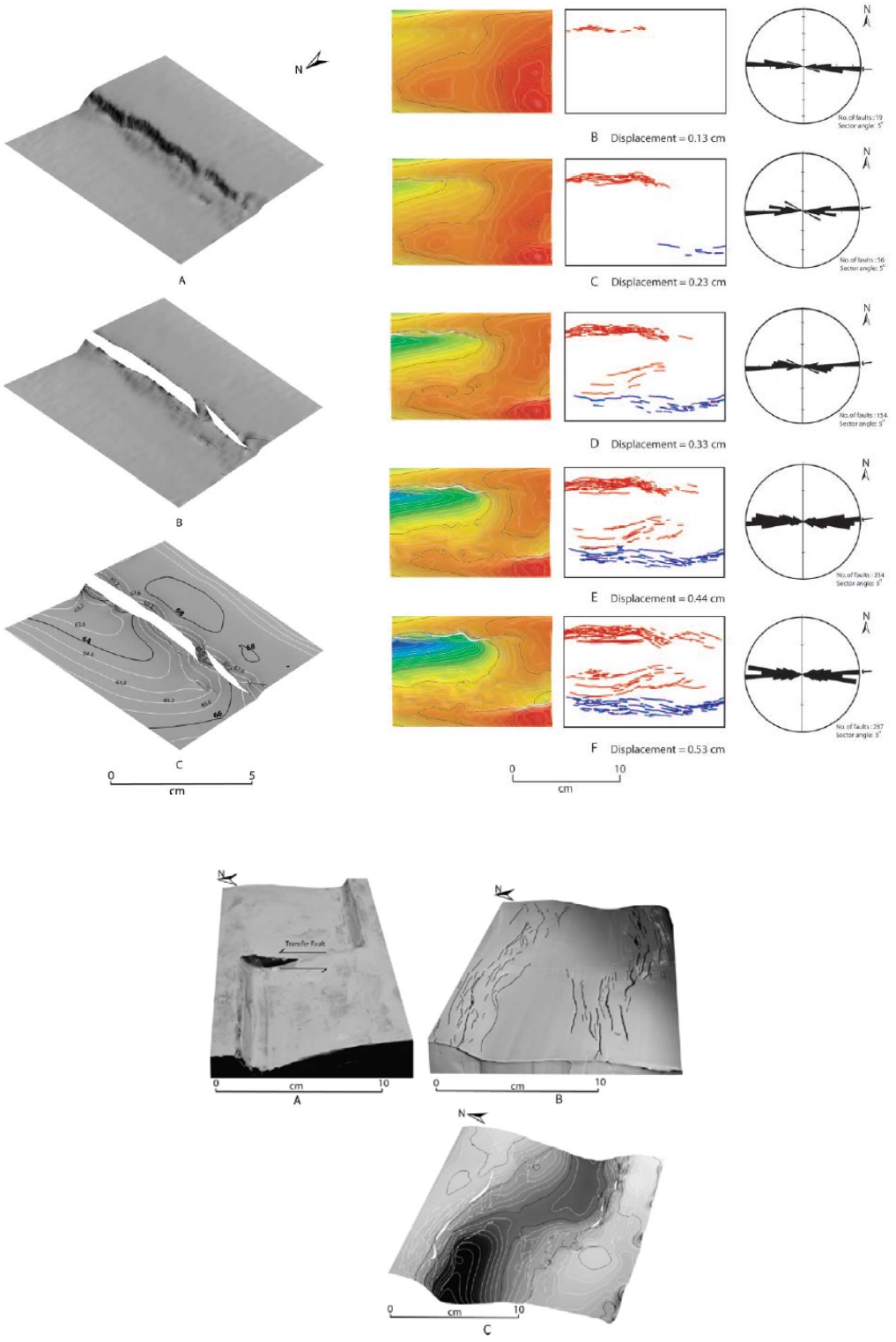

Fig.28 – (top-left) method of incorporating faults in 3-D surfaces; (top-right) progressive evolution of structural geometries and fault patterns; (bottom) oblique view of the clay experiment and the associated 3D model. (see paper for extended discussion).

Ramon et al. (2013) propose the use of X-ray computed tomography to reconstruct the geometry of analog models, inspired in the Balzes Anticline (External Sierras, Southern Pyrenees), and to characterize deformation patterns within the modeled structure in 3D.

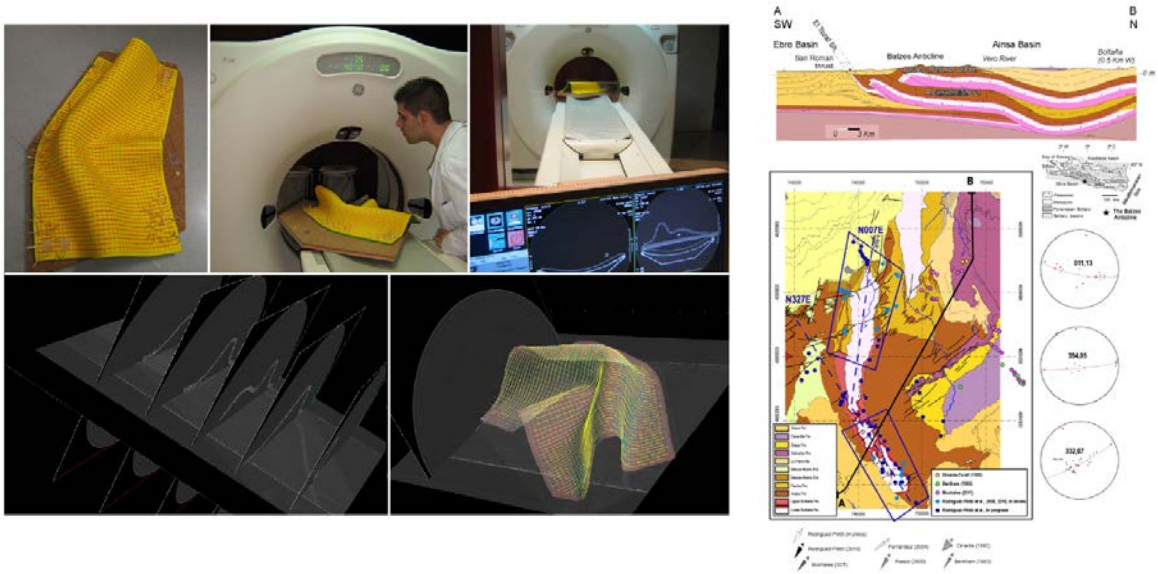

Fig.A29– (left) physical model and TAC apparatus/ methodology; (right) the Balzes Anticline structures (see paper for extended discussion).

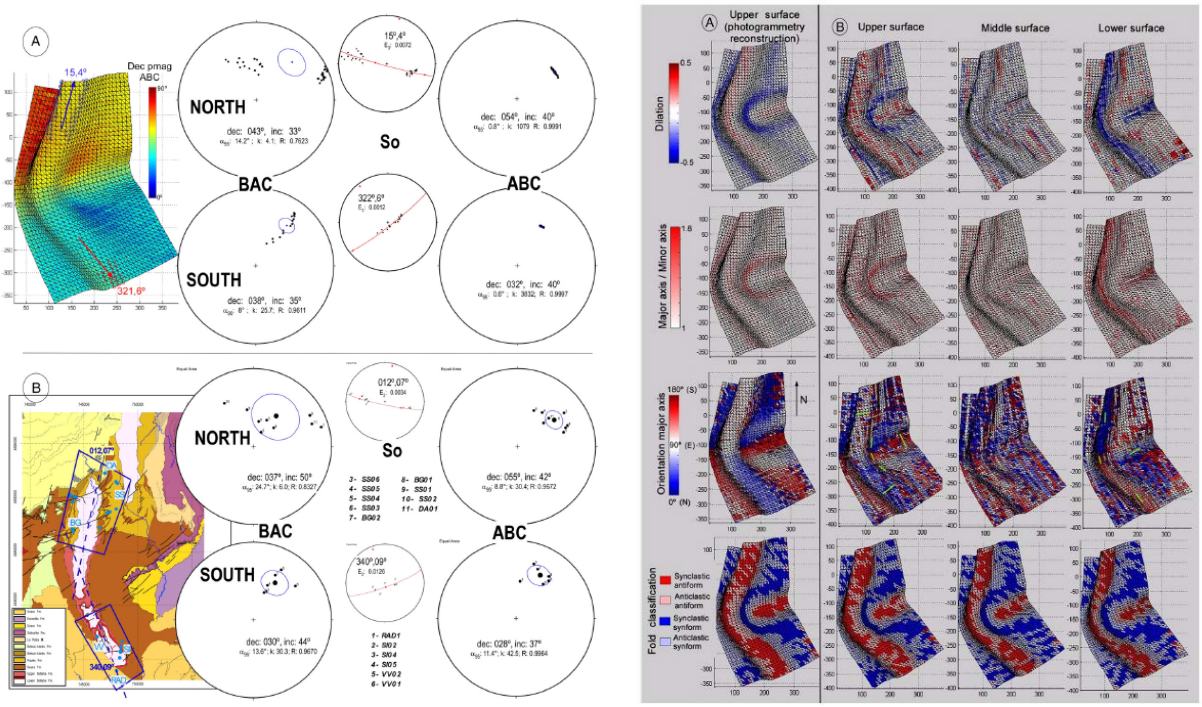

Fig.A30 – (left) 3D model vs outcrop structures; (right) 3D model surface analysis (see paper for extended discussion).

Sala et al. (2013) build a 3D structural model of the Chemery region (south-western Paris basin, France) exclusively based on borehole data (lithologies and velocities).

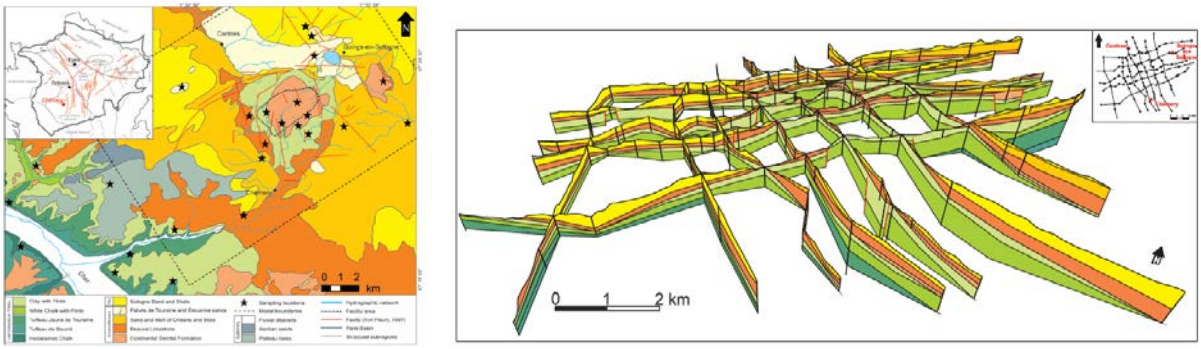

Fig.A31 – (left) location map; (right) fence diagram built on well stratigraphy correlation (see paper for extended discussion).

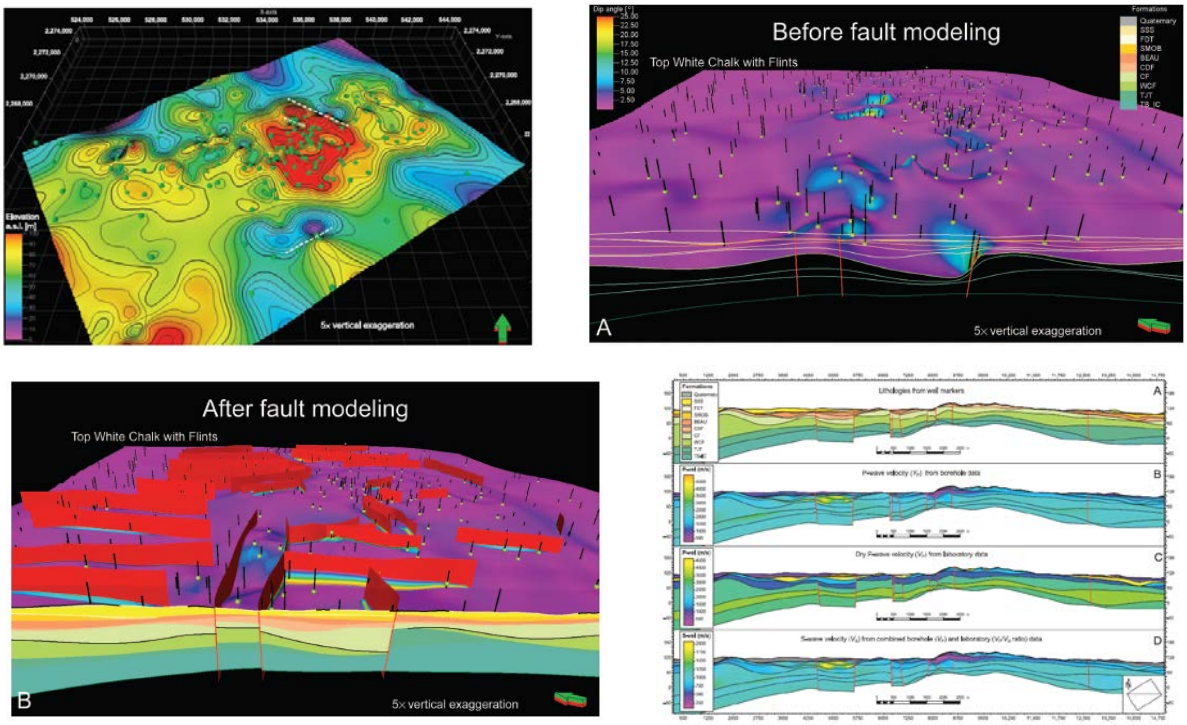

Fig.A32 – 3D model building by (top left) stratigraphic well-top gridding, (top right) velocity distribution and (bottom left) fault reconstruction: cross-section through the final model showing lithologies, structures and velocities (see paper for extended discussion).

Combining onshore and offshore information in the Bouillante zone that crosses the Guadeloupe Island coastline (French West Indies), **Calcagno et al. (2012)** propose a 3D fault model to evaluate the geothermal resources in the region.

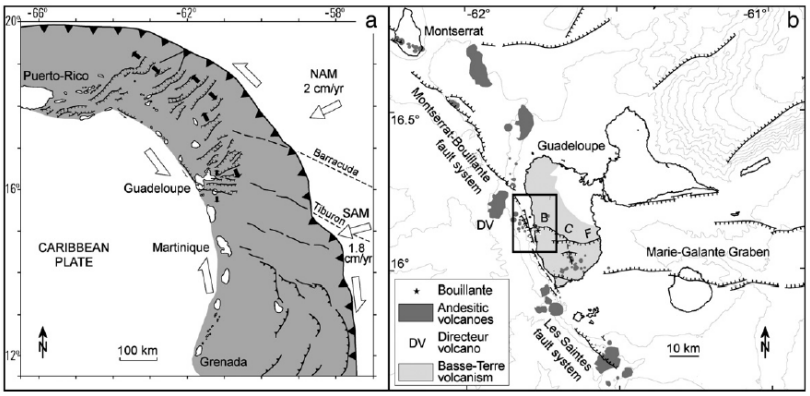

Fig.A33 – (top) location map.

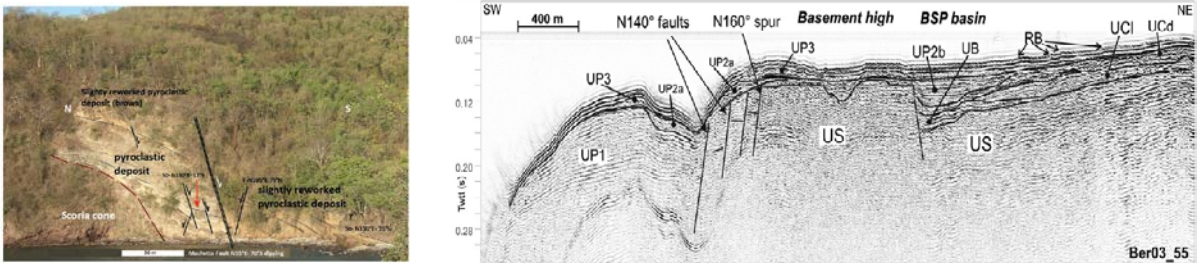

Fig.A34 – (left) outcrop structures; (right) seismic structures (see paper for extended discussion).

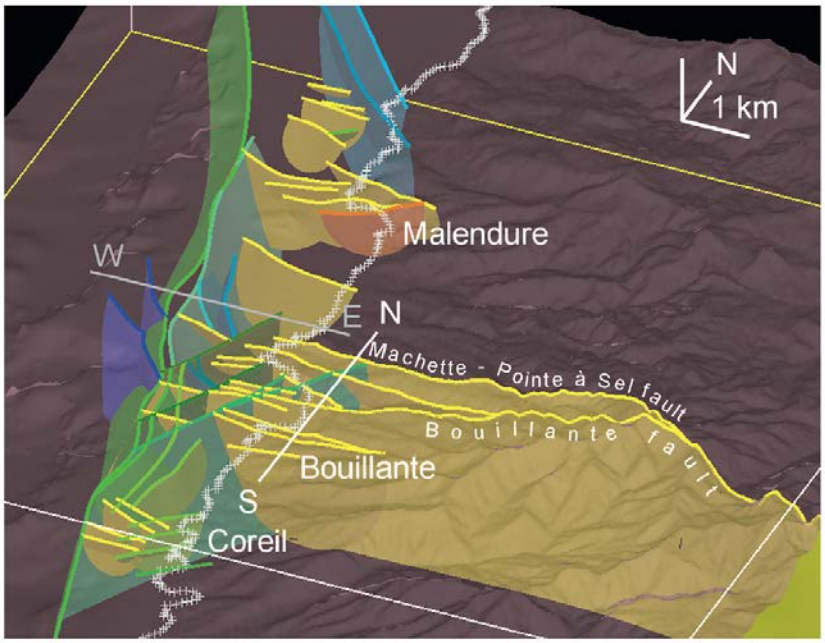

Fig.A35 – 3D fault model (see paper for extended discussion).

Vouillamoz et al (2012) built a 3D model of the Western Alps which provides a unique tool for the visualisation and analysis of the crustal units that form the belt.

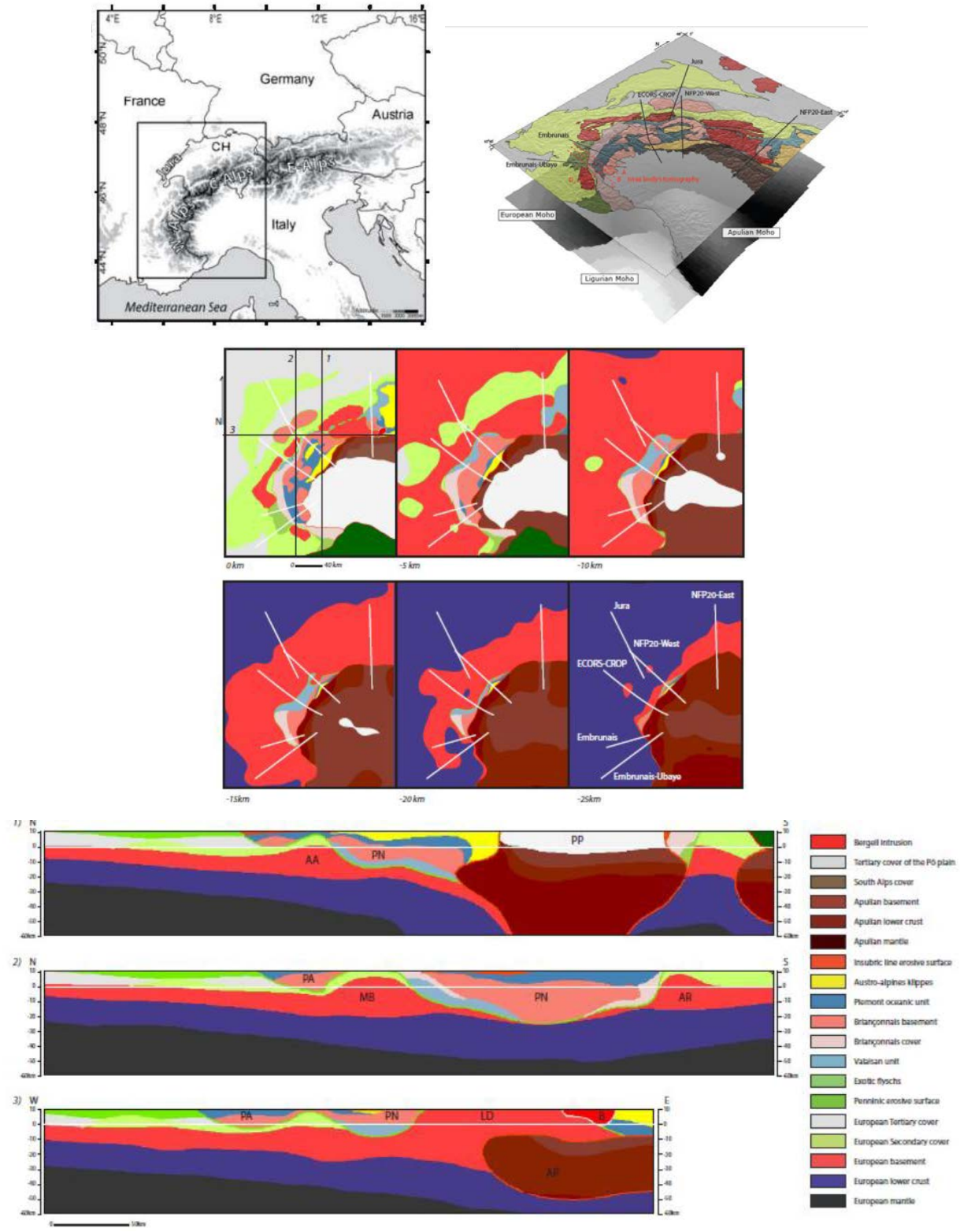

Fig.A36 – (top) location map and 3D model of the Western Alps; (centre) horizontal depth slices through the model; (bottom) vertical slices through the model (see paper for extended discussion).

Durand-Riard et al. (2011) present a new approach combining sequential decompaction with 3D restoration to allow for a true 3D basin analysis. Decompaction is performed in 3D after each restoration step, thus taking into account possible tectonic events and lateral thickness variations. Care is taken to apply decompaction to ensure volume continuity especially around faults. This approach is particularly suitable for syn-depositional folds whose growth strata constrain tectonic evolution through time.

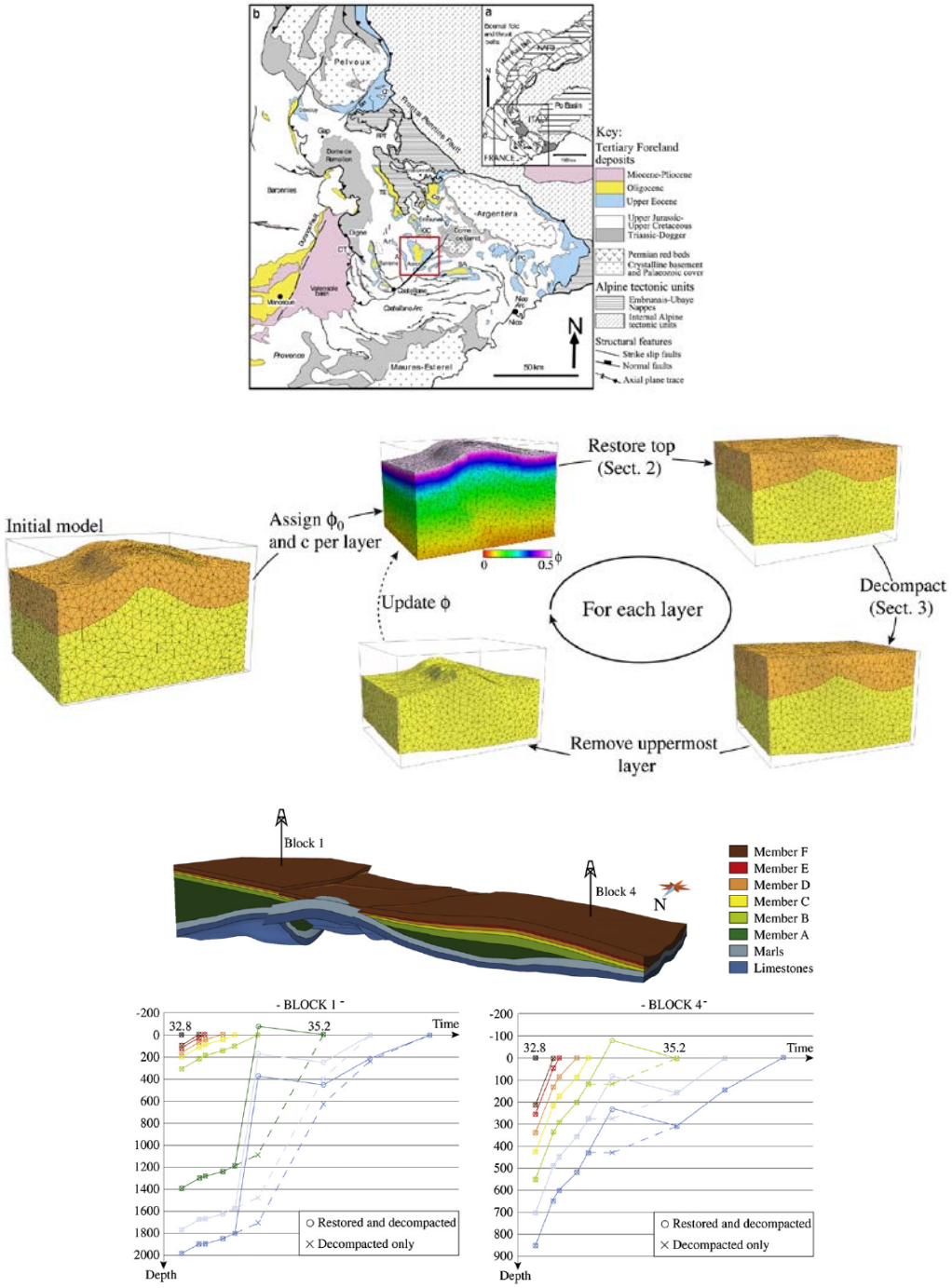

Fig.A37 – (top) workflow, (center) location map, (bottom) results from the methodology applied to the well burial history (see paper for extended discussion).

Lapponi et al. (2011) used outcrop data derived from fieldwork, remote sensing satellite and LiDAR-derived 3D models to build an integrated dual porosity-permeability static reservoir model which captured stratigraphic, diagenetic and structural heterogeneities of the Mishrif-Mauddud/Sarvak interval, one of the most prolific reservoir units in the Zagros region.

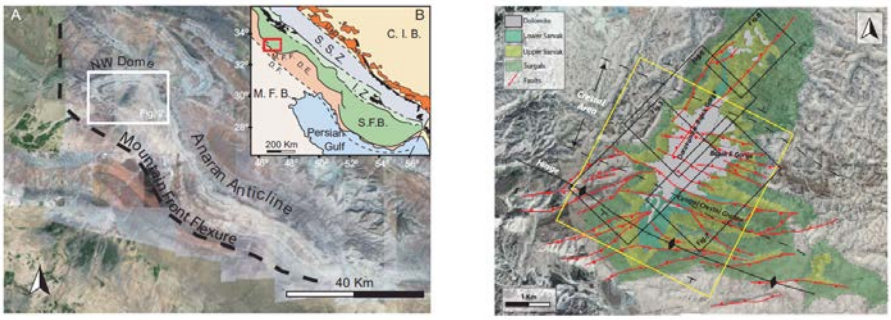

Fig.A38 –location and geological map of the study area (see paper for extended discussion).

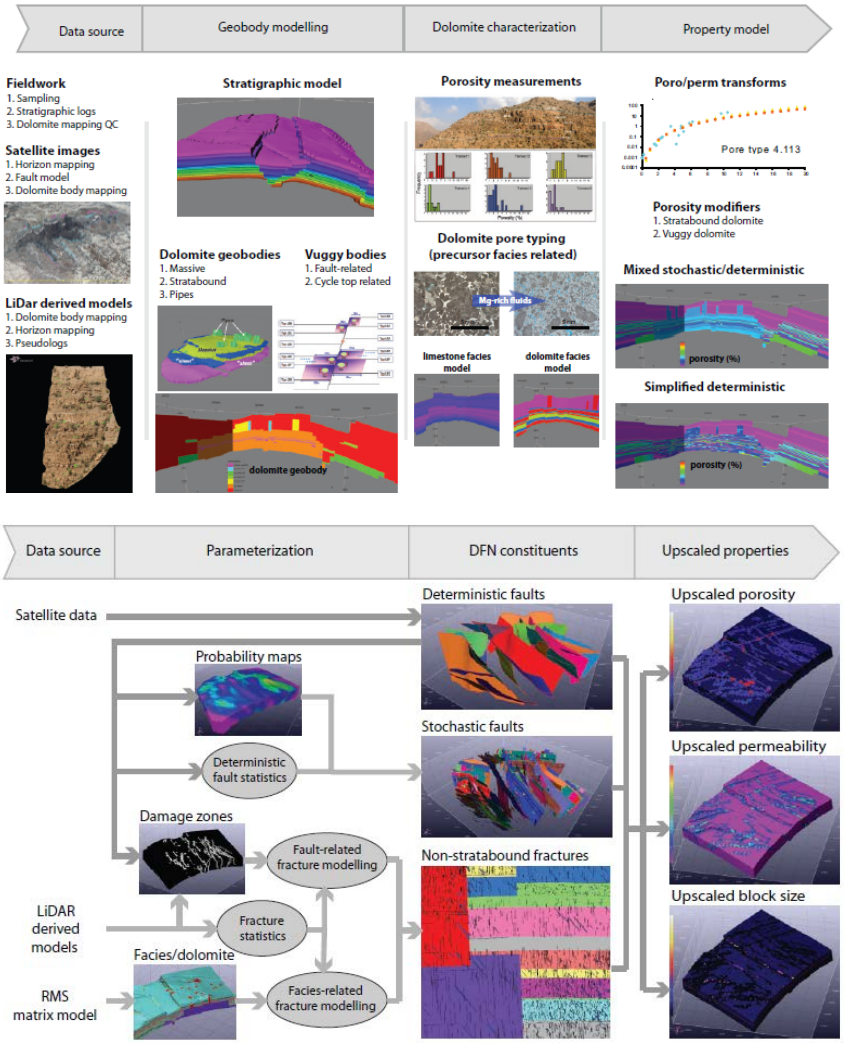

Fig.A39 – (top) workflow from data source to reservoir property modelling; (bottom) workflow from data source to fracture modelling and upscaling (see paper for extended discussion).

In order to validate existing interpretations and improve understanding of the region structural setting, **Trocme et al., (2011)** integrated geological and geophysical data to construct a 3D model of the southern Zagros fold-and-thrust belt diapiric province.

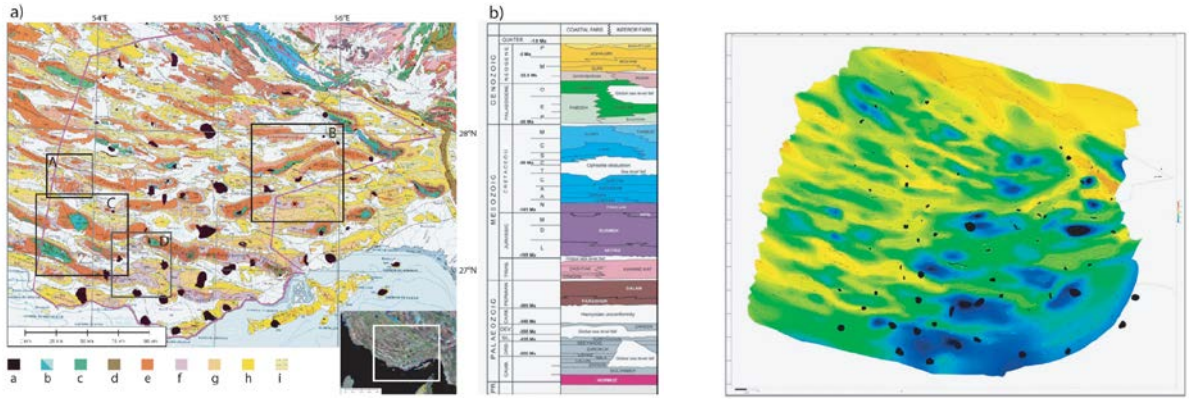

Fig.A40 – (left) location map; (right) near top Permian (i.e. the regional reservoir) depth structures from the 3D model (see paper for extended discussion).

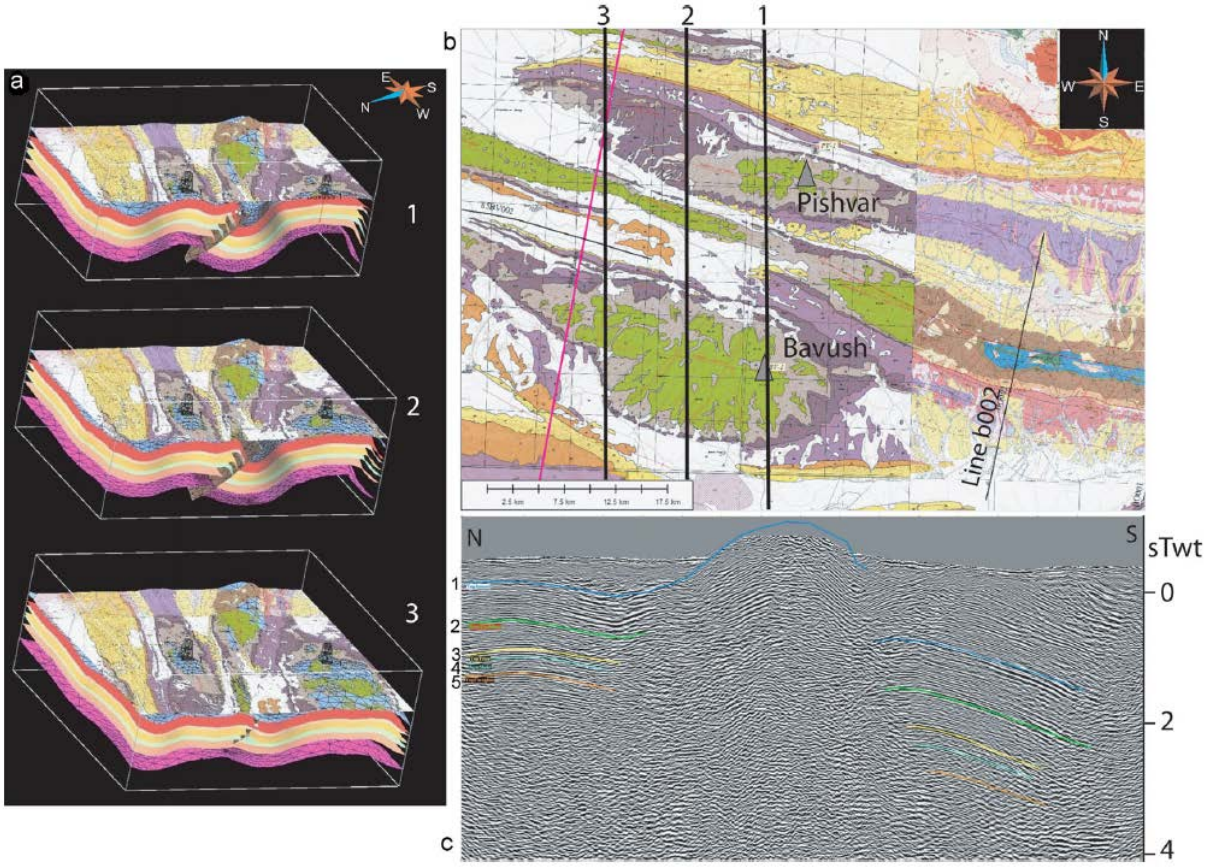

Fig.A41 – 3D model, map view and seismic line on the Bavush & Pishvar anticlines (see paper for extended discussion).

In order to understand the tectonic evolution of the Allauch Massif (SE France) **Guyonnet-Benaize et al. (2010)** developed a 3D structural model from field data and restored the associated units to their pre-Pyrenean-Alpine deformation geometry.

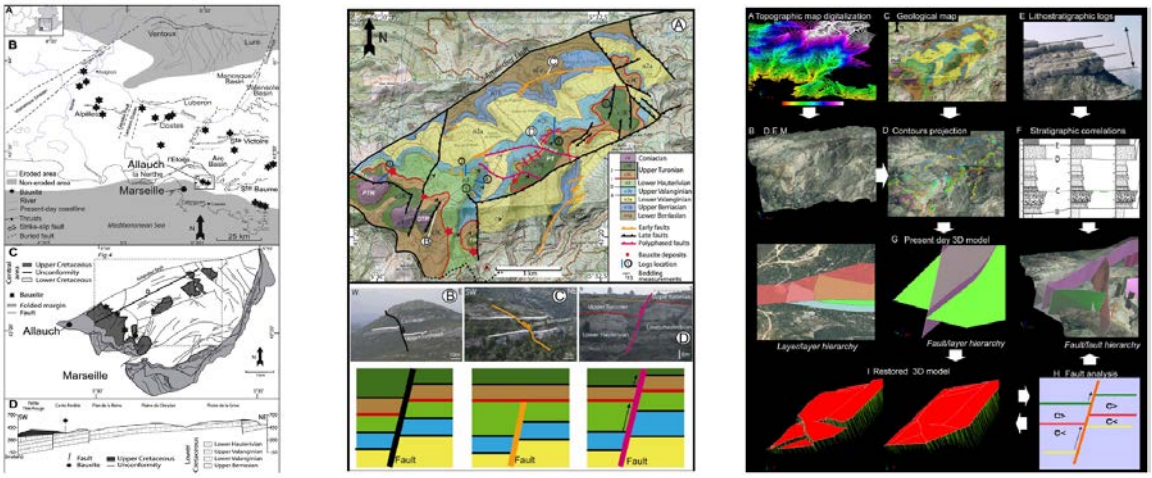

Fig.A42 – (left) location map, (center) field-geology structures and (right) workflow for the study (see paper for extended discussion).

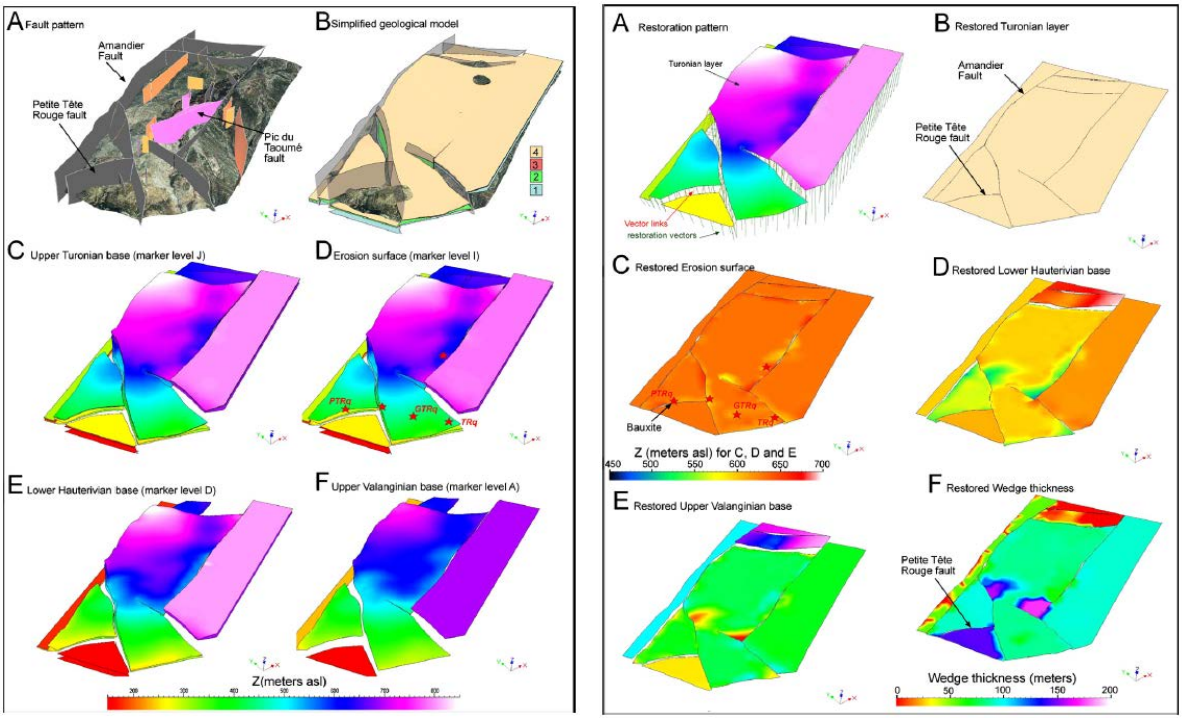

Fig.A43 – (left) 3D model units, (right) block-restoration of the modeled units (see paper for extended discussion).

Schreiber et al. (2009) present and discuss a 3-D geometrical model of the Moho topography in the Southwestern Alps by combining gravity, seismic and seismological constraints in a same and coherent 3-D space.

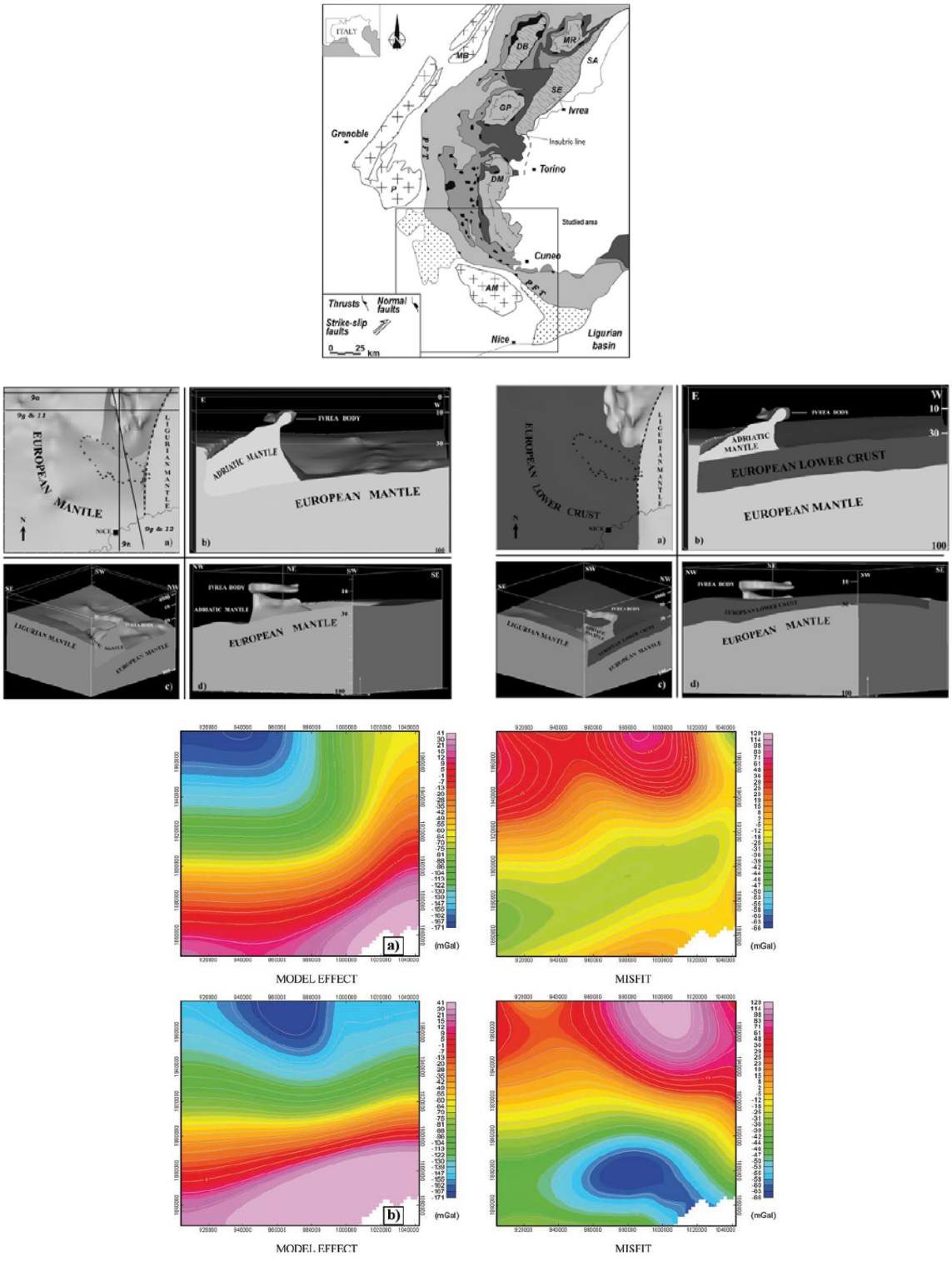

Fig.A44 – (top) location map; (center) 3D model alternative solutions; (bottom) gravity effect of the performed structural models and misfit in comparison with the regional gravity anomaly (see paper for extended discussion).

Sue et al. (2010) developed a 3D structural model of a key area in the southwestern Alps and used it as a structural frame to plot the earthquakes of the GéoFrance3D database, allowing to precisely and quantitatively investigating the relationships between crustal structures and current seismic activity of the belt.

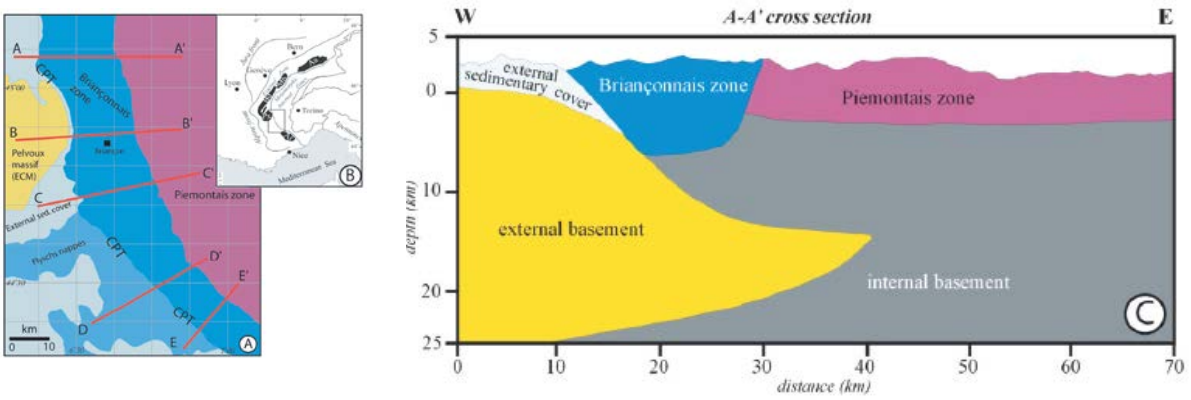

Fig.A45 – (left) location map; (right) crustal section across the study area (see paper for extended discussion).

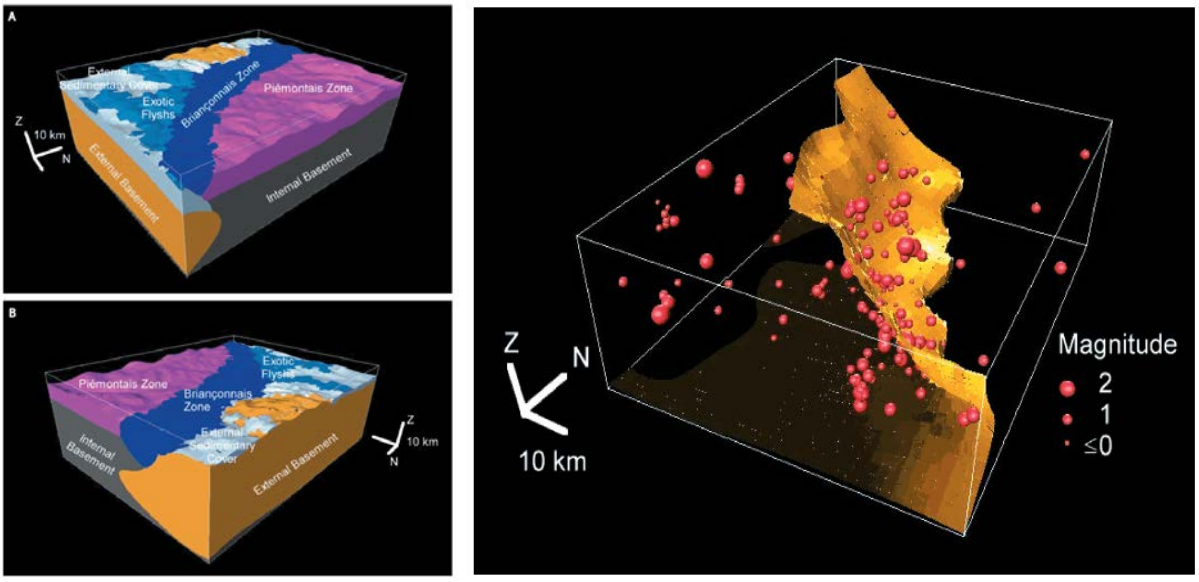

Fig.A46 – (left) 3D model; (right) earthquake hypocenters location with respect to one of the major crustal thrust from the 3D model (see paper for extended discussion).

Fredman et al. (2008) present numerical 3-D volumetric Fault-Facies modeling of fault envelopes based on a) three-dimensional (3-D) fault zone characterization, b) facies modeling of fault rocks and c) fluid flow simulation.

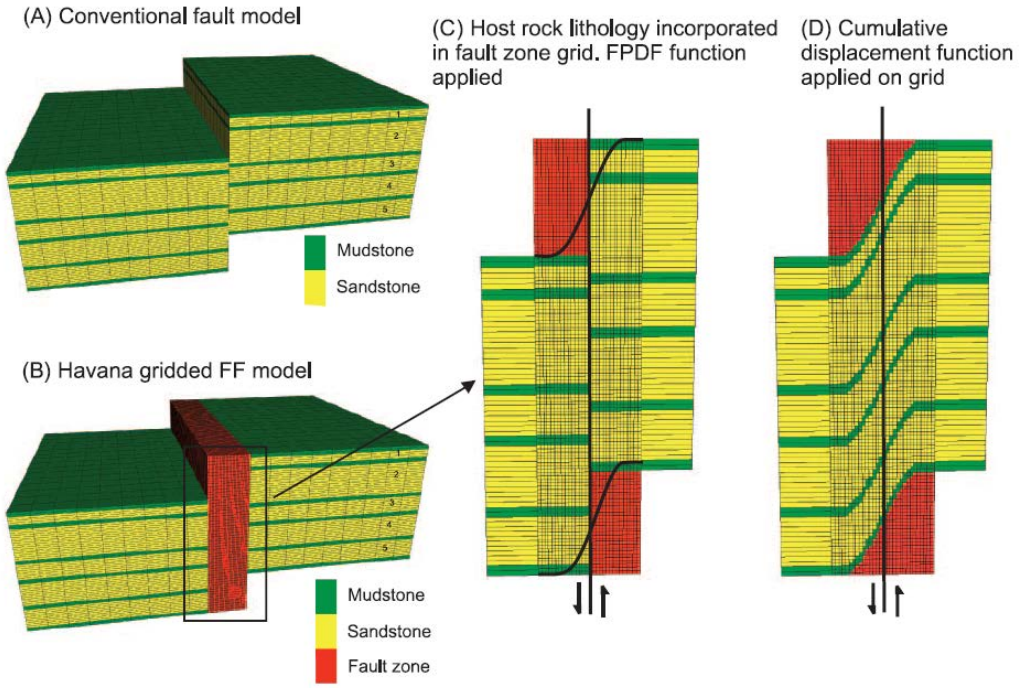

Fig.A47 – fault model criteria used to build the Fault-Facies model (see paper for extended discussion).

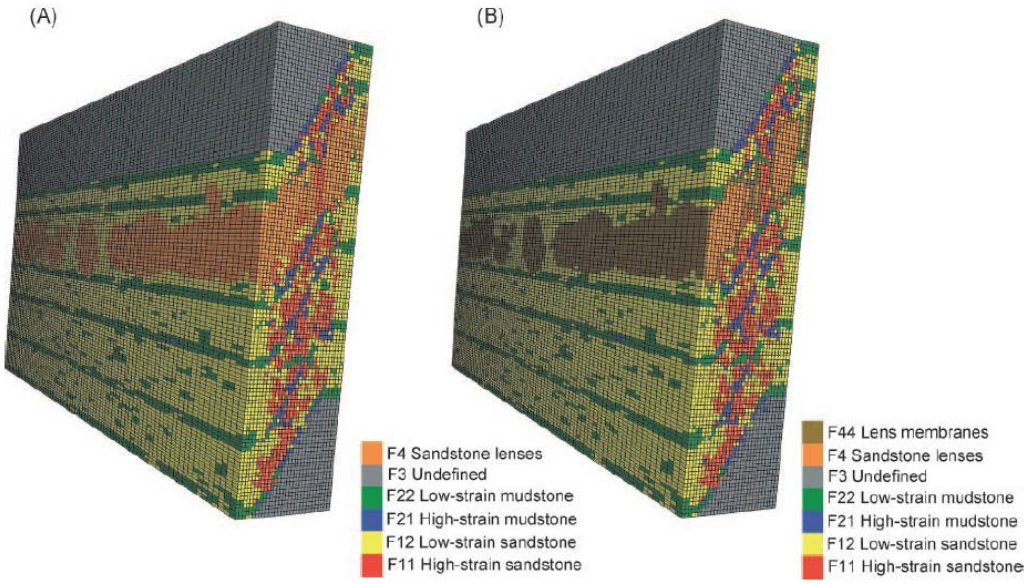

Fig.A48 – 3D view of different Fault-Facies models (see paper for extended discussion).

To accurately interpret the geometry of the depositional sequences and to determine the factors influencing the sedimentation in the Tremp basin (south-central Pyrenees), **Guillaume et al. (2008)** have developed a 3D model produced mainly from the interpretation and combination of surface data (including bedding dip and strike and a mosaic of aerial photographs), digital elevation model and balanced cross sections.

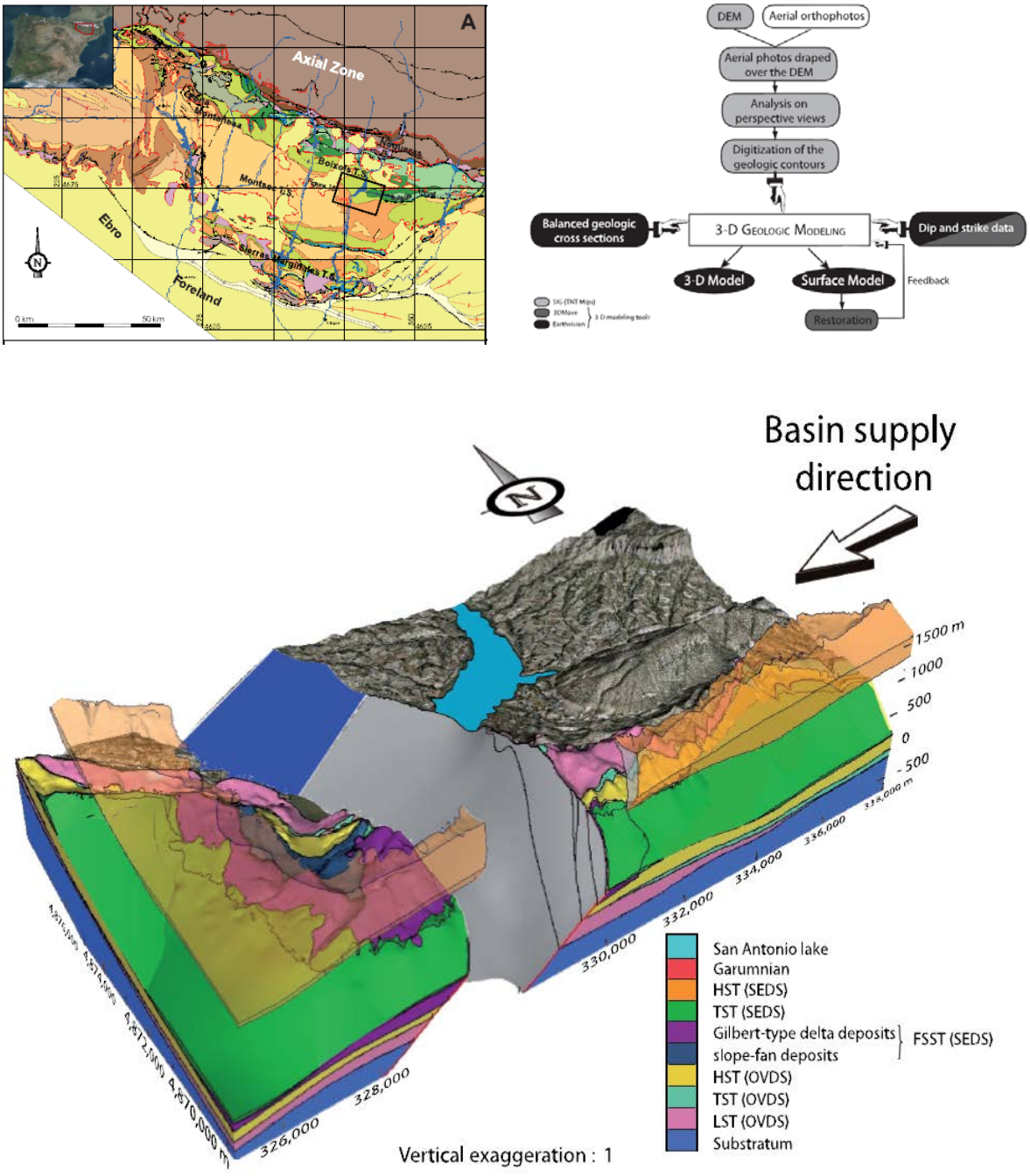

Fig.A49 –location map (top left), workflow (top right) and 3D model (bottom) of the study area (see paper for extended discussion).

In order to enhance understanding of deformation geometries and kinematics of the Morges massif (western Alps), **Calcagno et al. (2007)** built and restored a 3D geometric model from map and cross-section data derived from field structural and kinematic observations.

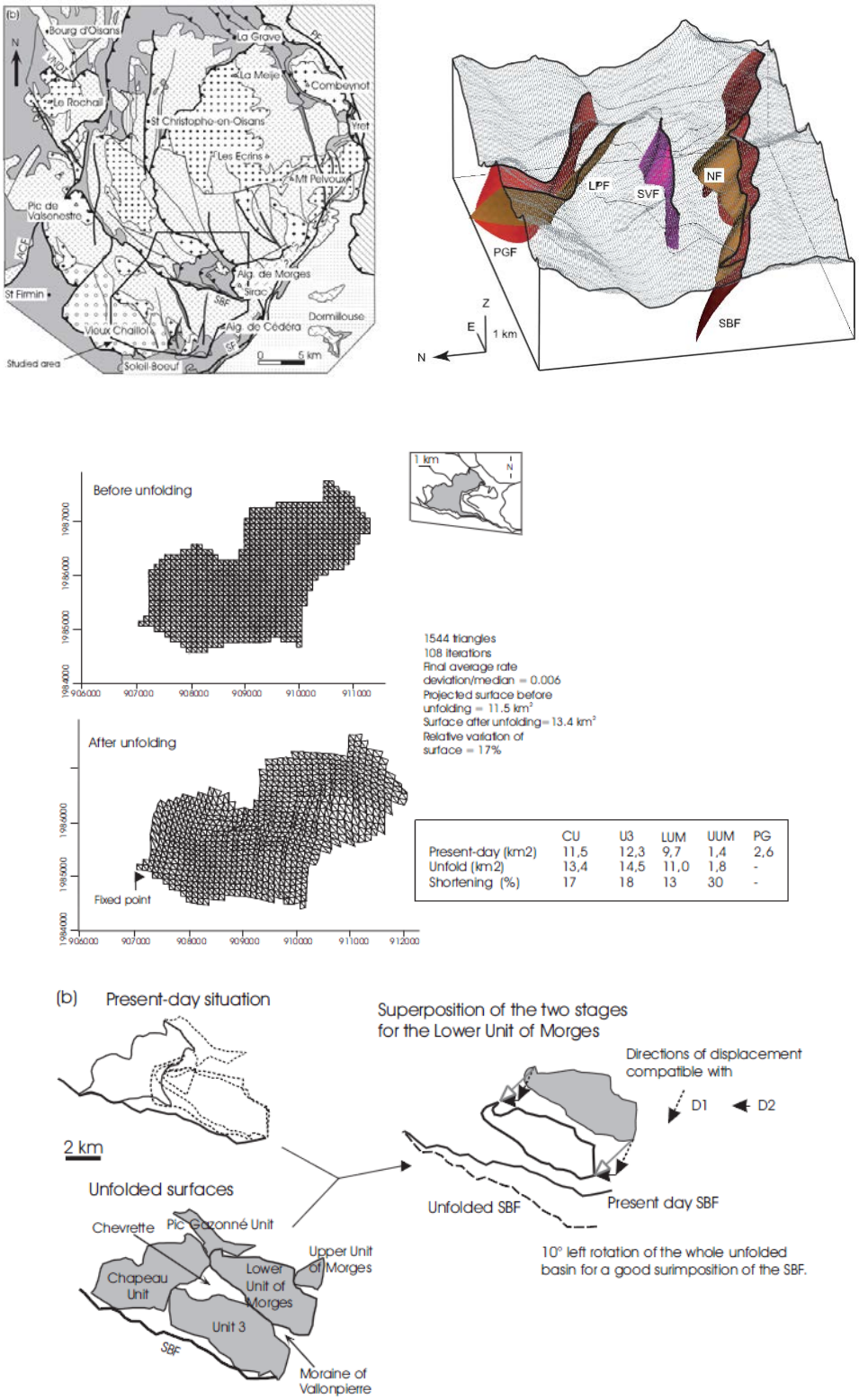

Fig.A50 – (top) location map of the study area 3D fault model; restoration of the interpreted structures (see paper for extended discussion).

Lohr et al. (2007) performed a three-dimensional (3-D) retrodeformation on a detailed interpreted 3-D structural model (German basin), to simulate strain in the hanging-wall at the time of faulting, at a scale below seismic resolution.

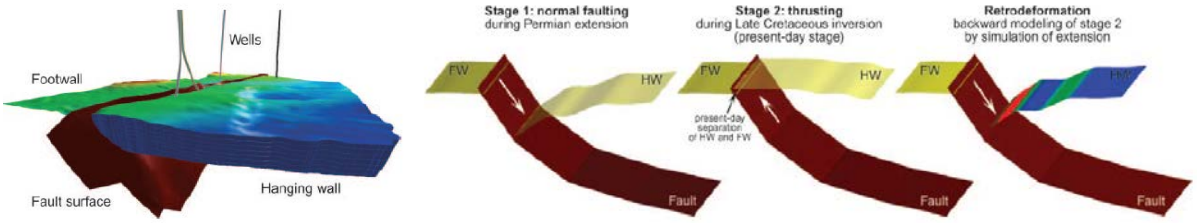

Fig.A51 – (left) 3D structural model; (right) methodology used for the study (see paper for extended discussion).

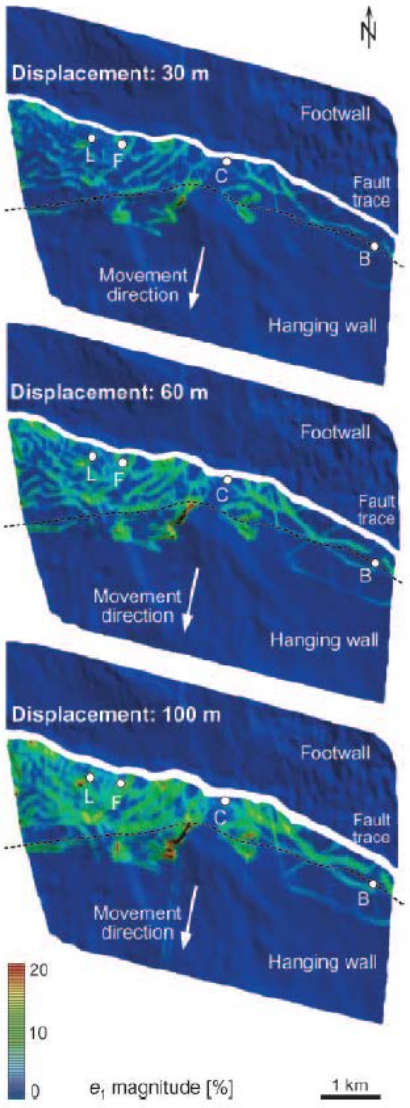

Fig.A52 – results of 3D retrodeformation of the model and the derived maximum strain distribution (see paper for extended discussion).

Based on field examples, **Yin and Groshong (2007)** present the results of a finite-thickness, three-dimensional (3-D) kinematic model for the fault-related deformation above an active diapir.

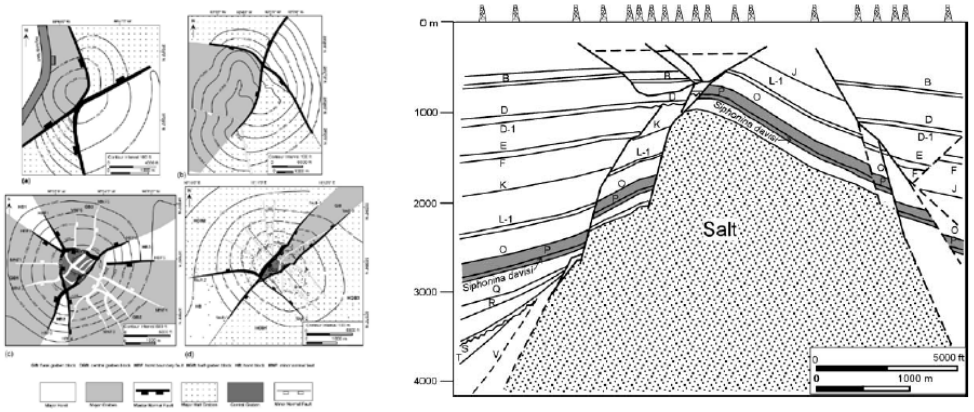

Fig.A53 – (left) fault map patterns for circular domes; (right) salt-dome-related structures on cross-section (see paper for extended discussion).

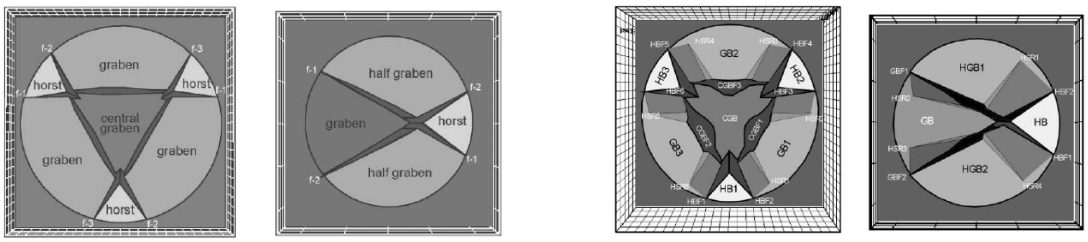

Fig.A54 – (left) model with faulted top of salt; (right) model with unfaulted top of salt (see paper for extended discussion).

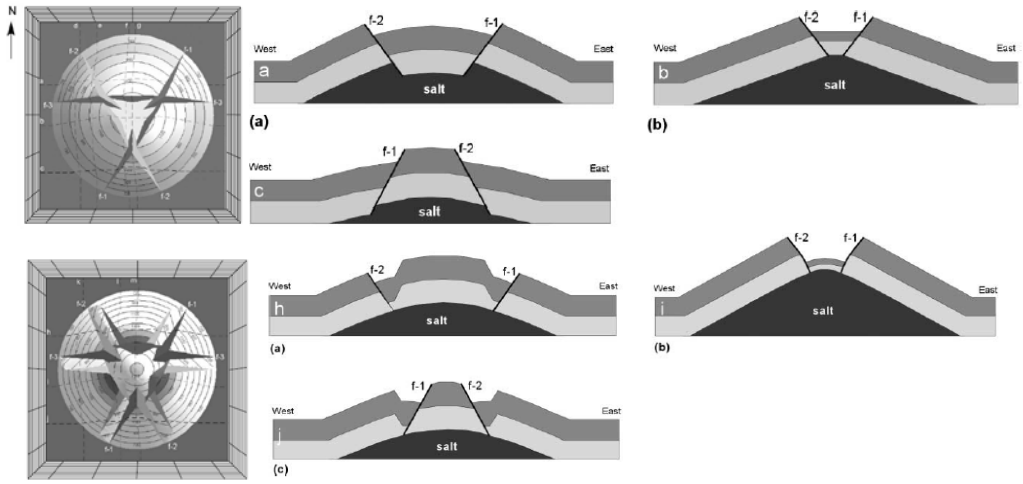

Fig.A55 –3D model with faulted (top) and unfaulted (bottom) top of salt; only EW cross-sections are illustrated (see paper for extended discussion).

Mitra et al. (2006) built 3D models to provide an understanding of the geometry and evolution of the Ku Zaap and Maloob structures (offshore Mexico) by integrating 3-D seismic interpretation, well data, and a series of balanced structural cross-sections.

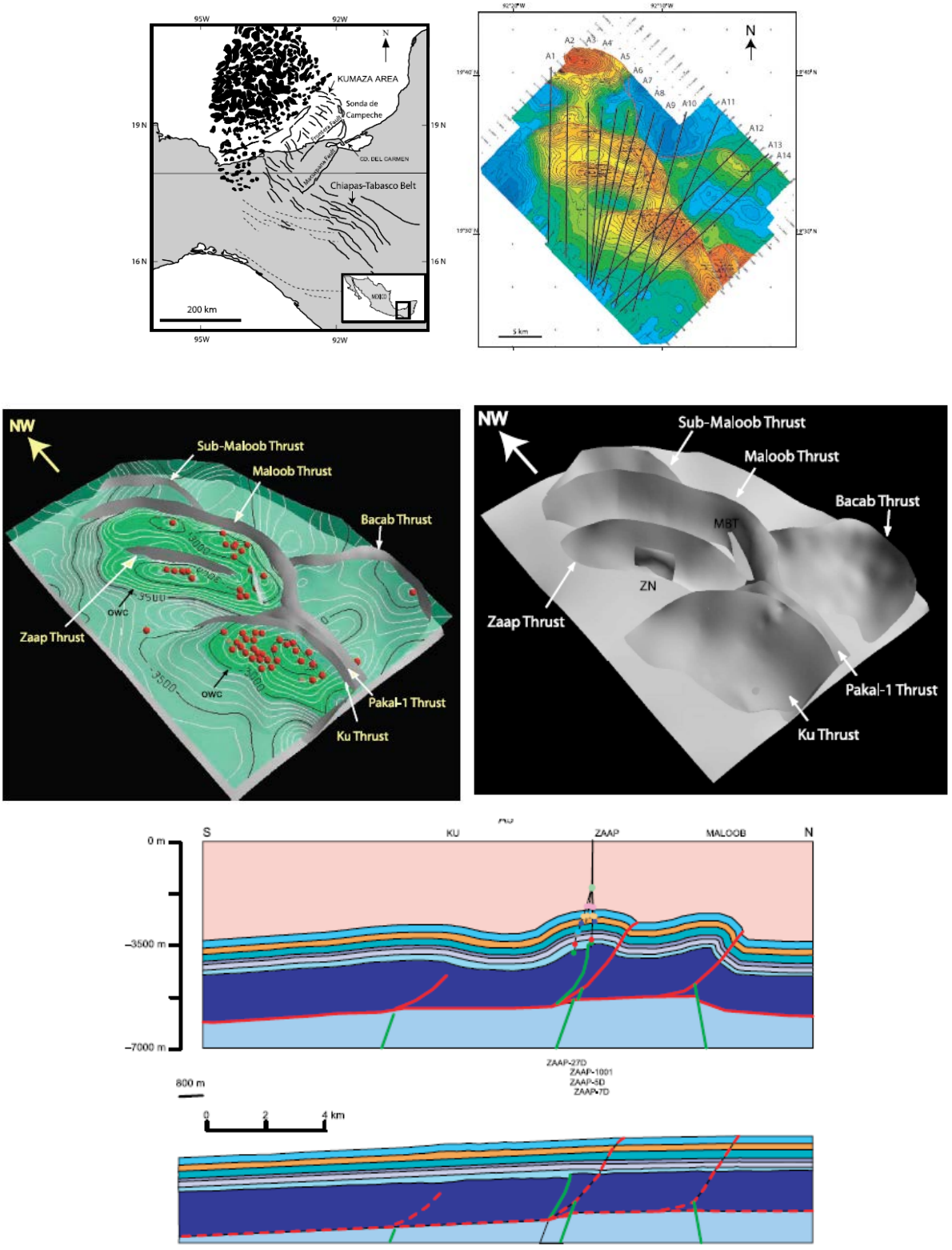

Fig.A56 – (top) Location map and reservoir depth map;(center) 3D structural model; (bottom) kinematic2D model (see paper for extended discussion).

Valcarce et al. (2006) constructed a 3D structural model of the El Porton field (Neuquen basin, Argentina) using 3-D seismic data and well information to plan new horizontal wells in steeply dipping to overturned limbs, through 50–60 m (164–196 ft) of productive reservoir avoiding pilot and sidetrack wells.

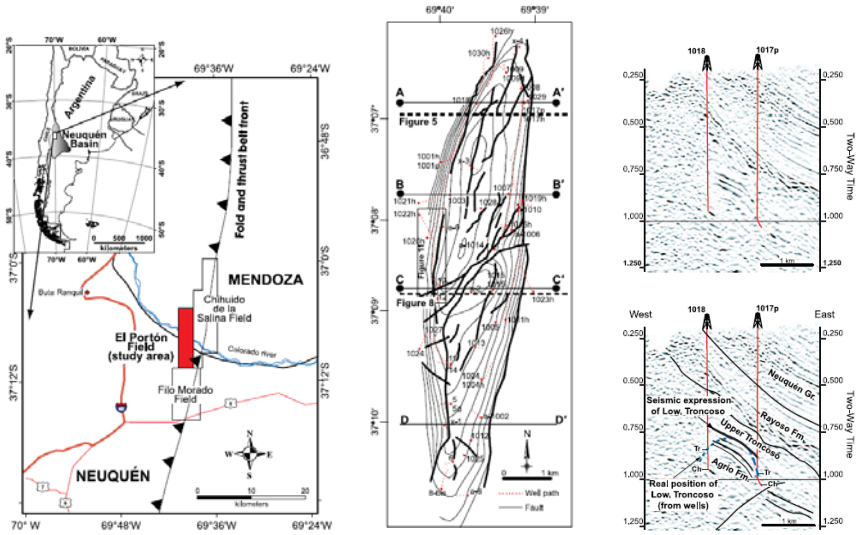

Fig.A57 – (left) location map; (center) top reservoir structural map; (right) seismic and wells across the El Porton field (see paper for extended discussion).

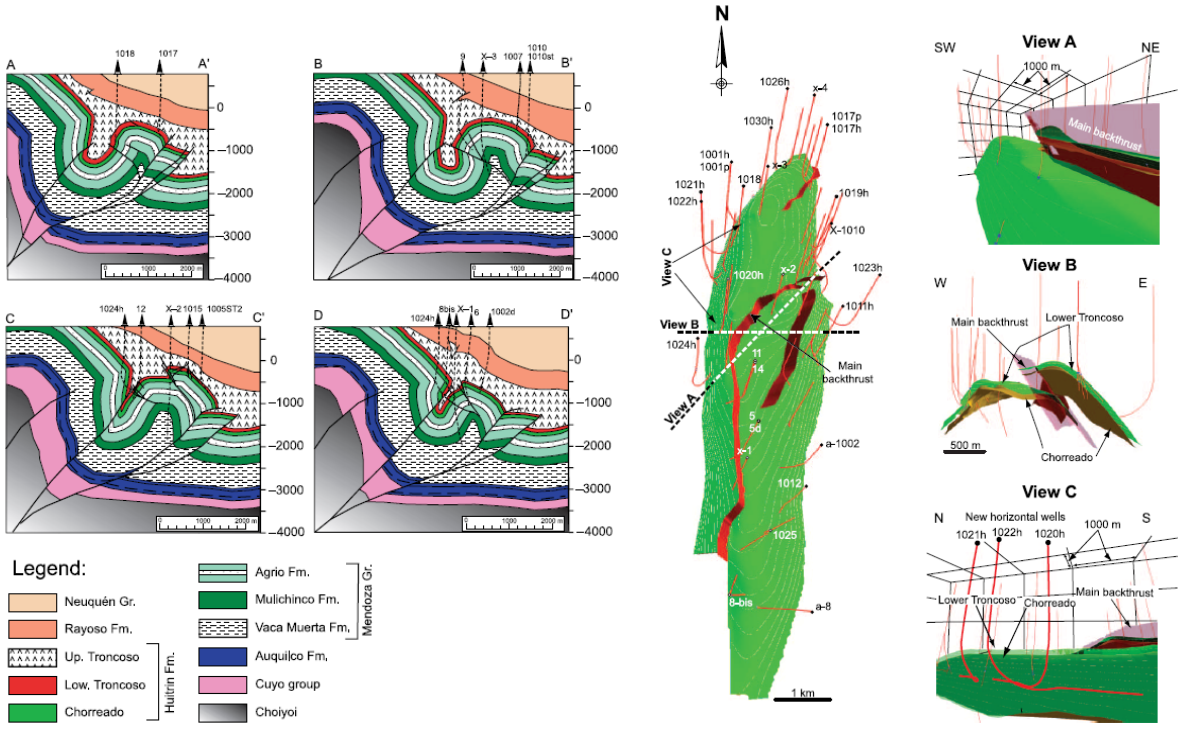

Fig.A58 – (left) structural sections and (right)3D model of the El Porton field (see paper for extended discussion).

Lamarche and Scheck-Wenderoth (2005) performed a 3D structural modelling of the Permian–Mesozoic Polish Basin in order to understand its structural and sedimentary evolution, which led to basin maturation (Permian–Cretaceous) and its tectonic inversion (Late Cretaceous–Paleogene).

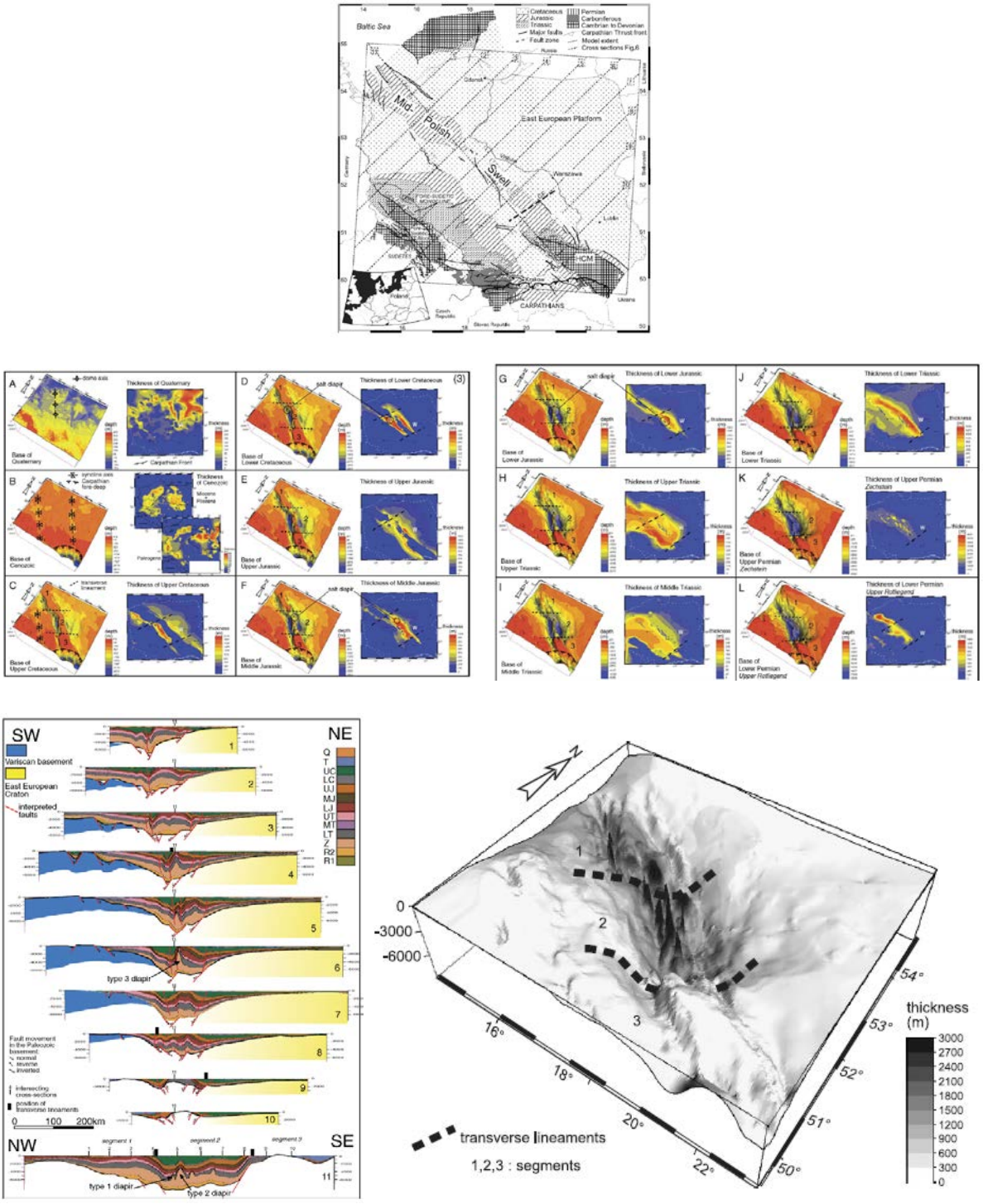

Fig.A59 – (top) location map and tectonics, (center) 3D model of the different layers and related isopach maps; (bottom-left) sections across the 3D model; (bottom-right) 3D structures and thickness of Zechstein salt (see paper for extended discussion).

To provide new understanding of the Southern Apennines thrust-belt architecture while constraining the derived interpretation of buried structure, **Turrini & Rennison (2004)** have built a 3D structural model of the region by integrating data from seismic-reflection, wells, surface geology, and sandbox simulations.

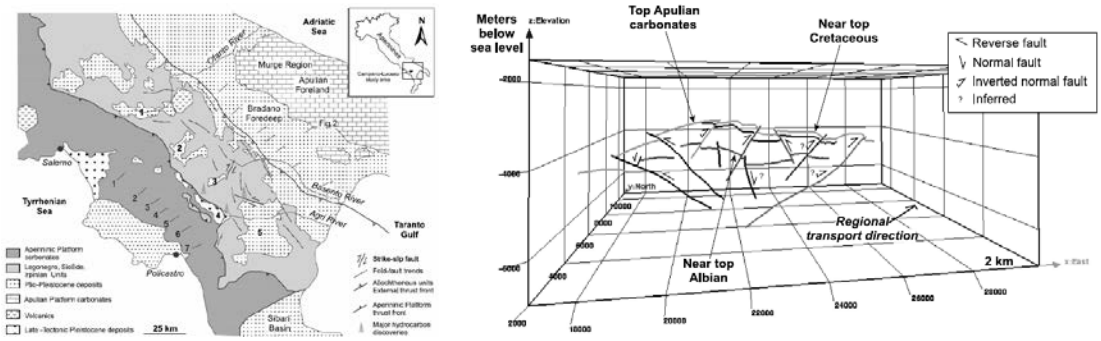

Fig.A60 – (left) location map of the study region; (right) 3D view of the Tempa Rossa field (see paper for extended discussion).

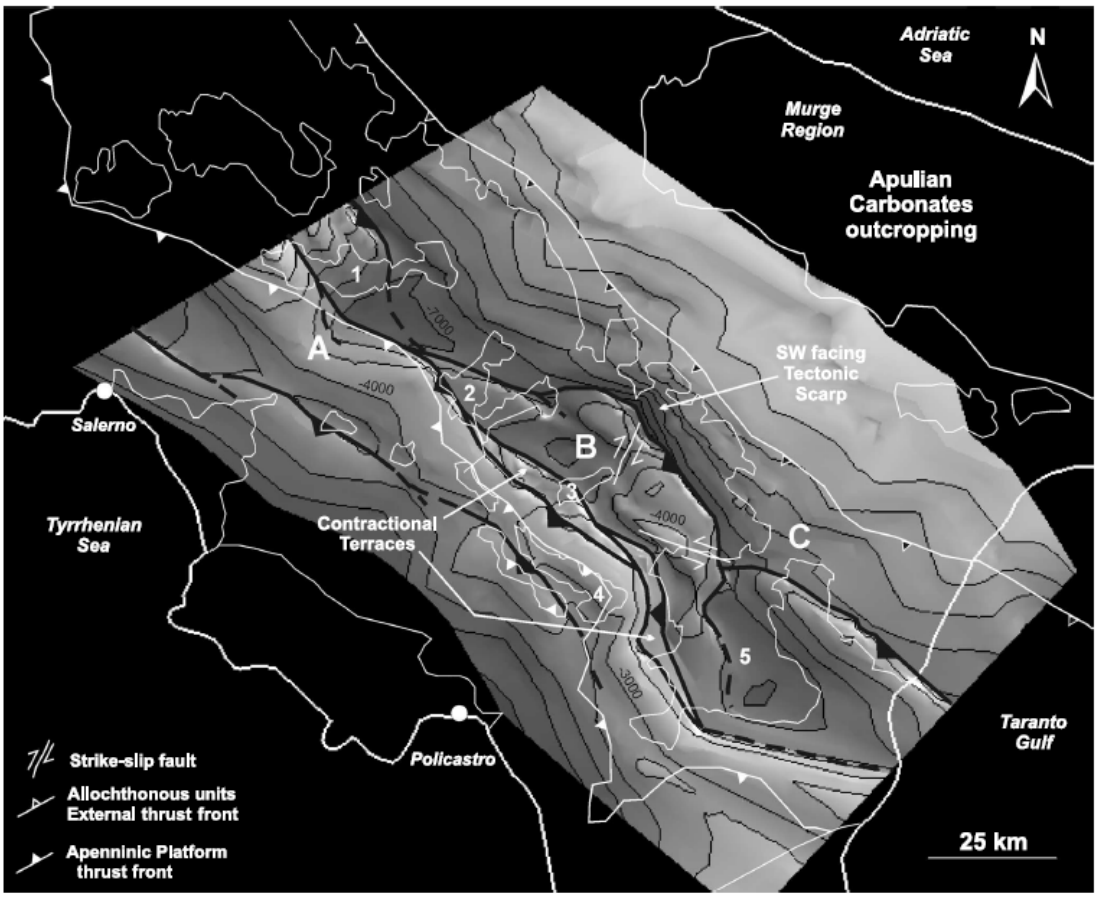

Fig.A61 – 3D structural model of the top Apula carbonate exploration target (see paper for extended discussion).

By using 3D seismic data **Masaferro et al. (2003)** built a 3D structural model of the Valle Morado faulted anticline (northwest Argentina) to analyze the deformation geometries and kinematics while aiming to understand the associated fracture network.

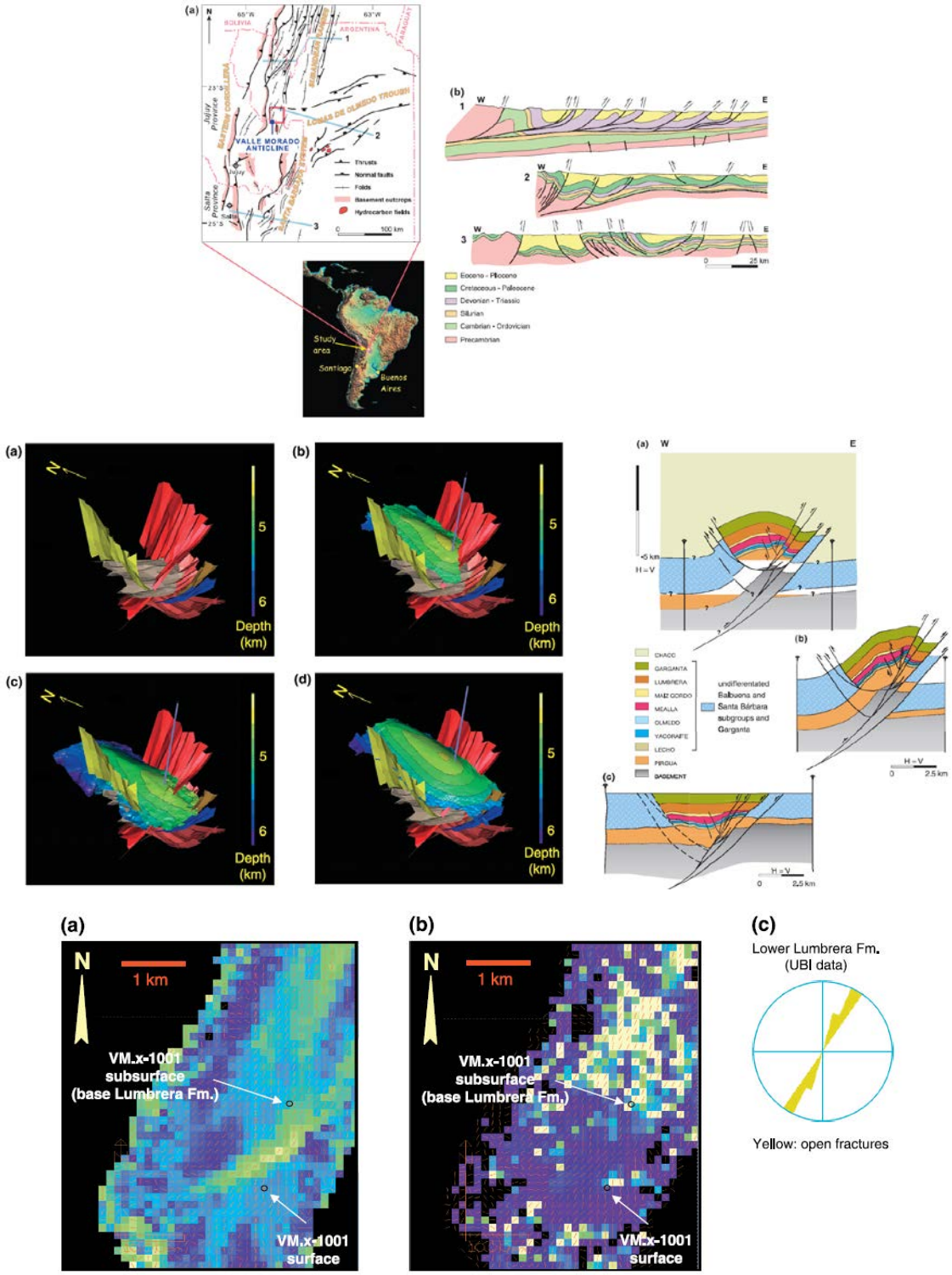

Fig.A62 – (top) location map and tectonics of the study area; (center) 3D structural model; (bottom) curvature analysis and fracture orientation prognosis (see paper for extended discussion).

Bailey et al. (2002) tested the connectivity of reservoir bodies in unfaulted and variably faulted, high resolution 3D geocellular stratigraphic models from the East Pennine Coalfield, UK. These deterministic stratigraphic–structural models are underpinned by high density borehole and mine plan data.

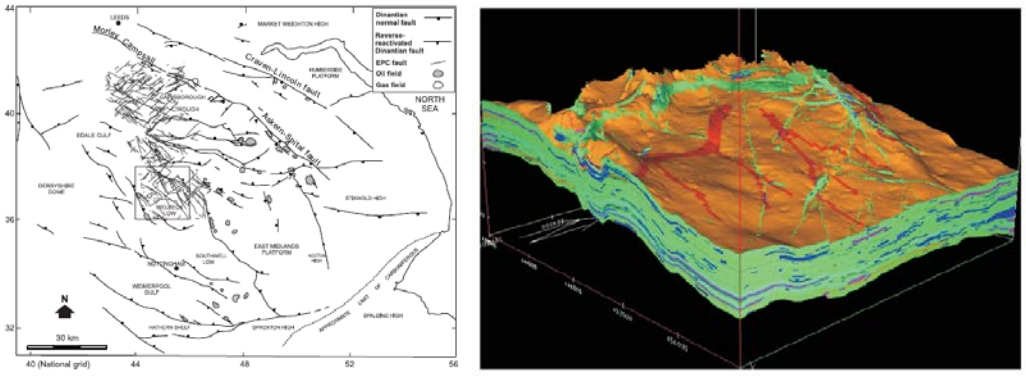

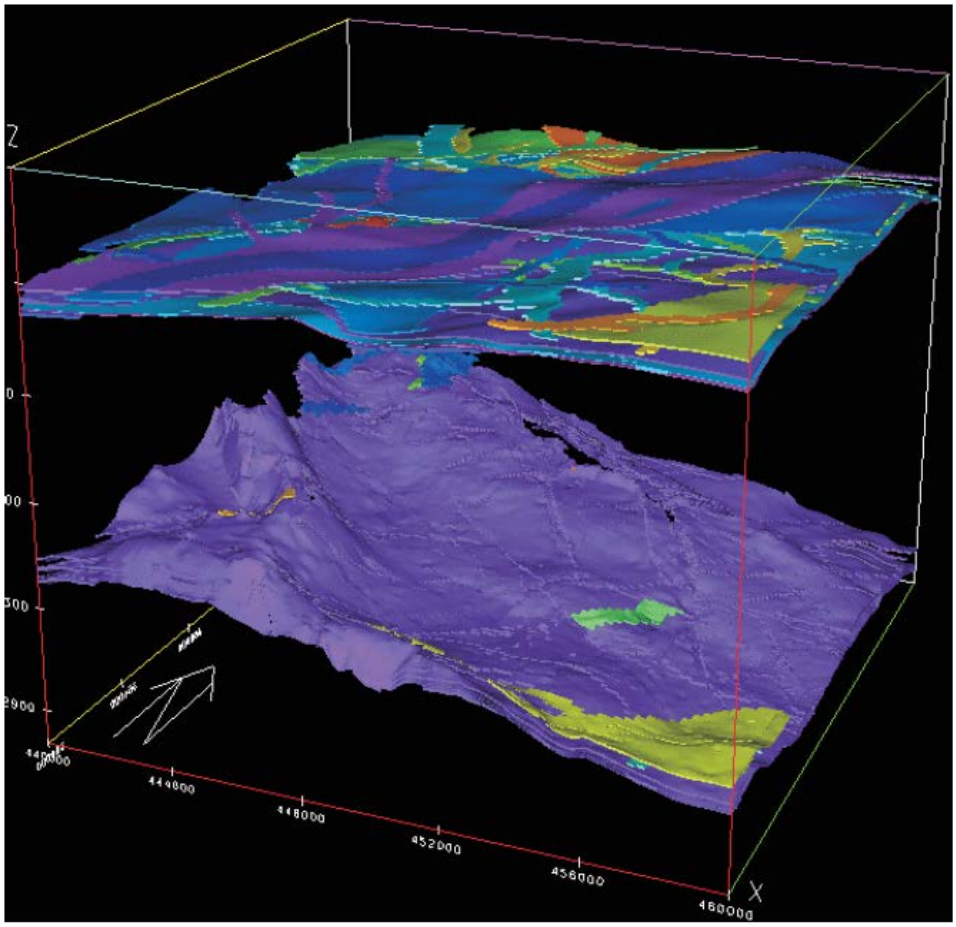

Fig.A63 – (top) location map and 3D model of the study area; (bottom) 3D visualization of the 20 _20 km model area illustrating the size and distribution of connected volumes (see paper for extended discussion).

Johannesen et al. (2002) performed a 3D structural and oil migration modelling of the Statfjord area of the Northern North Sea to increased understanding of the migration routes and definition of oil migration fairways.

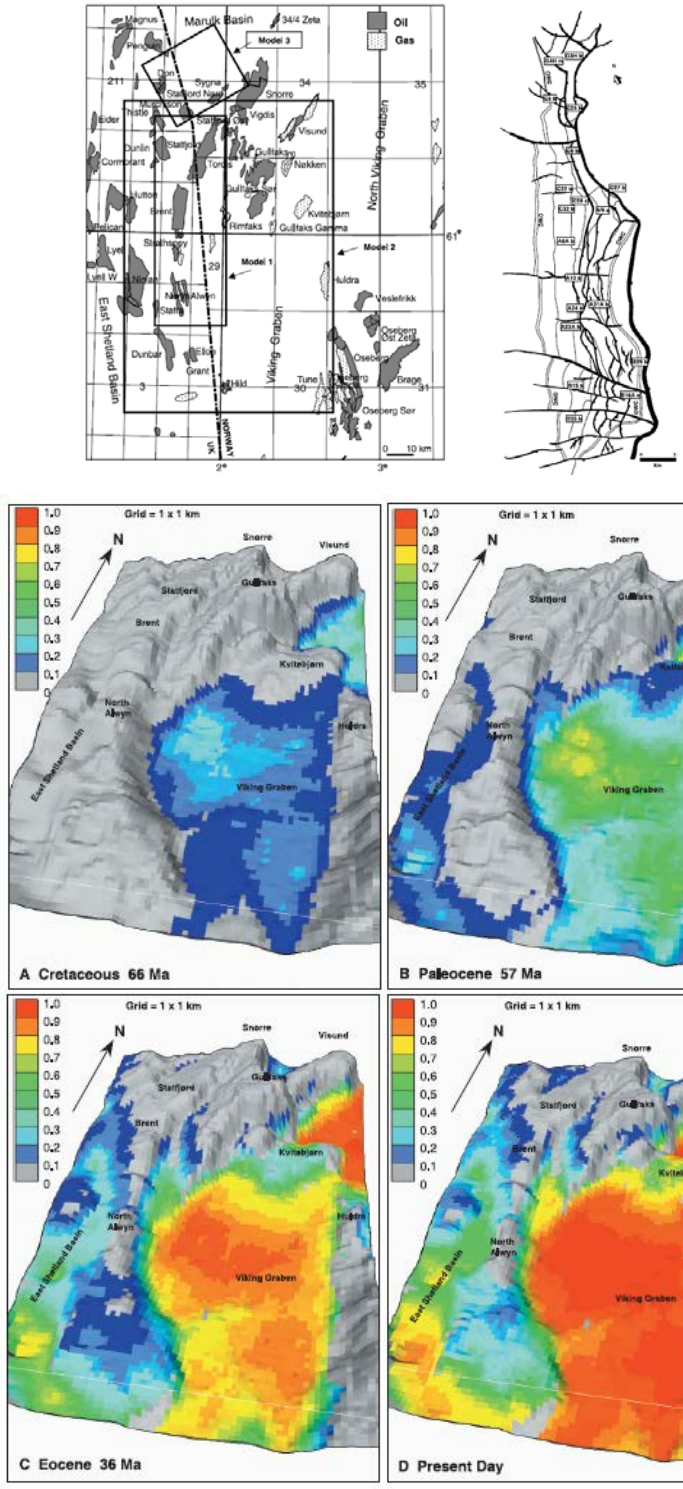

Fig.A64 – (top) location map and structures of the study area; (bottom) 3D visualization of the model illustrating the development of source rock transformation ratio for main source rock around the Statfjord area (see paper for extended discussion).

McClay and Bonora (2001) built 3D models from sand-box geometries about strike-slip tectonics to provide detailed templates for seismic interpretation of complex contractional structures in offset strike-slip fault system.

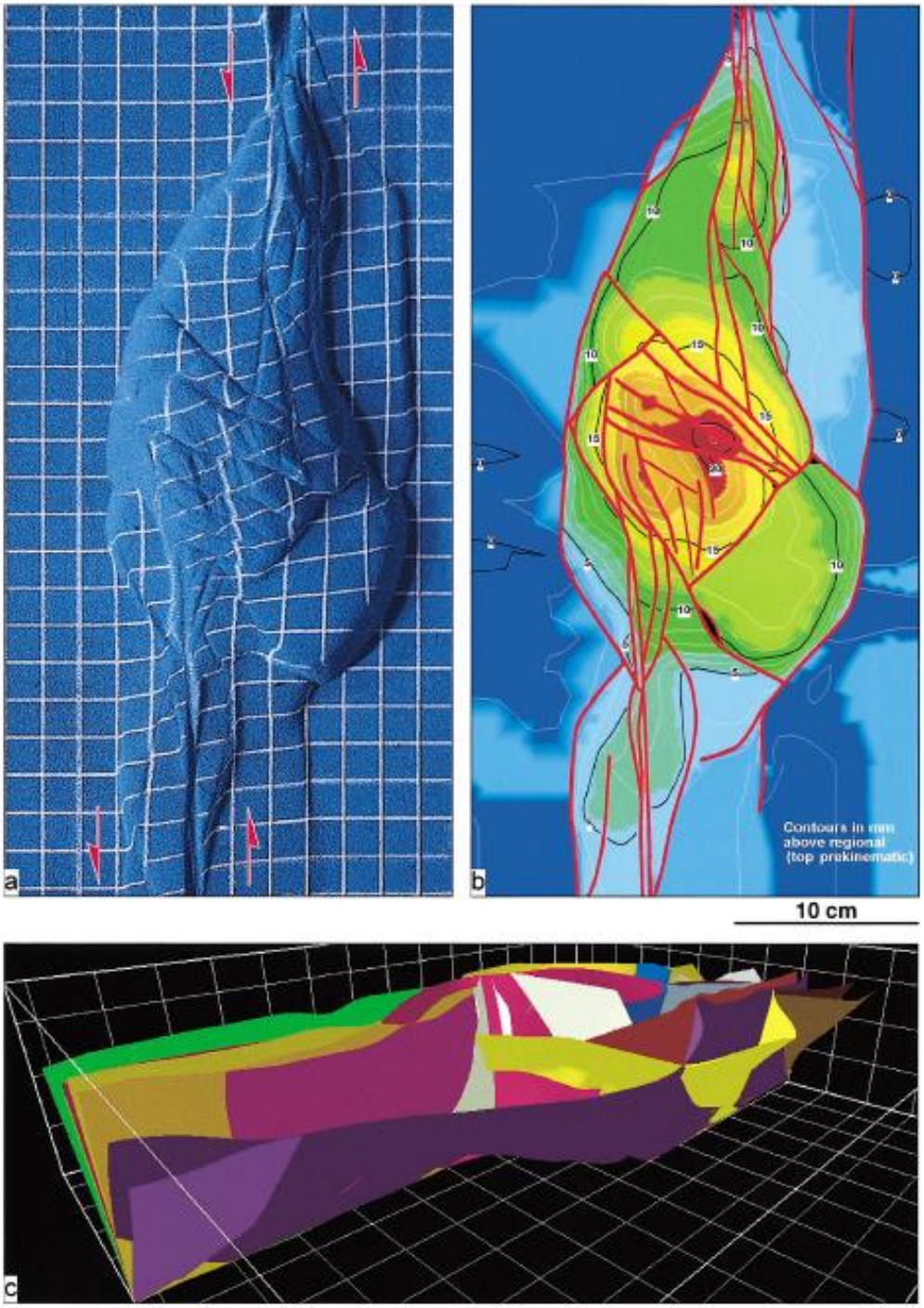

Fig.A65 - (a) Photograph of the upper surface of the model after 10 cm displacement on the basement faults. (b) Structure contours of the upper surface of the model as interpolated from fifty serial sections across the completed model. (c) Perspective view of a 3-Dvisualization of the faults in model W307 (see paper for extended discussion).

Guglielmo et al. (1997) performed 3D modelling to display and analyze a physical model simulating salt-related structures produced during gravity spreading and gliding.

Fig.A66 – (top) 2D experiment; (bottom) 3D model reconstruction at the different level of the model (see paper for extended discussion).

References

Andreatta, C., Dal Piaz, Gb., Vardabasso, S., Fabiani, R., Dal Piaz, G., 1957. Carta geologica delle Tre Venezie, scale 1:100,000, Map "10-Bolzano".

Alcalde, J., Marzán, I., Saura, E., Martí, D., Ayarza, P., Juhlin, C., Pérez-Estaún, A., Carbonell, R., 2014. 3D geological characterization of the Hontomín CO2 storage site, Spain: Multidisciplinary approach from seismic, well-log and regional data. Tectonophysics 627, 6–25; doi.org/10.1016/j.tecto.2014.04.025.

Allan,U.S., 1989. Model for hydrocarbon migration and entrapment within faulted structures. Am AssocPet Geol Bull 73, 803–81.

Argnani, A., Ricci Lucchi, F., 2001. Terziary silicoclastic turbidite systems of the Northern Apennines, in: Vai, G. B. and I. P. Martini (Eds.), Anatomy of an Orogen: the Apennines and adjacent mediterranean basins, Kluwer Academic Publishers, 327-350.

Assereto, R., Jadoul, F., Omenetto, P., 1977. Stratigrafia e metallogenesi del settore occidentale del distretto a Pb, Zn, fluorite e barite di Gorno (Alpi bergamasche)- Riv. Ital. Paleont., 83,3, pp.395-532.

Autin, J., Scheck-Wenderoth, M., Loegering, M.J., Anka, Z., Vallejo, E., Rodriguez, J.F., Dominguez, F., Marchal, Reichert, C., di Primio, R., D., Götze, H.-J., 2013. Colorado Basin 3D structure and evolution, Argentine passive margin. Tectonophysics 604, 264–279; doi.org/10.1016/j.tecto.2013.05.019.

Autin, J., Scheck-Wenderoth, M., Götze, H.-J., Reichert, C., Marchal, D., 2015. Deep structure of the Argentine margin inferred from 3D gravity and temperature modelling, Colorado Basin. Tectonophysics……; doi.org/10.1016/j.tecto.2015.11.023.

Badics, B., Uhrin, A., Veto, I., Bartha, A., Sajgó, C., 2004. Basin-centred gas in the Makó Trough, Hungary: a 3D basin and petroleum system modelling investigation. Petroleum Geoscience, 17, 405–416; doi: 10.1144/1354-079310-063.

Bailey, W. R., Manzocchi, T., Walsh, J. J., Keogh, K., Hodgetts, D. Rippon, J., Nell, P. A. R., Flint, S., Strand, J. A., 2002. The effect of faults on the 3D connectivity of reservoir bodies: a case study from the East Pennine Coalfield, UK. Petroleum Geoscience, Vol. 8 2002, pp. 263–277 1354-0793/02/$15.00.

Bally, A. W., Burbi, L. Cooper, C., Ghelardoni, R., 1986. Balanced sections and seismic reflection profiles across the Central Apennines, Mem. Soc. Geol. It., 35, 257-310.

Barba, S., Finocchio, D., Sikdar, E., Burrato, P., 2013. Modelling the interseismic deformation of a thrust system: seismogenic potential of the Southern Alps. Terra Nova, doi: 10.1111/ter.12026.

Barbieri, C., Bertotti, G., Di Giulio, A., Fantoni, R., Zoetermeijer, R., 2004. Flexural response of the Venetian foreland to the Southalpine tectonics along the TRANSALP profile. Terra Nova, 16, 5, 273-280, doi: 10.1111/j.1365-3121.2004.00561.x.

Bartolini, C., Caputo, R., Pieri, M., 1996. Pliocene-Quaternary sedimentation in the Northern Apennine Foredeep and related denudation, Geological Magazine, 133, 255-273, doi:10.1017/S0016756800009006.

Basili, R., Valensise, G., Vannoli, P., Burrato, P., Fracassi, U., Mariano, S., Tiberti, M. M., Boschi, E., 2008. The Database of Individual Seismogenic Sources (DISS), version 3: Summarizing 20 years of research on Italy's earthquake geology. Tectonophysics, 453, 1-4, 20-43, doi: 10.1016/j.tecto.2007.04.014.

Beaumont, C., Ellis, S., Pfiffner, A., 1999. Dynamics of sediment subduction-accretion at convergent margins: short-term modes, long-term deformation, and tectonic implications. Journal of Geophysical Research, 104, 17573-17601.

Bechtold, M., Battaglia, M., Tanner, D. C., Zuliani, D., 2009. Constraints on the active tectonics of the Friuli/NW Slovenia area from CGPS measurements and three-dimensional kinematic modeling. Journal of Geophysical Research, 114, B03408, doi:10.1029/2008JB005638, 2009.

Bello, M., Fantoni, R., 2002. Deep oil plays in the Po Valley: Deformation and hydrocarbon generation in a deformed foreland – AAPG Hedberg Conference, "Deformation History, Fluid Flow Reconstruction and Reservoir Appraisal in Foreland Fold and Thrust Belts" May 14-18, 2002, Palermo – Mondello (Sicily, Italy).

Benedetti, L. C., Tapponnier, P., Gaudemer, Y., Manighetti, I., and Van der Woerd, J., 2003. Geomorphic evidence for an emergent active thrust along the edge of the Po Plain: the Broni-Stradella fault, Journal of Geophysical Research, 108 (B5), 2238, doi:10.1029/2001JB001546.

Bennett, R.A., Serpelloni, E., Hreinsdóttir, S., Brandon, M.T., Buble, G., Basic, T., Casale, G., Cavaliere, A., Anzidei, M., Marjonovic, M., Minelli, G., Molli, G., Montanari, A., 2012. Syn-convergence extension observed using the RETREAT GPS network, northern Apennines, Italy. J. Geophys. Res., 117, B04408, doi:10.1029/2011JB008744.

Berg, R.C., Russell, H., Thorleifson, L.H., 2004. (Eds.): Three-dimensional Geological Mapping for Groundwater Applications – Workshop. Extended Abstracts, Illinois State Geological Survey. Open-File Series 2004-8. http://library.isgs.uiuc.edu/Pubs/pdfs/ofs/2009/ofs2009-04.pdf.

Bernoulli, D., Giger, M., Muller, D.W., Ziegler, U.R.F., 1993. Sr-isotope stratigraphy of the Gonfolite Lombarda Group (South-alpine molasse, northern Italy) and radiometric constraints for its age of deposition. Ecl. Geol. Helv., 86-3, 751-767.

Berra F., Galli M.T., Reghellin F., Torricelli S. & Fantoni R., 2009. Stratigraphic evolution of the Triassic-Jurassic succession in the Western Southern Alps (Italy) : the record of the two-stage rifting on the distal passive margin of Adria– Basin Research, 21, 335-353.

Berra, F., Carminati, E., 2010. Subsidence history from a backstripping analysis of the Permo-Mesozoic succession of the Central Southern Alps (Northern Italy). Basin Research, 22, 952-975.

Bersezio, R. & Bellantani, G., 1997. The thermal maturity of the Southalpine mesozoic succession north of Bergamo by vitrinite reflectance data. Atti Tic.Sc.Terra, 5, 101-114.

Bertello. F., Fantoni, R., Franciosi, R., Gatti, V, Ghielmi, M., Pugliese, A., 2010. From thrust-and-fold belt to foreland: hydrocarbon occurrences in Italy. Vining, BA & Pickering, S. C. (eds) Petroleum Geology: From Mature Basins to New Frontiers – Proceedings of the 7th Petroleum Geology Conference, 113–126; doi: 10.1144/0070113 # Petroleum Geology Conferences Ltd. Published by the Geological Society, London.

Bertotti G., Picotti V., Bernoulli D., Castellarin A., 1993. From rifting to drifting: tectonic evolution of the South-Alpine upper crust from the Triassic to the Early Cretaceous – Sedimentary Geology, 86, 53-76.

Bertotti, G., Capozzi, R., Picotti, V., 1997. Extension controls Quaternary tectonics, geomorphology and sedimentations of the N-Apennines foothills and adjacent Po Plain (Italy), Tectonophysics, 282, 291-301.

Béthoux, N., Theunissen, T., Beslier, M.O., Font, Y., Thouvenot, F., Dessa, J.X., Simon, S., Courrioux, G., Guillen, A., 2016. Earthquake relocation using a 3D a-priori geological velocitymodel from the western Alps to Corsica: Implication for seismic hazard. Tectonophysics 670, 82–100; doi.org/10.1016/j.tecto.2015.12.016.

Beydoun, Z.R., Clarke, M.W.H., Stoneley, R., 1992. Petroleum in the Zagros Basin: a late Tertiary foreland basin overprinted onto the outer edge of a vast hydrocarbon-rich Paleozoic–Mesozoic passive-margin shelf. In: Macqueen, R.W., Leckie, D.A. (Eds.), Foreland Basins and Fold Belts. Am. Assoc. Pet. Geol. Memoir, 55, 309–339.

Bigi,G., Castellarin, A., Catalano,R., Coli, M., Cosentino, D., Dal Piaz, G.V., Lentini, F., Parotto, M., Patacca, E., Praturlon, A., Salvini,F., Sartori, R., Scandone, P., & Vai, G.B., 1989. Synthetic structural-kinematic map of Italy, scale 1:2.000.000. CNR, Progetto Finalizzato Geodinamica, Roma.

Bignami, C., Burrato, P., Cannelli, V., Chini, M., Falcucci, E., Ferretti, A., Gori, S., Kyriakopoulos, C., Melini, D., Moro, M., Novali, F., Saroli, M., Stramondo, S, Valensise, G., Vannoli, P., 2012. Coseismic deformation pattern of the Emilia 2012 seismic sequence imaged by Radarsat-1 interferometry, Ann. Geophys. 55, 4, 789–795, doi:10.4401/ag6157.

Boccaletti, M., Coli, M., Eva, C., Ferrari, G., Giglia, G., Lazzarotto, A., Merlanti, F., Nicolich, R., Papani, G., Postpischl, D., 1985. Considerations on the seismotectonics of the Northern Apennines. Tectonophysics 117, 7–38, doi:10.1016/0040-1951(85)90234-3.

Boccaletti, M., Ciaranfi, N., Cosentino, D., Deiana, G., Gelati, R., Lentini, F., Massari, F., Moratti, G., Pescatore, T., Ricci Lucchi, F., Tortorici, L., 1990. Palinspastic restoration and paleogeographic reconstruction of the peri-Tyrrhenian area during the Neogene. Palaeogeography, Palaeoclimatology, Palaeoecology, 77, 1, pp. 41-50.

Boccaletti, M., Corti, G., Martelli, L., 2010. Recent and active tectonics of the external zone of the Northern Apennines (Italy) - International Journal Earth Science (Geol Rundsch), doi:10.1007/s00531-010-0545-y.

Bond, R.M.G., McClay, K.R., 1995. Inversion of Lower Cretaceous extensional basin, south central Pyrenees, Spain. In: Buchanan, J.G and Buchanan, P.G. (Eds), Basin Inversion, Geol. Soc. London Spec. Pub., 88, 415-431.

Bond, C.E., Shipton, Z.K., Gibbs, A.D., Jones, S., 2008. Structural mod- els: Optimizing risk analysis by understanding conceptual uncertainty. First Break, 26, 6, 65−71.

Bongiorni, D., 1987. La ricerca di idrocarburo negli alti strutturali mesozoici della Pianura Padana: l'esempio di Gaggiano – Atti Tic. Sc. Terra Vol. XXXI, pp. 125-141.

Bonini, L., Toscani, G., Seno, S., 2014. Three-dimensional segmentation and different rupture behavior during the 2012 Emilia seismic sequence (Northern Italy). Tectonophysics, 630, 33-42, doi:http://dx.doi.org/10.1016/j.tecto.2014.05.006.

Bosica, B., Shiner, P., 2013. Petroleum systems and Miocene turbidites leads in the Western Po Valley". 11th Offshore Mediterranean Conference and Exhibition. Ravenna, Italy March 20-22, 2013.

Brack, P., Rieber, H., 1993. Towards a better definition of the Anisian/Ladinian boundary : New biostratigraphic data and correlations of boundary sections from the Southern Alps. Eclogae geol. Helv. 86/2: 415-527.

Braga, Gp., Castellarin, A., Corsi, M., De Vecchi, Gp., Gatto, Gino., Gatti, Giuseppe, Largaiolli, T., Monese, A., Mozzi, G., Rui, A., Sassi, F.P., Zirpoli, G., 1968. Carta Geologica D'Italia, scale 1:100,000, Map "36-Schio".

Bresciani, I., Perotti, C.R., 2014. An active deformation structure in the Po Plain (N Italy): The Romanengo anticline. Tectonics, 33, doi:10.1002/2013TC003422.

Bressan G., De Franco R., Gentile F., 1992. Seismotectonic study of the Friuli (Italy) area based on tomographic inversion and geophysical data. Tectonophysics, 207: 383-400, Amsterdam.

Bressan.G., Snidarcig, A., Venturini, C., 1998. Present state of tectonic stress of the Friuli area (eastern Southern Alps). Tectonophysics 292 211–227.

Bressan, G., Bragato, L.P., Venturini, C., 2003. Stress and strain tensors based on focal mechanisms in the seismotectonic framework of th Friuli-Venezia Giulia region (Northeastern Italy). Bull. Seismol. Soc. America, 93/3: 1280-1297, Los Alamos.

Burnham, A.K., and Sweeney, J.J., 1989, A chemical kinetic model of vitrinite maturation and reflectance: Geochimica et Cosmochimica Acta, v. 53, p. 2649–2657.

Burrato, P., Ciucci, F., Valensise, G., 2003. An inventory of river anomalies in the Po Plain, Northern Italy: evidence for active blind thrust faulting. Annals of Geophysics, 46, 5, 865-882.

Burrato, P., Poli, M.E., Vannoli, P., Zanferrari, A., Basili, R., Galadini, F., 2008. Sources of Mw 5+ earthquakes in northeastern Italy and western Slovenia: An updated view based on geological and seismological evidence. Tectonophysics 453, 157–176.

Burrato, P., Maesano, F.E., D'Ambrogi, C., Toscani, G., Valensise, G., 2012. From drawing anticline axes to 3d modelling of seismogenic sources: evolution of seismotectonic mapping in the Po Plain. 7° EUropean Congress on REgional GEOscientific Cartography and Information Systems (EUREGEO), 12-15 June 2012, Bologna. Available from: http://ambiente.regione.emilia-romagna.it/geologia-en/temi/euregeo2012/presentations/09_Burrato_etal_Euregeo.pdf.

Burrato, P., D'Ambrogi, C., Maesano, F.E., and Toscani, G., 2014. Regional earthquake source model of the Po Plain based on full 3D definition of active faults. GeolMol Mid-term Conference, Montanuniversität Leoben, 5-6 June, 2014.

Calabrò R., Ceriani A., Di Giulio A., Fantoni R., F. Lino, Scotti P, 2003. Thermal history of syn-rift successions between the Iseo Basin and the Trento Plateau: results from the integrated study of organic matter maturity and fluid inclusions. Atti Tic. Sc. Terra, serie sp. v. 9, pp. 88-91.

Calcagno, P., Bouchot, V., Thinon, I., Bourgine, B., 2012. A new 3D fault model of the Bouillante geothermal province combining onshore and offshore structural knowledge (French West Indies). Tectonophysics 526–529, pp.185–195. ; doi:10.1016/j.tecto.2011.08.012.

Calcagno, P.; Chiles, J. P.; Courrioux, G, Guillen, A., 2008. Geological modelling from field data and geological knowledge Part I. Modelling method coupling 3D potential-field interpolation and geological rules . Physics of the Earth and Planetary Interiors. 171, 1-4, pp.147-157.

Calcagno, P., Lazarre, J., Courrioux, G., Ledru, P., 2007. 3D geometric modelling of an external orogenic domain: a case history from the western Alps (massif de Morges, Pelvoux). Bull. Soc. géol. Fr., 178, 4, pp. 263-274.

Campani, M., Mancktelow, N., Courrioux, G., 2014. The 3D interplay between folding and faulting in a syn-orogenic extensional system: the Simplon Fault Zone in the Central Alps (Switzerland and Italy). Swiss Journal of Geosciences, 107, 2-3, pp. 251-271.

Cantelli, C., Carloni, G.C., Castellarin, A., Ceretti, E., Colantoni, P., Cremonini, G., Elmi, C., Frascari, F., Monesi, F., Pisa, G., Rabbi, E., Tomadin, L., Vai, G.B., Braga, Gp., Corsi, M., Gatto, G., Locatelli, D., Rui, A., Sassi, P., Zirpoli, G., Dal Cin, R., Largaiolli, T., Gatto, G.O., 1971. Carta Geologica D'Italia, scale 1:100 000, Map "4C-13- Monte Cavallino-Ampezzo".

Caputo, R., Poli, M.E., Zanferrari, A., 2010. Neogene-Quaternary tectonic stratigraphy of the eastern Southern Alps, NE Italy. J. Struct. Geol., 32 (7), 1009-1027, doi: 10.1016/j.jsg.2010.06.004.

Carannante, C., Argnani, A., Massa, M., D'Alema, E., Lovati, S., Moretti, M., Cattaneo, M., Augliera, P., 21015. The May 20 (MW 6.1) and 29 (MW 6.0), 2012, Emilia (Po Plain, northern Italy) earthquakes: New seismotectonic implications from subsurface geology and high-quality hypocenter location. Tectonophysics 655, 107–123.

Cardozo, N., Montes, C., Marín, D., Gutierrez, I., Palenci, A., 2016. Structural analysis of the Tabaco anticline, Cerrej_on open-cast coal mine, Colombia, South America. Journal of Structural Geology 87, 115-133; doi.org/10.1016/j.jsg.2016.04.010.

Caricchi, C., Cifelli, F., Sagnotti, L., Sani, F., Speranza, F., Mattei, M., 2014. Paleomagnetic evidence for a post-Eocene 90° CCW rotation of internal Apennine units: A linkage with Corsica-Sardinia rotation? Tectonics, 33 (4), 374-392.

Carminati, E., 2009. Neglected basement ductile deformation in balanced-section restoration: An example from the Central Southern Alps (Northern Italy). Tectonophysics 463 (2009) 161–166 ; doi:10.1016/j.tecto.2008.09.042.

Carminati, E., Doglioni, C., Scrocca, D., 2003. Apennines subduction-related subsidence of Venice (Italy). Geophys. Res. Lett. 30 (13), 1717. http://dx.doi.org/10.1029/2003GL017001.

Carminati, E., Enzi, S., Camuffo, D., 2007. A study on the effects of seismicity on subsidence in foreland basins: An application to the Venice area. Global and Planetary Change 55, 237–250.

Carminati, E., Scrocca, D., Doglioni, C., 2010. Compaction-induced stress variations with depth in an active anticline: Northern Apennines, Italy. Journal of Geophysical Research, 115, B02401, doi:10.1029/2009JB006395.

Carminati, E., Cavazza, D., Scrocca, D., Fantoni, R., Scotti, P., Doglioni, C., 2010. Thermal and tectonic evolution of the Southern Alps (northern Italy) rifting: Coupled organic matter maturity analysis and thermo-kinematic modeling. AAPG Bulletin, v. 94, no. 3 (March 2010), pp. 369–397.

Carminati, E., Doglioni,C., 2012. Alps vs. Apennines: the paradigm of a tectonically asymmetric Earth. Earth-Science Reviews, 112, 67-96.

Carminati, E., Lustrino, M., Doglioni, C., 2012. Geodynamic evolution of the central and western Mediterranean: Tectonics vs. igneous petrology constraints. Tectonophysics, 579, 173-192, doi: 10.1016/j.tecto.2012.01.026.

Carr, A.D, 1998. Integrated maturation, hydrocarbon generation and diagenetic modelling in overpressured basins: Case study from the Central Graben, North Sea. Pau: Bull. Centre Rech. Elf Explor. Prod.Mem., 77–81.

Carr, A.D., 1999. A vitrinite reflectance kinetic model incorporating overpressure retardation. Marine and Petroleum Geology, 16, 355-377.

Carrapa, B., Di Giulio, A., 2001. The sedimentary record of the exhumation of a granite intrusion into a collisional setting: the lower Gonfolite Group, Southern Alps, Italy. Sedim. Geol., 139, 3-4, 217-228, doi: 10.1016/S0037-0738(00)00167-6.

Carulli G.B., Ponton, M., 1992. Interpretazione strutturale profonda del settore centrale Carnico-Friulano. Studi Geologici Camerti. Special Volume, CROP 1-1A, 275-284.

Carulli, G.B, Salvador, G.L., Ponton, M., Podda, F., 1997. La dolomia di forni: evoluzione di un bacino euxinico tardo triassico nelle prealpi carniche. Boll. Soc. Geol. It., 116, 95-107.

Casati, P., Assereto, R., Comizzoli, G., Passeri, L.D., Boni, A., Cassinis, G., Cerro, A., Rosetti, R., Accordi, B., Dieni, I., Malaroda, R., Bianchi, A., Cevales, G., Dal Piaz, Gb., Morgante, S., 1970. Carta Geologica D'Italia scale 1:100,000, Map "34- Breno".

Casero P., Rigamonti A., Iocca, M., 1990. Paleogeographic relationship during Cretaceous between the Northern Adriatic area and the Eastern Southern Alps; Mem.Soc.Geol.It. 45, 807-814.

Casero, P., 2004. Structural setting of petroleum exploration plays in Italy. Crescenti, V., D'Offizi, S., Merlino, S., Sacchi, L., (eds): Geology of Italy, Special Volume of the Italian Geological Society for the IGC 32 – Florence.

Cassano, E., Anelli, L., Fichera, R., Cappelli, V., 1986. Pianura Padana, interpretazione integrata di dati Geofisici e Geologici. - 73° congresso Soc. Geol. It., Roma.

Cassola, T., Battaglia, M., Doglioni. C., Zuliani, D., 2007. A two dimensional elastic deformation model of the strain accumulation in Friuli – Venezia Giulia (Julian Alps). Excerpt from the Proceedings of the COMSOL Users Conference 2007 Grenoble.

Castaldini, D., Panizza, M., 1991. Inventario delle faglie attive tra I fiumi Po e Piave e il lago di Como (Italia Settentrionale). Il Quaternario, 4(2), 333-410.

Castellarin, A., Vai, G.B., 1982. Introduzione alla geologia strutturale del Sudalpino. In: Castellarin, A., Vai,G.B., - Guida alla gelogia del Sudalpino centro orientale. Guide Geol. Reg., Soc.Geol.It., 1-22.

Castellarin A., Eva C., Giglia, G., Vai, G. B., 1985. Analisi strutturale del Fronte Appenninico Padano. Giornale di Geologia, Sez. 3°, 47/1-2, 47-75.

Castellarin, A., Vai, G. B., 1986. Southalpine versus Po Plain Apenninic arcs, in: The origin of arcs, Development in Geotectonic, Wezel, F. C. (Ed), 253-280, Elsevier Amsterdam.

Castellarin A., Vai, G.B., 1986. In Wezel F.C., ed., The origin of arcs, Elsevier Sc. Pul., 253-280.

Castellarin A., Eva C., Giglia, G., Vai, G. B., 1986. Analisi strutturale del Fronte Appenninico Padano. Giornale di Geologia, Sez. 3°, 47/1-2, 47-75.

Castellarin A., Cantelli L., Fesce A.M., Mercier J.L., Picotti V., Pini G.A., Prosser G. & Selli L., 1992. Alpine compressional tectonics in the Southern Alps. Relationships with the N-Appenines. Annales Tectonicae, 6: 62-94.

Castellarin, A., 2001. Alps-Apennines and Po Plain-Frontal Apennines relationships. In: Vai G. B. and Martini I. P. (Eds.), Anatomy of an Orogen. The Apennines and adjacent Mediterranean Basins, Kluver, London, 177- 196.

Castellarin, A., Nicolich, R., Fantoni, R., Cantelli, L., Sella, M., Selli, L., 2006. Structure of the litosphere beneath the Eastern Alps (southern sector of the TRANSALP transect). Tectonophysics, 414: 259-282.

Castellarin, A., Cantelli, L., 2010. Geology and evolution of the Northern Adriatic structural triangle between Alps and Apennines – Rend.Fis.Acc.Lincei, 21, (Suppl 1):S3-S14; doi:10.1007/s12210-010-0086-0.

Castello, B., Selvaggi, G., Chiarabba, C., Amato, A., 2006. CSI Catalogo della sismicità italiana 1981-2002, versione 1.1. INGV-CNT, Roma http://csi.rm.ingv.it/.

Castiglioni,B., Leonardi, P., Merla, G., Trevisan., Zenari, S., 1940. Carta geologica delle Tre Venezie, scale 1:100,000, Map "12- Pieve di Cadore"

Castiglioni, B., Boyer, G., Leonardi, P., Venzio, S., Dal Piaz, G., Vialli, V., Zenari, S., 1941. Carta geologica delle Tre Venezie, scale 1:100,000, Map "23- Belluno".

Caumon, G., Collon-Drouaillet, P., Le Carlier, C., Viseur, S., Sausse, J., 2009. Surface-Based 3D Modeling of Geological Structures. Math Geosci 41 : DOI 10.1007/s11004-009-9244-2, 927-945.

Cati, A., Sartorio, D., Venturini, S., 1987. Carbonate platforms in the subsurface of the northern Adriatic area. Mem.Soc. Geol.It., v.40. pp. 295-308.

Channell, J.E.T., D'Argenio, B., Horvath, F., 1979. Adria, the African promontory, in Mesozoic Mediterranean palaeogeography, Earth Sci. Rev. 15, 213-292.

Cherpeau, N., Caumon, G., 2015. Stochastic structural modelling in sparse data situations. Petroleum Geoscience, 21, 233-247; doi:10.1144/petgeo2013-030.

Chiarabba, C., Jovane, L., DiStefano, R., 2005. A new view of Italian seismicity using 20 years of instrumental recordings. Tectonophysics 395, 251– 268.

Chiaraluce, L., Valoroso, L., Anselmi, M., Bagh, S., Chiarabba, C., 2009. A decade of passive seismic monitoring experiments with local networks in four Italian regions; Tectonophysics 476 - 85–98.

Chiaramonte, M.,A., Novelli, L., 1986. Organic matter maturation in Northern Italy: some determining agents. Org. Geochem., 10, 281-290.

Ciarapica, G., Cirilli, S., D'Argenio, B., Marsella, E., Passeri, L., Zaninetti, L., 1986. Late Triassic open and euxinic basins in Italy. Rend.Soc.Geol.It., 9, pp.157-166.

Cibin, U., Di Giulio, A., Martelli, L., 2003. Oligocene-Early Miocene evolution of the Northern Apennines (northwestern Italy) traced through provenance of piggy-back basin fill successions. In: T. McCann & Saintot (Eds) Tracing tectonic deformation using the sedimentary record, Geol. Soc. London Spec. Pub., 208, 269-287. doi: 10.1144/GSL.SP.2003.208.01.13

Cibin, U., Di Giulio, A., Martelli, L., Catanzariti, R., Poccianti, S., Rosselli, C., Sani, F., 2004. Factors controlling foredeep turbidite deposition: the case of Northern Apennines (Oligocene-Miocene, Italy). In: S. Lomas & P. Joseph (Eds.), Confined turbidite systems, Geol. Soc. London Spec. Pub., 222, 115-134. doi: 10.1144/GSL.SP.2004.222.01.07.

Çiftçi, N.B., Giger, S.B., Clennell, M.B., 2011. Three-dimensional structure of experimentally produced clay smears: Implications for fault seal analysis. AAPG Bulletin, 97, 5, 733–757; doi:10.1306/10161211192.

Cimolino, A., Della Vedova, B., Nicolich, R., Barison, E., Brancatelli, G., 2010. New evidence of the outer Dinaric deformation front in the Grado area (NE-Italy) - Rend.Fis.Acc.Lincei, 21, (Suppl 1):S67-S179, DOI 10.1007/s12210-010-0096-y.

Civile, D., Zecchin, M., Forlin, E., Donda, F., Volpi, V., Merson, B., Persoglia, S., 2013. CO2geological storage in the Italian carbonate successions. International Journal of Greenhouse Gas Control 19, 101–116; doi:.org/10.1016/j.ijggc.2013.08.010.

Cloetingh, S., Ziegler, P., Beekman, F., Andriessen, P., Matenco, L., Bada, G., Garcia-Castellanos, D., Hardebol, N., Dezes, P., Sokoutis, D. 2005. Lithospheric memory, state of stress and rheology: neotectonic controls on Europe's intraplate continental topography, Quaternary Science Reviews 24, 3-4, 241–304.

CROP Project, 1st Edition, 2004. Deep seismic exploration of the Central mediterranean and Italy.. Editor: I. Finetti, ISBN: 9780080457604, Elsevier, Amsterdam.

Coward, M.P., Dietrich, D., Park, R.G. (eds.) 1989. Alpine Tectonics. Geol. Soc. London, Spec. Pub., 45, 449 pp.

Cuffaro, M., Riguzzi, F., Scrocca, D., Antonioli, F., Carminati, E., Livani, M., Doglioni, C., 2010. On the geodynamics of the northern Adriatic plate - Rend. Fis. Acc. Lincei (2010) 21 (Suppl 1): S253–S279; doi:10.1007/s12210-010-0098-9.

D'Ambrogi, C., Scrocca, D., Pantaloni, M., Valeri, V., Doglioni., 2010. Exploring Italian geological data in 3D; Journal of the Virtual Explorer, Electronic Edition, ISSN 1441-8142, volume 36, paper 33. In: (Eds.) Marco Beltrando, Angelo Peccerillo, Massimo Mattei, Sandro Conticelli, and Carlo Doglioni, The Geology of Italy, 2010. ftp://ftp.ingv.it/pub/filippo.muccini/SGI_VIRTUAL%20EXPLORER/exploring-italian-geological-data-in-3d.pdf.

Dal Piaz, G.V., Bistacchi, A., Massironi, M., 2004. Geological outline of the Alps. Episodes 26, 175e180.

Dal Piaz, G., Venzo,S., Fabiani, R., Trevisan, L., Pia, J., 1946. Carta geologica delle Tre Venezie, scale 1:100,000, Map "37-Bassano del Grappa".

Dahlstrom, C.D., 1969. Balanced cross-sections. Canadian Journal of Earth Science, 6, 743-757.

De Celles, P.G., Giles, K.A., 1996. Foreland basin systems. Basin Res. 8 (2), 105–123.

Defant, A., 1961. Physical Oceanography, Vol. 1, Pergamon Press, 728 pp.

Delacou, B., Sue, C., Champagnac, J.D., Burkhard, M., 2004. Present-day geodynamics in the bend of the western and central Alps as constrained by earthquake analysis. Geophys. J. Int., 158, 753–774 doi: 10.1111/j.1365-246X.2004.02320.x

Della Vedova, B., Bellani, S., Pellis, G., Squarci, P., 2001. Deep temperatures and surface heat flow distribution. In: Vai, G.B. & Martini, I.P. (Eds.): "Anatomy of an orogen: the Apenninesand adjacent Mediterranean basins". Kluwer Academic Publishers: 65-76, Dordrecht, The Netherlands.

Dercourt, J., Zonenshain, L.P., Ricou, L.-E., Kazmin, V.G., Le Pichon, X., Knipper, A.L., Grandjacquet, C., Sbortshikov, I.M., Geyssant, J., Lepvrier, C., Pechersky, D.H., Boulin, J., Sibuet, J.-C., Savostin, L.A., Sorokhtin, 0., Westphal, M., Bazhenov, M.L., Laurer, J.P., Biju-Duval, B., 1986. Geological evolution of the Tethys belt from Atlantic to Pamirs since the Lias. Tectonophysics, 123, 241-315.

Desegaulx, P., Roure, F., Villien, A., 1990. Structural evolution of the Pyrenees tectonic heritage and flexural behavior of the continental crust. J. Letouzey (Editor) and Editions Technip, Petroleum and Tectonics in Mobile Belts, 31-48.

Desio, A., Venzo, S., 1954. Carta Geologica D'Italia, scale 1:100,000, Map "33- Bergamo".

Devoti, R., Esposito, A., Pietrantonio, G., PisaniI, A.R., Riguzzi, F., 2011. Evidence of large scale deformation patterns from GPS data in the Italian subduction boundary, Earth Planet. Sc. Lett. 311, 3–4, 230–241, doi:10.1016/j.epsl.2011.09.034.

Dèzes, P. and Ziegler, P.A., 2004. Moho depth map of Western and Central Europe (2004) EUCOR-URGENT home page (http://www.unibas.ch/eucor-urgent).

Dèzes, P., Schmid, S.M. and Ziegler, P.A., 2004. Evolution of the European Cenozoic Rift System: interaction of the Alpine and Pyrenean orogens with their foreland lithosphere. Tectonophysics, 389, 1–33.

Dewey, J.F.; Pitman, C., Ryan, B. F., Bonnin, J. 1973. Plate tectonics and the evolution of the Alpine systems. Geological Society of America Bulletin, 84, 3,137-80.

De Zanche, V., Gianolla, P., Roghi, G., 2000. Carnian stratigraphy in the Raibl/Cave del Predil area (Julian Alps, Italy). Eclogae. Geol. Helv., 93, 331–347.

Dhont, D., Monod, B., Hervouet, Y., Backé, G., Klarica, S., 2012. 3D geological modeling of the Trujillo block: Insights for crustal escape models of the Venezuelan Andes . Journal of South America Earth Science, 39, pp. 245-251.

Di Bucci, D., Angeloni, P., 2012. Adria seismicity and seismotectonics: Review and critical discussion. Marine and Petroleum Geology, http://dx.doi.org/10.1016/j.marpetgeo.2012.09.005.

Di Capua, A., Vezzoli, G., Cavallo, A., Groppelli, G., 2015. Clastic sedimentation in the Late Oligocene Southalpine Foredeep: From tectonically controlled melting to tectonically driven erosion. Geological Journal, doi: 10.1002/gj.2632.

Di Giovambattista, R., Tyupkin, Y., 1999. The fine structure of the dynamics of seismicity before M>4.5 earthquakes in the area of Reggio Emilia (Northern Italy). Annali di Geofisica, 42, 5.

Di Giulio, A., Carrapa, B., Fantoni, R., Gorla, L., Valdisturlo, A., 2001. Middle Eocene-Early Miocene sedimentary evolution of the Western Lombardy South Alpine foredeep (Italy). Int. Jour. of Earth Sc., 90, 3, 534-548. doi: 10.1007/s005310000186.

Di Giulio, A., Mancin, N., Martelli, L., Sani, F., 2013. Foredeep palaeobathymetry and subsidence trends during advancing then retreating subduction. The Northern Apennine case (Oligocene-Miocene, Italy). Basin Res., 25, 6, 260-284, doi: 10.1111/bre.12002.

Di Manna, P., Guerrieri, L., Piccardi, L., Vittori, E., Castaldini, D., Berlusconi, A., Bonadeo, L., Comerci, V., Ferrario, F., Gambillara, R., Livio, F., Lucarini M., Michetti, A., 2012. Ground effects induced by the 2012 seismic sequence in Emilia: implications for seismic hazard assessment in the Po Plain. Annals of Geophysics, 55, No 4. doi: 10.4401/ag-6143.

Dischinger J.D., Mitra S., 2006. Three-dimensional structural model of the Painter and East Painter reservoir structures, Wyoming fold and thrust belt - AAPG Bulletin, v. 90, no. 8 (August 2006), pp. 1171–1185.

DISS Working Group, 2015. Database of Individual Seismogenic Sources (DISS), Version 3.2.0: A compilation of potential sources for earthquakes larger than M 5.5 in Italy and surrounding areas. http://diss.rm.ingv.it/diss/, © INGV 2015 - Istituto Nazionale di Geofisica e Vulcanologia - All rights reserved; doi:10.6092/INGV.IT-DISS3.2.0.

Doglioni, C., Bosellini, A., 1987. Eoalpine and mesoalpine tectonics in the Southern Alps. *Geol. Rund*., 76(3): 735-754, Stuttgart.

Doglioni, C., 1991. A proposal of kinematic modelling for W-dipping subductions - possible applications to the Tyrrhenian-Apennines system. Terra Nova, 3, 423-434.

Doglioni, C., 1994. The Puglia uplift (SE Italy): an anomaly in the foreland of the Apenninic subduction due to buckling of a thick continental lithosphere. Tectonics, 13, n°5, 1309-1321.

Doglioni, C., 1995. Geological remarks on the relationships between extension and convergent geodynamic settings. Tectonophysics, 252 (1-4), 253-267, doi: 10.1016/0040-1951(95)00087-9.

Doglioni, C., Harabaglia,P., Martinelli, G., Mongelli, F., Zito, G., 1996. A geodynamic model of the Southern Apennines accretionary prism. Terra Nova, 8, 540-547.

Doglioni C., Carminati E., 2008. Structural style and Dolomites field trip – Memorie descrittive della carta geologica d'italia, LXXXII.

Dondi, L., D'Andrea, G., 1986. La Pianura Padana e Veneta dall'Oligocene superiore al Pleistocene. Giornale di Geologia, Ser. 3, 48, 1–2, 197-225.

Drakatosa, G., Karastathisa, T, V., Makrisb, J., Papouliac, J., Stavrakakisa, G., 2005. 3D crustal structure in the neotectonic basin of the Gulf of Saronikos (Greece). Tectonophysics 400 (2005) 55– 65 ; doi:10.1016/j.tecto.2005.02.004.

Dunkel, K.M., Mickelson, D.M., Anderson, M.P, Fienen, M.N., 2009. Troy Valley glacial aquifer; 3D hydrostratigraphic model aiding water management in southern Wisconsin, USA. In Three-Dimensional Geological Mapping Workshop Extended Abstract 2009 Annual Meeting, Geological Society of America Portland, Oregon – October 17, 2009. https://www.ideals.illinois.edu/bitstream/handle/2142/50267/ofs2009-04.pdf?sequence=2.

Durand-Riard, P., Salles, L., Ford, M., Caumon, G., Pellerin, J., 2011. Understanding the evolution of syn-depositional folds: Coupling decompaction and 3D sequential restoration. Marine and Petroleum Geology, 28, 1530 -1539; doi:10.1016/j.marpetgeo.2011.04.001.

Ellis, J., Armstrong, N., 2015. Interpretation of geophysical data using structural principles to build geological models. First Break, 33, 79-86.

Egan, S.S., Kane, S., Buddin, T.S., Williams, G.D. and Hodgetts, D., 1999. Computer modelling and visualisation of the structural deformation caused by movement along geological faults. Computers & Geosciences, 25, 3, 283–297.

Elter, P., Pertusati, P., 1973. Considerazioni sul limite Alpi-Appennino e sulle sue relazioni con l'arco delle Alpi occidentali. Mem. Soc. Geol. Ital., 12: 359-375.

Errico G., Groppi G., Savelli S., Vaghi G.C., 1980. Malossa Field: a deep discovery in the Po Valley, Italy – AAPG Memoir 30, 525-538.

Fantoni, R., Bello, M., Ronchi, P., Scotti, P., 2002. Po Valley oil play – From the Villafortuna-Trecate field to South-Alpine and Northern Apennine exploration. EAGE 64th Conference & Exhibition — Florence, Italy, 27 - 30 May 2002.

Fantoni, R., Decarlis, A., Fantoni, E., 2003. L'Estensione Mesozoica al Margine occidentale delle Alpi Meridionali – Atti Ticinensi di Scienze della Terra, Vol.44, 97-110.

Fantoni R, Scotti P., 2003 – Thermal record of the Mesozoic extensional tectonics in the Southern Alps – Atti ticinensi Sc. Terra, SS9, 96-101.

Fantoni, R., Bersezio, R., Forcella, F., 2004. Alpine structure and deformation chronology at the Southern Alps-Po Plain border in Lombardy. Boll.Soc.Geol.It., 123 (2004), 463-476.

Fantoni R., Franciosi R., 2010. Tectono-sedimentary setting of the Po Plain and Adriatic foreland - Rend.Fis.Acc.Lincei, 21, (Suppl 1):S197-S209, DOI 10.1007/s12210-010-0102-4.

Farrington, R.J., Stegman, D.R., Moresi, L.N., Sandiford, M., May, D.A., 2010. Interactions of 3D mantle flow and continental lithosphere near passive margins. Tectonophysics 483, 20–28; doi:10.1016/j.tecto.2009.10.008.

Franciosi, R., Vignolo, A., 2002. Northern Adriatic foreland – A promising setting for the Southalpine Mid-Triassic petroleum system. EAGE, 64th Conference & Exhibition, Florence, Italy, 27-30 May, H-25.

Fernandez, N.; Kaus, B., 2014. Fold interaction and wavelength selection in 3D models of multilayer detachment folding. Tectonophysics 632, 199–217; doi.org/10.1016/j.tecto.2014.06.013.

Ferrer, O., Roca, E., Vendeville, B.C., 2014. The role of salt layers in the hangingwall deformation of kinked-planar extensional faults: Insights from 3D analogue models and comparison with the Parentis Basin. Tectonophysics, 636, 338–350; doi.org/10.1016/j.tecto.2014.09.013.

Fredman, N., Tveranger, J., Cardozo, N., Braathen, A., Soleng, H., Røe, P., Skorstad, A., Syversveen, A. R., 2008. Fault facies modeling: Technique and approach for 3-D conditioning and modeling of faulted grids. AAPG Bulletin, 92, 11, 1457–1478; doi:10.1306/06090807073.

Frisch, W., Meschede, M., Blakey, R.C., 2011. Plate Tectonics.Continental Drift and Mountain Building. Springer, ISBN 978-3-540-76503-5, doi, 10.1007/978-3-540-76504-2.

Galadini F., Poli M.E., Zanferrari A., 2005. Seismogenic sources potentially responsible for earthquakes with M>6 in the eastern Southern Alps (Thiene-Udine sector, NE Italy). Geoph. J. Int., 161: 739-762, Oxford.

Galli, M.T., Jadoul, F., Bernasconi, S.M., Cirilli, S., Weissert, H., 2007. Stratigraphy and palaeoenvironmental analysis of the Triassic-Jurassic transition in the western Southern Alps (Northern Italy). Paleogeography, Palaeoclimatology, Palaeoecology, 44, 52-70.

Galuppo, C., Toscani, G., Turrini, C., Bonini, L, Seno, S., 2016. Fracture patterns evolution in sandbox fault-related anticlines. Ital. J. Geosci., 135, 1, 5-16; doi: 10.3301/IJG.2014.39.

Gatto, G.O., Gatto, P., Baggio, P., De Vecchi, Gp., Mezzacasa, G., Piccirillo, E., Zirpoli, G., Friz., Gatto, G., Corsi, M., Sassi, F.P., Monese,A., Gregnanin, A., Zilian, T., Largaiolli, T., 1969. Carta Geologica D'Italia, scale 1:100,000, Map "1 & 4A- Passo del Brennero and Bressanone".

Gatto, P., Rui, A., Dal Pra,A., De Zanche,V., Gatto, G., Gatto, G.O., Corsi, M., Nardin, M., Sacerdoti, M., Largaiolli, T., Ghezzo, C., D'Amico, C., 1968. Carta Geologica D'Italia, scale 1:100,000, Map "21-Trento".

Gelati.R., Gnaccolini, 1982. Evoluzione tettonico-sedimentaria della zona al limite tra Alpi a Appennino tra l'inizio dell'Ologocene e il Miocene medio. Mem. Soc. Geol. It., 24, 183-191.

GEOMOL project: Assessing subsurface potentials of the Alpine Foreland Basins for sustainable planning and use of natural resources; 2015. http://geomol.eu/home/index_html.

Gerdes, M.L., Baumgartner, L.P., Valley, J.W., 1999. Stable isotopic evidence for limited fluid flow through dolomitic marble in the Adamello contact aureole, Cima Uzza, Italy. Journal of Petrology;40:853-872.

Ghielmi, M., Minervini, M., Nini, C., Rogledi, S., Rossi, M., Vignolo, A., 2010. Sedimentary and tectonic evolution in the eastern Po-Plain and northern Adriatic Sea area from Messinian to Middle Pleistocene (Italy). Rend. Fis. Acc. Lincei 21 (Suppl 1):S131–S166; doi: 10.1007/s12210-010-0101-5.

Ghielmi, M., Minervini, M., Nini, C., Rogledi, S., Rossi, M., 2012. Late Miocenee Middle Pleistocene sequences in the Po Plain and Northern Adriatic Sea (Italy): The stratigraphic record of modification phases affecting a complex foreland basin. Marine and Petroleum Geology, 1-32; http://dx.doi.org/ 10.1016/j.marpetgeo.2012.11.007.

Gianolla, P., De Zanche, V., Mietto, P., 2012. Triassic sequence stratigraphy in the Southern Alps (Northern Italy): definition of sequences and basin evolution. SEPM Special Publication No. 60, ISBN 1-56576-043-3.

Gibbs, A.D., 1983. Balanced cross-section construction from seismic sections in areas of extensional tectonics. J. Struct. Geol. 5, 153-169.

Gisquet, F., Lamarche, J., Floquet, M., Borgomano, J., Masse, J.P., Caline, B., 2013. Three-dimensional structural model of composite dolomite bodies in folded area (Upper Jurassic of the Etoile massif, southeastern France). AAPG Bulletin, 97, 9, 1477–1501; doi:10.1306/04021312016.

Gnaccolini, M., Jadoul, F., 1990. Carbonate platform, lagoon and delta "high-frequency" cycles from the Carnian of Lombardy (Southern Alps, Italy). Sedimentary Geology, 67, 143-159.

Gortani, M., Desio, A., 1925. Carta geologica delle Tre Venezie, scale 1:100,000, Map "14- Pontebba" .

Govoni, A., Marchetti, A., De Gori, P., Di Bona, M., Lucente, F. P., Improta, L., Chiarabba, C., Nardi, A., Margheriti, L., Agostinetti, N. P., Di Giovanbattista, R., Latorre, D., Anselmi, M., Ciaccio, M. G., Moretti, M., Castellano, C., Piccinini, D., 2014. The 2012 Emilia seismic sequence (Northern Italy): Imaging the thrust fault system by accurate aftershock location, Tectonophysics, doi: http://dx.doi.org/10.1016/j.tecto.2014.02.013.

Grad, M., Polkowsky, M., Ostaficzuk, S., 2016. High-resolution 3D seismic model of the crustal and uppermost mantle structure in Poland. Tectonophysics 666 (2016) 188–210 ; doi.org/10.1016/j.tecto.2015.10.022.

Graham Wall, B.R., Girbacea, R., Mesonjesi, A., Aydin, A., 2006. Evolution of fracture and fault-controlled fluid pathways in carbonates of the Albanides fold-thrust belt. AAPG Bulletin, 90, 8, pp. 1227 –1249.

Greber E., Leu W., Bernoulli D., Schumacher M.E., Wyss R., 1997. Hydrocarbon Provinces in the Swiss Southern Alps – a gas geochemistry and basin modelling study. Mar. and Pet. Geol., 14, 1, 3 -25.

Gretener, P.E., 1981. Geothermics: using temperature in hydrocarbon exploration. AAPG, Short Course Notes, 17

Grobe, A., Littke, R., Sachse, V., Leythaeuser, D., 2015. Burial history and thermal maturity of Mesozoic rocks of the Dolomites, Northern Italy. Swiss Geological Society, doi 10.1007/s00015-015-0191-2.

Guglielmetti, L., Comina, C., Abdelfettah, Y., Schill, E., Mandrone, G., 2013. Integration of 3D geological modeling and gravity surveys for geothermal prospection in an Alpine region. Tectonophysics 608, 1025–1036; doi.org/10.1016/j.tecto.2013.07.012.

Guglielmo, G., Jackson, M., Vendeville, B., 1997. Three-dimensional Visualization of Salt Walls and Associated Fault Systems. AAPG Bulletin, 81-1, 46-61.

Guillaume, B., Dhont, D., Brusset, S., 2008. Three-dimensional geologic imaging and tectonic control on stratigraphic architecture : Upper Cretaceous of the Tremp Basin (south-central Pyrenees, Spain). AAPG Bulletin, 92, 2, 249-269.

Guillen, A., Calcagno, Ph., Courrioux, G., Joly, A., Ledru, P., 2008. Geological modelling from field data and geological knowledge Part II. Modelling validation using gravity and magnetic data inversion . Physics of the Earth and Planetary Interiors. 171, 1-4, pp.158-169.

Guimera, J., Alonso, A., Mas, J.R.., 1995. Inversion of an extensional-ramp basin by a newly formed thrust: the Cameros basin (N.Spain). In: Buchanan, J.G and Buchanan, P.G. (Eds), Geol. Soc. London Spec. Pub., 88, 433-453.

Gusterhuber, J., Hinsch, R., Sachsenhofer, R.F., 2014. Evaluation of hydrocarbon generation and migration in the Molasse fold and thrust belt (Central Eastern Alps, Austria) using structural and thermal basin models. AAPG Bulletin, v. 98, no. 2, pp. 253–277.

Gunderson, K.L., Pazzaglia, F.J., Picotti, V., Anastasio, D.A., Kodama, K.P., Rittenour, T., Frankael, K.F., Ponza, A., Berti, C., Negri, A., Sabbatini, A., 2013. Unraveling tectonic and climatic controls on synorogenic growth strata (Northern Apennines, Italy), Geol. Soc. Am. Bull. 126, 3–4, 532–552, doi:10. 1130/B30902.1.

Guyonnet-Benaize, C., Lamarche, J., Masse J.P., Villeneuve, M., Viseur, S., 2010. 3D structural modelling of small-deformations in poly-phase faults pattern. Application to the Mid-Cretaceous Durance uplift, Provence (SE France). Journal of Geodynamics 50, 81–93; doi:10.1016/j.jog.2010.03.003.

Guyonnet-Benaize, C., Lamarche, J., Hollender, F., Viseur, S., Münch, P., Borgomano, J., 2015. Three-dimensional structural modeling of an active fault zone based on complex outcrop and subsurface data: The Middle Durance Fault Zone inherited from polyphase Meso-Cenozoic tectonics (southeastern France). Tectonics, 34, 2, 265-289; doi: 10.1002/2014TC003749.

Han,J., Yeon, Y., Hyun,H., Hwang, D., 2011. 3D Geological Model of Mining Area;http://www.asiageospatialforum.org/2011/proceeding/pps/Jonggyu%20Han_AGF.pdf.

Handy, M.R., Ustaszewski, K., Kissling, E., 2014. Reconstructing the Alps–Carpathians–Dinarides as a key to understanding switches in subduction polarity, slab gaps and surface motion. International Journal of Earth Sciences, 104 (1), 1-26; doi: 10.1007/s00531-014-1060-3.

Handy, M.R., Schmid, S.M., Bousquet, R., Kissling, E., Bernoulli, D., 2010. Reconciling plate-tectonic reconstructions of Alpine Tethys with the geological–geophysical record of spreading and subduction in the Alps. Earth-Science Reviews 102, 121–158.

Hossack, J.R., 1979. The use of balanced cross-sections in the calculation of orogenic contraction: a review. Journal of the Geological Society of London, 136, 705-711.

Klein, P., Richard,L., James,H., 2008. 3D curvature attributes: a new approach
for seismic interpretation. First break, 26, 105-112.

Klitzke, P., Faleide, I., Scheck-Wenderoth, M., Sippel, J., 2015. A lithosphere-scale structural model of the Barents Sea and Kara Sea region. Solid Earth, 6, 153–172; doi:10.5194/se-6-153-2015.

Koike, K., Kubo, T., Liu, C., Masoud, A., Amano, K., Kurihara, A., Matsuoka, T., Lanyon, B., 2015. 3D geostatistical modeling of fracture system in a granitic massif to characterize hydraulic properties and fracture distribution. Tectonophysics, 660, 1–16. doi.org/10.1016/j.tecto.2015.06.008.

Kruse, S.E., Royden, L.H., 1994. Bending and unbending of an elastic lithosphere: the Cenozoic history of the Apennine and Dinaride foredeep basins. Tectonics, 13 (2), 278-302, doi: 10.1029/93TC01935.

Jadoul, F., Rossi, P.M., 1982. Evoluzione paleogeografico-structturale e vulcanismo triassico nella Lombardia centro-occidentale. In A.Castellarin & G.B. Vai : Guida alla geologia del Sudalpino centro-occidentale. Guide geol.reg. S.G.I., 143-155, Bologna.

Jadoul, F., 1986. Stratigrafia e Paleogeografia del Norico nelle Prealpi bergamasche occidentali. Riv.It.Paleoont.Strat, v.91, 4 pp.479-512.

Jadoul, F., Berra, F., Frisia, S., 1992. Stratigraphic and palaeogeographic evolution of a carbonate platform in an extensional tectonic regime: the example of the Dolomia Principale in Lombardy (Italy). Rivista Italiana di Paleontologia e Stratigrafia 98, 1, 29-44.

Jadoul, F., Nicora A., Ortenzi A., Pohar C., 2002. Ladinian stratigraphy and paleogeography of the Southern Val Canale (Pontebbano-Tarvisiano, Julian Alps, Italy). Mem Soc.geol It., v57, pp29-43.

Jahn, A., Riller, U., 2009. A 3D model of first-order structural elements of the Vredefort Dome, South Africa — Importance for understanding central uplift formation of large impact structures. Tectonophysics 478, 221–229; doi:10.1016/j.tecto.2009.08.007.

Jarvie, D.M.., Claxton, B.L., Henk, F., Breyer, J.T., 2001. Oil and Shale Gas from the Barnett Shale, Ft. Worth Basin, Texas, AAPG National Convention, June 3-6, 2001, Denver, CO, AAPG Bull. Vol. 85, No. 13 (Supplement), p.A100.

Johannesen, J., Hay1, S. J., Milne1, J. K., Jebsen, C., Gunnesdal, S. C., Vayssaire, A., 2002. 3D oil migration modelling of the Jurassic petroleum system of the Statfjord area, Norwegian North Sea. Petroleum Geoscience, 8, 37–50; doi:1354-0793/02/$15.00.

Karakitsios, V., 2013. Western Greece and Ionian Sea petroleum systems. AAPG Bulletin, 97, 9, 1567-1595.

Kastelich V., Vrabek M., Cunningnam D. & Gosar A., 2008. Neo-alpine Structural Evolution and present-day Tectonic activity of the Eastern Southern Alps: the case of the Ravne Fault, NW Slovenia. *J. Struct. Geol.,* 30: 963-975.

Katz, B.J., Dittmar, E.I., Ehret, G.E., 2000. A geochemical review of carbonate source rocks in Italy. Journal of Petroleum Geology, v.23 (4), pp.399-424.

Keim, L., Spötl, C., and Brandner, R., 2006. The aftermath of the Carnian carbonate platform demise: a basinal perspective (Dolomites, Southern Alps): Sedimentology, v. 53 p. 361-386, doi: 10.1111/j.1365-3091.2006.00768.x.

Lacombe, O., Mouthereau, F., Angelier, J., Chu, H.T., Lee, J.C., 2003. Frontal belt curvature and oblique ramp development at an obliquely collided irregular margin: geometry and kinematics of the NW Taiwan fold–thrust belt. Tectonics 22, 3, 1025.

Lacombe, O., Bellahsen, N., 2016. Thick-skinned tectonics and basement-involved fold-thrust belts. Insight from selected Cenozoic orogens. Geological Magazine, Special Issue 'Tectonic evolution and mechanics of basement-involved fold-thrust belts' (O. Lacombe, J. Ruh, D. Brown and F. Nilfouroushan eds), doi: 10.1017/S0016756816000078.

Lamarche, J., Scheck-Wenderoth, M., 2005. 3D structural model of the Polish Basin. Tectonophysics, 397, 73-91; doi:10.1016/j.tecto.2004.10.013.

Lapponi, F., Casini, G., Sharp, I., Blendinger, W., Fernández, N., Romaire, I., Hunt, D., 2011. From outcrop to 3D modelling: a case study of a dolomitized carbonate reservoir, Zagros Mountains, Iran. Petroleum Geoscience, 17, 283–307 ; doi : 10.1144/1354-079310-040.

Larroque, C., 2009. Aléa sismique dans une région intraplaque à sismicité modérée: la junction Alpes-Bassin Ligure. Memoire d'Habilitation à Diriger des Recherches. UMR 6526 Géosciences Azur, CNRS.

Laubscher, H.P., 1996. Shallow and deep rotations in the Miocene Alps Tectonics, 15, 1022-1035.

Lecour, M., Cognot, R., Dvinage, I., Thore, P., Dulac, JP., 2001. Modelling of stochastic faults and fault network in a structural uncertainty study. Petroleum Geoscience, 7, S31-S42.

Leslie, G., Krabbendam, M., Kearsey, T., 2012. Assynt Culmination Geological 3D Model. British Geological Survey, http://www.bgs.ac.uk/research/ukgeology/assyntCulmination.html.

Letouzey, J., 1990. Fault Reactivation, Inversion and Fold-Thrust Belt. In: J. Letouzey (Ed) and Editions Technip, Petroleum and Tectonics in Mobile Belts, 101-128.

Lin, A.T., Watts, A.B., 2002. Origin of the West Taiwan basin by orogenic loading and flexure of the rifted continental margin. J. Geophys. Res., 107(B9), doi: 10.1029/2001JB000669.

Lindquist, S.J., 1999. Petroleum systems of the Po Basin province of northern Italy and the northern Adriatic Sea: Porto Garibaldi (biogenic), Meride/Riva di Solto (thermal), and Marnoso Arenacea (thermal): U.S. Geological Survey Open-File Report 99-50-M, 19 p., 15 figs., 3 tables.

Lindsay, M., Aillères, L., Jessell, M., de Kemp, E., Betts, P., 2012. Locating and quantifying geological uncertainty in three-dimensional models: Analysis of the Gippsland Basin, southeastern Australia. Tectonophysics, doi:10.1016/j.tecto.2012.04.007.

Lipparini, T., Perrella, G., Medioli, F., Venzo,S., Barbier, F., Malaroda, R., Sturani, C., Carraro, F., Zanella, E., Corsi, M., Gatto, G., Piccoli, G., 1969. Carta Geologica D'Italia, scale 1:100,000, Map "48-Peschiera del Garda".

Livio, F.A., Berlusconi, A., Michetti, A.M., Sileo, G., Zerboni, A., Trombino, L., Cremaschi, M., Mueller, K., Vittori, E., Carcano, C., Rogledi, S., 2009a. Active fault-related folding in the epicentral area of the December 25, 1222 (Io=IX MCS) Brescia earthquake (Northern Italy): Seismotectonic implications. Tectonophysics 476 (1–2), 320–335, doi:10.1016/j.tecto.2009.03.019.

Livio, F., Michetti, A.M., Sileo, G., Carcano, C., Mueller, K., Rogledi, S., Serva, L., Vittori, E., Berlusconi, A., 2009b. Quaternary capable folds and seismic hazard in Lombardia (Northern Italy): the Castenedolo structure near Brescia. Ital. J. Geosci. . (Boll. Soc. Geol. It.) 128 (1), 191–200.

Lohr, T., Krawczyk, C.M., Tanner, D.C., Samiee, R., Endres, H., Thierer, P.O., Oncken, O., Trappe, H., Bachmann, R., Kukla, P.A. 2008. Prediction of subseismic faults and fractures: Integration of three-dimensional seismic data, three-dimensional retrodeformation, and well data on an example of deformation around an inverted fault. AAPG Bulletin, 92, 4,473–485; doi:10.1306/11260707046.

Lowell, J.D., 1995. Mechanisms of basin inversion from worldwide examples. In: Buchanan, J.G and Buchanan, P.G. (Eds), Geol. Soc. London Spec. Pub., 88, 39-57.

Mackenzie, A. S., & Quigley, T. M. (1988). Principles of geochemical prospect appraisal. AAPG Bulletin, 72(4), 399-415.

Maesano, F., D'Ambrogi, C., Burrato, P., Toscani, G., 2010. Long-term geological slip rates of the Emilia thrust front (Northern Apennines) from 3D modelling of key buried horizons. 85° Congresso Nazionale della

Società Geologica Italiana, “L'Appennino nella geologia del Mediterraneo Centrale”, 6-8 September 2010, Pisa.

Maesano, F.E., D'Ambrogi, C., Burrato, P., Toscani, G., 2011. Slip-rates of the buried Northern Apennines thrust fronts from 3d modeling of key geological horizons (Po Plain, Northern Italy). VIII Forum della Federazione Italiana di Scienze della Terra, Geoitalia, 19-23 September 2011, Torino. (Plio-Pleistocene only & few pseudo 3D blocks from sections).

Maesano, F. E., Toscani, G., Burrato, P., Mirabella, F., D’Ambrogi, C., Basili, R., 2013. Deriving thrust fault slip rates from geological modeling: examples from the Marche coastal and offshore contraction belt, Northern Apennines, Italy, Marine Petr. Geol., 42, 122-134, doi:10.1016/j.marpetgeo.2012.10.008.

Maesano, F.E., The Italian Geomol Team, 2014. Integrating data sources for 3D modeling: the Italian activity in the GeoMol Project, Rend. Online Soc. Geol. It., 30, 28-32, 3 figs. (doi: 10.3301/ROL.2014.07).

Maesano, F.E., D’Ambrogi C., 2015. Coupling sedimentation and tectonic control: Pleistocene evolution of the central Po Basin. Italian Journal of Geosciences. In press. doi:10.3301/IJG.2015.17.

Maesano, F.E., D'Ambrogi, C., Burrato, P., Toscani, G., 2015. Slip-rates of blind thrusts in slow deforming areas: Examples from the Po Plain (Italy). Tectonophysics, 643, 8-25, doi: 10.1016/j.tecto.2014.12.007.

Maino, M., Decarlis, A., Felletti, F., Seno, S., 2013. Tectono-sedimentary evolution of the Tertiary Piedmont Basin (NW Italy) within the Oligo-Miocene central Mediterranean geodynamics. Tectonics, 32, 3, 593-619 doi: 10.1002/tect.20047.

Malusà, M., Anfinson, O., Dafov, L. & Stockli, D., 2016. Tracking Adria indentation beneath the Alps by detrital zircon U-Pb geochronology: Implications for the Oligocene-Miocene dynamics of the Adriatic microplate. Geology, 44, 155-158, doi: 10.1130/G37407.1.

Mann, D. M., Mackenzie, A. S., 1990. Prediction of pore fluid pressures in sedimentary basins: Marine and Petroleum Geology, 7, no. 1, 55–65, http://dx.doi.org/10.1016/0264-8172(90)90056-M.

Mann, P., Escalona, A., Castillo, M.V., 2006. Regional geologic and tectonic setting of the Maracaibo supergiant basin, western Venezuela. AAPG Bulletin, 90, 4, 445–477.

Mancin, N., Di Giulio, A., Cobianchi, M., 2009. Tectonic vs. climate forcing in the Cenozoic sedimentary evolution of a foreland basin (Eastern Southalpine system, Italy). Bas. Res., 21, 6, 799-823. doi: 10.1111/j.1365-2117.2009.00402.x

Mantovani, E., Viti, M., Cenni, N., Babbucci, D., Tamburelli, C., 2015. Present Velocity Field in the Italian Region by GPS Data: Geodynamic/Tectonic Implications. *International Journal of Geosciences*, **6**, 1285-1316. http://dx.doi.org/10.4236/ijg.2015.612103.

Margheriti, L., Pondrelli. S, Piccinini, D., Piana Agostinetti, N., Giovani, L., Salimbeni, S., Lucente, F.P., Amato, A., Baccheschi, P., Park, J., Brandon, M., Levin, V., Plomerová, J., Jedlicˇka, P., Vecsey, L., Babusˇka, V., Fiaschi, A., Carpani, B., Ulbricht, P., 2006. The subduction structure of the Northern Apennines: results from the RETREAT seismic deployment. Annals of Geophysics, 49, 4/5. http://earth.geology.yale.edu/~jjpark/Margheriti_etal_Annali_2006.pdf.

Mariotti, G., Doglioni, C., 2000. The dip of the foreland monocline in the Alps and Apennines. Earth Planet. Sci. Lett. 181, 191-202.

Márton, E., Zampieri, D., Kázmér, M., Dunkl, I., Frisch, W.. 2011. New Paleocene–Eocene paleomagnetic results from the foreland of the Southern Alps confirm decoupling of stable Adria from the African plate, Tectonophysics, 504, 89–99.

Masaferro, J., Bulnes, M., Poblet, J., Casson, N., 2003. Kinematic evolution and fracture prediction of the Valle Morado structure inferred from 3-D seismic data, Salta province, northwest Argentina. AAPG Bulletin, 87, 7, 1083–1104; doi:10.1306/02070301102.

Masetti, D., Fantoni, R., Romano, R., Sartorio, D., Trevisani, E., 2012. Tectonostratigraphic evolution of the Jurassic extensional basins of the eastern southern Alps and Adriatic foreland based on an integrated study of surface and subsurface data. AAPG Bulletin, v. 96, no. 11, pp. 2065–2089.

Maţenco, L., Bertotti, G., Dinu, C., Cloetingh, S., 1997. Tertiary tectonic evolution of the external South Carpathians and the adjacent Moesian platform (Romania). Tectonics, 16 (6), 896-911.

Matenco, L., Bertotti, G., Cloetingh, S., Dinu, C., 2003. Subsidence analysis and tectonic evolution of the external Carpathian - Moesian Platforn region during Neogene times. Sedimentary Geology, 156 (1-4), 71-94, doi: 10.1016/S0037-0738(02)00283-X.

Mattavelli, L., Novelli, L., 1987. Origin of the Po basin hydrocarbons – Memoires de la Societe Geologique de France, nouvelle serie. 151; 97-106.

Mattavelli, L., Novelli, L., 1990. Geochemistry and habitat of the oils in Italy: American Association of Petroleum Geologists Bulletin, 74, 10, 1623-1639.

Mattavelli, L., Margarucci, V., 1992. Malossa Field – Italy, Po Basin, in Foster, N.H., and Beaumont, E.A., Treatise of Petroleum Geology, Atlas of Oil and Gas Fields, Structural Traps VII: Tulsa, OK, American Association of Petroleum Geologists, p. 119-137.

Mattavelli, L., Pieri, M., Groppi, G., 1993. Petroleum exploration in Italy: a review. Mar. and Pet. Geol., 10, 410-425.

Mattirolo, E. Novarese, V., Franchi, S., Stella, A., 1927. Carta Geologica D'Italia, scale 1:100 000, Map "30-Varallo".

Maystrenko, Y., Bayer, U., Scheck-Wenderoth, M., 2013. Salt as a 3D element in structural modeling — Example from the Central European Basin System. Tectonophysics 591, 62–82 ; doi.org/10.1016/j.tecto.2012.06.030.

Maystrenko, Y., Scheck-Wenderoth, M., Hartwig, A., Anka, Z., Watts, A., Hirsch, K., Fishwick, S., 2013. Structural features of the Southwest African continental margin according to results of lithosphere-scale 3D gravity and thermal modelling. Tectonophysics, 604, 104–121. doi.org/10.1016/j.tecto.2013.04.014.

McClay, K., Bonora, M., 2001. Analog models of restraining stepovers in strike-slip fault systems. AAPG Bulletin, 85, 2, 233–260.

McDermott, K., Gillbard, E., Clarke, N., 2015. From Basalt to Skeletons – the 200 million-year history of the Namibian margin uncovered by new seismic data. *First break* volume 33, December 2015.

McQuarrie, N., Horton, B.K., Zandt, G., Beck, S., DeCelles, P.G., 2005. Lithospheric evolution of the Andean fold-thrust belt, Bolivia, and the origin of the central Andean plateau. Tectonophysics, 399 (1-4 SPEC. ISS.), 15-37, doi: 10.1016/j.tecto.2004.12.013.

Merlini S., Doglioni C., Fantoni R., Ponton M., 2002. Analisi strutturale lungo un profilo geologico tra la linea Fella Sava e l'avampaese adriatico (Friuli Venezia Giulia - Italia). Mem. Soc. Geol. It., 57: 293-300, Roma.

Michetti, A.M., Giardina, F., Livio, F., Mueller, K., Serva, L., Sileo, G., Vittori, E., Devoti, R., Riguzzi, F., Carcano, C., Rogledi, S., Bonadeo, L., Brunamonte, F., Fioraso, G., 2012. Active compressional tectonics, Quaternary capable faults and the seismic landscape of the Po Plain (N Italy), Annals of Geophysics, 55, 5, 969-1001, doi: 10.4401/ag-5462.

Middleton M. (1993) A transient method of measuring the thermal properties of rocks. Geophysics, 58, 357-365.

Mitra S., Leslie, W., 2003. Three-dimensional structural model of the Rhourde el Baguel - AAPG Bulletin, 87, 2, 231–250.

Mitra S., Figueroa G.C., Hernandez Garcia J., Murillo Alvarado A., 2005. Three-dimensional structural model of the Cantarell and Sihil structures, Campeche Bay, Mexico - AAPG Bulletin, 89, 1, 1–26.

Mitra S., Gonzalez, A., Hernandez Garcia, J., Kajari, G., 2007. Ek-Balam field: A structure related to multiple stages of salt tectonics and extension field, Algeria - AAPG Bulletin, 91, 11, 1619–1636.

Molinari, I., Argnani, A.; Morelli, A., 2015. Development and testing of a 3D seismic velocity model of the Po Plain sedimentary basin, Italy. Bulletin of the Seismological Society of America. 105, 2A, 753-764; doi: 10.1785/0120140204.

Montone, P., Mariucci, M.T., Pondrelli, S., Amato, A., 2004. An improved stress map for Italy and surrounding regions (central Mediterranean). Journal of Geophysical Research, 109, B10410, doi:10.1029/2003JB002703.

Moratto, l., Suhadolc, P., Costa, G., 2012. Finite-fault parameters of the September 1976 M>5 aftershocks in Friuli (NE Italy). Tectonophysics 536-537, 44-60.

Moretti, I., Triboulet, S., Endignoux, L, 1990. Some remarks on the geometrical modeling of geological deformations. In: J. Letouzey (Ed.) and Editions Technip, Petroleum and Tectonics in Mobile Belts, 155–162.

Moretti, I., and Raoult, JJ., 1990. Geological restoration of seismic depth images. First Break, 8, 7, 271-275.

Moretti, I., 2008. Working in complex areas: new restoration workflow based on quality control, 2D and 3D restoration. Marine and Petroleum Geology, 25, 205-217; doi: 10.1016/j.marpetgeo.2007.07.001.

Mosca, P., Polino, R., Rogledi, S., Rossi, M., 2010. New data for the kinematic interpretation of the Alps–Apennines junction (Northwestern Italy) - Int J Earth Sci (Geol Rundsch), 99:833–849, DOI 10.1007/s00531-009-0428-2.

Mouthereau, F., Watts, A. B., Burov, E., 2013. Structure of orogenic belts controlled by lithosphere age. *Nature Geoscience,* **6**, 785-789, doi: 10.1038/NGEO1902.

Muñoz-Jiménez, A.,Casas-Sainz, A.M., 1997. The Rioja Trough (N Spain): tectono sedimentary evolution of a symmetric foreland basin. Basin Research 9 (1), 65–85. http://dx.doi.org/10.1046/j.1365-2117.1997.00031.x.

Naylor, M., Sinclair, H. D., 2008. Pro- vs. retro-foreland basins. Basin Research 20 (3), 285-303. doi: 10.1111/j.1365-2117.2008.00366.x

Nardin, M., Rossi, D., Sommavilla, E., Largaiolli, T., Mozzi, G., Gregnanin, A., Zulian, T., Zirpoli, G., Corsi, M., Gatto, G.O., Gatto, P., Graga, Gp., Rui, a., 1970. Carta Geologica D'Italia, scale 1:100,000, Map "22-Feltre".

Nardon, S., Marzorati, D., Bernasconi, A., Cornini, S., Gonfalini, M., Mosconi, S., Romano, A., and Terdich, P., 1991. Fractured carbonate reservoir characterization and modeling a multidisciplinary case study from the Cavone oil field, Italy: First Break, 9, 12, 553-565.

Neumaier, M., Littke, R., Hantschel, T., Maerten, L., Joonnekindt, T., Kukla, P., 2014. Integrated charge and seal assessment in the Monagas fold and thrust belt of Venezuela. AAPG Bulletin, v. 98, no. 7, pp. 1325–1350.

Nicolai,C. & Gambini,R., 2007. Structural architecture of the Adria platform-and-basin system. Boll.Soc.Geol.It. (Ital.J.Geosci.), Spec. Issue No. 7, 21-37, 15 figs., 1 pl., CROP-04 (ed. by A. Mazzotti, E. Patacca and P. Scandone).

Nicolich, R., 2010. Geophysical investigation of the crust of the Upper Adriatic and neighbouring chains - Rend.Fis.Acc.Lincei, 21, (Suppl 1):S181-S196, DOI 10.1007/s12210-010-0093-y.

Norman Kent, W., Dasgupta, U., 2004. Structural evolution in response to fold and thrust belt tectonics in northern Assam. A key to hydrocarbon exploration in the Jaipur anticline area. Mar. and Pet. Geol. 21, 785–803. http://dx.doi.org/10.1016/j.marpetgeo.2003. 12.006.

Novelli, L., Chiaramonte, M. A., Mattavelli, L., Pizzi, G., Sartori, L., Scotti, P., 1987. Oil habitat in the northwestern Po Basin. In: B. Doligez, (Ed.) and Editions Technip, Migration of hydrocarbons in sedimentary basins, 27–57.

Nunns, A., 1991. Structural Restoration of Seismic and Geologic Sections in Extensional Regimes, AAPG Bulletin, 75, 2.

Oszczypko, N., 2006. Late Jurassic-Miocene evolution of the Outer Carpathian fold-and-thrust belt and its foredeep basin (Western Carpathians, Poland). Geological Quarterly, 50 (1), 169-194.

Pasquale,V., Gola, G., Chiozzi,P., Verdoya, M., 2011. Thermophysical properties of the Po Basin rocks. Geophys. J. Int., 186, 69–81. doi: 10.1111/j.1365-246X.2011.05040.x

Pasquale,V., Chiozzi, P., Verdoya, M., Gola, G., 2012. Heat flow in theWestern Po Basin and the surrounding orogenic belts. Geophys. J. Int., 190, 8–22. doi: 10.1111/j.1365-246X.2012.05486.x.

Passeri, L.D., Comizzoli, G., Assereto, R., 1967. Carta Geologica D'Italia, scale 1:100,000, Map "14 A-Tarvisio".

Paul, D., Mitra, S., 2013. Experimental models of transfer zones in rift systems. AAPG Bulletin, 97, 5, 759–780: doi:10.1306/10161212105.

Pennacchioni, G., Di Toro, G., Brack, P., Menegon, L., Villa, I.M., 2006. Brittle–ductile–brittle deformation during cooling of tonalite (Adamello, Southern Italian Alps). Tectonophysics 427, 171–197.

Pepper, A. S., Corvi, P.J., 1995a. Simple kinetic models of petroleum formation. Part I: Oil and Gas generation from kerogen. Marine and Petroleum Geology, v. 12, no. 3, p. 291-319.

Pepper, A. S., Corvi, P.J., 1995b. Simple kinetic models of petroleum formation. Part III: Modelling an open system. Marine and Petroleum Geology, v. 12, no. 4, p. 417-452.

Pepper, A.S., Dodd, T.A., 1995. Simple kinetic models of petroleum formation. Part II : oil-gas cracking. Marine and Petroleum Geology, v. 12, no. 3, p. 321-340.Perotti C. R., 1991. Osservazioni sull'assetto strutturale del versante padano dell'Appennino Nord-Occidentale, Atti Tic. Sc. Terra, 34, 11-22.

Perotti, C. R., Vercesi, P. L., 1991. Assetto tettonico ed evoluzione strutturale recente della porzione nord-occidentale dell'Appennino emiliano, Memorie Descrittive Carta Geologica d'Italia, XLVI, 313-326.

Peruzza, L., Poli, M.E., Rebez, A., Renner, G., Rogledi, S., Slejko, D., Zanferrari, A., 2002. The 1976-1977 seismic sequence in Friuli: new seismotectonic aspects. Mem. Soc. Geol. It., 57: 391-400, Roma.

Petersen, M. Seeber, L., Sykes, L., Nabelek, J., Armbruster, J., Pacheco, J., Hudnut, K., 1991. Seismicity and fault interaction, southern San Jacinto fault zone and adjacent faults, southern California: implications for seismic hazard. Tectonics, 10, 6, pp. 1187-1203.

Petricca, P, Carminati, E., 2014. Present-day stress field in subduction zones: Insights from 3D viscoelastic models and data. Tectonophysics 667, 48–62 ; doi.org/10.1016/j.tecto.2015.11.010.

Pfiffner, A., 2014. Geology of the Alps. Wiley and Sons Ed, New York. 368 pp.

Picotti, V., Pazzaglia, F. J., 2008. A new active tectonic model for the construction of the Northern Apennines mountain front near Bologna (Italy). Journal of Geophysical Research. V. 113 (B8), 1-24.

Pieri, M., Groppi,G., 1981. Subsurface geological structure of the Po Plain, Italy. Prog.Fin. Geodinamica CNR, pubbl.414, 1-113, Roma.

Pieri M., 1984. Storia delle ricerche nel sottosuolo padano fino alle ricostruzioni attuali – Cento anni di geologia Italiana, Volume Giubilare, 1° Centenario della Soc.Geol.Ital. 1881-1981, Roma, 155-177.

Pieri, M., 2001, Italian petroleum geology- In: G.B.Vai and I.P. Martini (eds), Anatomy of an Orogen: the Apennines and Adjacent Mediterranean Basins, pp.533-550.

Pietro, B., Raffaele, D., & Diego, G. (1979, January 1). Deep Drilling In Po Valley : Planning Criteria And Field Results. Society of Petroleum Engineers. doi:10.2118/7847-MS

PLACER, L., 1999. Contribution to the macrotectonic subdivisionof the border region between Southern Alps and External Dinarides. Geologija, 41, 223-255, Ljubljana.

PLACER, L., VRABEC, M., CELARC, B., 2010. The bases for understanding of the NW Dinarides and Istria Peninsula tectonics. Geologija 53/1 55-86 Ljubljana.Contribution to the macrotectonic subdivisionof the border region between Southern Alps and External Dinarides. Geologija, 41, 223-255, Ljubljana.

Pola, M., Ricciato, A., Fantoni, R., Fabbri, P., Zampieri, D., 2014. Architecture of the western margin of the North Adriatic foreland: The Schio-Vicenza fault system. Italian Journal of Geosciences, 133 (2), 223-234, doi: 10.3301/IJG.2014.04.

Poli, M.E., Peruzza, L., Rebez, A., Renner, G., Slejko, D., Zanferrari, A., 2002. New seismotectonic evidence from the analysis of the 1976-1977 and 1977-1999 seismicity in Friuli (NE Italy). Boll. Geof. Teor. Appl., 43: 53-78, Trieste.

Ponton, M., 2010. Architettura delle Alpi Friulane. Museo Friulano di Storia Naturale, Publ. N° 52, Udine, ISBN 9788888192529.

Ponza, A., Pazzaglia, F.J., Picotti, V., 2010. Thrust-fold activity at the mountain front of the Northern Apennines (Italy) from quantitative landscape analysis. Geomorphology 123 (3–4), 211–231, doi:10.1016/j.geomorph.2010.06.008.

Porro, C., 1921. In tema di ricerche di petrolio in Italia; La miniera italiana, 5, 137-156, 10 ff, Roma.

Ramón, M., Pueyo, E., Rodríguez-Pintó, A., Ros, L., Pocoví, A., Briz, J., Ciria, J., 2013. A computed tomography approach for understanding 3D deformation patterns in complex folds. Tectonophysics 593, 57–72 ; doi.org/10.1016/j.tecto.2013.02.027.

Ravaglia, A., Turrini, C., Seno, S., 2004. Mechanical stratigraphy as a factor controlling the development of a sandbox transfer zone: A three-dimensional analysis. J. Struct. Geol. 26, 2269-2283.

Ravaglia, A., Seno, S., Toscani, G., Fantoni, R., 2006. Mesozoic extension controlling the Southern Alps thrust front geometry under the Po Plain, Italy: Insights from sandbox models. Journal of Structural Geology 28, 2084e2096.

Resor, P., 2008. Deformation associated with a continental normal fault system, western Grand Canyon, Arizona. GSA Bulletin; 120, n° 3/4; 414–430.

Ricci Lucchi, F., 1986. The Oligocene to recent foreland basins of the northern Apennines, In: Allen, P. A., and P. Homewood (Eds), Foreland basins, I.A.S. Special Publication, 8, 105-139.

Rigo, F., 1991, Italy to open 'exclusive' Po basin area in 1992. Oil and Gas Journal, v. 89, no. 21 102-106.

Riva, A., Salvatori, T., Cavaliere, R., Ricchiuto, T., Novelli, L., 1986. Origin of oils in Po Valley, Northern Italy – Organic Geochemistry, 10, 391-400.

Rivenæs, J., Otterlei, C., Zachariassen, E., Dart, C., Sjøholm, J., 2005. A 3D stochastic model integrating depth, fault and property uncertainty for planning robust wells, Njord Field, offshore Norway. Petroleum Geoscience, 11, 57–65.

Rizzini, A., Dondi, L., 1978. Erosional surface of Messinian age in the subsurface of the Lombardian Plain (Italy). Mar. Geol., 27 (3-4), 303-325.

Roberts, A., 2001. Curvature attributes and their application to 3D interpreted horizons. First break,19, 85-100.

Roeder, D., 1991. Structure and tectonic evolution of alpine lithosphere – EUG VI Symposium, the European geotraverse (EGT) final results, Strasbourg.

Rogledi, S., 2010. Assetto strutturale delle unità alpine nella pianura tra il lago d'Iseo e il Garda. Rischio sismico nella Pianura Padana. http://cesia.ing.unibs.it/index.php/it/eventi/giornate-di-studio/119.

Rossi, M., Minervini, M., Ghielmi, M. & Rogledi, S., 2015. Messinian and Pliocene erosional surfaces in the Po Plain-Adriatic Basin: Insights from allostratigraphy and sequence stratigraphy in assessing play concepts related to accommodation and gateway turnarounds in tectonically active margins. Mar. and Pet. Geol., 66, 192-216.

Roure, F., Polino, R., Nicolich, R., 1989. Poinçonnements, rétrocharriages et chevauchements post-basculement dans les Alpes occidentales: evolution intracontinentale d'une chaîne de collision. CR Acad. Sci. Paris, 309, II, 283-290.

Roure, F., Polino, R., Nicolich, R., 1990. Early Neogene deformation beneath the Po plain: constraints on the post-collisional Alpine evolution. In: Deep structure of the Alps. Eds: Roure, F., Heitzmann, P., Polino, R.,. Mem.Soc.Geol.France 156, 309-322.

Roure F., Casero P., Vially R., 1991. Growth processes and mélange formation in the southern Apennine accretionary wedge..Earth and Planet. Sc. Lets, 102, 395-412.

Roure F., Choukroune P., Polino R., 1996. Deep seismic reflection data and new insights on the bulk geometry of mountain ranges. Comptes Rendus de l'Académie des Sciences, série IIa, 322, 345-359.

Roure, F., Nazaj, S., Mushka, K., Fili, I., Cadet, J.P., Bonneau, M., 2004. Kinematic evolution and petroleum systems—An appraisal of the Outer Albanides, in K. R. McClay, ed., Thrust tectonics and hydrocarbon systems: AAPG Memoir 82, 474 – 493.

Roure F., Casero P., Addoum B., 2012. Alpine inversion of the North African Margin, and delamination of its continental crust. Tectonics, 31, TC3006. Doi: 10.1029/2011TC002989.

Rovida, R., Camassi, R., Gasperini, P., Stucchi, M., (Eds), 2011. CPTI11, the 2011 version of the Parametric Catalogue of Italian Earthquakes, Milano, Bologna, http://emidius.mi.ingv.it/CPTI/.

Sala, P., Frehner, M., Tisato, N., Pfiffner, A., 2013. Building a three-dimensional near-surface geologic and petrophysical model based on borehole data : a case study from Chemery, Paris Basin, France. AAPG Bulletin, 97, 8, 1303-1324.

Sassi, F.P., Zirpoli, G., Nardin, M., Sacerdoti, M., Bosellini, A., Largaiolli, T., Leonardi, P., Sommavilla, E., MOzzi, G., Rossi, D., Proto Decima, F., Dal Monte, M., Paganelli, L., Simboli, G., Gatto, P., 1970. Carta Geologica D'Italia, scale 1:100,000, Map "11- M. Marmolada".

Scardia, G., Festa,A., Monegato, G., Pini, R., Rogledi, S., Tremolada, F., Galadini., F., 2014. Evidences for the late Alpine tectonics in the Lake Garda area (northern Italy) and seismogenic implications. Geol.Soc.of America Bulletin, doi: 10.1130/B30990.1.

Schmid, S.M., Kissling, E., 2000. The arc of the Western Alps in the light of geophysical data on deep crustal structure. Tectonics, 19, 62-85.

Schmid, S., Fugenschuh, B., Kissling, E., Schuster, R., 2004. Tectonic map and overall architecture of the Alpine orogen. Eclogae Geologicae Helvetiae 97, 93-117.

Schonborn, G., 1992. Alpine tectonics and kinematic models of the central southern Alps. Memorie di Scienze Geologiche, 44, 229-393.

Schonborn,G., 1999. Balancing cross sections with kinematic constraints: the Dolomites (northern Italy). Tectonics, 18, 3, pp. 527-545.

Schöpfer, M., Childs, C., Walsh, J., Manzocchi, T., 2016. Evolution of the internal structure of fault zones in three-dimensional numerical models of normal faults. Tectonophysics 666, 158–163; doi.org/10.1016/j.tecto.2015.11.003.

Schreiber, D., Lardeaux, J.M., Martelet, G., Courrioux, G., Guillen, A., 2010. 3-D modelling of Alpine Mohos in Southern Alps. Geophys. J. Int.; doi: 10.1111/j.1365-246X.2009.04486.x.

Schumacher, M.E., Laubscher, H.P., 1996. 3D crustal architecture of the Alps-Apennines join: a new view on seismic data. Tectonophysics, 260, 349-363.

Scotti, P., Fantoni, R., 2008. Thermal modeling of the extensional Mesozoic succession of the Southern Alps and implications for oil exploration in the Po Plain foredeep. 70th EAGE Congerence & Exhibition – Rome, Italy, 0-12 June, 2008.

Scrocca, D., Doglioni, C., Innocenti, F., 2003. Contraints for an interpretation of the italian geodynamics: a review. *Mem. Descr. Carta Geol. d'It.*LXII, 15-46.

Sekiguchi, K., 1984. A method for determining terrestrial heat flow in oil basinal areas. Tectonophysics, 103, 67etho.

Serpelloni, E., Anzidei, M., Baldi, P., Casula, G., & Galvani, A., 2005. Crustal velocity and strain-rate fields in Italy and surrounding regions: new results from the analysis of permanent and non-permanent GPS networks. Geophysical Journal International, Volume 161, Issue 3, pp. 861-880.

Serpelloni, E., Vannucci, G., Pondrelli, S., Argnani, A., Casula, G., Anzidei, M., Baldi, P., Gasperini, P., 2007. Kinematics of the Western Africa-Eurasia plate boundary from focal mechanisms and GPS data. Geophys. J. Int. 169, 1180–1200, doi:10.1111/j.1365-246X.2007.03367.x.

Serpelloni, E., Anderlini, L., Avallone, A., Cannelli, V., Cavaliere, A., Cheloni, D., D'Ambrosio, C., D'Anastasio, E., Esposito, A., Pietrantonio, G., Pisani, A.R., Anzidei, M., Cecere, G., D'Agostino, N., Del Mese, S., Devoti, R., Galvani, A., Massucci, A., Melini, D., Riguzzi, F., Selvaggi, G., Sepe, V., 2012. GPS observations of coseismic deformation following the May 20 and 29, 2012, Emilia seismic events (northern Italy): data, analysis and preliminary models, Ann. Geophys. 55, 4, doi:10.4401/ag-6168.

Serpelloni, E., Faccenna, C., Spada, G., Dong, D., D. P. Williams, S., 2013. Vertical GPS ground motion rates in the Euro-Mediterranean region: New evidence of velocity gradients at different spatial scales along the Nubia-Eurasia plate boundary. Journal of Geophysical Research, 118, 6003–6024, doi:10.1002/2013JB010102.

Shao, Y., Zheng, A., He, Y., Xiao, K., 2012. 3D Geological Modeling under Extremely , Complex Geological Conditions. Journal of Computers, 3, 699-705.

Shiner, P., Bosica, B., Turrini, C., 2013. The slope carbonates of the Apulian Platform – an under-explored play in the Central Adriatic. http://www.petroceltic.com/~/media/Files/P/Petroceltic-V2/pdf/AAPG-barcelona-2013-slope-carbonates-of-the-apulian-platform.pdf.

Stefani, M., and Burchell, M., 1990. Upper Triassic (Rhaetic) argillaceous sequences in northern Italy: depositional dynamics and source potential, *in* Hue, A.Y., ed., Deposition of Organic Facies, AAPG Studies in Geology #30: Tulsa, OK, American Association of Petroleum Geologists, p. 93-106.

Sue, C., Calcagno, P., Courrioux, G., Tricart, P., Frechet, J., Thouvenot, F., 2010. Relationships between inherited crustal structures and seismicity in the western Alps inferred from 3D structural modeling. *Bull. Soc. géol. Fr.*, 181, 6, 583-590.

Sweeney, J.J., and Burnham, A.K., 1990. Evaluation of a simple model of vitrinite reflectance based on chemical kinetics: American Association of Petroleum Geologists Bulletin, v. 74, p. 1559–1570.

Tensi J., Mouthereau F., Lacombe O., 2006. Lithospheric bulge in the West Taiwan basin. Basin Research, 18, 277–299, doi:10.1111/j.1365-2117.2006.00296x.

Tissot, B. P., and D. H. Welte, 1984, Petroleum formation and occurrence, 2nd ed: New-York, Springer Verlag, 699 p.

Toscani, G., Seno, S., Fantoni, R., Rogledi, S., 2006. Geometry and timing of deformation inside a structural arc; the case of the western Emilian folds (Northern Apennine front, Italy). Boll. della Soc. Geol. Ital. 125 (1), 59–65.

Toscani, G., Burrato, P., Di Bucci, D., Seno, S., Valensise, G., 2009. Plio-Quaternary tectonic evolution of the Northern Apennines thrust fronts (Bologna-Ferrara section, Italy): seismotectonic implications. Ital. J. Geosci. (Boll. della Soc. Geol. Ital.) 128 (2), 605–613, doi:10.3301/IJG.2009.128.2.605.

Toscani, G., Bonini, L., Ahmad, M.I., Bucci, D.D., Giulio, A.D., Seno, S., Galuppo, C., 2014. Opposite verging chains sharing the same foreland: Kinematics and interactions through analogue models (Central Po Plain, Italy). Tectonophysics, 633 (1), 268-282.

Toscani, G., Marchesini, A., Barbieri, C., Di Giulio, A., Fantoni, R., Mancin, N. & Zanferrari, A., 2016. The Friulian-Venetian Basin I: architecture and sediment flux into a shared foreland basin. Ital. J. Geosci., 135(3), doi: 10.3301/IJG.2015.35.

Trocme, V., Albouy, E., Callot, JP., Letouzey, J., Rolland, N., Goodarzi, H., Jahani, S., 2011. 3D structural modelling of the southern Zagros fold-and-thrust belt diapiric province. Geol. Mag. 148, 5–6, 879–900; doi:10.1017/S0016756811000446.

Trumpy, R., 1973. The timing of orogenic events in the Central Alps. In: De Jong, K.A., Scholten, R. (Eds.), Gravity and Tectonics. Wiley and Sons, New York, pp. 229e251.

Turrini, C., Rennison, P., 2004. Structural style from the Southern Apennines' hydrocarbon province—An integrated view, in K. R. McClay, ed., Thrust tectonics and hydrocarbon systems: AAPG Memoir 82, 558 – 578.

Turrini, C., Dups, K., Pullan, C., 2009. 2D and 3D structural modelling in the Swiss-French Jura Mountains. First break, 27, 65-71.

Turrini, C., Lacombe, O., Roure, F., 2014. Present-day 3D structural model of the Po Valley basin, Northern Italy. Mar. Pet. Geol. 56, 266–289. http://dx.doi.org/10.1016/j.marpetgeo.2014.02.006.

Turrini, C., Angeloni, P., Lacombe, O., Ponton, M., Roure, F., 2015. Three-dimensional seismo-tectonics in the Po Valley basin, Northern Italy Tectonophysics, 661, pp. 156-179, doi: 10.1016/j.tecto.2015.08.033.

Turrini, C., Angeloni, P., Lacombe, O., Ponton, M., Roure, F., 2015. Three-dimensional seismo-tectonics in the Po Valley basin, northern Italy. Geophysical Research Abstract, EGU, Vienna.

Uliana, M.A., Arteaga, M.E., Legarreta, L., Cerdan, J.J., Peroni, G.O., 1995. Inversion structures and hydrocarbon occurrence in Argentina. In Buchanan, J.G and Buchanan, P.G. (Eds), Geol. Soc. London Spec. Pub.,88, 211-233.

Valcarce, G., Zapata T., Ansa A., Selva G., 2006. Three-dimensional structural modeling and its application for development of the El Porto´n field, Argentina - AAPG Bulletin, 90, 3, 307–319.

Vaghi, G.C., Torricelli, L., Pulga, M., Giacca, D., Chierici, G.L., and Bilgeri, D., 1980, Production in the very deep Malossa field, Italy: Proceedings 10th World Petroleum Congress, Bucharest, v. 3, p. 371-388.

Van Hinsbergen, D.J.J., Mensink, M., Langereis, C.G., Maffione, M., Spalluto, L., Tropeano, M., Sabato, L., 2014. Did Adria rotate relative to Africa? Solid Earth, 5 (2), pp. 611-629. doi: 10.5194/se-5-611-2014.

Vannoli, P., Burrato, P., Valensise, G., 2014. The seismotectonics of the Po Plain (northern Italy): tectonic diversity in a blind faulting domain. Pure Appl. Geophys., doi:10.1007/s00024-014-0873-0.

Vanossi, M., Cortesogno, L., Galbiati, B., Messiga, B., Piccardo, G. B., Vannoli, P., Burrato P., Valensise, G., 2014. The Seismotectonics of the Po Plain (Northern Italy): Tectonic Diversity in a Blind Faulting Domain. Pure Appl. Geophys, doi 10.1007/s00024-014-0873-0.

Vannucci, R., 1986. Geologia delle Alpi Liguri: dati, problemi, ipotesi, Mem. Soc. Geol. It., 28, 5–75.

Waples, D.W., Waples, J.S., 2004 A review and evaluation of specific heat capacities of rocks, minerals, and subsurface fluids. Part 2, fluids and porous rocks. Nat Resour Res 13:123–130.

Venturini C., 1991. Cinematica neogenico-quaternaria del sudalpino orientale (settore friulano). *Studi Geol. Camerti*, vol. spec. (1990), 109-113, Camerino.

Vergés, J. (2007) Drainage Responses to Oblique and Lateral Thrust Ramps: A Review, in Sedimentary Processes, Environments and Basins: A Tribute to Peter Friend (eds G. Nichols, E. Williams and C. Paola), Blackwell Publishing Ltd., Oxford, UK. doi: 10.1002/9781444304411.ch3.

ViDEPI Project (http://unmig.sviluppoeconomico.gov.it/videpi/kml/webgis.asp).

Winterer, E. L., Bosellini, A., 1981. Subsidence and sedimentation on Jurassic passive continental margin, Southern Alps, Italy: AAPG Bulletin, v. 65, p. 394-421.

Wygrala, B.P., 1988. Integrated computer-aided basin modelling applied to analysis of hydrocarbon generation history in a Northern Italian oil field. Advances in Organic Geochemistry, 13, 1-3, pp. 187-197.

Viganò, A., Della Vedova, B., Ranalli, G., Martin, S., Scafidi, D., 2011. Geothermal and rheological regime in the Po plain sector of Adria (Northern Italy). Italian Journal of Geosciences, 131 (2), 228-240.

Vignaroli, G., Faccenna, C., Jolivet, L., Piromallo, C., Rossetti, F., 2008. Subduction polarity reversal at the junction between the Western Alps and the Northern Apennines, Italy; Tectonophysics 450, 34–50.

Vouillamoz, N., Sue, C., Champagnac, J., Calcagno, P., 2012. 3D cartography modeling of the Alpine Arc. Tectonophysics (2012), doi: 10.1016/j.tecto.2012.06.012.

Wang, C.Y, Shin T.C, 1998. Illustrating 100 years of Taiwan seismicity. TAO, 9, 4, 589-614 . http://tao.cgu.org.tw/pdf/v94p589.pdf

Watts A.B., 1992. The effective elastic thickness of the lithosphere and the evolution of foreland basins. Basin Research, 4, 169-178.

Weber, J., Vrabec, M., Pavlovcic-Preseren, P., Dixon, T., Jiang,Y., and Stopar, R, B., 2010. GPS derived motion of the Adriatic microplate from Istria Peninsula and Po Plain sites, and geodynamic implications, Tectonophysics 483, 213–222, doi:10.1016/j.tecto.2009.09.001.

Zanchi, A., Chinaglia, N., Conti, M., De Toni, S., Ferliga,C., Tsegaye, A., Valenti, L. & Bottin, R., 1990. Analisi strutturale lungo il fronte della dolomia principale in bassa val Seriana (Bergamo). Mem. Soc. Geol. It, 45, 83-92.

Zappaterra, E., 1994. Source-Rock distribution Model of the Periadriatic Region. AAPG Bullettin, v.78, n.3, pp.333-35.

Zattin, M., Cuman, A., Fantoni, R., Martin, S., Scotti, P., Stefani, C., 2006. From middle Jurassic heating to Neogene cooling: the thermochronological evolution of the Southern Alps. Tectonophysics, 414, 191-202.

Ziegler, P.A., 1989. Geodynamic model for Alpine intra-plate compressional deformation in Western and Central Europe. In Cooper M.A. and Williams, G.D (Eds), Geol. Soc. London Spec. Pub., 44(1):63-85.

Ziegler, P.A., Bertotti, G., Cloetingh.S., 2002. Dynamic processes controlling foreland development – the role of mechanical (de)coupling of orogenic wedges and forelands. EGU Stephan Mueller Special Publication Series, 1, 17–56.

Zoetemeijer R., Sassi, W., Cloetingh, S., 1992. Stratigraphic and kinematic modeling of thrust evolution, northern Appennines, Italy. Geology, 20, 1035-1038.

Zou Yan-Rong, Peng Ping'an, 2001. Overpressure retardation of organic-matter maturation : a kinetic model and its application. Marine and Petroleum Geology, 18, 707-713.

Yin, H., Groshong, R.H., 2007. A three-dimensional kinematic model for the deformation above an active diapir. AAPG Bulletin, 91, 3, 343–363; doi:10.1306/10240606034.